DNA REPAIR MACHINERY IN INNATE AND ADAPTIVE IMMUNITY

EDITED BY: Feilong Meng, Teng Ma, Zhenkun Lou, Xiaoyan Qiu, Ping-Kun Zhou and Weihua Zhou

PUBLISHED IN: Frontiers in Cell and Developmental Biology

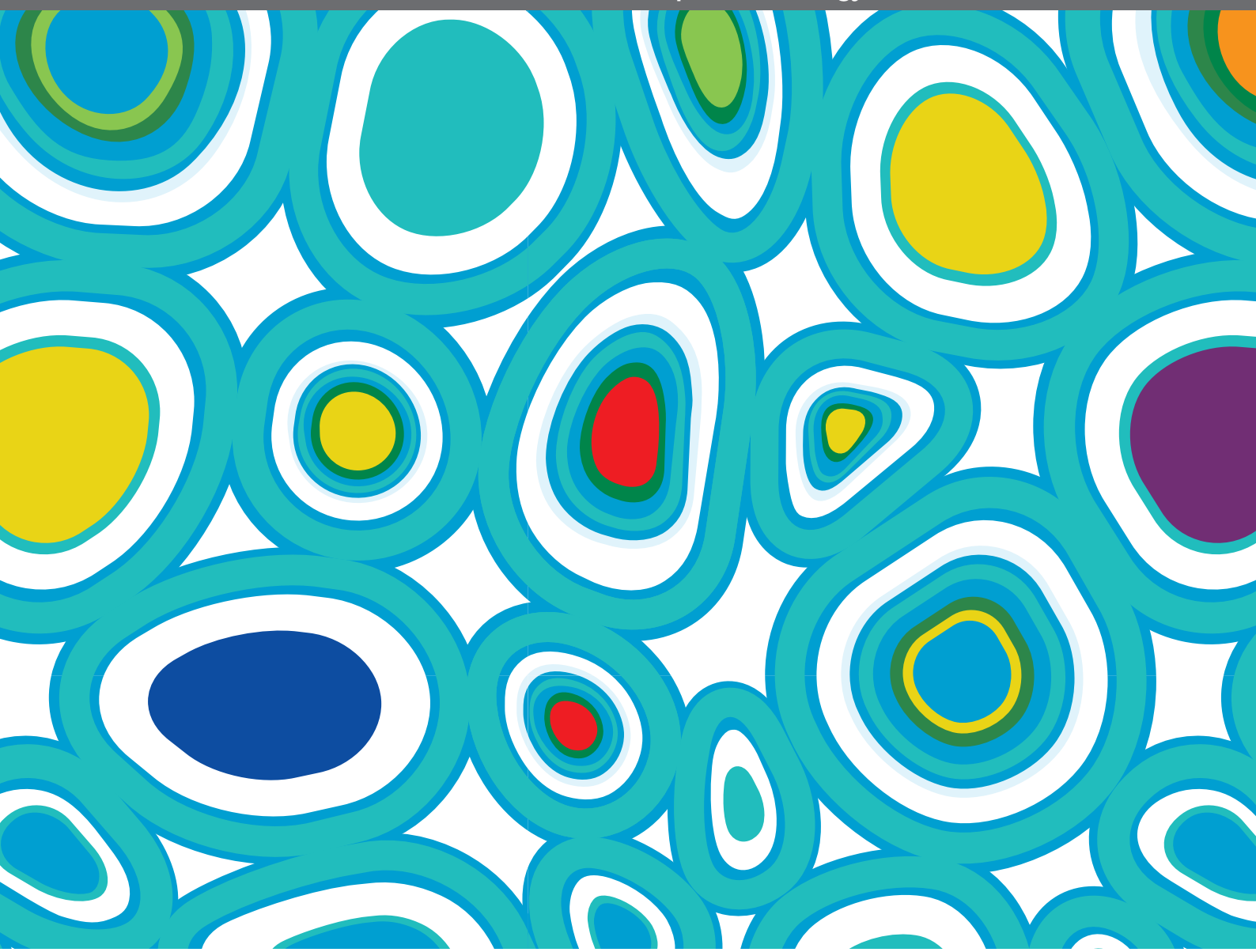

frontiers Research Topics

frontiers

ISSN 1664-8714
ISBN 978-2-88976-885-1
DOI 10.3389/978-2-88976-885-1

About Frontiers

Frontiers is more than just an open-access publisher of scholarly articles: it is a pioneering approach to the world of academia, radically improving the way scholarly research is managed. The grand vision of Frontiers is a world where all people have an equal opportunity to seek, share and generate knowledge. Frontiers provides immediate and permanent online open access to all its publications, but this alone is not enough to realize our grand goals.

Frontiers Journal Series

The Frontiers Journal Series is a multi-tier and interdisciplinary set of open-access, online journals, promising a paradigm shift from the current review, selection and dissemination processes in academic publishing. All Frontiers journals are driven by researchers for researchers; therefore, they constitute a service to the scholarly community. At the same time, the Frontiers Journal Series operates on a revolutionary invention, the tiered publishing system, initially addressing specific communities of scholars, and gradually climbing up to broader public understanding, thus serving the interests of the lay society, too.

Dedication to Quality

Each Frontiers article is a landmark of the highest quality, thanks to genuinely collaborative interactions between authors and review editors, who include some of the world's best academicians. Research must be certified by peers before entering a stream of knowledge that may eventually reach the public - and shape society; therefore, Frontiers only applies the most rigorous and unbiased reviews.
Frontiers revolutionizes research publishing by freely delivering the most outstanding research, evaluated with no bias from both the academic and social point of view. By applying the most advanced information technologies, Frontiers is catapulting scholarly publishing into a new generation.

What are Frontiers Research Topics?

Frontiers Research Topics are very popular trademarks of the Frontiers Journals Series: they are collections of at least ten articles, all centered on a particular subject. With their unique mix of varied contributions from Original Research to Review Articles, Frontiers Research Topics unify the most influential researchers, the latest key findings and historical advances in a hot research area! Find out more on how to host your own Frontiers Research Topic or contribute to one as an author by contacting the Frontiers Editorial Office: frontiersin.org/about/contact

DNA REPAIR MACHINERY IN INNATE AND ADAPTIVE IMMUNITY

Topic Editors:
Feilong Meng, Chinese Academy of Sciences (CAS), China
Teng Ma, Capital Medical University, China
Zhenkun Lou, Mayo Clinic, United States
Xiaoyan Qiu, Peking University, China
Ping-Kun Zhou, Department of Radiation Biology, Beijing Key laboratory for Radiobiology, Beijing Institute of Radiation Medicine, China
Weihua Zhou, University of Michigan, United States

Citation: Meng, F., Ma, T., Lou, Z., Qiu, X., Zhou, P.-K., Zhou, W., eds. (2022). DNA Repair Machinery in Innate and Adaptive Immunity. Lausanne: Frontiers Media SA. doi: 10.3389/978-2-88976-885-1

Table of Contents

frontiers in Cell and Developmental Biology

ORIGINAL RESEARCH
published: 04 October 2021
doi: 10.3389/fcell.2021.761300

Single-Cell RNA Sequencing Revealed CD14$^+$ Monocytes Increased in Patients With Takayasu's Arteritis Requiring Surgical Management

Gao Qing[1,2,3,4], Wu Zhiyuan[2], Yu Jinge[5], Miao Yuqing[1,2], Chen Zuoguan[2], Diao Yongpeng[2], Yin Jinfeng[3,4], Jia Junnan[4], Guo Yijia[3,4], Li Weimin[3,4†] and Li Yongjun[1,2*†]*

[1] Graduate School of Peking Union Medical College, Chinese Academy of Medical Science, Beijing, China, [2] Department of Vascular Surgery, National Centre of Gerontology, Beijing Hospital, Beijing, China, [3] National Tuberculosis Clinical Lab of China, Beijing Chest Hospital, Beijing Tuberculosis and Thoracic Tumor Research Institute, Capital Medical University, Beijing, China, [4] Beijing Key Laboratory in Drug Resistance Tuberculosis Research, Beijing Chest Hospital, Capital Medical University, Beijing, China, [5] Institute of Statistics and Big Data, Renmin University of China, Beijing, China

Objectives: Takayasu Arteritis (TA) is a highly specific vascular inflammation and poses threat to patients' health. Although some patients have accepted medical treatment, their culprit lesions require surgical management (TARSM). This study aimed at dissecting the transcriptomes of peripheral blood mononuclear cells (PBMCs) in these patients and to explore potential clinical markers for TA development and progression.

Methods: Peripheral blood were collected from four TA patients requiring surgical management and four age-sex matched healthy donors. Single cell RNA sequencing (scRNA-seq) was adopted to explore the transcriptomic diversity and function of their PBMCs. ELISA, qPCR, and FACS were conducted to validate the results of the analysis.

Results: A total of 29918 qualified cells were included for downstream analysis. Nine major cell types were confirmed, including CD14$^+$ monocytes, CD8$^+$ T cells, NK cells, CD4$^+$ T cells, B cells, CD16$^+$ monocytes, megakaryocytes, dendritic cells and plasmacytoid dendritic cells. CD14$^+$ monocytes (50.0 vs. 39.3%, $p < 0.05$) increased in TA patients, as validated by FACS results. TXNIP, AREG, THBS1, and CD163 increased in TA patients. ILs like IL-6, IL-6STP1, IL-6ST, IL-15, and IL-15RA increased in TA group.

Conclusion: Transcriptome heterogeneities of PBMCs in TA patients requiring surgical management were revealed in the present study. In the patients with TA, CD14$^+$ monocytes and gene expressions involved in oxidative stress were increased, indicating a new treatment and research direction in this field.

Keywords: takayasu arteritis, single-cell RNA sequencing, monocytes, CD163, clinical marker

OPEN ACCESS

Edited by:
Teng Ma,
Capital Medical University, China

Reviewed by:
Jing Li,
Peking Union Medical College Hospital (CAMS), China
Lei Li,
Tsinghua University, China

****Correspondence:***
Li Weimin
lwm_18@aliyun.com
Li Yongjun
liyongjun4679@bjhmoh.cn
† These authors share senior authorship

Specialty section:
This article was submitted to Signaling, a section of the journal Frontiers in Cell and Developmental Biology

Received: *19 August 2021*
Accepted: *13 September 2021*
Published: *04 October 2021*

Citation:
Qing G, Zhiyuan W, Jinge Y, Yuqing M, Zuoguan C, Yongpeng D, Jinfeng Y, Junnan J, Yijia G, Weimin L and Yongjun L (2021) Single-Cell RNA Sequencing Revealed CD14$^+$ Monocytes Increased in Patients With Takayasu's Arteritis Requiring Surgical Management. Front. Cell Dev. Biol. 9:761300. doi: 10.3389/fcell.2021.761300

INTRODUCTION

Takayasu arteritis (TA), which prevails in East Asia, is a highly specific vasculitis that exclusively involves the large arteries and the main branches. In its early stage, patients with TA are barely manifest specific symptoms or signs, making the diagnosis very challenging. However, during the disease progression or in its late stage, the culprit lesion can lead to severe organ ischemia, such as cerebral infarction and myocardial infarction. This may be due to that these patients with TA in early stage are not timely diagnosed and treated.

Currently, medical treatment for TA mainly includes glucocorticoids (Comarmond et al., 2017), methotrexate (Hoffman et al., 1994), and mycophenolate mofetil (Li et al., 2016; Dai et al., 2017). In recent years, biological agents such as tocilizumab (Zhou et al., 2017) and infliximab (Torp et al., 2021) have also been used as candidate drugs for TA. However, the active inflammation of some patients cannot be effectively controlled following medical treatment; thus, the stenosis of the culprit vessels continues to progress, and these patients with TA ultimately requiring surgical management, including endovascular treatment and open surgical repair (Chen et al., 2018; Diao et al., 2020).

Recently, pathological studies investigated on the role of $CD4^+$ T cells and interleukin (IL)-6 signaling pathway in the development and progression of TA (Sagar et al., 1992; Saadoun et al., 2015; Misra et al., 2016). IL-6 promotes the differentiation of $CD4^+$ T cells into Th17 cells, which then secrete cytokines, such as IL-17, IL-21, and IL-22, and induce an autoimmune response (Ruzt et al., 2013; Sutherland et al., 2013; Camporeale and Poli, 2018). Current medical treatment are based on these mechanisms. However, as mentioned previously, it remains unclear why the culprit lesions still progress in patients with TA requiring surgical management (TARSM), even though these patients have already accepted medical drugs.

Nowadays, single-cell RNA sequencing (scRNA-seq), a high-throughput technology, has been utilized to dissect cellular heterogeneities in many immune diseases at the single-cell level (Papalexi and Satija, 2018; See et al., 2018). This new technology may provide a more precisely method to explore immune disease in different clinical stages. In this study, we adopted this state-of-the-art technique to dissect the transcriptomes of peripheral blood mononuclear cells (PBMCs) in patients with TARSM and explore potential clinical markers for the development and progression of TA.

MATERIALS AND METHODS

Study Participants

Four female patients (27.75 ± 7.75 years old) who were admitted to Beijing Hospital Vascular Surgery Department from October 2019 to May 2020 were diagnosed with TA according to the American College of Rheumatology standard suggested by the American Rheumatism Association in 1990 (Arend et al., 1990). All patients including 3 active and 1 inactive had accepted medical treatment, but their clinical presentations still deteriorated and finally underwent surgical repair. Detailed clinical descriptions of the four patients and four age-sex-matched healthy donors are presented in **Supplementary Table 1**. The surgical classification of the patients with TA is also described in **Supplementary Table 1**. Peripheral blood samples were collected from the patients and healthy donors and used for scRNA-seq experiments. On the other hand, seven blood samples from outpatients with TA were collected for fluorescence-activated cell sorting (FACS), and four of the samples were used for quantitative PCR (qPCR).

Written consent was obtained from patients, healthy individuals, or their families. All the contents of this study met the relevant requirements of the ethics committee of Beijing Hospital. All experiments involving human samples were performed in accordance with the relevant regulations and current guidelines.

Single-Cell Suspensions Preparation

Density gradient centrifugation method was performed to obtain PBMCs. Phosphate buffered saline (PBS; Solarbio, P1022-500) was used to dilute the whole blood sample at a ratio of 1:1, and then the sample was added into a tube with approximately 2/3 volume of Ficoll (GE Healthcare, 17-1440-02). After centrifugation at 400× *g* for 35 min, three layers were obtained based on the size and density. The middle cell suspension layer was transferred into a new 15-ml centrifuge tube, added with PBS, and then centrifuged at 300× *g* for 7 min. The supernatant was discarded, the pellet containing PBMCs was washed twice and then resuspended in PBS to obtain a final concentration of 1×10^5 cells/ml. Viability staining using 0.4% Trypan blue solution (Sigma, T8154) was performed, and viable cells were counted under a microscope. The experimental procedure is shown in **Figure 1A**.

Single Cell RNA Sequencing

Single-cell suspensions were then loaded onto microfluidic devices, and scRNA-seq libraries were constructed according to the Singleron GEXSCOPETM protocol using the GEXSCOPETM Single-Cell RNA Library Kit (Singleron Biotechnologies). Individual libraries were diluted to 4 nM and pooled for sequencing. Pools were sequenced on an Illumina HiSeq X with 150 bp paired-end reads.

Data Analysis

The Seurat package (v.4.0.1) (Butler et al., 2018; Stuart et al., 2019) was used for quality control (QC), processing, and analysis. Each Seurat object was generated with genes that were expressed in more than three cells. QC conditions were set as follows: (Comarmond et al., 2017) genes within 200 and 3,000, and (Hoffman et al., 1994) the percentage of mitochondrial genes less than 20% were included for downstream analysis. After QC, the remaining cells were used for further analysis. A total of 29,918 qualified cells were included in the computational analysis. Among them, the case (TA) group had 8,965 cells, and the healthy control (HC) group had 20,953 cells.

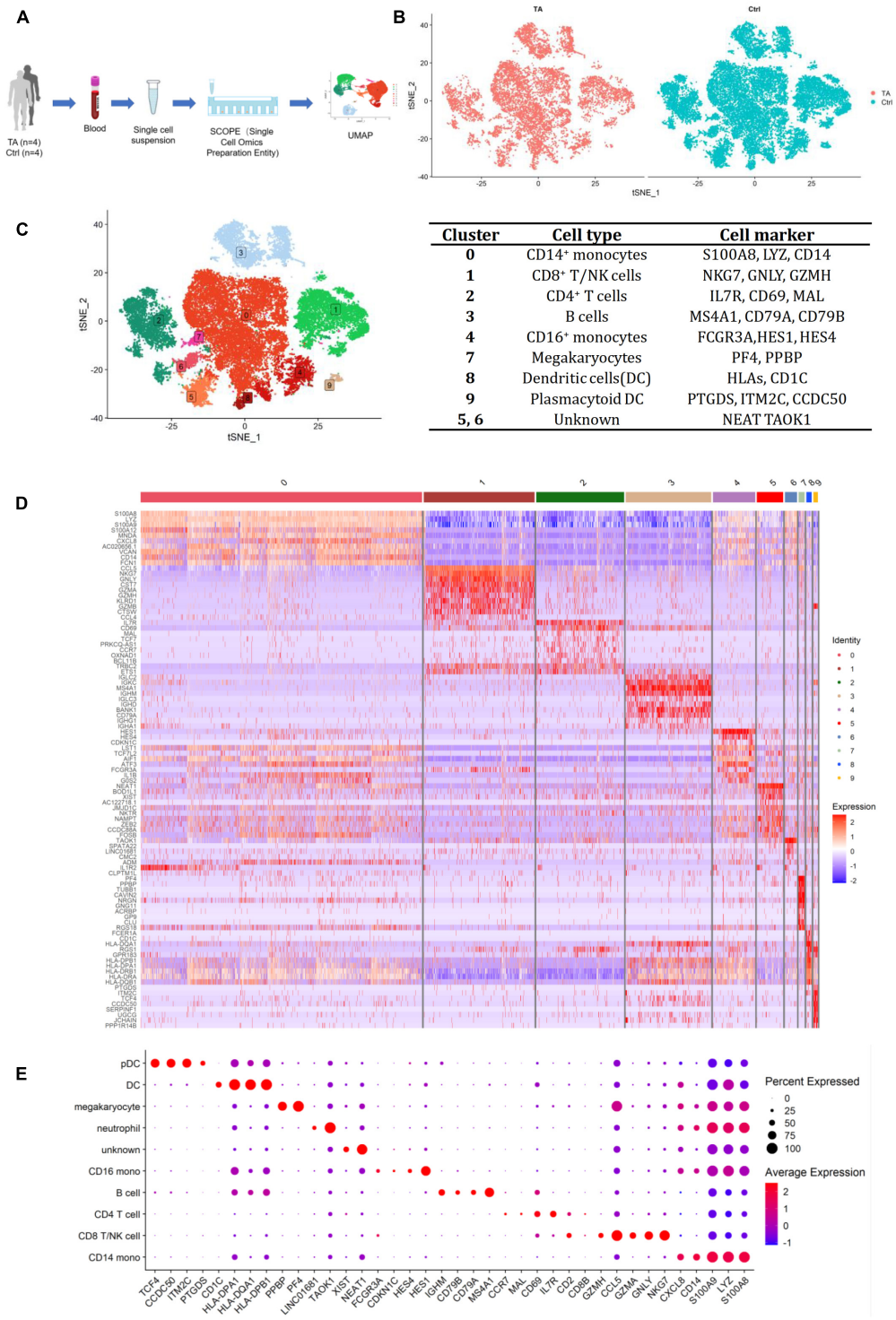

Cluster	Cell type	Cell marker
0	CD14⁺ monocytes	S100A8, LYZ, CD14
1	CD8⁺ T/NK cells	NKG7, GNLY, GZMH
2	CD4⁺ T cells	IL7R, CD69, MAL
3	B cells	MS4A1, CD79A, CD79B
4	CD16⁺ monocytes	FCGR3A,HES1, HES4
7	Megakaryocytes	PF4, PPBP
8	Dendritic cells(DC)	HLAs, CD1C
9	Plasmacytoid DC	PTGDS, ITM2C, CCDC50
5, 6	Unknown	NEAT TAOK1

FIGURE 1 | (A) The process of scRNA-seq. **(B)** Heterogeneity of TA and Ctrl group. **(C)** tSNE of 4 TA and 4 control samples and representative cell markers for each cluster, all cells were divided into 10 clusters. **(D)** Heatmap for 10 clusters. **(E)** Dotplot for 10 clusters. We chose 38 most representative markers for each cell type for dot plot construction. According to different expressed genes (DEGs) in heatmap, feature plots and dot plot, we verified CD14^{+} monocytes (cluster 0) by S100A8, LYZ, CD14; CD8^{+} T/NK cells (cluster 1) by NKG7, GNLY, GZMH; CD4^{+} T cells (cluster 2) by IL7R, CD69, MAL; B cells (cluster 3) by MS4A1, CD79A, CD79B; CD16^{+} monocytes (cluster 4) by HES1, HES4, FCGR3A; Megakaryocytes (cluster 7) by PF4, PPBP; Dendritic cells (cluster 8) by HLA-DPB1, HLA-DQA1, CD1C; Plasmacytoid dendritic cells (cluster 9) by PTGDS, ITM2C, CCDC50 and Undefined cells (cluster 5, 6) by NEAT1, XIST, TAOK1.

The CellCycleScoring function was used to calculate the cell cycle phase scores. SCTransform (Hafemeister and Satija, 2019) was adopted to reduce potential batch effects or technical variations. The principal component analysis was set at 1:20, and unsupervised cell clustering was performed.

The FindAllMarkers function with default settings was used to obtain the differentially expressed genes (DEGs) specific in each cluster, and the representative markers (genes with the high avg_logFC and adjusted p-value < 0.05) were then chosen for cluster labeling. DEGs between TA and HC in each cluster were identified using the FindMarkers function with the MAST method.

To determine the differences in cell composition between TA and HC, we used χ^2 analyses to analyze the differences in the composition ratios of various cell types, and cells with higher composition ratios in TA were used. GraphPad Prism (v.8.0.2) was also used to plot the figures.

Fluorescence-Activated Cell Sorting

FACS was used to test some significant markers and cell composition identified by scRNA-seq analysis. Another seven confirmed PBMCs from patients with TARSM were collected from Beijing Hospital outpatients. All samples were used for cell type and CD163 analyses. The antibodies included CD45 APC/Fire810 (HI30, 304076), CD3 FITC (SK7, 344803), CD4 PE/Cy7 (SK3, 344611), CD8 APC/Cy7 (SK1, 344713), CD19 PE/Dazzle 594 (SJ25C1, 363031), CD16 Brilliant Violet 650 (3G8, 302041), CD14 Brilliant Violet 785 (M5E2, 301839), CD56 Brilliant Violet 750 (5.1H11, 362555), and CD11c Alexa Fluor® 647 (S-HCL-3, 371525). All antibodies were obtained from BioLegend. FACS was conducted using Cytek Aurora, and data were analyzed using SpectroFlo software (v.2.2.0.4).

Enzyme-Linked Immunosorbent Assay

Serum samples were collected from TA and HC, and cytokine levels of thioredoxin-interacting protein (TXNIP), amphiregulin (AREG), Thrombospondin-1 (THBS1), and CD163 were measured using a 96T human ELISA kit (Dogesce, DG94224Q, DG96088Q, DG11739H, DG96191Q).

Quantitative PCR

Total RNA was isolated from TA and HC groups using the RNAprep pure Cell/Bacteria Kit (TIANGEN, DP430), and reverse transcription was performed using the FastKing RT Kit (TIANGEN, KR116). Four mRNA genes (TXNIP, AREG, THBS1, and CD163) were amplified using qPCR, and the primer pairs were: TXNIP (Yang et al., 2019) (F: 5′-GCCACA CTTACCTTGCCAAT-3′; R: 5′-TTGGATCCAGGAACGCTA AC-3′), AREG (Hachim et al., 2020) (F: 5′-GAGCACCT GGAAGCAGTAAC-3'; R: 5′-GGATCACAGCAGACATAAA GGC-3′), THBS1 (Khosravi et al., 2019) (F: 5′-AGGACTG CGTTGGTGATGTA-3′; R: 5′-TCAGGCACTTCTTTGCACTC AT-3′), and CD163 (Sanhurjo et al., 2018) (F: 5′-CACCAGT TCTCTTGGAGGAACA-3′; R: 5′-TTTCACTTCCACTCTCC CGC-3′). The qPCR was conducted using SuperReal PreMix Plus (SYBR Green) (TIANGEN, FP205).

Statistic Statement

We compared cell proportion of PBMCs between TARSM and healthy Ctrl. We also compared the levels of RNA and protein in these two groups. The statistical analysis of scRNA-seq were performed by R studio (v.1.2.1335) and results of cell proportion, ELISA, FACS and qPCR were managed by GraphPad Prism (v.8.0.2). All tests were two-sided and a p-value < 0.05 was considered to be significant.

RESULTS

scRNA-Seq Analysis of Blood Samples

We analyzed PBMCs from four patients with TA and four healthy controls. After QC, a total of 29,918 qualified cells were included for downstream computational analysis, among which 8,965 cells were from TA group and 20,953 cells from HC group. A preliminary estimation of the cell composition in each sample revealed a similar distribution for each cluster (**Figure 1B** and **Supplementary Figures 1A,B**). Data from the eight samples were integrated for further analysis.

Eight Major Cell Types

After unsupervised clustering, 10 clusters were initially obtained and identified by typical markers highly expressed in each cluster, including $CD14^+$ monocytes (cluster 0), $CD8^+$ T/natural killer (NK) cells (cluster 1), $CD4^+$ T cells (cluster 2), B cells (cluster 3), $CD16^+$ monocytes (cluster 4), megakaryocytes (cluster 7), dendritic cells (cluster 8), plasmacytoid dendritic cells (cluster 9), and undefined cells (clusters 5 and 6) (**Figures 1C–E**, **Supplementary Figure 1C**, and **Supplementary Table 2**).

To distinguish $CD8^+$ T cells and NK cells, we further analyzed cells from Cluster 1 (**Figure 2A** and **Supplementary Table 3**) and obtained $CD8^+$ T cells (subcluster 0) and NK cells (subcluster 1) according to the gene expression of each subcluster (**Figure 2B** and **Supplementary Figure 2A**).

Analysis of $CD4^+$ T cells was also conducted (**Figure 2C** and **Supplementary Table 4**). According to the gene expression of each subcluster, we obtained five cell populations, including memory $CD4^+$ T cells (subcluster 0) using TMSB4X, LTB, GIMAP7, IL32, and MYL12A; naïve $CD4^+$ T cells (subcluster 1) using CCR7, CXCR4, MAL, and SARAF; cytotoxic $CD4^+$ T cell (subcluster 2) using GZMA, GZMB, GZMH, and CCL5; early TCR response (subcluster 3) using EGR1, FOSB, FOS, IER2; and unidentified cluster using TAOK1 and LINC01681 (Ding et al., 2020; **Figure 2C** and **Supplementary Figure 2**).

Cellular Proportions of TARSM and HC

Next, we compared the cellular proportions between TA and HC groups. As shown in **Figure 2D**, compared with those in HC group, memory $CD4^+$ T cells in TA group increased (54.57 vs. 42.04%, $p < 0.05$). Meanwhile, the proportion of naïve $CD4^+$ T cells (14.93 vs. 30.62%, $p < 0.05$) and cytotoxic $CD4^+$ T cell decreased (11.57 vs. 13.32%, $p < 0.05$), moreover, $CD4^+$ T cells (10.6 vs. 14.4%, $p < 0.05$), $CD8^+$ T cells (7.2 vs. 9.9%, $p < 0.05$), and NK cells (5.5 vs. 7.0%, $p < 0.05$) (**Figure 2E**).

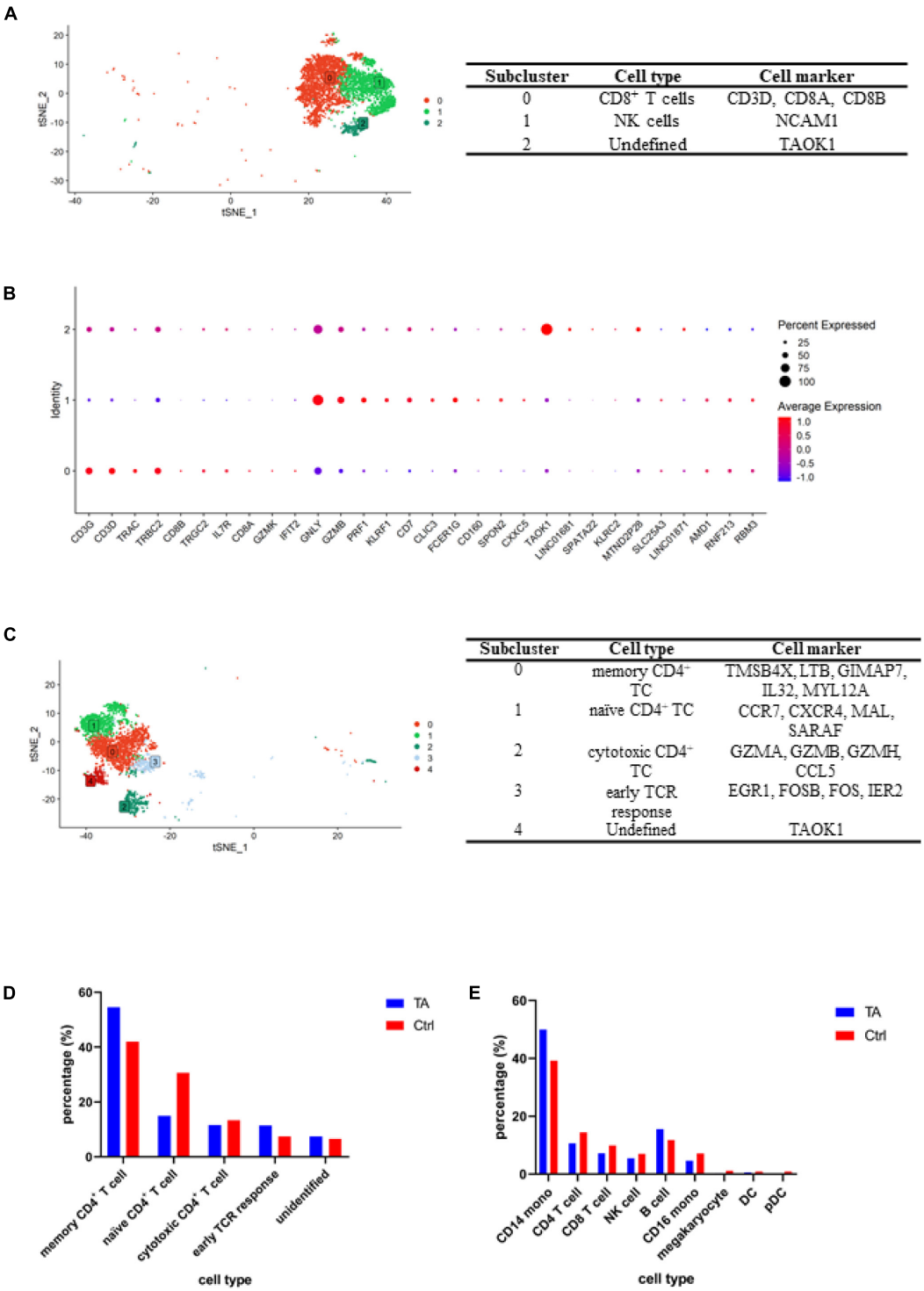

Subcluster	Cell type	Cell marker
0	$CD8^+$ T cells	CD3D, CD8A, CD8B
1	NK cells	NCAM1
2	Undefined	TAOK1

Subcluster	Cell type	Cell marker
0	memory $CD4^+$ TC	TMSB4X, LTB, GIMAP7, IL32, MYL12A
1	naïve $CD4^+$ TC	CCR7, CXCR4, MAL, SARAF
2	cytotoxic $CD4^+$ TC	GZMA, GZMB, GZMH, CCL5
3	early TCR response	EGR1, FOSB, FOS, IER2
4	Undefined	TAOK1

FIGURE 2 | (A) tSNE for $CD8^+$ T/NK cell clusters and representative cell markers for each cluster. **(B)** Dotplot for $CD8^+$ T/NK cell clusters. To further separate $CD8^+$ T cells and NK cells, we conducted an independent analysis for cluster 1, and according to the expression of specific genes, including CD8A, CD8B, NCAM1 (CD56), we obtained $CD8^+$ T cells (subcluster 0) and NK cells (subcluster 1). **(C)** tSNE for $CD4^+$ T cell clusters and representative cell markers for each cluster. We verified memory $CD4^+$ T cell (subcluster 0) by TMSB4X, LTB, GIMAP7, IL32, MYL12A; naïve $CD4^+$ T cell (subcluster 1) by CCR7, CXCR4, MAL, SARAF; cytotoxic $CD4^+$ T cell (subcluster 2) by GZMA, GZMB, GZMH, CCL5; early TCR response (subcluster 3) by EGR1, FOSB, FOS, IER2. **(D)** Comparation of $CD4^+$ T cells composition between TA and Ctrl group. It can be found the percentages of memory $CD4^+$ T cell were higher in TA than Ctrl. **(E)** Comparation of each cell type percentage between TA and Ctrl group and $CD14^+$ monocyte and B cell were higher in TA than Ctrl.

The data also revealed that $CD14^+$ monocytes (50.0 vs. 39.3%, $p < 0.05$) and B cells increased significantly (15.5 vs. 11.8%, $p < 0.05$), while $CD16^+$ monocytes (4.6 vs. 7.1%, $p < 0.05$), megakaryocytes (0.3 vs. 1.1%, $p < 0.05$), dendritic cells (0.6 vs. 0.9%, $p < 0.05$), and plasmacytoid dendritic cell (0.2 vs. 0.9%, $p < 0.05$) populations decreased in patients with TARSM.

Transcriptomics Altered in TARSM

We then explored DEGs between the two groups. In TA group, 251 genes were significantly highly expressed (avg_logFC > 0.25 and adjusted *P*-value $< 10^{-10}$; **Supplementary Table 5**). We also performed the same analysis in each cell type to explore the DEGs between the TA and HC groups. Four differentially expressed genes (TXNIP, AREG, THBS1, and CD163) were selected for further analysis (**Figure 3A**). Results revealed that CD163, AREG, THBS1, and TXNIP have higher expression in $CD14^+$ and $CD16^+$ monocytes.

We also performed gene orthology (GO) analysis in each cluster, and pathway analysis based on the DEGs was conducted using GO in $CD14^+$ monocytes. Among these, binding of the receptor for advanced glycation end products (RAGE) was observed in $CD14^+$ monocytes (**Figure 3B**) and dendritic cells (DCs) (**Supplementary Figure 3A**), indicating that this receptor pathway may be widely activated in antigen-presenting cells (APCs) of patients with TARSM.

Interleukin Family Genes in TARSM

Since IL family genes play significant roles in TA diseases (Mirault et al., 2017), we next explored how ILs changed from HC group to TA group. We listed the IL- or IL-related genes included in our datasets and explored their expression in the cell types among PBMCs. As shown in **Figure 4A**, each cell type possessed highly expressed IL-related gene clusters. For example, IL-1R2, IL-5, IL-17RA, and IL-1RAP were highly expressed in $CD14^+$ monocytes. Then, we also compared the expression of these genes between the two groups. We observed that some IL genes were highly expressed in TA group such as IL-6, IL-6STP1, IL-6ST, IL-15, IL-15RA, IL-18, IL-18RAP, and IL-18R1 (**Figures 4B,C**). We also observed that IL-6 was highly expressed in B cells and $CD16^+$ monocytes. In addition, IL-6 levels significantly increased in CD16 monocytes of TA group (**Supplementary Figure 3B**). However, how the IL genes contribute to the progression of TA remains to be elucidated.

FACS Revealed Similar Results

We then utilized FACS to validate our observations from the scRNA-seq results. First, different cell types were used in this study, and the results are shown in **Figure 5** and **Supplementary Figure 4**. Nine antibodies were used for identification **(Supplementary Figure 4A**). We compared the proportion of monocytes and B cells between TA and HC groups and observed that the proportion of monocytes increased (13.34 ± 5.307% vs. 5.31 ± 4.836%, $p = 0.0121$), but the difference in that of B cells was not significant (12.40 ± 9.822% vs. 15.71 ± 11.60%, $p = 0.5755$) in TA group (**Figure 5A**). Then, we used the integrated median fluorescence intensity (iMFI) value (Darrah et al., 2007) to compare and assess the expression of CD163 in the membrane of APCs (**Supplementary Figures 4B,C**) and found that CD163 was highly expressed in both monocytes (33,272 ± 18,904 vs. 6,252 ± 1,505, $p = 0.0292$) and DCs (12,619 ± 6,188 vs. 2,943 ± 1,580, $p = 0.0231$) in TA group (**Figure 5B**).

Quantitative PCR and ELISA

We also evaluated the expression of TXNIP, AREG, THBS1, and CD163. First, qPCR was performed, as shown in **Supplementary Figure 5A**. All four genes showed higher expression in TA group than in HC group, which was consistent with scRNA-seq. Then, we validated their expression by ELISA, as shown in **Supplementary Figure 5B**. Results showed that the levels of TXNIP (3.862 ± 0.4976 ng/ml vs. 3.478 ± 0.3369 ng/ml) and AREG (186.4 ± 26.33 pg/ml vs. 168.5 ± 20.34 pg/ml) were higher in TA group, which was similar to scRNA-seq results. However, THBS1 (64.32 ± 13.48 ng/ml vs. 69.38 ± 4.524 ng/ml) and CD163 (122.4 ± 10.21 ng/ml vs. 124.9 ± 11.28 ng/ml) levels were lower, indicating they were not increased in serum.

DISCUSSION

At present, research on the pathogenesis of TA has mainly focused on genes (Terao, 2016) and proteins (Mirault et al., 2017) of the peripheral blood of patients, especially in T cells (Regnier et al., 2020). However, it remains unclear how the other types of inflammatory cells in the peripheral blood contribute to the progression and development of TA. Kotaro found that IL-1 pathway expression was elevated in the peripheral blood of patients with refractory large vessel vasculitis by analyzing bulk-seq data, but the author failed to elucidate the relationship between the IL-1 pathway and different types of immune cells (Matsumoto et al., 2021). Compared with bulk-seq, scRNA-seq technology can analyze the transcriptome in each cell type, which provides more comprehensive information on the function of different inflammatory cells. To the best of our knowledge, this is the first time that scRNA-seq was used to detect the pathogenesis in the peripheral blood of patients with TA and identify potential cell markers.

In this study, it was revealed that the proportion of monocytes in patients with TARSM was higher in TA group than in HC group, which was similar in other immune-related diseases such as tuberculosis (Naranbhai et al., 2014), rheumatoid arthritis (Du et al., 2017), and vitiligo (Demirbas et al., 2020). This phenomenon observed in this study might be due to the following mechanism: **(a)** $CD14^+$ monocytes trigger immune responses, and **(b)** CD163 can inhibit the activation and proliferation of lymphocytes and reduce the absolute value of lymphocytes (Baeten et al., 2004). CD163 is a transmembrane scavenger receptor (Law et al., 1993) and is known to be elevated in patients with systemic lupus erythematosus (Borgia et al., 2018), systemic juvenile idiopathic arthritis (Minoia et al., 2015), and Kawasaki disease (Garcia-Pavon et al., 2017). CD163 is also considered as a potential marker for macrophage activation syndrome, which promotes the transition from monocytes/macrophages to M1 proinflammatory macrophages (Porcheray et al., 2005;

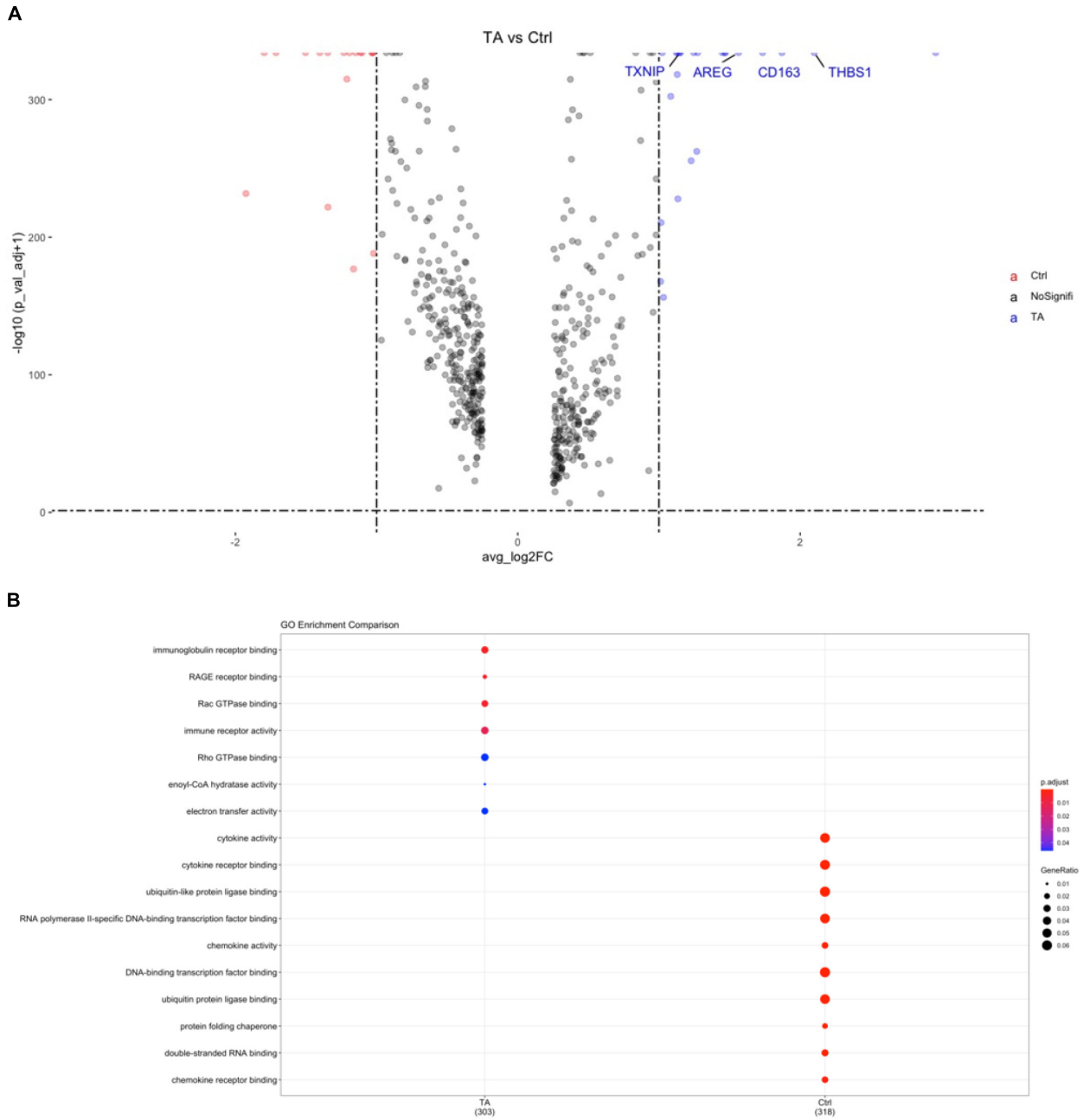

FIGURE 3 | (A) Volcano plot for gene expression of cell markers in PBMCs between TA and Ctrl group. TXNIP, AREG, THBS1, CD163 were significantly higher in TA group. **(B)** GO analysis of CD14^{+} monocytes. RAGE pathway can be found in TA group.

Avcin et al., 2006). In the present study, the elevated CD163 in APC membranes in patients with TA indicates that these cells are in an active state of inflammation, suggesting that APCs may play an important role in patients with TARSM and they are activated even earlier than CD4^{+} T cells.

Other cell markers highly expressed in the APCs of patients with TA were also analyzed, including TXNIP, THBS1, and AREG. Among these three markers, TXNIP and AREG showed consistent results in ELISA. TXNIP is a binding protein of thioredoxin (TXN) and can inhibit the antioxidant capacity of TXN and promote cell stress (Tinkov et al., 2018). TXNIP promotes the formation of reactive oxygen species (ROS)-NLRP3 inflammasomes by inhibiting the transfer of ROS by TXN, thereby increasing the concentration of IL-18 (Kim et al., 2019), which has also been shown to increase in patients with TARSM (Alibaz-Oner et al., 2015). NLRP3 inflammasomes

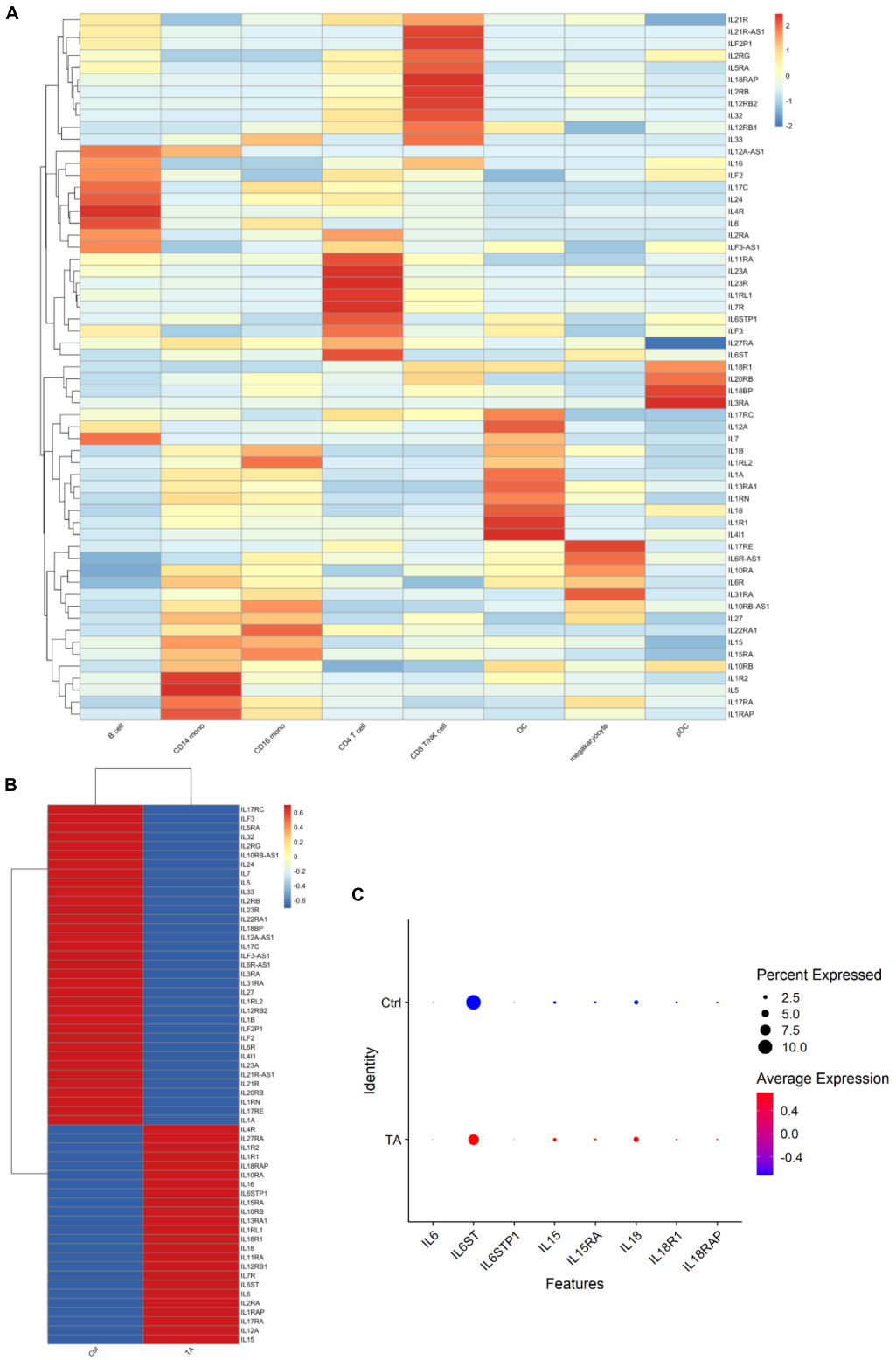

FIGURE 4 | (A) The expression of ILs in each cell type. **(B)** The expression of ILs in TA and Ctrl group. **(C)** Dotplot of 8 IL genes. It can be found IL-6, IL-6STP1, IL-6ST, IL-15, IL-15RA, IL-18, IL-18RAP, and IL-18R1 were detected in TA group.

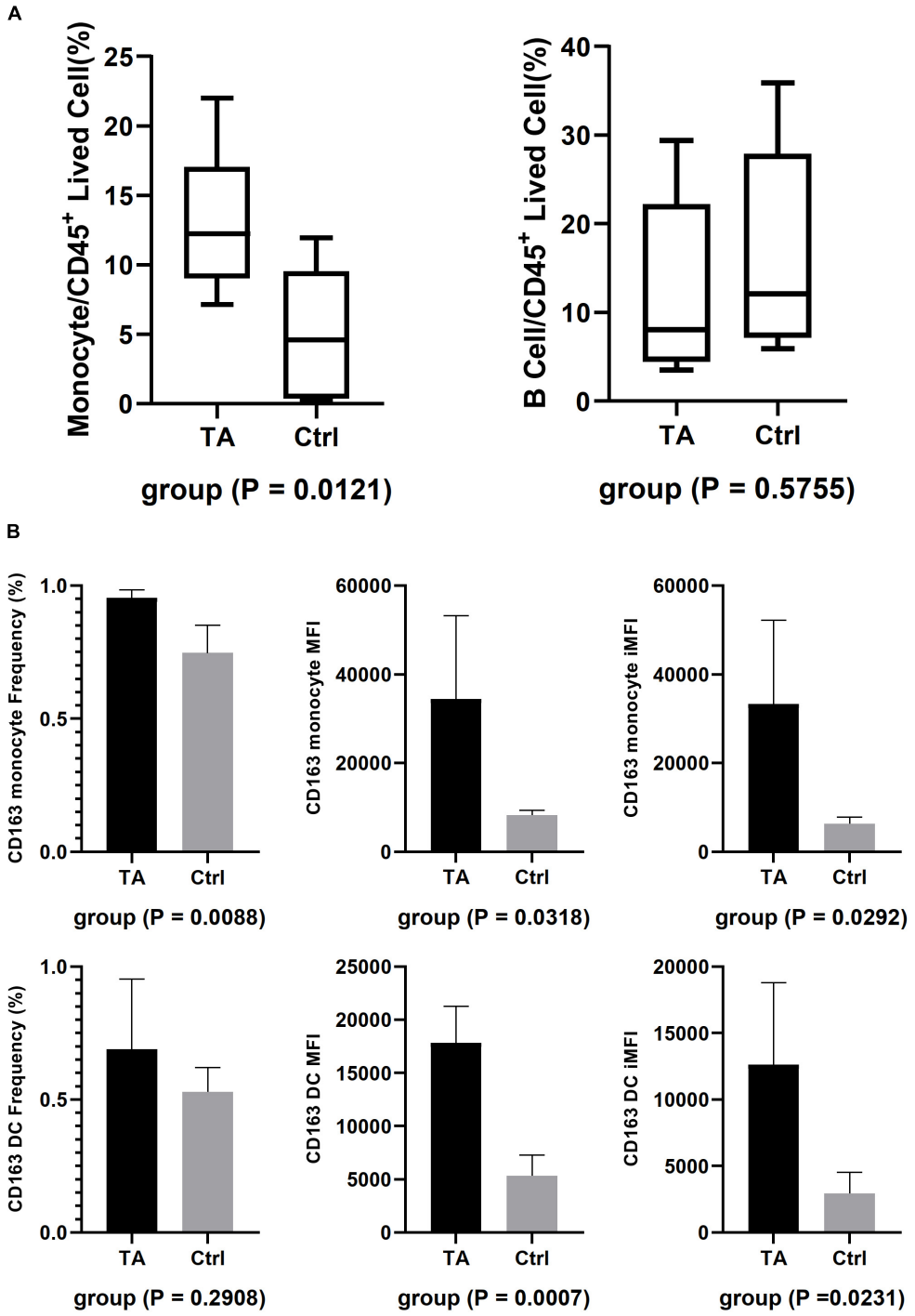

FIGURE 5 | FACS results. **(A)** The composition of CD14$^+$ monocyte and B cell in TA and Ctrl group. Only CD14$^+$ monocyte had higher composition in TA than Ctrl. **(B)** iMFI showed both monocytes and DC had a higher expression on their membrane in TA group.

are mainly secreted by activated macrophages (Kelley et al., 2019). At the same time, TXNIP is a negative regulator of thioredoxin, a key antioxidant protein to remove reactive oxygen and promote DNA repair (Lu and Holmgren, 2014). It means the high expression of TXNIP would results in a severe oxidative stress in the patient's body (Yu et al., 2013). The increased expression of TXNIP in TARSM monocytes is closely related to their function.

AREG, as one of the main ligands of the EFGR pathway, mainly participates in the regulation of proliferation,

apoptosis, and metastasis of various cells (Berasain and Avila, 2014). AREG expression is mainly elevated in pathological conditions, such as cirrhosis (Perugorria et al., 2008) and chronic obstructive pulmonary disease (Val et al., 2012). Recent studies on mouse models of glomerulonephritis also showed that AREG can enhance the function of Treg cells, inhibit the growth of $CD4^+$ T cells, and promote the recruitment of myeloid cells, proliferation, and cytokine secretion of M1 cells (Melderis et al., 2020). The increase in AREG in patients with TARSM might serve as an activation signal for monocytes.

Recent studies have shown the important roles of IL family genes in the progression of TA. Among them, IL-6 has received the most attention (Sagar et al., 1992), and anti-IL-6R biologics have also been widely used in clinical practice (Zhou et al., 2017). In this study, IL-6 was not only highly expressed in APCs, but also in B cells and even autocrine in $CD4^+$ T cells, indicating that B cells and $CD4^+$ T cells may have other unknown functions in TA. Interestingly, IL-15 and its receptor gene IL-15RA, which are widely expressed in a variety of cells (Patidar et al., 2016) and play a bridge between innate immunity and adaptive immunity (Pagliari et al., 2013), were also detected in our study. IL-15 can also activate the maturation and functional expression of T cells, DCs, and NK cells (Mattei et al., 2001; Saikh et al., 2001; Ali et al., 2015). In this study, IL-15 and its receptor IL-15RA were both highly expressed in APCs, indicating that their antigen presentation function is activated. IL-18 is mainly synthesized by APCs; meanwhile, its receptor genes, IL-18Rα and IL-18Rβ, are expressed in T cells and DCs. The main function of this pathway is to activate the NF-κB pathway and promote the synthesis of IFN-γ in Th1 cells (Nakanishi et al., 2001; Dinarello et al., 2013; Turner et al., 2014). As previously mentioned, IL-18 has been proven to be elevated in patients with TA (Minoia et al., 2015). In this study, IL-18 was found to be highly expressed in the DCs of patients with TA, and its receptor gene was highly expressed in $CD8^+$ T/NK cells, indicating that the IL-18 pathways may also occur in the PBMCs of patients with TARSM.

RAGE is a cell transmembrane receptor used to recognize and bind AGEs (Schmidt et al., 1992). AGEs refer to a kind of glycosylated molecules produced by oxidative stress or metabolism, which include not only cytokines but also some metabolites. After RAGE recognizes and binds to the corresponding ligand, it can activate the NF-κB pathway, thereby promoting the secretion of cytokines by inflammatory cells, such as IL-6 and TNF-α (Shen et al., 2020). By the way, the activation of RAGE and NFκB also send a message to reactive oxidant species (ROS), a key role in oxidative stress, by NADPH oxidase (Daffu et al., 2013). In this study, according to the GO analysis results of different cell types, it was found that APCs, such as $CD14^+$ monocytes and DCs, have prominent expression of RAGE pathways, indicating that activation of this pathway may be an important reason for APC activation.

Both TXNIP and RAGE are closely related to oxidative stress. Oxidative stress has been proposed as a root cause in development of many cardiovascular diseases, including atherosclerotic (Marchio et al., 2019), aneurysm (Emeto et al., 2016) and even TA (Mahajan et al., 2010). In human vessel, endothelial cells have become the major character of antioxidative, and the secreted endothelial nitric oxide synthase (eNOS) can produce NO, a vasoprotective molecule that can resist oxidation and inhibit the immune response of blood vessel walls (Forstermann et al., 2017). However, as the body is in an immune response or infection state, NADPH oxidase produced by immune cells can directly act on endothelial cells, destroy the stability of eNOS and inhibit the activity of NO, which finally produce a large amount of superoxide anion (Ghosh et al., 2017). The high expression of TXNIP and RAGE in monocyte suggested that oxidative stress may also be a cause of vascular intimal damage, and the trigger role played by monocyte cannot be ignored.

As previously mentioned, this is the first study to explore transcriptomics using scRNA-seq techniques in patients with TARSM. However, some limitations of this study should not be ignored. First, it is hardly to find TARSM patients without medical treatment for the following reasons: **(a)** For these patients, they are still unable to control the inflammatory activity even after receiving medical treatment, causing the disease progressing, and the vascular lumen continues to narrow, which finally to be occluded, then surgical treatment is required. **(b)** For the treatment strategy, medical therapy is still the first choice for TA treatment, while surgical operation is mainly for patients who have complications such as insufficient blood supply due to vascular occlusion. Second, the number of patients in this study was also limited, both in the scRNA-seq studies and in the validation studies, such as ELISA, qPCR, and FACS. In addition, the scRNA-seq technique adopted in this study only reflected a snapshot scene for this complex disease, and how the culprit lesion evolves requires further demonstration by longitudinal studies. Another issue that remains to be elucidated is the role of ILs in TA; that is, the correlation between the observation of ILs in this study and clinical studies needs to be explored and established. A validation cohort from another center would be an important next step in future research.

CONCLUSION

In conclusion, we used single-cell RNA technology to detect peripheral blood cells in patients with TARSM. Our study showed that the proportion of $CD14^+$ monocytes, function, and functional receptors increased in patients with TARSM after medical treatment, which suppressed $CD4^+$ T cell function. Moreover, monocytes have become a major factor in inflammation, and the inhibition of monocyte population and function can be used as a new direction for medical treatment. We also found that TXNIP and AREG can be used as diagnostic markers for TA development and progression, and highly expressed CD163 may be an important characteristic of APCs in patients with TARSM.

DATA AVAILABILITY STATEMENT

The data presented in the study are deposited in the Genome Sequence Archive for Human, accession number HRA001329 (https://bigd.big.ac.cn/gsa-human/browse/HRA001329).

ETHICS STATEMENT

The studies involving human participants were reviewed and approved by the Beijing Hospital Ethics Committee. Written informed consent to participate in this study was provided by the participants' legal guardian/next of kin.

AUTHOR CONTRIBUTIONS

GQ, LW, and LY designed the study. GQ did the experiments. WZ, YJG, and YJF analyzed the scRNA-seq data. CZ, DY, MY, GY, and JJ checked the case history. LW and LY revise the manuscript. All authors contributed to the article and approved the submitted version.

FUNDING

This work was supported by a grant from the National Science and Technology Major Project of China (No. 2018ZX10302 302001004), the National Natural Science Foundation of China (No. U1903118), the Beijing Hospital Clinical Research 121 Project (No. BJ-2018-089), Peking Union Medical College Graduate Innovation Fund (No. 2019-1002-23), and the Fundamental Research Funds for the Central Universities (No. 3332018174).

SUPPLEMENTARY MATERIAL

The Supplementary Material for this article can be found online at: https://www.frontiersin.org/articles/10.3389/fcell.2021.761300/full#supplementary-material

Supplementary Figure 1 | (A) tSNE of 8 samples. **(B)** Composition of 8 samples. The cell composition and cluster distribution were similar in 8 sample, which allowed for further analysis. **(C)** Feature plot of 16 cell markers.

Supplementary Figure 2 | (A) Feature plot for CD8+ T/NK cell clusters. **(B)** Dotplot for CD4+ T cells.

Supplementary Figure 3 | (A) GO analysis of DC. RAGE pathway can be found with higher expression in TA group in both CD14+ monocytes and DCs. **(B)** The comparation of ILs expression in each cell type between TA and Ctrl group.

Supplementary Figure 4 | FACS results. **(A)** The flow charts of FACS. We used 9 following antibodies to confirm each cell type found in scRNA-seq: CD4+ T cell (CD45+ CD3+ CD4+), CD8+ T cell (CD45+ CD3+ CD8+), NKT cell (CD45+ CD3+ CD56+), B cell (CD45+ CD3- CD19+), NK cell (CD45+ CD3- CD56+), CD14+ monocyte (CD45+ CD3- CD14+ CD16-), CD16+ monocyte (CD45+ CD3- CD14+ CD16+), DC (CD45+ CD3- CD14- CD19- CD16- CD56- CD11C+). **(B)** The expression of CD163 on monocyte membrane. I, II, III, IV are TA group and V, VI, VII, VIII are Ctrl group. These figures show that the crests of curves in TA group are closer to the right side than Ctrl group, which means CD163 have a higher expression on TA patients' monocyte surface. **(C)** The expression of CD163 on DC membrane. Similar to B, I, II, III, IV belong to TA group and V, VI, VII, VIII belong to Ctrl group. These figures show that CD163 express higher on TA patients' DC surface.

Supplementary Figure 5 | (A) qPCR results of 4 genes (TXNIP, AREG, THBS1, CD163). All genes were higher expressed in TA group. **(B)** ELISA results of 4 protein (TXNIP, AREG, THBS1, CD163). The serum levels of TXNIP and AREG were higher in TA group, however, THBS1 and CD163 were lower.

Supplementary Table 1 | Clinical information for the peripheral blood mononuclear cells.

Supplementary Table 2 | Cell markers for all cell clusters.

Supplementary Table 3 | Cell markers for CD8+ T/NK cells.

Supplementary Table 4 | Cell markers for CD4+ T cells.

Supplementary Table 5 | DEGs for all cell types.

REFERENCES

Ali, A. K., Nandagopal, N., and Lee, S. H. (2015). IL-15-PI3K-AKT-mTOR: a critical pathway in the life journey of natural killer cells. *Front. Immunol.* 6:355. doi: 10.3389/fimmu.2015.00355

Alibaz-Oner, F., Yentur, S. P., Saruhan-Direskeneli, G., and Direskeneli, H. (2015). Serum cytokine profiles in Takayasu's arteritis: search for biomarkers. *Clin. Exp. Rheumatol.* 33(2 Suppl. 89), S–32–5.

Arend, W. P., Michel, B. A., Bloch, D. A., Hunder, G. G., Calabrese, L. H., Edworthy, S. M., et al. (1990). The american college of rheumatology 1990 criteria for the classification of Takayasu arteritis. *Arthritis Rheum.* 33, 1129–1134.

Avcin, T., Tse, S. M., Schneider, R., Ngan, B., and Silverman, E. D. (2006). Macrophage activation syndrome as the presenting manifestation of rheumatic diseases in childhood. *J. Pediatr.* 148, 683–686.

Baeten, D., Moller, H. J., Delanghe, J., Veys, E. M., Moestrup, S. K., and De Keyser, F. (2004). Association of CD163+ macrophages and local production of soluble CD163 with decreased lymphocyte activation in spondylarthropathy synovitis. *Arthritis Rheum.* 50, 1611–1623. doi: 10.1002/art.20174

Berasain, C., and Avila, M. A. (2014). Amphiregulin. *Semin. Cell Dev. Biol.* 28, 31–41.

Borgia, R. E., Gerstein, M., Levy, D. M., Silverman, E. D., and Hiraki, L. T. (2018). Features, treatment, and outcomes of macrophage activation syndrome in childhood-onset systemic lupus erythematosus. *Arthritis Rheumatol.* 70, 616–624.

Butler, A., Hoffman, P., Smibert, P., Papalexi, E., and Satija, R. (2018). Integrating single-cell transcriptomic data across different conditions, technologies, and species. *Nat. Biotechnol.* 36, 411–420. doi: 10.1038/nbt.4096

Camporeale, A., and Poli, V. (2018). IL-6, IL-17 and STAT3: a holy trinity in auto-immunity? *Front. Biosci.* 17:2306–2326. doi: 10.2741/4054

Chen, Z. G., Chen, Y. X., Diao, Y. P., Wu, Z. Y., Yan, S., Ma, L., et al. (2018). Simultaneous multi-supra-aortic artery bypass successfully implemented in 17 patients with type I Takayasu arteritis. *Eur. J. Vasc. Endovasc. Surg.* 56, 903–909. doi: 10.1016/j.ejvs.2018.08.044

Comarmond, C., Biard, L., Lambert, M., Mekinian, A., Ferfar, Y., Kahn, J. E., et al. (2017). Long-term outcomes and prognostic factors of complications in Takayasu arteritis: a multicenter study of 318 patients. *Circulation* 136, 1114–1122. doi: 10.1161/circulationaha.116.027094

Daffu, G., del Pozo, C. H., O'Shea, K. M., Ananthakrishnan, R., Ramasamy, R., and Schmidt, A. M. (2013). Radical roles for RAGE in the pathogenesis of oxidative stress in cardiovascular diseases and beyond. *Int. J. Mol. Sci.* 14, 19891–19910. doi: 10.3390/ijms141019891

Dai, D., Wang, Y., Jin, H., Mao, Y., and Sun, H. (2017). The efficacy of mycophenolate mofetil in treating Takayasu arteritis: a systematic review and meta-analysis. *Rheumatol. Int.* 37, 1083–1088. doi: 10.1007/s00296-017-3704-7

Darrah, P. A., Patel, D. T., De Luca, P. M., Lindsay, R. W., Davey, D. F., Flynn, B. J., et al. (2007). Multifunctional TH1 cells define a correlate of vaccine-mediated protection against Leishmania major. *Nat. Med.* 13, 843–850. doi: 10.1038/nm1592

Demirbas, A., Elmas, O. F., Atasoy, M., Tursen, U., and Lotti, T. (2020). Can monocyte to HDL cholesterol ratio and monocyte to lymphocyte ratio be markers for inflammation and oxidative stress in patients with vitiligo? a preliminary study. *Arch. Dermatol. Res.* 313, 491–498. doi: 10.1007/s00403-020-02129-3

Diao, Y., Yan, S., Premaratne, S., Chen, Y., Tian, X., Chen, Z., et al. (2020). Surgery and endovascular management in patients with Takayasu's arteritis: a ten-year retrospective study. *Ann. Vasc. Surg.* 63, 34–44. doi: 10.1016/j.avsg.2019.07.009

Dinarello, C. A., Novick, D., Kim, S., and Kaplanski, G. (2013). Interleukin-18 and IL-18 binding protein. *Front. Immunol.* 4:289. doi: 10.3389/fimmu.2013.00289

Ding, J., Smith, S. L., Orozco, G., Barton, A., Eyre, S., and Martin, P. (2020). Characterisation of CD4+ T-cell subtypes using single cell RNA sequencing and the impact of cell number and sequencing depth. *Sci. Rep.* 10:19825. doi: 10.1038/s41598-020-76972-9

Du, J., Chen, S., Shi, J., Zhu, X., Ying, H., Zhang, Y., et al. (2017). The association between the lymphocyte-monocyte ratio and disease activity in rheumatoid arthritis. *Clin. Rheumatol.* 36, 2689–2695. doi: 10.1007/s10067-017-3815-2

Emeto, T. I., Moxon, J. V., Au, M., and Golledge, J. (2016). Oxidative stress and abdominal aortic aneurysm: potential treatment targets. *Clin. Sci.* 130, 301–315. doi: 10.1042/cs20150547

Forstermann, U., Xia, N., and Li, H. (2017). Roles of vascular oxidative stress and nitric oxide in the pathogenesis of atherosclerosis. *Circ. Res.* 120, 713–735. doi: 10.1161/circresaha.116.309326

Garcia-Pavon, S., Yamazaki-Nakashimada, M. A., Baez, M., Borjas-Aguilar, K. L., and Murata, C. (2017). Kawasaki disease complicated with macrophage activation syndrome: a systematic review. *J. Pediatr. Hematol. Oncol.* 39, 445–451.

Ghosh, A., Gao, L., Thakur, A., Siu, P. M., and Lai, C. W. K. (2017). Role of free fatty acids in endothelial dysfunction. *J. Biomed. Sci.* 24:50.

Hachim, M. Y., Elemam, N. M., Ramakrishnan, R. K., Salameh, L., Olivenstein, R., Hachim, I. Y., et al. (2020). Blood and salivary amphiregulin levels as biomarkers for asthma. *Front. Med.* 7:561866. doi: 10.3389/fmed.2020.561866

Hafemeister, C., and Satija, R. (2019). Normalization and variance stabilization of single-cell RNA-seq data using regularized negative binomial regression. *Genome Biol.* 20:296. doi: 10.1186/s13059-019-1874-1

Hoffman, G. S., Leavitt, R. Y., Kerr, G. S., Rottem, M., Sneller, M. C., and Fauci, A. S. (1994). Treatment of glucocorticoid-resistant or relapsing Takayasu arteritis with methotrexate. *Arthritis Rheum.* 37, 578–582.

Kelley, N., Jeltema, D., Duan, Y., and He, Y. (2019). The NLRP3 inflammasome: an overview of mechanisms of activation and regulation. *Int. J. Mol. Sci.* 20:3328.

Khosravi, M., Najafi, M., Amirfarhangi, A., Karimi, M., Fattah, F., and Shabani, M. (2019). The increase of pFAK and THBS1 protein and gene expression levels in vascular smooth muscle cells by histamine-treated M1 macrophages. *Iran. J. Allergy Asthma Immunol.* 18, 72–79.

Kim, S. K., Choe, J. Y., and Park, K. Y. (2019). TXNIP mediated nuclear factor-kappaB signaling pathway and intracellular shifting of TXNIP in uric acid-induced NLRP3 inflammasome. *Biochem. Biophys. Res. Commun.* 511, 725–731. doi: 10.1016/j.bbrc.2019.02.141

Law, S. K., Micklem, K. J., Shaw, J. M., Zhang, X. P., Dong, Y., Willis, A. C., et al. (1993). A new macrophage differentiation antigen which is a member of the scavenger receptor superfamily. *Eur. J. Immunol.* 23, 2320–2325. doi: 10.1002/eji.1830230940

Li, J., Yang, Y., Zhao, J., Li, M., Tian, X., and Zeng, X. (2016). The efficacy of mycophenolate mofetil for the treatment of chinese Takayasu's arteritis. *Sci. Rep.* 6:38687.

Lu, J., and Holmgren, A. (2014). The thioredoxin antioxidant system. *Free Radic. Biol. Med.* 66, 75–87.

Mahajan, N., Dhawan, V., Malik, S., and Jain, S. (2010). Implication of oxidative stress and its correlation with activity of matrix metalloproteinases in patients with Takayasu's arteritis disease. *Int. J. Cardiol.* 145, 286–288. doi: 10.1016/j.ijcard.2009.09.557

Marchio, P., Guerra-Ojeda, S., Vila, J. M., Aldasoro, M., Victor, V. M., and Mauricio, M. D. (2019). Targeting early atherosclerosis: a focus on oxidative stress and inflammation. *Oxid. Med. Cell. Longev.* 2019:8563845.

Matsumoto, K., Suzuki, K., Yoshimoto, K., Ishigaki, S., Yoshida, H., Magi, M., et al. (2021). Interleukin-1 pathway in active large vessel vasculitis patients with a poor prognosis: a longitudinal transcriptome analysis. *Clin. Transl. Immunol.* 10:e1307. doi: 10.1002/cti2.1307

Mattei, F., Schiavoni, G., Belardelli, F., and Tough, D. F. (2001). IL-15 is expressed by dendritic cells in response to type I IFN, double-stranded RNA, or lipopolysaccharide and promotes dendritic cell activation. *J. Immunol.* 167, 1179–1187. doi: 10.4049/jimmunol.167.3.1179

Melderis, S., Hagenstein, J., Warkotsch, M. T., Dang, J., Herrnstadt, G. R., Niehus, C. B., et al. (2020). Amphiregulin aggravates glomerulonephritis via recruitment and activation of myeloid cells. *J. Am. Soc. Nephrol.* 31, 1996–2012. doi: 10.1681/asn.2019111215

Minoia, F., Davi, S., Horne, A., Bovis, F., Demirkaya, E., Akikusa, J., et al. (2015). Dissecting the heterogeneity of macrophage activation syndrome complicating systemic juvenile idiopathic arthritis. *J. Rheumatol.* 42, 994–1001.

Mirault, T., Guillet, H., and Messas, E. (2017). Immune response in Takayasu arteritis. *Presse. Med* 48(7-8 Pt 2), e189–e196.

Misra, D. P., Chaurasia, S., and Misra, R. (2016). Increased circulating Th17 cells, serum IL-17A, and IL-23 in Takayasu arteritis. *Autoimmune Dis.* 2016:7841718.

Nakanishi, K., Yoshimoto, T., Tsutsui, H., and Okamura, H. (2001). Interleukin-18 regulates both Th1 and Th2 responses. *Annu. Rev. Immunol.* 19, 423–474.

Naranbhai, V., Kim, S., Fletcher, H., Cotton, M. F., Violari, A., Mitchell, C., et al. (2014). The association between the ratio of monocytes: lymphocytes at age 3 months and risk of tuberculosis (TB) in the first two years of life. *BMC Med.* 12:120. doi: 10.1186/s12916-014-0120-7

Pagliari, D., Cianci, R., Frosali, S., Landolfi, R., Cammarota, G., Newton, E. E., et al. (2013). The role of IL-15 in gastrointestinal diseases: a bridge between innate and adaptive immune response. *Cytokine Growth Factor Rev.* 24, 455–466. doi: 10.1016/j.cytogfr.2013.05.004

Papalexi, E., and Satija, R. (2018). Single-cell RNA sequencing to explore immune cell heterogeneity. *Nat. Rev. Immunol.* 18, 35–45. doi: 10.1038/nri.2017.76

Patidar, M., Yadav, N., and Dalai, S. K. (2016). Lnterleukin 15: a key cytokine for immunotherapy. *Cytokine Growth Factor Rev.* 31, 49–59. doi: 10.1016/j.cytogfr.2016.06.001

Perugorria, M. J., Latasa, M. U., Nicou, A., Cartagena-Lirola, H., Castillo, J., Goni, S., et al. (2008). The epidermal growth factor receptor ligand amphiregulin participates in the development of mouse liver fibrosis. *Hepatology* 48, 1251–1261. doi: 10.1002/hep.22437

Porcheray, F., Viaud, S., Rimaniol, A. C., Leone, C., Samah, B., Dereuddre-Bosquet, N., et al. (2005). Macrophage activation switching: an asset for the resolution of inflammation. *Clin. Exp. Immunol.* 142, 481–489. doi: 10.1111/j.1365-2249.2005.02934.x

Regnier, P., Le Joncour, A., Maciejewski-Duval, A., Desbois, A. C., Comarmond, C., Rosenzwajg, M., et al. (2020). Targeting JAK/STAT pathway in Takayasu's arteritis. *Ann. Rheum. Dis.* 79, 951–959.

Ruzt, S., Eidenschenk, C., and Ouyang, W. (2013). IL-22, not simply a Th17 cytokine. *Immunol. Rev.* 252, 116–132. doi: 10.1111/imr.12027

Saadoun, D., Garrido, M., Comarmond, C., Desbois, A. C., Domont, F., Savey, L., et al. (2015). Th1 and Th17 cytokines drive inflammation in Takayasu arteritis. *Arthritis Rheumatol.* 67, 1353–1360. doi: 10.1002/art.39037

Sagar, S., Ganguly, N. K., Koicha, M., and Sharma, B. K. (1992). Immunopathogenesis of Takayasu arteritis. *Heart Vessels* 7, 85–90. doi: 10.1007/bf01744550

Saikh, K. U., Khan, A. S., Kissner, T., and Ulrich, R. G. (2001). IL-15-induced conversion of monocytes to mature dendritic cells. *Clin. Exp. Immunol.* 126, 447–455. doi: 10.1046/j.1365-2249.2001.01672.x

Sanhurjo, L., Aran, G., Tellez, E., Amezaga, N., Armengol, C., Lopez, D., et al. (2018). CD5L promotes M2 macrophage polarization through autophagy-mediated upregulation of ID3. *Front. Immunol.* 9:480. doi: 10.3389/fimmu.2018.00480

Schmidt, A. M., Vianna, M., Gerlach, M., Brett, J., Ryan, J., Kao, J., et al. (1992). Isolation and characterization of two binding proteins for advanced glycosylation end products from bovine lung which are present on the endothelial cell surface. *J. Biol. Chem.* 267, 14987–14997. doi: 10.1016/s0021-9258(18)42137-0

See, P., Lum, J., Chen, J., and Ginhoux, F. A. (2018). Single-cell sequencing guide for immunologists. *Front. Immunol.* 9:2425. doi: 10.3389/fimmu.2018.02425

Shen, C. Y., Lu, C. H., Wu, C. H., Li, K. J., Kuo, Y. M., Hsieh, S. C., et al. (2020). The development of maillard reaction, and advanced glycation end product (AGE)-receptor for AGE (RAGE) signaling inhibitors as novel therapeutic strategies for patients with AGE-related diseases. *Molecules* 25:5591. doi: 10.3390/molecules25235591

Stuart, T., Butler, A., Hoffman, P., Hafemeister, C., Papalexi, E., Mauck, W. M. III, et al. (2019). Comprehensive integration of single-cell data. *Cell* 177, 1888–1902.e21.

Sutherland, A. P., Joller, N., Michaud, M., Liu, S. M., Kuchroo, V. K., and Grusby, M. J. (2013). IL-21 promotes CD8+ CTL activity via the transcription factor T-bet. *J. Immunol.* 190, 3977–3984. doi: 10.4049/jimmunol.1201730

Terao, C. (2016). Revisited HLA and non-HLA genetics of Takayasu arteritis–where are we? *J. Hum. Genet.* 61, 27–32. doi: 10.1038/jhg.2015.87

Tinkov, A. A., Bjorklund, G., Skalny, A. V., Holmgren, A., Skalnaya, M. G., Chirumbolo, S., et al. (2018). The role of the thioredoxin/thioredoxin reductase system in the metabolic syndrome: towards a possible prognostic marker? *Cell. Mol. Life Sci.* 75, 1567–1586. doi: 10.1007/s00018-018-2745-8

Torp, C. K., Bruner, M., Keller, K. K., Brouwer, E., Hauge, E. M., McGonagle, D., et al. (2021). Vasculitis therapy refines vasculitis mechanistic classification. *Autoimmun. Rev.* 20:102829. doi: 10.1016/j.autrev.2021.102829

Turner, M. D., Nedjai, B., Hurst, T., and Penington, D. J. (2014). Cytokines and chemokines: at the crossroads of cell signalling and inflammatory disease. *Biochim. Biophys. Acta* 1843, 2563–2582. doi: 10.1016/j.bbamcr.2014.05.014

Val, S., Belade, E., George, I., Boczkowski, J., and Baeza-Squiban, A. (2012). Fine PM induce airway MUC5AC expression through the autocrine effect of amphiregulin. *Arch. Toxicol.* 86, 1851–1859. doi: 10.1007/s00204-012-0903-6

Yang, C., Xia, W., Liu, X., Lin, J., and Wu, A. (2019). Role of TXNIP/NLRP3 in sepsis-induced myocardial dysfunction. *Int. J. Mol. Med.* 44, 417–426. doi: 10.3892/ijmm.2019.4232

Yu, Y., Xing, K., Badamas, R., Kuszynski, C. A., Wu, H., and Lou, M. F. (2013). Overexpression of thioredoxin-binding protein 2 increases oxidation sensitivity and apoptosis in human lens epithelial cells. *Free Radic. Biol. Med.* 57, 92–104.

Zhou, J., Chen, Z., Li, J., Yang, Y., Zhao, J., Chen, H., et al. (2017). The efficacy of tocilizumab for the treatment of Chinese Takayasu's arteritis. *Clin. Exp. Rheumatol.* 35, 171–175.

Conflict of Interest: The authors declare that the research was conducted in the absence of any commercial or financial relationships that could be construed as a potential conflict of interest.

Publisher's Note: All claims expressed in this article are solely those of the authors and do not necessarily represent those of their affiliated organizations, or those of the publisher, the editors and the reviewers. Any product that may be evaluated in this article, or claim that may be made by its manufacturer, is not guaranteed or endorsed by the publisher.

frontiers in Cell and Developmental Biology

ORIGINAL RESEARCH
published: 24 November 2021
doi: 10.3389/fcell.2021.773048

Halofuginone Sensitizes Lung Cancer Organoids to Cisplatin *via* Suppressing PI3K/AKT and MAPK Signaling Pathways

Hefei Li[1†], Yushan Zhang[2†], Xiaomei Lan[3†], Jianhua Yu[4], Changshuang Yang[3], Zhijian Sun[3], Ping Kang[3], Yi Han[2] and Daping Yu[2*]*

[1]Department of Thoracic Surgery, Affiliated Hospital of Hebei University, Baoding, China, [2]Department of Thoracic Surgery, Beijing Chest Hospital, Beijing Tuberculosis and Thoracic Tumor Research Institute, Capital Medical University, Beijing, China, [3]K2 Oncology Co. Ltd., Beijing, China, [4]Oncology Department, Wang Jing Hospital of China Academy of Chinese Medical Sciences, Beijing, China

OPEN ACCESS

Edited by:
Weihua Zhou,
University of Michigan, United States

Reviewed by:
Fan Yao,
Huazhong Agricultural University, China
Yuxiong Feng,
Zhejiang University, China

***Correspondence:**
Yi Han
hanyi@mail.ccmu.edu.cn
Daping Yu
ydpjsz@mail.ccmu.edu.cn

[†]These authors have contributed equally to this work and share first authorship

Specialty section:
This article was submitted to Signaling, a section of the journal Frontiers in Cell and Developmental Biology

Received: 09 September 2021
Accepted: 04 November 2021
Published: 24 November 2021

Citation:
Li H, Zhang Y, Lan X, Yu J, Yang C, Sun Z, Kang P, Han Y and Yu D (2021) Halofuginone Sensitizes Lung Cancer Organoids to Cisplatin via Suppressing PI3K/AKT and MAPK Signaling Pathways. Front. Cell Dev. Biol. 9:773048. doi: 10.3389/fcell.2021.773048

Lung cancer is the leading cause of cancer death worldwide. Cisplatin is the major DNA-damaging anticancer drug that cross-links the DNA in cancer cells, but many patients inevitably develop resistance with treatment. Identification of a cisplatin sensitizer might postpone or even reverse the development of cisplatin resistance. Halofuginone (HF), a natural small molecule isolated from *Dichroa febrifuga*, has been found to play an antitumor role. In this study, we found that HF inhibited the proliferation, induced G0/G1 phase arrest, and promoted apoptosis in lung cancer cells in a dose-dependent manner. To explore the underlying mechanism of this antitumor effect of halofuginone, we performed RNA sequencing to profile transcriptomes of NSCLC cells treated with or without halofuginone. Gene expression profiling and KEGG analysis indicated that PI3K/AKT and MAPK signaling pathways were top-ranked pathways affected by halofuginone. Moreover, combination of cisplatin and HF revealed that HF could sensitize the cisplatin-resistant patient-derived lung cancer organoids and lung cancer cells to cisplatin treatment. Taken together, this study identified HF as a cisplatin sensitizer and a dual pathway inhibitor, which might provide a new strategy to improve prognosis of patients with cisplatin-resistant lung cancer.

Keywords: lung cancer, patient-derived organoid, halofuginone, PI3K/AKT, MAPK

INTRODUCTION

Lung cancer is the most commonly diagnosed cancer (11.4% of the total cases) and the leading cause of cancer death (18% of the total cancer deaths) worldwide (Sung et al., 2021). Although obvious progression has been made in surgical and pharmacological therapies for lung cancer, relapses of lung cancer are frequently documented with stronger drug resistance than primary tumor (Chen H.-Z. et al., 2021). Up to now, platinum and its derivatives are still the major choice for chemotherapy against cancers. However, platinum-based chemotherapy drugs are often confronted with the problem of drug resistance, and the cancers with drug resistance are usually incurable. Therefore, finding novel sensitizers which can be used in combination with platinum to improve the clinical utility of platinum has attracted close attention from researchers in oncology, pharmacology, and chemistry worldwide.

Increasing evidence suggests that the development of platinum resistance requires orchestration of multiple signaling pathways, including the PI3K/AKT and MAPK pathway (Fang et al., 2017; Liang et al., 2019). Inhibition of key pathways responsible for platinum resistance with a single multi-pathway inhibitor might result in better efficacy with low toxicity than combination of inhibitors targeting individual pathway (Chen et al., 2016; Sanchez et al., 2019). Therefore, phenotypic screening of large chemical libraries in clinically relevant disease models could be used to fulfill this purpose. The establishment of a 3D preclinical model, which could well recapitulate the derived primary tumor and portray the *in vivo* response more accurately, is urgently needed to screen potential natural molecules to resolve the issue of cisplatin resistance. Patient-derived organoids (PDOs) are novel preclinical models and closely resemble their primary tumors in both historical features and molecular characteristics, which have attracted more and more attention in both high-throughput drug screening, personalized drug design, and companion diagnostics for patients (Puca et al., 2018; Ooft et al., 2019; Pasch et al., 2019; Shi et al., 2019; Driehuis et al., 2020; Yao et al., 2020).

Halofuginone (HF) is a febrifugine-derivative alkaloid extracted from *Dichroa febrifuga*. It has been reported that HF possesses marked antimalarial (Hewitt et al., 2017), anti-coccidial (Matus and Boison, 2016), and anticancer activities (Akhtar et al., 2018; Xia et al., 2018). The anticancer properties of HF might be attributed to promote infiltration of favorable immune cells (Huang and Brekken, 2019), suppressing pathways on Smad3/TGF-β (Cui et al., 2016), AKT/mTOR, and/or p53 signaling (Akhtar et al., 2018; Xia et al., 2018), preventing the differentiation of fibroblasts to myofibroblasts and the transition of epithelial cells to mesenchymal cells in mammals, inhibiting prolyl-tRNA synthetase, activating the amino acid starvation response, preventing the differentiation of TH17 cells to blunt autoimmune responses, and triggering the autophagy (Chen et al., 2017; Xia et al., 2018). However, the evidence on the response of PDOs to HF in modeling the *in vivo* drug response remains missing.

In this study, we evaluated the effects of HF on cisplatin-resistant lung cancer PDOs and cells to determine whether it acted as a sensitizer. RNA sequencing of NCI-H1299 and NCI-H460, two lung cancer cell lines, treated with HF exhibited significant transcriptional alterations of genes involved in PI3K/AKT and MAPK signaling pathways. *In vitro* functional assays showed strong growth inhibition of HF. Thus, we proposed a hypothesis that HF exhibited anticancer properties in lung cancer cell lines by the dual regulation of MAPK and PI3K/AKT signaling pathways. Of note, HF exhibited a synergy effect with cisplatin in our studied cell lines. Taken together, our investigation illustrated that HF is a promising anticancer hit and sensitizer for cisplatin in lung cancer.

MATERIALS AND METHODS

Tissue Processing and Organoid Culture

Lung cancer organoids were derived from surgery samples or transbronchial biopsies of lung cancer patients at Beijing Chest Hospital, Capital Medical University, Beijing, China. The study has got the approval of the Ethical Committee of Beijing Chest Hospital, Capital Medical University (Trial No. 11, 2020). Patients participating in this study signed informed consent forms. On arrival, tumor tissues were washed with cold PBS, cut into small pieces, washed with Advanced DMEM/F12 (Thermo Fisher Scientific, Waltham, MA, United States; containing 1× Glutamax, 10 mM HEPES and antibiotics), and digested with collagenase (Sigma-Aldrich, Cat #C9407, 2 mg/ml) for 1–2 h at 37°C. After washing twice with fresh medium (2% fetal calf serum, FCS) and centrifugation (400 rcf, 4 min), dissociated cells were seeded into growth factor reduced Matrigel (Corning, Cat # 356252) with the presence of Advanced DMEM/F12 at 37°C for 30 min. Next, the surface of the solidified mixture of cell suspension/Matrigel was sealed with complete human organoid medium (HOM, 500 μL), which comprised Advanced DMEM/F12 supplementing with series additives as described by Lampis et al. (2017) and Puca et al. (2018), replacing every 3 days. When the organoids ranged up to 200–500 μm in diameter (about 1 week), organoids were dissociated and passaged weekly using TrypLE Express (Gibco, Grand Island, NY, United States). The PDOs (2×10^6 cells/tube, P3) were frozen using the Recovery Cell Culture Freezing Medium (Gibco) and stored at −80°C before drug screening.

Compound Screening

A collection of almost 1,100 natural products were obtained from MedChemExpress (Shanghai, China). The natural product library was reformatted into 96-well source plates with concentration of 3.3 mM for automated robotic screening. At parallel, the cells were also treated with an equal volume (0.1%) of DMSO as a negative control and 1 μM final of staurosporine (MCE, shanghai, China) as a positive control. Plate-to-plate normalization and assay quality control were calculated according to them. A 3D cell viability assay was implemented, which determines the number of cell viability according to the ATP level using commercially available luminescence detection reagent (CellTiter-Glo 3D, #G9683, Promega, Madison, WI). In brief, organoids were processed as described earlier and plated in a 96-well low binding assay plate at a density of 6,000 cells per well in 50 μL comprising 10% growth factor reduced Matrigel. Additional 40 μL culture medium without Matrigel was added. Organoids were maintained in medium described earlier and drugged 2 days later by adding 10 μL culture medium comprising 33 μM natural product to get a final concentration of 3.3 μM (**Supplementary Figure S1A**). The assay was terminated at day 5 by adding 50 μL CellTiter-Glo. Assay quality and robustness were evaluated with the signal window (SW) and Z factor. Triplicate wells treated with staurosporine and vehicle solution (DMSO) were employed as bottom wells and top wells, respectively (**Supplementary Figure S1B**). The assay showed the signal windows (SW) were much larger than 10, and the Z factor values were between 0.5 and 1, which indicated that the assay was qualified for high-throughput screening (**Supplementary Figures S1C,D**).

Cell Lines and Cell Culture

Human lung cancer cell lines NCI-H1299 (ATCC Cat# CRL-5803, RRID: CVCL_0060) and NCI-H460 (ATCC Cat# HTB-177, RRID: CVCL_0459) were purchased from the American Type Culture Collection (ATCC; Manassas, VA, United States). Cells were maintained in RPMI-1640/1641/1642 medium (Gibco) supplemented with 10% FCS (Gibco) and 1% penicillin–streptavidin (Gibco) at 37°C in 5% CO_2.

Cell Viability Assay and Foci Assay

NCI-H460 (0.75×10^3 cells/well) and NCI-H1299 (0.75×10^3 cells/well) cell lines were seeded into 96-well plates and treated with vehicle or HF for 1, 3, and 5 days. After incubation, cell viability was detected using luminescence detection reagent (CellTiter-Glo, #G9243, Promega, Madison, WI). The CellTiter-Glo assay determines the number of viable cells in culture by quantifying ATP, which indicates the presence of metabolically active cells. Luminescence readout is directly proportional to the number of viable cells in culture. As for the foci assay, NCI-H460 (2×10^3 cells/well) and NCI-H1299 (2×10^3 cells/well) were seeded into 6-well plates, treated with HF as the way of cell viability assay, then fixed and stained the cells with crystal violet solution, and took photos with a camera and bright-field microscope. Each vial of frozen cells was thawed and maintained for a maximum of 10 passages.

Analysis of Cell Cycle Arrest and Apoptosis

The cell cycle and apoptosis were detected as previously described (Shi et al., 2018). Cells were cultured and treated with DMSO and HF (0.05 and 0.2 μM) in both NCI-H460 and NCI-H1299 for 24 h, followed by single staining with PI (Beyotime) for cell cycle analysis and double staining with PI and Annexin V-FITC (Beyotime) for apoptosis analysis. Data analysis was performed using NovoExpress v1.3.4.

Western Blot Analysis

A standard Western blot analysis of whole-cell protein lysates was performed using primary antibodies against cleaved PARP, PARP (Cell Signaling Technology, #9542, 1:1,000, RRID:AB_2160739), cleaved caspase-3 (Cell Signaling Technology Cat# 9661, 1:1,000, RRID:AB_2341188), caspase-3 (Cell Signaling Technology Cat# 9662, 1:1,000, RRID:AB_331439), cylclinD1 (Cell Signaling Technology Cat# 2978, 1:1,000, RRID:AB_2259616), p27 (Cell Signaling Technology Cat# 3686, 1:1,000, RRID:AB_2077850), p21 (Cell Signaling Technology Cat# 2947, 1:1,000, RRID: AB_823586), pRb (Cell Signaling Technology Cat# 8516, 1: 1,000, RRID:AB_11178658), and Rb (Cell Signaling Technology Cat# 9309, 1:1,000, RRID:AB_823629) to check the changes of apoptosis and G0/G1 phase markers. As well, for the alteration of effectors, the signaling pathways were examined with the primary antibodies including p-AKT1/2 (Cell Signaling Technology Cat# 4060, 1:1,000, RRID: AB_2315049), AKT1/2 (Proteintech Cat# 10176-2-AP, 1:2000, RRID:AB_2224574), p-ERK (Cell Signaling Technology Cat# 4370, 1:1,000, RRID:AB_2315112), and ERK (Proteintech Cat# 16443-1-AP, 1:2000, RRID:AB_10603369). Equal amounts of protein, which were blotted with an anti-β-actin antibody (Proteintech Cat# 60008-1-Ig, 1:2000, RRID: AB _2289225), was used as loading control.

RNA-Seq Analysis

NCI-H460 and NCI-H1299 cells were incubated with DMSO or HF (0.05 and 0.2 μM) for 48 h; after harvest, total RNA was isolated using the TriZolTM UP Plus RNA Kit. RNA was sent to BGI (Beijing, China) for sequencing and analysis. In brief, after total RNA was fragmented into short fragments, mRNA was enriched using oligo (dT) magnetic beads, followed by cDNA synthesis. Double-stranded cDNA was purified and enriched by PCR amplification, after which the library products were sequenced using BGIseq-500. The heatmap of DEGs ($\log_2 FC \geq 1, p \leq 0.001$) and KEGG analysis ($\log_2 FC \geq 1, p \leq 0.05$) in NSCLC cell lines were performed by the BGI using the Dr. TOM approach, a customized data mining system from BGI. Altered (upregulated or downregulated) expression of genes was expressed as $\log_2 FC$, which represents log-transformed fold change ($\log_2 FC = \log_2[B] - \log_2[A]$, while A and B represent values of gene expression for different treatment conditions).

Dual Drug Combination Assay

NCI-H1299 and NCI-H460 cells were plated in 96-well plates and treated with various concentrations of cisplatin or/and HF, either alone or in combination, for 72 h. Cell viability was determined as described before. The synergy effect was evaluated by measuring the IC_{50} and highest single agent (HSA) reference model (Yadav et al., 2015). In addition, Western blotting analysis and flow cytometry assay were performed to detect the effect of drug combination on signaling pathways and cell cycle arrest.

Cisplatin-resistant PDOs (PDO-R1 and PDO-R2) were derived from two cisplatin-resistant patients and were plated in 96-well plates and treated with various concentrations of HF and cisplatin. Synergistic effects were observed under a microscope, and Western blotting assay was performed to detect the effect of drug combination on signaling pathways.

Statistical Analysis

Data statistical analysis was performed using GraphPad Prism 8.0. The HF IC_{50} values were analyzed using non-linear regression (curve fit). The cell cycle and apoptosis data were analyzed using Excel using Student's t test. A p value < 0.05 was considered as statistically significant. All data subjected to statistical evaluations were gathered with at least three independent repeats of experiments.

RESULTS

Compound Screening and the Characterization of Cisplatin-Resistant NSCLC PDOs

PDOs have been reported for applications in preclinical drug discovery (Raja et al., 2016; Huang et al., 2017; Choudhury et al., 2020; Maloney et al., 2020; Skardal et al., 2020). A Two-stage screening strategy was employed whereby almost 1,100

A

Patient number	PDO number	Gender	Pathological pattern	Age	therapeutic regimen	clinical evaluation	Tissue type	T	N	M	Stage
Patient-R1	PDO-R1	male	squamous cell carcinoma	60	gemcitabine and nedaplatin, 2 cycles	PD	biopsy sample	2b	0	1c	IVb
Patient-R2	PDO-R2	male	squamous cell carcinoma	53	carrelizumab, Albumin-bound paclitaxel and carboplatin, 2 cycles, neoadjuvant therapy	PD	surgery sample	4	0	0	IIIa

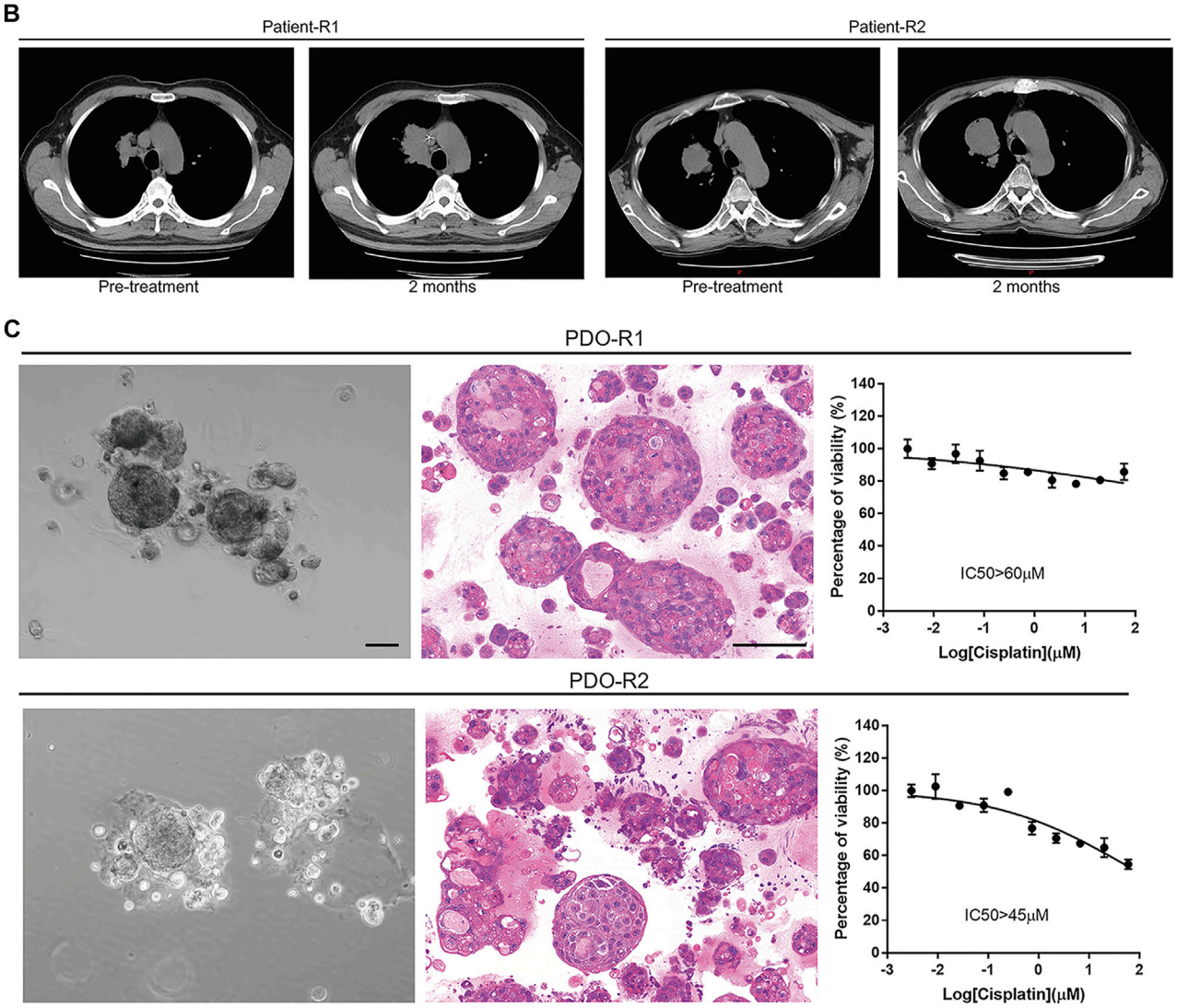

FIGURE 1 | Patient-derived lung cancer organoids were generated and phenotypically represent the tumors from which they were derived. **(A)** Table of patients, diagnosis, clinical evaluation, and treatment status at time of surgery/biopsy where parent tumor was obtained. **(B)** Evaluation of patients' clinical outcomes (computed tomography imaging of the subjects' lung cancer tumors before and 2 months after treatment with platinum). **(C)** Bright-field images, H and E–stained images, and cisplatin-resistant characterization of PDO-R1 and PDO-R2.

natural products were primarily screened in 1 PDO and then validated in six PDO models which completed by K2 Oncology Co., Ltd. (Beijing 100061, P.R. China). The screening process is illustrated in **Supplementary Figures S1A–D**, and the results showed that HF is exactly one of the top hits with strong anticancer potential (**Supplementary Figure S1E**). Then we performed further anticancer effect verification of HF in two cisplatin-resistant lung cancer PDOs. The clinical information and data of these two PDOs are summarized in **Figure 1A**. Both patients were treated with the platinum-based regimen, and the RECIST evaluation was performed after two cycles (**Figure 1B**). The cisplatin

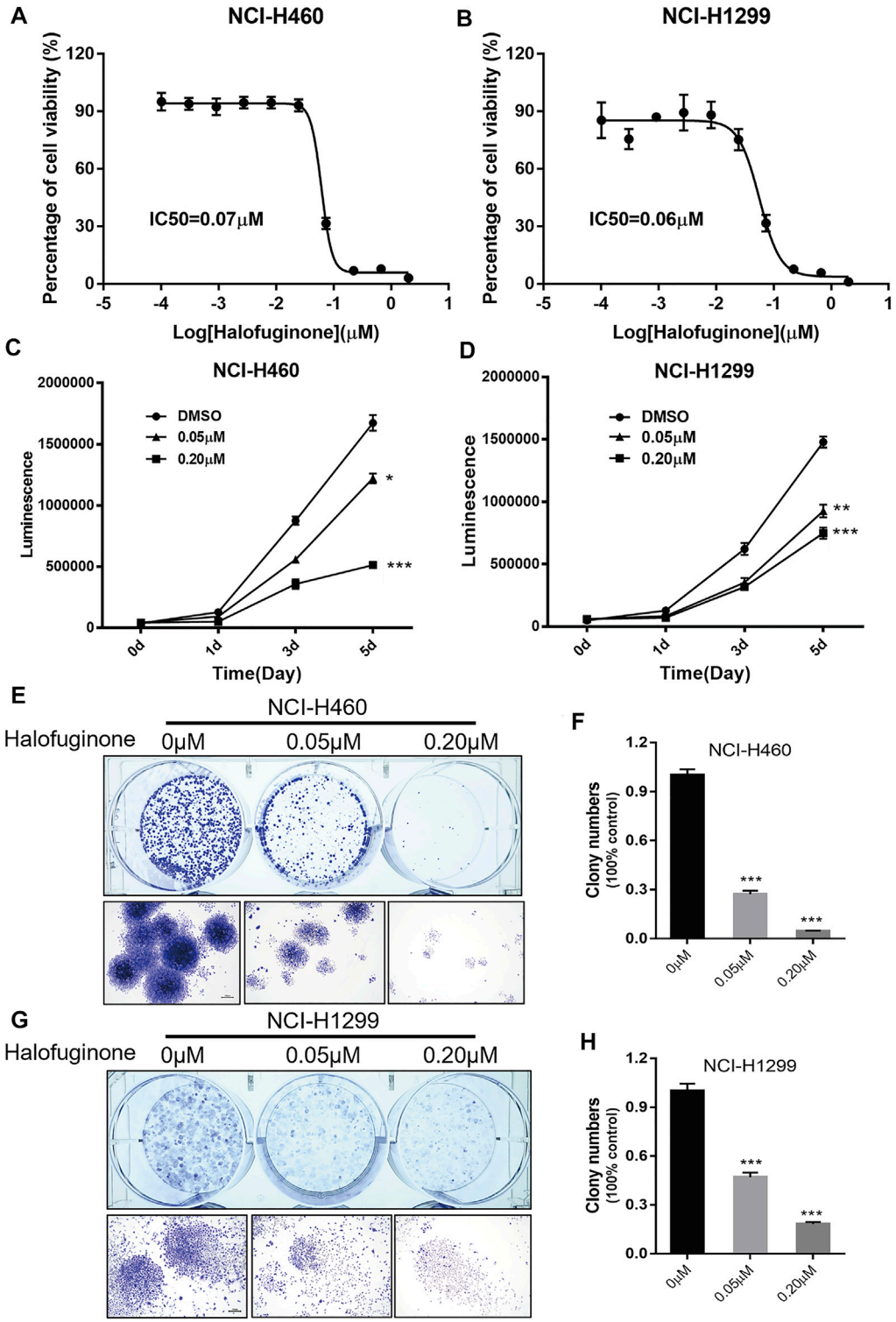

FIGURE 2 | Halofuginone significantly inhibited cell growth in NCI-H460 and NCI-H1299 cells. **(A,B)** The dose–response curves and IC50 values of halofuginone in NCI-H460 and NCI-H1299, respectively. **(C,D)** Cell proliferation suppression in NCI-H460 and NCI-H1299 with the treatment of halofuginone at the concentration of 0.05 and 0.2 μM for 5 days. (**E–H)** Halofuginone inhibited the colony formation in NCI-H460 and NCI-H1299 cells at the concentration of 0.05 and 0.2 μM for 7 days. Cells were stained with crystal violet solution at the endpoint. (*$p < 0.05$, **$p < 0.01$, ***$p < 0.001$).

resistance were maintained after PDOs were successfully established (**Figures 1C,D**).

HF Inhibited Cell Growth in Lung Cancer Cell Lines

Next, we verified the effect of HF in lung cancer cell lines, NCI-H1299 and NCI-H460. NCI-H460 showed partial cisplatin sensitivity, but the maximal inhibition rate was very limited (**Figure 4B**). NCI-H1299 is a cisplatin-resistant lung cancer cell line (Fan et al., 2020) (Chen M. et al., 2021), and its cisplatin resistance is also validated in this study (**Figure 4D**). The dose–response curve of HF in both cell lines exhibited identical IC_{50} (0.07 μM) (**Figures 2A,B**). The significant dose-dependent and time-dependent inhibition of HF on lung cancer cell proliferation were observed in both cell lines (**Figures 2C,D**). In addition, HF remarkably suppressed colony formation of the two cell lines in a dose-dependent manner (**Figures 2E–H**). Thus, these results indicated a remarkable growth inhibition of HF in lung cancer cell lines.

HF Induced G0/G1 Phase Arrest and Apoptosis in Lung Cancer Cell Lines

To explore the reasons for growth inhibition of lung cancer cells by HF, cell cycle distribution, and apoptosis induction were evaluated on HF-treated lung cancer cell lines. Through flow-cytometry assay, we noticed a dose-dependent G0/G1 phase arrest (**Figures 3A–D**) in both NCI-H1299 and NCI-H460 following 24-h treatment of HF. Additionally, HF induced dose-dependent apoptosis in both cell lines (**Figures 3E–H**). In detail, both the early and late apoptosis were significantly induced by HF (**Supplementary Figure S2**). Cyclin D1 (Sherr, 1996; Lukas et al., 1996) and p21 (Cheng et al., 1999; Pestell et al., 1999) are two canonical cell cycle markers for the G1 phase. Western blotting confirmed G0/G1 phase arrest with the decreased cyclin D1 expression and increased p21 expression in accordance with the flow cytometry tendency (**Figure 3I**). PARP (Lu et al., 2019) and caspase (Julien and Wells, 2017) activation are the key events of apoptosis, and the expression levels of their full-length and cleaved forms were examined with Western blotting. The decreased PARP and caspase 3 and the increased cleaved PARP and cleaved caspase3 suggested that HF induced apoptosis in a dose-dependent manner as well (**Figure 3J**). Taken together, HF induced G0/G1 phase arrest and apoptosis in a dose-dependent manner in NCI-H460 and NCI-H1299, which well explained the significant lung cancer cells growth inhibition.

HF Sensitized Lung Cancer Cell Lines to Cisplatin

To further investigate the impact of HF on cisplatin resistance in lung cancer, lung cancer cell lines, NCI-H1299 and NCI-H460, were employed for the dural drug synergy test. NCI-H1299 shows resistance to cisplatin, with IC_{50} larger than 100 mM and maximal inhibition rate smaller than 10%. NCI-H460 showed limited response to cisplatin, with maximal inhibition rate of about 20%, which induced the absolute IC_{50} larger than 10 mM and indicated a very low efficacy (**Figures 4B,D**). The synergy effect was evaluated by measuring the IC_{50} and the highest single agent (HSA) reference model (Yadav et al., 2015). With the existence of HF, significant left shift of dose–efficacy curve and decrease in IC_{50} were observed (**Figures 4B,D**). By adding 5, 14, and 41 nM of HF, the IC_{50} of cisplatin decreased from larger than 10 mM to 8, 2.4, and 0.4 μM for NIC-H460 and 9, 2.5, and 0.5 μM for NCI-H1299, respectively. Consistently, by adding serial diluted cisplatin to HF, the IC_{50} of HF also decreased, respectively (**Figures 4A,C**). To further analyze the synergy effect of cisplatin with HF, synergy score matrixes were calculated with the highest single agent (HSA) reference model. The average synergy score of cisplatin with HF is 21.585 and 24.851 for NCI-H1299 and NCI-H460, respectively. The HSA synergy scores were visualized with heatmap (red areas in the model graph) and 3D hillmap (**Figures 4E–H**). These data suggest the synergic effect of HF and cisplatin in lung cancer cell lines.

To further explore the potential value and the underlying synergy mechanism of HF with cisplatin, 1 and 10 μM of cisplatin and 50 and 200 nM HF were selected for cell cycle, apoptosis, and pathway markers detection using Western blot in NCI-H460 and NCI-H1299. When HF was combined with 1 μM of cisplatin, significant G0/G1 phase arrest was observed with the increase in p21 and p27 and the decrease in p-Rb and cyclin D1 in a dose-dependent manner (**Figure 5** upper). HF combined with 10 μM of cisplatin showed similar trend but a stronger dose-dependent synergistic effect than low-dose cisplatin. In addition, the apoptosis markers also showed similar synergy effect with the indicator of caspase 3 and cleaved caspase 3 (**Figure 5** middle). Similar tendency of G0/G1 phase arrest was further approved using flow cytometry with cell models treated with cisplatin alone, HF alone, and cisplatin combined with HF (**Figures 6A–C**). Obviously, cisplatin alone barely changed the cell cycle progression, but HF could induce prominent G0/G1 phase arrest at 200 nM. Altogether, these data demonstrated that HF would be a potential cisplatin sensitizer *via* G0/G1 phase arrest and apoptosis.

HF Altered Genome-Wide Gene Expression in Lung Cancer Cell Lines

RNA sequencing was performed to profile gene expression in both NCI-H460 and NCI-H1299 with the treatment of HF at 0.05 and 0.2 μM, respectively. (The datasets presented in this study can be found in online repositories. The names of the repository and accession number can be found below: http://www.ncbi.nlm.nih.gov/sra, accession number PRJNA769938). In both cell lines, >4000 genes were differentially expressed under the two concentrations. We observed substantial overlap between the two cell lines with regard to the genes that were differentially expressed following incubation with HF-1798 genes (DEGs, $\log_2FC \geq 1$, $p \leq 0.001$) were shared in NCI-H460 and NCI-H1299 with the treatment of different concentration of HF (**Figure 7A**). In addition, HF led to alterations of 5478 DEGs in NCI-H460 cells and 3523 DEGs

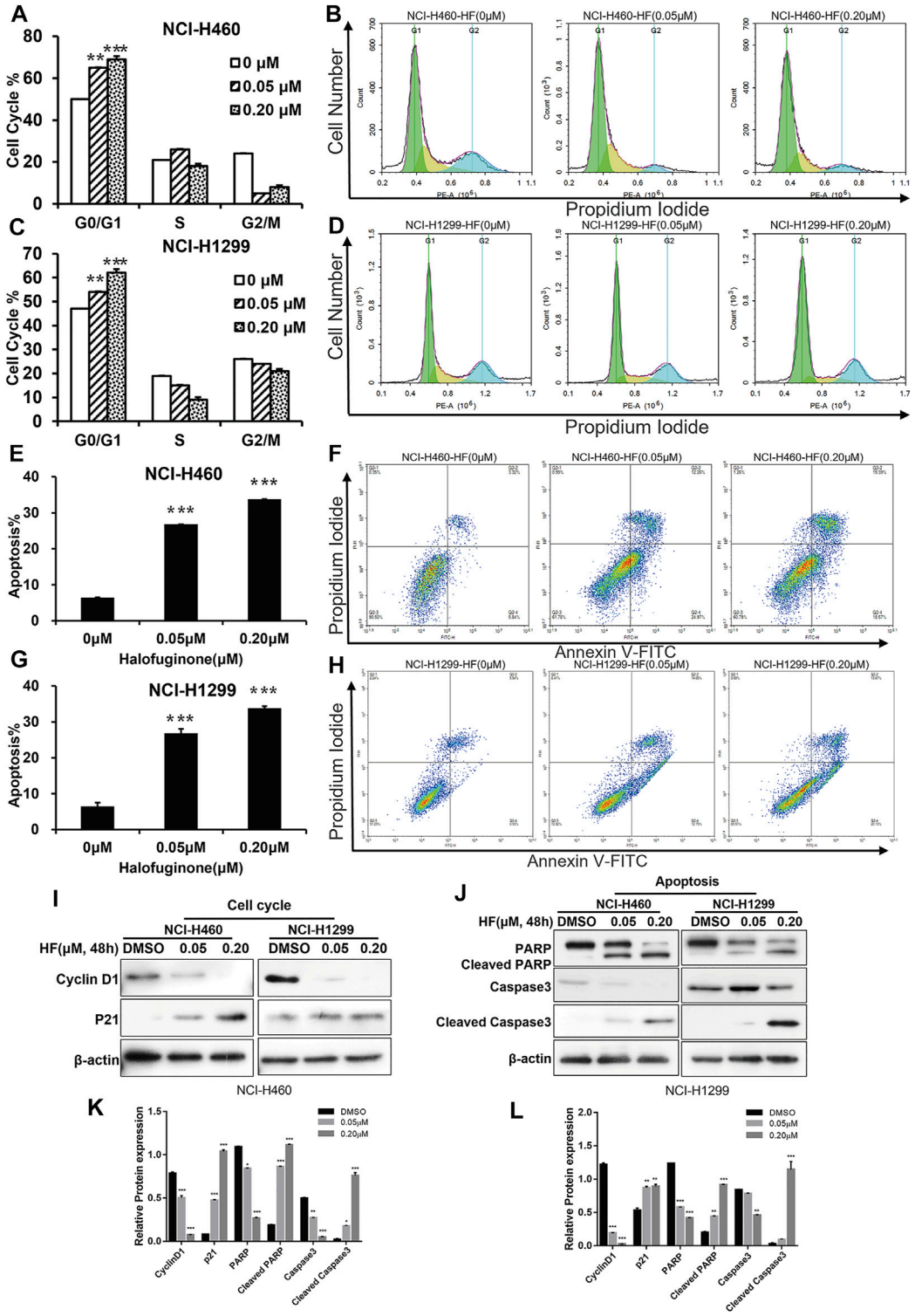

FIGURE 3 | Halofuginone induced G0/G1 arrest and apoptosis in NCI-H460 and NCI-H1299 cells. **(A–D)** Flow cytometry analysis of the cell cycle by PI staining in NCI-H460 and NCI-H 1299 cells with treatment of DMSO or halofuginone for 48 h ($n = 3$). **(E–H)** Flow cytometry analysis of apoptosis analysis by PI/Annexin V-FITC staining in both NCI-H460 and NCI-H1299 cells with treatment of DMSO or halofuginone for 48 h ($n = 3$). **(I–L)** Cell cycle and apoptosis markers (cyclin D1, p21, PARP, cleaved PARP, and cleaved caspase 3) analysis by Western blot. β-actin was used as a loading control ($n = 3$) (*$p < 0.05$, **$p < 0.01$, ***$p < 0.001$).

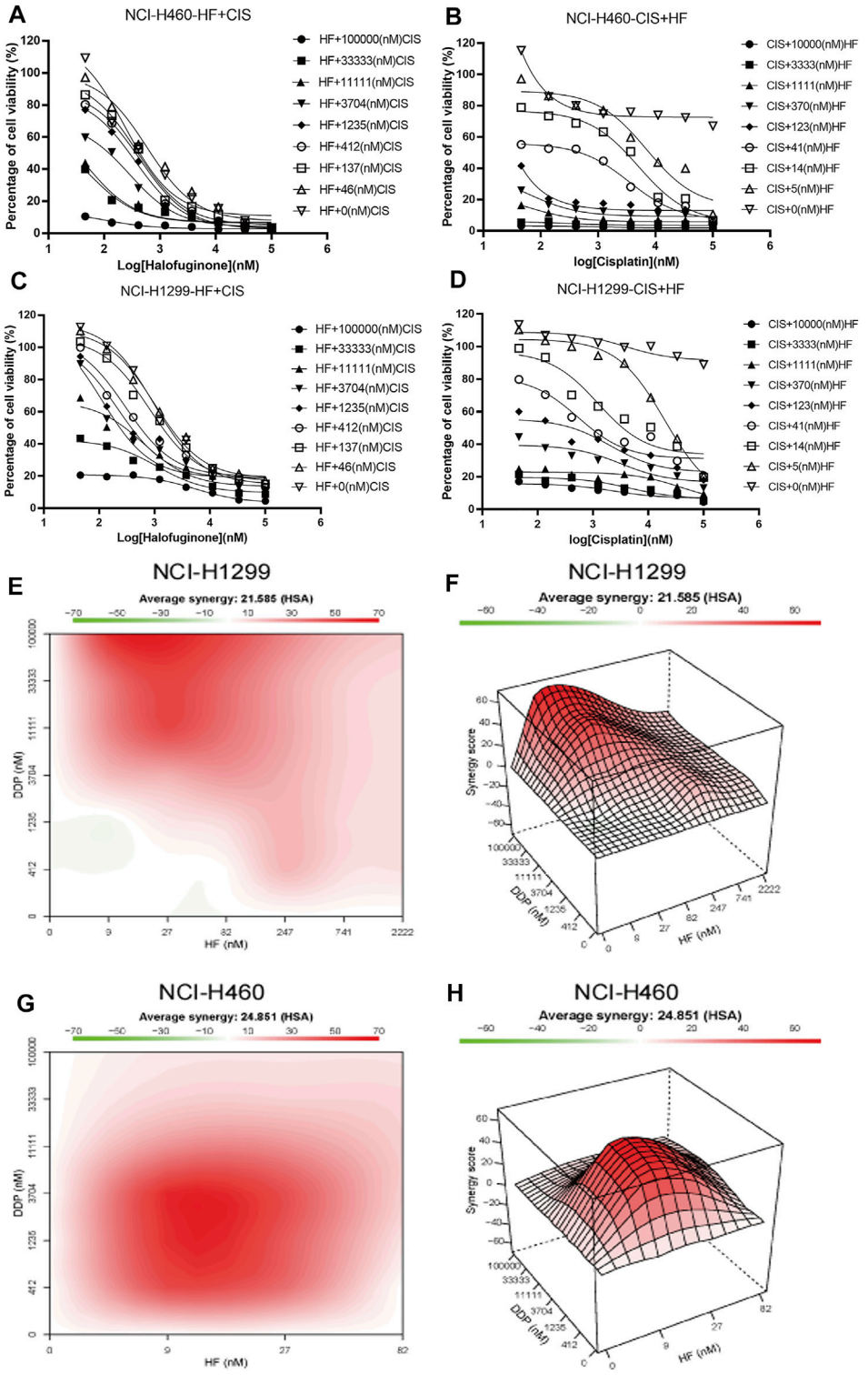

FIGURE 4 | Synergy effects of halofuginone and cisplatin on cell viability of NCI-H460 and NCI-H1299. **(A–D)** The dose–response curves of NCI-H460 and NCI-H1299 cells treated with the combination of halofuginone and cisplatin. **(E–H)** The surface plot and heatmap show the Excess over the highest single agent (EOHSA) of halofuginone and cisplatin combination in NCI-H460 and NCI-H1299 cells.

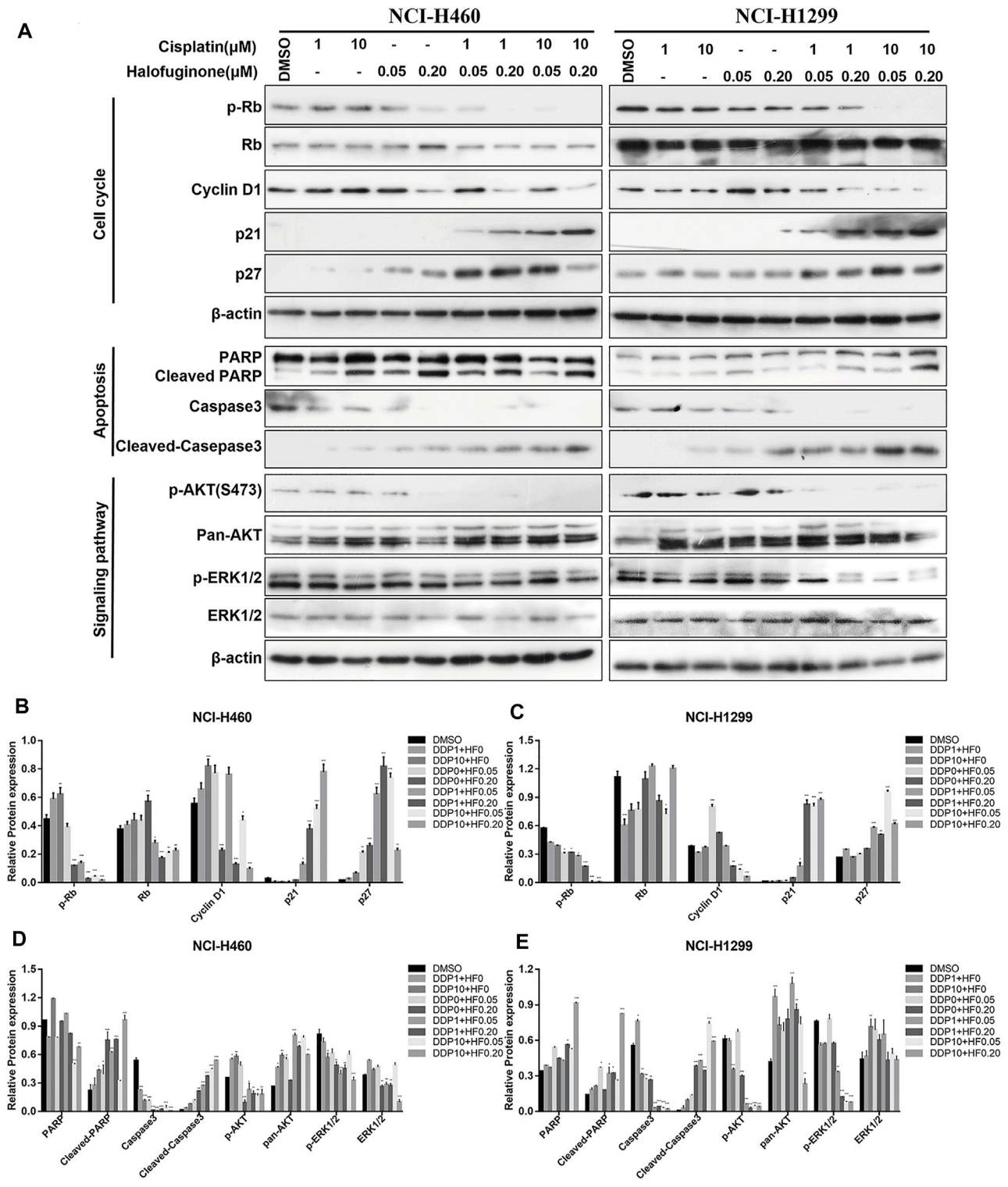

FIGURE 5 | Expression of markers related to cell cycle, apoptosis, and proliferation was detected by Western blotting in NCI-H460 and NCI-H1299 cells treated with the combination of halofuginone and cisplatin. **(A)** The cell lysates from NCI-H460 and NCI-H1299 cells were analyzed by Western blotting using the indicated antibodies. **(B-E)** Relative protein expressions were quantified by Image J software. ($n = 3$, $^{*}p < 0.05$, $^{**}p < 0.01$, $^{***}p < 0.001$).

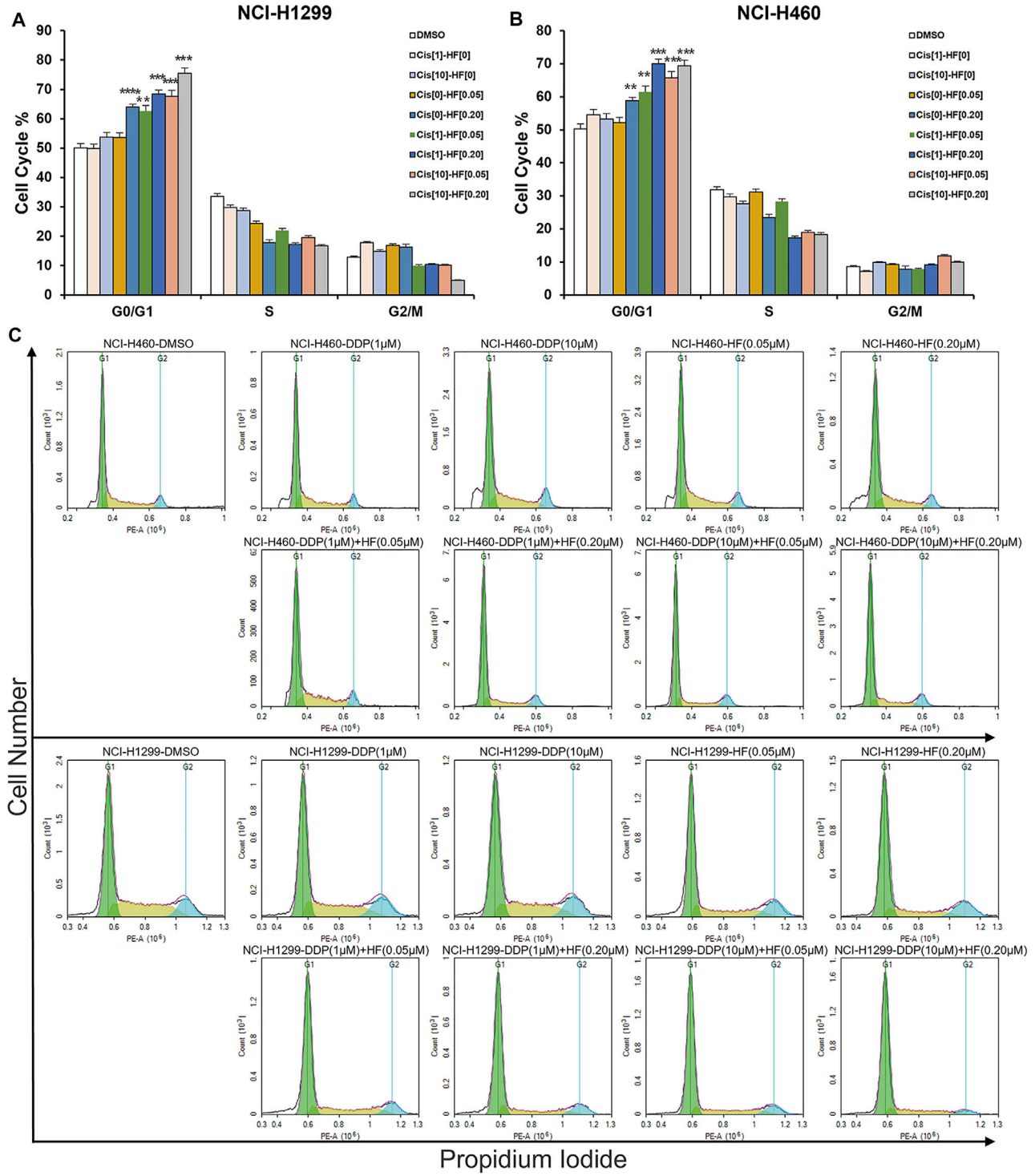

FIGURE 6 | Halofuginone/cisplatin combination significantly induced G0/G1 arrest in NCI-H1299 and NCI-H460 cells ($n = 3$, $^{*}p < 0.05$, $^{**}p < 0.01$, $^{***}p < 0.001$).

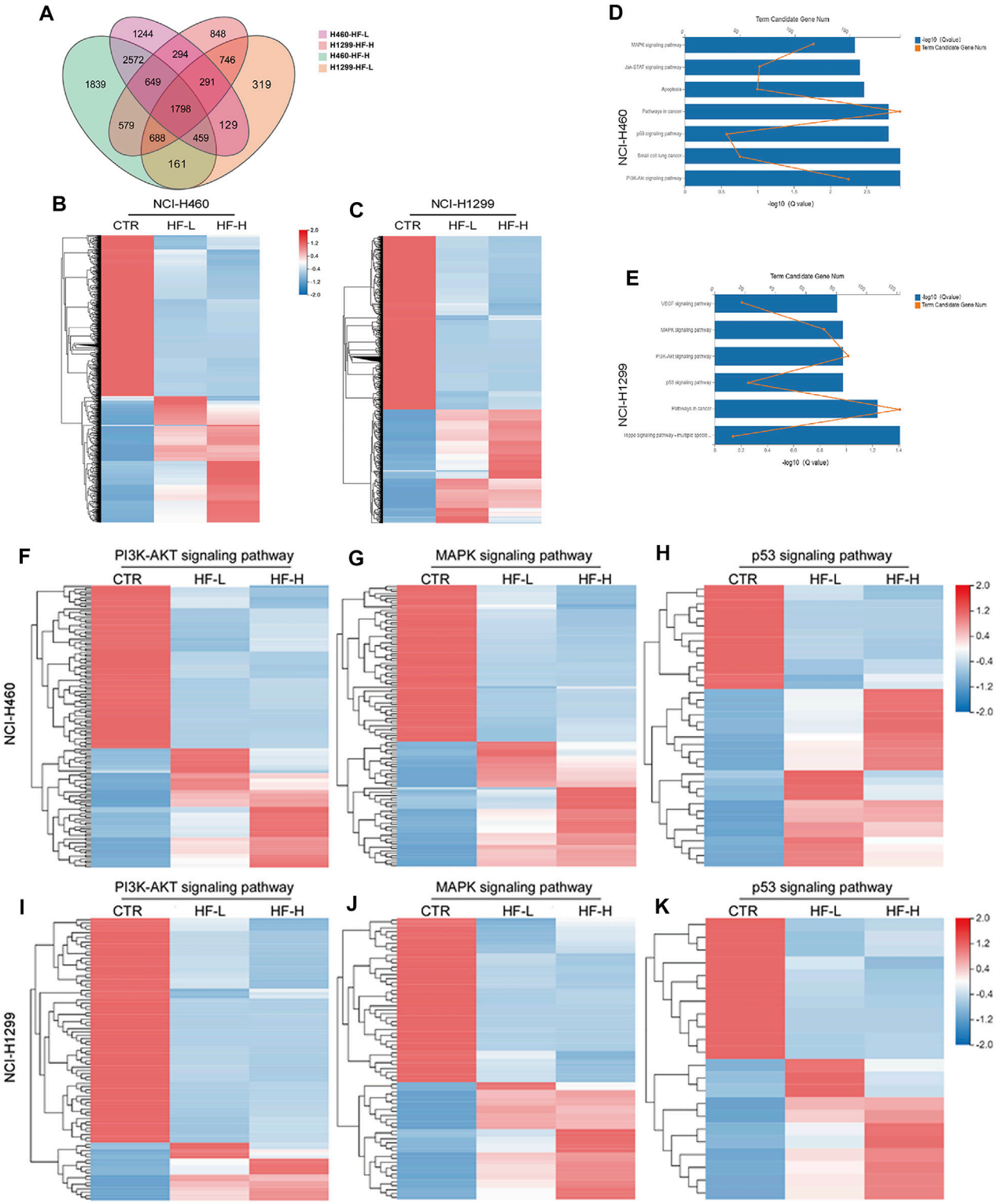

FIGURE 7 | Halofuginone induced genome-wide gene alteration in NCI-H1299 and NCI-H460 cells ($n = 3$). **(A)** 1798 different expression genes (DEGs, $\log_2FC \geq 1$, $p \leq 0.001$) were identified both in NCI-H460 and NCI-H1299 with the treatment of different concentration of HF. **(B,C)** Heatmap of the differential expressed genes for NCI-H460 and NCI-H1299 cells. HF led to alterations of 5478 DEGs in NCI-H460 cells and 3523 DEGs in NCI-H1299 cells *versus* each corresponding control group. Red indicates high expression, and green indicates low expression. **(D,E)** KEGG analysis of the DEGs revealed enrichments of cancer-associated pathways, including PI3K/AKT and MAPK signaling pathways. **(F–J)** Heatmap of the differential expressed genes related with PI3K/AKT MAPK and p53 signaling pathways.

in NCI-H1299 cells *versus* each corresponding control group (**Figures 7B,C**). The KEGG analysis of the DEGs revealed enrichments of cancer-associated pathways, including PI3K/AKT and MAPK signaling pathways (**Figures 7D,E**). Moreover, the genes related with PI3K/AKT and MAPK signaling pathways were sensitive to HF exposure (**Figures 7F,G,I,J**).

HF Blocked PI3K/AKT Signaling Pathway in Lung Cancer Cell Lines

Upregulation of p-AKT might enhance tumor progression and mediate resistance to drugs (Liu R. et al., 2020), and it has been well known that the binding of ligand to a transmembrane receptor, receptor tyrosine kinase (RTK), activates both PI3K/AKT and MAPK pathways to promote cell survival (Cao et al., 2019). Herein, we hypothesized that dual inhibition on the two pathways would exert a more stable and stronger growth and survival suppression than targeting individual pathway. The ratio of p-AKT (S473) to total Akt examined by Western blot was decreased by HF in a dose-dependent manner (**Figure 5** lower). Here, the observed downregulation of p-Akt in our cisplatin-resistant lung cancer cell lines by HF, indicating possible tumor suppression. Together, HF inhibited the cisplatin-resistant cell models growth *via* blocking the PI3K/AKT signaling pathway.

HF Blocked MAPK Signaling Pathway in Lung Cancer Cell Lines

The identical analysis and assays as before were performed to examine the effect of HF on the MAPK signaling pathway, which includes a small G protein (Ras) and three protein kinases (Raf, Mek, and Erk) and is activated with translocation of Erk (MAPK) to the nucleus (McCain, 2013). In protein level, p-Erk/Erk examined by Western blot exhibited dose-dependent decrease with the exposure of HF (**Figure 5** lower). Activation of the MAPK signaling pathway would strengthen tumor progression and mediate drug resistance as well (Cocco et al., 2019; Li et al., 2019). The decline of p-Erk1/2 indicated the potential activity of HF in lung cancer suppression. Thus, HF inhibited the cell models growth simultaneously *via* blocking the MAPK signaling pathway.

HF Sensitized Cisplatin in Cisplatin-Resistant PDOs

To study the response to the combination treatment of cisplatin and HF, the efficiency of tumor destruction was observed under a microscope, and exposure of PDOs to HF and combination of cisplatin and HF led to substantially reduced survival (**Figure 8A**). In addition, significant p-AKT (S473) and p-ERK decrease *via* Western blot appeared in cisplatin and HF combination groups compared to single drug treatment groups or control group (**Figures 8B–E**). Therefore, the results suggested that HF had the capacity to expand its sensitizer effect for cisplatin to preclinical cisplatin-resistant PDO models.

DISCUSSION

Cisplatin is one of the most widely used chemotherapy agents in the treatment of lung tumors. The mechanism of action for cisplatin is considered as damaging DNA and inhibiting DNA synthesis. However, cancer cells would develop multi-type resistance to overcome DNA damage and synthesis suppression to diminish the therapeutics efficacy (Liao et al., 2020; Yang et al., 2020). Therefore, combination strategy with cisplatin and cisplatin sensitizer will be of promising clinical value. Accumulating evidence has indicated that activation of cell proliferation and survival pathways, such as PI3K/AKT and MAPK signaling pathways, contribute to cisplatin resistance (J, 2013). PDOs of cancers derived from cisplatin-resistant tumor tissue can be used to facilitate discovery of anticancer leading compounds for their close morphological and genetic features of the original tumor (Lancaster and Knoblich, 2014; Weeber et al., 2015; Boretto et al., 2019; Ooft et al., 2019; Ubink et al., 2019). Besides, the (pre)clinical efficiency and safety of multi-target natural products with potential capacity for multi-target drug discovery have been characterized by more and more studies (Koeberle and Werz, 2014; Chen et al., 2016; Gonçalves and Romeiro, 2019; Liu X. et al., 2020; Ren et al., 2020). Especially, for some complicated diseases, such as acute ischemic stroke (Chen et al., 2016), tissue plasminogen activator is the only FDA-approved drug for treatment, but its clinical use is limited by the narrow therapeutic time window and severe side effects. Adjunct therapies *via* a multi-target strategy are warranted in reducing the side effects and extending tissue plasminogen activator's therapeutic time window with the consideration of the unsatisfaction of single target modulating. In addition, phenotype alteration induced by multi-target natural products could provide valuable information for drug combination (Sanchez et al., 2019).

Previous studies have reported that HF exhibited anticancer effects on various tumor types (Cui et al., 2016; Koohestani et al., 2016; Chen et al., 2017; Tsuchida et al., 2017; Akhtar et al., 2018; Xia et al., 2018; Huang and Brekken, 2019; Kunimi et al., 2019), which strongly supports the hypothesis that the therapeutic potential of HF is mainly through inducing anti-proliferation, autophagy, and apoptosis. However, the role and underlying mechanism of HF in cisplatin-resistant lung cancer cells have rarely been investigated. In this study, HF was found to be one of the top hits among 1,100 natural products in reducing cell viability of PDO models established by K2 Oncology Co., Ltd. (Beijing 100061, China).

Mechanically, we observed HF remarkably induced G0/G1 phase arrest and apoptosis in lung cancer cell lines. Subsequently, RNA sequencing was introduced for gene expression profiling regulated by HF. DEG analysis and KEGG analysis indicated that PI3K/AKT, MAPK, and p53 signaling pathways were affected. HF was once reported as a positive control drug that showed modest interaction of −6.91 kcal/mol having a Ki value of 8.61 μM with unbound p53 but expressed significant inhibition (Ki = 3.88 μM) against $p21^{Waf1/Cip1}$ with binding energy of −7.38 kcal/mol. A multiplex analysis of phosphorylation of diverse

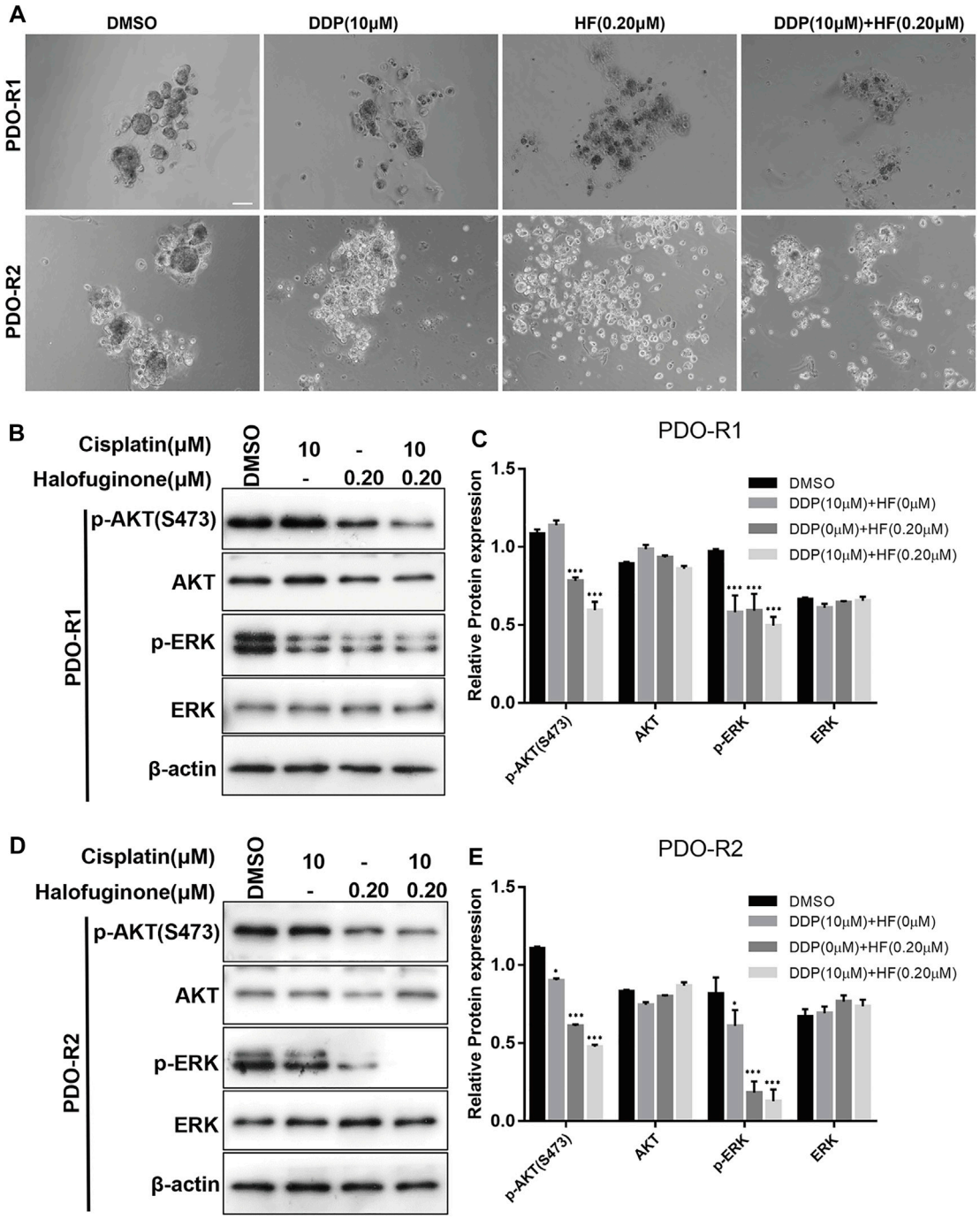

FIGURE 8 | Synergy effects of halofuginone and cisplatin on cell viability of PDO. **(A)** Microphotograph images of cisplatin-resistant PDOs (PDO-R1 and PDO-R2) at indicated time points of treated by cisplatin alone, halofuginone alone, and cisplatin/halofuginone combination. **(B–E)** the expression levels of pAKT and p-ERK were detected by Western blotting in cisplatin-resistant PDOs treated with cisplatin, halofuginone alone, and halofuginone/cisplatin combination ($n = 3$) (*$p < 0.05$, **$p < 0.01$, ***$p < 0.001$).

components of signaling cascades revealed that HF induced changes in P38 MAPK activation and increased phosphorylation of c-Jun and p53. Our data exhibited significantly p27 and p21 increase, p-Rb and cyclin D1 decrease with the combination of cisplatin and HF. p27 and p21 are two downstream effectors of PI3K/AKT that led to G0/G1 phase arrest. Moreover, the p53 signaling pathway is a downstream part of the p38/MAPK signaling pathway which contributed to G0/G1 phase arrest. As the G0/G1 phase is the most sensitive period for tumor cells to cisplatin, disruption of

the cell cycle at this period might be part of the reasons for cisplatin-resistant sensitization.

HF dose-dependently suppressed Akt and ERK signaling pathways, which indicated that HF suppressed the cisplatin-resistant cells by the dual targeting of PI3K/AKT and MAPK signaling pathways. Moreover, the combination study between cisplatin and HF qualitatively evaluated in lung cancer cell lines showed increased sensitivity to cisplatin with HF exposure, and the combination of cisplatin with both Akt inhibitor and ERK inhibitor also simulated this phenomenon. To further validate the preclinical synergy, two cisplatin-resistant PDO models were employed with the treatment of vehicle, HF alone, cisplatin alone, or HF combined with cisplatin. Additionally, the growth inhibition and dual signaling pathway suppression in the HF alone group and combination group in cisplatin-resistant PDOs were in line with that in lung cancer cell lines. Thus, HF might be a potential sensitizer to cisplatin by its dual pathway targeting effects.

Although this study showed that HF suppressed the cisplatin-resistant cells by the dual targeting of PI3K/Akt and MAPK signaling pathways, a broader insight into its multi-mechanistic nature requires a system-wide screening approach. As we all know, resistance to cisplatin is attributed to three molecular mechanisms: increased DNA repair, altered cellular accumulation, and increased drug inactivation. One of the most predominant mechanisms is the increase in DNA damage repair, among which nucleotide excision repair (NER) and mismatch repair (MMR) are included. Wang et al. indicated that HF significantly promoted DNA damage-related protein g-H2AX, pATM, and pATR expression in human esophageal cancer cell lines (Wang et al., 2020), informing HF is probably involved in the balance of DNA damage and DNA repair which decide cell death versus survival. So, further studies are required to examine the influence of HF on DNA damage repair.

P53 signaling is also associated with cisplatin resistance based on the literature evidence, and it was reported that HF could decrease the expression of p53 to suppress the migration and invasion in breast cancer cells (Xia et al., 2018). In this study, the RNAseq also indicted that the p53 pathway was regulated by HF treatment. The effect of HF on the p53 pathway will be further investigated in follow-up studies, which may provide a new vision of HF on p53 pathway drug discovery. There is still no specific p53 agonist in clinical development, which restricts the clinical translation of this study. By understanding the dural inhibitor effect to these pathways also provides evidence the clinical application of PI3Ki/AKTi and ERKi in cisplatin-resistant lung cancer.

Collectively, natural product has a huge multi-target library for synergy study and multi-target lead finding. By high-throughput clinical associated PDO models screening and RNA sequencing, we could get better understanding of multi-pathway networks and obtain more precious natural anticancer molecules. Altogether, this study demonstrated that HF might act as a promising therapeutic agent to sensitize cisplatin in the clinical chemotherapy strategy in cisplatin-resistant lung cancer and could be applied in clinical in future.

DATA AVAILABILITY STATEMENT

The datasets presented in this study can be found in online repositories. The names of the repository/repositories and accession number(s) can be found NCBI with accession PRJNA769938.

ETHICS STATEMENT

The studies involving human participants were reviewed and approved by the Ethical Committee of Beijing Chest Hospital, Capital Medical University. The patients/participants provided their written informed consent to participate in this study.

AUTHOR CONTRIBUTIONS

YH and DY designed and supervised the study. HL and YZ collected the samples and interpreted the data. XL, JY, and CY performed the *in vitro* experiments. XL wrote the manuscript with the help of ZS and PK. All authors have read and approved the manuscript.

FUNDING

This work was supported by the Capital Health Research and Development of Special' (No. shoufa 2020-2Z-2164), Beijing Tongzhou District Science and Technology Project (No. KJ2021CX009), and Huzhou Science and Technology Bureau Tackling key industrial projects (No. 2020GG11).

SUPPLEMENTARY MATERIAL

The Supplementary Material for this article can be found online at: https://www.frontiersin.org/articles/10.3389/fcell.2021.773048/full#supplementary-material

REFERENCES

Akhtar, S., Khan, M. K. A., and Arif, J. M. (2018). Evaluation and Elucidation Studies of Natural Aglycones for Anticancer Potential Using Apoptosis-Related Markers: An In Silico Study. *Interdiscip. Sci. Comput. Life Sci.* 10 (2), 297–310. doi:10.1007/s12539-016-0191-6

Boretto, M., Maenhoudt, N., Luo, X., Hennes, A., Boeckx, B., Bui, B., et al. (2019). Patient-derived Organoids from Endometrial Disease Capture Clinical Heterogeneity and Are Amenable to Drug Screening. *Nat. Cel Biol* 21 (8), 1041–1051. doi:10.1038/s41556-019-0360-z

Cao, Z., Liao, Q., Su, M., Huang, K., Jin, J., and Cao, D. (2019). AKT and ERK Dual Inhibitors: The Way Forward?. *Cancer Lett.* 459, 30–40. doi:10.1016/j.canlet.2019.05.025

Chen, G.-Q., Gong, R.-H., Yang, D.-J., Zhang, G., Lu, A.-P., Yan, S.-C., et al. (2017). Halofuginone Dually Regulates Autophagic Flux through Nutrient-Sensing Pathways in Colorectal Cancer. *Cell Death Dis* 8 (5), e2789. doi:10.1038/cddis.2017.203

Chen, H.-S., Qi, S.-H., and Shen, J.-G. (2016). One-Compound-Multi-Target: Combination Prospect of Natural Compounds with Thrombolytic Therapy in Acute Ischemic Stroke. *Cn* 15 (1), 134–156. doi:10.2174/1570159x14666160620102055

Chen, H.-Z., Bonneville, R., Paruchuri, A., Reeser, J. W., Wing, M. R., Samorodnitsky, E., et al. (2021a). Genomic and Transcriptomic Characterization of Relapsed SCLC through Rapid Research Autopsy. *JTO Clin. Res. Rep.* 2 (4), 100164. doi:10.1016/j.jtocrr.2021.100164

Chen, M., Chen, Z., Castillo, J. B., Cui, L., Zhou, K., Shen, B., et al. (2021b). [18F]-C-SNAT4: an Improved Caspase-3-Sensitive Nanoaggregation PET Tracer for Imaging of Tumor Responses to Chemo- and Immunotherapies. *Eur. J. Nucl. Med. Mol. Imaging* 48 (11), 3386–3399. doi:10.1007/s00259-021-05297-0

Cheng, M., Olivier, P., Diehl, J. A., Fero, M., Roussel, M. F., Roberts, J. M., et al. (1999). The p21(Cip1) and p27(Kip1) CDK 'inhibitors' Are Essential Activators of Cyclin D-dependent Kinases in Murine Fibroblasts. *EMBO J.* 18 (6), 1571–1583. doi:10.1093/emboj/18.6.1571

Choudhury, D., Ashok, A., and Naing, M. W. (2020). Commercialization of Organoids. *Trends Molecular Medicine* 26 (3), 245–249. doi:10.1016/j.molmed.2019.12.002

Cocco, E., Schram, A. M., Kulick, A., Misale, S., Won, H. H., Yaeger, R., et al. (2019). Resistance to TRK Inhibition Mediated by Convergent MAPK Pathway Activation. *Nat. Med.* 25 (9), 1422–1427. doi:10.1038/s41591-019-0542-z

Cui, Z., Crane, J., Xie, H., Jin, X., Zhen, G., Li, C., et al. (2016). Halofuginone Attenuates Osteoarthritis by Inhibition of TGF-β Activity and H-type Vessel Formation in Subchondral Bone. *Ann. Rheum. Dis.* 75 (9), 1714–1721. doi:10.1136/annrheumdis-2015-207923

Driehuis, E., Kretzschmar, K., and Clevers, H. (2020). Establishment of Patient-Derived Cancer Organoids for Drug-Screening Applications. *Nat. Protoc.* 15 (10), 3380–3409. doi:10.1038/s41596-020-0379-4

Fan, C.-C., Tsai, S.-T., Lin, C.-Y., Chang, L.-C., Yang, J.-C., Chen, G. Y., et al. (2020). EFHD2 Contributes to Non-small Cell Lung Cancer Cisplatin Resistance by the Activation of NOX4-ROS-ABCC1 axis. *Redox Biol.* 34, 101571. doi:10.1016/j.redox.2020.101571

Fang, Y., Zhang, C., Wu, T., Wang, Q., Liu, J., and Dai, P. (2017). Transcriptome Sequencing Reveals Key Pathways and Genes Associated with Cisplatin Resistance in Lung Adenocarcinoma A549 Cells. *PLoS One* 12 (1), e0170609. doi:10.1371/journal.pone.0170609

Gonçalves, P. B., and Romeiro, N. C. (2019). Multi-target Natural Products as Alternatives against Oxidative Stress in Chronic Obstructive Pulmonary Disease (COPD). *Eur. J. Med. Chem.* 163, 911–931. doi:10.1016/j.ejmech.2018.12.020

Hewitt, S. N., Dranow, D. M., Horst, B. G., Abendroth, J. A., Forte, B., Hallyburton, I., et al. (2017). Biochemical and Structural Characterization of Selective Allosteric Inhibitors of the Plasmodium Falciparum Drug Target, Prolyl-tRNA-Synthetase. *ACS Infect. Dis.* 3 (1), 34–44. doi:10.1021/acsinfecdis.6b00078

Huang, H., and Brekken, R. A. (2019). The Next Wave of Stroma-Targeting Therapy in Pancreatic Cancer. *Cancer Res.* 79 (2), 328–330. doi:10.1158/0008-5472.CAN-18-3751

Huang, Y., Koues, O. I., Zhao, J.-y., Liu, R., Pyfrom, S. C., Payton, J. E., et al. (2017). Cis -Regulatory Circuits Regulating NEK6 Kinase Overexpression in Transformed B Cells Are Super-enhancer Independent. *Cel Rep.* 18 (12), 2918–2931. doi:10.1016/j.celrep.2017.02.067

Julien, O., and Wells, J. A. (2017). Caspases and Their Substrates. *Cell Death Differ* 24 (8), 1380–1389. doi:10.1038/cdd.2017.44

Koeberle, A., and Werz, O. (2014). Multi-target Approach for Natural Products in Inflammation. *Drug Discov. Today* 19 (12), 1871–1882. doi:10.1016/j.drudis.2014.08.006

Koohestani, F., Qiang, W., MacNeill, A. L., Druschitz, S. A., Serna, V. A., Adur, M., et al. (2016). Halofuginone Suppresses Growth of Human Uterine Leiomyoma Cells in a Mouse Xenograft Model. *Hum. Reprod.* 31 (7), 1540–1551. doi:10.1093/humrep/dew094

Kunimi, H., Miwa, Y., Inoue, H., Tsubota, K., and Kurihara, T. (2019). A Novel HIF Inhibitor Halofuginone Prevents Neurodegeneration in a Murine Model of Retinal Ischemia-Reperfusion. *Int. J. Mol. Sci.* 20 (13), 3171. doi:10.3390/ijms20133171

Lampis, A., Carotenuto, P., Vlachogiannis, G., Cascione, L., Hedayat, S., Burke, R., et al. (2017). MIR21 Drives Resistance to Heat Shock Protein 90 Inhibition in Cholangiocarcinoma. *Gastroenterology* 154 (4), 1066–e5. doi:10.1053/j.gastro.2017.10.043

Lancaster, M. A., and Knoblich, J. A. (2014). Organogenesis in a Dish: Modeling Development and Disease Using Organoid Technologies. *Science* 345 (6194), 1247125. doi:10.1126/science.1247125

Li, S., Fong, K.-w., Gritsina, G., Zhang, A., Zhao, J. C., Kim, J., et al. (2019). Activation of MAPK Signaling by CXCR7 Leads to Enzalutamide Resistance in Prostate Cancer. *Cancer Res.* 79 (10), 2580–2592. doi:10.1158/0008-5472.Can-18-2812

Liang, F., Ren, C., Wang, J., Wang, S., Yang, L., Han, X., et al. (2019). The Crosstalk between STAT3 and P53/RAS Signaling Controls Cancer Cell Metastasis and Cisplatin Resistance via the Slug/MAPK/PI3K/AKT-mediated Regulation of EMT and Autophagy. *Oncogenesis* 8 (10), 59. doi:10.1038/s41389-019-0165-8

Liao, X. Z., Gao, Y., Sun, L. L., Liu, J. H., Chen, H. R., Yu, L., et al. (2020). Rosmarinic Acid Reverses Non-small Cell Lung Cancer Cisplatin Resistance by Activating the MAPK Signaling Pathway. *Phytotherapy Res.* 34, 1142–1153. doi:10.1002/ptr.6584

Liu, R., Chen, Y., Liu, G., Li, C., Song, Y., Cao, Z., et al. (2020a). PI3K/AKT Pathway as a Key Link Modulates the Multidrug Resistance of Cancers. *Cel Death Dis* 11 (9), 797. doi:10.1038/s41419-020-02998-6

Liu, X., Zhou, Y., Peng, J., Xie, B., Shou, Q., and Wang, J. (2020b). Silencing C-Myc Enhances the Antitumor Activity of Bufalin by Suppressing the HIF-1α/SDF-1/CXCR4 Pathway in Pancreatic Cancer Cells. *Front. Pharmacol.* 11 (495). doi:10.3389/fphar.2020.00495

Lu, H., Bai, L., Zhou, Y., Lu, Y., Jiang, Z., and Shi, J. (2019). Recent Study of Dual HDAC/PARP Inhibitor for the Treatment of Tumor. *Ctmc* 19 (12), 1041–1050. doi:10.2174/1568026619666190603092407

Lukas, J., Bartkova, J., and Bartek, J. (1996). Convergence of Mitogenic Signalling Cascades from Diverse Classes of Receptors at the Cyclin D-cyclin-dependent Kinase-pRb-Controlled G1 Checkpoint. *Mol. Cel Biol* 16 (12), 6917–6925. doi:10.1128/mcb.16.12.6917

Maloney, E., Clark, C., Sivakumar, H., Yoo, K., Aleman, J., Rajan, S. A. P., et al. (2020). Immersion Bioprinting of Tumor Organoids in Multi-Well Plates for Increasing Chemotherapy Screening Throughput. *Micromachines* 11 (2), 208. doi:10.3390/mi11020208

Matus, J. L., and Boison, J. O. (2016). A Multi-Residue Method for 17 Anticoccidial Drugs and Ractopamine in Animal Tissues by Liquid Chromatography-Tandem Mass Spectrometry and Time-Of-Flight Mass Spectrometry. *Drug Test. Anal.* 8 (5-6), 465–476. doi:10.1002/dta.2019

McCain, J. (2013). The MAPK (ERK) Pathway: Investigational Combinations for the Treatment of BRAF-Mutated Metastatic Melanoma. *P T : a peer-reviewed J. formulary Manag.* 38 (2), 96–108.

Ooft, S. N., Weeber, F., Dijkstra, K. K., McLean, C. M., Kaing, S., van Werkhoven, E., et al. (2019). Patient-derived Organoids Can Predict Response to Chemotherapy in Metastatic Colorectal Cancer Patients. *Sci. Transl. Med.* 11 (513), 2574. doi:10.1126/scitranslmed.aay2574

Pasch, C. A., Favreau, P. F., Yueh, A. E., Babiarz, C. P., Gillette, A. A., Sharick, J. T., et al. (2019). Patient-Derived Cancer Organoid Cultures to Predict Sensitivity to Chemotherapy and Radiation. *Clin. Cancer Res.* 25 (17), 5376–5387. doi:10.1158/1078-0432.CCR-18-3590

Pestell, R. G., Albanese, C., Reutens, A. T., Segall, J. E., Lee, R. J., and Arnold, A. (1999). The Cyclins and Cyclin-dependent Kinase Inhibitors in Hormonal Regulation of Proliferation and Differentiation. *Endocr. Rev.* 20 (4), 501–534. doi:10.1210/edrv.20.4.0373

Puca, L., Bareja, R., Prandi, D., Shaw, R., Benelli, M., Karthaus, W. R., et al. (2018). Patient Derived Organoids to Model Rare Prostate Cancer Phenotypes. *Nat. Commun.* 9 (1), 2404. doi:10.1038/s41467-018-04495-z

Raja, W. K., Mungenast, A. E., Lin, Y.-T., Ko, T., Abdurrob, F., Seo, J., et al. (2016). Self-Organizing 3D Human Neural Tissue Derived from Induced Pluripotent Stem Cells Recapitulate Alzheimer's Disease Phenotypes. *PLoS One* 11 (9), e0161969. doi:10.1371/journal.pone.0161969

Ren, F., Wu, K., Yang, Y., Yang, Y., Wang, Y., and Li, J. (2020). Dandelion Polysaccharide Exerts Anti-angiogenesis Effect on Hepatocellular Carcinoma by Regulating VEGF/HIF-1α Expression. *Front. Pharmacol.* 11 (460), e00460. doi:10.3389/fphar.2020.00460

Sanchez, B. G., Bort, A., Mateos-Gomez, P. A., Rodriguez-Henche, N., and Diaz-Laviada, I. (2019). Combination of the Natural Product Capsaicin and Docetaxel Synergistically Kills Human Prostate Cancer Cells through the Metabolic Regulator AMP-Activated Kinase. *Cancer Cel Int* 19, 54. doi:10.1186/s12935-019-0769-2

Sherr, C. J. (1996). Cancer Cell Cycles. *Science* 274 (5293), 1672–1677. doi:10.1126/science.274.5293.1672

Shi, R., Radulovich, N., Ng, C., Liu, N., Notsuda, H., Cabanero, M., et al. (2019). Organoid Cultures as Preclinical Models of Non-small Cell Lung Cancer. *Clin. Cancer Res.* 26, 1162. doi:10.1158/1078-0432.CCR-19-1376

Shi, Y., Liu, X., Fredimoses, M., Song, M., Chen, H., Liu, K., et al. (2018). FGFR2 Regulation by Picrasidine Q Inhibits the Cell Growth and Induces Apoptosis in Esophageal Squamous Cell Carcinoma. *J. Cel Biochem* 119 (2), 2231–2239. doi:10.1002/jcb.26385

Skardal, A., Aleman, J., Forsythe, S., Rajan, S., Murphy, S., Devarasetty, M., et al. (2020). Drug Compound Screening in Single and Integrated Multi-Organoid Body-On-A-Chip Systems. *Biofabrication* 12 (2), 025017. doi:10.1088/1758-5090/ab6d36

Sung, H., Ferlay, J., Siegel, R. L., Laversanne, M., Soerjomataram, I., Jemal, A., et al. (2021). Global Cancer Statistics 2020: GLOBOCAN Estimates of Incidence and Mortality Worldwide for 36 Cancers in 185 Countries. *CA Cancer J. Clin.* 71 (3), 209–249. doi:10.3322/caac.21660

Tsuchida, K., Tsujita, T., Hayashi, M., Ojima, A., Keleku-Lukwete, N., Katsuoka, F., et al. (2017). Halofuginone Enhances the Chemo-Sensitivity of Cancer Cells by Suppressing NRF2 Accumulation. *Free Radic. Biol. Med.* 103, 236–247. doi:10.1016/j.freeradbiomed.2016.12.041

Ubink, I., Bolhaqueiro, A. C. F., Elias, S. G., Raats, D. A. E., Peters, N. A., et al. (2019). Organoids from Colorectal Peritoneal Metastases as a Platform for Improving Hyperthermic Intraperitoneal Chemotherapy. *Br. J. Surg.* 106 (10), 1404–1414. doi:10.1002/bjs.11206

Wang, Y., Xie, Z., and Lu, H. (2020). Significance of Halofuginone in Esophageal Squamous Carcinoma Cell Apoptosis through HIF-1α-FOXO3a Pathway. *Life Sci.* 257, 118104. doi:10.1016/j.lfs.2020.118104

Weeber, F., van de Wetering, M., Hoogstraat, M., Dijkstra, K. K., Krijgsman, O., Kuilman, T., et al. (2015). Preserved Genetic Diversity in Organoids Cultured from Biopsies of Human Colorectal Cancer Metastases. *Proc. Natl. Acad. Sci. United States America* 112 (43), 13308–13311. doi:10.1073/pnas.1516689112

Xia, X., Wang, L., Zhang, X., Wang, S., Lei, L., Cheng, L., et al. (2018). Halofuginone-induced Autophagy Suppresses the Migration and Invasion of MCF-7 Cells via Regulation of STMN1 and P53. *J. Cel Biochem* 119 (5), 4009–4020. doi:10.1002/jcb.26559

Yadav, B., Wennerberg, K., Aittokallio, T., and Tang, J. (2015). Searching for Drug Synergy in Complex Dose-Response Landscapes Using an Interaction Potency Model. *Comput. Struct. Biotechnol. J.* 13, 504–513. doi:10.1016/j.csbj.2015.09.001

Yang, W., Xiao, W., Cai, Z., Jin, S., and Li, T. (2020). miR-1269b Drives Cisplatin Resistance of Human Non-small Cell Lung Cancer via Modulating the PTEN/PI3K/AKT Signaling Pathway. *Onco Targets Ther.* 13, 109–118. doi:10.2147/OTT.S225010

Yao, Y., Xu, X., Yang, L., Zhu, J., Wan, J., Shen, L., et al. (2020). Patient-Derived Organoids Predict Chemoradiation Responses of Locally Advanced Rectal Cancer. *Cell Stem Cell* 26 (1), 17–26. doi:10.1016/j.stem.2019.10.010

Conflict of Interest: XL, CY, ZS, and PK were employed by K2 Oncology Co. Ltd.

The remaining authors declare that the research was conducted in the absence of any commercial or financial relationships that could be construed as a potential conflict of interest.

The handling editor declared a shared affiliation with several of the authors YZ, YH, and DY at time of review.

Publisher's Note: All claims expressed in this article are solely those of the authors and do not necessarily represent those of their affiliated organizations, or those of the publisher, the editors, and the reviewers. Any product that may be evaluated in this article, or claim that may be made by its manufacturer, is not guaranteed or endorsed by the publisher.

frontiers in Cell and Developmental Biology

ORIGINAL RESEARCH
published: 26 November 2021
doi: 10.3389/fcell.2021.767624

Multiple DSB Resection Activities Redundantly Promote Alternative End Joining-Mediated Class Switch Recombination

Xikui Sun[1,2], Jingning Bai[1,2], Jiejie Xu[1,2], Xiaoli Xi[3], Mingyu Gu[1,2], Chengming Zhu[4], Hongman Xue[5], Chun Chen[5] and Junchao Dong[1,2,5]**

[1]Department of Immunology, Zhongshan School of Medicine, Sun Yat-sen University, Guangzhou, China, [2]Key Laboratory of Tropical Disease Control (Sun Yat-sen University), Ministry of Education, Guangzhou, China, [3]Department of Gastroenterology, the Third Affiliated Hospital of Sun Yat-sen University, Guangzhou, China, [4]Research Center of the Seventh Affiliated Hospital, Sun Yat-sen University, Shenzhen, China, [5]Department of Pediatrics, the Seventh Affiliated Hospital of Sun Yat-Sen University, Shenzhen, China

Alternative end joining (A-EJ) catalyzes substantial level of antibody class switch recombination (CSR) in B cells deficient for classical non-homologous end joining, featuring increased switch (S) region DSB resection and junctional microhomology (MH). While resection has been suggested to initiate A-EJ in model DSB repair systems using engineered endonucleases, the contribution of resection factors to A-EJ-mediated CSR remains unclear. In this study, we systematically dissected the requirement for individual DSB resection factors in A-EJ-mediated class switching with a cell-based assay system and high-throughput sequencing. We show that while CtIP and Mre11 both are mildly required for CSR in WT cells, they play more critical roles in mediating A-EJ CSR, which depend on the exonuclease activity of Mre11. While DNA2 and the helicase/HRDC domain of BLM are required for A-EJ by mediating long S region DSB resection, in contrast, Exo1's resection-related function does not play any obvious roles for class switching in either c-NHEJ or A-EJ cells, or mediated in an AID-independent manner by joining of Cas9 breaks. Furthermore, ATM and its kinase activity functions at least in part independent of CtIP/Mre11 to mediate A-EJ switching in Lig4-deficient cells. In stark contrast to Lig4 deficiency, 53BP1-deficient cells do not depend on ATM/Mre11/CtIP for residual joining. We discuss the roles for each resection factor in A-EJ-mediated CSR and suggest that the extent of requirements for resection is context dependent.

Keywords: DNA double-strand breaks repair, alternative end joining, class switch recombination, DSB end resection, microhomology

OPEN ACCESS

Edited by:
Teng Ma,
Capital Medical University, China

Reviewed by:
Valentyn Oksenych,
University of Oslo, Norway
Jian Yuan,
Tongji University, China

****Correspondence:***
Junchao Dong
dongjch@mail.sysu.edu.cn
Chun Chen
chenchun69@126.com

Specialty section:
This article was submitted to Signaling, a section of the journal Frontiers in Cell and Developmental Biology

Received: *31 August 2021*
Accepted: *25 October 2021*
Published: *26 November 2021*

Citation:
Sun X, Bai J, Xu J, Xi X, Gu M, Zhu C, Xue H, Chen C and Dong J (2021) Multiple DSB Resection Activities Redundantly Promote Alternative End Joining-Mediated Class Switch Recombination. Front. Cell Dev. Biol. 9:767624. doi: 10.3389/fcell.2021.767624

INTRODUCTION

Mature B cells undergo immunoglobulin heavy chain (*IgH*) class switch recombination (CSR) to mediate different antibody effector functions. CSR replaces the initially expressed μ constant gene (Cμ) with a downstream constant gene through genomic DNA recombination (Xu et al., 2012). In the mouse *IgH* locus, six independently transcribed C_H genes, Cγ3, Cγ1, Cγ2b, Cγ2a, Cε, and Cα, line up to 200 kb downstream of Cμ. A long and repetitive intronic switch region (4–12 kb) with tandem G-rich repeat sequences on the non-template strand lies between each C_H gene and its I promoter.

Stimulating B cells with combinations of activators and cytokines directs CSR to particular C_H genes by modulating germline transcription to recruit AID, which introduces into S regions multiple C to U mutations that are subsequently converted to staggered double-strand breaks (DSBs) by base excision and mismatch repair with yet unclear mechanisms (Hwang et al., 2015; Yu and Lieber, 2019). CSR is completed by joining donor Sμ and acceptor S region DSBs in a deletion-preferred fashion to promote antibody production (Dong et al., 2015).

AID-initiated S region DSBs are efficiently repaired by the classical non-homologous end joining (c-NHEJ) pathway, which simply aligns and religates two broken ends with minor modification. Ku/DNA-PKcs and Lig4/XRCC4 complexes are the core components of c-NHEJ and depletion of any of these factors in mature B cells significantly, but not completely reduces CSR efficiency (Boboila et al., 2010; Boboila et al., 2012). In fact, CSR to IgG in cells deficient for Ku, Lig4, or both can still occur at levels to ~30% of WT cells with altered kinetics, strongly implicating alternative end joining (A-EJ) pathways for residual switching (Yan et al., 2007; Boboila et al., 2010). Sanger and high-throughput sequencing of the junctions of residual Sμ-Sx joins revealed elevated usage of microhomology (MH) sequences (usually 1–5 bp in length) shared between donor and acceptor DSBs in the absence of Ku and/or Lig4, indicating that A-EJ preferred microhomology-mediated end joining (MMEJ). It is noteworthy that MH represents a significant feature but does not serve as a defining factor for A-EJ, as NHEJ repair in WT cells also utilizes MH in a significant portion of junctions. It has been proposed that PARP1 and the Lig3/XRCC1 complex are requisite A-EJ factors (Frit et al., 2014). Early evidence supporting this notion came from ligation of DNA substrates with protruding overhang ends (Vogel et al., 2003; Audebert et al., 2004). However, *in vivo* study with activated primary B cells only revealed a rather minor role for PARP1 in MH usage and no impact on IgG switching efficiency *per se* (Robert et al., 2009). In addition, conditional knockout of XRCC1 in both WT and Lig4-deficient B cells did not affect either CSR or chromosomal translocations (Boboila et al., 2012). The latter finding raised the possibility that DNA ligase I also plays a role in A-EJ, which was supported by later studies that deleting either nuclear Lig3 or Lig1 in Lig4-deficient CH12F3 cells conferred no additional CSR defect than Lig4 deletion alone. As mammals only have these three ligases, this suggests that Lig1 and Lig3 are redundant in A-EJ (Lu et al., 2016; Masani et al., 2016). As Lig1 and nuclear-form Lig3 deletion alone in WT did not render the cells obvious defect in end joining and CSR (Han et al., 2014; Masani et al., 2016), whether and how A-EJ occurs in WT cells are currently difficult to assess and awaits more careful dissection. AID-initiated S region DSBs also trigger activation of DNA damage response (DDR) kinase Ataxia telangiectasia-mutated (ATM), which phosphorylates a series of downstream substrates including histone variant, H2AX, MDC1, 53BP1, etc., that assemble into macromolecular foci surrounding DSBs to amplify damage signals and tether DSB ends for efficient repair (Xu et al., 2012). Deficiency for DDR factors has been shown to severely impair end joining during V(D)J recombination (Helmink et al., 2011; Zha et al., 2011; Liu et al., 2012; Oksenych et al., 2013) and leads to impaired CSR at 30–50% of corresponding wild type cells and accumulation of substantial AID-dependent *IgH* breaks, indicating a role for ATM/H2AX in the joining phase of CSR (Reina-San-Martin et al., 2004; Franco et al., 2006; Boboila et al., 2012). Ablation of 53BP1 results in the most profound CSR defect where only about 5% of wild type switching level is observed accompanied by increased intra-S joining and *IgH* specific break burden (Manis et al., 2004; Ward et al., 2004; Reina-San-Martin et al., 2007; Bothmer et al., 2011). Recently, Rif1 has been identified as a phosphor-53BP1-associating effector protein that suppresses DSB resection, a 5'->3′ nucleolytic process to expose 3′ single-stranded overhangs at broken ends (Escribano-Díaz et al., 2013; Zimmermann et al., 2013); accordingly, Rif1-deficient cells display largely impaired CSR to downstream S regions (Callen et al., 2013; Chapman et al., 2013; Di Virgilio et al., 2013). In this regard, ATM-dependent DDR has been shown to promote c-NHEJ during CSR at least in part by preventing extensive S-region DSBs end resection and MMEJ (Yamane et al., 2013; Dong et al., 2015; Panchakshari et al., 2018).

It has been well documented that 5'->3′ DSB end resection is required for homologous recombination (HR) and MMEJ of DSB repair in yeast and higher eukaryotes (Symington, 2016). While HR requires longer homology to the sequence around DSB ends for base pairing, MMEJ may, in principle, involve shorter resection to expose MH sequences for annealing. DSB resection is initiated by the coordinated action of DNA nuclease complex MRN and CtIP. MRN complex consists of RAD50, NBS1, and Mre11 that renders the complex endonuclease and 3′-5′ exonuclease activity, an orientation opposite to the ongoing resection (Garcia et al., 2011). Recent study revealed that Mre11 uses its endonuclease activity to nick DNA at 3′ downstream vicinity of DSB and its exo-activity to degrade DNA strand towards the break to expose single-stranded DNA (Paull, 2018). While Mre11 has been shown to be critical for both c-NHEJ and A-EJ-mediated CSR (Dinkelmann et al., 2009), the exact role for CtIP in CSR is less clear (Lee-Theilen et al., 2011; Bothmer et al., 2013; Liu et al., 2019). Human *CtIP* encodes a 5′-flap endonuclease on branched DNA structure that participates in resection initiation mainly by stimulating Mre11's endonuclease activity independent of its endonuclease activity (Sartori et al., 2007; Makharashvili et al., 2014), and CtIP phosphorylation at T855 by ATM is critical for its role in resection (Peterson et al., 2013; Wang et al., 2013). A recently identified exonuclease EXD2 has been shown to functionally interact with MRN to accelerate DSB resection with its 3′-5′ exonuclease activity and is required for efficient HR (Broderick et al., 2016), but its role in MMEJ/A-EJ remains to be exploited. After Mre11/CtIP-mediated initiation to degrade up to hundred nucleotides close to the break, helicase BLM/WRN and endonuclease DNA2 switches on to promote long range resection up to tens of kilobases away from the break, and this activity appears redundant with exonuclease Exo1 (Symington, 2016).

The observation that both $lig4^{-/-}$ and $53bp1^{-/-}$ cells exhibit greatly increased DSB resection and similarly elevated MH usage in Sμ-Sx junctions raised the question of which activities are involved in S region DSB resection in these cells and whether DSB

resection accounts for all or part of CSR defect. In this regard, thorough investigation on the role for DSB resection in A-EJ-mediated CSR is still lacking. In this study, we systematically examined the requirements for each individual protein involved in DSB resection machinery in activated B cells proficient or deficient for Lig4 or 53BP1. Our results revealed that resection factors play important roles in A-EJ mediated CSR, and ATM kinase activity with CtIP/Mre11 in A-EJ. In addition, although both Lig4 and 53BP1 deficiency lead to c-NHEJ defect with remarkably similar MH patterns (Panchakshari et al., 2018), their need for DSB resection to assist residual joining varied greatly. In summary, our work indicated that B cells harness multiple DSB resection activities to engage A-EJ-mediated CSR in a context-dependent manner.

MATERIALS AND METHODS

Cell Culture

All of CH12F3 cell lines in this study were cultured with in RPMI 1640 (10-040-CV, Corning) supplemented with 15% FBS (FSP500, ExCell Bio), 100 mM β-mercaptoethanol (0482-250 ml, Amresco), 20 μM HEPS (25-060-CI, Corning), 2 mM L-Glutamine (25-005-CI, Corning), 1× MEM non-essential amino acid (25-025-CI, Corning), 1 mM sodium pyruvate (25-000-CI, Corning), 1× penicillin streptomycin (30-002-CI, Corning). 293T and Phoenix Ampho were maintained in DMEM (10-013-CV, Corning) supplemented with 10% FBS (ExCell Bio) and 1× penicillin streptomycin.

Plasmids

PSpCas9(BB)-2A-GFP (pX458) plasmid was obtained from Addgene (#48138). All the gRNA oligonucleotides were cloned into pX458. All the oligonucleotides sequences were listed in Appendix information, **Supplementary Table S1**. pMSCV-IRES-GFP II (pMIG II) plasmid was obtained from Addgene (#52107). pLKO.1 puro plasmid was obtained from Addgene (#8453). pMD2.G and psPAX2 plasmids were kindly gifted by the F.W.A. laboratory.

Construction of Gene Knockout Cell Lines.

The gene deletion strategies were performed according to the essential domain of genes reported (Taccioli et al., 1998; Babbe et al., 2009; Schaetzlein et al., 2013; Broderick et al., 2016; Panchakshari et al., 2018; van Wietmarschen et al., 2018). WT CH12F3 cell line or its mutants were nucleofected with a pair of pX458 vector with two gRNAs flanking one or two exons using the 4D Nucleofector Kit (solution SF, protocol CA-137; Lonza). At 24–48 h post-nucleofection, the GFP positive cells were sorted with Beckman Coulter MoFlo Astrios EQs and plated into 96-well plates. Single cell clones were marked and screened by PCR. Positive clones were further confirmed by western blot analysis or T-A cloning and sequencing.

Antibody

The primary antibodies used in this study were as follows: anti-ATM Rabbit antibody (D2E2, #2873, Cell Signaling Technology), anti-γ-Tubulin antibody (#5886, Cell Signaling Technology), anti-Mre11 Antibody (#4895, Cell Signaling Technology), anti-DNA-PKcs (G-12, SC-390849, Santa Cruz), anti-CtIP (D-4, SC-271339, Santa Cruz), anti-EXD2 antibody (20138-1-AP, Proteintech), anti-phospho KAP1 (S824) antibody (A304-146A-M, Bethyl Laboratories), anti-β-Actin antibody (66009-1-Ig, Proteintech), anti-AID monoclonal antibody (mAID-2, 14-5959-82, eBioscience), and anti-Flag M2 antibody (F1804-50UG, Sigma-Aldrich). The antibodies for flow cytometry analysis were anti-Mouse lgM-APC (17-5790-82, eBioscience), anti-Mouse lgA-PE (12-4204-83, eBioscience), and anti-Mouse lgG1-PE (406608, Biolegend).

Chemicals and DNA Damaging Treatments

Mirin (M9948-5 MG, Sigma-Aldrich), PFM01 (SML1735-5mg, Sigma-Aldrich), Ku55933 (SML 1109-5 mg, Sigma-Aldrich), and AZD1390(S8680-5 mg, Selleck) were dissolved in DMSO and stored at −20°C. Cells were exposed to X-rays generated by a Rad Source RS2000 Irradiator (160 kv, 25 mA) to induce DNA damage.

Short Hairpin RNA-Mediated Gene Silencing

ShRNAs specific to Mre11, CTIP, and DNA2 were cloned into pLKO.1 puro vector. All the shRNA sequences were listed in Appendix information, **Supplementary Table S1**. The plko.1 vector cloned with specific shRNA sequence and the packaging plasmids pMD2. G and psPAX2 were co-transfected into HEK293T cell to produce lentiviruses with polyethylenimine (PEI) transfection reagent. Cell supernatants were collected after 48 h post-transfection and filtered with a sterile 0.45-μm syringe filter to remove cell debris. The lentiviruses were concentrated by virus precipitation Solution (ExCell Bio) and resuspended in complete medium. CH12F3 or its mutants were infected with lentivirus by centrifuging at 32°C 1,000×*g* 60 min. After transduction for 48 h, the cells were selected with 0.5 μg/ml puromycin for 5–7 days.

$EXO1^{WT}$/$EXO1^{EK}$ Rescue Experiment

The EXO1 cDNA sequence was obtained using reverse transcription from total RNA extracted from WT CH12F3 cell line. EXO1 mutants $EXO1^{EK}$ was obtained with site-directed mutagenesis. The C terminus of cDNA was added with 3× flag tag by two sequential PCR rounds. The EXO1/$EXO1^{EK}$-3× flag were cloned into pMIG II. Retrovirus vector pMIG II-$EXO1^{WT}$/$EXO1^{EK}$-3× flag were transfected into Phoenix Ampho cell to produce retrovirus with PEI. Retrovirus was concentrated as lentivirus did. EXO1-deficient CH12F3 were transduced with retrovirus by centrifuging at 32°C 1,000×*g* for 60 min. After transduction for 3–4 days, the GFP positive cells were sorted with Beckman Coulter MoFlo Astrios EQs. To confirm the expression of $EXO1^{WT}$/$EXO1^{EK}$ in EXO1-deficient CH12F3 was rescued, the infected cells were lysed for western blot analysis with anti-flag primary antibody.

Class Switch Recombination Assay

WT CH12F3 cell line or its mutants at a density of 5×10^4 cells/mL or 1×10^5 cells/mL were stimulated with 1 μg/ml anti-CD40

(16-0401-86, eBioscience), 20 ng/ml IL4 (214-14, PeproTech), and 1 ng/ml TGF-β (96-100-21-10, PeproTech) for 72 h. Cells were collected and analyzed by flow cytometry. Data were presented as mean ± SD from independent experiments (Student's *t*-test, *$p < 0.05$, **$p < 0.01$, ***$p < 0.001$, ****$p < 0.0001$, n. s indicates non-significant differences).

Cas9-Initiated Class Switch Recombination Assay

For CRISPR/Cas9-initiated CSR (Cas-CSR) in CH12F3 cells, sgRNAs targeting up- and down-stream S regions (Sμ and Sγ1) were transfected into CH12F3 cells via electroporation. SgRNAs were cloned into px458 plasmids. After transfection, CSR to IgG will increase gradually. CSR level to other Ig in KO cells was normalized to the GFP + ratio of 24 h after transfection.

Western Blotting

Cells were collected and lysed in RIPA buffer with fresh proteinase inhibitors. The cell lysate was centrifuged and quantified by the BCA assay (23225, Thermo). The collected cell lysate was denatured by boiling in loading buffer at 100°C for 10 min, loaded into the wells of SDS/PAGE to separate, and transferred to PVDF membranes (IPVH00010, Merck). The membranes were blocked by 5% skim milk in PBST for 1 h at room temperature, probed with indicated primary antibodies overnight at 4°C, washed 3 times with PBST, incubated with recommended HRP-conjugated second antibody (7074s, Cell Signaling Technology) for 1 h at room temperature, washed 3 times with PBST, and visualized with HRP substrate peroxide solution.

Quantitative RT-PCR

Total RNA was extracted using TRIzol reagent (15596026, Invitrogen). RNA was reverse transcribed into cDNA by the reverse transcription system (RR037A, Takara). SYBR Premix Ex Taq kit (RR820A, Takara) was used to perform qRT-PCR on LightCycler480 Real-Time PCR System (Roche). Relative gene expression levels were obtained based on the $2^{-\Delta\Delta Ct}$ method with Hprt as internal reference control. Primers for qRT-PCR are listed in **Supplementary Table S1**.

HTGTS

HTGTS libraries were constructed as described (Dong et al., 2015). Briefly, genomic DNA of CH12F3 or its mutants were extracted after stimulation for 3 days. The genomic DNA was sonicated and amplified by LAM-PCR with 5′ Sμ biotin primer (5′-CAGACCTGGGAATGTATGGT-3′). The Biotinylated products of PCR were captured by Dynabeads MyOne streptavidin C1 beads (Invitrogen), ligated with bridge adapters on-bead. The ligated products were amplified by second-PCR to add adaptor. Then, the products of PCR were blocking with endonuclease Afill to remove germline genomic DNA fragment. The third round PCR was performed to add Illumina Miseq-compatible adapters to conduct MiSeq sequencing. The HTGTS data were analyzed as described (Dong et al., 2015; Panchakshari et al., 2018). Data were presented as mean ± SEM (Student's *t*-test, *$p < 0.05$, **$p < 0.01$, ***$p < 0.001$).

Statistical Analysis

Statistical analysis was performed in GraphPad Prism 7.01. Data was reported as mean and SD except that the HTGTS analysis was reported as mean and SEM. Unpaired two-tailed Student *t* test or two-way ANOVA was used to examine the significant difference between samples. The asterisks stand for significant differences (*$p < 0.05$, **$p < 0.01$, ***$p < 0.001$, ****$p < 0.0001$, n. s indicates non-significant differences).

Data and Code Availability

HTGTS sequencing data have been deposited at the Sequence Read Archive (SRA) with a project #PRJNA728565, with an access URL:https://dataview.ncbi.nlm.nih.gov/object/PRJNA728565.

RESULTS

Mre11 and CtIP are Required for A-EJ Mediated Class Switch Recombination to IgA

Previous reports indicated that germline deletion of Mre11 or CtIP confers early embryonic lethality in mice, and mutant MEF cells showed altered proliferation and genome instability (Buis et al., 2008; Chen et al., 2005). To first examine the role of Mre11 in class switching, we utilized two different short hairpin RNAs (shRNA) expressed from lentiviral vectors to silence its expression in mouse mature B cell lymphoma cell line CH12F3 that can be stimulated to specifically undergo isotype switching to IgA (**Figure 1A**). ShRNA-mediated knock down of Mre11 expression in CH12F3 appears not affecting the overall proliferation of cells (**Supplementary Figure S1A**). When stimulated by the combination of αCD40/IL-4/TGF-β, shMre11 cells showed similar level of mature Iμ and Iα germline transcription, and the protein level of AID was not perturbed by Mre11 silencing (**Supplementary Figures S1B,S1C**). IgA expression in shMre11 cells showed a mild defect by surface staining (**Figures 1B,C**, **Supplementary Figure S2A**). To distinguish whether the endonuclease or exonuclease of Mre11 is involved in CSR by c-NHEJ, we treated CH12F3 cells with small chemical inhibitor Mirin or PFM01 that specifically inhibit Mre11's exo- or endonuclease activity, respectively (Shibata et al., 2014), and discovered that only Mirin, but not PFM01 treatment conferred a mild but significant defect in IgA levels (**Figure 1D**, **Supplementary Figure S2B**). Next, we used three different shRNA to silence expression of CtIP in CH12F3 cell (**Figure 1E**). While CtIP knockdown did not affect the Iμ and Iα germline transcription, AID protein level and cell proliferation rate did exhibit small decline by shCtIP-3# (**Supplementary Figures S1D-F**). However, all three shCtIP-infected cells showed similar IgA levels at around 70–80% of values of WT, implying that CtIP contributes to class switching in WT cells

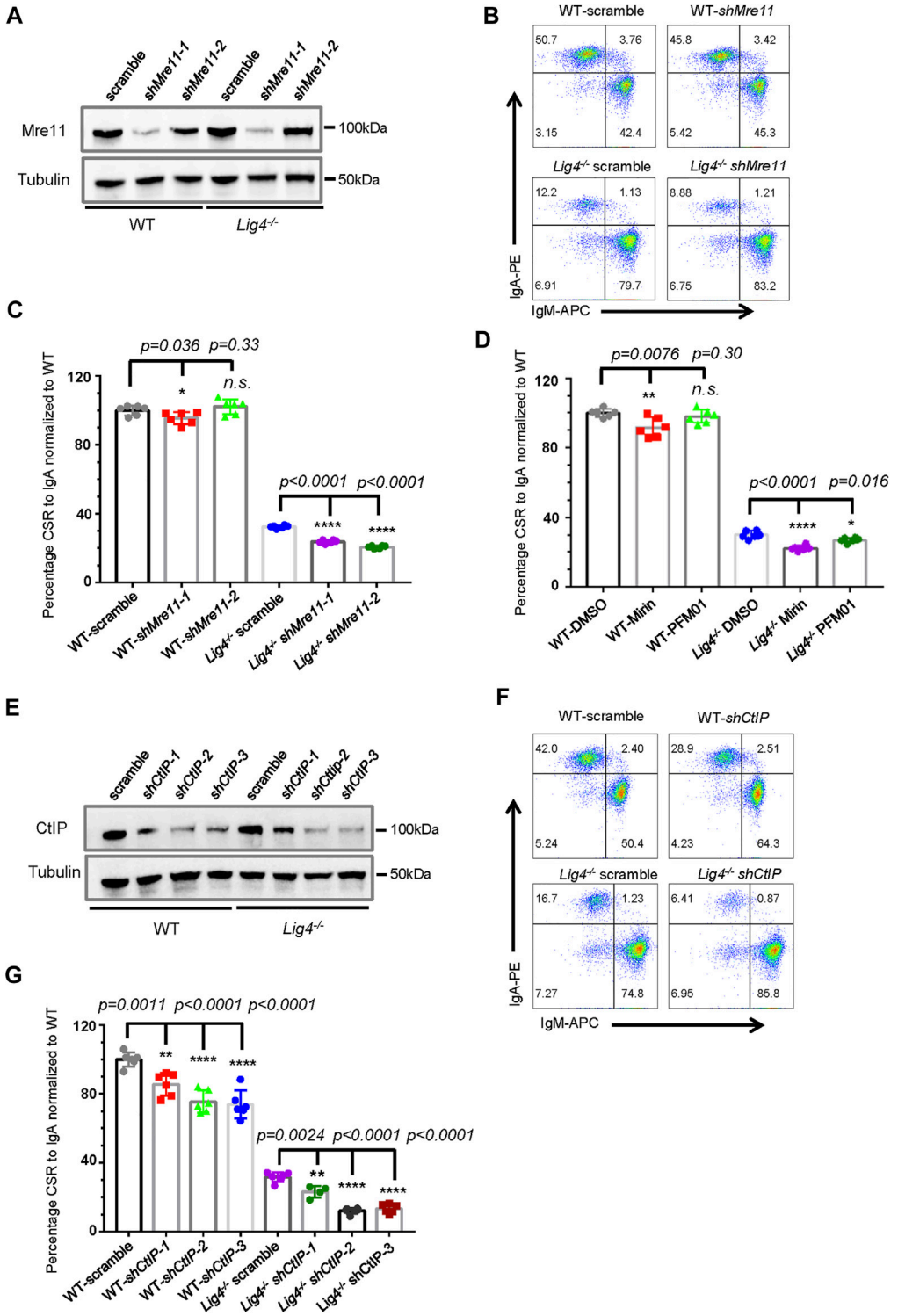

FIGURE 1 | Mre11 and CtIP are essential for A-EJ mediated CSR. **(A)** Western blot analysis of Mre11 expression in WT and *Lig4*$^{-/-}$ CH12F3 cells transduced with lentivirus expressing the indicated shRNA. **(B)** Representative flow cytometry analysis of CSR to IgA in Mre11-silenced WT and *Lig4*$^{-/-}$ cells. **(C)** Quantification of IgA switching efficiency in Mre11-silenced WT and *Lig4*$^{-/-}$ cells normalized to that scramble control. Data were presented as mean ± SD from six independent experiments (Student's *t*-test, **p* < 0.05, ***p* < 0.01, ****p* < 0.001, *****p* < 0.0001, n. s. (*p* > 0.05) indicates non-significant differences). **(D)** Normalized CSR to IgA in WT and *Lig4*$^{-/-}$ cells pretreated with 10 μM exonuclease inhibitor (Mirin), 10 μM endonuclease inhibitor (PFM01). Data were presented as mean ± SD from six independent experiments (Student's *t*-test, **p* < 0.05, ***p* < 0.01, ****p* < 0.001, *****p* < 0.0001, n. s. (*p* > 0.05) indicates non-significant differences). **(E)** Western blot analysis of CtIP

(*Continued*)

FIGURE 1 | expression in WT and *Lig4*$^{-/-}$ cells transduced with lentivirus expressing the indicated shRNA. **(F)** Representative flow cytometry analysis of IgA switching in CtIP-knockdown WT and *Lig4*$^{-/-}$ cells. **(G)** Quantification of IgA CSR efficiency in CtIP knockdown WT and *Lig4*$^{-/-}$ cells. CSR was assayed at 72 h after stimulation with α-CD40/IL-4/TGF-β. Scramble represented control shRNA targeting a non-mouse sequence. Data were presented as mean ± SD from six independent experiments (Student's *t*-test, *$p < 0.05$, **$p < 0.01$, ***$p < 0.001$, ****$p < 0.0001$, n. s. ($p > 0.05$) indicates non-significant differences).

largely independent of AID protein regulation. A recent study reported EXD2 as an exonuclease that functions with Mre11 for DSB resection and HR (Broderick et al., 2016). We generated EXD2 knockout CH12F3 cells by CRISPR/Cas9 (**Supplementary Figures S3A–S3C**), and surface staining indicated that EXD2 was not required for IgA switching by c-NHEJ (**Supplementary Figure S3D**).

To further investigate whether these resection initiation proteins are required for CSR by A-EJ, we knocked-down Mre11 in *Lig4*$^{-/-}$ CH12F3 cells (**Figure 1A**). Again, Mre11 silencing in *Lig4*$^{-/-}$ cells did not change Iμ/Iα germline transcription and AID protein level, or overall proliferation (**Supplementary Figures S1A–S1C**). As previously reported, *Lig4*$^{-/-}$ cells switched to IgA at an efficiency about ~30% of that of WT CH12F3 cells. Mre11 silencing by two different hairpin RNAs significantly further reduced IgA levels by about one third to half (**Figures 1B,C**). Treating *Lig4*$^{-/-}$ cells with either Mirin or PFM01 also reduced IgA switching levels to close to 50% of DMSO-treated control cells (**Figure 1D**, **Supplementary Figure S2B**). Similarly, shRNA-mediated knockdown of CtIP in *Lig4*$^{-/-}$ cells further impairs IgA switching by more than 50% (**Figures 1F,G**, **Supplementary Figure S2C**). A rather mild effect on A-EJ was observed by *Exd2* deletion in *Lig4*$^{-/-}$ cells (**Supplementary Figures S3C,S3D**), suggesting that the stimulation of Mre11's exonuclease activity by Exd2 is negligible during B cell class switching. Taken together, these data suggest that while efficient CSR in wild type cells requires Mre11/CtIP to various extent, Mre11 and CtIP play more important roles in A-EJ-mediated CSR.

S-S Joining Pattern and MH Usage in c-NHEJ and A-EJ in the Absence of Mre11 or CtIP

To further explore the molecular signature of end joining in cells deficient for Mre11 or CtIP, we utilized High Throughput Genome-wide Translocation Sequencing (HTGTS) to characterize Sμ-Sα junctions and MH usage pattern in stimulated CH12F3 wild type and mutant cells (**Figure 2A**). HTGTS with a 5' Sμ anchor primer fine-maps joining from AID-initiated DSBs occurring in upstream Sμ to those in Sα region and genome wide. Consistent with no or moderate defect in c-NHEJ CSR by FACS in WT CH12F3 cells, Mre11 or CtIP knockdown cells showed nearly no difference in the percentage of Sμ-Sα joining compared with scramble controls (**Supplementary Figure S4**). When examining junctions mapped to the Sα region for details, however, we indeed observed a small but significant decrease in the ratio of direct versus inversional Sμ-Sα joining in shMre11 cells (**Figures 2B,C**). The percentages of junctions falling into Cα represents joining of Sμ to Sα DSBs resected into distal region (**Figure 2A**). In shMre11 cells, we observed a small but significant increase in the Sα DSBs long resection (**Figure 2D**), and MH usage of Sμ-Sα joining showed a slight decrease in "blunt" (MH = 0) and increase in MH = 1 joins (**Figure 2E**), consistent with a role for Mre11 in activating DDR kinase ATM that is critical for suppressing resection and MH usage. In contrast, CtIP-silenced CH12F3 cells showed identical Sα DSB resection and MH pattern in Sμ-Sα junctions compared with control cells (**Figures 2D,E**), indicating that CtIP does not play a critical role in the joining step of c-NHEJ-mediated CSR.

We then analyzed S-S joining pattern of Mre11 or CtIP-silenced *Lig4*$^{-/-}$ cells with HTGTS. Scramble control virus transduced *Lig4*$^{-/-}$ cells had significantly decreased in direct Sα joining and concomitant decrease in the ratio of direct versus inversional Sα junctions (**Figures 2B–D**). Mre11 or CtIP knockdown further decreased direct Sα joining percentage, consistent with IgA surface staining data (**Figure 2B**). Interestingly, we found no significant difference in Cα distal junctions and MH usage between *Lig4*$^{-/-}$ cells infected with scramble or shMre11/shCtIP virus (**Figures 2D,E**), indicating that while Mre11/CtIP is partly required for A-EJ events in Lig4-deficient cells, they are not required for the long resection activity into Cα region in these cells. In addition, we indeed discovered an obviously decreased ratio of direct versus inversional Sα junctions in shCtIP infected *Lig4*$^{-/-}$ cells (**Figures 2B,C**), implicating a unique role for CtIP in A-EJ in this context.

BLM/DNA2-Mediated Long-Range Resection is Required for A-EJ Class Switch Recombination

To study the role of long range DSB resection factors in CSR, we first deleted Exo1 by CRISPR/Cas9 in CH12F3 cells (**Supplementary Figures S5A,B**). Consistent with previous reports, IgA switching in Exo1 knockout cells in both WT and *Lig4*$^{-/-}$ backgrounds was extremely low (**Supplementary Figure S5C**) due to severe defect in mismatch repair that is critical to convert AID-initiated lesions into DSBs (Bardwell et al., 2004). Except for its exonuclease activity, Exo1 also has a structural function to facilitate the assembly of high-order protein complex. The Exo1^{E109K} mutation that is exonuclease-dead has been shown to retain mismatch repair activity but is defective in DSB resection and HR-related functions (Schaetzlein et al., 2013). We thus reintroduced the Exo1^{E109K} (referred to as Exo1^{EK} hereafter) mutation by retrovirus back to *Exo1*-deleted WT and *Lig4*$^{-/-}$ cells (**Supplementary Figure S5D**), and both Exo1^{WT} and Exo1^{EK} fully rescued the near-null IgA switching in not only *Exo1*$^{-/-}$ cells, but also *Lig4*$^{-/-}$ *Exo1*$^{-/-}$ cells (**Figure 3A**, **Supplementary Figure S5E**), indicating that exonuclease-embedded DSB resection function of Exo1 is not required for either c-NHEJ or A-EJ-mediated CSR. To further test whether Exo1 plays any role in joining of non-AID initiated

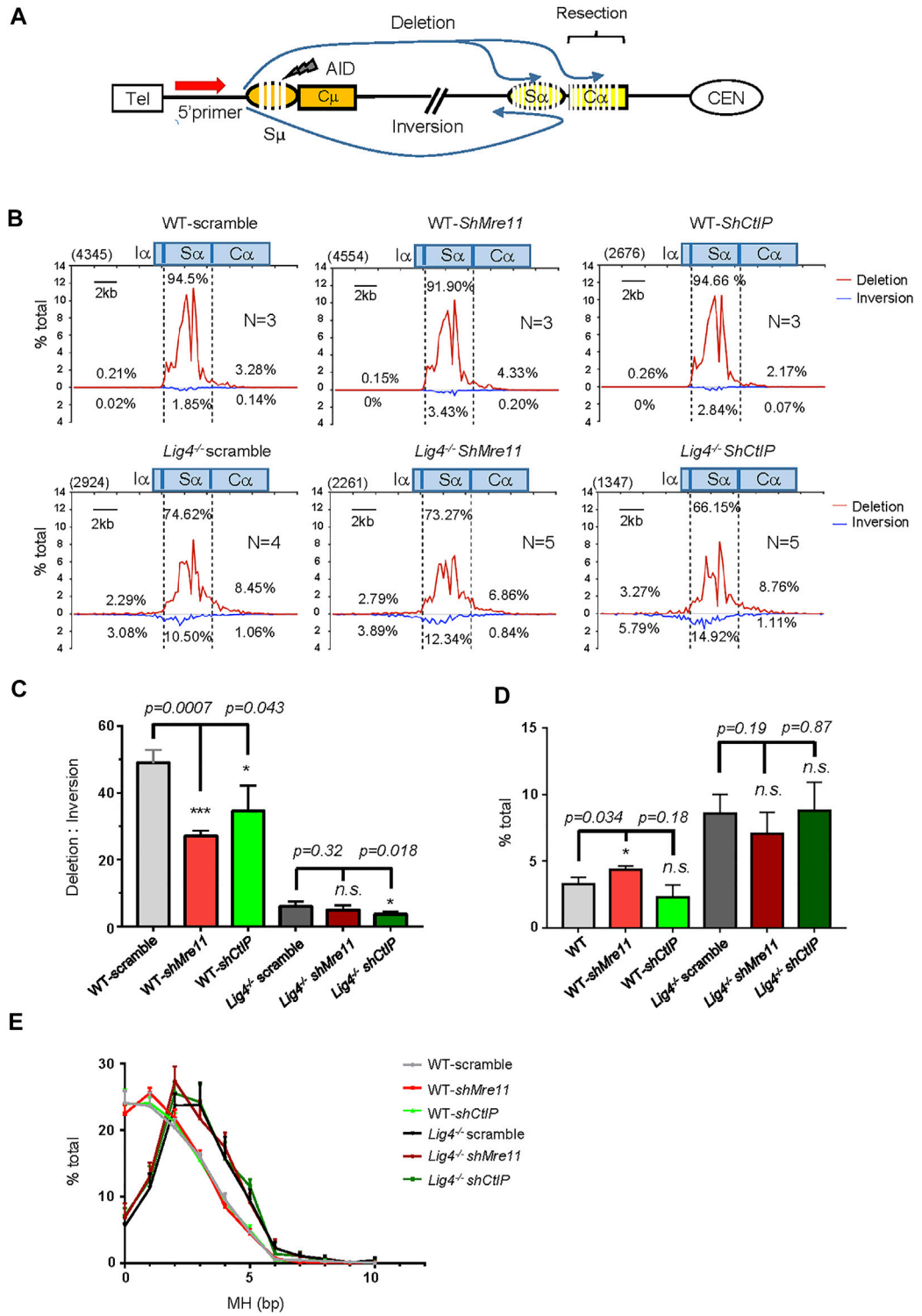

FIGURE 2 | S-S junction profile and MH usage pattern in Mre11/CtIP-silenced WT and *Lig4–/–* cells. **(A)** Diagram of the joining outcomes between Sμ and Sα DSB sequenced by HTGTS. Joining from 5′ Sμ bait DSB to Sα broken end reading in the telomere to centromere orientation are designated as deletion and represent productive joining, whereas those from 5′ Sμ to Sα broken end reading from centromere telomere orientation are designated as inversion and represent non-productive joining. Junctions falling into distal Cα region are denoted as long resection. **(B)** Linear distribution of pooled Sμ-Sα junctions recovered from Mre11/CtIP-silenced WT and *Lig4*$^{-/-}$ cells with indicated numbers (*N*) of experiment repeats are shown in the form of deletion or inversion along a 20-kb region centered at core Sα (Chr12: 114491001–114511000). Bin size is 200 bp and 100 bins are presented in each plot. Numbers in the parenthesis represent total unique junctions in the indicated region.

(*Continued*)

FIGURE 2 | (C) The ratio of deletion versus inversion for Sα junctions in Mre11/CtIP-silenced WT and *Lig4*$^{-/-}$ cells. Data were presented as mean ± SEM (Student's *t*-test, **p* < 0.05, ***p* < 0.01, ****p* < 0.001, n. s. (*p* > 0.05) indicates non-significant differences). **(D)** Percentage of long resection junctions in Mre11/CtIP-silenced WT and *Lig4*$^{-/-}$ cells. Data were presented as mean ± SEM (Student's *t*-test, **p* < 0.05, n. s. (*p* > 0.05) indicates non-significant differences). **(E)** The MH pattern of Sμ-Sα junctions in Mre11/CtIP-silenced WT and *Lig4*$^{-/-}$ cells. HTGTS analyses were performed with indicated cells stimulated with α-CD40/IL-4/TGF-β for 72 h. Data were presented as mean ± SEM.

DSBs, we introduced simultaneous blunt end breaks at Sμ and Sγ1 by CRISPR/Cas9 (**Supplementary Figure S5F**) and tested switching to IgG1 in WT, *Lig4*$^{-/-}$, *Exo1*$^{-/-}$, or double-mutant cells at 24, 48, and 72 h post-transfection. After normalization with transfection efficiency, efficient joining of Sμ-Cas9 DSBs to Sγ1-Cas9 breaks generated 40–60% of IgG1+ cells; as expected, Lig4 ablation reduced IgG1 switching efficiency by more than half to only 10–20% (**Figure 3B**, **Supplementary Figures S5G,5H**). In addition, we found that *Exo1* deletion in either in WT or *Lig4*$^{-/-}$ cells did not reduce Cas9-mediated IgG1 switching than the corresponding controls (**Figure 3B**). Taken together, we conclude that Exo1 is not required for joining AID or Cas9-generated DSBs by either c-NHEJ or A-EJ pathways.

We then asked whether DNA2/BLM-mediated long range resection is required for efficient A-EJ. Two specific shRNA efficiently knocked down the mRNA expression of DNA2 by 50–70% in both wild type and *Lig4*$^{-/-}$ CH12F3 cells (**Supplementary Figure S6A**); accordingly, the IgA CSR efficiency in WT cells was slightly decreased by about 20%, and *Lig4*$^{-/-}$ cells with shDNA2 exhibited an IgA CSR decline by 30% (**Figure 3C**, **Supplementary Figure S6H**). This deficiency can be at least partly attributed to impaired proliferation caused by DNA2 knockdown in WT and *Lig4*$^{-/-}$ cells (**Supplementary Figure S6B**). To test the role of BLM in A-EJ, we first deleted with CRISPR/Cas9 the exon 8 of *Blm* gene upstream of the helicase domain; this mutation rendered ablation of BLM by premature termination of translation (Babbe et al., 2009) (**Supplementary Figures S6C,S6D**). The resultant BLM$^{\Delta helicase}$ cells were indistinguishable in IgA switching compared with WT cells, whilst BLM$^{\Delta helicase}$ in the *Lig4*$^{-/-}$ background slightly but significantly reduced IgA CSR compared to control cells (**Supplementary Figure S6E**). Due to severe slow proliferation caused by helicase domain disruption, we generated another *Blm* mutation by Cas9 to delete the exon 19 that encodes Helicase-and-RNaseD-like-C-terminal (HRDC) domain of BLM (**Supplementary Figures S6F,G**). The HRDC domain interacts with the ATPase domain of BLM that may affect its helicase activity (Newman et al., 2015) and has been shown to be required for annealing of complementary single-strand DNA and Holliday junction resolution (Wu et al., 2005; Newman et al., 2015; van Wietmarschen et al., 2018). Although BLM$^{\Delta HRDC}$ CH12F3 cells proliferate and switch to IgA normally, BLM$^{\Delta HRDC}$ in *Lig4*$^{-/-}$ background displayed a substantial decrease in CSR efficiency (**Figure 3D**, **Supplementary Figures S6l**), indicating that the HRDC domain of BLM is required for A-EJ, but not c-NHEJ-mediated class switching.

To gain more insights on the mechanism of how BLM participates in A-EJ, we performed HTGTS assay in WT and *Lig4*$^{-/-}$ cells with BLM$^{\Delta HRDC}$ mutation and analyzed the pattern of S-S joining and MH in these cells (**Supplementary Figure S7**). Compared with WT cells, the BLM$^{\Delta HRDC}$ mutant exhibited a slightly decrease in the proportion of Sα junctions and a mild increase in junctions involving long Sα resection (**Supplementary Figures S7B,C**). When examining MH pattern of Sμ-Sα junctions, we recovered no significant difference between WT and BLM$^{\Delta HRDC}$ mutant cells (**Supplementary Figure S7D**). In contrast, a significant decrease in the proportion of long Sα resection junctions in *Lig4*$^{-/-}$ cells with BLM$^{\Delta HRDC}$ mutation was observed (**Figures 3E,F**), indicating the HRDC activity is required for the joining of long-resected Sα breaks in *Lig4*$^{-/-}$ cells. Similar to aforementioned cells in WT background, no significant difference in the MH profile in Sμ-Sα junctions was observed in BLM$^{\Delta HRDC}$ cells compared with the corresponding *Lig4*$^{-/-}$ control (**Figure 3G**).

ATM Kinase Activity is Required for Both c-NHEJ and A-EJ-Mediated Class Switch Recombination

AID-initiated DSB recruits and activates ATM. While ATM positively regulates c-NHEJ-mediated CSR, its role in A-EJ has not been carefully examined. To this end, we first applied a highly selective ATM inhibitor AZD1390 that suppressed c-NHEJ mediated CSR at low concentrations with no effect on germline transcription and AID expression (**Figure 4A**, **Supplementary Figures S8C,E**). Treating *Lig4*$^{-/-}$ cells with AZD1390 further reduced IgA switching by about half (**Figure 4A**). The CSR reduction by AZD1390 treatment in *Lig4*$^{-/-}$ cells was phenocopied by *Atm* knockout (**Figure 4B**, **Supplementary Figure S8A**). In addition, we observed more phosphorylation of KAP1 that was ATM-dependent in IR-irradiated Lig4-deficient cells compared with WT control, indicating persistent ATM activation in A-EJ cells (**Supplementary Figure S8B**). Together, we concluded that ATM kinase activity is required for both c-NHEJ and A-EJ-mediated CSR.

We then examined the Sμ-Sα joining pattern with ATM deletion and ATM kinase inhibition by the HTGTS assay. *Atm* knockout or kinase activity inhibition in CH12F3 cells similarly resulted in increased Sα DSBs resection, increased MH usage, and decreased ratio of deletional versus inversional Sμ-Sα joining (**Figures 4C–E**). Surprisingly, in *Lig4*$^{-/-}$ cells with *Atm* ablation, although the percentage of Sα deletional joining over total *IgH* junctions decreased (**Supplementary Figures S8F-H**) that was consistent with further reduced IgA surface expression than *Lig4*$^{-/-}$ cells by flow cytometry, other parameters including Sα DSBs long resection, MH usage, and ratio of deletional versus inversional Sμ-Sα junctions remained unchanged compared with controls (**Figures 4C–E**). We concluded that while ATM plays important roles in both c-NHEJ and A-EJ-mediated CSR, it did not appear to control Sα long resection in Lig4-deficient cells. We also examine the potential role of another PIKK, DNA-PKcs in CSR. Consistent with the reported role of DNA-

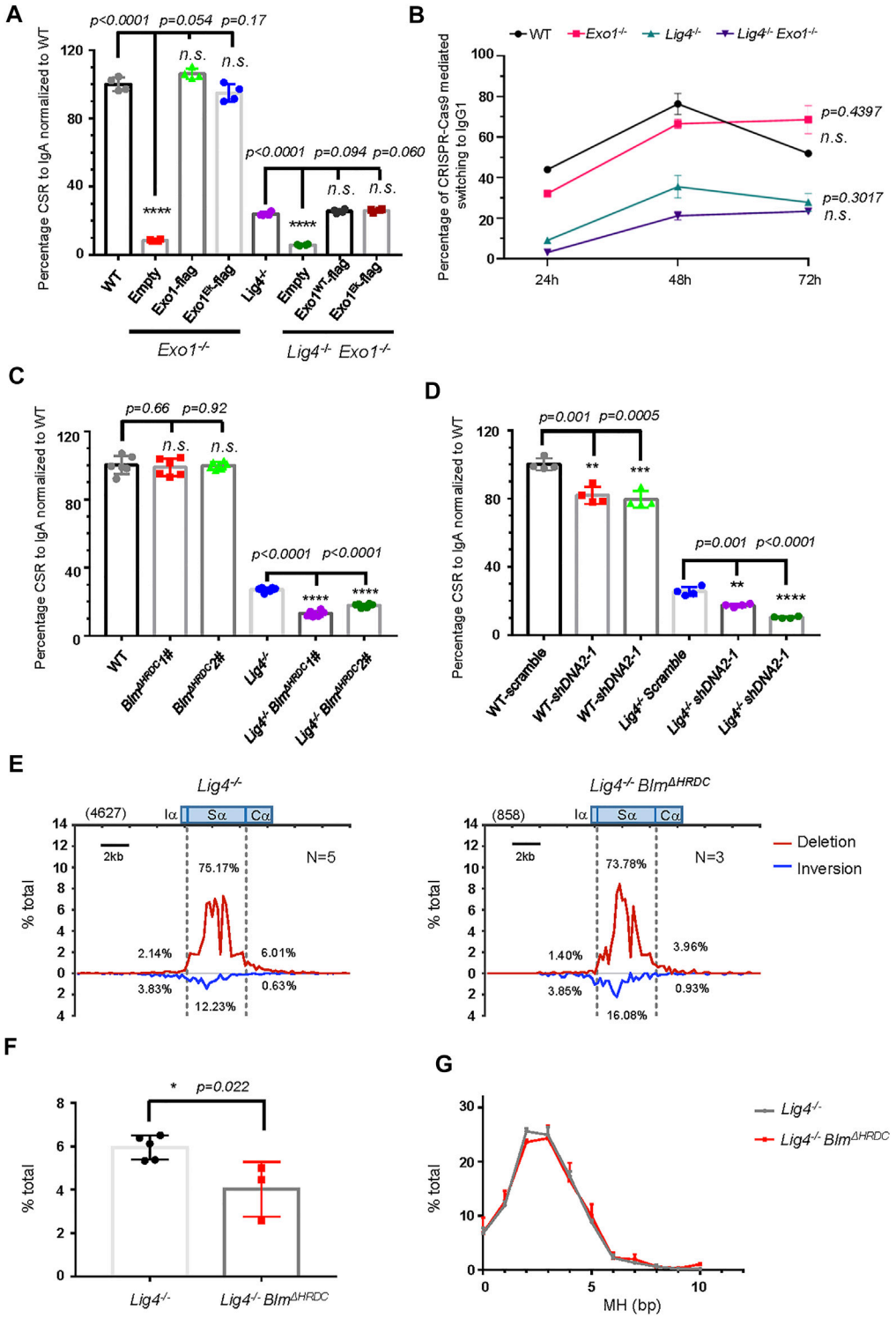

FIGURE 3 | Long resection factors BLM/DNA2 are involved in A-EJ mediated CSR. **(A)** Normalized CSR to IgA in Exo1-deficient B cell reconstituted with retrovirus expressing indicated constructs. Data were presented as mean ± SD from four independent experiments (Student's *t*-test, *$p < 0.05$, **$p < 0.01$, ***$p < 0.001$, ****$p < 0.0001$, n. s. ($p > 0.05$) indicates non-significant differences). **(B)** Efficiency of switching to IgG1 with CRISPR/Cas9 targeting Sμ and Sγ1, respectively, in Exo1-deficient WT and *Lig4*$^{-/-}$ cells. Data were presented as mean ± SD from three independent experiments (two-way ANOVA, n. s. ($p > 0.05$) indicates non-significant differences). **(C)** Normalized IgA CSR efficiency in *DNA2*-silenced WT and *Lig4*$^{-/-}$ cells. Data were presented as mean ± SD from four independent experiments (Student's *t*-test, *$p < 0.05$, **$p < 0.01$, ***$p < 0.001$, ****$p < 0.0001$, n. s. ($p > 0.05$) indicates non-significant differences). **(D)** Normalized IgA CSR efficiency in *Blm* HRDC

(*Continued*)

FIGURE 3 | domain deleted WT and *Lig4*$^{-/-}$ cells. Data were presented as mean ± SD from six independent experiments (Student's *t*-test, *$p < 0.05$, **$p < 0.01$, ***$p < 0.001$, ****$p < 0.0001$, n. s. ($p > 0.05$) indicates non-significant differences). **(E)** Linear distribution of pooled Sμ-Sα junctions recovered from HTGTS libraries with CSR activated *Lig4*$^{-/-}$ *Blm*$^{\Delta HRDC}$ cells. Numbers (*N*) indicated experiment repeats. **(F)** Percentage of long resection junctions in *Lig4*$^{-/-}$ *Blm*$^{\Delta HRDC}$ cells. Data were presented as mean ± SEM (Student's *t*-test, *$p < 0.05$, n. s. ($p > 0.05$) indicates non-significant differences). **(G)** The MH pattern of Sμ-Sα junctions in *Lig4*$^{-/-}$ *Blm*$^{\Delta HRDC}$ cells. Data were presented as mean ± SEM.

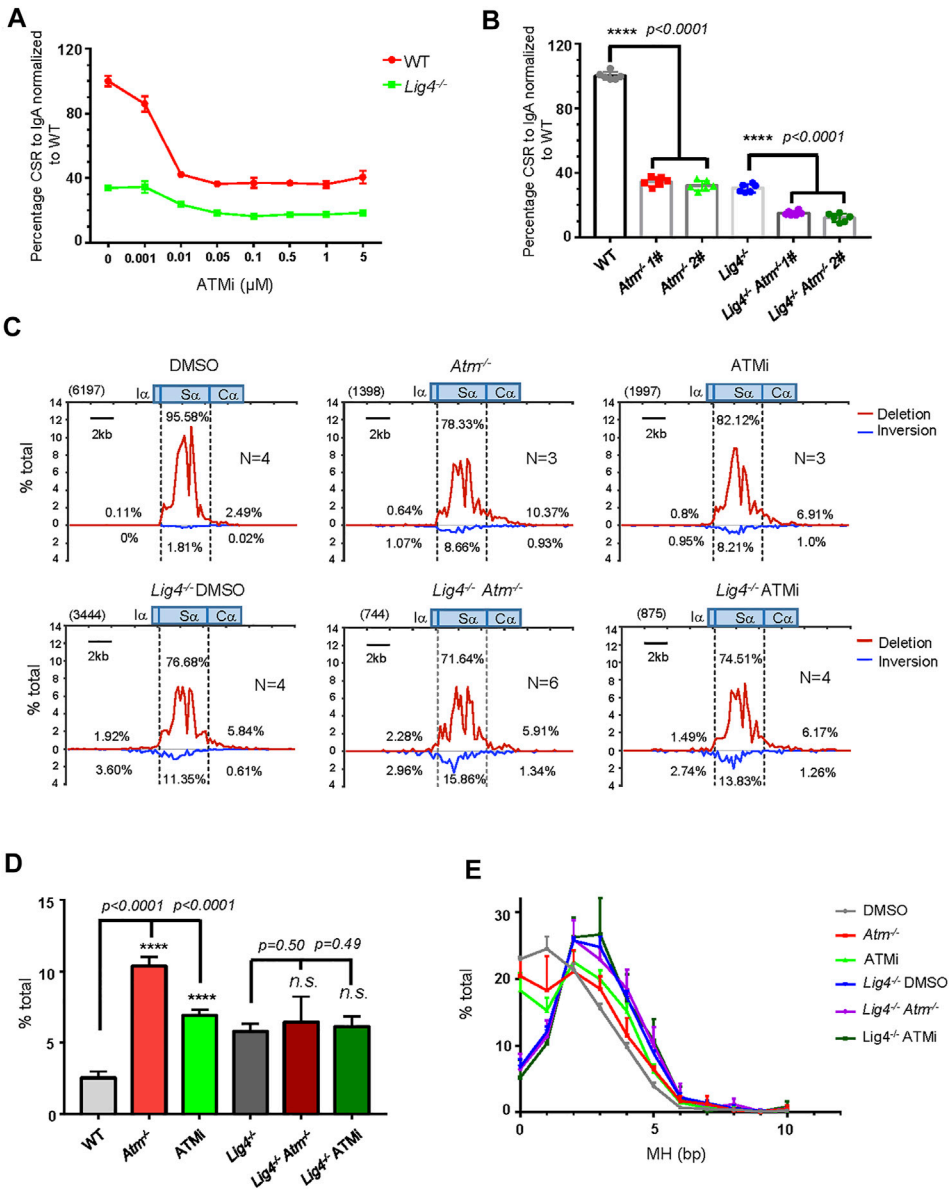

FIGURE 4 | ATM and its kinases activity play important role in A-EJ mediated CSR. **(A)** Normalized IgA switching efficiency in WT and *Lig4*$^{-/-}$ cells treated with ATM inhibitor AZD1390 at gradient concentrations ranging from 0 μM, 0.001 μM, 0.01 μM, 0.05 μM, 0.1 μM, 0.5 μM, and 1–5 μM. Data were presented as mean ± SD from three independent experiments. **(B)** Normalized IgA switching efficiency in *Atm* deleted WT and *Lig4*$^{-/-}$ cells. Data were presented as mean ± SD from six independent experiments (Student's *t*-test, *$p < 0.05$, **$p < 0.01$, ***$p < 0.001$, ****$p < 0.0001$, n. s. ($p > 0.05$) indicates non-significant differences). **(C)** Linear distribution of pooled Sμ-Sα junctions recovered from HTGTS libraries with CSR activated DMSO or 0.1 μM AZD1390-treated ATM-deficient WT and *Lig4*$^{-/-}$ cells. Numbers (*N*) indicated experiment repeats. **(D)** Percentage of long resection junctions in ATM inhibitor-treated and ATM-deficient WT and *Lig4*$^{-/-}$ cells. Data were presented as mean ± SEM (Student's *t*-test, *$p < 0.05$, **$p < 0.01$, ***$p < 0.001$, ****$p < 0.0001$, n. s. ($p > 0.05$) indicates non-significant differences). **(E)**The usage of MH among Sμ-Sα junctions recovered from HTGTS libraries ATM inhibitor-treated and ATM-deficient WT and *Lig4*$^{-/-}$ cells. Data were presented as mean ± SEM.

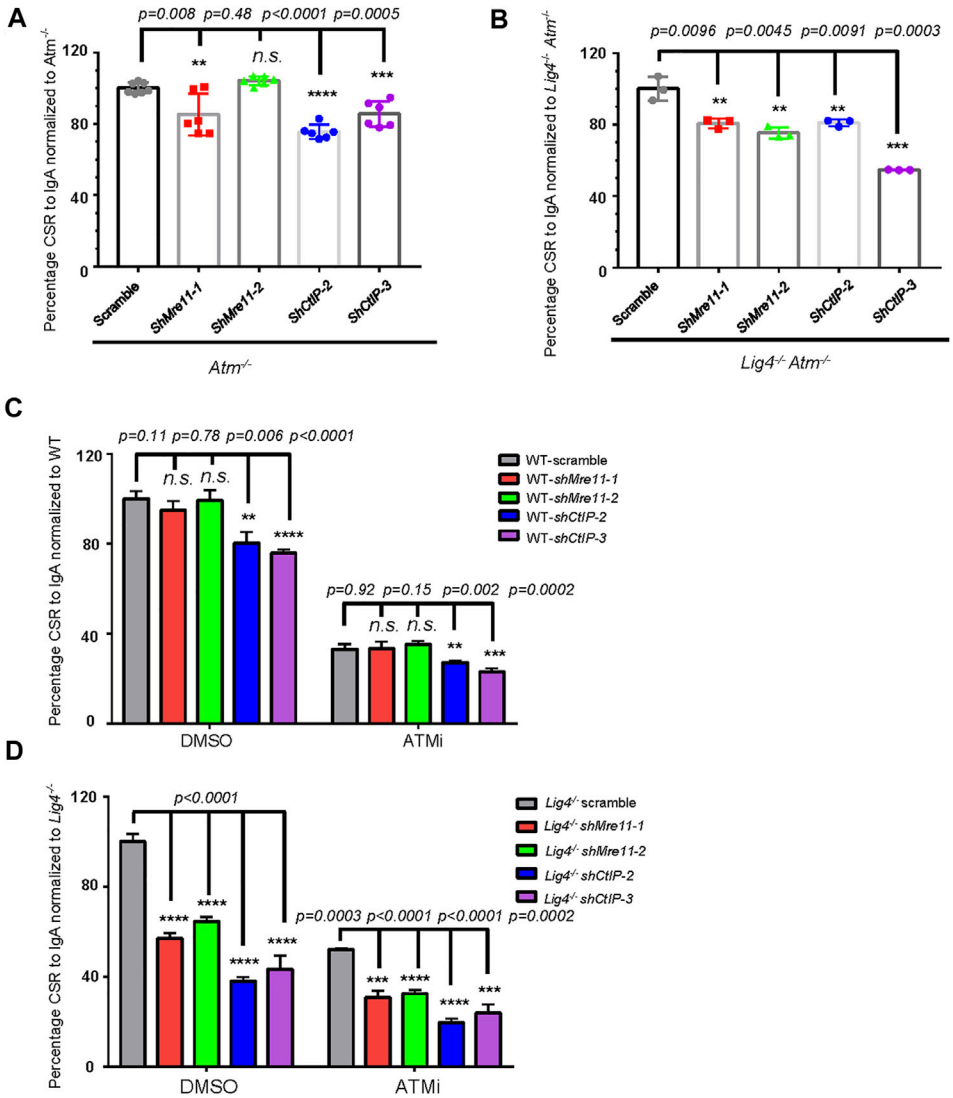

FIGURE 5 | ATM and Mre11/CtIP promote A-EJ mediated CSR independently of each other. **(A, B)** Silencing Mre11/CtIP by different shRNAs further reduced CSR in both *Atm*$^{-/-}$ cells (**A**) and *Lig4*$^{-/-}$ *Atm*$^{-/-}$ cells (**B**). Data were presented as mean ± SD from six in **A**, three in **B** independent experiments (Student's *t*-test, **p* < 0.05, ***p* < 0.01, ****p* < 0.001, *****p* < 0.0001, n. s. (*p* > 0.05) indicates non-significant differences). **(C)** Inhibition of ATM kinase activity with AZD1390 (100 nM) could reduce CSR in Mre11/CtIP-silenced WT CH12F3 cells. Data were presented as mean ± SD from three independent experiments (Student's *t*-test, **p* < 0.05, ***p* < 0.01, ****p* < 0.001, *****p* < 0.0001, n. s. (*p* > 0.05) indicates non-significant differences). **(D)** Inhibition of ATM kinase activity with AZD1390 could further reduce IgA CSR in Mre11/CtIP-silenced *Lig4*$^{-/-}$ cells. Data were presented as mean ± SD from three independent experiments (Student's *t*-test, **p* < 0.05, ***p* < 0.01, ****p* < 0.001, *****p* < 0.0001, n. s. (*p* > 0.05) indicates non-significant differences).

PKcs in promoting c-NHEJ to IgG in primary mouse B cells (Franco et al., 2008; Callén et al., 2009), while deleting DNA-PKcs by CRISPR/Cas9 (**Supplementary Figures S9A–D**) significantly diminished IgA in WT CH12F3 cells, knocking out DNA-PKcs in *Lig4*$^{-/-}$ cells did not further reduce IgA CSR (**Supplementary Figure S9E**), indicating that DNA-PKcs does not play a role in A-EJ.

ATM Functions Independently of Mre11/CtIP in Promoting A-EJ

Previous reports suggested ATM may promote DSBs resection through phosphorylating CtIP as the CtIP-T859A mutant compromised resection and HR repair (Peterson et al., 2013; Wang et al., 2013). To investigate the relationship between ATM and Mre11/CtIP in end joining during CSR, we first silenced Mre11 or CtIP expression by shRNA in *ATM*$^{-/-}$ cells (**Supplementary Figure S10A**). While shMre11 in *ATM*$^{-/-}$ cells showed only a mild effect on IgA + cells by surface staining, silencing CtIP slightly decreased (~20%) IgA switching compared with scramble control (**Figure 5A**). However, in *Lig4*$^{-/-}$ *ATM*$^{-/-}$ cells, silencing either Mre11 or CtIP (**Supplementary Figure S10B**) conferred significantly more defect in CSR up to 50% lower than scramble control, a phenotype much more severe than that in *Atm* deletion alone

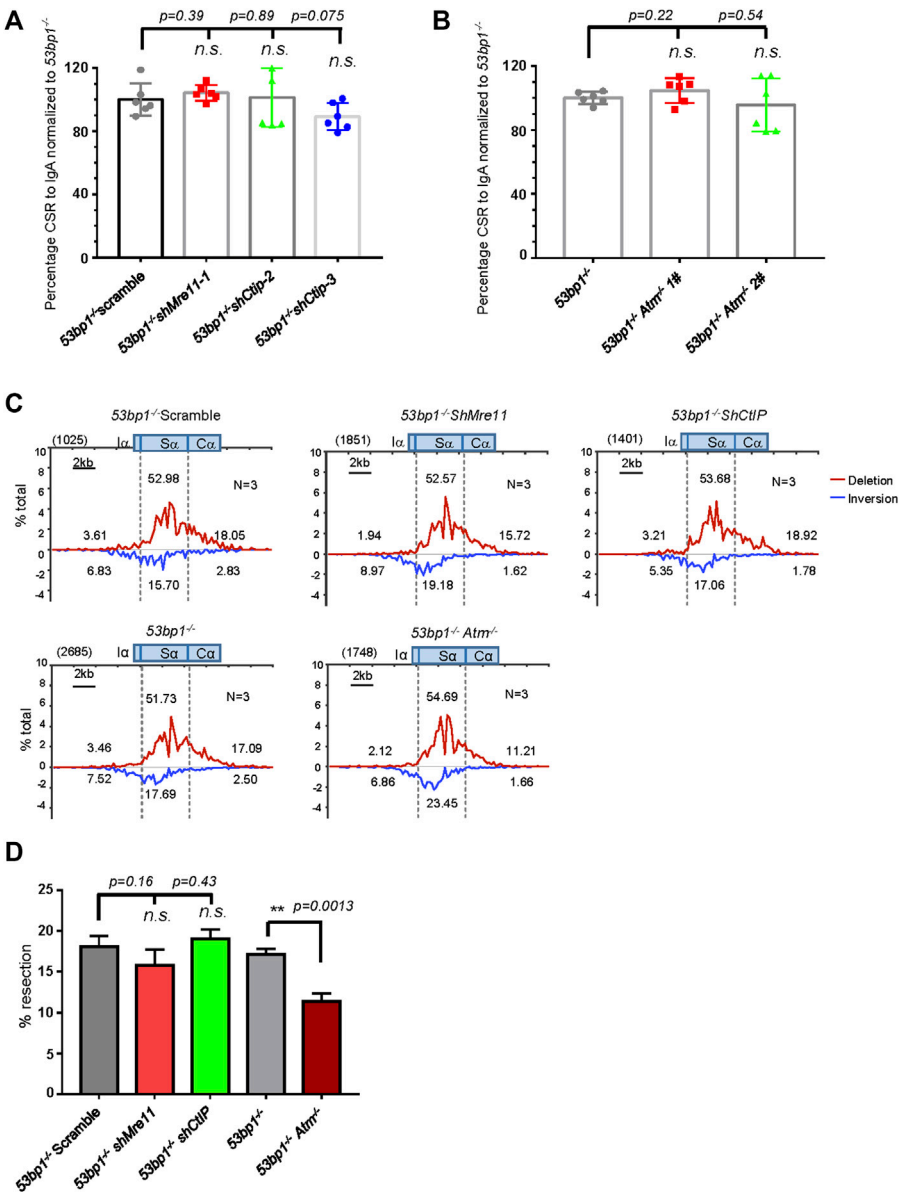

FIGURE 6 | Mre11/CtIP and ATM are not required for CSR in 53bp1$^{-/-}$ cells. **(A)** Silencing Mre11/CtIP did not affect IgA CSR in *53bp1*$^{-/-}$ cells. Data were presented as mean ± SD from six independent experiments (Student's *t*-test, n. s. ($p > 0.05$) indicates non-significant differences). **(B)** Normalized IgA switching efficiency in *Atm*-deleted *53bp1*$^{-/-}$ cells. Data were presented as mean ± SD from six independent experiments (Student's *t*-test, n. s. ($p > 0.05$) indicates non-significant differences). **(C)** Linear distribution of pooled Sμ-Sα junctions recovered from HTGTS libraries with CSR activated Mre11/CtIP-silenced and ATM knockout *53bp1*$^{-/-}$ cells. Numbers (*N*) indicated experiment repeats. **(D)** Percentage of long resection junction in Sμ-Sα junctions recovered from HTGTS libraries with Mre11/CtIP-silenced and ATM-deficient *53bp1*$^{-/-}$ cells. CSR and HTGTS analysis were assayed at 72 h after stimulation with α-CD40/IL-4/TGF-β. Data were presented as mean ± SEM (Student's *t*-test, $^{*}p < 0.05$, $^{**}p < 0.01$, n. s. ($p > 0.05$) indicates non-significant differences).

(**Figure 5B**), suggesting that Mre11 and CtIP function in part via different pathways than ATM in promoting A-EJ in Lig4-deficient cells.

To further confirm the above observation, we treated Mre11 or CtIP-silenced WT or *Lig4*$^{-/-}$ cells with DMSO or AZD1390 before stimulating them for CSR. Consistent with aforementioned findings, silencing only CtIP but not Mre11 in DMSO-treated WT cells resulted in a mild IgA switching defect (**Figure 5C**). As expected, ATMi treatment decreased IgA switching of scramble control cells compared with DMSO treatment; no significant difference in switch efficiency was observed between ATMi-treated control and shMre11 cells (**Figure 5C**). In contrast, ATMi-treated shCtIP cells showed further IgA defect than scramble control cells under the same treatment (**Figure 5C**). These data confirmed an epistatic effect between ATM and Mre11, and a non-overlapping function of ATM and CtIP in c-NHEJ-mediated cells. In stark contrast, ATMi treatment indeed caused more severe switching defect

in *Lig4*$^{-/-}$ cells infected with either shMre11 or shCtIP compared with that of scramble control (**Figure 5D**). Taken together, these data implicated that while ATM and Mre11 are epistatic in c-NHEJ-mediated CSR, it functions at least in part independent of Mre11 and CtIP in promoting A-EJ-mediated CSR in *Lig4*$^{-/-}$ cells.

Less Dependency on Mre11/CtIP-Mediated Resection for Class Switch Recombination in *53bp1*$^{-/-}$ Cells

Ours and others' previous reports had indicated that 53BP1-deficient B cells underwent greatly impaired CSR characterized by significantly increased S region DSB resection and MH usage in S-S junctions (Bothmer et al., 2013; Dong et al., 2015), representing a scenario similar to A-EJ comparing to c-NHEJ factor ablation. To investigate whether Mre11/CtIP-mediated resection plays any role in A-EJ in 53BP1-deficient cells, we first silenced these two factors with lentiviral expressed shRNA (**Supplementary Figure S11A**) and stimulated them for switching. However, in contrast to what we observed in *Lig4*$^{-/-}$ cells, silencing Mre11 or CtIP in *53bp1*$^{-/-}$ cells did not lead to further defect in IgA switching compared with that of scramble control (**Figure 6A**). ATM kinase inhibition by AZD1390 in *53bp1*$^{-/-}$ cells resulted in very mild, if there was any, additive decline in switching than DMSO controls (**Supplementary Figure S11B**). Similarly, *Atm* gene knockout by CRISPR/Cas9 in *53bp1*$^{-/-}$ cells (**Supplementary Figures S11C,D**) did not change its switching efficiency (**Figure 6B**), suggesting that ATM and its kinase activity are not required for A-EJ in this setting.

We also deleted resection factor EXD2 in *53bp1*$^{-/-}$ cells and results showed EXD2 depletion did not further reduce IgA switching (**Supplementary Figures S11E,F**). Similar to the observations with WT CH12F3 cells, deleting Exo1 in *53bp1*$^{-/-}$ nearly completely abolished switching, and re-introducing either EXO1^{WT} or Exo1^{E109K} mutants back to the *53bp1*$^{-/-}$ *Exo1*$^{-/-}$ double-mutant cells restored IgA switching to the *53bp1*$^{-/-}$ level (**Supplementary Figures S11G–I**), suggesting that Exo1-mediated DSB resection was not required for A-EJ in 53BP1-deficient cells. Taken together, it appears that neither short-range nor long-range resections factors were critical for A-EJ in 53BP1-deficient cells, and the requirement for resection activity in A-EJ-mediated CSR is context dependent.

To gain more insight into the effect of Mre11/CtIP and ATM kinase on class switch in *53bp1*$^{-/-}$ cells, we applied HTGTS assay with Mre11/CtIP-silenced or *Atm*-deleted *53bp1*$^{-/-}$ cells. Consistent with the IgA FACS staining data, HTGTS revealed similar levels of Sμ-Sα joining in all cells with shMre11 or shCtIP or *ATM* deletion compared with *53bp1*$^{-/-}$ control cells (**Supplementary Figures S12A,B**). Surprisingly, we found that Mre11 or CtIP silencing did not change the overall pattern of Sα joining in *53bp1*$^{-/-}$ cells in that deletional versus inversional Sα joins and levels of SαDSB resection were similar in shMre11 and shCtIP-infected *53bp1*$^{-/-}$ cells compared with those in scramble control cells (**Figures 6C,D**, **Supplementary Figure S12C**). However, we indeed observed a significant increase in the percentage of direct junctions and junctions with 1 base pair of microhomology sequences in shMre11 cells (**Supplementary Figure S12D**), implicating that Mre11 and CtIP may have different roles in mediating MH-mediated joining in this context. *Atm* gene deletion, on the other hand, resulted in significantly decreased Sα DSB long resection without changing MH usage in Sα junctions (**Figures 6C,D**, **Supplementary Figure S12D**). Taken together, we concluded that while only ATM activity is required for Sα DSB resection in 53BP1-deficient cells, neither Mre11/CtIP nor ATM is required for the residual switching in this setting.

DISCUSSION

Our previous studies reported elevated S region DSB resection and MH usage in 53*bp1*$^{-/-}$ or *Lig4*$^{-/-}$ than that in wild type cells (Dong et al., 2015; Panchakshari et al., 2018). In this study, we continue to demonstrate that DSB resection factors together with ATM play important roles in meditating A-EJ in the absence of Lig4. Based on the findings from this study and others' reports, we summarize the roles of each individual factor in CSR in the absence of Lig4 or 53BP1. Consistent with a prior report (Dinkelmann et al., 2009), the mild increase in resection and MH usage in Mre11-silenced cells that resembled (but not as severe) ATM-deficient cells supports the notion that Mre11 has a minor role in meditating c-NHEJ in wild type B cells through activating ATM-dependent DDR. In contrast, CtIP deficiency impaired CSR but the nearly identical resection and junctional MH as control cells indicates that CtIP is not strictly required for end joining in WT cells. The mild CSR defect in CtIP-deficient WT cells had been attributed to impaired cellular proliferation or AID expression (Lee-Theilen et al., 2011; Liu et al., 2019). Our data that several shCtIP clones with different proliferation rates and AID levels showed similar efficiency indicated other mechanisms may underlie CtIP's role in CSR. An interesting hypothesis is that CtIP facilitates DSB end bridging independent of resection initiation, as a recent study suggested (Öz et al., 2020), likely through multimerization (Wang et al., 2012; Andres et al., 2015; Davies et al., 2015). Furthermore, our data clearly supported roles for Mre11/CtIP in A-EJ-mediated CSR in *Lig4*$^{-/-}$ cells. However, it appeared that Mre11/CtIP silencing did not affect S region DSB long resection indicated by the distal Cα junctions in HTGTS assay. As AID-initiated Sα breaks are highly enriched in the core, joining of Sα breaks into Cα would require an Sα DSBs to be resected over a thousand base pairs away from the core region. Thus, the lack of change in Cα junctions in shMre11/shCtIP cells can be explained as that they do not affect Sα DSB "long" resection, and their potential roles in mediating Sα short resection in Lig4-deficient cells cannot be ruled out. In addition, CtIP may have additional Mre11-independent roles in A-EJ in *Lig4*$^{-/-}$ cells in the same fashion in WT cells. In this regard, we indeed found that shCtIP *Lig4*$^{-/-}$ cells showed further decreased ratio of Sα direct versus inversional junctions that was not seen in shMre11 cells, indicating CtIP can participate in A-EJ by promoting deletional Sμ-Sα joining independent of Mre11.

As Mre11 or CtIP silencing further reduced but not completely abolished CSR, there exists Mre11/CtIP-independent A-EJ activities

in Lig4-deficient cells that include BLM/DNA2-mediated long range resection, as deleting *Blm* or silencing DNA2 in *Lig4*$^{-/-}$ cells reduced residual switching. BLM may participate in A-EJ-mediated CSR through two mechanisms. First, it contributes to S region DSB resection in *Lig4*$^{-/-}$ cells by using its helicase activity and in conjunction with DNA2. However, the severe proliferation defect due to impaired S phase DSB repair in Lig4-deficient CSR-activated cells hindered further investigation on this function. Second, BLM may promote resection-generated ssDNA to anneal with each other by its HRDC domain (Wu et al., 2005). We cannot prove or exclude at this point the possibility that the HRDC domain may affect the helicase activity through intramolecular interaction (Newman et al., 2015). To our surprise, the DSB resection activity of Exo1 is not strictly required for A-EJ in this context, an observation consistent with a prior report that the separation-of-function mutation Exo1^{E109K} can still support A-EJ activity in an I-SceI-based assay system (Schaetzlein et al., 2013). This finding was further confirmed by a CRISPR/Cas9-mediated end joining assay that does not rely on Exo1 to generate S region DSBs, supporting the notion that Exo1 and associated resection activity is not required for A-EJ in general.

Corresponding to a recent report (Wang et al., 2020), our data demonstrated that ATM and its intrinsic kinase activity were required for both c-NHEJ and A-EJ-mediated CSR, and there were no obvious differences between ATM kinase inhibition and *Atm* deletion in A-EJ efficiency in Lig4-deficient cells. In c-NHEJ, ATM functions in part to recruit 53BP1-Rif1 to prevent BRCA1/CtIP-mediated S region DSB resection. However, we did not find significant changes in Sα DSBs resection and MH usage in *Atm* deleted or kinase inhibited *Lig4*$^{-/-}$ cells. Prior reports have suggested that ATM promotes CtIP-dependent DSB resection by direct phosphorylation (Wang et al., 2020), our finding with additive CSR impairment in Lig4-deficient cells defective with both ATM and CtIP clearly indicated that ATM activates additional targets in A-EJ other than CtIP.

Lastly, our data revealed the differential needs for Mre11/CtIP/ATM between Lig4-deficient and 53BP1-deficient cells that could stem from the readiness of these cells to undergo resection. In Lig4-deficient cells, 53BP1 is still present at DSBs to recruit Rif1 to counteract CtIP-mediated resection in G1, and a fraction of cells may proceed to S/G2 phase for CtIP/BRCA1 to block Rif1 recruitment to enable resection (Daley and Sung, 2013; Di Virgilio et al., 2013). It is thus conceivable that silencing Mre11 or CtIP in *Lig4*$^{-/-}$ cells can lead to resection inhibition and dampen A-EJ efficiency. On the other hand, in *53bp1*$^{-/-}$ cells the requirement for CtIP to exclude 53BP1/Rif1 becomes minimal as resection suppression by Rif1 has been canceled out. Consistent with the minimal effect of resection on CSR efficiency we observed in *53bp1*$^{-/-}$ cells, a recent report revealed that resection can be largely uncoupled with CSR (Sundaravinayagam et al., 2019) and suggested that higher order chromatin structure by 53BP1 oligomerization is essential to enforce the 3-D architecture of *IgH* locus for efficient class switching (Dong et al., 2015; Fernandez and Chaudhuri, 2019). In this context, resection inhibition in *53bp1*$^{-/-}$ cells by either Mre11/CtIP silencing or ATM ablation did not change A-EJ efficiency, as the requisite *IgH* loops for efficient CSR has already greatly collapsed (Wuerffel et al., 2007; Feldman et al., 2017; Zhang et al., 2019) (Cortizas et al., 2013).

DATA AVAILABILITY STATEMENT

The datasets presented in this study can be found in online repositories. The names of the repository/repositories and accession number(s) can be found in the article/Supplementary Material.

AUTHOR CONTRIBUTIONS

JD, CC, and XS designed the experiments; XS, JB, JX, XX, and MG performed the experiments; XS and J.X. conducted the HTGTS analyses; XS, JB, and JD analyzed the data; and JD and XS wrote the manuscript. Other authors provided reagents, designed or performed specific experiments, and helped revise the paper.

FUNDING

This work is supported by funding from National Natural Science Foundation of China (81871304, 32070892), Guangdong Innovative and Entrepreneurial Research Team Program (grant 2016ZT06S252), Guangzhou Municipal Science and Technology Bureau (202002030064), and funding from the Fundamental Research Funds for the Central Universities (18ykzd11), Sanming Project of Medicine in Shenzhen (SZSM202011004), and Open project of Key Laboratory of Tropical Disease Control (Sun Yat-sen University), Ministry of Education (2020ZX01).

ACKNOWLEDGMENTS

We thank Xingui Wu and Nan Dong for the assistance in bioinformatics analysis.

SUPPLEMENTARY MATERIAL

The Supplementary Material for this article can be found online at: https://www.frontiersin.org/articles/10.3389/fcell.2021.767624/full#supplementary-material

REFERENCES

Andres, S. N., Appel, C. D., Westmoreland, J. W., Williams, J. S., Nguyen, Y., Robertson, P. D., et al. (2015). Tetrameric Ctp1 Coordinates DNA Binding and DNA Bridging in DNA Double-Strand-Break Repair. *Nat. Struct. Mol. Biol.* 22 (2), 158–166. doi:10.1038/nsmb.2945

Audebert, M., Salles, B., and Calsou, P. (2004). Involvement of poly(ADP-Ribose) Polymerase-1 and XRCC1/DNA Ligase III in an Alternative Route for DNA Double-Strand Breaks Rejoining. *J. Biol. Chem.* 279 (53), 55117–55126. doi:10.1074/jbc.m404524200

Babbe, H., McMenamin, J., Hobeika, E., Wang, J., Rodig, S. J., Reth, M., et al. (2009). Genomic Instability Resulting from Blm Deficiency Compromises Development, Maintenance, and Function of the

B Cell Lineage. *J. Immunol.* 182 (1), 347–360. doi:10.4049/jimmunol.182.1.347

Bardwell, P. D., Woo, C. J., Wei, K., Li, Z., Martin, A., Sack, S. Z., et al. (2004). Altered Somatic Hypermutation and Reduced Class-Switch Recombination in Exonuclease 1-mutant Mice. *Nat. Immunol.* 5 (2), 224–229. doi:10.1038/ni1031

Boboila, C., Alt, F. W., and Schwer, B. (2012). Classical and Alternative End-Joining Pathways for Repair of Lymphocyte-specific and General DNA Double-Strand Breaks. *Adv. Immunol.* 116, 1–49. doi:10.1016/b978-0-12-394300-2.00001-6

Boboila, C., Jankovic, M., Yan, C. T., Wang, J. H., Wesemann, D. R., Zhang, T., et al. (2010). Alternative End-Joining Catalyzes Robust IgH Locus Deletions and Translocations in the Combined Absence of Ligase 4 and Ku70. *Proc. Natl. Acad. Sci.* 107 (7), 3034–3039. doi:10.1073/pnas.0915067107

Bothmer, A., Robbiani, D. F., Di Virgilio, M., Bunting, S. F., Klein, I. A., Feldhahn, N., et al. (2011). Regulation of DNA End Joining, Resection, and Immunoglobulin Class Switch Recombination by 53BP1. *Mol. Cel* 42 (3), 319–329. doi:10.1016/j.molcel.2011.03.019

Bothmer, A., Rommel, P. C., Gazumyan, A., Polato, F., Reczek, C. R., Muellenbeck, M. F., et al. (2013). Mechanism of DNA Resection during Intrachromosomal Recombination and Immunoglobulin Class Switching. *J. Exp. Med.* 210 (1), 115–123. doi:10.1084/jem.20121975

Broderick, R., Nieminuszczy, J., Baddock, H. T., Deshpande, R. A., Gileadi, O., Paull, T. T., et al. (2016). EXD2 Promotes Homologous Recombination by Facilitating DNA End Resection. *Nat. Cel Biol* 18 (3), 271–280. doi:10.1038/ncb3303

Buis, J., Wu, Y., Deng, Y., Leddon, J., Westfield, G., Eckersdorff, M., et al. (2008). Mre11 Nuclease Activity Has Essential Roles in DNA Repair and Genomic Stability Distinct from ATM Activation. *Cell* 135 (1), 85–96. doi:10.1016/j.cell.2008.08.015

Callen, E., Di Virgilio, M., Kruhlak, M. J., Nieto-Soler, M., Wong, N., Chen, H. T., et al. (2013). 53BP1 Mediates Productive and Mutagenic DNA Repair through Distinct Phosphoprotein Interactions. *Cell* 153, 1266–1280. English. doi:10.1016/j.cell.2013.05.023

Callén, E., Jankovic, M., Wong, N., Zha, S., Chen, H.-T., Difilippantonio, S., et al. (2009). Essential Role for DNA-PKcs in DNA Double-Strand Break Repair and Apoptosis in ATM-Deficient Lymphocytes. *Mol. Cel* 34 (3), 285–297. doi:10.1016/j.molcel.2009.04.025

Chapman, J. R., Barral, P., Vannier, J.-B., Borel, V., Steger, M., Tomas-Loba, A., et al. (2013). RIF1 Is Essential for 53BP1-dependent Nonhomologous End Joining and Suppression of DNA Double-Strand Break Resection. *Mol. Cel* 49 (5), 858–871. doi:10.1016/j.molcel.2013.01.002

Chen, P.-L., Liu, F., Cai, S., Lin, X., Li, A., Chen, Y., et al. (2005). Inactivation of CtIP Leads to Early Embryonic Lethality Mediated by G 1 Restraint and to Tumorigenesis by Haploid Insufficiency. *Mol. Cel Biol* 25 (9), 3535–3542. doi:10.1128/mcb.25.9.3535-3542.2005

Cortizas, E. M., Zahn, A., Hajjar, M. E., Patenaude, A.-M., Di Noia, J. M., and Verdun, R. E. (2013). Alternative End-Joining and Classical Nonhomologous End-Joining Pathways Repair Different Types of Double-Strand Breaks during Class-Switch Recombination. *J. Immunol.* 191 (11), 5751–5763. doi:10.4049/jimmunol.1301300

Daley, J. M., and Sung, P. (2013). RIF1 in DNA Break Repair Pathway Choice. *Mol. Cel* 49 (5), 840–841. doi:10.1016/j.molcel.2013.02.019

Davies, O. R., Forment, J. V., Sun, M., Belotserkovskaya, R., Coates, J., Galanty, Y., et al. (2015). CtIP Tetramer Assembly Is Required for DNA-End Resection and Repair. *Nat. Struct. Mol. Biol.* 22 (2), 150–157. Epub 2015/01/07. doi:10.1038/nsmb.2937

Di Virgilio, M., Callen, E., Yamane, A., Zhang, W., Jankovic, M., Gitlin, A. D., et al. (2013). Rif1 Prevents Resection of DNA Breaks and Promotes Immunoglobulin Class Switching. *Science* 339 (6120), 711–715. doi:10.1126/science.1230624

Dinkelmann, M., Spehalski, E., Stoneham, T., Buis, J., Wu, Y., Sekiguchi, J. M., et al. (2009). Multiple Functions of MRN in End-Joining Pathways during Isotype Class Switching. *Nat. Struct. Mol. Biol.* 16 (8), 808–813. doi:10.1038/nsmb.1639

Dong, J., Panchakshari, R. A., Zhang, T., Zhang, Y., Hu, J., Volpi, S. A., et al. (2015). Orientation-specific Joining of AID-Initiated DNA Breaks Promotes Antibody Class Switching. *Nature* 525 (7567), 134–139. Epub 2015/08/27. doi:10.1038/nature14970

Escribano-Díaz, C., Orthwein, A., Fradet-Turcotte, A., Xing, M., Young, J. T. F., Tkáč, J., et al. (2013). A Cell Cycle-dependent Regulatory Circuit Composed of 53BP1-RIF1 and BRCA1-CtIP Controls DNA Repair Pathway Choice. *Mol. Cel* 49 (5), 872–883. doi:10.1016/j.molcel.2013.01.001

Feldman, S., Wuerffel, R., Achour, I., Wang, L., Carpenter, P. B., and Kenter, A. L. (2017). 53BP1 Contributes to Igh Locus Chromatin Topology during Class Switch Recombination. *J. Immunol.* 198 (6), 2434–2444. doi:10.4049/jimmunol.1601947

Fernandez, K. C., and Chaudhuri, J. (2019). Uncoupling the DSB End-Protecting and CSR-Promoting Functions of 53BP1. *Cel Rep.* 28 (6), 1387–1388. doi:10.1016/j.celrep.2019.07.076

Franco, S., Gostissa, M., Zha, S., Lombard, D. B., Murphy, M. M., Zarrin, A. A., et al. (2006). H2AX Prevents DNA Breaks from Progressing to Chromosome Breaks and Translocations. *Mol. Cel* 21 (2), 201–214. doi:10.1016/j.molcel.2006.01.005

Franco, S., Murphy, M. M., Li, G., Borjeson, T., Boboila, C., and Alt, F. W. (2008). DNA-PKcs and Artemis Function in the End-Joining Phase of Immunoglobulin Heavy Chain Class Switch Recombination. *J. Exp. Med.* 205 (3), 557–564. doi:10.1084/jem.20080044

Frit, P., Barboule, N., Yuan, Y., Gomez, D., and Calsou, P. (2014). Alternative End-Joining Pathway(s): Bricolage at DNA Breaks. *DNA Repair* 17, 81–97. doi:10.1016/j.dnarep.2014.02.007

Garcia, V., Phelps, S. E. L., Gray, S., and Neale, M. J. (2011). Bidirectional Resection of DNA Double-Strand Breaks by Mre11 and Exo1. *Nature* 479 (7372), 241–244. doi:10.1038/nature10515

Han, L., Masani, S., Hsieh, C.-l., and Yu, K. (2014). DNA Ligase I Is Not Essential for Mammalian Cell Viability. *Cel Rep.* 7 (2), 316–320. doi:10.1016/j.celrep.2014.03.024

Helmink, B. A., Tubbs, A. T., Dorsett, Y., Bednarski, J. J., Walker, L. M., Feng, Z., et al. (2011). H2AX Prevents CtIP-Mediated DNA End Resection and Aberrant Repair in G1-phase Lymphocytes. *Nature* 469 (7329), 245–249. doi:10.1038/nature09585

Hwang, J. K., Alt, F. W., and Yeap, L. S. (2015). Related Mechanisms of Antibody Somatic Hypermutation and Class Switch Recombination. *Microbiol. Spectr.* 3, MDNA3 0037 2014. doi:10.1128/microbiolspec.MDNA3-0037-2014

Lee-Theilen, M., Matthews, A. J., Kelly, D., Zheng, S., and Chaudhuri, J. (2011). CtIP Promotes Microhomology-Mediated Alternative End Joining during Class-Switch Recombination. *Nat. Struct. Mol. Biol.* 18 (1), 75–79. doi:10.1038/nsmb.1942

Liu, X., Jiang, W., Dubois, R. L., Yamamoto, K., Wolner, Z., and Zha, S. (2012). Overlapping Functions between XLF Repair Protein and 53BP1 DNA Damage Response Factor in End Joining and Lymphocyte Development. *Proc. Natl. Acad. Sci.* 109 (10), 3903–3908. English. doi:10.1073/pnas.1120160109

Liu, X., Wang, X. S., Lee, B. J., Wu-Baer, F. K., Lin, X., Shao, Z., et al. (2019). CtIP Is Essential for Early B Cell Proliferation and Development in Mice. *J. Exp. Med.* 216 (7), 1648–1663. English. doi:10.1084/jem.20181139

Lu, G., Duan, J., Shu, S., Wang, X., Gao, L., Guo, J., et al. (2016). Ligase I and Ligase III Mediate the DNA Double-Strand Break Ligation in Alternative End-Joining. *Proc. Natl. Acad. Sci. USA* 113 (5), 1256–1260. doi:10.1073/pnas.1521597113

Makharashvili, N., Tubbs, A. T., Yang, S.-H., Wang, H., Barton, O., Zhou, Y., et al. (2014). Catalytic and Noncatalytic Roles of the CtIP Endonuclease in Double-Strand Break End Resection. *Mol. Cel* 54 (6), 1022–1033. English. doi:10.1016/j.molcel.2014.04.011

Manis, J. P., Morales, J. C., Xia, Z., Kutok, J. L., Alt, F. W., and Carpenter, P. B. (2004). 53BP1 Links DNA Damage-Response Pathways to Immunoglobulin Heavy Chain Class-Switch Recombination. *Nat. Immunol.* 5 (5), 481–487. doi:10.1038/ni1067

Masani, S., Han, L., Meek, K., and Yu, K. (2016). Redundant Function of DNA Ligase 1 and 3 in Alternative End-Joining during Immunoglobulin Class Switch Recombination. *Proc. Natl. Acad. Sci. USA* 113 (5), 1261–1266. doi:10.1073/pnas.1521630113

Newman, J. A., Savitsky, P., Allerston, C. K., Bizard, A. H., Özer, Ö., Sarlós, K., et al. (2015). Crystal Structure of the Bloom's Syndrome Helicase Indicates a Role for the HRDC Domain in Conformational Changes. *Nucleic Acids Res.* 43 (10), 5221–5235. doi:10.1093/nar/gkv373

Oksenych, V., Kumar, V., Liu, X., Guo, C., Schwer, B., Zha, S., et al. (2013). Functional Redundancy between the XLF and DNA-PKcs DNA Repair Factors in V(D)J Recombination and Nonhomologous DNA End Joining. *Proc. Natl. Acad. Sci.* 110 (6), 2234–2239. doi:10.1073/pnas.1222573110

Öz, R., Howard, S. M., Sharma, R., Törnkvist, H., Ceppi, I., Kk, S., et al. (2020). Phosphorylated CtIP Bridges DNA to Promote Annealing of Broken Ends. *Proc. Natl. Acad. Sci. USA* 117 (35), 21403–21412. doi:10.1073/pnas.2008645117

Panchakshari, R. A., Zhang, X., Kumar, V., Du, Z., Wei, P.-C., Kao, J., et al. (2018). DNA Double-Strand Break Response Factors Influence End-Joining Features of IgH Class Switch and General Translocation Junctions. *Proc. Natl. Acad. Sci. USA* 115 (4), 762–767. doi:10.1073/pnas.1719988115

Paull, T. T. (2018). 20 Years of Mre11 Biology: No End in Sight. *Mol. Cel* 71 (3), 419–427. doi:10.1016/j.molcel.2018.06.033

Peterson, S. E., Li, Y., Wu-Baer, F., Chait, B. T., Baer, R., Yan, H., et al. (2013). Activation of DSB Processing Requires Phosphorylation of CtIP by ATR. *Mol. Cel* 49 (4), 657–667. doi:10.1016/j.molcel.2012.11.020

Reina-San-Martin, B., Chen, H. T., Nussenzweig, A., and Nussenzweig, M. C. (2004). ATM Is Required for Efficient Recombination between Immunoglobulin Switch Regions. *J. Exp. Med.* 200 (9), 1103–1110. English. doi:10.1084/jem.20041162

Reina-San-Martin, B., Chen, J., Nussenzweig, A., and Nussenzweig, M. C. (2007). Enhanced Intra-switch Region Recombination during Immunoglobulin Class Switch Recombination in 53BP1-/- B Cells. *Eur. J. Immunol.* 37 (1), 235–239. doi:10.1002/eji.200636789

Robert, I., Dantzer, F., and Reina-San-Martin, B. (2009). Parp1 Facilitates Alternative NHEJ, whereas Parp2 Suppresses IgH/c-Myc Translocations during Immunoglobulin Class Switch Recombination. *J. Exp. Med.* 206 (5), 1047–1056. doi:10.1084/jem.20082468

Sartori, A. A., Lukas, C., Coates, J., Mistrik, M., Fu, S., Bartek, J., et al. (2007). Human CtIP Promotes DNA End Resection. *Nature* 450 (7169), 509–514. doi:10.1038/nature06337

Schaetzlein, S., Chahwan, R., Avdievich, E., Roa, S., Wei, K., Eoff, R. L., et al. (2013). Mammalian Exo1 Encodes Both Structural and Catalytic Functions that Play Distinct Roles in Essential Biological Processes. *Proc. Natl. Acad. Sci.* 110 (27), E2470–E2479. English. doi:10.1073/pnas.1308512110

Shibata, A., Moiani, D., Arvai, A. S., Perry, J., Harding, S. M., Genois, M.-M., et al. (2014). DNA Double-Strand Break Repair Pathway Choice Is Directed by Distinct MRE11 Nuclease Activities. *Mol. Cel* 53 (2), 361. doi:10.1016/j.molcel.2014.01.008

Sundaravinayagam, D., Rahjouei, A., Andreani, M., Tupiņa, D., Balasubramanian, S., Saha, T., et al. (2019). 53BP1 Supports Immunoglobulin Class Switch Recombination Independently of its DNA Double-Strand Break End Protection Function. *Cel Rep.* 28 (6), 1389–1399. doi:10.1016/j.celrep.2019.06.035

Symington, L. S. (2016). Mechanism and Regulation of DNA End Resection in Eukaryotes. *Crit. Rev. Biochem. Mol. Biol.* 51 (3), 195–212. doi:10.3109/10409238.2016.1172552

Taccioli, G. E., Amatucci, A. G., Beamish, H. J., Gell, D., Xiang, X. H., Arzayus, M. I. T., et al. (1998). Targeted Disruption of the Catalytic Subunit of the DNA-PK Gene in Mice Confers Severe Combined Immunodeficiency and Radiosensitivity. *Immunity* 9 (3), 355–366. doi:10.1016/s1074-7613(00)80618-4

van Wietmarschen, N., Merzouk, S., Halsema, N., Spierings, D. C. J., Guryev, V., and Lansdorp, P. M. (2018). BLM Helicase Suppresses Recombination at G-Quadruplex Motifs in Transcribed Genes. *Nat. Commun.* 9, 271. doi:10.1038/s41467-017-02760-1

Vogel, J., Bartels, V., Tang, T. H., Churakov, G., Slagter-Jager, J. G., Huttenhofer, A., et al. (2003). RNomics in *Escherichia coli* Detects New sRNA Species and Indicates Parallel Transcriptional Output in Bacteria. *Nucleic Acids Res.* 31 (22), 6435–6443. doi:10.1093/nar/gkg867

Wang, H., Shao, Z., Shi, L. Z., Hwang, P. Y.-H., Truong, L. N., Berns, M. W., et al. (2012). CtIP Protein Dimerization Is Critical for its Recruitment to Chromosomal DNA Double-Stranded Breaks. *J. Biol. Chem.* 287 (25), 21471–21480. doi:10.1074/jbc.m112.355354

Wang, H., Shi, L. Z., Wong, C. C. L., Han, X., Hwang, P. Y.-H., Truong, L. N., et al. (2013). The Interaction of CtIP and Nbs1 Connects CDK and ATM to Regulate HR-Mediated Double-Strand Break Repair. *Plos Genet.* 9 (2), e1003277. doi:10.1371/journal.pgen.1003277

Wang, X. S., Zhao, J., Wu-Baer, F., Shao, Z., Lee, B. J., Cupo, O. M., et al. (2020). CtIP-mediated DNA Resection Is Dispensable for IgH Class Switch Recombination by Alternative End-Joining. *Proc. Natl. Acad. Sci. USA* 117 (41), 25700–25711. doi:10.1073/pnas.2010972117

Ward, I. M., Reina-San-Martin, B., Olaru, A., Minn, K., Tamada, K., Lau, J. S., et al. (2004). 53BP1 Is Required for Class Switch Recombination. *J. Cel Biol* 165 (4), 459–464. doi:10.1083/jcb.200403021

Wu, L., Lung Chan, K., Ralf, C., Bernstein, D. A., Garcia, P. L., Bohr, V. A., et al. (2005). The HRDC Domain of BLM Is Required for the Dissolution of Double Holliday Junctions. *Embo J.* 24 (14), 2679–2687. doi:10.1038/sj.emboj.7600740

Wuerffel, R., Wang, L., Grigera, F., Manis, J., Selsing, E., Perlot, T., et al. (2007). S-S Synapsis during Class Switch Recombination Is Promoted by Distantly Located Transcriptional Elements and Activation-Induced Deaminase. *Immunity* 27 (5), 711–722. English. doi:10.1016/j.immuni.2007.09.007

Xu, Z., Zan, H., Pone, E. J., Mai, T., and Casali, P. (2012). Immunoglobulin Class-Switch DNA Recombination: Induction, Targeting and beyond. *Nat. Rev. Immunol.* 12 (7), 517–531. doi:10.1038/nri3216

Yamane, A., Robbiani, D. F., Resch, W., Bothmer, A., Nakahashi, H., Oliveira, T., et al. (2013). RPA Accumulation during Class Switch Recombination Represents 5′-3′ DNA-End Resection during the S-G2/M Phase of the Cell Cycle. *Cel Rep.* 3 (1), 138–147. doi:10.1016/j.celrep.2012.12.006

Yan, C. T., Boboila, C., Souza, E. K., Franco, S., Hickernell, T. R., Murphy, M., et al. (2007). IgH Class Switching and Translocations Use a Robust Non-classical End-Joining Pathway. *Nature* 449 (7161), 478–U9. doi:10.1038/nature06020

Yu, K. F., and Lieber, M. R. (2019). Current Insights into the Mechanism of Mammalian Immunoglobulin Class Switch Recombination. *Crit. Rev. Biochem. Mol.* 12 (4), 333–351. doi:10.1080/10409238.2019.1659227

Zha, S., Guo, C., Boboila, C., Oksenych, V., Cheng, H.-L., Zhang, Y., et al. (2011). ATM Damage Response and XLF Repair Factor Are Functionally Redundant in Joining DNA Breaks. *Nature* 469 (7329), 250–254. doi:10.1038/nature09604

Zhang, X., Zhang, Y., Ba, Z., Kyritsis, N., Casellas, R., and Alt, F. W. (2019). Fundamental Roles of Chromatin Loop Extrusion in Antibody Class Switching. *Nature* 575 (7782), 385–389. doi:10.1038/s41586-019-1723-0

Zimmermann, M., Lottersberger, F., Buonomo, S. B., Sfeir, A., and de Lange, T. (2013). 53BP1 Regulates DSB Repair Using Rif1 to Control 5′ End Resection. *Science* 339 (6120), 700–704. English. doi:10.1126/science.1231573

Conflict of Interest: The authors declare that the research was conducted in the absence of any commercial or financial relationships that could be construed as a potential conflict of interest.

Publisher's Note: All claims expressed in this article are solely those of the authors and do not necessarily represent those of their affiliated organizations, or those of the publisher, the editors and the reviewers. Any product that may be evaluated in this article, or claim that may be made by its manufacturer, is not guaranteed or endorsed by the publisher.

frontiers in Cell and Developmental Biology

REVIEW
published: 20 December 2021
doi: 10.3389/fcell.2021.794754

RNA m^{6}A Modification in Immunocytes and DNA Repair: The Biological Functions and Prospects in Clinical Application

Mingjie Zhou[1,2,3†], *Wei Liu*[2†], *Jieyan Zhang*[4] *and Nan Sun*[1*]

[1]Department of Blood Transfusion, The Fourth Hospital of Hebei Medical University, Shijiazhuang, China, [2]Department of Immunology, Hebei Medical University, Shijiazhuang, China, [3]Department of Hand Surgery, Huashan Hospital, Fudan University, Shanghai, China, [4]Department of Orthopaedics, Wuxi Branch of Zhongda Hospital Southeast University, Wuxi, China

As the most prevalent internal modification in mRNA, N^6-methyladenosine (m^{6}A) plays broad biological functions *via* fine-tuning gene expression at the post-transcription level. Such modifications are deposited by methyltransferases (i.e., m^{6}A Writers), removed by demethylases (i.e., m^{6}A Erasers), and recognized by m^{6}A binding proteins (i.e., m^{6}A Readers). The m^{6}A decorations regulate the stability, splicing, translocation, and translation efficiency of mRNAs, and exert crucial effects on proliferation, differentiation, and immunologic functions of immunocytes, such as T lymphocyte, B lymphocyte, dendritic cell (DC), and macrophage. Recent studies have revealed the association of dysregulated m^{6}A modification machinery with various types of diseases, including AIDS, cancer, autoimmune disease, and atherosclerosis. Given the crucial roles of m^{6}A modification in activating immunocytes and promoting DNA repair in cells under physiological or pathological states, targeting dysregulated m^{6}A machinery holds therapeutic potential in clinical application. Here, we summarize the biological functions of m^{6}A machinery in immunocytes and the potential clinical applications *via* targeting m^{6}A machinery.

Keywords: m^{6}A (N^6-methyladenosine), immunocyte, epigenetics, immunotherapy, DNA repair

OPEN ACCESS

Edited by:
Teng Ma,
Capital Medical University, China

Reviewed by:
Lei Gao,
City of Hope National Medical Center, United States
Qi Cui,
Beckman Research Institute, City of Hope, United States

****Correspondence:***
Nan Sun
sunnantheone@163.com

†These authors have contributed equally to this work

Specialty section:
This article was submitted to Signaling, a section of the journal Frontiers in Cell and Developmental Biology

Received: *14 October 2021*
Accepted: *01 November 2021*
Published: *20 December 2021*

Citation:
Zhou M, Liu W, Zhang J and Sun N (2021) RNA m^{6}A Modification in Immunocytes and DNA Repair: The Biological Functions and Prospects in Clinical Application. Front. Cell Dev. Biol. 9:794754. doi: 10.3389/fcell.2021.794754

INTRODUCTION

While RNA modification was first identified in 1970s, it becomes a research focus in recent years. It broadly exists in different species, including fungi (Bodi et al., 2015), plants (Yue et al., 2019), and animals (Yoon et al., 2017; Xia et al., 2018). During the past decades, researchers have found that RNA methylation is a widespread modification in coding sequence and non-coding sequence (Huang et al., 2020), most of which are located at the amine group outside ring, special nitrogen and carbon positions of purine and pyrimidine, and the oxygen atom of the 2′-OH moiety (Liu and Jia, 2014). If classified by the modified position, RNA methylation mainly consists of N^6-methyladenosine (m^{6}A), 5-methylcytosine (m^{5}C), N^7-methylguanosine (m^{7}G), etc., among which m^{7}G cap at the 5′end of RNA sequence has been rigorously studied for decades (Devarkar et al., 2016; Pandolfini et al., 2019). However, m^{6}A modification, representing the most abundant modification, needs further study.

As reported, m^{6}A modifications are localized in the conversed DRACH motifs (D = G/A/U, R = G/A, H = A/U/C). The distribution of m^{6}A is usually in the coding and 3′ untranslated regions,

especially enriched in the upstream of stop codon in mRNA (Roundtree et al., 2017). Recent researches find that m^{6}A modification is also an important biological mark of endogenous circular RNA (circRNA) (Chen et al., 2019). Moreover, m^{6}A modification in lncRNA can regulate the efficiency of glycolysis (Liu J et al., 2019) or promote oncogenesis (Chen et al., 2020). Since m^{6}A modification is dynamic and reversible, the biological function and molecular mechanism of m^{6}A modification have become a research hotspot in many medical fields.

WRITERS, ERASERS, AND READERS

The most momentous breakthrough in this field is the discovery of the m^{6}A machinery involved in m^{6}A modification, including "Writers," "Erasers" and "Readers," performing the function of methyltransferase, demethylase, and recognizing the m^{6}A structure, respectively. They dynamically regulate the homeostasis of m^{6}A and its functions in cells.

Writers

With the function of forming m^{6}A structure, "Writers" protein is a 1 MDa complex composed of multiple subunits, containing Methyltransferase like-3 (METTL3) (Liu et al., 2014), Methyltransferase like-14 (METTL14) (Weng et al., 2018), Wilm's Tumor 1-associating protein (WTAP) (Ping et al., 2014; Sorci et al., 2018), etc. METTL3 is responsible for catalyzing the transfer of methyl group with the support of S-adenosyl-methionine (SAM) in many types of RNA including mRNA and miRNA, while METTL14 is a catalytic cofactor capable of recognizing and binding the target mRNA. WTAP is in charge of recruiting the targeting RNA and locating the METTL3/METTL14/WTAP complex into the nuclear speckles, which is relevant to the prognosis and cisplatin resistance (Ma et al., 2021) of cancer and the infiltration of T lymphocyte within tumors (Li H et al., 2020). New subunits, termed RBM15/RBM15B (Knuckles et al., 2018), KIAA1429 (Lan et al., 2019), ZFP217 (Song et al., 2019), and ZC3H3 (Silla et al., 2020), have been identified, and their functions involve in the recruitment, m^{6}A modification of mRNA or lncRNA, and regulation of the m^{6}A catalytic efficiency. Different types of "Writers" may interact with each other, as a result of which may influence the progression of some diseases such as colorectal cancer (Chen H et al., 2021).

Erasers

The m^{6}A structure can be erased by the "Erasers" protein. Fat mass and obesity-associated protein (FTO) (Jia et al., 2011) was supposed to be the first demethylase discovered, whose existence confirmed the reversibility of m^{6}A modification. FTO and the second identified "Erasers" called AlkB Homolog 5 (ALKBH5) (Zheng et al., 2013) jointly counter the m^{6}A modification of "Writers," thus maintaining the homeostasis of m^{6}A level in cells, whereas the distribution of the two proteins are tissue-specific. The amino acid sequence HXDXnH and RXXXXXR (X = any amino acid) with demethylase activity are contained in their mutual AlkB domain. Both of them remove the m^{6}A methylation from mRNA with the Fe (II)/α-ketoglutarate-dependent dioxygenase (Fedeles et al., 2015). The demonstration of "Writers" and "Erasers" initiates a new branch, namely, m^{6}A research, in the field of epigenetics. Recent studies on ALKBH5 gradually elucidate its multiple functions in disease progressing and therapeutic efficacy, including CD4$^+$ T cell pathogenicity in autoimmunity (Zhou et al., 2021), anti PD-1 response in tumor treatment (Li N et al., 2020), glucocorticoid resistance in T-cell acute lymphoblastic leukemia cell treatment (Gong et al., 2021), etc.

Readers

The level of m^{6}A in cells is dynamically modulated by "Writers" and "Erasers," while "Readers" can recognize the m^{6}A structure and regulate the subsequent cell processes such as translation and stability of mRNA. The YTH domain-containing family is the first confirmed component of "Readers," characterized by the YTH domain at C terminus. YTHDF1~3 and YTHDC1~2 (Kasowitz et al., 2018; Zhou et al., 2020) are identified as m^{6}A binding proteins, among which researches concerning YTHDF are more detailed. Generally speaking, the aforementioned m^{6}A "Readers" proteins have the same function of binding the m^{6}A-modified mRNA with the consensus YTH domain at C terminus, while YTHDF1 promote translation by binding the m^{6}A at translation initiation site (Zhuang et al., 2019); YTHDF2, characterized by the P/Q/N-rich domain at N terminus, recruits the CCR4-NOT deadenylase complex and brings the target mRNA to cytoplasmic P bodies (Du et al., 2016), resulting in the destabilization of mRNA (Paris et al., 2019); YTHDF3 is also related to mRNA decay, but it is regarded to have a synergistic effect on YTHDF1 and YTHDF2 (Ni et al., 2019). In contrast to YTHDF, additional Readers such as insulin-like growth factor 2 mRNA-binding proteins (IGF2BPs) (Hanniford et al., 2020) can uniquely stabilize the target mRNA, while the eukaryotic initiation factor 3 (eIF3) (Meyer et al., 2015; Wolf et al., 2020) can promote cap-independent translation of mRNA with 5′-UTR m^{6}A modified. Moreover, other m^{6}A Readers like ELAVL1 (Zhang et al., 2017) are being studied recently.

ROLES OF M^{6}A MODIFICATION IN IMMUNOCYTES

Immunocytes play a crucial role in a variety of bioprocesses, such as recognizing and presenting the pathogen and immune response, whose depletion or dysfunction is the important pathological basis of tumorigenesis, viral infection, and autoimmune diseases, etc. Previous researches focused on the function of m^{6}A in cancer cells, including endometrial cancer (Liu et al., 2018), breast cancer (Cai et al., 2018), bladder cancer (Cheng et al., 2019), hepatocellular cancer (Zhao X et al., 2018), nasopharyngeal cancer (Zhang et al., 2018), glioblastoma stem cells (Cui et al., 2017), acute myeloid leukemia (Cui et al., 2017), etc. Nevertheless, recent m^{6}A researches on T lymphocyte, B lymphocyte, DC, and macrophage broaden our cognition

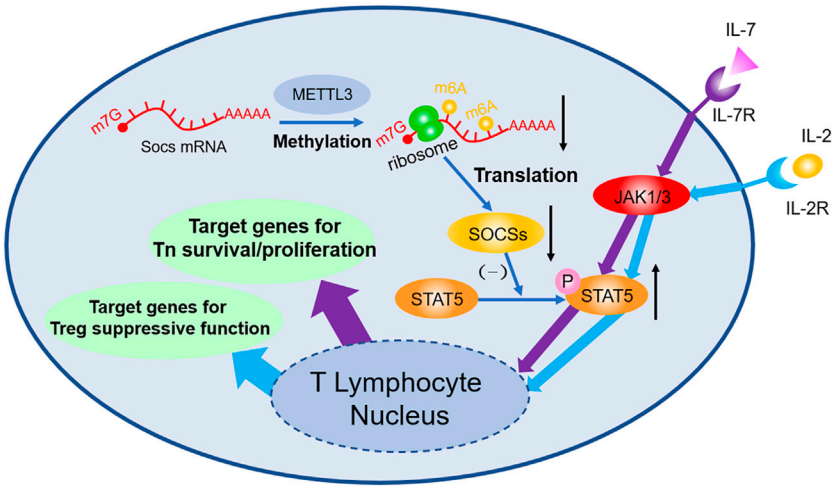

FIGURE 1 | m^{6}A decoration contributes to the regulation of Tn differentiation and Treg function both through JAK-STAT5 pathway. m^{6}A modifications in *Soc1*, *Soc3*, and *Cish* mRNA accelerate their degradation, thus decreasing the expression of SOCS. As a consequence, through the JAK/STAT5 pathway, IL-7 induced differentiation of Tn and IL-2 induced suppressive function of Treg are both influenced afterwards.

towards the human immune system, which are the latest achievements of m^{6}A modification.

T Lymphocyte

T lymphocyte is the executant of human adaptive immune system, which is related to antitumor immunity and autoimmune diseases. Furthermore, T lymphocyte is likely to have interaction with neural stem cells, thus inhibiting its proliferation and resulting in age-related brain disease (Dulken et al., 2019); the abnormal level of m5C, another form of RNA methylation, in CD^{4+} T lymphocytes may have a potential link with the pathogenesis of systemic lupus erythematosus (SLE) (Guo G et al., 2020). According to the differences in function and phenotype, T lymphocyte can be divided into subtypes including naïve T cell (Tn), cytotoxic T cell, regulatory T cell (Treg), helper T cell (Th), etc., which is mainly driven by the stimulation of inflammation factor such as interleukin (IL) and tumor necrosis factor (TNF). Recently, bile acid has been proved to be an accessional regulator of Th17 (Hang et al., 2019) and Treg differentiation. The newly discovered subtype termed exhausted T cell (Tex) along with its key transcription factor called thymocyte selection-associated high mobility group box (TOX) (Scott et al., 2019) is a breakthrough in antitumor study, although the connection between Tex and m^{6}A remains to be explored.

Studies focusing on m^{6}A in T lymphocyte mark the initiation of m^{6}A study in adaptive immune field. Li H-B et al. (2017) found that 5 weeks after transplant of wild type Tn, Rag$^{-/-}$ mice develop colitis due to the differentiation of Tn into effector T cell, whereas Rag$^{-/-}$ mice with Mettl3$^{-/-}$ transplanted exhibit no sign of similar symptoms and no T cell infiltration or inflammation inside spleen and colon can be observed. FACS shows the dysfunction of Mettl3$^{-/-}$ Tn differentiation. Molecular biology studies indicate that *Soc1*, *Soc3*, and *Cish* mRNA are stabilized owing to the lack of m^{6}A modification; afterwards, elevated SOCS protein inhibits the phosphorylation of STAT5, then the IL-7 mediated JAK-STAT5 pathway will be blocked, and thus the differentiation of Tn is suffocated. However, because Mettl3$^{-/-}$ strengthen ERK and APK pathway simultaneously, no obvious increase in T cell apoptosis can be observed. Follow-up study (Tong et al., 2018) found that Tn homeostasis of Mettl3$^{f/f}$; CD4-Cre mice can be destroyed and have colitis 3 months after being born, because Treg's suppression of effector T cell is faulted. During this process, genetic depletion of *Mettl3* reduces the m^{6}A modification of *Socs* mRNA, then stabilizes mRNA, and upregulates its expression. High level SOCS protein inhibits IL-2-STAT5 pathway, resulting in the dysfunction of Treg. Additionally, it is demonstrated that Treg can strengthen type-II DC's ability of presenting antigen (Binnewies et al., 2019), enhance antitumor response, and improve prognosis of checkpoint blockade such as PD-1 block immunotherapy (shown in **Figure 1**).

Another study (Lu et al., 2020) unveils the function of *Mettl14* in T lymphocytes. In this research, CD4-Cre$^{+/Tg}$ Mettl14$^{FL/FL}$ conditional knockout mice have found to develop spontaneous colitis due to the increased level in Th1 cytokines, such as IFN-γ and TNF-α. Follow-up studies show that RORγt expression in *Mettl14* deficient Tregs is downregulated compared to the wild-type Tregs and the induction efficacy of *Mettl14* deficient Tn to iTreg is obviously impaired. As a consequence, both the reduction of iTregs, whose function has reported to be controlling the experimental colitis, and the dysfunctional Mettl14 deficient Tregs lead to the development of spontaneous colitis. With the function of METTL3 in T follicular helper cell differentiation being clarified recently (Yao et al., 2021), plenty of evidences have persuade us that m^{6}A may play an irreplaceable role in all subtypes of T cells.

Furthermore, in acute myeloid leukemia (AML), FTO inhibition can lead to downregulation of leukocyte immunoglobulin-like receptor subfamily B member 4 (LILRB4), render AML cells vulnerable to activated T cells,

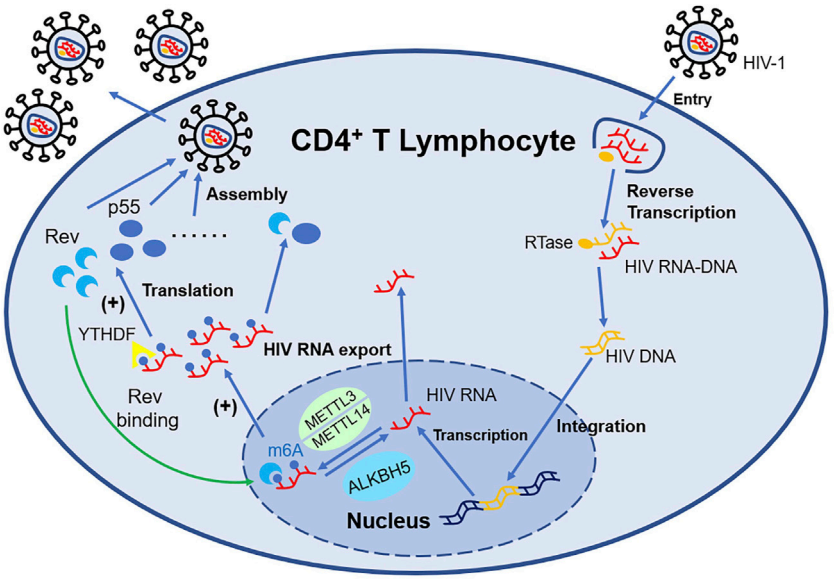

FIGURE 2 | m^{6}A-associated proteins in HIV-infected T lymphocytes regulate the expression of HIV mRNA. METTL3/METTL14 can install m^{6}A decoration on HIV mRNA, while ALKBH5 can remove such modification. YTHDF1-3 recognize the m^{6}A structure and influence the expression of HIV mRNA such as Rev and p55. With the support of Rev, HIV mRNA modified by m^{6}A can export nucleus more easily, which promote the replication of HIV.

and simultaneously overcome hypomethylating agent (HMA)-induced immune evasion. FTO's function in anti-tumor immunity, especially its function in T cells, can be a promising therapeutic strategy in the field of m^{6}A research (Su et al., 2020).

In addition, when CD4$^+$ T cell is infected by the Human Immunodeficiency Virus (HIV), both HIV RNA and intrinsic RNA will be obviously increased (Lichinchi et al., 2016) independent of virus replication. Only gp120 will upregulate the level of m^{6}A without influencing the expression of Writers and Erasers (Tirumuru and Wu, 2019). The m^{6}A modification position of HIV RNA mainly distributes at 3′-UTR (Kennedy et al., 2016), which is directly involved in the regulation of viral mRNA nuclear export and protein synthesis. The m^{6}A modification machinery, such as YTHDF (Tirumuru et al., 2016), METTL3/METTL14, and ALKBH5 (Lichinchi et al., 2016), act as a crucial regulator of this process. The m^{6}A modification of HIV RNA will affect the expression of viral proteins including p55 (the product of gene *gag*) and Rev, consequently impacting the viral infectivity and replication, while suppressing the expression of IFN-I in monocytic cells and macrophages at the same time (Chen S et al., 2021). Therefore, antibodies neutralizing gp120 or CD4$^+$ probably have the potential to counter HIV. Besides, Fu et al. (2019) for the first time applied HIV transgenic rats for m^{6}A research and elucidated the role of m^{6}A modification in mRNA in chronic HIV diseases, especially neurologic disorder (shown in **Figure 2**).

In conclusion, the effect of YTHDF2 on virus remains to be ascertained or can be bidirectional (Toro-Ascuy et al., 2016; Lu W et al., 2018); YTHDF3 weakens the viral infectivity and inhibits the viral replication. Uniquely, YTHDF3 can be incorporated into the virion and still keep its antiviral activation, but the HIV protease can cleave the virion containing YTHDF3. This mechanism prevents HIV from being killed thoroughly and provides a new thought for HIV treatment (Jurczyszak et al., 2020).

All the researches above reveal that m^{6}A along with associated protein can alter the stability of mRNA and regulate nuclear export and translation of mRNA, thus influencing the bioprocess of T cell with different phenotype and promoting the progression of certain diseases.

B Lymphocyte

B lymphocyte is involved in the humoral immunity by producing antibodies. Applying bioengineering technology to design special improbable immunogen can induce the synthesis of antibodies with high affinity, which have the potential to treat virus infection, such as HIV (Saunders et al., 2019). A recent clinical study suggests that m^{6}A modification is closely related to the oncogenesis and progress of mantle cell lymphoma (Zhang W et al., 2019). Mantle cell lymphocyte is a kind of non-hodgkin B cell lymphoma characterized by aggressive phenotype and rapid rate of progression. After analysis of 123 samples of clinical patients, the hazard ratios of YTHDF3, METTL3, FTO, METTL14, ALKBH5, YTHDF2, and WTAP are below 1, while those of YTHDF1, KIAA1429, and ELAVL1 are above 1, among which the maximum is ELAVL while the minimum is YTHDF3, implying that ELAVL and YTHDF3 might be the most important regulators of mantle cell lymphoma. Moreover, "m^{6}A index" is proposed to evaluate the prognosis of patients. Without much available biology research data, this statistical study directs a path for the following m^{6}A research concerning B lymphocyte.

Recent studies have shown that the deletion of *Mettl14* can decrease the m^{6}A level in developing B cells and inhibit some

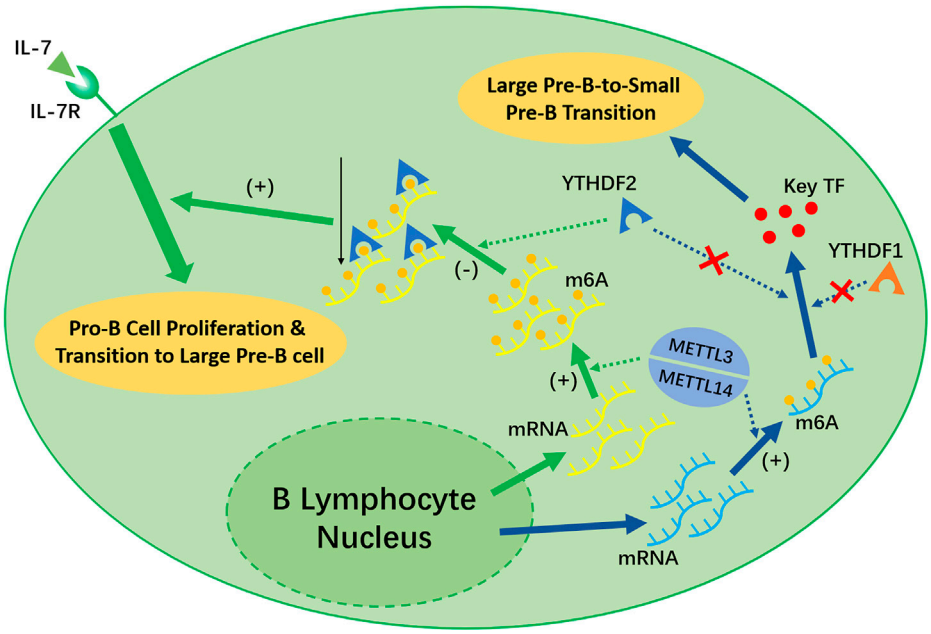

FIGURE 3 | METTL3/METTL14 complex and YTHDF1 is necessary for the early development of B lymphocytes. METTL14 plays an unreplaceable role in the IL-7 induced Pro-B lymphocyte proliferation, Pro-B-to-Large-Pre-B transition, and Large-Pre-B-to-Small-Pre-B transition. YTHDF2 will recognize the m^{6}A modification afterwards and decrease the transcripts as a result, which promote early B lymphocyte development. Notably, YTHDF2 only facilitate in the first two process. The Large-Pre-B-to Small-Pre-B Transition is independent of YTHDF1 or YTHDF2.

important processes, such as the IL-7-induced Pro-B cell proliferation and the transition to the Large Pre-B Stage, which depends on the function of YTHDF2 (Zheng et al., 2020) (shown in **Figure 3**). However, the Large-Pre-B-to-Small-Pre-B Transition depends on METTL14, but is independent of YTHDF1 or YTHDF2 (shown in **Figure 3**).

The pathogenesis of diffuse large B-cell lymphoma (DLBCL), which is the most common subtype of lymphoma derived from B lymphocytes, has been illustrated to have a link with upregulated METTL3 and the m^{6}A level of the mRNA of pigment epithelium-derived factor (Cheng et al., 2020), while PIWI-interacting RNAs have been identified to function in this process recently (Han et al., 2021). The association between B lymphocytes and other m^{6}A methylation-related proteins remains to be explored.

Besides, Kaposi's sarcoma (KS) is evidently associated with infection of HIV and Kaposi's sarcoma-associated herpesvirus (KSHV). KSHV shows strong lymphotropic and invades B cells in the circulation (Myoung and Ganem, 2011). During this process, m^{6}A Reader protein YTHDF2 plays a positive role in KSHV replication (Hesser et al., 2018). However, inconsistent with its feature *in vivo*, KSHV exhibits weaken infectivity and proliferation in B cells lines *in vitro*, so the role of m^{6}A and associated protein in the oncogenesis of KS remains to be explored.

DC

As the bridge between the innate and adaptive immune, DCs function as antigen-presenting cells and can also produce VEGF-α for the recruitment of neutrophil to control cutaneous bacterial infections (Janela et al., 2019). Therefore, DCs play a core role in the eradication of pathogen and inducement of immune tolerance. It has been evidenced that the dysfunction of DC activation is involved in the progression of multiple inflammation, cancer, and autoimmune diseases. Tyrosine kinase AXL can induce the expression of PD-1. IFN-γ and IL-4 can respectively promote and inhibit the production of IL-12; thus, blockade of IL-4 receptor can strengthen antitumor response by expanding the infiltration of T lymphocyte at tumor position (Maier et al., 2020). Though the association between the suppression of DCs and extracellular m^{6}A-modified RNA has been confirmed for decades (Karikó et al., 2005), studies concerning m^{6}A in DCs are still at its infant stage.

Wang H et al. (2019) found that total level of m^{6}A in DCs is increasing parallel with its maturation. The distribution of m^{6}A is mainly located in NLR, TNF, and NF-κB pathways, which are responsible for the induction of co-stimulatory factors and pro-inflammation factors which promote maturation of DCs. METTL3 was involved in this physiological process. Distinct from most of the previous laboratory findings, the fundamental mechanism is the upregulation of translation efficiency, but not the stability of mRNA (Wang H et al., 2019) (shown in **Figure 4**).

Han et al. (2019) discovered the connection between upregulated translation and YTHDF1. The depletion of YTHDF1 in DCs will limit the expression of lysosomal protease, which decelerates the degradation of antigen, thus improving DCs' ability of presenting antigen and activating

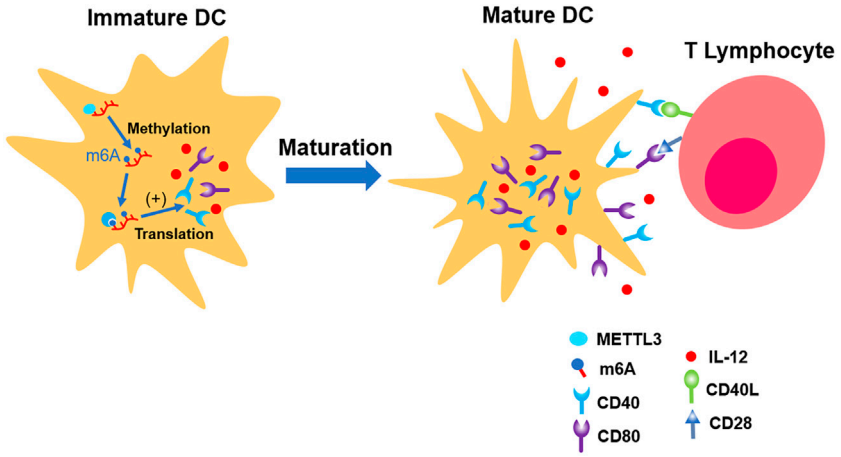

FIGURE 4 | METTL3 up-regulates the expression of CD40, CD80, and IL-12, which promote the maturation of immature DC. In the end, its ability of presenting antigen and interaction with T lymphocytes are strengthened.

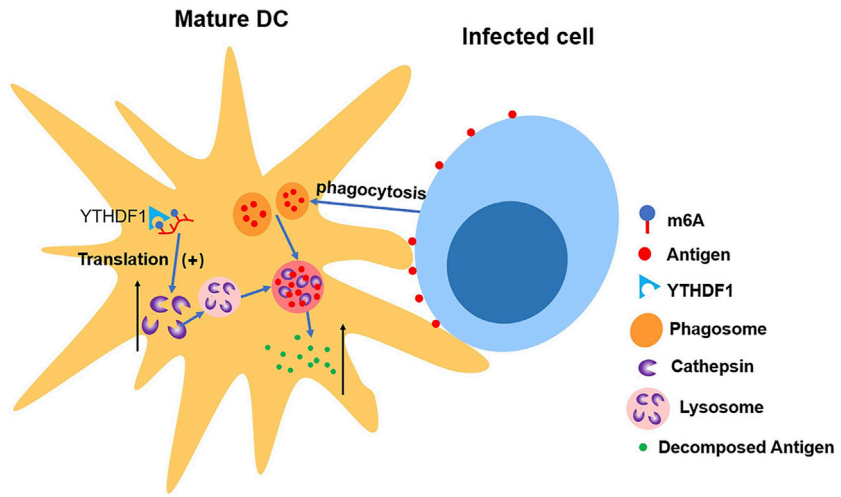

FIGURE 5 | YTHDF1 increases the level of cathepsin in mature DCs, which accelerates the cleavage of antigens in phagosome, making DCs' ability of presenting antigen impaired.

$CD8^+$ T cell. This suggests a new mechanism of immune escape as well as an important reason for weak antitumor immune response in certain clinical cases (Han et al., 2019) (shown in **Figure 5**).

Macrophage

Macrophage is a kind of innate immune cell dwelling in various tissues with multiple subtypes, which can be classified into classically activated macrophages (M1) and alternatively activated macrophages (M2). Early researches have implied the possibility of m^{6}A weakening immune response (Durbin et al., 2016). However, recent researches indicate that m^{6}A modification plays an important role in antivirus, negative feedback control of macrophage activation (Du et al., 2020), and the polarization of macrophages. Roles of m^{6}A Writers, Erasers, and Readers in macrophages are summarized in **Table 1**.

In detail, "Writers" METTL3 catalyzes the m^{6}A methylation at coding sequence (CDS) and 3′-UTR of *STAT1* mRNA, facilitating the polarization of M1, but having opposite impact on M2 (Liu Y et al., 2019). Another study has also illustrated METTL3's function in promoting M1 differentiation, which afterwards benefits bone marrow mesenchymal stem cells (Lei et al., 2021). Moreover, METTL3 can methylate hnRNPA2B1 and *Cgas*, *Ifi16*, and *Sting* mRNA simultaneously, and then the affinity of hnRNPA2B1 to three mRNA above is improved, which ultimately increases the production of IFN-β and amplifies the immune response to DNA virus (Wang L et al., 2019). In addition, METTL3 deficiency have proved to impede the activation of macrophages through TLR4 signaling pathway

TABLE 1 | Roles of m^{6}A Writers, Erasers, and Readers in macrophages.

m^{6}A regulator	Cell subtype	Target genes	Biological function
Writers			
METTL3	M1	*STAT1*	Promote polarization
	M2	*STAT1*	Inhibit polarization
	M1/M2	*Cgas, Ifi16, Sting, hnRNPA2B1*	Increase the production of IFN-β Amplify the immune response to DNA virus
		Irakm	Promote activation
METTL14	M1/M2	*Ebi3*	suppress CD8$^+$ T cell dysfunction and tumor growth
Erasers			
FTO	M1	*STAT1*	Promote polarization
	M2	*STAT6, PPAR-γ*	
ALKBH5	M1/M2	*Mavs, Traf3, Traf6*	Inhibit translation and production of IFN
Readers			
YTHDF2	M1/M2	*STAT1, PPAR-γ*	Impede macrophage activation
		MAP2K4, MAP4K4	Inhibit the expression of pro-inflammatory cytokine and inflammatory response
YTHDF3		*FOX O 3*	Impede the expression of IFN-stimulated genes and immunity response to VSV
IGF2BP2		*TSC1, PPAR-γ*	regulate macrophage phenotypic activation and inflammatory diseases

by stabilizing *Irakm* transcripts (Tong et al., 2021). As for METTL14, there is also indirect evidence indicating its function in suppressing CD8$^+$ T cell dysfunction and tumor growth (Dong et al., 2021).

After knockout of "Erasers" *FTO*, the polarization of both M1 and M2 can be inhibited, during which the expression of STAT1 in M1 was decreased, while the degradation of *STAT6* and *PPAR-γ* mRNA is increased (Gu et al., 2020). Furthermore, ALKBH5 demethylate DDX46-binded *Mavs*, *Traf3*, and *Traf6* mRNAs, leading to the retention of these mRNAs inside nuclear, indirectly inhibiting translation and reducing the production of IFN. In the end, antiviral activation of macrophages is weakened (Zheng et al., 2017).

Knockdown of "Readers" *YTHDF2* can stimulate the expression of *STAT1* (Huangfu et al., 2020) and *PPAR-γ* mRNA (Gu et al., 2020), while forced expression of YTHDF2 could destabilize *MAP2K4* and *MAP4K4* mRNA and activate the NF-κB and MAPK pathway (Yu et al., 2019), which will facilitate LPS-induced osteoclastogenesis and inflammatory response (Fang et al., 2021). YTHDF3 was regarded as a negative regulator of antivirus. With the assistance of PABP1 and elF4G2, YTHDF3 can bind the translation initiation site of *FOXO3* mRNA and promote translation. As a result, the expression of IFN-stimulated genes is inhibited, which weakens the immunity response to Vesicular stomatitis virus (VSV) (Zhang Y et al., 2019). Moreover, another reader IGF2BP2 has also proved to be associated with the phenotypic activation of macrophage (Wang X et al., 2021).

Researches focusing on m^{6}A modification in macrophages reveal its association with some diseases. The occurrence of atherosclerosis (AS) has proved to be linked with m^{6}A modification. During this progress, ox-LDL induces the expression of DDX5 in macrophages and limits the function of METTL3 which transfers the methyl group to macrophages scavenger receptor A (*MSR1*) mRNA. Ultimately, *MSR1* mRNA is stabilized, and more MSR1 is synthesized. Uptake of more lipids further facilitates the formation of foam cells, resulting in the progression of AS (Zhao W et al., 2018). In another study, Zhang X et al. (2021) has also identified the function of METTL3 in promoting ox-LDL-induced inflammation and mitochondrial dysfunction by methylating peroxisome proliferator-activated receptor-γ coactivator 1-alpha (PGC-1α) mRNA with the assistance of YTHDF2. Intriguingly, m5C, another form of RNA methylation, can deteriorate AS induced by hyper-homocysteinemia (Wang et al., 2017), while acute coronary syndrome, whose main pathological basis is AS, is also related to the m^{6}A modification of circ-0029589 in macrophage (Guo M et al., 2020).

The dysfunction of m^{6}A in macrophages is also a pathogenesis factor of autoimmune diseases. Wang J et al. (2019) found that in patients with rheumatoid arthritis, METTL3 in macrophages is obviously improved and positively associated with CRP and ESR. Moreover, lipopolysaccharide (LPS) can stimulate the expression of METTL3 in macrophages and then slack the immune response to inflammation through NF-κB pathway (Wang J et al., 2019). Other autoimmune diseases such as osteoarthritis (Liu Q et al., 2019) and SLE (Li et al., 2018) show possibility of having connection with m^{6}A dysfunction in macrophages.

THE APPLICATION OF M^{6}A MODIFICATION AND ITS DEVELOPMENT PROSPECT

Given the identification of aberrant m^{6}A modification in various diseases, targeting m^{6}A machinery in specific cells can be regarded as a new treatment for viral infection, cancer, and autoimmune diseases. However, changes in m^{6}A levels in different diseases are lack of consistency, so treatment targeting m^{6}A should be supposed to modulating m^{6}A level to normal level, instead of simply accelerating or decelerating m^{6}A modification (Wang et al., 2018).

m^{6}A-Associated Proteins Modulating DNA Repair

Plenty of researches have confirmed the correlation between m^{6}A and DNA repair in different situations. Zhang et al. have reported the

TABLE 2 | m^{6}A-associated proteins in DNA repair.

m^{6}A regulator	Biological function
Writers	
METTL3	Modulate DNA-RNA hybrid accumulation Regulate accumulation of the three-stranded R-loops Regulate the m^{6}A modification in ultraviolet-induced DNA damage Direct the recruitment of Pol κ to the DNA damage sites
METTL14	Enhance translation of DNA repair genes Suppress ultraviolet-induced skin tumorigenesis
KIAA1429	Interfere with DNA damage response in cisplatin-treated germ cell tumor
Erasers	
FTO	Regulate the m^{6}A modification in ultraviolet-induced DNA damage
ALKBH5	Regulate ROS-induced DNA damage response
Readers	
YTHDC1	Modulate DNA-RNA hybrid accumulation
YTHDF2	Regulate accumulation of the three-stranded R-loops
IGF2BP2	Extend mRNA half time in ROS-induced DNA damage response

METTL3-m^{6}A-YTHDC1 axis which promotes the double-strand breaks by modulating DNA-RNA hybrid accumulation (Zhang et al., 2020). Other researches indicate that accumulation of the three-stranded R-loops, formed by RNA: DNA hybrid and single stranded DNA, is regulated by YTHDF2 (Abakir et al., 2020), METTL3, and tonicity-responsive enhancer binding protein (TonEBP) (Kang et al., 2021). More surprisingly, the arginine substrates of METTL14 itself at intrinsically disordered C terminus can also be methylated. It proved to be an initial signal of interaction between METTL14 and RNA polymerase II, which will afterwards implement the m^{6}A modification of target mRNA. Subsequent studies have confirmed that METTL14 arginine methylation is associated with the enhanced translation of DNA repair genes (Wang Z et al., 2021). Recent studies even clarified the correlation between DNA damage repair and m^{6}A-modified retrotransposable element (RTE) RNAs, in which intronic Long Interspersed Element-1 (LINE-1) interacts with the hosting gene transcription, resulting in the downregulation of its expression (Xiong et al., 2021). KIAA1429 was also recently discovered to have close links with the modulation of response to cisplatin in germ cell tumor by interfering with DNA damage response (Miranda-Gonçalves et al., 2021).

As for Erasers, the homologs of AlkB (ALKBHs), which originally function as repair proteins in *E. coli*, are also important regulators of DNA repair and m^{6}A modification at the same time in mammalian cells (Müller et al., 2017; Müller et al., 2018). Recently, the ERK/JNK/ALKBH5-PTMs/m^{6}A axis has been reported to participate in the regulation of ROS-induced DNA damage response, in which progress IGF2BP also plays a part in extending mRNA half time (Yu et al., 2021). METTL3 and FTO can jointly regulate the m^{6}A modification in RNA at DNA damage sites induced by ultraviolet. The function of DNA polymerase κ (Pol κ), which is the key DNA repair enzyme, require the catalytic activity of METTL3, implying the m^{6}A modification directs the recruitment of Pol κ to the DNA damage sites (Xiang et al., 2017). Furthermore, METTL14 has proved to play a tumor-suppressive role in ultraviolet-induced skin tumorigenesis (Yang et al., 2021). All the m^{6}A-associated proteins which regulate DNA repair are summarized in **Table 2**.

In conclusion, since m^{6}A, along with its associated proteins, plays an important role in the pathogenesis and facilitating DNA repair, attaching m^{6}A-targeted therapy to traditional chemo- or radiotherapy may improve the prognosis of some diseases such as carcinoma through two mechanisms.

Medication Targeting m^{6}A

Abnormally elevated m^{6}A level is the feature of most malignant tumor, so developing new drugs inhibiting m^{6}A modification is the most fundamental idea to treat these diseases. Actually, this kind of drugs has been developed for decades. 3-Deaza-Adenosine (DAA) with its analogue can block S-adenosylhomocysteine (SAH) hydrolase, which results in the accumulation of SAH and feedback suppression of SAM (Chiang, 1998). So DAA can indirectly inhibit the m^{6}A modification of mRNA. However, since DAA can suppress the m^{6}A modification in many physiological or pathological processes, there will be many unexpected side effects, such as the prevention of T lymphocyte activation, hypotensive effect, and activation of gene expression. At present, DAA is mainly used for the treatment of AIDS (Kennedy et al., 2016).

Moreover, some diseases like acute myeloid leukemia (AML) are characterized by the aberrant decrease of m^{6}A (Li Z et al., 2017). Rhein (Chen et al., 2012), curcumin (Lu N et al., 2018), meclofenamic acid (Huang et al., 2015), and Saikosaponin-D (Sun et al., 2021) can inhibit the function of FTO by binding the active site of FTO or m^{6}A position of mRNA. Two emerging small molecules targeting FTO demethylase called FB32 and FB32-2, which can dramatically inhibit the progression of AML cells *in vitro* and *in vivo*, have been developed recently (Huang et al., 2019). Coupled with the latest advancement called STM2457, which is a highly potent and selective first-in-class catalytic inhibitor of METTL3 (Yankova et al., 2021),

we can foresee that the era of treating AML or other diseases featured by m^{6}A level unbalance using m^{6}A-targeted method is coming.

Immunotherapy Targeting m^{6}A

Although solid researches data is unavailable, the regulatory function of m^{6}A modification to immunocytes makes it possible for m^{6}A to be a new target for immunotherapy. It has been demonstrated that m^{6}A is a regulator of Tn differentiation, T lymphocyte homeostasis (Li H-B et al., 2017), and suppressive function of Tregs (Tong et al., 2018). Recent studies have found that loss of METTL3 in myeloid cells reprograms the macrophages and increases Treg infiltration into tumors by influencing the YTHDF1-mediated translation of SPRED2 (Yin et al., 2021). Therefore, inhibiting mRNA m^{6}A modification of Tregs at tumor site or myeloid cells can motivate the antitumor activation of CD8$^+$ T cell, which can be a promising immunotherapy. Meanwhile, inhibiting mRNA m^{6}A modification in Tn can reduce the formation of effector T cell, which is helpful for the treatment for autoimmune diseases. Furthermore, regulating the expression of METTL3 (Wang H et al., 2019) and YTHDF1 to a suitable level can improve DCs' ability of presenting tumor neoantigen. More importantly, depletion of YTHDF1 and blockade of checkpoint have a synergistic effect on strengthening antitumor immunity (Han et al., 2019), and ALKBH5 (Li N et al., 2020) and METTL3/14 (Wang et al., 2020) have also proved to regulate anti PD-1 response. So as for patients resistant to the PD-1 immunotherapy, targeting m^{6}A can be a new alternative treatment. Since m^{6}A decoration of viral double-stranded RNA can also downregulate the innate sensing pathway of antiviral response (Qiu et al., 2021), immunotherapy targeting m^{6}A is bound to be a promising therapy for various diseases including viral infections, autoimmune disorders, cancers, etc.

DISCUSSION

As the most abundant post-transcriptional mRNA modification in mammals, m^{6}A is involved in the occurrence of several diseases. Recently, an enormous amount of m^{6}A related studies in immunocytes highlight the fact that targeting m^{6}A can be a promising new treatment strategy for viral infection, cancer, and autoimmune diseases. However, in different cell lines, diseases, even different types of the same diseases, the changes of m^{6}A level, as well as functions of three m^{6}A-associated enzymes lack consistency. Moreover, m^{6}A modification is widely involved in a variety of cellular processes and medication targeting m^{6}A is not selective. All these reasons indicate that clinical treatment *via* targeting m^{6}A modification may be not safe enough. Thus, there is unmet need to develop more sophisticated techniques for m^{6}A detection (Dai et al., 2018; Castellanos-Rubio et al., 2019). Moreover, detailed studies on disease mechanisms are required to realize the clinical application of m^{6}A-targeting treatment. Pharmaceutical researches on drugs with high selectivity or combination of existing drugs and targeted drug delivery system can also promote the accurate treatment of diseases through the m^{6}A-targeting method. Some recent experimental results have indicated the promising prospects of this field (Zhu et al., 2021). Last but not least, m^{6}A modification is supposed to be highly relevant to gut microbiota (Jabs et al., 2020), heat shock proteins (Feng et al., 2020), sepsis (Sun et al., 2020; Xing et al., 2021), and pulmonary hypertension (Pan et al., 2020) and even peripheral nerve injury (Zhang L et al., 2021). These studies can provide valuable experimental basis for development of new treatments.

AUTHOR CONTRIBUTIONS

WL and NS contributed to the design of the topic. MZ and JZ searched and organized the relevant papers. MZ and JZ wrote the first draft of the manuscript. MZ drew the figures and tables in the manuscript. WL and NS contributed to the polish of the manuscript. All authors contributed to manuscript revision, read, and approved the submitted version.

FUNDING

This work was supported by Medical Research Project of Health Commission of Heibei Province. Development of a novel HER2-targeting CAR-T and its efficacy and safety in solid tumors (No. 20200037). Natural Science Foundation of Hebei Province. GM-CSF rich exosomes from local X-ray irradiated breast tumors mediate lung metastasis by enhancing MDSC recruitment (No. H2020206424).

REFERENCES

Abakir, A., Giles, T. C., Cristini, A., Foster, J. M., Dai, N., Starczak, M., et al. (2020). N6-methyladenosine Regulates the Stability of RNA:DNA Hybrids in Human Cells. *Nat. Genet.* 52 (1), 48–55. doi:10.1038/s41588-019-0549-x

Binnewies, M., Mujal, A. M., Pollack, J. L., Combes, A. J., Hardison, E. A., Barry, K. C., et al. (2019). Unleashing Type-2 Dendritic Cells to Drive Protective Antitumor CD4+ T Cell Immunity. *Cell* 177 (3), 556–571. doi:10.1016/j.cell.2019.02.005

Bodi, Z., Bottley, A., Archer, N., May, S. T., and Fray, R. G. (2015). Yeast m6A Methylated mRNAs Are Enriched on Translating Ribosomes during Meiosis, and under Rapamycin Treatment. *PLoS One* 10, e0132090. doi:10.1371/journal.pone.0132090

Cai, X., Wang, X., Cao, C., Gao, Y., Zhang, S., Yang, Z., et al. (2018). HBXIP-elevated Methyltransferase METTL3 Promotes the Progression of Breast Cancer via Inhibiting Tumor Suppressor Let-7g. *Cancer Lett.* 415, 11–19. doi:10.1016/j.canlet.2017.11.018

Castellanos-Rubio, A., Santin, I., Olazagoitia-Garmendia, A., Romero-Garmendia, I., Jauregi-Miguel, A., Legarda, M., et al. (2019). A Novel RT-QPCR-Based Assay for the Relative Quantification of Residue Specific m6A RNA Methylation. *Sci. Rep.* 9 (1), 4220. doi:10.1038/s41598-019-40018-6

Chen, B., Ye, F., Yu, L., Jia, G., Huang, X., Zhang, X., et al. (2012). Development of Cell-Active N6-Methyladenosine RNA Demethylase FTO Inhibitor. *J. Am. Chem. Soc.* 134 (43), 17963–17971. doi:10.1021/ja3064149

Chen, H., Yao, J., Bao, R., Dong, Y., Zhang, T., Du, Y., et al. (2021). Cross-talk of Four Types of RNA Modification Writers Defines Tumor Microenvironment and Pharmacogenomic Landscape in Colorectal Cancer. *Mol. Cancer* 20 (1), 29. doi:10.1186/s12943-021-01322-w

Chen, S., Kumar, S., Espada, C. E., Tirumuru, N., Cahill, M. P., Hu, L., et al. (2021). N6-methyladenosine Modification of HIV-1 RNA Suppresses Type-I

Interferon Induction in Differentiated Monocytic Cells and Primary Macrophages. *Plos Pathog.* 17, e1009421. doi:10.1371/journal.ppat.1009421

Chen, S., Zhou, L., and Wang, Y. (2020). ALKBH5-mediated m6A Demethylation of lncRNA PVT1 Plays an Oncogenic Role in Osteosarcoma. *Cancer Cel Int* 20, 34. doi:10.1186/s12935-020-1105-6

Chen, Y. G., Chen, R., Ahmad, S., Verma, R., Kasturi, S. P., Amaya, L., et al. (2019). N6-Methyladenosine Modification Controls Circular RNA Immunity. *Mol. Cel* 76 (1), 96–109. doi:10.1016/j.molcel.2019.07.016

Cheng, M., Sheng, L., Gao, Q., Xiong, Q., Zhang, H., Wu, M., et al. (2019). The m6A Methyltransferase METTL3 Promotes Bladder Cancer Progression via AFF4/NF-Kb/MYC Signaling Network. *Oncogene* 38 (19), 3667–3680. doi:10.1038/s41388-019-0683-z

Cheng, Y., Fu, Y., Wang, Y., and Wang, J. (2020). The m6A Methyltransferase METTL3 Is Functionally Implicated in DLBCL Development by Regulating m6A Modification in PEDF. *Front. Genet.* 11, 955. doi:10.3389/fgene.2020.00955

Chiang, P. K. (1998). Biological Effects of Inhibitors of S-Adenosylhomocysteine Hydrolase. *Pharmacol. Ther.* 77 (2), 115–134. doi:10.1016/s0163-7258(97)00089-2

Cui, Q., Shi, H., Ye, P., Li, L., Qu, Q., Sun, G., et al. (2017). m 6 A RNA Methylation Regulates the Self-Renewal and Tumorigenesis of Glioblastoma Stem Cells. *Cel Rep.* 18 (11), 2622–2634. doi:10.1016/j.celrep.2017.02.059

Dai, T., Pu, Q., Guo, Y., Zuo, C., Bai, S., Yang, Y., et al. (2018). Analogous Modified DNA Probe and Immune Competition Method-Based Electrochemical Biosensor for RNA Modification. *Biosens. Bioelectron.* 114, 72–77. doi:10.1016/j.bios.2018.05.018

Devarkar, S. C., Wang, C., Miller, M. T., Ramanathan, A., Jiang, F., Khan, A. G., et al. (2016). Structural Basis for m7G Recognition and 2′-O-Methyl Discrimination in Capped RNAs by the Innate Immune Receptor RIG-I. *Proc. Natl. Acad. Sci. USA* 113 (3), 596–601. doi:10.1073/pnas.1515152113

Dong, L., Chen, C., Zhang, Y., Guo, P., Wang, Z., Li, J., et al. (2021). The Loss of RNA N6-Adenosine Methyltransferase Mettl14 in Tumor-Associated Macrophages Promotes CD8+ T Cell Dysfunction and Tumor Growth. *Cancer Cell* 39 (7), 945–957. doi:10.1016/j.ccell.2021.04.016

Du, H., Zhao, Y., He, J., Zhang, Y., Xi, H., Liu, M., et al. (2016). YTHDF2 Destabilizes m6A-Containing RNA through Direct Recruitment of the CCR4-Not Deadenylase Complex. *Nat. Commun.* 7, 12626. doi:10.1038/ncomms12626

Du, J., Liao, W., Liu, W., Deb, D. K., He, L., Hsu, P. J., et al. (2020). N6-Adenosine Methylation of Socs1 mRNA Is Required to Sustain the Negative Feedback Control of Macrophage Activation. *Developmental Cel* 55 (6), 737–753. doi:10.1016/j.devcel.2020.10.023

Dulken, B. W., Buckley, M. T., Navarro Negredo, P., Saligrama, N., Cayrol, R., Leeman, D. S., et al. (2019). Single-cell Analysis Reveals T Cell Infiltration in Old Neurogenic Niches. *Nature* 571 (7764), 205–210. doi:10.1038/s41586-019-1362-5

Durbin, A. F., Wang, C., Marcotrigiano, J., and Gehrke, L. (2016). RNAs Containing Modified Nucleotides Fail to Trigger RIG-I Conformational Changes for Innate Immune Signaling. *mBio* 7, e00833–16. doi:10.1128/mBio.00833-16

Fang, C., He, M., Li, D., and Xu, Q. (2021). YTHDF2 Mediates LPS-Induced Osteoclastogenesis and Inflammatory Response via the NF-Kb and MAPK Signaling Pathways. *Cell Signal.* 85, 110060. doi:10.1016/j.cellsig.2021.110060

Fedeles, B. I., Singh, V., Delaney, J. C., Li, D., and Essigmann, J. M. (2015). The AlkB Family of Fe(II)/α-Ketoglutarate-dependent Dioxygenases: Repairing Nucleic Acid Alkylation Damage and beyond. *J. Biol. Chem.* 290 (34), 20734–20742. doi:10.1074/jbc.r115.656462

Feng, Y., Hu, Y., Hou, Z., Sun, Q., Jia, Y., and Zhao, R. (2020). Chronic Corticosterone Exposure Induces Liver Inflammation and Fibrosis in Association with m6A-Linked post-transcriptional Suppression of Heat Shock Proteins in Chicken. *Cell Stress and Chaperones* 25 (1), 47–56. doi:10.1007/s12192-019-01034-7

Fu, Y., Zorman, B., Sumazin, P., Sanna, P. P., and Repunte-Canonigo, V. (2019). Epitranscriptomics: Correlation of N6-Methyladenosine RNA Methylation and Pathway Dysregulation in the hippocampus of HIV Transgenic Rats. *PLoS One* 14, e0203566. doi:10.1371/journal.pone.0203566

Gong, H., Liu, L., Cui, L., Ma, H., and Shen, L. (2021). ALKBH5-mediated m6A-demethylation of USP1 Regulated T-cell Acute Lymphoblastic Leukemia Cell Glucocorticoid Resistance by Aurora B. *Mol. Carcinogenesis* 60 (9), 644–657. doi:10.1002/mc.23330

Gu, X., Zhang, Y., Li, D., Cai, H., Cai, L., and Xu, Q. (2020). N6-methyladenosine Demethylase FTO Promotes M1 and M2 Macrophage Activation. *Cell Signal.* 69, 109553. doi:10.1016/j.cellsig.2020.109553

Guo, G., Wang, H., Shi, X., Ye, L., Yan, K., Chen, Z., et al. (2020). Disease Activity-Associated Alteration of mRNA M5 C Methylation in CD4+ T Cells of Systemic Lupus Erythematosus. *Front. Cel Dev. Biol.* 8, 430. doi:10.3389/fcell.2020.00430

Guo, M., Yan, R., Ji, Q., Yao, H., Sun, M., Duan, L., et al. (2020). IFN Regulatory Factor-1 Induced Macrophage Pyroptosis by Modulating m6A Modification of Circ_0029589 in Patients with Acute Coronary Syndrome. *Int. Immunopharmacology* 86, 106800. doi:10.1016/j.intimp.2020.106800

Han, D., Liu, J., Chen, C., Dong, L., Liu, Y., Chang, R., et al. (2019). Anti-tumour Immunity Controlled through mRNA m6A Methylation and YTHDF1 in Dendritic Cells. *Nature* 566 (7743), 270–274. doi:10.1038/s41586-019-0916-x

Han, H., Fan, G., Song, S., Jiang, Y., Qian, C. a., Zhang, W., et al. (2021). piRNA-30473 Contributes to Tumorigenesis and Poor Prognosis by Regulating m6A RNA Methylation in DLBCL. *Blood* 137 (12), 1603–1614. doi:10.1182/blood.2019003764

Hang, S., Paik, D., Yao, L., Kim, E., Trinath, J., Lu, J., et al. (2019). Bile Acid Metabolites Control TH17 and Treg Cell Differentiation. *Nature* 576 (7785), 143–148. doi:10.1038/s41586-019-1785-z

Hanniford, D., Ulloa-Morales, A., Karz, A., Berzoti-Coelho, M. G., Moubarak, R. S., Sánchez-Sendra, B., et al. (2020). Epigenetic Silencing of CDR1as Drives IGF2BP3-Mediated Melanoma Invasion and Metastasis. *Cancer Cell* 37 (1), 55–70. doi:10.1016/j.ccell.2019.12.007

Hesser, C. R., Karijolich, J., Dominissini, D., He, C., and Glaunsinger, B. A. (2018). N6-methyladenosine Modification and the YTHDF2 Reader Protein Play Cell Type Specific Roles in Lytic Viral Gene Expression during Kaposi's Sarcoma-Associated Herpesvirus Infection. *Plos Pathog.* 14, e1006995. doi:10.1371/journal.ppat.1006995

Huang, H., Weng, H., and Chen, J. (2020). m6A Modification in Coding and Non-coding RNAs: Roles and Therapeutic Implications in Cancer. *Cancer Cell* 37 (3), 270–288. doi:10.1016/j.ccell.2020.02.004

Huang, Y., Su, R., Sheng, Y., Dong, L., Dong, Z., Xu, H., et al. (2019). Small-Molecule Targeting of Oncogenic FTO Demethylase in Acute Myeloid Leukemia. *Cancer Cell* 35 (4), 677–691. doi:10.1016/j.ccell.2019.03.006

Huang, Y., Yan, J., Li, Q., Li, J., Gong, S., Zhou, H., et al. (2015). Meclofenamic Acid Selectively Inhibits FTO Demethylation of m6A over ALKBH5. *Nucleic Acids Res.* 43 (1), 373–384. doi:10.1093/nar/gku1276

Huangfu, N., Zheng, W., Xu, Z., Wang, S., Wang, Y., Cheng, J., et al. (2020). RBM4 Regulates M1 Macrophages Polarization through Targeting STAT1-Mediated Glycolysis. *Int. Immunopharmacology* 83, 106432. doi:10.1016/j.intimp.2020.106432

Jabs, S., Biton, A., Bécavin, C., Nahori, M.-A., Ghozlane, A., Pagliuso, A., et al. (2020). Impact of the Gut Microbiota on the m6A Epitranscriptome of Mouse Cecum and Liver. *Nat. Commun.* 11 (1), 1344. doi:10.1038/s41467-020-15126-x

Janela, B., Patel, A. A., Lau, M. C., Goh, C. C., Msallam, R., Kong, W. T., et al. (2019). A Subset of Type I Conventional Dendritic Cells Controls Cutaneous Bacterial Infections through VEGFα-Mediated Recruitment of Neutrophils. *Immunity* 50 (4), 1069–1083. doi:10.1016/j.immuni.2019.03.001

Jia, G., Fu, Y., Zhao, X., Dai, Q., Zheng, G., Yang, Y., et al. (2011). N6-methyladenosine in Nuclear RNA Is a Major Substrate of the Obesity-Associated FTO. *Nat. Chem. Biol.* 7 (12), 885–887. doi:10.1038/nchembio.687

Jurczyszak, D., Zhang, W., Terry, S. N., Kehrer, T., Bermúdez González, M. C., McGregor, E., et al. (2020). HIV Protease Cleaves the Antiviral m6A Reader Protein YTHDF3 in the Viral Particle. *Plos Pathog.* 16, e1008305. doi:10.1371/journal.ppat.1008305

Kang, H. J., Cheon, N. Y., Park, H., Jeong, G. W., Ye, B. J., Yoo, E. J., et al. (2021). TonEBP Recognizes R-Loops and Initiates m6A RNA Methylation for R-Loop Resolution. *Nucleic Acids Res.* 49 (1), 269–284. doi:10.1093/nar/gkaa1162

Karikó, K., Buckstein, M., Ni, H., and Weissman, D. (2005). Suppression of RNA Recognition by Toll-like Receptors: the Impact of Nucleoside Modification and the Evolutionary Origin of RNA. *Immunity* 23 (2), 165–175. doi:10.1016/j.immuni.2005.06.008

Kasowitz, S. D., Ma, J., Anderson, S. J., Leu, N. A., Xu, Y., Gregory, B. D., et al. (2018). Nuclear m6A Reader YTHDC1 Regulates Alternative Polyadenylation

and Splicing during Mouse Oocyte Development. *Plos Genet.* 14, e1007412. doi:10.1371/journal.pgen.1007412

Kennedy, E. M., Bogerd, H. P., Kornepati, A. V. R., Kang, D., Ghoshal, D., Marshall, J. B., et al. (2016). Posttranscriptional M 6 A Editing of HIV-1 mRNAs Enhances Viral Gene Expression. *Cell Host & Microbe* 19 (5), 675–685. doi:10.1016/j.chom.2016.04.002

Knuckles, P., Lence, T., Haussmann, I. U., Jacob, D., Kreim, N., Carl, S. H., et al. (2018). Zc3h13/Flacc Is Required for Adenosine Methylation by Bridging the mRNA-Binding Factor Rbm15/Spenito to the m6A Machinery Component Wtap/Fl(2)d. *Genes Dev.* 32 (5-6), 415–429. doi:10.1101/gad.309146.117

Lan, T., Li, H., Zhang, D., Xu, L., Liu, H., Hao, X., et al. (2019). KIAA1429 Contributes to Liver Cancer Progression through N6-methyladenosine-dependent post-transcriptional Modification of GATA3. *Mol. Cancer* 18 (1), 186. doi:10.1186/s12943-019-1106-z

Lei, H., He, M., He, X., Li, G., Wang, Y., Gao, Y., et al. (2021). METTL3 Induces Bone Marrow Mesenchymal Stem Cells Osteogenic Differentiation and Migration through Facilitating M1 Macrophage Differentiation. *Am. J. Transl Res.* 13 (5), 4376–4388.

Li, H.-B., Tong, J., Zhu, S., Batista, P. J., Duffy, E. E., Zhao, J., et al. (2017). m6A mRNA Methylation Controls T Cell Homeostasis by Targeting the IL-7/STAT5/SOCS Pathways. *Nature* 548 (7667), 338–342. doi:10.1038/nature23450

Li, H., Su, Q., Li, B., Lan, L., Wang, C., Li, W., et al. (2020). High Expression of WTAP Leads to Poor Prognosis of Gastric Cancer by Influencing Tumour-associated T Lymphocyte Infiltration. *J. Cel Mol Med* 24 (8), 4452–4465. doi:10.1111/jcmm.15104

Li, L.-J., Fan, Y.-G., Leng, R.-X., Pan, H.-F., and Ye, D.-Q. (2018). Potential Link between M 6 A Modification and Systemic Lupus Erythematosus. *Mol. Immunol.* 93, 55–63. doi:10.1016/j.molimm.2017.11.009

Li, N., Kang, Y., Wang, L., Huff, S., Tang, R., Hui, H., et al. (2020). ALKBH5 Regulates Anti-PD-1 Therapy Response by Modulating Lactate and Suppressive Immune Cell Accumulation in Tumor Microenvironment. *Proc. Natl. Acad. Sci. USA* 117 (33), 20159–20170. doi:10.1073/pnas.1918986117

Li, Z., Weng, H., Su, R., Weng, X., Zuo, Z., Li, C., et al. (2017). FTO Plays an Oncogenic Role in Acute Myeloid Leukemia as a N 6 -Methyladenosine RNA Demethylase. *Cancer Cell* 31 (1), 127–141. doi:10.1016/j.ccell.2016.11.017

Lichinchi, G., Gao, S., Saletore, Y., Gonzalez, G. M., Bansal, V., Wang, Y., et al. (2016). Dynamics of the Human and Viral m6A RNA Methylomes during HIV-1 Infection of T Cells. *Nat. Microbiol.* 1, 16011. doi:10.1038/nmicrobiol.2016.11

Liu, J., Eckert, M. A., Harada, B. T., Liu, S.-M., Lu, Z., Yu, K., et al. (2018). m6A mRNA Methylation Regulates AKT Activity to Promote the Proliferation and Tumorigenicity of Endometrial Cancer. *Nat. Cel Biol* 20 (9), 1074–1083. doi:10.1038/s41556-018-0174-4

Liu, J., and Jia, G. (2014). Methylation Modifications in Eukaryotic Messenger RNA. *J. Genet. Genomics* 41 (1), 21–33. doi:10.1016/j.jgg.2013.10.002

Liu, J., Yue, Y., Han, D., Wang, X., Fu, Y., Zhang, L., et al. (2014). A METTL3-METTL14 Complex Mediates Mammalian Nuclear RNA N6-Adenosine Methylation. *Nat. Chem. Biol.* 10 (2), 93–95. doi:10.1038/nchembio.1432

Liu, J., Zhang, X., Chen, K., Cheng, Y., Liu, S., Xia, M., et al. (2019). CCR7 Chemokine Receptor-Inducible Lnc-Dpf3 Restrains Dendritic Cell Migration by Inhibiting HIF-1α-Mediated Glycolysis. *Immunity* 50 (3), 600–615. doi:10.1016/j.immuni.2019.01.021

Liu, Q., Li, M., Jiang, L., Jiang, R., and Fu, B. (2019). METTL3 Promotes Experimental Osteoarthritis Development by Regulating Inflammatory Response and Apoptosis in Chondrocyte. *Biochem. Biophysical Res. Commun.* 516 (1), 22–27. doi:10.1016/j.bbrc.2019.05.168

Liu, Y., Liu, Z., Tang, H., Shen, Y., Gong, Z., Xie, N., et al. (2019). The N6-Methyladenosine (m6A)-Forming Enzyme METTL3 Facilitates M1 Macrophage Polarization through the Methylation of STAT1 mRNA. *Am. J. Physiol. Cel Physiol* 317, C762. doi:10.1152/ajpcell.00212.2019

Lu, N., Li, X., Yu, J., Li, Y., Wang, C., Zhang, L., et al. (2018). Curcumin Attenuates Lipopolysaccharide-Induced Hepatic Lipid Metabolism Disorder by Modification of M6 A RNA Methylation in Piglets. *Lipids* 53 (1), 53–63. doi:10.1002/lipd.12023

Lu, T. X., Zheng, Z., Zhang, L., Sun, H.-L., Bissonnette, M., Huang, H., et al. (2020). A New Model of Spontaneous Colitis in Mice Induced by Deletion of an RNA m6A Methyltransferase Component METTL14 in T Cells. *Cell Mol. Gastroenterol. Hepatol.* 10 (4), 747–761. doi:10.1016/j.jcmgh.2020.07.001

Lu, W., Tirumuru, N., St. Gelais, C., Koneru, P. C., Liu, C., Kvaratskhelia, M., et al. (2018). N6-Methyladenosine-binding Proteins Suppress HIV-1 Infectivity and Viral Production. *J. Biol. Chem.* 293 (34), 12992–13005. doi:10.1074/jbc.ra118.004215

Ma, H., Shen, L., Yang, H., Gong, H., Du, X., and Li, J. (2021). m6A Methyltransferase Wilms' Tumor 1-associated Protein Facilitates Cell Proliferation and Cisplatin Resistance in NK/T Cell Lymphoma by Regulating Dual-specificity Phosphatases 6 Expression via m6A RNA Methylation. *IUBMB Life* 73 (1), 108–117. doi:10.1002/iub.2410

Maier, B., Leader, A. M., Chen, S. T., Tung, N., Chang, C., LeBerichel, J., et al. (2020). A Conserved Dendritic-Cell Regulatory Program Limits Antitumour Immunity. *Nature* 580 (7802), 257–262. doi:10.1038/s41586-020-2134-y

Meyer, K. D., Patil, D. P., Zhou, J., Zinoviev, A., Skabkin, M. A., Elemento, O., et al. (2015). 5′ UTR m6A Promotes Cap-independent Translation. *Cell* 163 (4), 999–1010. doi:10.1016/j.cell.2015.10.012

Miranda-Gonçalves, V., Lobo, J., Guimarães-Teixeira, C., Barros-Silva, D., Guimarães, R., Cantante, M., et al. (2021). The Component of the m6A Writer Complex VIRMA Is Implicated in Aggressive Tumor Phenotype, DNA Damage Response and Cisplatin Resistance in Germ Cell Tumors. *J. Exp. Clin. Cancer Res.* 40 (1), 268. doi:10.1186/s13046-021-02072-9

Müller, T. A., Struble, S. L., Meek, K., and Hausinger, R. P. (2018). Characterization of Human AlkB Homolog 1 Produced in Mammalian Cells and Demonstration of Mitochondrial Dysfunction in ALKBH1-Deficient Cells. *Biochem. Biophysical Res. Commun.* 495 (1), 98–103. doi:10.1016/j.bbrc.2017.10.158

Müller, T. A., Tobar, M. A., Perian, M. N., and Hausinger, R. P. (2017). Biochemical Characterization of AP Lyase and m6A Demethylase Activities of Human AlkB Homologue 1 (ALKBH1). *Biochemistry* 56 (13), 1899–1910. doi:10.1021/acs.biochem.7b00060

Myoung, J., and Ganem, D. (2011). Infection of Lymphoblastoid Cell Lines by Kaposi's Sarcoma. *J. Virol.* 85 (19), 9767–9777. doi:10.1128/jvi.05136-11

Ni, W., Yao, S., Zhou, Y., Liu, Y., Huang, P., Zhou, A., et al. (2019). Long Noncoding RNA GAS5 Inhibits Progression of Colorectal Cancer by Interacting with and Triggering YAP Phosphorylation and Degradation and Is Negatively Regulated by the m6A Reader YTHDF3. *Mol. Cancer* 18 (1), 143. doi:10.1186/s12943-019-1079-y

Pan, Y. Y., Yang, J. X., Xu, Y. F., and Mao, W. (2020). Yin Yang-1 Suppresses CD40 ligand-CD40 Signaling-mediated Anti-inflammatory Cytokine Interleukin-10 Expression in Pulmonary Adventitial Fibroblasts by Promoting Histone H3 Tri-methylation at Lysine 27 Modification on Interleukin-10 Promoter. *Cell Biol Int* 44 (7), 1544–1555. doi:10.1002/cbin.11351

Pandolfini, L., Barbieri, I., Bannister, A. J., Hendrick, A., Andrews, B., Webster, N., et al. (2019). METTL1 Promotes Let-7 MicroRNA Processing via m7G Methylation. *Mol. Cel* 74 (6), 1278–1290. doi:10.1016/j.molcel.2019.03.040

Paris, J., Morgan, M., Campos, J., Spencer, G. J., Shmakova, A., Ivanova, I., et al. (2019). Targeting the RNA m6A Reader YTHDF2 Selectively Compromises Cancer Stem Cells in Acute Myeloid Leukemia. *Cell Stem Cell* 25 (1), 137–148. doi:10.1016/j.stem.2019.03.021

Ping, X.-L., Sun, B.-F., Wang, L., Xiao, W., Yang, X., Wang, W.-J., et al. (2014). Mammalian WTAP Is a Regulatory Subunit of the RNA N6-Methyladenosine Methyltransferase. *Cell Res* 24 (2), 177–189. doi:10.1038/cr.2014.3

Qiu, W., Zhang, Q., Zhang, R., Lu, Y., Wang, X., Tian, H., et al. (2021). N6-methyladenosine RNA Modification Suppresses Antiviral Innate Sensing Pathways via Reshaping Double-Stranded RNA. *Nat. Commun.* 12 (1), 1582. doi:10.1038/s41467-021-21904-y

Roundtree, I. A., Evans, M. E., Pan, T., and He, C. (2017). Dynamic RNA Modifications in Gene Expression Regulation. *Cell* 169 (7), 1187–1200. doi:10.1016/j.cell.2017.05.045

Saunders, K. O., Wiehe, K., Tian, M., Acharya, P., Bradley, T., Alam, S. M., et al. (2019). Targeted Selection of HIV-specific Antibody Mutations by Engineering B Cell Maturation. *Science* 366, e7199. doi:10.1126/science.aay7199

Scott, A. C., Dündar, F., Zumbo, P., Chandran, S. S., Klebanoff, C. A., Shakiba, M., et al. (2019). TOX Is a Critical Regulator of Tumour-specific T Cell Differentiation. *Nature* 571 (7764), 270–274. doi:10.1038/s41586-019-1324-y

Silla, T., Schmid, M., Dou, Y., Garland, W., Milek, M., Imami, K., et al. (2020). The Human ZC3H3 and RBM26/27 Proteins Are Critical for PAXT-Mediated Nuclear RNA Decay. *Nucleic Acids Res.* 48 (5), 2518–2530. doi:10.1093/nar/gkz1238

Song, T., Yang, Y., Wei, H., Xie, X., Lu, J., Zeng, Q., et al. (2019). Zfp217 Mediates m6A mRNA Methylation to Orchestrate Transcriptional and post-transcriptional Regulation to Promote Adipogenic Differentiation. *Nucleic Acids Res.* 47 (12), 6130–6144. doi:10.1093/nar/gkz312

Sorci, M., Ianniello, Z., Cruciani, S., Larivera, S., Ginistrelli, L. C., Capuano, E., et al. (2018). METTL3 Regulates WTAP Protein Homeostasis. *Cell Death Dis* 9 (8), 796. doi:10.1038/s41419-018-0843-z

Su, R., Dong, L., Li, Y., Gao, M., Han, L., Wunderlich, M., et al. (2020). Targeting FTO Suppresses Cancer Stem Cell Maintenance and Immune Evasion. *Cancer Cell* 38 (1), 79–96. doi:10.1016/j.ccell.2020.04.017

Sun, K., Du, Y., Hou, Y., Zhao, M., Li, J., Du, Y., et al. (2021). Saikosaponin D Exhibits Anti-leukemic Activity by Targeting FTO/m6A Signaling. *Theranostics* 11 (12), 5831–5846. doi:10.7150/thno.55574

Sun, X., Dai, Y., Tan, G., Liu, Y., and Li, N. (2020). Integration Analysis of m6A-SNPs and eQTLs Associated with Sepsis Reveals Platelet Degranulation and *Staphylococcus aureus* Infection Are Mediated by m6A mRNA Methylation. *Front. Genet.* 11, 7. doi:10.3389/fgene.2020.00007

Tirumuru, N., Zhao, B. S., Lu, W., Lu, Z., He, C., and Wu, L. (2016). N(6)-methyladenosine of HIV-1 RNA Regulates Viral Infection and HIV-1 Gag Protein Expression. *eLife* 5, e15528. doi:10.7554/eLife.15528

Tirumuru, N., and Wu, L. (2019). HIV-1 Envelope Proteins Up-Regulate N6-Methyladenosine Levels of Cellular RNA Independently of Viral Replication. *J. Biol. Chem.* 294 (9), 3249–3260. doi:10.1074/jbc.ra118.005608

Tong, J., Wang, X., Liu, Y., Ren, X., Wang, A., Chen, Z., et al. (2021). Pooled CRISPR Screening Identifies m6A as a Positive Regulator of Macrophage Activation. *Sci. Adv.* 7, eabd4742. doi:10.1126/sciadv.abd4742

Tong, J., Cao, G., Zhang, T., Sefik, E., Amezcua Vesely, M. C., Broughton, J. P., et al. (2018). m6A mRNA Methylation Sustains Treg Suppressive Functions. *Cel Res* 28 (2), 253–256. doi:10.1038/cr.2018.7

Toro-Ascuy, D., Rojas-Araya, B., Valiente-Echeverría, F., and Soto-Rifo, R. (2016). Interactions between the HIV-1 Unspliced mRNA and Host mRNA Decay Machineries. *Viruses* 8 (11), 320. doi:10.3390/v8110320

Wang, H., Hu, X., Huang, M., Liu, J., Gu, Y., Ma, L., et al. (2019). Mettl3-mediated mRNA m6A Methylation Promotes Dendritic Cell Activation. *Nat. Commun.* 10 (1), 1898. doi:10.1038/s41467-019-09903-6

Wang, J., Yan, S., Lu, H., Wang, S., and Xu, D. (2019). METTL3 Attenuates LPS-Induced Inflammatory Response in Macrophages via NF-Kb Signaling Pathway. *Mediators Inflamm.* 2019, 3120391. doi:10.1155/2019/3120391

Wang, L., Hui, H., Agrawal, K., Kang, Y., Li, N., Tang, R., et al. (2020). m6 A RNA Methyltransferases METTL3/14 Regulate Immune Responses to Anti-PD-1 Therapy. *EMBO J.* 39, e104514. doi:10.15252/embj.2020104514

Wang, L., Wen, M., and Cao, X. (2019). Nuclear hnRNPA2B1 Initiates and Amplifies the Innate Immune Response to DNA Viruses. *Science* 365, eaav0758. doi:10.1126/science.aav0758

Wang, N., Tang, H., Wang, X., Wang, W., and Feng, J. (2017). Homocysteine Upregulates interleukin-17A Expression via NSun2-Mediated RNA Methylation in T Lymphocytes. *Biochem. Biophysical Res. Commun.* 493 (1), 94–99. doi:10.1016/j.bbrc.2017.09.069

Wang, S., Chai, P., Jia, R., and Jia, R. (2018). Novel Insights on m6A RNA Methylation in Tumorigenesis: a Double-Edged Sword. *Mol. Cancer* 17 (1), 101. doi:10.1186/s12943-018-0847-4

Wang, X., Ji, Y., Feng, P., Liu, R., Li, G., Zheng, J., et al. (2021). The m6A Reader IGF2BP2 Regulates Macrophage Phenotypic Activation and Inflammatory Diseases by Stabilizing TSC1 and PPAR γ. *Adv. Sci.* 8 (13), 2100209. doi:10.1002/advs.202100209

Wang, Z., Pan, Z., Adhikari, S., Harada, B. T., Shen, L., Yuan, W., et al. (2021). m(6) A Deposition Is Regulated by PRMT1-Mediated Arginine Methylation of METTL14 in its Disordered C-Terminal Region. *EMBO J.* 40 (5), e106309. doi:10.15252/embj.2020106309

Weng, H., Huang, H., Wu, H., Qin, X., Zhao, B. S., Dong, L., et al. (2018). METTL14 Inhibits Hematopoietic Stem/Progenitor Differentiation and Promotes Leukemogenesis via mRNA m6A Modification. *Cell Stem Cell* 22 (2), 191–205. doi:10.1016/j.stem.2017.11.016

Wolf, D. A., Lin, Y., Duan, H., and Cheng, Y. (2020). eIF-Three to Tango: Emerging Functions of Translation Initiation Factor eIF3 in Protein Synthesis and Disease. *J. Mol. Cel Biol* 12 (6), 403–409. doi:10.1093/jmcb/mjaa018

Xia, H., Zhong, C., Wu, X., Chen, J., Tao, B., Xia, X., et al. (2018). Mettl3 Mutation Disrupts Gamete Maturation and Reduces Fertility in Zebrafish. *Genetics* 208 (2), 729–743. doi:10.1534/genetics.117.300574

Xiang, Y., Laurent, B., Hsu, C.-H., Nachtergaele, S., Lu, Z., Sheng, W., et al. (2017). RNA m6A Methylation Regulates the Ultraviolet-Induced DNA Damage Response. *Nature* 543 (7646), 573–576. doi:10.1038/nature21671

Xing, Y., Cheng, D., Shi, C., and Shen, Z. (2021). The Protective Role of YTHDF1-Knock Down Macrophages on the Immune Paralysis of Severe Sepsis Rats with ECMO. *Microvasc. Res.* 137, 104178. doi:10.1016/j.mvr.2021.104178

Xiong, F., Wang, R., Lee, J.-H., Li, S., Chen, S.-F., Liao, Z., et al. (2021). RNA m6A Modification Orchestrates a LINE-1-Host Interaction that Facilitates Retrotransposition and Contributes to Long Gene Vulnerability. *Cel Res* 31 (8), 861–885. doi:10.1038/s41422-021-00515-8

Yang, Z., Yang, S., Cui, Y-H., Wei, J., Shah, P., Park, G., et al. (2021). METTL14 Facilitates Global Genome Repair and Suppresses Skin Tumorigenesis. *Proc. Natl. Acad. Sci. U S A.* 118 (35), e2025948118. doi:10.1073/pnas.2025948118

Yankova, E., Blackaby, W., Albertella, M., Rak, J., De Braekeleer, E., Tsagkogeorga, G., et al. (2021). Small-molecule Inhibition of METTL3 as a Strategy against Myeloid Leukaemia. *Nature* 593 (7860), 597–601. doi:10.1038/s41586-021-03536-w

Yao, Y., Yang, Y., Guo, W., Xu, L., You, M., Zhang, Y.-C., et al. (2021). METTL3-dependent m6A Modification Programs T Follicular Helper Cell Differentiation. *Nat. Commun.* 12 (1), 1333. doi:10.1038/s41467-021-21594-6

Yin, H., Zhang, X., Yang, P., Zhang, X., Peng, Y., Li, D., et al. (2021). RNA m6A Methylation Orchestrates Cancer Growth and Metastasis via Macrophage Reprogramming. *Nat. Commun.* 12 (1), 1394. doi:10.1038/s41467-021-21514-8

Yoon, K.-J., Ringeling, F. R., Vissers, C., Jacob, F., Pokrass, M., Jimenez-Cyrus, D., et al. (2017). Temporal Control of Mammalian Cortical Neurogenesis by m6A Methylation. *Cell* 171 (4), 877–889. doi:10.1016/j.cell.2017.09.003

Yu, F., Wei, J., Cui, X., Yu, C., Ni, W., Bungert, J., et al. (2021). Post-translational Modification of RNA m6A Demethylase ALKBH5 Regulates ROS-Induced DNA Damage Response. *Nucleic Acids Res.* 49 (10), 5779–5797. doi:10.1093/nar/gkab415

Yu, R., Li, Q., Feng, Z., Cai, L., and Xu, Q. (2019). m6A Reader YTHDF2 Regulates LPS-Induced Inflammatory Response. *Ijms* 20 (6), 1323. doi:10.3390/ijms20061323

Yue, H., Nie, X., Yan, Z., and Weining, S. (2019). N6-methyladenosine Regulatory Machinery in Plants: Composition, Function and Evolution. *Plant Biotechnol. J.* 17 (7), 1194–1208. doi:10.1111/pbi.13149

Zhang, C., Chen, L., Peng, D., Jiang, A., He, Y., Zeng, Y., et al. (2020). METTL3 and N6-Methyladenosine Promote Homologous Recombination-Mediated Repair of DSBs by Modulating DNA-RNA Hybrid Accumulation. *Mol. Cel* 79 (3), 425–442. doi:10.1016/j.molcel.2020.06.017

Zhang, J., Kong, L., Guo, S., Bu, M., Guo, Q., Xiong, Y., et al. (2017). hnRNPs and ELAVL1 Cooperate with uORFs to Inhibit Protein Translation. *Nucleic Acids Res.* 45 (5), 2849–2864. doi:10.1093/nar/gkw991

Zhang, L., Hao, D., Ma, P., Ma, B., Qin, J., Tian, G., et al. (2021). Epitranscriptomic Analysis of m6A Methylome after Peripheral Nerve Injury. *Front. Genet.* 12, 686000. doi:10.3389/fgene.2021.686000

Zhang, P., He, Q., Lei, Y., Li, Y., Wen, X., Hong, M., et al. (2018). m6A-mediated ZNF750 Repression Facilitates Nasopharyngeal Carcinoma Progression. *Cel Death Dis* 9 (12), 1169. doi:10.1038/s41419-018-1224-3

Zhang, W., He, X., Hu, J., Yang, P., Liu, C., Wang, J., et al. (2019). Dysregulation of N6-Methyladenosine Regulators Predicts Poor Patient Survival in Mantle Cell Lymphoma. *Oncol. Lett.* 18 (4), 3682–3690. doi:10.3892/ol.2019.10708

Zhang, X., Li, X., Jia, H., An, G., and Ni, J. (2021). The m6A Methyltransferase METTL3 Modifies PGC-1α mRNA Promoting Mitochondrial Dysfunction and oxLDL-Induced Inflammation in Monocytes. *J. Biol. Chem.* 297, 101058. doi:10.1016/j.jbc.2021.101058

Zhang, Y., Wang, X., Zhang, X., Wang, J., Ma, Y., Zhang, L., et al. (2019). RNA-binding Protein YTHDF3 Suppresses Interferon-dependent Antiviral Responses by Promoting FOXO3 Translation. *Proc. Natl. Acad. Sci. USA* 116 (3), 976–981. doi:10.1073/pnas.1812536116

Zhao, W., Wang, Z., Sun, Z., He, Y., Jian, D., Hu, X., et al. (2018). RNA Helicase DDX5 Participates in oxLDL-Induced Macrophage Scavenger Receptor 1

Expression by Suppressing mRNA Degradation. *Exp. Cel Res.* 366 (2), 114–120. doi:10.1016/j.yexcr.2018.03.003

Zhao, X., Chen, Y., Mao, Q., Jiang, X., Jiang, W., Chen, J., et al. (2018). Overexpression of YTHDF1 Is Associated with Poor Prognosis in Patients with Hepatocellular Carcinoma. *Cbm* 21 (4), 859–868. doi:10.3233/cbm-170791

Zheng, G., Dahl, J. A., Niu, Y., Fedorcsak, P., Huang, C.-M., Li, C. J., et al. (2013). ALKBH5 Is a Mammalian RNA Demethylase that Impacts RNA Metabolism and Mouse Fertility. *Mol. Cel* 49 (1), 18–29. doi:10.1016/j.molcel.2012.10.015

Zheng, Q., Hou, J., Zhou, Y., Li, Z., and Cao, X. (2017). The RNA Helicase DDX46 Inhibits Innate Immunity by Entrapping m6A-Demethylated Antiviral Transcripts in the Nucleus. *Nat. Immunol.* 18 (10), 1094–1103. doi:10.1038/ni.3830

Zheng, Z., Zhang, L., Cui, X.-L., Yu, X., Hsu, P. J., Lyu, R., et al. (2020). Control of Early B Cell Development by the RNA N6-Methyladenosine Methylation. *Cel Rep.* 31 (13), 107819. doi:10.1016/j.celrep.2020.107819

Zhou, B., Liu, C., Xu, L., Yuan, Y., Zhao, J., Zhao, W., et al. (2020). N 6 -Methyladenosine Reader Protein YT521-B Homology Domain-Containing 2 Suppresses Liver Steatosis by Regulation of mRNA Stability of Lipogenic Genes. *Hepatology* 73 (1), 91–103. doi:10.1002/hep.31220

Zhou, J., Zhang, X., Hu, J., Qu, R., Yu, Z., Xu, H., et al. (2021). m6A Demethylase ALKBH5 Controls CD4+ T Cell Pathogenicity and Promotes Autoimmunity. *Sci. Adv.* 7, eabg0470. doi:10.1126/sciadv.abg0470

Zhu, X. J., Feng, J. Q., Zheng, M. Z., Yang, Z. R., Zhao, L., Zhang, W., et al. (2021). Metal-Protein Nanoparticles Facilitate Anti-VSV and H1N1 Viruses through the Coordinative Actions on Innate Immune Responses and METTL14. *Macromol Biosci.* 21, e2000382. doi:10.1002/mabi.202000382

Zhuang, M., Li, X., Zhu, J., Zhang, J., Niu, F., Liang, F., et al. (2019). The m6A Reader YTHDF1 Regulates Axon Guidance through Translational Control of Robo3.1 Expression. *Nucleic Acids Res.* 47 (9), 4765–4777. doi:10.1093/nar/gkz157

Conflict of Interest: The authors declare that the research was conducted in the absence of any commercial or financial relationships that could be construed as a potential conflict of interest.

Publisher's Note: All claims expressed in this article are solely those of the authors and do not necessarily represent those of their affiliated organizations, or those of the publisher, the editors and the reviewers. Any product that may be evaluated in this article, or claim that may be made by its manufacturer, is not guaranteed or endorsed by the publisher.

frontiers in Cell and Developmental Biology

REVIEW
published: 21 February 2022
doi: 10.3389/fcell.2021.828657

DNA Damage and Activation of cGAS/STING Pathway Induce Tumor Microenvironment Remodeling

*Rong Shen[1†], Disheng Liu[2†], Xiaoning Wang[3], Zhao Guo[1], Haonan Sun[2], Yanfeng Song[1] and Degui Wang[1]**

[1]School of Basic Medical Sciences, Lanzhou University, Lanzhou, China, [2]The First Hospital of Lanzhou University, Lanzhou, China, [3]School of Medicine, Shandong University, Jinan, China

DNA damage occurs throughout tumorigenesis and development. The immunogenicity of DNA makes it an immune stimulatory molecule that initiates strong inflammatory responses. The cGAS/STING pathway has been investigated as a critical receptor in both exogenous and endogenous DNA sensing to activate the innate immune response. Growing lines of evidence have indicated that activation of the cGAS/STING pathway is critical in antitumor immunity. Recent studies have demonstrated the outstanding advancement of this pathway in tumor-combined immunotherapy; accordingly, increased studies focus on exploration of STING pathway agonists and analogues. However, current studies propose the potential use of the cGAS/STING pathway in tumor initiation and metastasis. Here, we review the molecular mechanisms and activation of the cGAS/STING pathway, and the relationship between DNA damage and this pathway, particularly highlighting the remodeling of immune contexture in tumor environment (TME) triggered by cascade inflammatory signals. A detailed understanding of TME reprogramming initiated by this pathway may pave the way for the development of new therapeutic strategies and rational clinical application.

Keywords: DNA damage, cGAS/STING, interferon, immune response, TME, remodeling, oncotherapy

OPEN ACCESS

Edited by:
Teng Ma,
Capital Medical University, China

Reviewed by:
Kun Xiong,
Central South University, China
Lili Yang,
Tianjin Medical University Cancer Institute and Hospital, China
Hiroshi Maekawa,
Northwestern University, United States

****Correspondence:***
Degui Wang
wangdegui@lzu.edu.cn

[†]These authors have contributed equally to this work and share first authorship

Specialty section:
This article was submitted to Signaling, a section of the journal Frontiers in Cell and Developmental Biology

Received: *03 December 2021*
Accepted: *27 December 2021*
Published: *21 February 2022*

Citation:
Shen R, Liu D, Wang X, Guo Z, Sun H, Song Y and Wang D (2022) DNA Damage and Activation of cGAS/STING Pathway Induce Tumor Microenvironment Remodeling. Front. Cell Dev. Biol. 9:828657. doi: 10.3389/fcell.2021.828657

1 INTRODUCTION

The tumor environment (TME) is known as a highly dynamic and constantly evolving system that is hard to predict. Interactions between various types of cells or cells with non-cells affect tumor growth and progression. In the process of tumor progression and oncotherapy, the DNA damage of tumor cells occurs frequently induced by various stresses; meanwhile, the immune system is activated continuously. DNA damage has been concluded as a critical factor in immune activation. Currently, inflammation response has become an important characteristic of tumor, and abnormal inflammatory mediator expression has been considered to be directly related to tumor prognosis (Qu et al., 2018; Greten and Grivennikov, 2019). The tumor could affect all systems in an organism, including the immune system, and when combined with radiotherapy or chemotherapy, it may lead to the collapse of the immune system. Experimental and clinical studies have suggested that a great part of deaths occurring in cancer are related to chronic infections, which are unmanageable and frequently in an advanced tumor stage. Indeed, interactional signals produced by tumor cells and immune cells in TME induce the changes of TME and build a tumor "preferred" TME to support growth and metastasis (Hinshaw and Shevde, 2019; Chen et al., 2021). Throughout the tumor process, the TME continues to evolve and reconstruct in the context of DNA damage, and the host

struggles against the tumor persistently. Researchers have attempted to reveal the relationship among DNA damage, inflammation, and tumors, but it remains unclear.

The cGAS/STING pathway, a cytosolic DNA receptor, has been regarded as an important mechanism to regulate inflammation-driven tumor progression (Ahn et al., 2014). The cyclic GMP-AMP synthase (cGAS) is known due to its specific ability of recognizing and responding to cytosolic DNA in a DNA-sequence-independent but DNA-length-dependent manner (Sun et al., 2013). STING is an adaptor in innate immune which inherits the activation signal of cGAS and triggers downstream immune inflammatory response to protect the host. The function of the cGAS/STING pathway in eliciting immunity against exogenous pathogenic microorganisms has been extensively reported. Recent lines of evidence have extended the role of this pathway to cancer, senescence, and autophagy. In this review, we focus on the dichotomous roles of cGAS/STING in TME remodeling and its profound influence as a potential therapeutic strategy against cancer.

2 OVERVIEW OF THE CGAS/STING PATHWAY

cGAS, a 522-amino-acid protein, contains an unstructured positively charged domain (N-terminal) and a nucleotidyltransferase domain (C-terminal), both of which are working to bind with DNA. The N-terminal domain is reported to be involved in cGAS nuclear translocation (Gentili et al., 2019). The C-terminal domain contains two lobes with an active site as the catalytic domain of cGAS. The N-terminal domain contributes to the separation of the cGAS/DNA complex to mediate the cGAS activation once bound with DNA (Du and Chen, 2018). After binding with DNA, cGAS assembles into a dimer, which is formed by two DNA fragments embedded into two cGAS molecules to maintain a stable active state. It was reported that the longer DNA performed more efficiently in cGAS activation and promotion of cGAS/DNA complex formation (Zhou et al., 2018).

It has been concluded that cGAS is located in the cytoplasm and is kept isolated from self-DNA in the nucleus and mitochondria to prevent cGAS activation. However, recent studies presented that cGAS could be observed in the nucleus in case of DNA damage (Liu H et al., 2018; Zierhut et al., 2019). What is more, it was indicated that cGAS was mainly localized in the nucleus but strictly separated from chromatin (Volkman et al., 2019). However, the mechanisms through which cGAS could remain inactive in the nucleus remain unclear. It is speculated that the predominant localization of cGAS in the nucleus might be a preparation for rapid response to guarantee sufficient signaling under conditions of DNA exposure (Hopfner and Hornung, 2020).

After binding with DNA, the cGAS dimer catalyzes ATP and GTP into 2′,3′-cyclic GMP-AMP (cGAMP), a second messenger, to activate stimulator of interferon genes (STING) at the endoplasmic reticulum (ER) and initiate STING re-localization in the cytoplasm. STING is a 40-kDa protein with four transmembrane domains in ER, which are responsible for binding kinase TANK-binding kinase 1 (TBK1) (Zhang et al., 2020). Upon binding to cGAMP, STING is activated through transforming the structure from a higher-order oligomerization to tetramers (Shang et al., 2019; Zhao et al., 2019). Then, STING is transferred from ER to Golgi, where STING recruits and activates TBK1, and then promotes interferon regulatory factor 3 (IRF3) and NFκB translocation into the nucleus and conducts transcriptional function further (Li et al., 2013; Liu et al., 2015; Zhang et al., 2019).

3 ACTIVATION OF THE CGAS/STING SIGNALING PATHWAY

3.1 cGAS Recognizes DNA Fragment

cGAS/STING pathway response is concluded to be activated *via* DNA fragments. It is clear that the DNA source of pathogenic microorganisms is the primary factor of the pathway activation. Recent studies indicated that cGAS can also interact with endogenous self-DNA fragments, including nuclear DNA, mitochondrial DNA, micronucleus, and chromatin free in cytoplasm.

It has been confirmed that cGAS could combine with double-stranded DNA (dsDNA), single-stranded DNA (ssDNA), and RNA–DNA hybrids in the cytoplasm (Herzner et al., 2015; Luecke et al., 2017). Various exogenous DNA that could bind with cGAS were suggested, including bacteria, viruses, and parasites (Hahn et al., 2018; Cohen et al., 2019; Song et al., 2020). cGAS expression is also detected in the nucleus; it is assumed that exogenous DNA from viruses might be identified in the nucleus by cGAS, due to the increased accessibility as the virus replicates in the nucleus (Lahaye et al., 2018). The exogenous DNA released into intercellular space could also activate immune cells and neighboring cells to initiate the defense response of the host (Nandakumar et al., 2019).

Recently, increasing lines of evidence indicate that endogenous self-DNA plays a crucial role in activating the cGAS/STING pathway, which is closely linked to health and disease. Self-DNA is commonly packaged or restricted in the nucleus and mitochondria to constrain the contact with cGAS (Boyer et al., 2020; Michalski et al., 2020). A recent study indicated that cGAS was not free in the cytoplasm but localized on the plasma membrane through the N-terminal domain (Barnett et al., 2019). If these restrictions are violated, thus triggering self-DNA or cGAS release into cytoplasm, judged as mislocation, a rapid and intense inflammatory reaction would be initiated *via* the cGAS/STING pathway (Zhang et al., 2019). Normally, the self-DNA mislocation could be induced by various stress factors, such as ultraviolet light, ionizing radiation, DNA damage agents, and replication stress; the subsequent DNA repair failure and cell death are the other important sources of free self-DNA (Bhattacharya et al., 2017; Mackenzie et al., 2017). In the process, increased genomic instability leads to exposure of chromatin and formation of abnormal micronucleus, which are also regarded as the agonist of the cGAS/STING pathway (**Figure 1**).

Another potential source of self-DNA in the cytoplasm is mitochondrial DNA (mtDNA) (**Figure 1**). Mitochondrial

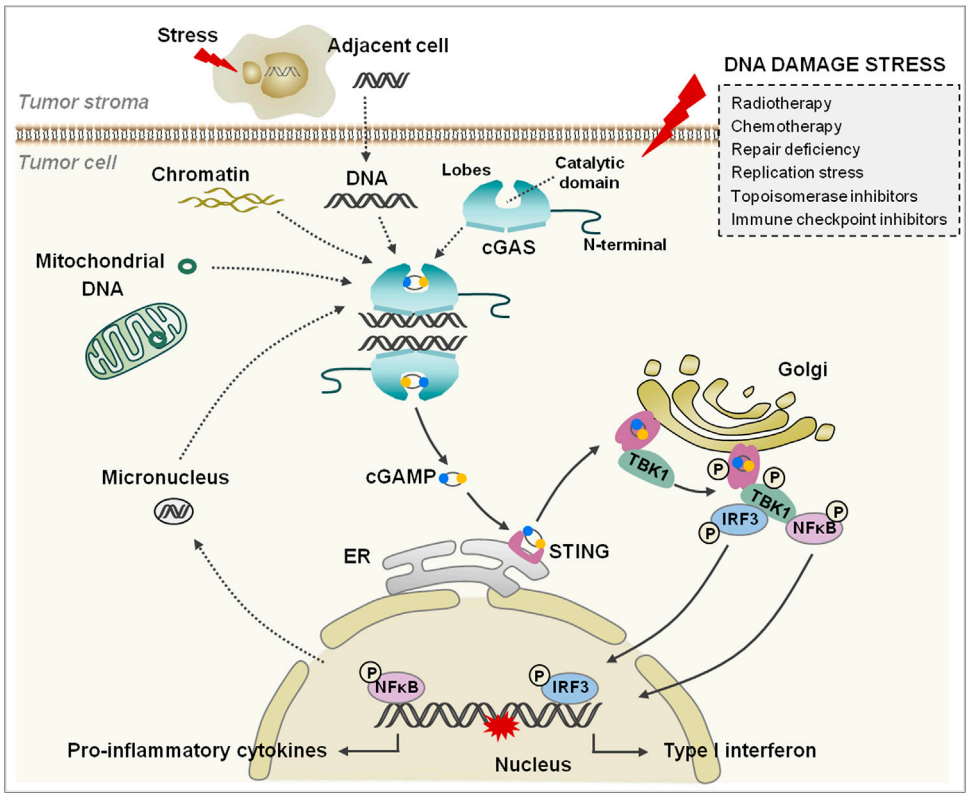

FIGURE 1 | The cGAS/STING signaling pathway. cGAS consists of an N-terminal domain and a C-terminal domain that contains two lobes and a catalytic domain. The tumor cells are damaged under various stresses (the box on the right); the free self-DNA from the nucleus, mitochondria, and dying tumor cells bind to and activate cGAS, and catalyze the synthesis cGAMP. cGAMP binds to and changes the conformation of STING, and then STING transfers from ER to Golgi apparatus and is phosphorylated by adjacent activated TBK1. Subsequently, IRF3 and NFκB are phosphorylated by TBK1 and translocate into the nucleus to regulate IFN-I and inflammatory cytokine generation.

degeneration and membrane potential reduction is the primary cause of mtDNA leaking into the cytoplasm. Studies have performed that the opening of mitochondrial permeability transition pore (mPTP) could lead to mtDNA release; voltage-dependent anion channel 1 (VDAC1) oligomers were also involved in the process through formation of pores in the mitochondrial outer membrane (Kim J et al., 2019). Consistently, a recent study showed that the hyperinflammatory responses were induced in amyotrophic lateral sclerosis through cGAS/STING pathway activation *via* mPTP- and VDAC1-mediated mtDNA release (Yu et al., 2020). In the process, the dimer in the mitochondrial outer membrane was formed by bax and bak, which contribute to open the pores on the membrane and free mtDNA from the mitochondrial matrix (White et al., 2014; McArthur et al., 2018). Simultaneously, the mitochondrial cytochrome c is also leaked into the cytoplasm and activates caspases to cleave cGAS and IRF3 to block inflammatory reactions (White et al., 2014; McArthur et al., 2018).

3.2 Activation of the cGAS/STING Pathway

The C-terminal of cGAS contains a motif with zinc ion binding module, which is involved in DNA binding and cGAS dimerization. The pocket between two lobes is the pivotal binding site of substrates (Hopfner and Hornung, 2020). Once cGAS binds with DNA, the pocket structure of cGAS would transform to cyclize ATP and GTP into cGAMP (**Figure 1**). The cGAMP contains two phosphodiester bonds; one connects 2′-hydroxyl of GMP to 5′-phosphate of AMP, and another connects 3′-hydroxyl of AMP to 5′-phosphate of GMP(Ablasser et al., 2013a; Zhang et al., 2013). Therefore, this unique isomer determines the specific activation of cGAS by dsDNA, although the ssDNA could also bind with cGAS, but the lack of specific phosphodiester bonds makes the activation impossible under the circumstances (Zhang et al., 2020).

Recent studies reported that interaction of cGAS and dsDNA induced the formation of micrometer-sized liquid-like droplets through liquid–liquid phase separation, in which cGAS was activated (Du and Chen, 2018). These lipid-like droplets enhance cGAMP generation through increasing the concentrations of reactants, and the process is reported to be dynamic and reversible, which is proposed to initiate or terminate inflammatory response to DNA in a timely manner (Du and Chen, 2018).

The cGAMP binds with STING to form a polymer, in which the pocket conformation of STING would be changed from an

open roof to a closed conformation (Shang et al., 2012; Zhang et al., 2013). Subsequently, STING leaves ER and transfers to the Golgi apparatus in the form of COP-II vesicles, where the STING dimer would be phosphorylated by the adjacent activated TBK1 but not the one bound itself (Liu et al., 2015). The phosphorylation of this complex provides a docking site for recruiting IRF3 *via* binding with the positively charged surface of IRF3, and then IRF3 is phosphorylated by TBK1; thus, the dimerized IRF3 translocates into the nucleus and turns on interferon-I (IFN-I) and inflammatory cytokines (Tao et al., 2016). Another alternative mechanism is to activate NFκB downstream of this pathway, but the contradictory models in the process have been previously proposed (Konno et al., 2013; Fang et al., 2017; de Oliveira Mann et al., 2019) (**Figure 1**).

4 DNA DAMAGE AND CGAS/STING

As the storage bank of genetic information, maintaining the integrity of DNA is of importance. Emerging lines of evidence have suggested that the cGAS/STING pathway plays a pivotal role in regulating DNA damage response and genomic instability, which is involved in the progression of multiple diseases including cancer.

4.1 DNA Damage Response and Genomic Instability

DNA damage of cells can be induced by exogenous and endogenous stress; cells establish a complex DNA damage response (DDR) system in the process, which involves multiple interactive or independent signaling pathways, and much of them remain unclear. Various cell biological processes are in connection with DDR, such as cell cycle regulation, DNA damage repair, cell metabolisms, senescence, and apoptosis. Timely and appropriate DDR has a positive effect on maintaining integrity and correctness of genome.

Genomic instability is an important indicator in disease events particularly in cancer, which has been observed in a variety of malignancies and precancerous lesions, and is related to prognosis, therapy, and overcome (Liu X et al., 2017; Kim J. H et al., 2019; Bao et al., 2021). Genomic instability elevation could be due to the defect of DDR and increased replication stress. Normally, the intracellular random errors produced by replication or stress exposure would trigger cell cycle checkpoints and DNA damage repair system to correct and rescue to ensure genetic stability. The abnormal damage response and repair could induce genomic instability occurrence through breaking the limited fidelity of DNA. It is realized that most of the human tumors are associated with genomic instabilities, which also indicate the tumor stage, metastasis, and recurrence (Chan-Seng-Yue et al., 2020; Bao et al., 2021). Genomic instability is related to the resistance of chemotherapy and radiotherapy in a clinical setting, such as taxol, 5-fluorouracil, and epirubicin used in breast cancer, colon cancer, and osteosarcoma (Telli et al., 2016; Hoglander et al., 2018). The increased genomic instability, abnormal chromosome copy numbers, and chromosome deficiency have also been verified in some metastasis of tumors (Pailler et al., 2015; Bakhoum et al., 2018).

As another result of DNA damage, small fragments of DNA leak out of the nucleus in mitosis and form the membrane-packaged micronuclei (Hintzsche et al., 2017). As mentioned previously, micronucleus is a pivotal source of self-DNA, through which cGAS is activated and triggers downstream signaling pathway to initiate inflammatory immune response. cGAS is confirmed to be co-localized with γH2AX, a DNA damage marker. Furthermore, researchers showed that the co-localization of cGAS with γH2AX did not exist only in micronuclei in the cytoplasm; it was also observed that cGAS was transferred into the nucleus and localized at the sites of damaged dsDNA (Liu H et al., 2018). The DDR to micronuclei that connected with the cGAS/STING pathway might guide the fate selected by cells to deal with, rescue or elimination; consequently, the irreparable DNA damage of cells leads to apoptosis but failed rescue induces mutation and tumor eventually (Gulen et al., 2017).

4.2 Interaction of the cGAS/STING Pathway and Tumor

Increased number of studies reveal the crucial role of the cGAS/STING pathway in innate antitumor immunity; however, evidence on the cGAS/STING pathway promoting tumor progression is also emerging.

The DNA of tumor cells is commonly released in the process of rapid proliferation and antitumor therapy; subsequently, cGAS recognizes the DNA source and responds quickly to activate STING and downstream cascade reaction to eliminate tumor cells through innate immune response (Wang et al., 2020). Researchers have shown that micronuclei are widespread in tumor cells and tumor stroma. Antigen-presenting cells (APC) are initiated and regulated by IFN-I, and then the tumor antigens yield to CD8 T cells and natural killer (NK) cells (Woo et al., 2014; Marcus et al., 2018). Recent studies have performed that the cGAS/STING pathway is activated in APC *via* free DNA in tumor, which renders tumor vulnerable to immunological surveillance (Marcus et al., 2018). cGAS/STING pathway activation in tumor cells forms an obstacle to the early-stage tumors through upregulating IFN-I and inflammatory cytokines for antitumor immunity, which is also closely related to induction of tumor cell senescence (Dou et al., 2017).

On the other hand, the tumor cells need to evade this signaling pathway detection to survive in the harsh living environment; thus, IFN-I deletion and the cGAS/STING axis are observed to be disrupted in tumors (Gajewski and Corrales, 2015). Previous studies showed that the cGAS/STING pathway could be rendered defectively by various mechanisms, such as the interrupted translocation from ER to Golgi, abnormal methylation at promoter regions of cGAS and STING, and improper posttranslational modification of these proteins (Xia et al., 2016a; Xia et al., 2016b). A recent study suggested that hypoxia in TME could inactivate the cGAS/STING pathway and induce immunosuppression through targeting an

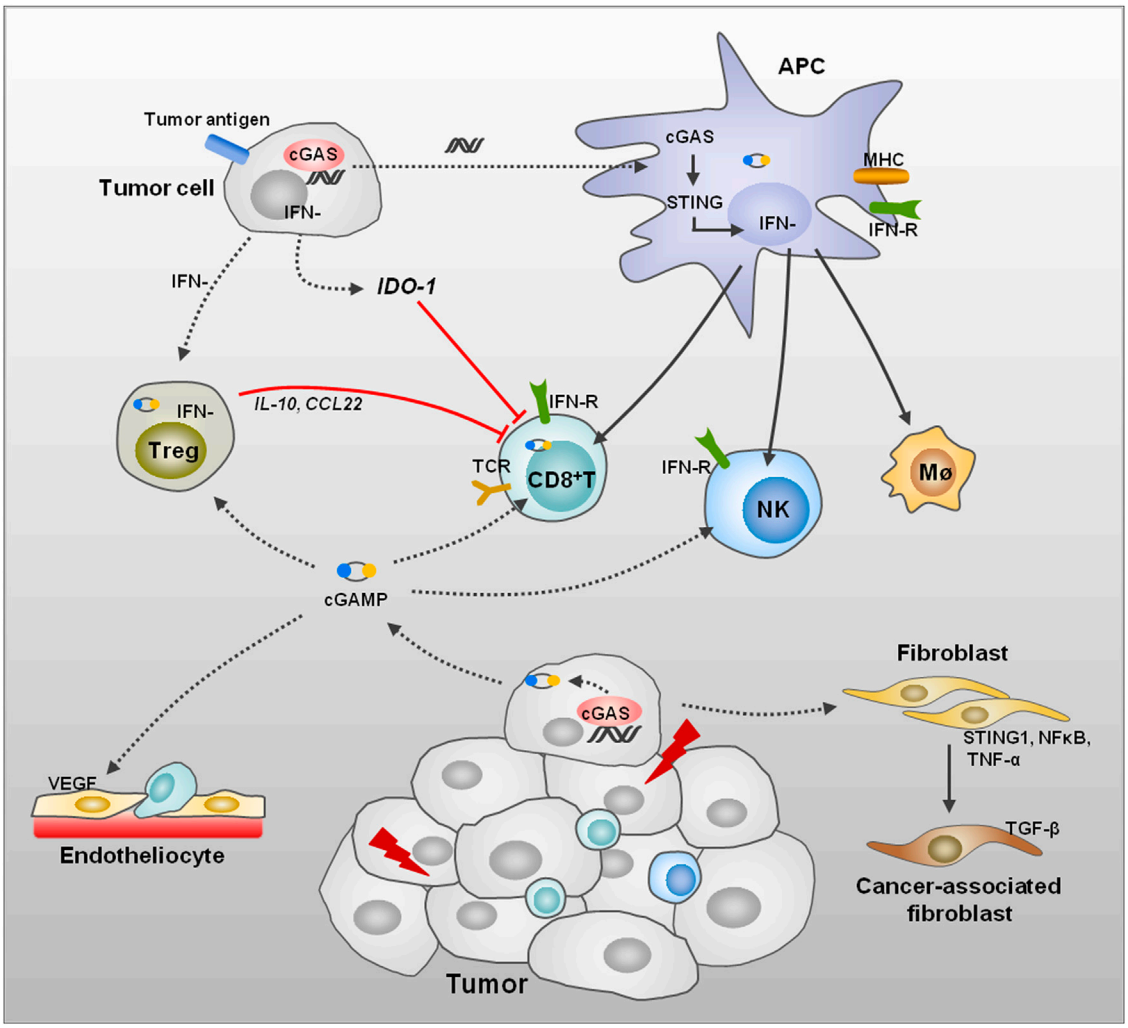

FIGURE 2 | Remodeling of TME induced by DNA damage. DNA damage of tumor cells leads to dsDNA, thus activating the cGAS/STING signaling pathway and promotes IFN generation in several kinds of cells. The APC activation can be induced through endocytosis of tumor-derived dsDNA, cGAMP, or extracellular vesicle. Then, APCs initiate $CD8^+$ T cells, NK cells, and macrophages to enhance the immune response in TME. The Treg cell activation induced by tumor cells performs immune suppression to T-cell proliferation and functions through anti-inflammatory factors. The tumor cells also induce IDO1 expression to enhance amino acid metabolism, thus suppressing T-cell function. STING activation promotes normalization of tumor vasculature and increases migration of T cells across endothelial barrier and enhances antitumor immunity. In addition, cGAS/STING pathway activation in fibroblasts affects the differentiation of fibroblasts to CAFs.

epigenetic factor NCOA3 by hypoxia-responsive miRNAs, which was necessary for basal levels of cGAS expression (Wu et al., 2017). As expected, restoring cGAS expression recovered the anti-tumor immune response (Wu et al., 2017). In addition, cGAS/STING pathway activation has also been indicated to regulate intrinsic cellular programs, including inducing tumor cell autophagy, apoptosis, necroptosis, and pyroptosis (Vanpouille-Box et al., 2018; Li et al., 2019; Zhang et al., 2020).

It seems certain that the success of radiotherapy and chemotherapy in tumor therapy is closely related to the innate immune signaling partially mediated by the cGAS/STING pathway. Meanwhile, evidence that the cGAS/STING pathway-mediated immune inflammation contributed to tumorigenesis, progression, and metastasis in some tumors was proposed; thus, the application involved in this pathway in oncotherapy became more complicated (see below). In general, the tumor immunotherapeutics need to achieve a rational balance between promoting potent antitumor response and preventing inflammation-mediated tumor progression.

5 REMODELING OF TME INDUCED BY DNA DAMAGE THROUGH THE CGAS/STING PATHWAY

5.1 Alternation of Metabolites in TME

The TME is as a nutrient-rich soil affording nutrition to tumor cell growth after reconstruction by tumor, in which the antitumor immunity is restrained. Proteins and amino acids are crucial for tumor proliferation and reconstruction of TME, which could

remodel tumor stroma and angiopoiesis as the tumor develops, to construct a proper environment for its growth (Bose et al., 2020; Hou et al., 2020; Winkler et al., 2020). The catabolism of amino acid tryptophan (Trp) is a common feature in antitumor immunity defeat (Garber, 2018; Mitchell et al., 2018). Trp can be catabolized by indoleamine 2,3 dioxygenase (IDO) enzyme produced from tumor cells; the metabolic kynurenine has been confirmed to suppress T-cell proliferation and function (Liu Y et al., 2018; Mitchell et al., 2018; Takenaka et al., 2019). Arginine (Arg) is catabolized into L-ornithine by arginase (ARG1) as well as nitric oxide synthetase (NOS), which performs immunoregulation of M2 macrophages and myeloid-derived suppressor cells (MDSCs); L-ornithine could mediate the tumor cell proliferation and suppression of antitumor immunity *via* converting into polyamines (Roci et al., 2019; Fultang et al., 2020; Carriche et al., 2021; Miska et al., 2021).

The increased cell death in TME induces the DNA release and cGAS/STING pathway activation to initiate innate immunity subsequently. The innate immune cells could produce IFN-I (IFN-α and IFN-β) and IFN-II (IFN-γ), which stimulate downstream gene production including gene encoding enzymes to catabolize Trp and Arg, inflammatory cytokines, and transforming growth factor-β (TGF-β) (Weiner, 2009). Both IFN-α and IFN-γ could induce IDO1 expression, but IDO1 is restrained by the regulation factors of IFN-β (Liu Y et al., 2017; Du et al., 2019; Shi et al., 2019; Cheng et al., 2020). In addition, the Trp catabolism is increased in cancer patients, as a precursor of 5-hydroxytryptamine, and its overexpression could lead to emotion changes and depressive behaviors in patients (Tang et al., 2020; Karmakar and Lal, 2021). IFN-γ promotes the inducible NOS (iNOS) expression, while cytokines IL-4 and IL-13 stimulate ARG1; moreover, TGF-β enhances both IDO1 and ARG1 response (Boutard et al., 1995; Ji et al., 2019; Baier et al., 2020). The current studies have indicated that these pathways are all involved in remodeling the expression of metabolites in TME that is activated *via* tumor-associated inflammation, and interfere with tumor therapy and prognosis; however, whether more metabolites play a synergy role in this process remains to be clarified.

5.2 Implication to Immune Cells in TME

5.2.1 Antigen-Presenting Cell (APC)

APCs play a critical role in the uptake and processing of antigens and then present to T cells for immune response. Generally, the damaged and dying non-tumorigenic cells could avoid activation of APCs to prevent the autoinflammatory disease because of chronic cytokine production. It has been confirmed that antigen presentation on the surface of tumor cells could be enhanced in radiotherapy and chemotherapy, and then T cells recognize antigen presented on major histocompatibility complex I (MHC-I) and respond rapidly.

Recent studies suggested that multiple oncotherapies were related to activation of the cGAS/STING pathway, as the tumor-derived DNA was detected in the cytoplasm of the tumor-infiltrating dendritic cells (DCs); meanwhile, tumor-specific antigen presentation and cytotoxic T-cell activation were increased (Chen et al., 2016b; Deng et al., 2014; Wang et al., 2017) (**Figure 2**). In chemotherapy of ovarian cancer, cisplatin exposure boosted tumor immunogenicity *via* elevating calreticulin, MHC-I, antigen presentation, and T-cell infiltration through activating the cGAS/STING pathway (Grabosch et al., 2019). In the process of photodynamic therapy (PDT), PDT enhanced MHC-II and CD80 expression and induced maturation of DCs in an IFN-I-dependent manner in melanoma (Lamberti et al., 2019). In TME, mtDNA of tumor cells were ingested by DCs and activate cGAS to increase IFN-I production in DC cytoplasm; inhibition of CD47 could suppress mtDNA degradation by phagosomes, which contributes to enhance antitumor adaptive immunity (Xu et al., 2017).

The IFN-I plays an important role in activating innate and adaptive immune through promoting maturation and activation of DCs and macrophages, thus enhancing the antigen presentation and T-cell infiltration (**Figure 2**). Manganese (Mn^{2+}) is a potent activator of cGAS, which could be released from mitochondria and Golgi and bind with cGAS in the cytoplasm to enhance enzymatic activity of cGAS (Wang et al., 2018). Mn^{2+} treatment stimulates IFN-I and cytokine production *via* the cGAS/STING pathway and improves response to clinical immunotherapy in patients (Lv et al., 2020). In a recent study, *Bacillus* Calmette-Guérin (BCG) instillations in urothelial carcinoma elevated STING and IFN as well as pro-inflammatory molecules, thus promoting M1 macrophages and T-cell infiltration in tumor (Lombardo et al., 2021). In addition, in non-muscle invasive bladder cancer, expression of STING was higher in patients who responded to BCG therapy, and elevated further after BCG treatment (Lombardo et al., 2021).

Studies have performed that the STING agonist (2′3′-cGAMP) could facilitate malignant B-cell apoptosis by phosphorylation and activation of STING on mice fibroblasts; subsequently, the tumor cell antigens are released to stimulate immune response in this manner (Tang et al., 2016). A recent study proposed that treatment with STING agonist decreased tumor burden in high-grade serous carcinoma, and mice were able to survive *via* the combination treatment of carboplatin, STING agonist, and anti-PD-1. In the process, STING agonist treatment enhanced IFN response, antigen presentation, and MHC II expression (Ghaffari et al., 2018).

5.2.2 T Cell

In solid tumor therapy, T-cell-based immunotherapy made a breakthrough but encountered multiple challenges; the specific targetable tumor antigen presentation is of importance to T-cell therapy (Lim and June, 2017; Sadelain et al., 2017). Current studies indicate that spontaneous initiation of tumor antigen-specific T cells is likely to be relevant to DC antigen presentation and IFN-I production in host cells (Diamond et al., 2011).

A recent research indicated that the cGAS/STING cascade was remarkably suppressed in peripheral blood $CD8^+$ T cells from tumor patients, STING agonist treatment promoted $CD8^+$ T cell stemness from patients with cancer; in addition, elevated STING activation enhanced oncotherapy of CAR-T cells in a xenograft model (Li W et al., 2020). In triple-negative breast cancer therapy, the PARP inhibitor olaparib induced T-cell infiltration *via* the

cGAS/STING pathway in tumor and paracrine activation of DCs was enhanced in the process; furthermore, activation of the pathway was more obvious in homologous recombination-deficient tumor cells (Pantelidou et al., 2019). Consistently, pro-inflammatory response and T-cell recruitment were abolished after knockout of STING in tumor cells (Pantelidou et al., 2019). In another study, $CD8^+$ T-cell infiltration in engrafted melanoma was lower than that in wild-type mice, but intratumoral injection of cGAMP facilitated immune response. Mechanistically, the cGAS/STING pathway was activated by STING agonist in endothelial cells instead of DCs and other immune cells, thus promoting the trafficking and infiltration of $CD8^+$ T cells into tumor (Demaria et al., 2015).

Based on the reported assay of immunogenic cell death and T-cell activation, a DNA topoisomerase II inhibitor was proposed to induce the protein HMGB1 release and IFN-I expression in tumor; subsequently, DCs were activated through both NFκB activation and the STING-dependent IFN-I pathway, and then T cells were recruited into the tumor to increase therapeutic efficacy (Wang et al., 2019). Ataxia telangiectasia mutated (ATM) is known as a critical factor in nucleus DNA damage repair; surprisingly, blockade of ATM is indicated to facilitate immune checkpoint blockade therapy. Mechanistically, inhibition of ATM promotes mtDNA leakage into the cytoplasm and activates the cGAS/STING pathway *via* suppressing mitochondrial transcription factor A (TFAM), thus enhancing T-cell infiltration into TME subsequently (Hu et al., 2021). Another critical kinase in DDR is ATR; the ATR inhibitor performs radiosensitization to tumor alongside remarkable infiltration of $CD3^+$ and NK cells in TME through activation of STING and inducing IFN response (Dillon et al., 2019). Furthermore, inhibition of RAD51, a critical component in DNA double-strand break repair, activated the cGAS sensing pathway and improved $CD8^+$ T-cell infiltration *via* increasing cytosolic dsDNA in small cell lung cancer (Jin et al., 2021). Majority of studies display the positive function of the cGAS/STING pathway in facilitating T-cell activation and recruitment in TME; undoubtedly, the negative regulation of this pathway to T cells is also presented (**Figure 2**) (see below).

5.2.3 Regulatory T Cell (Treg Cell)

Treg cells suppress immune reaction; generally, the ratio of Treg and T cells keeps a dynamic change to maintain immune response stability in the body. A previous study indicated that Treg cells can activate and facilitate proliferation by tumor-associated antigens in TME, which leads to immune tolerance and treatment resistance of tumors (Ahmadzadeh et al., 2019) (**Figure 2**). Combination therapy including STING agonist, anti-PD-1, and anti-CTLA-4 led to significant tumor regression in mice; the Treg cell ratio was suppressed obviously with increased $CD8^+$ T cells in oropharyngeal cancers (Dorta-Estremera et al., 2019). In a glioma study, using the tdTomato mice, it was indicated that the IFN-I signal triggered by STING blocked Treg cells and promoted $CD8^+$ T-cell response; furthermore, the efficacy of OVA-targeted peptide vaccine was enhanced by STING agonist (Ohkuri et al., 2014). A different opinion presented that IFN-β transcript sustained in resistant tumors induced PD-L1 and NOS2 expression in tumors and DCs that affected Treg cell accumulation in TME, thus enhancing the ratio of $CD8^+$T/Treg cells in the context of long-term anti-PD-1 treatment (Jacquelot et al., 2019).

5.3 Angiogenesis

In TME, tumor growth is dependent on angiogenesis and competitive nutrition, and the chronic immune response induces growth factors and results in angiogenesis and suppression of antitumor. Multiple proangiogenic factors in TME are involved in tumor angiogenesis to drive new blood vessel formation (Jiang et al., 2020; Ronca et al., 2017). Tumor blood vessels appear disorganized and immature, which reduces chemotaxis of immune cells into TME but increases the distant metastasis of tumor cells. A recent study proposed that T-cell transendothelial migration was regulated by endothelial STING in an IFN-I-dependent manner (Anastasiou et al., 2021). IFN-β was proposed to downregulate VEGF expression and suppress tumor angiogenesis (Takano et al., 2014), but it was also shown that IFN-α and IFN-β promoted vasculogenic mimicry formation and facilitated tumor growth (Jablonska et al., 2010; Yeh et al., 2018). Interestingly, STING activation plays a positive role, including promoting normalization of tumor vasculature and improving immune response in TME (**Figure 2**). Restoration of vascular structure results in increased migration of T cells across the endothelial barrier and enhances antitumor immunity (Yang et al., 2019). A genome-wide phenotype screen showed that TBK1, IRF3, and downstream signals were suggested to be the necessary proangiogenic factors (Korherr et al., 2006). However, another study showed that the activation of the cGAS/STING/IRF3 pathway induced by palmitic acid treatment suppressed angiogenesis mechanistically and activated IRF3 bound to the promoter of mammalian Ste20-like kinases 1 (MST1) gene, thus inhibiting endothelial cell proliferation (Yuan et al., 2017).

5.4 Reprogramming of Fibroblast in TME

Fibroblasts are of importance to maintain integrity in normal tissues, whereas, in inflammatory response, fibrotic disease and tumors are reprogrammed for different functions (Driskell and Watt, 2015; Sahai et al., 2020). The metabolites and proteins derived from tumor cells are indicated to alter the biological characteristics of fibroblasts by remodeling their metabolism and phenotype; in addition, studies have provided more evidence of the key metabolic connection between tumor cells and cancer-associated fibroblasts (CAFs) (Bertero et al., 2019; Li F et al., 2020; Zhang et al., 2021). TBK1, downstream of the cGAS/STING pathway, was recently reported as a potential regulator of fibroblast activation; inhibition of TBK1 activity reduced α-SMA stress fiber level and mitigated deposition of collagen and fibronectin in fibroblasts (Aravamudhan et al., 2020). A recent study that combined mass cytometry and single-cell mRNA sequencing analysis proposed that expression of CD105 was the distinctive indication in two diverse functional fibroblasts in both healthy tissues and tumors (Hutton et al., 2021). Interestingly, results showed that TGF-β signaling was enriched in CD105 positive cancer-associated fibroblasts (CAFs), which were permissive for tumor growth (**Figure 2**). However, in

CD105-negative CAFs, the STING1, NFκB, IL-6, TNF-α, JAK2, and LTBR signals observed high expression and remarkably performed tumor suppression (Hutton et al., 2021). In another important research, IFN-β1 was specifically upregulated in CAFs that contacted tumor cells through STING/IRF3 pathway activation due to the transcytosis of tumor cell cytoplasm into CAFs. Intriguingly, this reprogramming did not occur in CAFs that have no contact with tumor cells, which resulted in two different CAFs phenotypes and functions that coexisted in TME (Arwert et al., 2020).

6 EMERGING PRO-TUMOR ROLE OF THE CGAS/STING PATHWAY

The emerging lines of evidence show that the cGAS/STING pathway performs positive facilitation on immune response in tumors; nevertheless, current studies propose a potential promotion of this pathway in tumor initiation, progression, and metastasis (Chen et al., 2016a; Lemos et al., 2016).

Chronic and aberrant inflammation is closely related to tumorigenesis and development. In inflammatory colitis associated tumor model, deficiency of STING increased the susceptibility to tumorigenesis (Ahn et al., 2015), but in a non-inflammatory Lewis lung carcinoma (LLC), STING activation induced tumor growth (Lemos et al., 2016). It has been indicated that activated the cGAS/STING pathway accelerates initiation and activation of DCs and T cells, and recent studies showed that STING activation suppressed proliferation of T cells, which was independent with the TBK1/IRF3/IFN-I axis downstream, but in a manner of NFκB activation by the distinct C-terminal domain of STING in T cells (Cerboni et al., 2017). The STING agonist treatment induced initiation of IFN-I and T-cell-specific response involved in ER stress and cell death pathways, but only STING activation without cell antigen receptor would induce T-cell death in the process (Larkin et al., 2017). Researchers evaluated the relationship of STING expression and immune cell infiltration in malignant tumor, and suggested that pan-cancer expression of STING was positively correlated with immune cell infiltration including all types of immune cells (An et al., 2019). Inhibition of cGAS or STING expression in tumor cells could prevent metastasis in animal models (Chen et al., 2016a; Bakhoum et al., 2018).

The tumor metabolite in TME, such as the amino acids tryptophan and arginine, the common TME hallmarks in clinical oncotherapy, are proposed to respond to IFN and transforming growth factor-β (TGF-β) cytokines to suppress antitumor immunity and promote tumorigenesis (Rodriguez et al., 2007; Weiner, 2009; Opitz et al., 2011). An oral cancer study displayed that the oxidized mtDNA in cytosol induced IFN signaling through the cGAS/STING pathway and thus elevated PD-L1 and IDO-1 expression, which inhibited T-cell function through inducing IFN and IL-6 production from macrophages (Cheng et al., 2020). Another study indicated that STING activation did not impact cell viability in tongue squamous cell carcinoma, but facilitated IL-10, IDO, and CCL22 production, the immunosuppressive cytokines, thus inducing Treg cell infiltration and suppressing T-cell proliferation and activation (Liang et al., 2015). As previously mentioned, IDO plays a negative regulatory role in inflammatory response and T-cell activation. In mouse (LCC) models with STING knockout, suppressed IDO expression and MDSCs were observed, because IFN contributed to IDO induction. Furthermore, inhibition of IDO expression restrained tumor growth effectively, indicating the crucial role of IDO in TING-mediated tumor growth (Lemos et al., 2016). Therefore, IDO- and metabolite-induced immunosuppression in TME is an essential condition in the cGAS/STING pathway-involved tumorigenesis (Lemos et al., 2016).

A previous study indicated that tumor metastasis in mice brain was connected with the cGAMP transfer from tumor cells to astrocytes in an adjacent paracrine and endocytosis manner; in the process, the cGAS/STING pathway in astrocytes was activated as well as IFN-α and TNF-α, which contributed to establish a tumor growth advantage (Chen et al., 2016a). In addition, the activation of the STING/IFN-I pathway was also indicated to elevate CCR2 expression, and suppressive inflammation in colon tumors through recruiting MDSCs, CCR2 blockage-mitigated MDSC infiltration, and immunosuppression initiated by STING activation enhanced oncotherapy (Liang et al., 2017). Collectively, the potential immunosuppression of STING is emerging and is drawing more attention; in addition, the tumor cells surviving in antitumor therapy might change their tolerance and benefit from TME, which could facilitate tumor recurrence and metastasis. In this regard, sustaining dominance of the immunogenic process while minimizing the pro-tumor inflammation is of importance to oncotherapy.

7 THE CGAS/STING PATHWAY IN ONCOTHERAPY

In the process of growth, progression, and therapy, the tumor cells would undergo various stresses and induce immune response to be removed in host. Recent studies propose that the cGAS/STING pathway plays crucial roles in antitumor immune response and immune surveillance. In TME, the tumor-derived DNA have been observed in APCs' cytoplasm, and immune response is amplified though antigen presentation-induced recruitment of T cells and NK cells (Woo et al., 2014; Corrales et al., 2016). In addition, cGAMP was reported to be transmitted from cell to cell or to the extracellular area by some transport-associated and gap junction proteins, such as SLC19A1, CX43/CX45, LRRC8, and MerTK (Ablasser et al., 2013b; Chen et al., 2016a; Luteijn et al., 2019; Zhou C et al., 2020; Zhou Y et al., 2020).

The intensity of inflammation and the extent of cGAS/STING activation should be the critical factors in determining whether this pathway is antitumor or pro-tumor. Moreover, the genomic instability of tumor cells is another considerable element in cGAS/STING pathway-related pro-tumor and metastasis. In tumor progression, some tumor cells evolve to escape the host immune surveillance gradually; for example, the cGAS or STING expression is silenced or neglected so that the signal transduction

TABLE 1 | Clinical trials testing STING agonists in oncotherapy.

Agonists	Co-therapy	Tumor types	Phase	NCT Number
DMXAA	+Docetaxel	Advanced solid tumors	I	NCT01285453
	+Carboplatin + paclitaxel or docetaxel	Advanced solid tumors	I	NCT01240642
	+Carboplatin and paclitaxel	HNSCC	I	NCT00674102
	+Carboplatin and paclitaxel	HNSCC	I/II	NCT00832494
	+Carboplatin and paclitaxel	HNSCC	III	NCT00662597
	+Docetaxel	Prostate cancer	II	NCT00111618
	+Carboplatin and paclitaxel	SCLC	II	NCT01057342
ADU-S100	+Ipilimumab	Advanced solid tumors	I	NCT02675439
	+Spartalizumab	Advanced solid tumors or lymphoma	Ib	NCT03172936
	+Pembrolizumab	HNSCC	II	NCT03937141
MK-1454	+Pembrolizumab	Advanced solid tumors or lymphoma	I	NCT03010176
	+Pembrolizumab	HNSCC	II	NCT04220866
MK-2118	+Pembrolizumab	Advanced solid tumors or lymphoma	I	NCT03249792
SB11285	+Atezolizumab	Advanced solid tumors	Ia/Ib	NCT04096638
GSK3745417	+Pembrolizumab	Advanced solid tumors	I	NCT03843359
BMS-986301	+Nivolumab/ipilimumab	Advanced solid tumors	I	NCT03956680
E7766	Single agent	Advanced solid tumors, lymphomas, bladder cancer	I/Ib	NCT04144140

Abbreviations: HNSCC, head and neck squamous cell carcinoma, SCLC, small cell lung carcinoma.

cascade is interrupted and failed to trigger immune response (Xia et al., 2016a). Furthermore, DNA methylation has been proposed as a crucial factor to regulate the silencing of genes in tumor cells (Lai et al., 2021). As the crucial cytosolic DNA sensor of tumors, the ability to activate innate and adaptive immune responses of the cGAS/STING pathway attracts much attention for pharmacological target development. Currently, studies have mainly focused on the agonists of the cGAS/STING pathway and their usage as vaccine adjuvants for antitumor combined immunotherapy. The effect of tumor immunotherapy depends on expression of tumor-associated antigens and partially on antigen presentation; the cGAS/STING pathway has been used in combination immunotherapy in some tumors due to its enhancement of APC function.

Co-delivery of c-di-GMP and chimeric antigen receptor T (CAR-T) cells led to remarkably pancreatic tumor regression in mice (Smith et al., 2017). Combination of anti-PD-L1 and intramuscular injection of exogenous 2′3′-cGAMP suppressed melanoma growth and increased survival of mice harboring tumors (Wang et al., 2017). In pre-clinical models of ovarian tumor and aggressive lung cancer, combination therapy including anti-IL-10, 2′3′-cGAMP, and anti-PD-L1 targeting innate and adaptive immunity dramatically decreased MDSCs and improved DC activation and T-cell infiltration (Hartl et al., 2019). Breast tumor patients with high expression of CD47 showed poor survival and prognosis; cGAMP and anti-CD47 combination therapy effectively suppressed tumor growth, whereas monotherapy with anti-CD47 did not inhibit tumors (Kosaka et al., 2021). The flavone-8-acetic acid derivative 5,6-dimethylxanthenone-4-acetic acid (DMXAA), a selective STING agonist of mice, has outstanding antitumor characteristics in multiple tumor models (Curran et al., 2016; Weiss et al., 2017; Liu et al., 2020; Xu et al., 2021). In addition, ADU-S100, one of promising agonists of STING, exhibits significant inhibition on colon tumor and ascites in the case of synergistically cooperating with anti-PD-1 and anti-COX2 (Lee et al., 2021), which is investigated in clinical phase I trials of solid tumors and lymphomas (Sivick et al., 2018; Meric-Bernstam et al., 2021).

Over the past decade, more efforts are focused on the development of STING agonists that perform improved stability and binding capacity on human STING, some of which have been used in clinical trials of oncotherapy (**Table 1**). Correctively, antitumor immune therapy requires activating APCs by the cGAS/STING pathway as well as enhancing tumor-associated antigen presentation to T cells to improve efficiency.

8 CONCLUSION AND FUTURE PERSPECTIVE

The DNA damage repair responses of cells have profound influence on inflammatory response and tumorigenesis. Defective DDR allows genomic instability and micronuclei formation, the pivotal source of self-DNA, through which the DNA sensor cGAS is activated and triggering downstream signal cascade reaction; what is more, the variability of TME exacerbates DNA damage and genomic instability. Accumulating studies have elucidated the crucial role of the cGAS/STING pathway in surveillance of free self-DNA. Emerging lines of evidence have indicated that activation of the cGAS/STING pathway facilitates antitumor immune responses effectively, except for the established role in innate immunity under condition of exogenous pathogens. Rapid progress has been acquired for understanding the molecular basis and mechanisms in antitumor immune responses, which provide novel insight and references to guide oncotherapy.

Notably, the chronic activation of inflammatory *via* the cGAS/STING pathway is closely related to tumorigenesis and metastasis. Moreover, the intensity of inflammatory reaction and cGAS/STING pathway activation in different cells lead to the exact opposite results, whereby the TME is remodeled in the process. The challenges promoting immunostimulatory effects of

oncotherapy while blocking negative immunosuppression remain insurmountable. Hence, how to grasp the internal relationship among various objects in TME and balance the activation status of the pathway in cells with antithetical functions still needs in-depth investigation.

The discovery and investigation of the cGAS/STING pathway in tumor therapy and TME provide a novel framework for future therapeutic strategies. The inspiring potential of this pathway activation promotes intense investigation for the development of pharmacological compounds in this pathway. The agonists and analogues have been used as immune adjuvants in combined therapy such as chemotherapy, radiotherapy, and immune checkpoint blockade in preclinical trials to enhance efficacy. At present, the cGAS/STING pathway is considered to be a promising therapeutic target that might turn the immunologically "cold" tumor to a "hot" one. Although effective drugs have been used in trials, potential problems might hinder their application in the future. For example, the chemical property restrains the penetrating capacity, delivery mode, and bioavailability of drugs, including charged property, hydrophilicity, and metabolism. In addition, the cytotoxicity and narrow therapeutic windows restrict the application scope of drugs. Therefore, strategies to develop and screen potential agonists and to improve drug delivery carriers are urgently needed. On the other hand, emerging preclinical and clinical lines of evidence reveal that various antitumor drugs could activate this pathway through DNA damage; neglect of this potential may underestimate its contribution to therapeutic efficacy. Therefore, the combinatorial treatment for therapeutic benefit is considerable and promising.

AUTHOR CONTRIBUTIONS

RS and LD: investigation, visualization, and writing original draft. XW, ZG, and HS: investigation, formal analysis, and data compilation. GW, YS, RS, and DL: conceptualization, methodology, validation, resources, supervision, and funding acquisition. All authors approved the final version.

FUNDING

This work was financially supported by the National Natural Science Foundation of China (Nos. 82071695 and 82060535) (to DW); his major research direction is DNA damage and immune response. The Natural Science Foundation of Gansu Province (No. 21JR7RA450) supported RS; her major research direction is DNA damage and immune response. The Innovation Fund of Higher Education of Gansu Province (2021B-010) supported DL; his major research direction is renal fibrosis and epigenetic alteration.

REFERENCES

Ablasser, A., Goldeck, M., Cavlar, T., Deimling, T., Witte, G., Röhl, I., et al. (2013a). cGAS Produces a 2′-5′-linked Cyclic Dinucleotide Second Messenger that Activates STING. *Nature* 498 (7454), 380–384. doi:10.1038/nature12306

Ablasser, A., Schmid-Burgk, J. L., Hemmerling, I., Horvath, G. L., Schmidt, T., Latz, E., et al. (2013b). Cell Intrinsic Immunity Spreads to Bystander Cells via the Intercellular Transfer of cGAMP. *Nature* 503 (7477), 530–534. doi:10.1038/nature12640

Ahmadzadeh, M., Pasetto, A., Jia, L., Deniger, D. C., Stevanović, S., Robbins, P. F., et al. (2019). Tumor-infiltrating Human CD4 + Regulatory T Cells Display a Distinct TCR Repertoire and Exhibit Tumor and Neoantigen Reactivity. *Sci. Immunol.* 4 (31). doi:10.1126/sciimmunol.aao4310

Ahn, J., Xia, T., Konno, H., Konno, K., Ruiz, P., and Barber, G. N. (2014). Inflammation-driven Carcinogenesis Is Mediated through STING. *Nat. Commun.* 5, 5166. doi:10.1038/ncomms6166

Ahn, J., Konno, H., and Barber, G. N. (2015). Diverse Roles of STING-dependent Signaling on the Development of Cancer. *Oncogene* 34 (41), 5302–5308. doi:10.1038/onc.2014.457

An, X., Zhu, Y., Zheng, T., Wang, G., Zhang, M., Li, J., et al. (2019). An Analysis of the Expression and Association with Immune Cell Infiltration of the cGAS/STING Pathway in Pan-Cancer. *Mol. Ther. - Nucleic Acids* 14, 80–89. doi:10.1016/j.omtn.2018.11.003

Anastasiou, M., Newton, G. A., Kaur, K., Carrillo-Salinas, F. J., Smolgovsky, S. A., Bayer, A. L., et al. (2021). Endothelial STING Controls Tcell Transmigration in an IFN-I Dependent Manner. *JCI insight* 6 (15). doi:10.1172/jci.insight.149346

Aravamudhan, A., Haak, A. J., Choi, K. M., Meridew, J. A., Caporarello, N., Jones, D. L., et al. (2020). TBK1 Regulates YAP/TAZ and Fibrogenic Fibroblast Activation. *Am. J. Physiology-Lung Cell Mol. Physiol.* 318 (5), L852–L863. doi:10.1152/ajplung.00324.2019

Arwert, E. N., Milford, E. L., Rullan, A., Derzsi, S., Hooper, S., Kato, T., et al. (2020). STING and IRF3 in Stromal Fibroblasts Enable Sensing of Genomic Stress in Cancer Cells to Undermine Oncolytic Viral Therapy. *Nat. Cel Biol* 22 (7), 758–766. doi:10.1038/s41556-020-0527-7

Baier, J., Gänsbauer, M., Giessler, C., Arnold, H., Muske, M., Schleicher, U., et al. (2020). Arginase Impedes the Resolution of Colitis by Altering the Microbiome and Metabolome. *J. Clin. Invest.* 130 (11), 5703–5720. doi:10.1172/JCI126923

Bakhoum, S. F., Ngo, B., Laughney, A. M., Cavallo, J.-A., Murphy, C. J., Ly, P., et al. (2018). Chromosomal Instability Drives Metastasis through a Cytosolic DNA Response. *Nature* 553 (7689), 467–472. doi:10.1038/nature25432

Bao, S., Hu, T., Liu, J., Su, J., Sun, J., Ming, Y., et al. (2021). Genomic Instability-Derived Plasma Extracellular Vesicle-microRNA Signature as a Minimally Invasive Predictor of Risk and Unfavorable Prognosis in Breast Cancer. *J. Nanobiotechnol* 19 (1), 22. doi:10.1186/s12951-020-00767-3

Barnett, K. C., Coronas-Serna, J. M., Zhou, W., Ernandes, M. J., Cao, A., Kranzusch, P. J., et al. (2019). Phosphoinositide Interactions Position cGAS at the Plasma Membrane to Ensure Efficient Distinction between Self- and Viral DNA. *Cell* 176 (6), 1432–1446. e1411. doi:10.1016/j.cell.2019.01.049

Bertero, T., Oldham, W. M., Grasset, E. M., Bourget, I., Boulter, E., Pisano, S., et al. (2019). Tumor-Stroma Mechanics Coordinate Amino Acid Availability to Sustain Tumor Growth and Malignancy. *Cel Metab.* 29 (1), 124–140. doi:10.1016/j.cmet.2018.09.012

Bhattacharya, S., Srinivasan, K., Abdisalaam, S., Su, F., Raj, P., Dozmorov, I., et al. (2017). RAD51 Interconnects between DNA Replication, DNA Repair and Immunity. *Nucleic Acids Res.* 45 (8), 4590–4605. doi:10.1093/nar/gkx126

Bose, S., Allen, A. E., and Locasale, J. W. (2020). The Molecular Link from Diet to Cancer Cell Metabolism. *Mol. Cel.* 78 (6), 1034–1044. doi:10.1016/j.molcel.2020.05.018

Boutard, V., Havouis, R., Fouqueray, B., Philippe, C., Moulinoux, J. P., and Baud, L. (1995). Transforming Growth Factor-Beta Stimulates Arginase Activity in Macrophages. Implications for the Regulation of Macrophage Cytotoxicity. *J. Immunol.* 155 (4), 2077–2084.

Boyer, J. A., Spangler, C. J., Strauss, J. D., Cesmat, A. P., Liu, P., McGinty, R. K., et al. (2020). Structural Basis of Nucleosome-dependent cGAS Inhibition. *Science* 370 (6515), 450–454. doi:10.1126/science.abd0609

Carriche, G. M., Almeida, L., Stüve, P., Velasquez, L., Dhillon-LaBrooy, A., Roy, U., et al. (2021). Regulating T-Cell Differentiation through the Polyamine Spermidine. *J. Allergy Clin. Immunol.* 147 (1), 335–348. doi:10.1016/j.jaci.2020.04.037

Cerboni, S., Jeremiah, N., Gentili, M., Gehrmann, U., Conrad, C., Stolzenberg, M.-C., et al. (2017). Intrinsic Antiproliferative Activity of the Innate Sensor STING in T Lymphocytes. *J. Exp. Med.* 214 (6), 1769–1785. doi:10.1084/jem.20161674

Chan-Seng-Yue, M., Kim, J. C., Wilson, G. W., Ng, K., Figueroa, E. F., O'Kane, G. M., et al. (2020). Transcription Phenotypes of Pancreatic Cancer Are Driven by Genomic Events during Tumor Evolution. *Nat. Genet.* 52 (2), 231–240. doi:10.1038/s41588-019-0566-9

Chen, D., Zhang, X., Li, Z., and Zhu, B. (2021). Metabolic Regulatory Crosstalk between Tumor Microenvironment and Tumor-Associated Macrophages. *Theranostics* 11 (3), 1016–1030. doi:10.7150/thno.51777

Chen, Q., Boire, A., Jin, X., Valiente, M., Er, E. E., Lopez-Soto, A., et al. (2016a). Carcinoma-astrocyte gap Junctions Promote Brain Metastasis by cGAMP Transfer. *Nature* 533 (7604), 493–498. doi:10.1038/nature18268

Chen, Q., Sun, L., and Chen, Z. J. (2016b). Regulation and Function of the cGAS-STING Pathway of Cytosolic DNA Sensing. *Nat. Immunol.* 17 (10), 1142–1149. doi:10.1038/ni.3558

Cheng, A. N., Cheng, L.-C., Kuo, C.-L., Lo, Y. K., Chou, H.-Y., Chen, C.-H., et al. (2020). Mitochondrial Lon-Induced mtDNA Leakage Contributes to PD-L1-Mediated Immunoescape via STING-IFN Signaling and Extracellular Vesicles. *J. Immunother. Cancer* 8 (2), e001372. doi:10.1136/jitc-2020-001372

Cohen, D., Melamed, S., Millman, A., Shulman, G., Oppenheimer-Shaanan, Y., Kacen, A., et al. (2019). Cyclic GMP-AMP Signalling Protects Bacteria against Viral Infection. *Nature* 574 (7780), 691–695. doi:10.1038/s41586-019-1605-5

Corrales, L., McWhirter, S. M., Dubensky, T. W., Jr., and Gajewski, T. F. (2016). The Host STING Pathway at the Interface of Cancer and Immunity. *J. Clin. Invest.* 126 (7), 2404–2411. doi:10.1172/JCI86892

Curran, E., Chen, X., Corrales, L., Kline, D. E., Dubensky, T. W., Jr., Duttagupta, P., et al. (2016). STING Pathway Activation Stimulates Potent Immunity against Acute Myeloid Leukemia. *Cel Rep.* 15 (11), 2357–2366. doi:10.1016/j.celrep.2016.05.023

de Oliveira Mann, C. C., Orzalli, M. H., King, D. S., Kagan, J. C., Lee, A. S. Y., and Kranzusch, P. J. (2019). Modular Architecture of the STING C-Terminal Tail Allows Interferon and NF-Kb Signaling Adaptation. *Cel Rep.* 27 (4), 1165–1175. e1165. doi:10.1016/j.celrep.2019.03.098

Demaria, O., De Gassart, A., Coso, S., Gestermann, N., Di Domizio, J., Flatz, L., et al. (2015). STING Activation of Tumor Endothelial Cells Initiates Spontaneous and Therapeutic Antitumor Immunity. *Proc. Natl. Acad. Sci. USA* 112 (50), 15408–15413. doi:10.1073/pnas.1512832112

Deng, L., Liang, H., Xu, M., Yang, X., Burnette, B., Arina, A., et al. (2014). STING-dependent Cytosolic DNA Sensing Promotes Radiation-Induced Type I Interferon-dependent Antitumor Immunity in Immunogenic Tumors. *Immunity* 41 (5), 843–852. doi:10.1016/j.immuni.2014.10.019

Diamond, M. S., Kinder, M., Matsushita, H., Mashayekhi, M., Dunn, G. P., Archambault, J. M., et al. (2011). Type I Interferon Is Selectively Required by Dendritic Cells for Immune Rejection of Tumors. *J. Exp. Med.* 208 (10), 1989–2003. doi:10.1084/jem.20101158

Dillon, M. T., Bergerhoff, K. F., Pedersen, M., Whittock, H., Crespo-Rodriguez, E., Patin, E. C., et al. (2019). ATR Inhibition Potentiates the Radiation-Induced Inflammatory Tumor Microenvironment. *Clin. Cancer Res.* 25 (11), 3392–3403. doi:10.1158/1078-0432.CCR-18-1821

Dorta-Estremera, S., Hegde, V. L., Slay, R. B., Sun, R., Yanamandra, A. V., Nicholas, C., et al. (2019). Targeting Interferon Signaling and CTLA-4 Enhance the Therapeutic Efficacy of Anti-PD-1 Immunotherapy in Preclinical Model of HPV+ Oral Cancer. *J. Immunotherapy Cancer* 7 (1), 252. doi:10.1186/s40425-019-0728-4

Dou, Z., Ghosh, K., Vizioli, M. G., Zhu, J., Sen, P., Wangensteen, K. J., et al. (2017). Cytoplasmic Chromatin Triggers Inflammation in Senescence and Cancer. *Nature* 550 (7676), 402–406. doi:10.1038/nature24050

Driskell, R. R., and Watt, F. M. (2015). Understanding Fibroblast Heterogeneity in the Skin. *Trends Cell Biology* 25 (2), 92–99. doi:10.1016/j.tcb.2014.10.001

Du, J., Liu, A., Zhu, R., Zhou, C., Su, H., Xie, G., et al. (2019). The Different Effects of IFN-β and IFN-γ on the Tumor-Suppressive Activity of Human Amniotic Fluid-Derived Mesenchymal Stem Cells. *Stem Cell Int.* 2019, 1–15. doi:10.1155/2019/4592701

Du, M., and Chen, Z. J. (2018). DNA-induced Liquid Phase Condensation of cGAS Activates Innate Immune Signaling. *Science* 361 (6403), 704–709. doi:10.1126/science.aat1022

Fang, R., Wang, C., Jiang, Q., Lv, M., Gao, P., Yu, X., et al. (2017). NEMO-IKKβ Are Essential for IRF3 and NF-Kb Activation in the cGAS-STING Pathway. *J.I.* 199 (9), 3222–3233. doi:10.4049/jimmunol.1700699

Fultang, L., Booth, S., Yogev, O., Martins da Costa, B., Tubb, V., Panetti, S., et al. (2020). Metabolic Engineering against the Arginine Microenvironment Enhances CAR-T Cell Proliferation and Therapeutic Activity. *Blood* 136 (10), 1155–1160. doi:10.1182/blood.2019004500

Gajewski, T. F., and Corrales, L. (2015). New Perspectives on Type I IFNs in Cancer. *Cytokine Growth Factor. Rev.* 26 (2), 175–178. doi:10.1016/j.cytogfr.2015.01.001

Garber, K. (2018). A New Cancer Immunotherapy Suffers a Setback. *Science* 360 (6389), 588. doi:10.1126/science.360.6389.588

Gentili, M., Lahaye, X., Nadalin, F., Nader, G. P. F., Lombardi, E. P., Herve, S., et al. (2019). The N-Terminal Domain of cGAS Determines Preferential Association with Centromeric DNA and Innate Immune Activation in the Nucleus. *Cel Rep.* 26 (13), 3798. doi:10.1016/j.celrep.2019.03.049

Ghaffari, A., Peterson, N., Khalaj, K., Vitkin, N., Robinson, A., Francis, J.-A., et al. (2018). STING Agonist Therapy in Combination with PD-1 Immune Checkpoint Blockade Enhances Response to Carboplatin Chemotherapy in High-Grade Serous Ovarian Cancer. *Br. J. Cancer* 119 (4), 440–449. doi:10.1038/s41416-018-0188-5

Grabosch, S., Bulatovic, M., Zeng, F., Ma, T., Zhang, L., Ross, M., et al. (2019). Cisplatin-induced Immune Modulation in Ovarian Cancer Mouse Models with Distinct Inflammation Profiles. *Oncogene* 38 (13), 2380–2393. doi:10.1038/s41388-018-0581-9

Greten, F. R., and Grivennikov, S. I. (2019). Inflammation and Cancer: Triggers, Mechanisms, and Consequences. *Immunity* 51 (1), 27–41. doi:10.1016/j.immuni.2019.06.025

Gulen, M. F., Koch, U., Haag, S. M., Schuler, F., Apetoh, L., Villunger, A., et al. (2017). Signalling Strength Determines Proapoptotic Functions of STING. *Nat. Commun.* 8 (1), 427. doi:10.1038/s41467-017-00573-w

Hahn, W. O., Butler, N. S., Lindner, S. E., Akilesh, H. M., Sather, D. N., Kappe, S. H. I., et al. (2018). cGAS-mediated Control of Blood-Stage Malaria Promotes Plasmodium-specific Germinal center Responses. *JCI insight* 3 (2). doi:10.1172/jci.insight.94142

Hartl, C. A., Bertschi, A., Puerto, R. B., Andresen, C., Cheney, E. M., Mittendorf, E. A., et al. (2019). Combination Therapy Targeting Both Innate and Adaptive Immunity Improves Survival in a Pre-clinical Model of Ovarian Cancer. *J. Immunotherapy Cancer* 7 (1), 199. doi:10.1186/s40425-019-0654-5

Herzner, A.-M., Hagmann, C. A., Goldeck, M., Wolter, S., Kübler, K., Wittmann, S., et al. (2015). Sequence-specific Activation of the DNA Sensor cGAS by Y-form DNA Structures as Found in Primary HIV-1 cDNA. *Nat. Immunol.* 16 (10), 1025–1033. doi:10.1038/ni.3267

Hinshaw, D. C., and Shevde, L. A. (2019). The Tumor Microenvironment Innately Modulates Cancer Progression. *Cancer Res.* 79 (18), 4557–4566. doi:10.1158/0008-5472.CAN-18-3962

Hintzsche, H., Hemmann, U., Poth, A., Utesch, D., Lott, J., Stopper, H., et al. (2017). Fate of Micronuclei and Micronucleated Cells. *Mutat. Research/Reviews Mutat. Res.* 771, 85–98. doi:10.1016/j.mrrev.2017.02.002

Höglander, E. K., Nord, S., Wedge, D. C., Lingjærde, O. C., Silwal-Pandit, L., Gythfeldt, H. v., et al. (2018). Time Series Analysis of Neoadjuvant Chemotherapy and Bevacizumab-Treated Breast Carcinomas Reveals a Systemic Shift in Genomic Aberrations. *Genome Med.* 10 (1), 92. doi:10.1186/s13073-018-0601-y

Hopfner, K.-P., and Hornung, V. (2020). Molecular Mechanisms and Cellular Functions of cGAS-STING Signalling. *Nat. Rev. Mol. Cel Biol* 21 (9), 501–521. doi:10.1038/s41580-020-0244-x

Hou, P.-p., Luo, L.-j., Chen, H.-z., Chen, Q.-t., Bian, X.-l., Wu, S.-f., et al. (2020). Ectosomal PKM2 Promotes HCC by Inducing Macrophage Differentiation and Remodeling the Tumor Microenvironment. *Mol. Cel.* 78 (6), 1192–1206. doi:10.1016/j.molcel.2020.05.004

Hu, M., Zhou, M., Bao, X., Pan, D., Jiao, M., Liu, X., et al. (2021). ATM Inhibition Enhances Cancer Immunotherapy by Promoting mtDNA Leakage and cGAS/STING Activation. *J. Clin. Invest.* 131 (3). doi:10.1172/JCI139333

Hutton, C., Heider, F., Blanco-Gomez, A., Banyard, A., Kononov, A., Zhang, X., et al. (2021). Single-cell Analysis Defines a Pancreatic Fibroblast Lineage that Supports Anti-tumor Immunity. *Cancer cell* 39 (9), 1227–1244. doi:10.1016/j.ccell.2021.06.017

Jablonska, J., Leschner, S., Westphal, K., Lienenklaus, S., and Weiss, S. (2010). Neutrophils Responsive to Endogenous IFN-β Regulate Tumor Angiogenesis and Growth in a Mouse Tumor Model. *J. Clin. Invest.* 120 (4), 1151–1164. doi:10.1172/JCI37223

Jacquelot, N., Yamazaki, T., Roberti, M. P., Duong, C. P. M., Andrews, M. C., Verlingue, L., et al. (2019). Sustained Type I Interferon Signaling as a Mechanism of Resistance to PD-1 Blockade. *Cell Res* 29 (10), 846–861. doi:10.1038/s41422-019-0224-x

Ji, L., Zhao, X., Zhang, B., Kang, L., Song, W., Zhao, B., et al. (2019). Slc6a8-Mediated Creatine Uptake and Accumulation Reprogram Macrophage Polarization via Regulating Cytokine Responses. *Immunity* 51 (2), 272–284. doi:10.1016/j.immuni.2019.06.007

Jiang, X., Wang, J., Deng, X., Xiong, F., Zhang, S., Gong, Z., et al. (2020). The Role of Microenvironment in Tumor Angiogenesis. *J. Exp. Clin. Cancer Res.* 39 (1), 204. doi:10.1186/s13046-020-01709-5

Jin, R., Liu, B., Yu, M., Song, L., Gu, M., Wang, Z., et al. (2021). Profiling of DNA Damage and Repair Pathways in Small Cell Lung Cancer Reveals a Suppressive Role in the Immune Landscape. *Mol. Cancer* 20 (1), 130. doi:10.1186/s12943-021-01432-5

Karmakar, S., and Lal, G. (2021). Role of Serotonin Receptor Signaling in Cancer Cells and Anti-tumor Immunity. *Theranostics* 11 (11), 5296–5312. doi:10.7150/thno.55986

Kim, J., Gupta, R., Blanco, L. P., Yang, S., Shteinfer-Kuzmine, A., Wang, K., et al. (2019). VDAC Oligomers Form Mitochondrial Pores to Release mtDNA Fragments and Promote Lupus-like Disease. *Science* 366 (6472), 1531–1536. doi:10.1126/science.aav4011

Kim, J. H., Penson, A. V., Taylor, B. S., and Petrini, J. H. J. (2019). Nbn–Mre11 Interaction Is Required for Tumor Suppression and Genomic Integrity. *Proc. Natl. Acad. Sci. USA* 116 (30), 15178–15183. doi:10.1073/pnas.1905305116

Konno, H., Konno, K., and Barber, G. N. (2013). Cyclic Dinucleotides Trigger ULK1 (ATG1) Phosphorylation of STING to Prevent Sustained Innate Immune Signaling. *Cell* 155 (3), 688–698. doi:10.1016/j.cell.2013.09.049

Korherr, C., Gille, H., Schafer, R., Koenig-Hoffmann, K., Dixelius, J., Egland, K. A., et al. (2006). Identification of Proangiogenic Genes and Pathways by High-Throughput Functional Genomics: TBK1 and the IRF3 Pathway. *Proc. Natl. Acad. Sci.* 103 (11), 4240–4245. doi:10.1073/pnas.0511319103

Kosaka, A., Ishibashi, K., Nagato, T., Kitamura, H., Fujiwara, Y., Yasuda, S., et al. (2021). CD47 Blockade Enhances the Efficacy of Intratumoral STING-Targeting Therapy by Activating Phagocytes. *J. Exp. Med.* 218 (11). doi:10.1084/jem.20200792

Lahaye, X., Gentili, M., Silvin, A., Conrad, C., Picard, L., Jouve, M., et al. (2018). NONO Detects the Nuclear HIV Capsid to Promote cGAS-Mediated Innate Immune Activation. *Cell* 175 (2), 488–501. e422. doi:10.1016/j.cell.2018.08.062

Lai, J., Fu, Y., Tian, S., Huang, S., Luo, X., Lin, L., et al. (2021). Zebularine Elevates STING Expression and Enhances cGAMP Cancer Immunotherapy in Mice. *Mol. Ther.* 29 (5), 1758–1771. doi:10.1016/j.ymthe.2021.02.005

Lamberti, M. J., Mentucci, F. M., Roselli, E., Araya, P., Rivarola, V. A., Rumie Vittar, N. B., et al. (2019). Photodynamic Modulation of Type 1 Interferon Pathway on Melanoma Cells Promotes Dendritic Cell Activation. *Front. Immunol.* 10, 2614. doi:10.3389/fimmu.2019.02614

Larkin, B., Ilyukha, V., Sorokin, M., Buzdin, A., Vannier, E., and Poltorak, A. (2017). Cutting Edge: Activation of STING in T Cells Induces Type I IFN Responses and Cell Death. *J.I.* 199 (2), 397–402. doi:10.4049/jimmunol.1601999

Lee, S. J., Yang, H., Kim, W. R., Lee, Y. S., Lee, W. S., Kong, S. J., et al. (2021). STING Activation Normalizes the Intraperitoneal Vascular-Immune Microenvironment and Suppresses Peritoneal Carcinomatosis of colon Cancer. *J. Immunother. Cancer* 9 (6), e002195. doi:10.1136/jitc-2020-002195

Lemos, H., Mohamed, E., Huang, L., Ou, R., Pacholczyk, G., Arbab, A. S., et al. (2016). STING Promotes the Growth of Tumors Characterized by Low Antigenicity via IDO Activation. *Cancer Res.* 76 (8), 2076–2081. doi:10.1158/0008-5472.CAN-15-1456

Li, A., Yi, M., Qin, S., Song, Y., Chu, Q., and Wu, K. (2019). Activating cGAS-STING Pathway for the Optimal Effect of Cancer Immunotherapy. *J. Hematol. Oncol.* 12 (1), 35. doi:10.1186/s13045-019-0721-x

Li, F., Huangyang, P., Burrows, M., Guo, K., Riscal, R., Godfrey, J., et al. (2020). FBP1 Loss Disrupts Liver Metabolism and Promotes Tumorigenesis through a Hepatic Stellate Cell Senescence Secretome. *Nat. Cel Biol* 22 (6), 728–739. doi:10.1038/s41556-020-0511-2

Li, W., Lu, L., Lu, J., Wang, X., Yang, C., Jin, J., et al. (2020). cGAS-STING-mediated DNA Sensing Maintains CD8 + T Cell Stemness and Promotes Antitumor T Cell Therapy. *Sci. Transl. Med.* 12 (549). doi:10.1126/scitranslmed.aay9013

Li, X.-D., Wu, J., Gao, D., Wang, H., Sun, L., and Chen, Z. J. (2013). Pivotal Roles of cGAS-cGAMP Signaling in Antiviral Defense and Immune Adjuvant Effects. *Science* 341 (6152), 1390–1394. doi:10.1126/science.1244040

Liang, D., Xiao-Feng, H., Guan-Jun, D., Er-Ling, H., Sheng, C., Ting-Ting, W., et al. (2015). Activated STING Enhances Tregs Infiltration in the HPV-Related Carcinogenesis of Tongue Squamous Cells via the C-jun/CCL22 Signal. *Biochim. Biophys. Acta (Bba) - Mol. Basis Dis.* 1852 (11), 2494–2503. doi:10.1016/j.bbadis.2015.08.011

Liang, H., Deng, L., Hou, Y., Meng, X., Huang, X., Rao, E., et al. (2017). Host STING-dependent MDSC Mobilization Drives Extrinsic Radiation Resistance. *Nat. Commun.* 8 (1), 1736. doi:10.1038/s41467-017-01566-5

Lim, W. A., and June, C. H. (2017). The Principles of Engineering Immune Cells to Treat Cancer. *Cell* 168 (4), 724–740. doi:10.1016/j.cell.2017.01.016

Liu, H., Zhang, H., Wu, X., Ma, D., Wu, J., Wang, L., et al. (2018). Nuclear cGAS Suppresses DNA Repair and Promotes Tumorigenesis. *Nature* 563 (7729), 131–136. doi:10.1038/s41586-018-0629-6

Liu, S., Cai, X., Wu, J., Cong, Q., Chen, X., Li, T., et al. (2015). Phosphorylation of Innate Immune Adaptor Proteins MAVS, STING, and TRIF Induces IRF3 Activation. *Science* 347 (6227), aaa2630. doi:10.1126/science.aaa2630

Liu, W., Kim, G. B., Krump, N. A., Zhou, Y., Riley, J. L., and You, J. (2020). Selective Reactivation of STING Signaling to Target Merkel Cell Carcinoma. *Proc. Natl. Acad. Sci. USA* 117 (24), 13730–13739. doi:10.1073/pnas.1919690117

Liu, X., Zhang, M., Ying, S., Zhang, C., Lin, R., Zheng, J., et al. (2017). Genetic Alterations in Esophageal Tissues from Squamous Dysplasia to Carcinoma. *Gastroenterology* 153 (1), 166–177. doi:10.1053/j.gastro.2017.03.033

Liu, Y., Liang, X., Dong, W., Fang, Y., Lv, J., Zhang, T., et al. (2018). Tumor-Repopulating Cells Induce PD-1 Expression in CD8+ T Cells by Transferring Kynurenine and AhR Activation. *Cancer cell* 33 (3), 480–494. doi:10.1016/j.ccell.2018.02.005

Liu, Y., Liang, X., Yin, X., Lv, J., Tang, K., Ma, J., et al. (2017). Blockade of IDO-kynurenine-AhR Metabolic Circuitry Abrogates IFN-γ-Induced Immunologic Dormancy of Tumor-Repopulating Cells. *Nat. Commun.* 8, 15207. doi:10.1038/ncomms15207

Lombardo, K. A., Obradovic, A., Singh, A. K., Liu, J. L., Joice, G., Kates, M., et al. (2021). BCG Invokes superior STING -mediated Innate Immune Response over Radiotherapy in a Carcinogen Murine Model of Urothelial Cancer. *J. Pathol.* doi:10.1002/path.5830

Luecke, S., Holleufer, A., Christensen, M. H., Jønsson, K. L., Boni, G. A., Sørensen, L. K., et al. (2017). cGAS Is Activated by DNA in a Length-dependent Manner. *EMBO Rep.* 18 (10), 1707–1715. doi:10.15252/embr.201744017

Luteijn, R. D., Zaver, S. A., Gowen, B. G., Wyman, S. K., Garelis, N. E., Onia, L., et al. (2019). SLC19A1 Transports Immunoreactive Cyclic Dinucleotides. *Nature* 573 (7774), 434–438. doi:10.1038/s41586-019-1553-0

Lv, M., Chen, M., Zhang, R., Zhang, W., Wang, C., Zhang, Y., et al. (2020). Manganese Is Critical for Antitumor Immune Responses via cGAS-STING and Improves the Efficacy of Clinical Immunotherapy. *Cel Res* 30 (11), 966–979. doi:10.1038/s41422-020-00395-4

Mackenzie, K. J., Carroll, P., Martin, C.-A., Murina, O., Fluteau, A., Simpson, D. J., et al. (2017). cGAS Surveillance of Micronuclei Links Genome Instability to Innate Immunity. *Nature* 548 (7668), 461–465. doi:10.1038/nature23449

Marcus, A., Mao, A. J., Lensink-Vasan, M., Wang, L., Vance, R. E., and Raulet, D. H. (2018). Tumor-Derived cGAMP Triggers a STING-Mediated Interferon Response in Non-tumor Cells to Activate the NK Cell Response. *Immunity* 49 (4), 754–763. e754. doi:10.1016/j.immuni.2018.09.016

McArthur, K., Whitehead, L. W., Heddleston, J. M., Li, L., Padman, B. S., Oorschot, V., et al. (2018). BAK/BAX Macropores Facilitate Mitochondrial Herniation and mtDNA Efflux during Apoptosis. *Science* 359 (6378). doi:10.1126/science.aao6047

Meric-Bernstam, F., Sweis, R. F., Hodi, F. S., Messersmith, W. A., Andtbacka, R. H. I., Ingham, M., et al. (2021). Phase I Dose-Escalation Trial of MIW815 (ADU-S100), an Intratumoral STING Agonist, in Patients with Advanced/Metastatic Solid Tumors or Lymphomas. *Clin. Cancer Res.*, CCR–21. doi:10.1158/1078-0432.CCR-21-1963

Michalski, S., de Oliveira Mann, C. C., Stafford, C. A., Witte, G., Bartho, J., Lammens, K., et al. (2020). Structural Basis for Sequestration and Autoinhibition of cGAS by Chromatin. *Nature* 587 (7835), 678–682. doi:10.1038/s41586-020-2748-0

Miska, J., Rashidi, A., Lee-Chang, C., Gao, P., Lopez-Rosas, A., Zhang, P., et al. (2021). Polyamines Drive Myeloid Cell Survival by Buffering Intracellular pH to Promote Immunosuppression in Glioblastoma. *Sci. Adv.* 7 (8). doi:10.1126/sciadv.abc8929

Mitchell, T. C., Hamid, O., Smith, D. C., Bauer, T. M., Wasser, J. S., Olszanski, A. J., et al. (2018). Epacadostat Plus Pembrolizumab in Patients with Advanced Solid Tumors: Phase I Results from a Multicenter, Open-Label Phase I/II Trial (ECHO-202/KEYNOTE-037). *Jco* 36 (32), 3223–3230. doi:10.1200/JCO.2018.78.9602

Nandakumar, R., Tschismarov, R., Meissner, F., Prabakaran, T., Krissanaprasit, A., Farahani, E., et al. (2019). Intracellular Bacteria Engage a STING-TBK1-MVB12b Pathway to Enable Paracrine cGAS-STING Signalling. *Nat. Microbiol.* 4 (4), 701–713. doi:10.1038/s41564-019-0367-z

Ohkuri, T., Ghosh, A., Kosaka, A., Zhu, J., Ikeura, M., David, M., et al. (2014). STING Contributes to Antiglioma Immunity via Triggering Type I IFN Signals in the Tumor Microenvironment. *Cancer Immunol. Res.* 2 (12), 1199–1208. doi:10.1158/2326-6066.CIR-14-0099

Opitz, C. A., Litzenburger, U. M., Sahm, F., Ott, M., Tritschler, I., Trump, S., et al. (2011). An Endogenous Tumour-Promoting Ligand of the Human Aryl Hydrocarbon Receptor. *Nature* 478 (7368), 197–203. doi:10.1038/nature10491

Pailler, E., Auger, N., Lindsay, C. R., Vielh, P., Islas-Morris-Hernandez, A., Borget, I., et al. (2015). High Level of Chromosomal Instability in Circulating Tumor Cells of ROS1-Rearranged Non-small-cell Lung Cancer. *Ann. Oncol.* 26 (7), 1408–1415. doi:10.1093/annonc/mdv165

Pantelidou, C., Sonzogni, O., De Oliveria Taveira, M., Mehta, A. K., Kothari, A., Wang, D., et al. (2019). PARP Inhibitor Efficacy Depends on CD8+ T-Cell Recruitment via Intratumoral STING Pathway Activation in BRCA-Deficient Models of Triple-Negative Breast Cancer. *Cancer Discov.* 9 (6), 722–737. doi:10.1158/2159-8290.CD-18-1218

Qu, X., Tang, Y., and Hua, S. (2018). Immunological Approaches towards Cancer and Inflammation: A Cross Talk. *Front. Immunol.* 9, 563. doi:10.3389/fimmu.2018.00563

Roci, I., Watrous, J. D., Lagerborg, K. A., Lafranchi, L., Lindqvist, A., Jain, M., et al. (2019). Mapping Metabolic Events in the Cancer Cell Cycle Reveals Arginine Catabolism in the Committed SG2M Phase. *Cel Rep.* 26 (7), 1691–1700. doi:10.1016/j.celrep.2019.01.059

Rodriguez, P. C., Quiceno, D. G., and Ochoa, A. C. (2007). L-arginine Availability Regulates T-Lymphocyte Cell-Cycle Progression. *Blood* 109 (4), 1568–1573. doi:10.1182/blood-2006-06-031856

Ronca, R., Benkheil, M., Mitola, S., Struyf, S., and Liekens, S. (2017). Tumor Angiogenesis Revisited: Regulators and Clinical Implications. *Med. Res. Rev.* 37 (6), 1231–1274. doi:10.1002/med.21452

Sadelain, M., Rivière, I., and Riddell, S. (2017). Therapeutic T Cell Engineering. *Nature* 545 (7655), 423–431. doi:10.1038/nature22395

Sahai, E., Astsaturov, I., Cukierman, E., DeNardo, D. G., Egeblad, M., Evans, R. M., et al. (2020). A Framework for Advancing Our Understanding of Cancer-Associated Fibroblasts. *Nat. Rev. Cancercancer* 20 (3), 174–186. doi:10.1038/s41568-019-0238-1

Shang, G., Zhang, C., Chen, Z. J., Bai, X.-c., and Zhang, X. (2019). Cryo-EM Structures of STING Reveal its Mechanism of Activation by Cyclic GMP-AMP. *Nature* 567 (7748), 389–393. doi:10.1038/s41586-019-0998-5

Shang, G., Zhu, D., Li, N., Zhang, J., Zhu, C., Lu, D., et al. (2012). Crystal Structures of STING Protein Reveal Basis for Recognition of Cyclic Di-GMP. *Nat. Struct. Mol. Biol.* 19 (7), 725–727. doi:10.1038/nsmb.2332

Shi, J., Chen, C., Ju, R., Wang, Q., Li, J., Guo, L., et al. (2019). Carboxyamidotriazole Combined with IDO1-Kyn-AhR Pathway Inhibitors Profoundly Enhances Cancer Immunotherapy. *J. Immunotherapy Cancer* 7 (1), 246. doi:10.1186/s40425-019-0725-7

Sivick, K. E., Desbien, A. L., Glickman, L. H., Reiner, G. L., Corrales, L., Surh, N. H., et al. (2018). Magnitude of Therapeutic STING Activation Determines CD8+ T Cell-Mediated Anti-tumor Immunity. *Cel Rep.* 25 (11), 3074–3085. doi:10.1016/j.celrep.2018.11.047

Smith, T. T., Moffett, H. F., Stephan, S. B., Opel, C. F., Dumigan, A. G., Jiang, X., et al. (2017). Biopolymers Codelivering Engineered T Cells and STING Agonists Can Eliminate Heterogeneous Tumors. *J. Clin. Invest.* 127 (6), 2176–2191. doi:10.1172/JCI87624

Song, Z.-M., Lin, H., Yi, X.-M., Guo, W., Hu, M.-M., and Shu, H.-B. (2020). KAT5 Acetylates cGAS to Promote Innate Immune Response to DNA Virus. *Proc. Natl. Acad. Sci. USA* 117 (35), 21568–21575. doi:10.1073/pnas.1922330117

Sun, L., Wu, J., Du, F., Chen, X., and Chen, Z. J. (2013). Cyclic GMP-AMP Synthase Is a Cytosolic DNA Sensor that Activates the Type I Interferon Pathway. *Science* 339 (6121), 786–791. doi:10.1126/science.1232458

Takano, S., Ishikawa, E., Matsuda, M., Yamamoto, T., and Matsumura, A. (2014). Interferon-β Inhibits Glioma Angiogenesis through Downregulation of Vascular Endothelial Growth Factor and Upregulation of Interferon Inducible Protein 10. *Int. J. Oncol.* 45 (5), 1837–1846. doi:10.3892/ijo.2014.2620

Takenaka, M. C., Gabriely, G., Rothhammer, V., Mascanfroni, I. D., Wheeler, M. A., Chao, C.-C., et al. (2019). Control of Tumor-Associated Macrophages and T Cells in Glioblastoma via AHR and CD39. *Nat. Neurosci.* 22 (5), 729–740. doi:10.1038/s41593-019-0370-y

Tang, C.-H. A., Zundell, J. A., Ranatunga, S., Lin, C., Nefedova, Y., Del Valle, J. R., et al. (2016). Agonist-Mediated Activation of STING Induces Apoptosis in Malignant B Cells. *Cancer Res.* 76 (8), 2137–2152. doi:10.1158/0008-5472.CAN-15-1885

Tang, L., Wang, Z., Mu, Q., Yu, Z., Jacobson, O., Li, L., et al. (2020). Targeting Neutrophils for Enhanced Cancer Theranostics. *Adv. Mater.* 32 (33), 2002739. doi:10.1002/adma.202002739

Tao, J., Zhou, X., and Jiang, Z. (2016). cGAS-cGAMP-STING: The Three Musketeers of Cytosolic DNA Sensing and Signaling. *IUBMB life* 68 (11), 858–870. doi:10.1002/iub.1566

Telli, M. L., Timms, K. M., Reid, J., Hennessy, B., Mills, G. B., Jensen, K. C., et al. (2016). Homologous Recombination Deficiency (HRD) Score Predicts Response to Platinum-Containing Neoadjuvant Chemotherapy in Patients with Triple-Negative Breast Cancer. *Clin. Cancer Res.* 22 (15), 3764–3773. doi:10.1158/1078-0432.CCR-15-2477

Vanpouille-Box, C., Demaria, S., Formenti, S. C., and Galluzzi, L. (2018). Cytosolic DNA Sensing in Organismal Tumor Control. *Cancer cell* 34 (3), 361–378. doi:10.1016/j.ccell.2018.05.013

Volkman, H. E., Cambier, S., Gray, E. E., and Stetson, D. B. (2019). Tight Nuclear Tethering of cGAS Is Essential for Preventing Autoreactivity. *eLife* 8. doi:10.7554/eLife.47491

Wang, C., Guan, Y., Lv, M., Zhang, R., Guo, Z., Wei, X., et al. (2018). Manganese Increases the Sensitivity of the cGAS-STING Pathway for Double-Stranded DNA and Is Required for the Host Defense against DNA Viruses. *Immunity* 48 (4), 675–687. doi:10.1016/j.immuni.2018.03.017

Wang, H., Hu, S., Chen, X., Shi, H., Chen, C., Sun, L., et al. (2017). cGAS Is Essential for the Antitumor Effect of Immune Checkpoint Blockade. *Proc. Natl. Acad. Sci. USA* 114 (7), 1637–1642. doi:10.1073/pnas.1621363114

Wang, Y., Luo, J., Alu, A., Han, X., Wei, Y., and Wei, X. (2020). cGAS-STING Pathway in Cancer Biotherapy. *Mol. Cancer* 19 (1), 136. doi:10.1186/s12943-020-01247-w

Wang, Z., Chen, J., Hu, J., Zhang, H., Xu, F., He, W., et al. (2019). cGAS/STING axis Mediates a Topoisomerase II Inhibitor-Induced Tumor Immunogenicity. *J. Clin. Invest.* 129 (11), 4850–4862. doi:10.1172/JCI127471

Weiner, G. J. (2009). CpG Oligodeoxynucleotide-Based Therapy of Lymphoid Malignancies. *Adv. Drug Deliv. Rev.* 61 (3), 263–267. doi:10.1016/j.addr.2008.12.006

Weiss, J. M., Guérin, M. V., Regnier, F., Renault, G., Galy-Fauroux, I., Vimeux, L., et al. (2017). The STING Agonist DMXAA Triggers a Cooperation between T Lymphocytes and Myeloid Cells that Leads to Tumor Regression. *Oncoimmunology* 6 (10), e1346765. doi:10.1080/2162402X.2017.1346765

White, M. J., McArthur, K., Metcalf, D., Lane, R. M., Cambier, J. C., Herold, M. J., et al. (2014). Apoptotic Caspases Suppress mtDNA-Induced STING-Mediated Type I IFN Production. *Cell* 159 (7), 1549–1562. doi:10.1016/j.cell.2014.11.036

Winkler, J., Abisoye-Ogunniyan, A., Metcalf, K. J., and Werb, Z. (2020). Concepts of Extracellular Matrix Remodelling in Tumour Progression and Metastasis. *Nat. Commun.* 11 (1), 5120. doi:10.1038/s41467-020-18794-x

Woo, S.-R., Fuertes, M. B., Corrales, L., Spranger, S., Furdyna, M. J., Leung, M. Y. K., et al. (2014). STING-dependent Cytosolic DNA Sensing Mediates Innate Immune Recognition of Immunogenic Tumors. *Immunity* 41 (5), 830–842. doi:10.1016/j.immuni.2014.10.017

Wu, M.-Z., Cheng, W.-C., Chen, S.-F., Nieh, S., O'Connor, C., Liu, C.-L., et al. (2017). miR-25/93 Mediates Hypoxia-Induced Immunosuppression by Repressing cGAS. *Nat. Cel Biol* 19 (10), 1286–1296. doi:10.1038/ncb3615

Xia, T., Konno, H., Ahn, J., and Barber, G. N. (2016a). Deregulation of STING Signaling in Colorectal Carcinoma Constrains DNA Damage Responses and

Correlates with Tumorigenesis. *Cel Rep.* 14 (2), 282–297. doi:10.1016/j.celrep.2015.12.029

Xia, T., Konno, H., and Barber, G. N. (2016b). Recurrent Loss of STING Signaling in Melanoma Correlates with Susceptibility to Viral Oncolysis. *Cancer Res.* 76 (22), 6747–6759. doi:10.1158/0008-5472.CAN-16-1404

Xu, M. M., Pu, Y., Han, D., Shi, Y., Cao, X., Liang, H., et al. (2017). Dendritic Cells but Not Macrophages Sense Tumor Mitochondrial DNA for Cross-Priming through Signal Regulatory Protein α Signaling. *Immunity* 47 (2), 363–373. doi:10.1016/j.immuni.2017.07.016

Xu, N., Palmer, D. C., Robeson, A. C., Shou, P., Bommiasamy, H., Laurie, S. J., et al. (2021). STING Agonist Promotes CAR T Cell Trafficking and Persistence in Breast Cancer. *J. Exp. Med.* 218 (2). doi:10.1084/jem.20200844

Yang, H., Lee, W. S., Kong, S. J., Kim, C. G., Kim, J. H., Chang, S. K., et al. (2019). STING Activation Reprograms Tumor Vasculatures and Synergizes with VEGFR2 Blockade. *J. Clin. Invest.* 129 (10), 4350–4364. doi:10.1172/JCI125413

Yeh, Y.-H., Hsiao, H.-F., Yeh, Y.-C., Chen, T.-W., and Li, T.-K. (2018). Inflammatory Interferon Activates HIF-1α-Mediated Epithelial-To-Mesenchymal Transition via PI3K/AKT/mTOR Pathway. *J. Exp. Clin. Cancer Res.* 37 (1), 70. doi:10.1186/s13046-018-0730-6

Yu, C.-H., Davidson, S., Harapas, C. R., Hilton, J. B., Mlodzianoski, M. J., Laohamonthonkul, P., et al. (2020). TDP-43 Triggers Mitochondrial DNA Release via mPTP to Activate cGAS/STING in ALS. *Cell* 183 (3), 636–649. doi:10.1016/j.cell.2020.09.020

Yuan, L., Mao, Y., Luo, W., Wu, W., Xu, H., Wang, X. L., et al. (2017). Palmitic Acid Dysregulates the Hippo-YAP Pathway and Inhibits Angiogenesis by Inducing Mitochondrial Damage and Activating the Cytosolic DNA Sensor cGAS-STING-IRF3 Signaling Mechanism. *J. Biol. Chem.* 292 (36), 15002–15015. doi:10.1074/jbc.M117.804005

Zhang, C., Shang, G., Gui, X., Zhang, X., Bai, X.-c., and Chen, Z. J. (2019). Structural Basis of STING Binding with and Phosphorylation by TBK1. *Nature* 567 (7748), 394–398. doi:10.1038/s41586-019-1000-2

Zhang, X., Bai, X.-c., and Chen, Z. J. (2020). Structures and Mechanisms in the cGAS-STING Innate Immunity Pathway. *Immunity* 53 (1), 43–53. doi:10.1016/j.immuni.2020.05.013

Zhang, X., Shi, H., Wu, J., Zhang, X., Sun, L., Chen, C., et al. (2013). Cyclic GMP-AMP Containing Mixed Phosphodiester Linkages Is an Endogenous High-Affinity Ligand for STING. *Mol. Cel.* 51 (2), 226–235. doi:10.1016/j.molcel.2013.05.022

Zhang, Y., Recouvreux, M. V., Jung, M., Galenkamp, K. M. O., Li, Y., Zagnitko, O., et al. (2021). Macropinocytosis in Cancer-Associated Fibroblasts Is Dependent on CaMKK2/ARHGEF2 Signaling and Functions to Support Tumor and Stromal Cell Fitness. *Cancer Discov.* 11 (7), 1808–1825. doi:10.1158/2159-8290.CD-20-0119

Zhao, B., Du, F., Xu, P., Shu, C., Sankaran, B., Bell, S. L., et al. (2019). A Conserved PLPLRT/SD Motif of STING Mediates the Recruitment and Activation of TBK1. *Nature* 569 (7758), 718–722. doi:10.1038/s41586-019-1228-x

Zhou, C., Chen, X., Planells-Cases, R., Chu, J., Wang, L., Cao, L., et al. (2020). Transfer of cGAMP into Bystander Cells via LRRC8 Volume-Regulated Anion Channels Augments STING-Mediated Interferon Responses and Anti-viral Immunity. *Immunity* 52 (5), 767–781. e766. doi:10.1016/j.immuni.2020.03.016

Zhou, W., Whiteley, A. T., de Oliveira Mann, C. C., Morehouse, B. R., Nowak, R. P., Fischer, E. S., et al. (2018). Structure of the Human cGAS-DNA Complex Reveals Enhanced Control of Immune Surveillance. *Cell* 174 (2), 300–311. e311. doi:10.1016/j.cell.2018.06.026

Zhou, Y., Fei, M., Zhang, G., Liang, W.-C., Lin, W., Wu, Y., et al. (2020). Blockade of the Phagocytic Receptor MerTK on Tumor-Associated Macrophages Enhances P2X7R-dependent STING Activation by Tumor-Derived cGAMP. *Immunity* 52 (2), 357–373. doi:10.1016/j.immuni.2020.01.014

Zierhut, C., Yamaguchi, N., Paredes, M., Luo, J.-D., Carroll, T., and Funabiki, H. (2019). The Cytoplasmic DNA Sensor cGAS Promotes Mitotic Cell Death. *Cell* 178 (2), 302–315. doi:10.1016/j.cell.2019.05.035

Conflict of Interest: The authors declare that the research was conducted in the absence of any commercial or financial relationships that could be construed as a potential conflict of interest.

Publisher's Note: All claims expressed in this article are solely those of the authors and do not necessarily represent those of their affiliated organizations, or those of the publisher, the editors, and the reviewers. Any product that may be evaluated in this article, or claim that may be made by its manufacturer, is not guaranteed or endorsed by the publisher.

frontiers | Frontiers in Cell and Developmental Biology

ORIGINAL RESEARCH
published: 20 April 2022
doi: 10.3389/fcell.2022.889656

The Apoptotic Resistance of BRCA1-Deficient Ovarian Cancer Cells is Mediated by cAMP

Wei Yue[1,2,3,4], *Jihong Ma*[1,2,3,4], *Yinan Xiao*[1,2,3,4], *Pan Wang*[1,2,3,4], *Xiaoyang Gu*[1,2,3,4], *Bingteng Xie*[5] *and Mo Li*[1,2,3,4]*

[1]Center for Reproductive Medicine, Department of Obstetrics and Gynecology, Peking University Third Hospital, Beijing, China, [2]National Clinical Research Center for Obstetrics and Gynecology (Peking University Third Hospital), Beijing, China, [3]Key Laboratory of Assisted Reproduction (Peking University), Ministry of Education, Beijing, China, [4]Beijing Key Laboratory of Reproductive Endocrinology and Assisted Reproductive Technology (Peking University Third Hospital), Beijing, China, [5]School of Life Science, Beijing Institute of Technology, Beijing, China

Breast cancer type 1 susceptibility protein (BRCA1) is essential for homologous recombination repair of DNA double-strand breaks. Loss of BRCA1 is lethal to embryos due to extreme genomic instability and the activation of p53-dependent apoptosis. However, the apoptosis is resisted in BRCA1-deficient cancer cells even though their p53 is proficient. In this study, by analysis of transcriptome data of ovarian cancer patients bearing BRCA1 defects in TCGA database, we found that cAMP signaling pathway was significantly activated. Experimentally, we found that BRCA1 deficiency caused an increased expression of ADRB1, a transmembrane receptor that can promote the generation of cAMP. The elevated cAMP not only inhibited DNA damage-induced apoptosis through abrogating p53 accumulation, but also suppressed the proliferation of cytotoxic T lymphocytes by enhancing the expression of immunosuppressive factors DKK1. Inhibition of ADRB1 effectively killed cancer cells by abolishing the apoptotic resistance. These findings uncover a novel mechanism of apoptotic resistance in BRCA1-deficient ovarian cancer cells and point to a potentially new strategy for treating BRCA1-mutated tumors.

Keywords: BRCA1-deficient tumor, ADRB1, cAMP, apoptosis, immune suppression

OPEN ACCESS

Edited by:
Teng Ma,
Capital Medical University, China

Reviewed by:
Yibin Chen,
University of Texas MD Anderson Cancer Center, United States
Hailong Wang,
Capital Normal University, China

***Correspondence:**
Mo Li
limo@hsc.pku.edu.cn

Specialty section:
This article was submitted to Signaling, a section of the journal Frontiers in Cell and Developmental Biology

Received: *04 March 2022*
Accepted: *23 March 2022*
Published: *20 April 2022*

Citation:
Yue W, Ma J, Xiao Y, Wang P, Gu X, Xie B and Li M (2022) The Apoptotic Resistance of BRCA1-Deficient Ovarian Cancer Cells is Mediated by cAMP. Front. Cell Dev. Biol. 10:889656. doi: 10.3389/fcell.2022.889656

INTRODUCTION

As a core homologous recombination (HR) factor, BRCA1 functions in the maintenance of genome integrity (Deng and Brodie, 2000; Huen et al., 2010; Tarsounas and Sung, 2020). Loss of BRCA1 causes a failure of repairing DNA double-strand breaks (DSBs) and leads to the accumulation of DNA lesions in cells (Eyfjord and Bodvarsdottir, 2005; Savage and Harkin, 2015). It has been reported that BRCA1 deficiency in mice causes early embryonic death before day E7.5 because of extreme genomic instability and p53-dependent apoptosis activation (Gowen et al., 1996; Hakem et al., 1996; Ludwig et al., 1997). BRCA1 null primary mouse embryonic fibroblast cells display severe growth arrest phenotypes and also activation of p53-depende nt apoptosis (Xu et al., 2001; Cao et al., 2006; Drost et al., 2011; Zhu et al., 2011). On the other hand, women carrying *BRCA1* mutations have a 50%–80% risk of developing breast cancer and a 40%–65% risk of developing ovarian cancer during their lifetime (Eastson et al., 1995; Rahman and Stratton, 1998; King et al., 2003). Interestingly, these *BRCA1*-mutated cancer cells resist apoptosis and proliferate smoothly (Elledge and Amon, 2002;

Monteiro, 2003). This paradox can be partially explained by the coexistence of *p53* mutations which abrogates p53-dependent apoptosis (Brodie and Deng, 2001; Aubrey et al., 2018; Hafner et al., 2019). However, a considerable proportion of cancer cells from BRCA1-deficient breast or ovarian cancer patients bear no p53 mutations (Ramus et al., 1999; Greenblatt et al., 2001; Manie et al., 2009; Jonsson et al., 2019). Thus, these cancer cells may evolve unknown abilities for tumor survival.

Apoptosis is a programmed cell death process that can be triggered by multiple stresses, such as DNA damage, cytotoxic chemicals, and oxidative stress. Apoptosis is essential for the elimination of genome-unstable cells and the maintenance of homeostasis (Carneiro and El-Deiry, 2020). However, various tumor types have developed specific approaches to alter apoptotic pathways, leading to defects in apoptosis (Ghobrial et al., 2005). Exploring the specific pathways that resist apoptosis in a certain tumor will be conducive to discover novel targeted drugs. Recent investigations reveal that cAMP participates in promoting cancer cell proliferation, migration, invasion, and metabolism, and is a potential apoptotic suppressor (Naderi et al., 2009; Sood et al., 2010; Creed et al., 2015; Pon et al., 2016; Zhang et al., 2019). As an intracellular second messenger, cAMP performs signal transduction roles in many biological processes, such as gene expression regulation, neurotransmitter synthesis, and cell metabolism (Yan et al., 2016; Patra et al., 2021). Of note, many proteins that can promote the generation of cAMP are up-regulated in cancers (Sales et al., 2001; Chang et al., 2004; Lehrer and Rheinstein, 2020).

In this study, by analyzing the transcriptome data from TCGA database, we found that cAMP signaling pathway was significantly activated in BRCA1-defective ovarian cancer patients. In addition, genes that involved in regulating this pathway, such as ADRB1, a β-adrenocepter that can promote the production of cAMP, were up-regulated in BRCA1-defective ovarian cancer patients. When BRCA1 was knocked down in ovarian cancer cell lines bearing wide-type BRCA1, the expression of ADRB1 was significantly increased. ADRB1 enhanced the level of cAMP in BRCA1 knock-down cells that resisted p53-dependent apoptosis induced by DNA damage. Moreover, cAMP could also induce the expression of DDK1, which is a secreted factor that can suppress the cytotoxic T lymphocytes to kill cancer cells. Inhibition of ADRB1 by its selective inhibitor abrogated its ability to inhibit p53-dependent apoptosis. In conclusion, our study uncovers an underlying mechanism by which BRCA1-deficient cancer cells resist apoptosis, and identifies possible therapeutic targets for *BRCA1*-mutated tumors.

MATERIALS AND METHODS

Bioinformatics Analysis

The integrated dataset containing clinical information, BRCA1 mutation information, transcriptome data of 594 ovarian cancer patients (TCGA, Firehose Legacy) was acquired from the cBioPortal database (https://www.cbioportal.org/). The overall survival analysis between BRCA1-deficient and -proficient group, differentially expressed genes analysis between BRCA1-deficient and -proficient group, gene expression correlation analysis between BRCA1 and DNA damage repair genes, and gene mutation frequency analysis between BRCA1-deficient and -proficient group were conducted using online tool in cBioPortal (Cerami et al., 2012; Gao et al., 2013). Gene Ontology (GO) and Kyoto Encyclopedia of Genes and Genomes (KEGG) enrichment analysis of up-regulated and down-regulated genes were performed by using the WebGestalt (http://www.webgestalt.org/#) (Liao et al., 2019). Gene set enrichment analysis (GSEA) was performed based on the normalized mRNA expression data (RNA Seq V2 RSEM) using GSEA software with default setting (http://www.broadinstitute.org/gsea) (Mootha et al., 2003; Subramanian et al., 2005). Normalized enrichment score (NES) and false discovery rate (FDR) of each gene sets were calculated.

Chemicals and Antibodies

All chemicals were purchased from Sigma except for those specifically mentioned. The CFSE (carboxyfluorescein succinimidyl ester, HY-D0938), dobutamine (HY-15746), atenolol (HY-17498), and epinephrine (HY-B0447B) were purchased from MCE. The 8-CPT-cAMP (BML-CN130-0020) was purchased from LDBIO. Anti-β-actin (66009-1-lg) antibody was purchased from Proteintech. Anti-cleaved Caspase-3 (Asp175) 9664 antibody was purchased from Cell Signaling Technology. Anti-Bax (6A7) (sc-23959) antibody was purchased from Santa Cruz Biotechnology. Anti-ADRB1 (ab85037) and Anti-DKK1 (ab93017) antibody was purchased from Abcam. Anti-P53 (NB200-103) antibody was purchased from Novus. Anti-BRCA1 (PA5-88149) antibody, Alexa Fluor™ 647 Phalloidin (A22287), Alexa FluorTM 488 goat anti-mouse IgG (A-11001), HRP goat anti-mouse IgG (H + L) secondary antibody (32430), and HRP goat anti-rabbit IgG (H + L) secondary antibody 31466) were purchased from Thermo Fisher Scientific.

Plasmid Construction

To knockdown the expression of *BRCA1*, oligos encoding *BRCA1* shRNA was cloned into pLKO.1 plasmid. shRNA sequence was designed using "shRNAs for Individual Genes" purchased from Sigma Aldrich. The sequences of negative control (NC) and gene targeting shRNA were provided in **Supplementary Table S2**.

Cell Culture, Chemicals Treatment, and IR Treatment

HEK-293T and A2780 cells were cultured in DMEM medium supplemented with 10% fetal bovine serum (FBS), and 100 U/ml penicillin-streptomycin in a 37°C incubator with 5% CO_2. OVCAR-5 and IGROV-1 cells were cultured in RPMI-1640 medium supplemented with 10% fetal bovine serum (FBS), and 100 U/ml penicillin-streptomycin in a 37°C incubator with 5% CO_2. For chemicals treatment, cells were incubated with epinephrine (10 μM), dobutamine (10 μM), atenolol (50 μM), ICI-118551 (50 μM), or 8-CPT-cAMP (200 μM) for 90 min before ELISA experiments or IR treatment. For IR treatment, cells were irradiated with a 137Cs source at a dose of 10 Gy. After

18 h, the cells were used for RTCA, flow cytometry, immunofluorescence, and western blot experiments.

Immunofluorescence

Cells were fixed in 4% paraformaldehyde in PBS (pH 7.4) for 30 min followed by permeabilization with PBS containing 0.5% Triton-X-100 for 25 min at room temperature. Cells were blocked with 1% bovine serum albumin-supplemented PBS for 1 h and then incubated with the indicated primary antibodies (1:200–1:500) diluted in 3% bovine serum albumin-supplemented PBS at 4°C overnight. After washing three times in PBS containing 0.1% Tween 20 and 0.01% Triton-X 100, cells were incubated with an appropriate fluorescent secondary antibody for 1 h at room temperature. After washing three times, samples' nuclear were stained with Hoechst 33342 (10 μg/ml) for 10 min and subsequently mounted on glass slides. Images were acquired using a confocal laser scanning microscope with a 63 x/1.40 oil objective (Carl Zeiss 880).

shRNA Lentivirus Generation and shRNA Knockdown

For shRNA lentivirus generation, the pLKO.1 plasmid comprising shRNA was co-transfected with the packaging plasmids (psPAX2 and pMD2. G) into HEK293T cells using Lipofectamine 3000™ according to the manufacturer's protocol. Six hours after transfection, the cells were washed and changed with fresh growth culture media and incubated for another 48 h. Then the culture media containing viral particles were harvested and centrifuged at 3,000 ×*g* for 5 min to remove the cell debris and filtered by a 0.45-μm filter. The viral supernatant was further concentrated with a Centricon Plus-20 Centrifugal Filter at 4,000 ×*g*. The concentrated lentivirus supernatant was aliquoted and kept at -80°C before use. To knock down *BRCA1* mRNA in indicated cells, 1×10^5 cells were seeded onto 6-well plates and incubated at 37°C with 5% CO_2 until reaching 30–40% confluence. The concentrated viral supernatant was added into the culture medium at a multiplicity of infection (MOI) of 20. After 72 h, puromycin was added to the medium at 1 μg/ml for stable knock-down selection.

Western Blot

Total protein was extracted from cell lysate by RIPA buffer. Protein samples were separated by sodium dodecyl sulfate polyacrylamide gel electrophoresis (SDS-PAGE) and then electrically transferred to polyvinylidene fluoride membranes. Following transfer, the membranes were blocked in TBST containing 5% skim milk for 1 h at room temperature, and then incubated with primary antibodies (1:500–1:1,000 dilution) overnight at 4°C. After washing in TBST three times, the membranes were incubated at 37°C for 1 h with a 1:1,000 dilution of HRP-conjugated secondary antibody. Finally, protein bands were visualized using an enhanced chemiluminescence detection system (Amersham Biosciences).

cAMP ELISA

cAMP level was measured with Human cAMP ELISA Kit (Sino BestBio, CK-E10885). In total, 5×10^6 cells were harvested, washed with PBS and lysed in 500 μL RIPA Lysis buffer (Pierce, 89900) on ice for 20 min. Then the samples were centrifuged at 1000 ×*g* at 4°C for 15 min, and the supernatant was used to measure cAMP concentration according to the manufacturer's protocol.

RT-qPCR

The total RNA of tumor cells was extracted by TRIzol reagent (Gibco, 15596026) and 2 μg RNA of each sample was reverse transcribed into cDNA with RevertAid RT Reverse Transcription Kit (Thermo, K1691). RT-qPCR was performed on the StepOnePlus system (ABI) with PowerUp™ SYBR™ Green Master Mix (Thermo, A25742). Conditions of RT-qPCR were 95°C for 2 min; 95°C for 3 s and 60°C for 30 s for 40 cycles. Relative expression values of each target genes were normalized to mRNA expression of the housekeeping gene GAPDH. The relative mRNA expression level was calculated through the comparative cycle threshold method ($2^{-\Delta\Delta Ct}$). The primers were provided in **Supplementary Table S2**.

Cell Proliferation Assay by xCELLigence RTCA System

Cell proliferation was assessed using the xCELLigence RTCA system (Acea Bioscience, San Diego, CA, United States, distributed by Roche Diagnostics) that allows long-term monitoring of live cells in a noninvasive manner (Heinecke et al., 2014; Al Nakouzi et al., 2016). In brief, 5,000–10,000 cells were seeded in each well of E-16-well plates (Roche). Cell proliferation was monitored for 40–70 h at 37°C in the incubator. Microelectrodes on the bottom of plates were used to detect impedance changes proportional to the number of adherent cells. The impedance value of each well was automatically recorded by Real-Time Cell Analyzer (RTCA) software. Two parallel wells were included for each sample in one replicate, and three independent replicates were conducted.

$CD8^+$ T Cells Proliferation Assay

Peripheral blood mononuclear cells (PBMCs) of human were obtained from healthy volunteers and used for isolation of $CD8^+$ T cells. The $CD8^+$ T cells were selected using the MagniSort™ Human $CD8^+$ T cell Enrichment Kit (Thermo fisher, 8804-6812-74) according to the manufacturer's protocol. 2×10^5 isolated cells were labeled with CFSE and cultured in the 96-well plate. After incubated with Human T-Activator CD3/CD28 Dynabeads (Thermo fisher, 11161D) for 3 days, the $CD8^+$ T cells were activated to proliferate. The activated $CD8^+$ T cells were continuously co-cultured with the culture supernatant for 3 days. Then, the cells were collected and analyzed by flow cytometry.

Flow Cytometry

For cell cycle analysis, cells were washed with PBS, trypsinized, and centrifuged at 1,500 rpm for 3 min. Then the cells were washed three times with 1% BSA in PBS at 1,500 rpm for 3 min followed by fixation in 70% ethanol at 4°C overnight. The fixed cells were washed with ice-cold PBS twice and

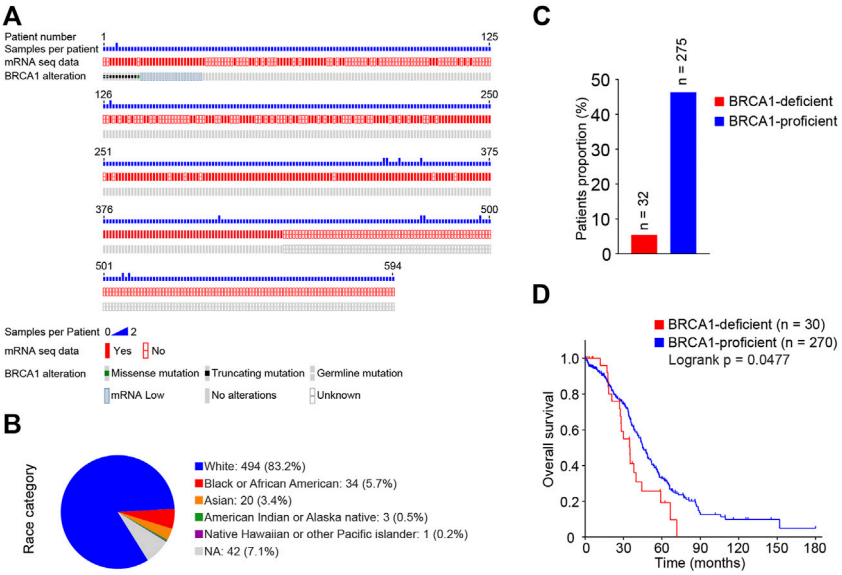

FIGURE 1 | Survival analysis of BRCA1-deficient ovarian cancer patients from TCGA database. **(A)** *BRCA1* mutations and mRNA transcriptome information plot of ovarian cancer patients from TCGA database downloaded from the cBioPortal. A total of 606 samples from 594 ovarian cancer patients in the dataset were recorded. **(B)** Race category of ovarian cancer patients from **(A)**. Of the 594 patients 83.2% were Caucasian, 5.7% were African American, 3.4% were Asian. **(C)** Proportions of BRCA1-deficient (mutated and mRNA low) and -proficient (wild-type and mRNA normal) patients. 32 BRCA1-deficient, 275 BRCA1-proficient were included. **(D)** Kaplan-Meier survival curve of overall survival between BRCA1-deficient patients (n = 30, red) and BRCA1-proficient patients (n = 270, blue). Patients with related clinical information were included. LogRank p = 0.0477.

incubated with RNaseA (50 μg/ml) at 37°C for 30 min. After staining with PI (10 μg/ml) for 30 min, a total of 10,000 cells of each sample was analyzed by a FACSCalibur™ Flow Cytometer (BD, Franklin Lakes, NJ, United States) and the data were analyzed using FlowJo software. Cell apoptosis analysis was performed using Annexin V-FITC/PI Apoptosis Detection Kit (Vazyme, Nanjing, China). Briefly, cells were washed with PBS, trypsinized, and centrifuged at 1,500 rpm for 3 min. Then the cells were washed with PBS followed by staining with annexin V-FITC and propidium iodide, a total of 10,000 cells of each sample was analyzed using a BD FACScan flow cytometry system (Becton Dickinson, Franklin, NJ, United States).

Statistical Analyses

All experiments were performed in triplicate unless indicated otherwise. Means and standard deviations were plotted. Student's t-test was used for statistical analyses. $p < 0.05$ was considered statistically significant. Statistical details are showed in figure legends.

RESULTS

BRCA1 Deficiency is Associated With Poor Survival Outcomes in Ovarian Cancer Patients

Through the cBioPortal database (https://www.cbioportal.org/), we obtained clinical information integrated with genome and transcriptome data for ovarian cancer patients [Ovarian Serous Cystadenocarcinoma (TCGA, Firehose Legacy)] (Cerami et al., 2012; Gao et al., 2013). A total of 606 tumor tissue samples from 594 patients, all with serous ovarian cancers, were recorded in this dataset (**Figure 1A**, **Supplementary Table S1**). Of the 594 patients 83.2% were Caucasian, 5.7% were African American, and 3.4% were Asian (**Figure 1B**). We found 12 patients with *BRCA1* mutations based on the genome sequence data, and each of them carried one type of BRCA1 mutation. Another 20 patients carrying a wild-type *BRCA1* gene had low levels of BRCA1 mRNA. Therefore, we summarized the 32 cases with defective BRCA1 function (BRCA1-deficient group); 29 of them had corresponding transcriptome data. A total of 275 cases carried the wild-type *BRCA1* gene and expressed normal levels of BRCA1 (BRCA1-proficient group) (**Figures 1A,C**). Next, we compared the survival status of ovarian cancer patients with or without BRCA1 deficiency. As shown in **Figure 1D**, cancer patients with defective BRCA1 had significantly shorter overall survival outcomes than those with normal BRCA1. This indicates that BRCA1 deficiency predicts poor outcomes for ovarian cancer patients.

BRCA1 Deficiency Impairs DNA Damage Repair in Ovarian Cancer Patients

Using the transcriptome data, we analyzed the correlation in mRNA expression levels of the *BRCA1* gene and genes related to DNA damage response among the ovarian cancer patients. We found that BRCA1 expression was positively correlated with that of each of the DNA damage responsive genes tested: *PARP1*, *RAD51AP1*, *E2F7*, *ATR*, *FBXO5*, *AURKA*, *E2F8*, *TIMELESS*, *RAD51*, and *POLQ* (**Figure 2A**). The results suggest that

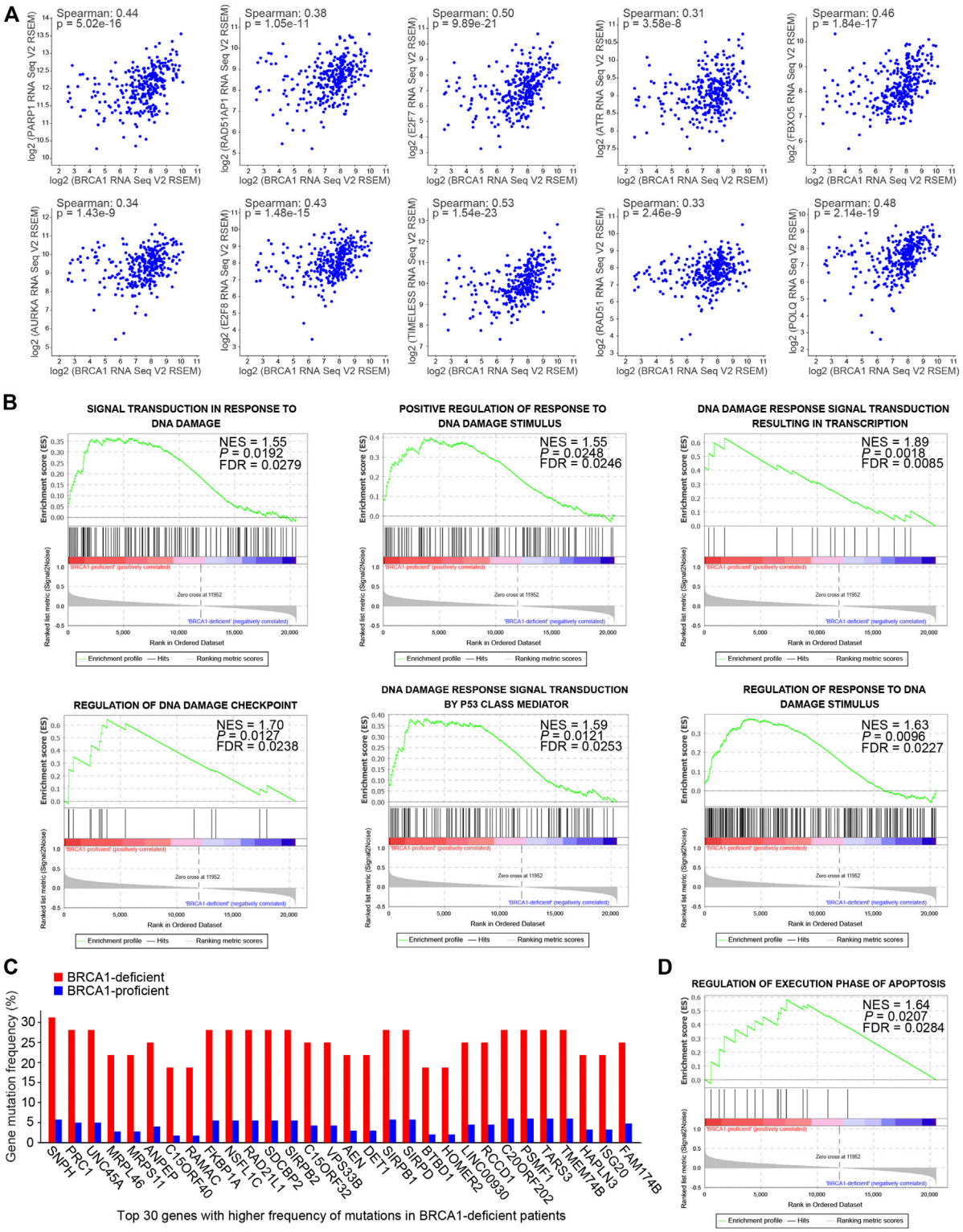

FIGURE 2 | DNA damage responses were compromised in BRCA1-deficient ovarian cancer patients. **(A)** mRNA expression correlation analysis of the *BRCA1* gene and genes related to DNA damage response among the ovarian cancer patients. *BRCA1* gene expression was positively correlated with these genes. Spearman: spearman correlation coefficient. **(B)** GSEA analysis of gene sets related to DNA damage responses based on the normalized mRNA expression data (RNA Seq V2 RSEM) between BRCA1-proficient (n = 275) and -deficient (n = 29) patients. NES, normalized enrichment score. FDR, false discovery rate. Positive NES indicates lower expression in BRCA1-deficient patients. **(C)** Gene mutation frequency analysis between BRCA1-deficient patients (red) and -proficient patients (blue). Top 30 genes with significantly higher frequency of mutations in BRCA1-deficient patients compared with BRCA1-proficient patients are shown. **(D)** GSEA analyses of gene set related to regulation of execution phase of apoptosis based on the normalized mRNA expression data (RNA Seq V2 RSEM) between BRCA1-proficient (n = 275) and -deficient (n = 29) patients. NES, normalized enrichment score. FDR, false discovery rate. Positive NES indicates lower expression in BRCA1-deficient patients.

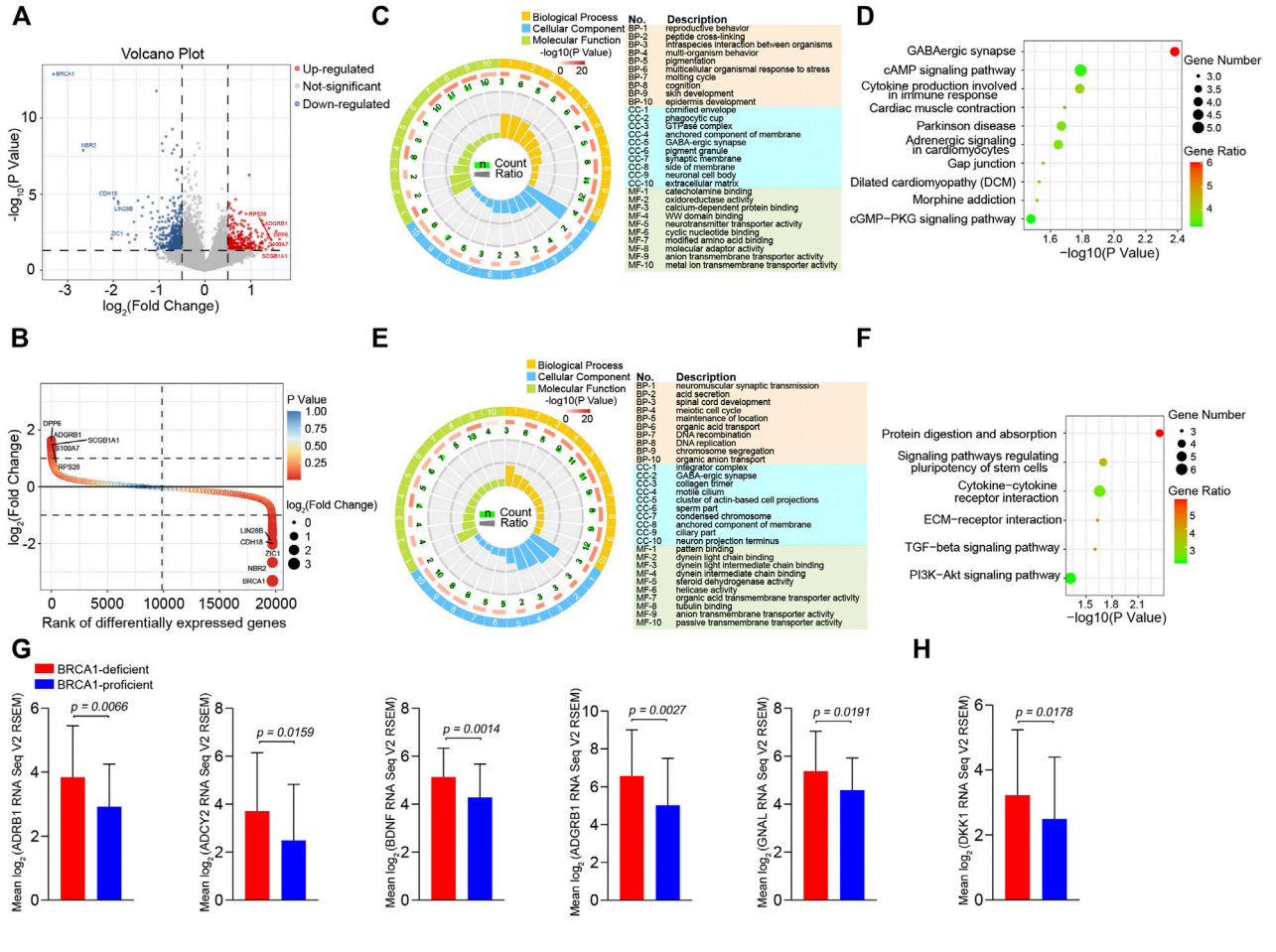

FIGURE 3 | Differentially expressed genes analysis between BRCA1-deficient and BRCA1-proficient ovarian cancer patients. **(A)** Volcano plot of differentially expressed genes (fold change >1.5, *p* value <0.05) between BRCA1-deficient (*n* = 29) and -proficient (*n* = 275) patients. In total, 447 differentially expressed genes including 176 up-regulated genes (red) and 271 down-regulated genes (blue) were identified in BRCA1-deficient ovarian cancer patients. **(B)** Rank plot of differentially expressed genes according to gene expressing difference. The highest five up-regulated and down-regulated genes in BRCA1-deficient patients are labelled in the left and right in the plot, respectively. **(C)** GO enrichment analysis of 176 up-regulated genes. The first lap indicates top 10 GO terms in "biological process," "cellular component," and "molecular function," the description of each item is listed in the right. *p* value and the number of the genes for corresponding GO terms are shown in the second and the third laps, respectively. Enrichment factors of each GO term are shown in the fourth lap. **(D)** KEGG analysis of 176 up-regulated genes. Top 10 most significantly pathways are shown in the plot. The color key from green to red represents the gene ratio. Dot size indicates the number of the genes in corresponding pathway. **(E)** GO enrichment analysis of 271 down-regulated genes. The first lap indicates top 10 GO terms in "biological process," "cellular component," and "molecular function," the description of each item is listed in the right. *p* value and the number of the genes for corresponding GO terms are shown in the second and the third laps, respectively. Enrichment factors of each GO term are shown in the fourth lap. **(F)** KEGG analysis of 271 down-regulated genes. Top six most significantly pathways are shown in the plot. The color key from green to red represents the gene ratio. Dot size indicates the number of the genes in corresponding pathway. **(G)** Comparison of *ADRB1*, *ADCY2*, *BDNF*, *ADGRB1*, and *GNAL* expression between BRCA1-deficient (*n* = 29, red) and -proficient (*n* = 275, blue) patients. **(H)** Comparison of *DKK1* expression between BRCA1-deficient (*n* = 29, red) and -proficient (*n* = 275, blue) patients.

BRCA1 deficiency may cause inadequate DNA damage repair due to the lack of DNA damage repair factors in ovarian cancer cells.

To explore the effects of BRCA1 deficiency in the ovarian cancer patients, we analyzed mRNA expression differences between the BRCA1-deficient and -proficient groups using Gene set enrichment analysis (GSEA) (Mootha et al., 2003; Subramanian et al., 2005). As shown in **Figure 2B**, gene sets related to DNA damage responses were enriched in the BRCA1-proficient group, including signal transduction in response to DNA damage (NES = 1.55), positive regulation of response to DNA damage stimulus (NES = 1.55), DNA damage response signal transduction resulting in transcription (NES = 1.89), regulation of DNA damage checkpoint (NES = 1.70), DNA damage response signal transduction by p53 class mediator (NES = 1.59), and regulation of response to DNA damage stimulus (NES = 1.63). The positive NES value indicates that genes in these gene sets are expressed lower in BRCA1-deficient patients than in BRCA1-proficient patients, which suggests that responses to DNA damage are attenuated in ovarian cancer cells with defective BRCA1. The lack or deficiency of DNA damage repair inevitably causes gene mutations, which are sources of genome instability in cancer cells. Therefore, we further analyzed

the gene mutations within the BRCA1-defective ovarian cancer patients. As expected, the gene mutation frequency in the BRCA1-deficient patients was much higher than that in patients with normal BRCA1 (**Figure 2C**). However, extreme genome instability caused by these mutations did not result in more obvious apoptosis in the BRCA1-defective ovarian cancer patients than that in patients with normal BRCA1 (**Figure 2D**). These results indicate that BRCA1-deficient cancer cells may have mechanisms that allow them to resist apoptosis, even in the presence of persistent DNA damage and extreme genome instability.

cAMP Signaling is Significantly Activated in the BRCA1-Deficient Ovarian Cancer Patients

To uncover the mechanism underlying the apoptotic resistance of BRCA1-deficient ovarian cancer cells, we analyzed the differentially expressed genes (DEGs) between the BRCA1-deficient and -proficient cases. We identified 447 DEGs (fold change >1.5, p value <0.05), 176 up-regulated and 271 down-regulated, in the BRCA1-deficient ovarian cancer patients (**Figure 3A**). Also, we ranked the DEGs according to difference in gene expression level (**Figure 3B**). The most significantly up-regulated genes were *DPP6*, *ADGRB1*, *SCGB1A1*, *S100A7*, and *RPS28*, and the most significantly down-regulated genes were *BRCA1*, *NBR2*, *ZIC1*, *CDH18*, and *LIN28B*. Based on these results, we can see that BRCA1-deficient ovarian cancer cells expressed lower levels of BRCA1 mRNA as expected.

Next, we performed Gene Ontology (GO) and Kyoto Encyclopedia of Genes and Genomes (KEGG) pathway enrichment analysis of the DEGs. The main enriched molecular function terms for the up-regulated genes in BRCA1-defective ovarian cancer cells were "catecholamine binding," "oxidoreductase activity, acting on the CH-NH group of donors," "calcium-dependent protein binding," "WW domain binding," "neurotransmitter transporter activity," and "cyclic nucleotide binding" (**Figure 3C**). KEGG analysis showed that the most significantly enriched pathways were "GABAergic synapse," "cAMP signaling pathway," "Cytokine production involved in immune response," and "Adrenergic signaling in cardiomyocytes" (**Figure 3D**). In the down-regulated gene analysis, molecular functions associated with "pattern binding," "dynein light chain binding," "steroid dehydrogenase activity," "helicase activity," and "organic acid transmembrane transporter activity," were enriched (**Figure 3E**). The "Protein digestion and absorption," "Signaling pathways regulating pluripotency of stem cells," "Cytokine-cytokine receptor interaction," and "ECM-receptor interaction" KEGG pathways were obviously enriched (**Figure 3F**). When inspecting the results above, we particularly noticed that genes involved in the ADRB1-mediated cAMP signaling pathway were dramatically up-regulated in BRCA1-deficient ovarian cancer patients (**Figures 3D,G**). In addition, genes that participate in regulating this pathway, including those involved in "catecholamine binding," "calcium-dependent protein binding," and "cyclic nucleotide binding," were also dramatically up-regulated (**Figure 3C**). These data demonstrate that cAMP signaling is significantly activated in BRCA1-deficient ovarian cancer patients. A series of studies have illustrated that cAMP can inhibit cancer cell apoptosis induced by DNA damage (Nishihara et al., 2003; Naderi et al., 2009). Besides, the expression of DKK1 in the "cytokine production involved in immune response" pathway was also elevated in BRCA1-deficient ovarian cancer patients (**Figures 3D,H**). DKK1 is a secreted factor that has immune inhibitory effects through suppressing the proliferation of $CD8^+$ T cells and NK cells, thus leading to immune evasion of cancer cells (Chu et al., 2021). Therefore, BRCA1-deficient ovarian cancer cells may develop two ways to resist cell death.

BRCA1 Knock-Down Induces Elevated Expression of ADRB1 for an Increased Generation of cAMP

We wanted to verify whether ovarian cancer cells express higher levels of ADRB1 and upon BRCA1 knock-down. We selected three ovarian cancer cell lines (OVCAR-5, IGROV-1, and A2780) bearing wild-type BRCA1 (Stordal et al., 2013) and knocked down endogenous BRCA1 using lentivirus-based shRNA. BRCA1 was successfully knocked down in the OVCAR-5, IGROV-1, and A2780 cells upon treatment with the BRCA1-targeting shRNA lentivirus, as determined by qPCR and western blot analysis (**Figures 4A,C**). When BRCA1 was knocked down, the mRNA and protein levels of ADRB1 in the three ovarian cancer cell lines increased compared with those in the control groups (**Figures 4B,C**), indicating that BRCA1 knock-down induces ADRB1 expression in ovarian cancer cells.

In vivo, catecholamine hormones including norepinephrine and epinephrine in the plasma can activate ADRB1, which can promote adenylyl cyclase to synthesize cAMP (Pon et al., 2016). In cultured cells, we found the level of cAMP is maintained at a relatively low concentration in the absence of stimulating factors. When stimulated ovarian cancer cells by the non-selective adrenoreceptor agonist epinephrine, the cAMP level was significantly elevated, indicating that activated adrenoreceptor can promote the production of cAMP. When BRCA1 was knocked down, cAMP generation was further increased compared with the control group after epinephrine treatment (**Figure 4D**). The enhanced effect on cAMP production in the BRCA1-deficient cancer cells may be due to the overexpression of ADRB1. To test this, we treated the ovarian cancer cells with the ADRB1 selective agonist dobutamine. Dobutamine treatment only induced mild cAMP production, indicating that ovarian cancer cells with normal BRCA1 maintain relatively low levels of ADRB1. However, cAMP generation dramatically increased in the ovarian cancer cells with knock-down of BRCA1 after dobutamine treatment. In addition, when we simultaneously treated the BRCA1 knock-down ovarian cancer cells with dobutamine and the ADRB1-specific antagonist atenolol, the levels of cAMP decreased to the basal level, whereas the ADRB2-specific antagonist ICI-118551 had no inhibitory effect (**Figure 4E**). On the other hand, we also detected the mRNA levels of DKK1 in BRCA1 knock-down ovarian cancer cell lines. No significant difference of DKK1 expression was observed between control and BRCA1 knock-down cancer cells

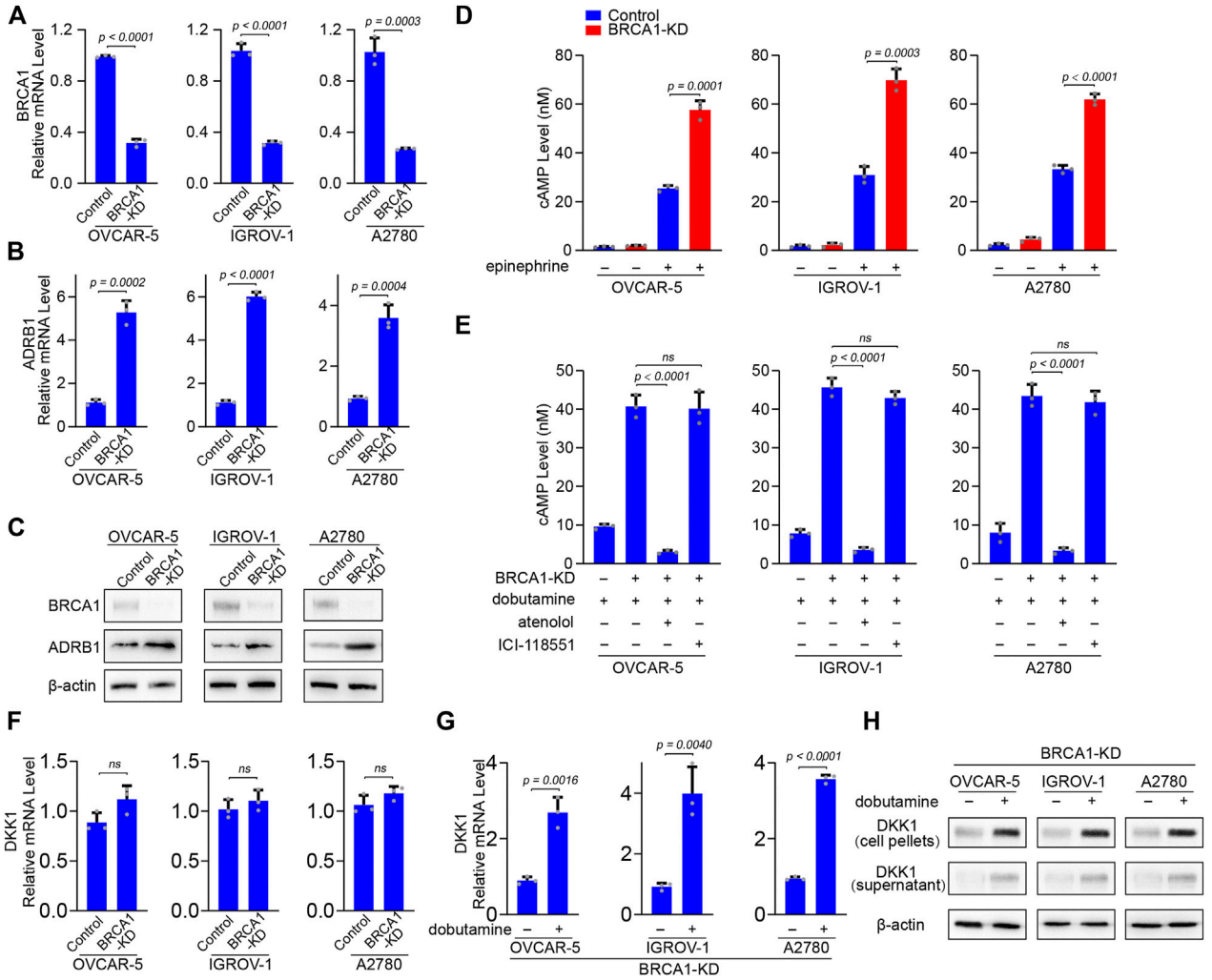

FIGURE 4 | BRCA1 knock-down promotes ADRB1 expression and cAMP production in ovarian cancer cells. **(A)** qPCR analysis of BRCA1 knock-down efficacy by shRNA lentivirus in OVCAR-5, IGROV-1, and A2780 ovarian cancer cells. KD: knock down. Data are presented as mean values ±SD. *p* values were calculated by unpaired two-tailed Student's *t*-tests. **(B)** qPCR analysis of ADRB1 mRNA expression level in control and BRCA1 knock-down OVCAR-5, IGROV-1, and A2780 ovarian cancer cells. Data are presented as mean values ±SD. *p* values were calculated by unpaired two-tailed Student's *t*-tests. **(C)** Western blot analysis of BRCA1 and ADRB1 proteins levels in control and BRCA1 knock-down OVCAR-5, IGROV-1, and A2780 ovarian cancer cells. β-actin was used as a loading control. **(D)** cAMP levels were determined by ELISA in control and BRCA1 knock-down OVCAR-5, IGROV-1, and A2780 ovarian cancer cells treated with or without epinephrine. Data are presented as mean values ±SD. *p* values were calculated by unpaired two-tailed Student's *t*-tests. **(E)** cAMP levels were determined by ELISA in control and BRCA1 knock-down OVCAR-5, IGROV-1, and A2780 ovarian cancer cells treated with or without dobutamine, atenolol or ICI-118551. Data are presented as mean values ±SD. *p* values were calculated by unpaired two-tailed Student's *t*-tests. **(F)** qPCR analysis of DKK1 mRNA expression level in control and BRCA1 knock-down OVCAR-5, IGROV-1, and A2780 ovarian cancer cells. Data are presented as mean values ±SD. *p* values were calculated by unpaired two-tailed Student's t-tests. **(G)** qPCR analysis of DKK1 mRNA expression level in BRCA1 knock-down OVCAR-5, IGROV-1, and A2780 ovarian cancer cells treated with or without dobutamine. Data are presented as mean values ±SD. *p* values were calculated by unpaired two-tailed Student's t-tests. **(H)** Western blot analysis of DKK1 protein levels in cell pellets and supernatant from BRCA1 knock-down OVCAR-5, IGROV-1, and A2780 ovarian cancer cells treated with or without dobutamine. β-actin was used as a loading control.

(**Figure 4F**). However, when the BRCA1 knock-down cells were treated with dobutamine, the expressional level of DKK1 was dramatically elevated (**Figures 4G,H**). Considering DKK1 is a secreted protein, we also detected the protein level of DKK1 in the culture medium. As expected, the protein level of DKK1 in the culture medium of dobutamine-treated BRCA1 knock-down cancer cells was elevated (**Figure 4H**). The results demonstrate that ovarian cancer cells deficient in BRCA1 express higher levels of ADRB1, which promotes the synthesis of cAMP. The elevated cAMP further induces the expression of DKK1 in these cancer cells.

Elevated cAMP Inhibits Apoptosis of BRCA1 Knock-Down Ovarian Cancer Cells and Proliferation of CD8$^+$ T Cells

To test the hypothesis that cellular cAMP suppress DNA damage-induced apoptosis in BRCA1-deficient ovarian cancer cells, we

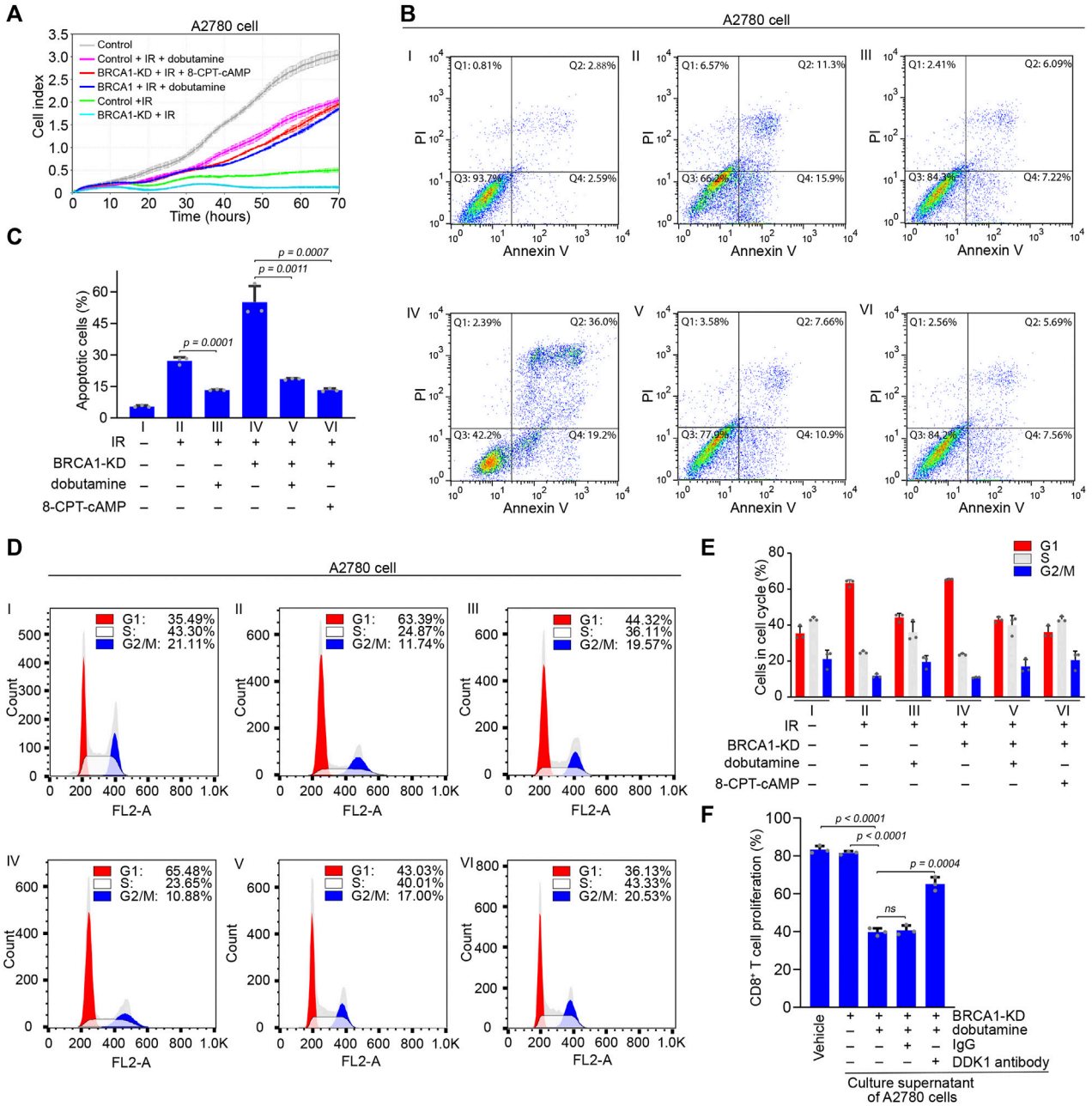

FIGURE 5 | The effects of cAMP on apoptosis of BRCA1 knock-down ovarian cancer cells and proliferation of $CD8^+$ T cells. **(A)** Control and BRCA1 knock-down A2780 cells were treated with or without dobutamine or 8-CPT-cAMP before IR irradiation, and the proliferation of these cells was monitored using the xCELLigence RTCA system. Cell proliferation was automatically monitored 70 h (i.e., until the control cells reached a growth plateau). Control cells are shown by grey line, IR irradiated control and BRCA1 knock-down cells are shown by green and cyan lines, dobutamine pre-treated control and BRCA1 knock-down cells irradiated by IR are shown by pink and blue lines, 8-CPT-cAMP pre-treated BRCA1 knock-down cells irradiated by IR are shown by red line. Error bars represent the standard deviation. **(B)** Control and BRCA1 knock-down A2780 cells were treated with or without dobutamine or 8-CPT-cAMP before exposed to 10 Gy IR. After 18 h, cell apoptosis analysis was performed through flow cytometry. **I**: control cells without IR treatment, **II**: control cells with IR treatment, **III**: dobutamine pre-treated control cells with IR treatment, **IV**: BRCA1 knock-down cells with IR treatment, **V**: dobutamine pre-treated BRCA1 knock-down cells with IR treatment, **VI**: 8-CPT-cAMP pre-treated BRCA1 knock-down cells with IR treatment. Q1: necrotic cells, Q2: early apoptotic cells, Q3: late apoptotic cells, Q4: viable cells. **(C)** Percentages of apoptotic A2780 cells, including early and late apoptotic cells, in each group from **(B)**. Three biologically independent replicates were performed. Data are presented as mean values ±SD. *p* values were calculated by unpaired two-tailed Student's *t*-tests. **(D)** Cell cycle analysis was performed to detect the effects of dobutamine or 8-CPT-cAMP on cells that were treated as described in **(B)** through flow cytometry. G1 phase: red, S phase: white, G2/M phase: blue. **(E)** Percentages of G1 phase, S phase, and G2/M phase cells in each group from **(D)**. Three biologically independent replicates were performed. Data are presented as mean values ±SD. **(F)** The inhibitory effect of secretion of dobutamine pre-treated BRCA1 knock-down A2780 cells on the proliferation of $CD8^+$ T cells *in vitro*. The proliferation of the cells was determined by CFSE dilution. Three biologically independent replicates were performed. Data are presented as mean values ±SD. *p* values were calculated by unpaired two-tailed Student's *t*-tests.

treated BRCA1 knock-down A2780 ovarian cancer cells with ionizing radiation (IR), which induces DNA double-strand breaks (Shikazono et al., 2009). After exposure to 10 Gy IR, the growth of the BRCA1 knock-down A2780 cells nearly ceased, whereas growth of IR-treated control cells was partially recovered to grow (**Figure 5A**). This suggests that cell cycle arrest or apoptosis induced by massive unrepaired DNA damage may lead to the arrested growth of BRCA1 knock-down A2780 cells, whereas cells with wild-type BRCA1 can recover after DNA damage repair. When A2780 cells were incubated with dobutamine or 8-CPT-cAMP (a membrane-permeable analog of cAMP) before IR treatment, the proliferation of the cells could be recovered to a large extent. As shown in **Figure 5A**, after incubation with dobutamine, IR-treated control and BRCA1 knock-down A2780 cells could proliferate normally. Similar to the effect of dobutamine, 8-CPT-cAMP also removed the inhibition on the BRCA1 knock-down A2780 cells proliferation. This suggests that endogenous cAMP in BRCA1 knock-down ovarian cancer cells can prevent cell death or cell cycle arrest caused by DNA damage.

Next, we investigated the apoptosis of A2780 cells after IR treatment using flow cytometry. Compared with control A2780 cells without IR treatment, which consisted of only 5.5% basal apoptotic cells, the proportions of control and BRCA1 knock-down A2780 cells that were apoptotic after IR treatment were 27.2 and 55.2%, respectively. This indicates that BRCA1 is essential for DNA damage repair, and that the lack of BRCA1 causes dramatic apoptosis in ovarian cancer cells bearing massive unrepaired DNA double-strand breaks. In contrast, in the presence of dobutamine, the percentages of control and BRCA1 knock-down A2780 cells that were apoptotic after IR treatment decreased to 13.3 and 18.5%, respectively. Similar to the effect of dobutamine, direct stimulation by 8-CPT-cAMP of IR-treated BRCA1 knock-down A2780 cells decreased the percentage of apoptotic cells to 13.25% (**Figures 5B,C**). At the same time, we also performed cell cycle analysis to determine the proportions of cells in each phase. The percentage of control A2780 cells in G1 phase was 35.49%. After exposure to IR, the percentages of control and BRCA1 knock-down A2780 cells in G1 phase were 63.39 and 65.48%, respectively, indicating that massive DNA damage arrested the cell cycle in G1. After dobutamine treatment, the percentages of G1 cells in IR-treated control and BRCA1 knock-down A2780 cells decreased to 44.32 and 43.03%, respectively, suggesting that cAMP terminated the cell cycle arrest caused by DNA damage. Treatment with 8-CPT-cAMP decreased the percentage of IR-treated BRCA1 knock-down A2780 cells in the G1 phase to 36.13%, a percentage similar to that of the control cells (**Figures 5D,E**). In addition, we tested whether DKK1 could inhibit the proliferation of $CD8^+$ T cell *in vitro*. Considering that DDK1 is a secreted protein, we collected culture supernatant of BRCA1 knock-down A2780 cells that were treated with or without dobutamine. Only the secretion of dobutamine treated BRCA1 knock-down A2780 cells could inhibited the proliferation of the $CD8^+$ T cells. The inhibitory effect could be compromised by adding the DKK1 antibody, but not the control IgG (**Figure 5F**), demonstrating that DKK1 can actually inhibit the proliferation of $CD8^+$ T cells. In general, we demonstrate that cAMP promoted by ADRB1 abolishes cell cycle arrest and DNA damage induced-apoptosis in BRCA1-deficient cancer cells. The secreted DKK1 from BRCA1-deficient cancer cells on the other hand confronts immune cells, assisting the apoptotic resistance.

cAMP Inhibits Apoptosis Through Abrogating p53 Accumulation

Using immunofluorescence staining, we determined the level of pro-apoptotic pore-forming protein BCL-2-associated X protein (BAX) in A2780 cells. Consistent with the previous results of flow cytometry, after exposure to IR, the BAX signal in A2780 cells was significantly enhanced in comparison with that in the control cells, and the percentages of BAX-positive cells in the two groups were 29.7 and 4.1%, respectively. As expected, a stronger BAX signal was detected in the BRCA1 knock-down cancer cells upon IR irradiation, and the percentage of BAX-positive cells increased to 61.2%. If the cells were treated with dobutamine beforehand, weaker BAX signals were observed in the IR-irradiated control and BRCA1 knock-down A2780 cells, and 13.7 and 14.5% cancer cells were BAX positive, respectively. In addition, the inhibitory effect of 8-CPT-cAMP on BAX protein accumulation was similar to that of dobutamine on the IR-treated BRCA1 knock-down ovarian cancer cells (**Figures 6A,B**). Immunoblotting against BAX and the activated (cleaved) form of the apoptotic executioner protein caspase-3 from A2780 ovarian cancer cells further verified the above results (**Figures 6C–E**), confirming that the inhibitory effect of cAMP on apoptosis of ovarian cancer cells is dependent on its ability to inhibit the apoptosis pathway.

Because of the essential role of p53 in apoptosis regulation (Carneiro and El-Deiry, 2020), p53 accumulation in response to DNA damage might be inhibited by the enhanced cAMP in the BRCA1-deficient ovarian cancer cells. After IR irradiation, p53 accumulation and caspase-3 cleavage were substantially elevated in the BRCA1 knock-down ovarian cancer cells. Dobutamine or 8-CPT-cAMP treatment dramatically decreased the levels of p53 and cleaved caspase-3. However, the inhibitory effect of dobutamine on p53 accumulation and caspase-3 cleavage was abrogated by the ADRB1 selective inhibitor atenolol (**Figures 6F,G**). The results show that cAMP antagonism of DNA damage-induced apoptosis is dependent on the inhibition of p53 accumulation in the BRCA1-deficient ovarian cancer cells. We also examined the inhibitory effects of cAMP on apoptosis in two other ovarian cells lines (OVCAR-5 and IGROV-1) with knock-down of BRCA1. IR-induced p53 accumulation and cleavage of caspase-3 in these cancer cells could also be attenuated by dobutamine (**Figure 6H**). In summary, these results show the relationship between the inhibitory effect of cAMP on apoptosis and DNA damage-induced p53 accumulation, BAX induction, and cleavage of caspase-3, demonstrating that ADRB1-mediated cAMP production negatively regulates DNA damage-induced apoptosis of the BRCA1-deficient ovarian cancer cells.

DISCUSSION

BRCA1 is an essential homologous recombination factor that plays fundamental functions in DNA damage repair and genomic

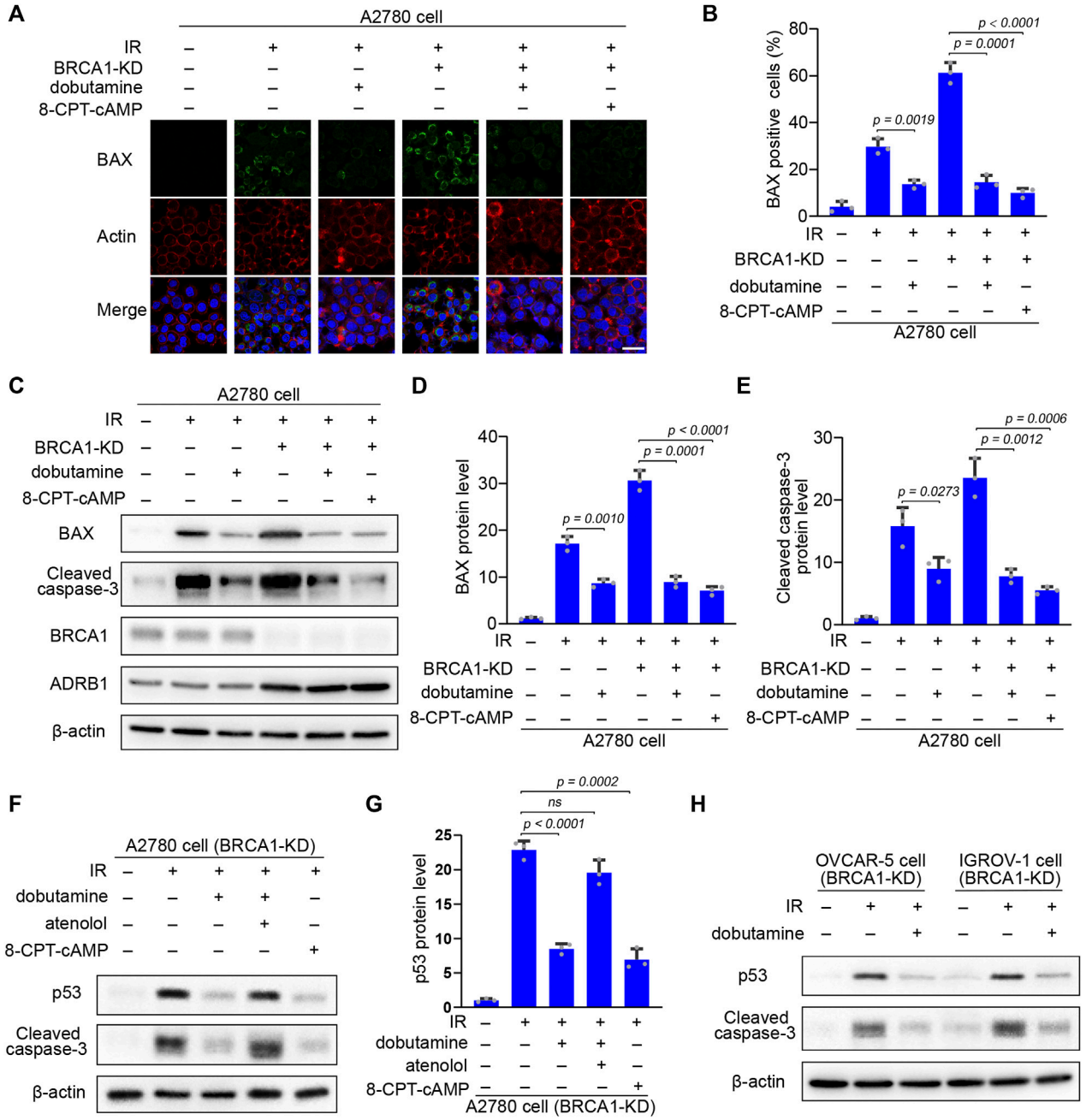

FIGURE 6 | The inhibitory effect of cAMP on IR-induced apoptosis is p53 dependent. **(A)** Control and BRCA1 knock-down A2780 cells were treated as described in **Panel 5C**. 18 h after IR, immunofluorescence staining of pro-apoptotic pore-forming protein BAX of each cells was performed. Scale bar, 25 μm. **(B)** Percentages of BAX positive cells in each group from **(A)**. At least 100 cells were included in each group. Three biologically independent replicates were performed. Data are presented as mean values ±SD. *p* values were calculated by unpaired two-tailed Student's *t*-tests. **(C)** Western blot analysis of BRCA1, ADRB1, BAX, and cleaved caspase-3 protein level in each group that were treated as described in **(A)**. β-actin was used as a loading control. **(D,E)** Protein levels of BAX and cleaved caspase-3 in each group from **(C)**. The relative intensities of BAX and cleaved caspase-3 bands were quantified by ImageJ. The experiments were performed three times. Data are presented as mean values ±SD. *p* values were calculated by unpaired two-tailed Student's *t*-tests. **(F)** BRCA1 knock-down A2780 cells were treated with or without dobutamine, atenolol, or 8-CPT-cAMP before exposed to 10 Gy IR. 18 h after IR, p53 and cleaved caspase-3 protein levels in each group were determined by western blot. β-actin was used as a loading control. **(G)** Protein levels of p53 in each group from **(F)**. The relative intensities of p53 bands were quantified by ImageJ. The experiments were performed three times. Data are presented as mean values ±SD. *p* values were calculated by unpaired two-tailed Student's *t*-tests. **(H)** BRCA1 knock-down OVCAR-5 and IGROV-1 cells were incubated with or without dobutamine before exposed to 10 Gy IR. 18 h after IR, p53 and cleaved caspase-3 protein levels in each group were determined by western blot. β-actin was used as a loading control.

integrity maintenance (Huen et al., 2010). BRCA1 deficiency results in defective DNA damage repair and accumulation of DNA lesions that is lethal to embryos and primary mouse embryonic fibroblast cells because of the activation of p53-dependent apoptosis (Gowen et al., 1996; Hakem et al., 1996; Ludwig et al., 1997; Xu et al., 2001). However, mutations in the *BRCA1* gene dramatically increase the incidence of breast and ovarian cancers in women (Eastson et al., 1995; Rahman and Stratton, 1998; King et al., 2003). In these patients, the *BRCA1*-mutated cancer cells resist apoptosis and grow normally even their p53 is proficient. Thus, the BRCA1-deficient cancer cells may evolve some apoptotic resistance skills *in vivo*. In this study, through retrospective analysis of ovarian cancer patients' transcriptome data, we found that ovarian cancer cells in BRCA1-deficient patients expressed higher levels of ADRB1, which can enable adenylyl cyclase to generate cAMP. Consistent with the results above, when BRCA1 was knocked down in BRCA1 wide-type ovarian cancer cell lines, the cells expressed higher levels of ADRB1, which promoted the production of cAMP. The elevated cAMP inhibited IR-induced cell apoptosis by abolishing the function of p53. On the other hand, the elevated cAMP also induced the expression of DDK1, which inhibited the proliferation of $CD8^+$ T lymphocytes that can promote the immune evasion of cancer cells. When ADRB1 was inhibited, the resistance ability of BRCA1-deficient ovarian cancer cells to p53-dependent apoptosis was abrogated.

It is well known that p53 is the key factor located in the center of the complex apoptosis pathway, which can be induced by cellular stresses, such as DNA damage, cytotoxic chemicals, and oxidative stress (Aubrey et al., 2018). Under normal conditions, p53 is maintained at a low level through continuous degradation by the proteasome. Upon a cellular stress, for example, persistent or irreparable DNA damage, p53 is stabilized and aggregates in the cell nucleus, where it initiates apoptosis to clear the cells with defective genomes (Hafner et al., 2019; Carneiro and El-Deiry, 2020). Therefore, circumvention of the p53-based apoptosis response is extremely important for the tumor formation and progression, especially in BRCA1-deficient ovarian and breast cancer cells, which are prone to accumulate DNA damages. In our retrospective analysis of transcriptome data from BRCA1-deficient ovarian cancer patients, we found that the DNA damage repair-related pathways were severely attenuated, and the gene mutation frequency was much higher than that in patients with normal BRCA1, suggesting that BRCA1 deficiency caused inefficient DNA damage repair, leading to a massive number of gene mutations and extreme genome instability. However, no obvious increase in apoptotic signals was detected in the BRCA1-deficient ovarian cancer patients, indicating that apoptosis was inhibited in the BRCA1-deficient ovarian cancer cells. Of course, mutation or deletion of p53 is the most direct mechanism to resist apoptosis, but not all BRCA1-deficient cancer patients carry defective p53 (Ramus et al., 1999; Greenblatt et al., 2001; Manie et al., 2009; Jonsson et al., 2019). We found that expression of ADRB1 in BRCA1-defective ovarian cancer cells was activated by extracellular catecholamine hormones. Activated ADRB1 generates abundant cAMP, which inhibits DNA damage-induced apoptosis. Therefore, it is also possible that characteristics of the specific physiological environment in the ovarian tissue, such as the existence of extracellular survival factors (e.g., extracellular catecholamine hormones) and/or BRCA1-defective ovarian cancer cells expressing higher levels of anti-apoptosis factors (e.g., ADRB1) overwhelm the p53-activated apoptosis.

In vivo, adrenergic receptors on the membranes of target cells can be bound and activated by the catecholamine hormones from the plasma, and then cAMP can be utilized to activate downstream pathways that regulate the associated biological processes (Antoni et al., 2006; Paravati et al., 2018). Studies have shown that β-adrenoreceptors, especially ADRB1 and ADRB2, are highly expressed in pan cancers that significantly reduce the overall survival of tumor patients (Lehrer and Rheinstein, 2020). From this side, the poor outcomes of BRCA1-deficient ovarian cancer patients are related to anti-apoptotic ability mediated by ADRB1. In addition to ADRB1, BRCA1-deficient ovarian cancer cells also express high levels of other factors related to catecholamine-adrenoceptor-cAMP pathway regulation, such as the adenylate cyclase ADCY2 and G protein-coupled receptor ADGRB1. Considering the role of BRCA1 in regulating gene transcription (Mullan et al., 2006; Rosen et al., 2006), we speculate that BRCA1 may act as a corepressor that inhibits the transcription of these genes. Moreover, the elevated cAMP induces an increased expression of the secretory protein DKK1, which was reported to promote tumor growth and metastasis in several tumor models (Kagey and He, 2017). In our study, we found that DKK1 secreted by BRCA1-deficient cancer cells could inhibit $CD8^+$ T cells proliferation, which impaired $CD8^+$ T cells activation. It has been reported that enhanced serum level of DKK1 is correlated with a poor prognosis in cancer patients (Chu et al., 2021). This effect may result from the immunoregulatory role of DKK1 in generating an immunosuppressive tumor microenvironment through suppressing the proliferation of $CD8^+$ T cells and other immune cells, thus facilitating the immune evasion of cancer cells. This enhances cAMP efficiency for apoptotic resistance in cancer cells. In the future, chemicals that can block the activities of these factors may be used as new therapeutic drugs against *BRCA1*-mutated tumors.

DATA AVAILABILITY STATEMENT

Publicly available datasets were analyzed in this study. This data can be found here: https://www.cbioportal.org/study/summary?id=ov_tcga.

AUTHOR CONTRIBUTIONS

ML conceived and designed the experiments; WY, BX and JM analyzed bioinformatics data; WY, YX, PW and XG performed the experiments; ML and WY wrote the manuscript.

FUNDING

This work was supported by the China Postdoctoral Science Foundation (2021M700289) to YX, and by the National Natural Science Foundation of China (82103106) to XG.

SUPPLEMENTARY MATERIAL

The Supplementary Material for this article can be found online at: https://www.frontiersin.org/articles/10.3389/fcell.2022.889656/full#supplementary-material

REFERENCES

Al Nakouzi, N., Wang, C. K., Beraldi, E., Jager, W., Ettinger, S., Fazli, L., et al. (2016). Clusterin Knockdown Sensitizes Prostate Cancer Cells to Taxane by Modulating Mitosis. *EMBO Mol. Med.* 8, 761–778. doi:10.15252/emmm.201506059

Antoni, M. H., Lutgendorf, S. K., Cole, S. W., Dhabhar, F. S., Sephton, S. E., Mcdonald, P. G., et al. (2006). The Influence of Bio-Behavioural Factors on Tumour Biology: Pathways and Mechanisms. *Nat. Rev. Cancer* 6, 240–248. doi:10.1038/nrc1820

Aubrey, B. J., Kelly, G. L., Janic, A., Herold, M. J., and Strasser, A. (2018). How Does P53 Induce Apoptosis and How Does This Relate to P53-Mediated Tumour Suppression? *Cell Death Differ* 25, 104–113. doi:10.1038/cdd.2017.169

Brodie, S. G., and Deng, C.-X. (2001). BRCA1-associated Tumorigenesis: what Have We Learned from Knockout Mice? *Trends Genet.* 17, S18–S22. doi:10.1016/s0168-9525(01)02451-9

Cao, L., Kim, S., Xiao, C., Wang, R.-H., Coumoul, X., Wang, X., et al. (2006). ATM-Chk2-p53 Activation Prevents Tumorigenesis at an Expense of Organ Homeostasis upon Brca1 Deficiency. *EMBO J.* 25, 2167–2177. doi:10.1038/sj.emboj.7601115

Carneiro, B. A., and El-Deiry, W. S. (2020). Targeting Apoptosis in Cancer Therapy. *Nat. Rev. Clin. Oncol.* 17, 395–417. doi:10.1038/s41571-020-0341-y

Cerami, E., Gao, J., Dogrusoz, U., Gross, B. E., Sumer, S. O., Aksoy, B. A., et al. (2012). The cBio Cancer Genomics portal: an Open Platform for Exploring Multidimensional Cancer Genomics Data. *Cancer Discov.* 2, 401–404. doi:10.1158/2159-8290.cd-12-0095

Chang, S.-H., Liu, C. H., Conway, R., Han, D. K., Nithipatikom, K., Trifan, O. C., et al. (2004). Role of Prostaglandin E 2 -dependent Angiogenic Switch in Cyclooxygenase 2-induced Breast Cancer Progression. *Proc. Natl. Acad. Sci. U.S.A.* 101, 591–596. doi:10.1073/pnas.2535911100

Chu, H. Y., Chen, Z., Wang, L., Zhang, Z.-K., Tan, X., Liu, S., et al. (2021). Dickkopf-1: a Promising Target for Cancer Immunotherapy. *Front. Immunol.* 12, 1850. doi:10.3389/fimmu.2021.658097

Creed, S. J., Le, C. P., Hassan, M., Pon, C. K., Albold, S., Chan, K. T., et al. (2015). β2-adrenoceptor Signaling Regulates Invadopodia Formation to Enhance Tumor Cell Invasion. *Breast Cancer Res.* 17, 145. doi:10.1186/s13058-015-0655-3

Deng, C.-X., and Brodie, S. G. (2000). Roles of BRCA1 and its Interacting Proteins. *Bioessays* 22, 728–737. doi:10.1002/1521-1878(200008)22:8<728:aid-bies6>3.0.co;2-b

Drost, R., Bouwman, P., Rottenberg, S., Boon, U., Schut, E., Klarenbeek, S., et al. (2011). BRCA1 RING Function Is Essential for Tumor Suppression but Dispensable for Therapy Resistance. *Cancer Cell* 20, 797–809. doi:10.1016/j.ccr.2011.11.014

Eastson, D., Ford, D., and Bishop, T. J. a. J. H. G. (1995). Breast and Ovarian Cancer Incidence in BRCA1-Mutations Carriers. *Am. J. Hum. Genet.* 56, 256–271.

Elledge, S. J., and Amon, A. (2002). The BRCA1 Suppressor Hypothesis: an Explanation for the Tissue-specific Tumor Development in BRCA1 Patients. *Cancer Cell* 1, 129–132. doi:10.1016/s1535-6108(02)00041-7

Eyfjord, J. E., and Bodvarsdottir, S. K. (2005). Genomic Instability and Cancer: Networks Involved in Response to DNA Damage. *Mutat. Res./Fund. Mol. Mech. Mutagen.* 592, 18–28. doi:10.1016/j.mrfmmm.2005.05.010

Gao, J., Aksoy, B. A., Dogrusoz, U., Dresdner, G., Gross, B., Sumer, S. O., et al. (2013). Integrative Analysis of Complex Cancer Genomics and Clinical Profiles Using the cBioPortal. *Sci. Signal.* 6, pl1. doi:10.1126/scisignal.2004088

Ghobrial, I. M., Witzig, T. E., and Adjei, A. A. (2005). Targeting Apoptosis Pathways in Cancer Therapy. *CA: A Cancer J. Clin.* 55, 178–194. doi:10.3322/canjclin.55.3.178

Gowen, L. C., Johnson, B. L., Latour, A. M., Sulik, K. K., and Koller, B. H. (1996). Brca1 Deficiency Results in Early Embryonic Lethality Characterized by Neuroepithelial Abnormalities. *Nat. Genet.* 12, 191–194. doi:10.1038/ng0296-191

Greenblatt, M. S., Chappuis, P. O., Bond, J. P., Hamel, N., and Foulkes, W. D. (2001). TP53 Mutations in Breast Cancer Associated with BRCA1 or BRCA2 Germ-Line Mutations: Distinctive Spectrum and Structural Distribution. *Cancer Res.* 61, 4092–4097.

Hafner, A., Bulyk, M. L., Jambhekar, A., and Lahav, G. (2019). The Multiple Mechanisms that Regulate P53 Activity and Cell Fate. *Nat. Rev. Mol. Cel Biol.* 20, 199–210. doi:10.1038/s41580-019-0110-x

Hakem, R., De La Pompa, J. L., Sirard, C., Mo, R., Woo, M., Hakem, A., et al. (1996). The Tumor Suppressor Gene Brca1 Is Required for Embryonic Cellular Proliferation in the Mouse. *Cell* 85, 1009–1023. doi:10.1016/s0092-8674(00)81302-1

Heinecke, J. L., Ridnour, L. A., Cheng, R. Y. S., Switzer, C. H., Lizardo, M. M., Khanna, C., et al. (2014). Tumor Microenvironment-Based Feed-Forward Regulation of NOS2 in Breast Cancer Progression. *Proc. Natl. Acad. Sci. U.S.A.* 111, 6323–6328. doi:10.1073/pnas.1401799111

Huen, M. S. Y., Sy, S. M. H., and Chen, J. (2010). BRCA1 and its Toolbox for the Maintenance of Genome Integrity. *Nat. Rev. Mol. Cel Biol.* 11, 138–148. doi:10.1038/nrm2831

Jonsson, P., Bandlamudi, C., Cheng, M. L., Srinivasan, P., Chavan, S. S., Friedman, N. D., et al. (2019). Tumour Lineage Shapes BRCA-Mediated Phenotypes. *Nature* 571, 576–579. doi:10.1038/s41586-019-1382-1

Kagey, M. H., and He, X. (2017). Rationale for Targeting the Wnt Signalling Modulator Dickkopf-1 for Oncology. *Br. J. Pharmacol.* 174, 4637–4650. doi:10.1111/bph.13894

King, M.-C., Marks, J. H., and Mandell, J. B.New York Breast Cancer Study Group (2003). Breast and Ovarian Cancer Risks Due to Inherited Mutations in BRCA1 and BRCA2. *Science* 302, 643–646. doi:10.1126/science.1088759

Lehrer, S., and Rheinstein, P. H. (2020). The ADRB1 (Adrenoceptor Beta 1) and ADRB2 Genes Significantly Co-express with Commonly Mutated Genes in Prostate Cancer. *Discov. Med.* 30, 163–171.

Liao, Y., Wang, J., Jaehnig, E. J., Shi, Z., and Zhang, B. (2019). WebGestalt 2019: Gene Set Analysis Toolkit with Revamped UIs and APIs. *Nucleic Acids Res.* 47, W199–W205. doi:10.1093/nar/gkz401

Ludwig, T., Chapman, D. L., Papaioannou, V. E., and Efstratiadis, A. (1997). Targeted Mutations of Breast Cancer Susceptibility Gene Homologs in Mice: Lethal Phenotypes of Brca1, Brca2, Brca1/Brca2, Brca1/p53, and Brca2/p53 Nullizygous Embryos. *Genes Dev.* 11, 1226–1241. doi:10.1101/gad.11.10.1226

Manié, E., Vincent-Salomon, A., Lehmann-Che, J., Pierron, G., Turpin, E., Warcoin, M., et al. (2009). High Frequency of TP53 Mutation in BRCA1 and Sporadic Basal-like Carcinomas but Not in BRCA1 Luminal Breast Tumors. *Cancer Res.* 69, 663–671. doi:10.1158/0008-5472.can-08-1560

Monteiro, A. N. A. (2003). BRCA1: the Enigma of Tissue-specific Tumor Development. *Trends Genet.* 19, 312–315. doi:10.1016/s0168-9525(03)00110-0

Mootha, V. K., Lindgren, C. M., Eriksson, K.-F., Subramanian, A., Sihag, S., Lehar, J., et al. (2003). PGC-1α-responsive Genes Involved in Oxidative Phosphorylation Are Coordinately Downregulated in Human Diabetes. *Nat. Genet.* 34, 267–273. doi:10.1038/ng1180

Mullan, P. B., Quinn, J. E., and Harkin, D. P. (2006). The Role of BRCA1 in Transcriptional Regulation and Cell Cycle Control. *Oncogene* 25, 5854–5863. doi:10.1038/sj.onc.1209872

Naderi, E. H., Findley, H. W., Ruud, E., Blomhoff, H. K., and Naderi, S. (2009). Activation of cAMP Signaling Inhibits DNA Damage-Induced Apoptosis in BCP-ALL Cells through Abrogation of P53 Accumulation. *Blood* 114, 608–618. doi:10.1182/blood-2009-02-204883

Nishihara, H., Kizaka-Kondoh, S., Insel, P. A., and Eckmann, L. (2003). Inhibition of Apoptosis in normal and Transformed Intestinal Epithelial Cells by cAMP

through Induction of Inhibitor of Apoptosis Protein (IAP)-2. *Proc. Natl. Acad. Sci. U.S.A.* 100, 8921–8926. doi:10.1073/pnas.1533221100

Paravati, S., Rosani, A., and Warrington, S. J. (2018). *Physiology, Catecholamines*. Treasure Island, FL: StatPearls Publishing.

Patra, C., Foster, K., Corley, J. E., Dimri, M., and Brady, M. F. J. S. (2021). *Biochemistry*. Treasure Island, FL: StatPearls Publishing. cAMP.

Pon, C. K., Lane, J. R., Sloan, E. K., and Halls, M. L. (2016). The β 2 -adrenoceptor Activates a Positive cAMP-calcium Feedforward Loop to Drive Breast Cancer Cell Invasion. *FASEB j.* 30, 1144–1154. doi:10.1096/fj.15-277798

Rahman, N., and Stratton, M. R. (1998). The Genetics of Breast Cancer Susceptibility. *Annu. Rev. Genet.* 32, 95–121. doi:10.1146/annurev.genet.32.1.95

Ramus, S. J., Bobrow, L. G., Pharoah, P. D. P., Finnigan, D. S., Fishman, A., Altaras, M., et al. (1999). Increased Frequency ofTP53 Mutations inBRCA1 andBRCA2 Ovarian Tumours. *Genes Chromosom. Cancer* 25, 91–96. doi:10.1002/(sici)1098-2264(199906)25:2<91:aid-gcc3>3.0.co;2-5

Rosen, E. M., Fan, S., and Ma, Y. (2006). BRCA1 Regulation of Transcription. *Cancer Lett.* 236, 175–185. doi:10.1016/j.canlet.2005.04.037

Sales, K. J., Katz, A. A., Davis, M., Hinz, S., Soeters, R. P., Hofmeyr, M. D., et al. (2001). Cyclooxygenase-2 Expression and Prostaglandin E2Synthesis Are Up-Regulated in Carcinomas of the Cervix: A Possible Autocrine/Paracrine Regulation of Neoplastic Cell Function via EP2/EP4 Receptors. *J. Clin. Endocrinol. Metab.* 86, 2243–2249. doi:10.1210/jcem.86.5.7442

Savage, K. I., and Harkin, D. P. (2015). BRCA1, a 'complex' Protein Involved in the Maintenance of Genomic Stability. *FEBS J.* 282, 630–646. doi:10.1111/febs.13150

Shikazono, N., Noguchi, M., Fujii, K., Urushibara, A., and Yokoya, A. (2009). The Yield, Processing, and Biological Consequences of Clustered DNA Damage Induced by Ionizing Radiation. *Jrr* 50, 27–36. doi:10.1269/jrr.08086

Sood, A. K., Armaiz-Pena, G. N., Halder, J., Nick, A. M., Stone, R. L., Hu, W., et al. (2010). Adrenergic Modulation of Focal Adhesion Kinase Protects Human Ovarian Cancer Cells from Anoikis. *J. Clin. Invest.* 120, 1515–1523. doi:10.1172/jci40802

Stordal, B., Timms, K., Farrelly, A., Gallagher, D., Busschots, S., Renaud, M., et al. (2013). BRCA1/2 Mutation Analysis in 41 Ovarian Cell Lines Reveals Only One Functionally Deleterious BRCA1 Mutation. *Mol. Oncol.* 7, 567–579. doi:10.1016/j.molonc.2012.12.007

Subramanian, A., Tamayo, P., Mootha, V. K., Mukherjee, S., Ebert, B. L., Gillette, M. A., et al. (2005). Gene Set Enrichment Analysis: a Knowledge-Based Approach for Interpreting Genome-wide Expression Profiles. *Proc. Natl. Acad. Sci. U.S.A.* 102, 15545–15550. doi:10.1073/pnas.0506580102

Tarsounas, M., and Sung, P. (2020). The Antitumorigenic Roles of BRCA1-BARD1 in DNA Repair and Replication. *Nat. Rev. Mol. Cel Biol.* 21, 284–299. doi:10.1038/s41580-020-0218-z

Xu, X., Qiao, W., Linke, S. P., Cao, L., Li, W.-M., Furth, P. A., et al. (2001). Genetic Interactions between Tumor Suppressors Brca1 and P53 in Apoptosis, Cell Cycle and Tumorigenesis. *Nat. Genet.* 28, 266–271. doi:10.1038/90108

Yan, K., Gao, L.-N., Cui, Y.-L., Zhang, Y., and Zhou, X. (2016). The Cyclic AMP Signaling Pathway: Exploring Targets for Successful Drug Discovery (Review). *Mol. Med. Rep.* 13, 3715–3723. doi:10.3892/mmr.2016.5005

Zhang, X., Zhang, Y., He, Z., Yin, K., Li, B., Zhang, L., et al. (2019). Chronic Stress Promotes Gastric Cancer Progression and Metastasis: an Essential Role for ADRB2. *Cell Death Dis.* 10, 788. doi:10.1038/s41419-019-2030-2

Zhu, Q., Pao, G. M., Huynh, A. M., Suh, H., Tonnu, N., Nederlof, P. M., et al. (2011). BRCA1 Tumour Suppression Occurs via Heterochromatin-Mediated Silencing. *Nature* 477, 179–184. doi:10.1038/nature10371

Conflict of Interest: The authors declare that the research was conducted in the absence of any commercial or financial relationships that could be construed as a potential conflict of interest.

Publisher's Note: All claims expressed in this article are solely those of the authors and do not necessarily represent those of their affiliated organizations, or those of the publisher, the editors, and the reviewers. Any product that may be evaluated in this article, or claim that may be made by its manufacturer, is not guaranteed or endorsed by the publisher.

frontiers | Frontiers in Cell and Developmental Biology

REVIEW
published: 26 April 2022
doi: 10.3389/fcell.2022.903781

Nucleic Acid Sensing Pathways in DNA Repair Targeted Cancer Therapy

Bingteng Xie[1,2]* *and Aiqin Luo*[1,2]*

[1]School of Life Science, Beijing Institute of Technology, Beijing, China, [2]Key Laboratory of Molecular Medicine and Biological Diagnosis and Treatment, Beijing Institute of Technology, Ministry of Industry and Information Technology, Beijing, China

The repair of DNA damage is a complex process, which helps to maintain genome fidelity, and the ability of cancer cells to repair therapeutically DNA damage induced by clinical treatments will affect the therapeutic efficacy. In the past decade, great success has been achieved by targeting the DNA repair network in tumors. Recent studies suggest that DNA damage impacts cellular innate and adaptive immune responses through nucleic acid-sensing pathways, which play essential roles in the efficacy of DNA repair targeted therapy. In this review, we summarize the current understanding of the molecular mechanism of innate immune response triggered by DNA damage through nucleic acid-sensing pathways, including DNA sensing *via* the cyclic GMP-AMP synthase (cGAS), Toll-like receptor 9 (TLR9), absent in melanoma 2 (AIM2), DNA-dependent protein kinase (DNA-PK), and Mre11-Rad50-Nbs1 complex (MRN) complex, and RNA sensing *via* the TLR3/7/8 and retinoic acid-inducible gene I (RIG-I)-like receptors (RLRs). Furthermore, we will focus on the recent developments in the impacts of nucleic acid-sensing pathways on the DNA damage response (DDR). Elucidating the DDR-immune response interplay will be critical to harness immunomodulatory effects to improve the efficacy of antitumor immunity therapeutic strategies and build future therapeutic approaches.

Keywords: DNA damage and repair, DDR inhibitors, nucleic acid-sensing pathways, innate immunity, immunotherapy

OPEN ACCESS

Edited by:
Teng Ma,
Capital Medical University, China

Reviewed by:
Jianyu Wang,
Chongqing Medical University, China
Yang Pu,
Chinese Academy of Medical Sciences and Peking Union Medical College, China

***Correspondence:**
Bingteng Xie
xiebingteng@bit.edu.cn
Aiqin Luo
aqluobit@163.com

Specialty section:
This article was submitted to Signaling, a section of the journal Frontiers in Cell and Developmental Biology

Received: *24 March 2022*
Accepted: *08 April 2022*
Published: *26 April 2022*

Citation:
Xie B and Luo A (2022) Nucleic Acid Sensing Pathways in DNA Repair Targeted Cancer Therapy. Front. Cell Dev. Biol. 10:903781. doi: 10.3389/fcell.2022.903781

1 OVERVIEW OF DNA DAMAGE AND REPAIR NETWORK

Up until now, chemotherapy and radiotherapy have remained the important treatment options for a variety of cancers (Hellmann et al., 2016; Chu et al., 2018; Qin et al., 2018; De Ruysscher et al., 2019; Grassberger et al., 2019; Galluzzi et al., 2020; Huang and Zhou, 2020; McLaughlin et al., 2020). The key mechanism of tumor cell death induced by standard chemotherapy and radiotherapy is DNA damage, leading to cell-cycle arrest and death directly or after S-phase DNA replication in the cell cycle. On the other hand, to deal with possible DNA lesions, tumors cells have evolved intricate repair mechanisms, and the ability to repair therapy-induced DNA damage would influence the therapeutic efficacy (Bouwman and Jonkers, 2012; Gavande et al., 2016). Here, we first overview the various types of DNA damage caused by radiotherapy and chemotherapy and the corresponding DNA damage repair pathways (see previous reviews for details) (Ciccia and Elledge, 2010; Giglia-Mari et al., 2011; Pinder et al., 2013; Chatterjee and Walker, 2017; Cussiol et al., 2019; Souliotis et al., 2020).

Some commonly used potent chemotherapy compounds (cyclophosphamide, dacarbazine, cisplatin, etc.) act by adding the alkyl groups to specific bases of DNA, yielding alkylated products such as O2-alkylthymine, O4-alkylthymine, O6-methylguanine, and O6-ethylguanine (Serrone et al., 2000; Emadi et al., 2009; Dasari and Tchounwou, 2014). Monofunctional alkylating agents have one active moiety and can only modify a single base, while bifunctional

alkylating agents have two reaction sites, which can crosslink DNA to protein or another DNA base resulting in intra-strand crosslinks or inter-strand crosslinks. Radiotherapy by ionizing radiation (IR) can attack DNA directly by breaking the phosphodiester bond and the deoxyribose, and other indirect means have also been confirmed, for example, highly reactive oxygen species (ROS) produced from water radiolysis could result in the oxidization of the DNA desoxyribose moiety and the four nitrogenous bases (Henner et al., 1982; Desouky et al., 2015). Thereby, chemotherapy and radiotherapy can result in various kinds of DNA damage including base damage, single-strand breaks (SSBs), and double-strand breaks (DSBs). Among them, DSBs are thought to be the most harmful to cell survival and are the main mechanism to promote the therapeutic effect.

To remedy various DNA damage types, there has developed a complex DNA damage response (DDR) network (Giglia-Mari et al., 2011). The pathways involved in DNA damage repair mainly include direct reversal, base excision repair (BER), nucleotide excision repair (NER), non-homologous end joining (NHEJ), and homologous recombination (HR) pathway. Direct reversal, the simplest DNA repair pathway, depends primarily on a single protein and does not involve nucleotide removal, resynthesis, or ligation. For example, the O6-alkyl group of guanines can be removed by O6-methylguanine DNA methyltransferase (MGMT). BER and NER pathways take part in the DNA SSBs repairment. BER often participates in the repair of the small but highly mutagenic DNA lesions, which usually significantly undermine genomic fidelity and stability (Dianov and Hübscher, 2013). The BER pathway is initiated with the excision of the damaged base by any of 11 DNA glycosylases (Krokan et al., 1997), after which the exposed gap will be filled by a different set of proteins, among which the repair of single-base gaps require the short-patch pathway while polybasic gaps are in need of the long-patch pathway (Woodrick et al., 2017; Biau et al., 2019; Caldecott 2020). The NER pathway involves multiple steps requiring more than 30 proteins and is the main pathway used by mammals to remove bulky DNA lesions, including numerous chemical adducts, intra-strand crosslinking of DNA, and some forms of oxidative damage. In the NER pathway, the damaged bases are first recognized, then the DNA double-strand is unwound, and then the excision repair complex will remove the damaged bases followed by filling and ligating of the gap (Gillet and Schärer, 2006; Shuck et al., 2008).

DSB is a highly toxic gene damage that seriously threatens cellular homeostasis by affecting the transcription of genes, DNA replication, and chromosome segregation. Failure in repairing DSBs can lead to devastating chromosomal instabilities, and result in the dysregulation of gene expression and an increased hazard of carcinogenesis (Kryston et al., 2011). In human cells, two pathways, HDR and NHEJ, take part in DNA DSBs repair (Chang et al., 2017). HDR is generally considered to be participated in DSBs repair only during the S and G2 phases of the cell cycle given that it needs a homologous template to replace the damaged DNA segment in the genome, but it has been shown that centromeric DSBs in the G1 phase can activate the HDR pathway to maintain centromeric integrity recently (Yilmaz et al., 2021). The canonical HDR pathway is relatively slow but error-free, which needs numerous factors involved in homology search, Holliday junction formation, DNA synthesis, and the final DNA ligation (San Filippo et al., 2008; Krejci et al., 2012). Unlike the HR pathway, the NHEJ pathway does not need a DNA template and is active throughout the whole cell cycle, therefore it responds relatively quickly but is error-prone (Chang et al., 2017). In NHEJ pathway, four specific steps are involved including DNA termini recognition, bridging of the DNA ends, DNA end processing, and DNA ligation.

2 DNA REPAIR TARGETED THERAPY

Given that tumor cells could repair DNA damage induced by chemotherapy and radiotherapy in order to survive, the use of inhibitors of specific DNA repair pathways combined with DNA-damaging treatment can be efficacious. Some DNA repair inhibitors have been exploited as clinical agents targeting the proteins involved in sensing and conducting DNA damage signals as well as other proteins in DNA repair pathways (Mateo et al., 2019; Cheng et al., 2022).

DNA damage sensor proteins are key functional proteins to initiate repair and can sense multiple DNA damage signals, in which poly (ADP-ribosyl) polymerase-1 (PARP-1) is widely recognized to be the primary responder to SSBs while it could also bind and signal DSBs (Li and Yu 2013; Ceccaldi et al., 2015; Mateos-Gomez et al., 2015; Pandey and Black, 2021). After rapidly detecting the DNA damage, PARP-1 synthesizes of poly (ADP-ribose) (PAR) chains on itself and many different proteins near the damage site initiating recruitment of DNA repair complexes. The formation of the PAR chain can promote the release of PARP-1 from the position where it binds to the damaged DNA so that the other repair proteins could contact with the damaged site. Inhibition of PARP will reduce the synthesis of PAR chains, making PARP unable to dissociate from damaged DNA, thus preventing the recruitment of other repair proteins (Zandarashvili et al., 2020). The failure of PAR chain formation and the release of PARP from damaged DNA will lead to the enrichment of SSBs, which can be transformed into single-sided DSBs during DNA replication (Bixel and Hays, 2015). However, in the cells with the absence of intact DSBs repair pathways, such as in BRCA1 and BRCA2 mutated cells, the persistent DSBs are toxic and even deadly. Many small molecule PARP inhibitors (PARPi) targeting the catalytic activity of PARP-1 are now approved and clinically used in patients with breast, ovarian, prostate, and pancreatic cancers deficient in other DDR components, and the expanded utilities of small molecule PARP inhibitors in other cancer types are under consideration (Ramakrishnan Geethakumari et al., 2017; Zimmer et al., 2018; Hammel et al., 2020; Xie et al., 2020).

For DSBs, lupus Ku autoantigen protein (Ku) and the Mre11-Rad50-Nbs1 complex (MRN) play important roles. Ku is a protein heterodimer composed of Ku70/Ku80, which takes part in the NHEJ pathway and binds to DNA DSBs (Chen et al., 2021). Upon recognition and binding of DSBs, Ku recruits the DNA-dependent protein kinase catalytic subunit (DNA-PKcs) that assists in classical NHEJ repair. A class of

compounds has been developed that abrogates the Ku-DNA end binding activity, inhibits cellular NHEJ, and enhances the cellular activity of radiomimetic agents and IR (Gavande et al., 2020). The MRN complex has nuclease activity and can bind DNA, so it can participate in the initial detection and processing of DSB (Rupnik et al., 2008), which is dependent on the nuclease activity of Mre11, the central factor of the MRN complex with endonuclease activity and 3′–5′ exonuclease activity (Stracker and Petrini, 2011). Upon bound to the damaged position, MRN recruits the DNA-damage signaling kinase ataxia-telangiectasia mutated (ATM), activates it, and triggers a series of signaling events that drive HR repair (Uziel et al., 2003). A class of inhibitors has been developed to selectively block the nuclease activity of Mre11 and prevent DNA damage repair (Dupré et al., 2008).

DNA damage signaling proteins trigger multiple post-translational modifications and the assembly of protein complexes, which amplify and diversify the DNA damage signals. Initially, one of three phosphatidylinositol-3 kinase-related kinases (PIKKs): DNA-PKcs, ATM, or ATM- and Rad3-Related (ATR) is activated by phosphorylation in response to DNA damage (Woods and Turchi, 2013). DNA-PKcs, forming a heterotrimeric complex with Ku, are required for proper DSBs repair by NHEJ. Using its activated kinase activity after being bound to the DNA terminus, it will phosphorylate itself and other target proteins to coordinates the NHEJ pathway (Falck et al., 2005; Uematsu et al., 2007). Following the appearance of DSB, the MRN complex activates ATM, which then phosphorylates histone H2AX as the main kinase (Burma et al., 2001). ATM could also phosphorylate checkpoint kinase 2 (Chk2) and p53 to impact cell cycle regulation and cytotoxicity (Cheng and Chen, 2010; Smith et al., 2010). ATR participates in HR, NER, long-patch BER, postreplication repair, interstrand cross-link repair, and replication fork restart after its activation by replication protein A (RPA)-coated ssDNA (Cimprich and Cortez, 2008). Several small molecules targeting three PIKKs such as VX-984 and CC-115 for DNA-PKcs, AZD0156 for ATM, VX-970, and AZD6738 for ATR are currently in different stages of clinical trials (Munster et al., 2016; Foote et al., 2018; Pike et al., 2018; Timme et al., 2018; Gorecki et al., 2020). In addition, checkpoint kinase 1 (Chk1) and Chk2, protein kinases that lie downstream of ATR and ATM, have also been utilized as therapeutic targets for drug development (Jobson et al., 2009; King et al., 2014).

3 NUCLEIC ACID-SENSING PATHWAYS CONNECT DNA DAMAGE TO INNATE IMMUNITY

Cancer chemotherapy and radiotherapy aim to induce catastrophic DNA damage such as DSBs to cause cancer cell apoptosis, which can further aggravate the degree of DNA damage and promote the therapeutic effect when combined with DNA damage repair inhibitors. According to the severity of the DNA damage, some cancer cells directly initiate programmed cell death to clear the damaged genome beyond endurance. Besides, nucleic acid released from dying cells can activate the innate immune response of surrounding cells (Wang et al., 2021b). Even if DNA damage does not directly kill cells, increasing evidence indicates that the accumulation of nucleic acids in the cytoplasm caused by DNA damage can also trigger an inflammatory response within the cells (Nastasi et al., 2020). DNA damage-induced cytosolic nucleic acid shares common receptors (pattern recognition receptors, PRRs) and downstream effectors with those induced by viral or bacterial infections (Takeuchi and Akira, 2010; Taffoni et al., 2021), which are summarized below (**Figure 1**). And some agonists of these nucleic acid-sensing pathways are already in clinical trials (**Table 1**). Strikingly, recent research has indicated that the proteins that participated in DNA repair also play active roles in innate immune signaling.

3.1 DNA Sensing Pathways

3.1.1 Cyclic GMP-AMP Synthase

Normally, DNA is trapped in the nucleus and mitochondria and rapidly degraded by nucleases in the cytoplasm and endolysosomes. DNA-sensing receptors could detect increased amounts of intracellular DNA. Currently, cyclic GMP-AMP synthase (cGAS), a nucleotidyltransferase (NTase), is the most widely accepted dsDNA sensor that acts followed by stimulator of interferon genes (STING) performing multiple functions (Kuchta et al., 2009; Sun et al., 2013; Wu et al., 2013). cGAS normally resides to be inactive. Initial studies considered cGAS as a cytoplasmic protein, in which cGAS could not interact with nuclear or mitochondrial DNA, but some recent works indicate that cGAS also resides in the nucleus constitutively (Gentili et al., 2019; Jiang et al., 2019; Volkman et al., 2019). cGAS can be activated not only by viral or bacterial infection-related DNA entering the cytoplasm but also by endogenous self-DNA, including cytosolic DNA from nucleus and mitochondria, DNA in cytoplasmic micronucleus, and chromatin in the nucleus (Li X.-D. et al., 2013; West et al., 2015; Dou et al., 2017; Glück et al., 2017; Harding et al., 2017; Mackenzie et al., 2017; Gratia et al., 2019). Upon binding to DNA, cGAS assembles into a dimer at an active state and converts ATP and GTP into the second messenger cyclic GMP-AMP (cGAMP) (Ablasser et al., 2013; Diner et al., 2013; Gao et al., 2013; Zhang et al., 2013). The complete activation and stabilization of cGAS-DNA complexes require DNA lengths to exceed a certain threshold, allowing two or more cGAS molecules to bind to the same DNA to form oligomeric structures or condensates (Li X. et al., 2013; Zhang J.-Z. et al., 2014; Andreeva et al., 2017; Luecke et al., 2017; Du and Chen, 2018; Hooy and Sohn, 2018). The cyclic-dinucleotide sensor STING, an ~40 kDa dimeric transmembrane protein located in the endoplasmic reticulum (ER), could detect and bind to cGAMP to make a conformational change, which results in its translocation from the ER to the Golgi apparatus and the activation of TANK-binding kinase 1 (TBK1) (Ishikawa and Barber, 2008; Burdette et al., 2011; Liu et al., 2015; Ergun et al., 2019; Shang et al., 2019; Zhang et al., 2019; Zhao et al., 2019). The activated TBK1 phosphorylates itself, STING, and the interferon regulatory factor 3 (IRF3), after which the active IRF3 dimer is transported to the nucleus to activate the expression of type I interferon genes. The cGAS-STING signaling can also lead to the transcription of pro-inflammatory cytokines-related genes

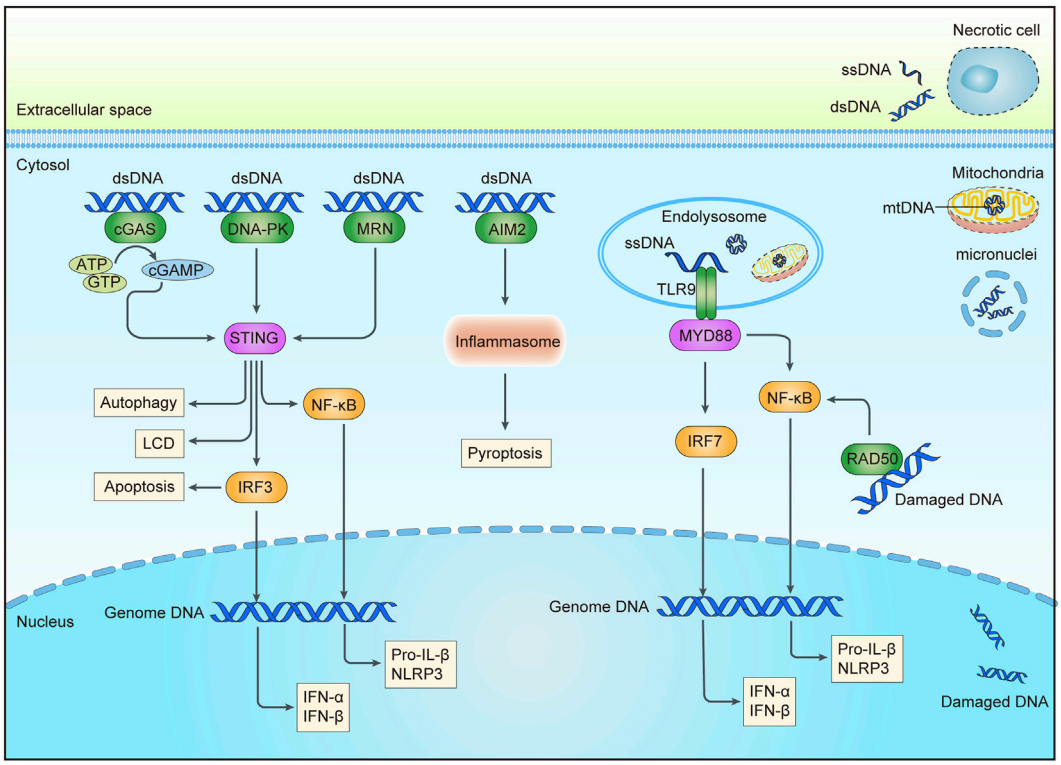

FIGURE 1 | DNA sensing pathways triggered by DNA damage. An abnormal increase of intracellular DNA could come from the nucleus, micronuclei, or mitochondria after chemotherapy or radiation. DNA in endosomal may be from extracellular DNA of necrotic cells through endocytosis or cytoplasmic DNA through autophagy. Sensors for DNA are shown in green, including cGAS, DNA-PK, MRN, AIM2, and RAD50 in the cytoplasm, and TLR9 in the endolysosome. Adaptor molecules are shown in pink and downstream signaling molecules are shown in yellow. Activation of these pathways may result in the production of interferon (IFN) and other cytokines, apoptosis, pyroptosis, autophagy, etc., cGAS, cyclic GMP-AMP synthase; DNA-PK, DNA-dependent protein kinase complex; MRN, Mre11-Rad50-Nbs1 complex; AIM2, absent in melanoma 2; TLR9, Toll-like receptor 9; cGAMP, cyclic GMP-AMP; STING, stimulator of interferon genes; MYD88, myeloid differentiation primary response protein 88; IRF3/7, interferon regulatory factor 3/7; NF-κB, nuclear factor-κB; NLRP3, NOD-, LRR- and pyrin domain-containing 3; LCD, a lytic cell death program; dsDNA, double stranded DNA; ssDNA, single stranded DNA; mtDNA, mitochondrial DNA.

via nuclear factor-κB (NF-κB) (de Oliveira Mann et al., 2019). In addition, STING is related to autophagy induction, however, its functional mechanism still remains to be elucidated (Watson et al., 2012). Growing studies suggest that the activation of STING can trigger cell death by various means. For example, STING could facilitate respective programmed cell death by inducing the production of many pro-apoptotic and pro-necroptotic molecules (Paludan et al., 2019). Furthermore, the accumulation of lysosomal STING could trigger lysosome membrane permeabilization, leading to the release of lysosomal hydrolases with cell death as a result (Gaidt et al., 2017). Besides, phosphorylated IRF3 downstream of STING can stimulate apoptosis by reducing the Bcl-xL-dependent suppression of the permeability of mitochondrial outer membrane in mitotic cells (Zierhut et al., 2019; Xie et al., 2021).

3.1.2 Toll-Like Receptors 9

Toll-like receptors (TLRs) are important components of innate immune responses induced by pathogenic microorganisms or tissue injury (Moresco et al., 2011). TLR, a highly conserved intracellular transmembrane protein, has emerged as a key PRR in the past 20 years. It exists in multiple types of cells, such as T cells, B cells, APC, epithelial cells, and endothelial cells (Chang 2010). All TLRs possess a leucine-rich-repeat (LRR) domain binding ligand extracellularly, a transmembrane domain, and a cytosolic Toll/IL-1 receptor (TIR) homology domain (Delneste et al., 2007). In all TLRs, TLR9 is found specifically in the endosomes and can be activated by single-stranded DNA containing unmethylated cytidine-phosphate-guanosine (CpG) dinucleotides escaping from the digestion of nucleases such as DNase II (Kumagai et al., 2008). TLR9 must undergo proteolytic processing in the endosomal compartments to complete ligand-mediated dimerization and activation (Majer et al., 2017). TLR9 not only triggers plasmacytoid dendritic cells to produce type I IFN and activate the polyclonal B cells through the myeloid differentiation primary response protein 88 (MYD88) and interferon-regulatory factor 7 (IRF7) signaling pathway, but also induces the production of inflammasome-related factors pro-interleukin-1β (pro-IL-1β) and NOD-, LRR- and pyrin domain-containing 3 (NLRP3) *via* NF-κB (Honda et al., 2005; Zhang X. et al., 2014). According to a recent study, TLR9 can sense mitochondrial DNA during mitophagy, and induce C-X-C motif chemokine ligand 10 (CXCL10) expression and $CD8^+$ T cell recruitment, which reveals a novel role of chemotherapy in the innate immune response (Limagne et al., 2022).

TABLE 1 | Summary of clinical trials of nucleic acid-sensing pathways-related agonists.

PRR	ClinicalTrials.gov Identifier	Agent(s)	Route of administration	Cancer type(s)	Clinical phase of development
STING	NCT04144140	E7766	Intratumoral	Lymphoma; advanced solid tumors	Phase 1/1b
STING	NCT04609579	SNX281 (or in combination with pembrolizumab)	Intravenous	Advanced solid tumor; advanced lymphoma	Phase 1
STING	NCT05070247	TAK-500 (or in combination with pembrolizumab)	Intravenous	Select locally advanced; metastatic solid tumors	Phase 1
TLR	NCT00960752	R848 gel (in combination with gp100 and MAGE-3 peptide vaccine)	Intradermally and subcutaneously	Melanoma	Phase 2
TLR	NCT02668770	MGN1703 (in combination with ipilimumab)	Subcutaneously and intratumoral injection	Advanced cancers; melanoma	Phase 1
TLR3	NCT03734692	Rintatolimod (in combination with cisplatin and pembrolizumab)	Intraperitoneal	Ovarian cancer recurrent	Phase 1; Phase 2
TLR7	NCT00899574	Imiquimod	Cream	Breast cancer; breast neoplasms	Phase 2
TLR7	NCT00941811	Imiquimod	Cream	HPV	Phase 2
TLR7	NCT01421017	Imiquimod (in combination with cyclophosphamide or radiotherapy)	Cream	Breast cancer; metastatic breast cancer; recurrent breast cancer	Phase 1; Phase 2
TLR7	NCT03416335	DSP-0509 (or in combination with pembrolizumab)	Intravenous	Neoplasms	Phase 1; Phase 2
TLR7	NCT04101357	BNT411 (or in combination with atezolizumab, carboplatin and etoposide)	Intravenous	Solid tumor; extensive-stage small cell lung cancer	Phase 1; Phase 2
TLR7	NCT04338685	RO7119929 (in combination with Tocilizumab)	Oral	Carcinoma; hepatocellular; biliary tract cancer; secondary liver cancer; liver metastases	Phase 1
TLR7	NCT04588324	SHR2150 (or in combination with chemotherapy plus PD-1 or CD47 antibody)	Oral	Solid tumor	Phase 1; Phase 2
TLR7/8	NCT00821652	Resiquimod (in combination with NY-ESO-1 protein vaccination)	Subcutaneously	Tumors	Phase 1
TLR7/8	NCT04278144	BDC-1001 (or in combination with nivolumabe)	Intravenous	HER2 positive solid tumors	Phase 1; Phase 2
TLR7/8	NCT04799054	TransCon (or in combination with pembrolizumab)	Intratumoral	Advanced solid tumor; locally advanced solid tumor; metastatic solid tumor	Phase 1; Phase 2
TLR7/8	NCT04840394	BDB018 (or in combination with pembrolizumab)	Intravenous	Advanced solid tumors	Phase 1
TLR8	NCT01294293	VTX-2337 (in combination with pegylated liposomal doxorubicin hydrochloride or paclitaxel)	Subcutaneously	Ovarian epithelial; fallopian tube; peritoneal cavity cancer	Phase 1
TLR8	NCT01334177	VTX-2337 (in combination with cetuximab)	Subcutaneously	Locally advanced; recurrent; metastatic squamous cell cancer of head and neck	Phase 1
TLR8	NCT01666444	VTX-2337 (in combination with pegylated liposomal doxorubicin)	Intravenous	Epithelial ovarian cancer; fallopian tube cancer; primary peritoneal cancer	Phase 2
TLR8	NCT01836029	VTX-2337 (in combination with chemotherapy and cetuximab)	Intravenous	Carcinoma; squamous cell of head and neck	Phase 2
TLR8	NCT03906526	VTX-2337 (or in combination with nivolumabe)	Subcutaneously or intratumoral injection	Carcinoma; squamous cell	Phase 1
TLR9	NCT00185965	CPG 7909 (in combination with radiation therapy)	Intratumoral	Recurrent low-grade lymphomas	Phase 1; Phase 2
TLR9	NCT02254772	SD-101 (in combination with ipilimumab and radiation therapy)	Intratumoral	Recurrent low-grade B-cell lymphoma	Phase 1; Phase 2
TLR9	NCT02927964	SD-101 (in combination with Ibrutinib and radiation therapy)	Intratumoral	Relapsed or refractory grade 1–3A follicular lymphoma	Phase 1; Phase 2
TLR9	NCT03410901	SD-101 (in combination with anti-OX40 antibody BMS 986178 and radiation therapy)	Intratumoral	Low-grade B-cell non-hodgkin lymphomas	Phase 1
TLR9	NCT03618641	CMP-001 (in combination with nivolumab)	Intravenous	Melanomal; lymph node cancer	Phase 2
TLR9	NCT03831295	SD-101 (in combination with anti-OX40 antibody BMS 986178)	Intratumoral	Advanced malignant solid neoplasm; extracranial solid neoplasm; metastatic malignant solid neoplasm	Phase 1
TLR9	NCT04050085	SD-101 (in combination with nivolumab and radiation therapy)	Intratumoral	Chemotherapy-refractory metastatic pancreatic cancer	Phase 1
TLR9	NCT04270864	Tilsotolimod (in combination with ipilimumab and nivolumab)	Intratumoral	Advanced cancer	Phase 1
TLR9	NCT04387071	CMP-001 (in combination with INCAGN01949)	Intratumoral	Stage IV pancreatic; other cancers except melanoma	Phase 1; Phase 2

(Continued on following page)

TABLE 1 | (*Continued*) Summary of clinical trials of nucleic acid-sensing pathways-related agonists.

PRR	ClinicalTrials.gov Identifier	Agent(s)	Route of administration	Cancer type(s)	Clinical phase of development
TLR9	NCT04401995	Vidutolimod (in combination with nivolumab)	Subcutaneously and intratumoral injection	Melanoma	Phase 2
TLR9	NCT04708418	CMP-001 (in combination with pembrolizumab)	Subcutaneously and intratumoral injection	Operable melanoma	Phase 2
TLR9	NCT04935229	SD-101 (or in combination with nivolumab or ipilimumab)	Pressure-enabled hepatic artery infusion	Metastatic uveal melanoma in the liver	Phase 1
TLR9	NCT05220722	SD-101 (in combination with checkpoint blockade)	Pressure-enabled hepatic artery infusion	Hepatocellular carcinoma; intrahepatic cholangiocarcinoma	Phase 1; Phase 2

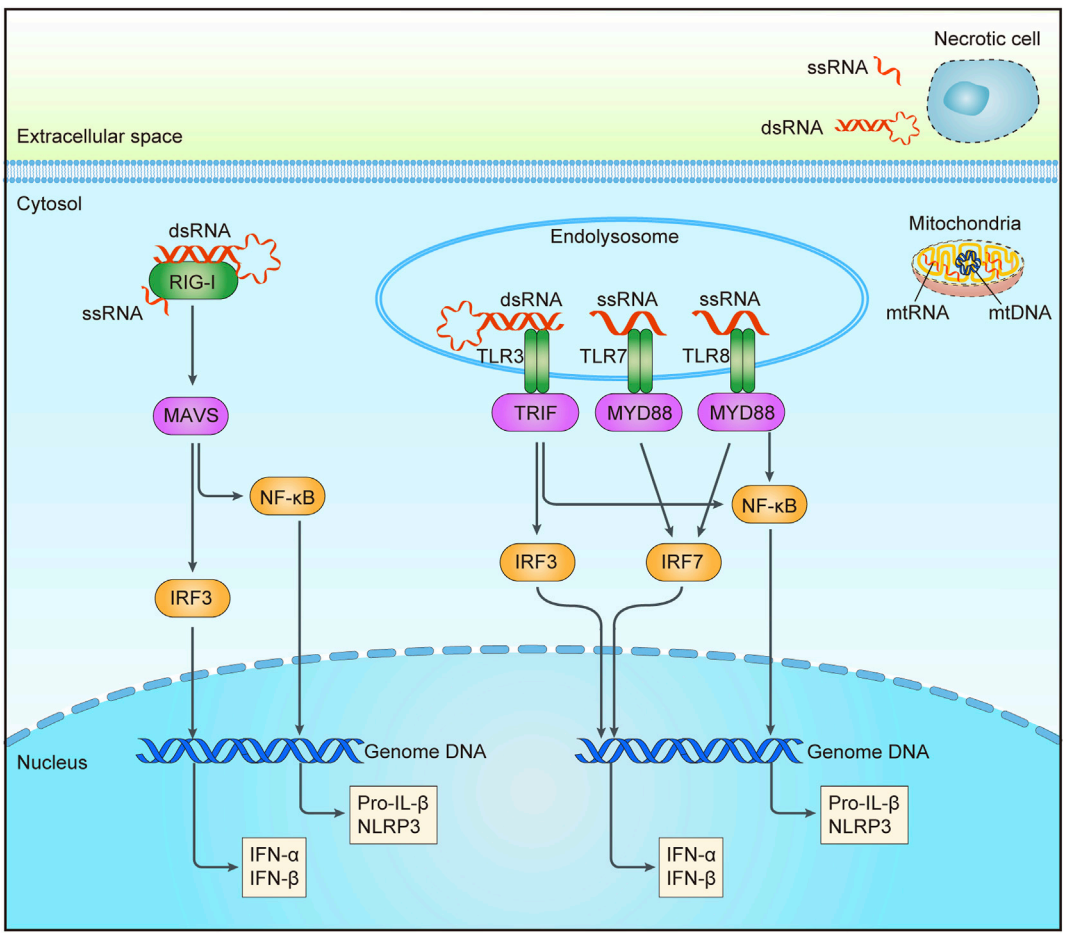

FIGURE 2 | RNA sensing pathways triggered by DNA damage. Aberrant increase of intracellular RNA could be from mitochondria after chemotherapy or radiation. RNA in endosomal may be from extracellular RNA of necrotic cells through endocytosis or cytoplasmic RNA through autophagy. Sensors for RNA are shown in green, including RIG-1 in the cytoplasm, and TLR3/7/8 in the endolysosome. Adaptor molecules are shown in pink and downstream signaling molecules are shown in yellow. Activation of these pathways may result in the production of interferon (IFN) and other cytokines, etc. RIG-I, a retinoic acid-inducible gene I; TLR3/7/8, Toll-like receptor 3/7/8; MAVS, mitochondrial antiviral signaling protein; TRIF, Toll-like receptor adaptor molecule 1; MYD88, myeloid differentiation primary response protein 88; IRF3/7, interferon regulatory factor 3/7; NF-κB, nuclear factor-κB; dsRNA, double stranded RNA; ssRNA, single stranded RNA; mtRNA, mitochondrial RNA; mtDNA, mitochondrial DNA.

3.1.3 Absent in Melanoma 2

The absent in melanoma 2 (AIM2), containing pyrin and HIN domains, takes an important part in inflammasome activation as the dsDNA-sensing receptor in the cytoplasm of cells (Fernandes-Alnemri et al., 2009; Hornung et al., 2009). The N-terminal pyrin domain (PYD) of AIM2 could interact with apoptosis-associated speck-like protein (ASC), which possesses a caspase recruitment domain (CARD) and a C-terminal HIN domain sensing cytoplasmic DNA (Hornung et al., 2009; Wang and Yin, 2017). The recruitment of ASC leads to the generation of fibrilar super-structures, to which Caspase-1 is bound by CARD-CARD interactions (Miao et al., 2011; Lugrin and Martinon, 2018). The oligomerization of ASC leads to the activation of some proteins such as the conversion of pro-IL-1β into the biologically active IL-1β. The inflammasome can also trigger pro-inflammatory pyroptosis (Liang et al., 2020). Gasdermins family proteins are the important factors mediating inflammatory cell death (Kovacs and Miao, 2017), in which Gasdermin D (GSDMD) can be cleaved by Caspase-1 to release the N-terminal of Gasdermin so that it can polymerize and cause perforation of the plasma membrane, allowing the intracellular substance to leak out, causing cell death (Lammert et al., 2020). It is well known that AIM2 can detect dsDNA in the cytosol, but recent studies have found that AIM2 can also sense DSBs directly within the nucleus to induce intestinal epithelial cells and bone marrow cells to initiate the caspase-1-dependent death (Hu et al., 2016).

3.1.4 DNA-PK Complex

Recent findings reveal that some proteins in DNA repair also take part in the sense of foreign DNA in the cytosol. DNA-dependent protein kinase (DNA-PK) complex assembled from Ku70/Ku80 heterodimer and the kinase subunit (DNA-PKcs) can sense DNA DSBs in response to repair the DNA damage in the NHEJ pathway, and Ku has also been reported to detect viral DNA in human cells as a PRR to induce type I and type III interferons or pro-inflammatory cytokines (Abe et al., 2019). DNA stimulates the Ku complex to translocate into the cytoplasm and bind to the dsDNA terminals using its middle domain independent of DNA sequence (Sui et al., 2021a; Sui et al., 2021b). Numerous studies have reported that STING is the downstream adaptor of Ku to induce type I/III interferons and inflammatory cytokines *via* phosphorylation of IRF3 (Sui et al., 2017). Ku complex is abundantly expressed in aged human and mouse $CD4^+$ T cells, and it recognizes accumulating cytoplasmic DNA in the cytoplasm, which facilitates the recruitment of DNA-PKcs and phosphorylation of the kinase ZAK, ultimately promoting the proliferation and activation of $CD4^+$ T cells (Wang et al., 2021a).

3.1.5 Mre11-Rad50-Nbs1 Complex

MRN complex consisting of two MRE11 subunits, two RAD50 units, and two NBS1 subunits, can sense and respond to DNA damage firstly in DDR to orchestrate DDR response in DSBs and replication fork collapse (Zhu et al., 2018; Tisi et al., 2020). The hetero-hexamers MRN complex could conduct ATP hydrolysis of RAD50, bind multiple DNA molecules, and link DNA molecules with exonuclease and endonuclease (Kondo et al., 2013). RAD50 could recognize cytosolic dsDNA and bind caspase-recruitment domain (CARD9), a pro-inflammatory signaling adaptor, to its zinc-hook region, which tends to recruit Bcl-10, leading to the activation of NF-κB and the generation of pro-inflammatory cytokine IL-1β (Roth et al., 2014).

3.2 RNA Sensing Pathways

3.2.1 Toll-Like Receptor 3/7/8

In mammalian cells, both single-stranded and double-stranded RNA can be recognized by PRR as pathogen-associated molecular patterns (PAMPs) or damage-associated molecular patterns (DAMPs) (**Figure 2**). RNA from necrotic cells may be internalized by cells *via* clathrin-dependent endocytosis, or it can enter cells after complexation with peptides or within immune complexes (Lövgren et al., 2004; Barrat et al., 2005; Itoh et al., 2008; Ganguly et al., 2009). The activation of TLR, a type I transmembrane protein, is required for inducing innate and adaptive immune responses, among which TLR3 can recognize double-stranded RNA and structured RNA containing a partial stem in secondary structures of single-stranded RNA, and TLR7/8 can recognize the fragments of single-stranded RNA (Alexopoulou et al., 2001; Karikó et al., 2004; Cavassani et al., 2008; Tatematsu et al., 2013). Depending on the intracellular compartments to recognize ligands, discriminate self-and non-self-derived nucleic acids, TLRs activate the downstream signaling pathways (Gay et al., 2014). Upon ligand binding, the dimers of TLRs will emerge after binding ligands to recruit the cytosolic adaptor proteins with TIR domain, such as MyD88 and Toll-like receptor adaptor molecule 1 (TRIF) (Yamamoto et al., 2003; Vyncke et al., 2016). The recruitment of MyD88 could activate NF-κB through type I interferon induction by IRF7 and tumor necrosis factor receptor-associated factor 6 (TRAF6). Intriguingly, among the TLRs, only TLR3 could signal to induce the generation of type I interferon and proinflammatory cytokines by the recruitment of TRIF rather than depending on MyD88 (Oshiumi et al., 2003).

3.2.2 (RIG-I)-Like Receptors

RLRs are composed of retinoic acid-inducible gene I (RIG-I), melanoma differentiation-associated protein 5 (MDA5), and laboratory of genetics and physiology2 (LGP2), which can help the innate immune system sense cytosolic RNA (Kang et al., 2004; Yoneyama et al., 2004; Yoneyama et al., 2005; Ori et al., 2017). RIG-I and MDA5 contain two CARDs at the N-terminus, a DExD/H box RNA helicase domain in the central and a C-terminal domain (CTD), which mediate downstream signaling by sensing RNA. MDA5 preferentially recognizes dsRNA longer than 1 kb unlike RIG-I, which could bind relatively short dsRNA (Kato et al., 2008; Goubau et al., 2014). The CARD domains of RIG-I and MDA5 oligomerize after binding to dsRNA and tend to interact with the CARD of mitochondrial antiviral signaling protein (MAVS) (Kawai et al., 2005; Seth et al., 2005). Then the oligomerization of MAVS occurs after binding to RIG-I or MDA5 to form prion-like aggregates, upon which the downstream signaling pathways

can be activated (Hou et al., 2011). Besides, MAVS could trigger the transcription of type I IFNs *via* IRF3 or IRF7 by activating TBK1, and the transcription of inflammatory cytokines *via* NF-κB by activating the IKK complex (IKKα, IKKβ, NEMO) (Goubau et al., 2013; Ori et al., 2017).

Recent research has found that the DNA fragments released from ionizing radiation-induced double-strand DNA breaks could activate both the cGAS/STING-dependent DNA-sensing pathway and the MAVS-dependent RNA sensing pathway (Feng et al., 2020). Interestingly, chemotherapeutic agents and ionizing radiation can also lead to mitochondrial DNA double-strand breaks (mtDSBs). After mtDNA breaks, BAX and BAK mediate herniation, then the mitochondrial RNA will be released into the cytoplasm, triggering the RIG-I-MAVS-dependent immune response (Tigano et al., 2021). These studies suggest that DNA damage can also activate innate immune responses through RNA sensing pathways.

4 THE IMPACTS OF NUCLEIC ACID-SENSING PATHWAYS ON DNA REPAIR

4.1 Cyclic GMP-AMP Synthase-Stimulator of Interferon Genes

As mentioned above, several DDR proteins, such as DNA-PK and MRN complex, can not only can participate in the DNA repair, but also take part in the onset of inflammatory responses. Conversely, PRRs, first discovered to sense immune-stimulatory nucleic acids, have also been found to take part in the regulation of DDR. Previously, cGAS-STING signaling was simply identified as a response pathway to cytosol dsDNA, however, they have recently been found to function in DNA repair, independent of interferon response. cGAS could inhibit the repair of DNA DSBs by HR without relying on STING and the catalytic activity of cGAS (Hopfner and Hornung, 2020). There are two mechanisms for cGAS-dependent HR inhibition. In one of them, because it has been found at the sites of chromosomal damage marked by PARP1 and γ-H2AX, cGAS could prevent the recruitment of proteins necessary for the HR process by interacting with γ-H2AX and PAR (Liu et al., 2018). On the other hand, subsequent work suggested that cGAS could prevent RAD51-DNA filaments to pair and the broken DNA strand from invading into the homologous strand by binding the homologous dsDNA template to form oligomeric clusters (Jiang et al., 2019). However, the detailed mechanism remains to be investigated further.

STING has been confirmed to promote DDR and enable cell survival without cGAS, though they are partners (Cheradame et al., 2021). Downregulation of STING increases cell death and makes breast cancer cells more sensitive to genotoxic treatment. Following chemotherapy regimens, some STINGs are found to be located at the inner nuclear membrane and bind the NHEJ proteins DNA-PKcs, Ku70, and Ku80, suggesting that STING may control NHEJ-mediated DNA repair by cooperating with DNA-PK (Ferguson et al., 2012; Morchikh et al., 2017; Sui et al., 2017; Cheradame et al., 2021). Regrettably, its specific mechanism remains unclear.

Recent research has proposed a novel mechanism that IR-induced DNA damages would trigger the phosphorylation and activation of phosphoribosyl pyrophosphate synthetases PRPS1/2 *via* ATM and cGAS/STING/TBK1, which could promote the synthesis of deoxyribonucleotide given that the PRPSs are the rate-limiting enzymes. Then the increased deoxyribonucleotide will help for DNA repair. Nevertheless, it remains to be clarified how the cells respond to DNA damage *via* the cGAS-STING pathway under different contexts (Kornberg et al., 1955; Hove-Jensen, 1988; Liu et al., 2021).

4.2 Toll-Like Receptors

TLRs are the key members of the innate immune system, functioning as the first line of defense against multiple injurious substances (Trinchieri and Sher, 2007; Barton and Kagan, 2009; Kawai and Akira, 2011). Recent literature has shown that activation of TLRs could also promote DNA repair by upregulating the expression of DNA repair genes, apart from upregulating cellular defense systems. Upon TLR9 stimulation, there is a significant increase of mRNAs to participate in adjusting cell cycles and DNA repair after CpG DNA is injected into the abdominal cavity (Zheng et al., 2008; Klaschik et al., 2010; Sommariva et al., 2011). And NER gene expression is increased by treating bone marrow-derived cell lines with the TLR7/8 agonist (Imiquimod) *in vitro* (Fishelevich et al., 2011). It has been deduced that TLR signaling pathways may result in transcriptional activation of DNA repair machinery through direct and indirect mechanisms. The promoter regions of many genes involved in DNA repair contain the binding sites of activator protein-1 (AP-1) (Xiao et al., 1993; Zhong et al., 2000). The transcriptional control of DNA repair might be linked to TLR agonist treatment through the transcriptional activation function of the AP-1. On the other hand, DNA repair can be promoted because the activated TLR could induce the generation of cytokines. The cytokines such as IL-12 may be sensed by their appropriate cytokine receptor, leading to the increased transcription levels of DNA repair genes (Majewski et al., 2010). However, increased DNA repair is detrimental for cancer treatment. The previous study has found that TLR9 agonist treatment upregulates the genes associated with DNA repair in immune cells but downregulates them in tumor cells, which is contributed to the death of cancer cells (Sommariva et al., 2011). Those conflicting data highlight the need for further research into how immune versus stromal cells, and normal versus cancerous cells respond to TLR agonists, as well as related DNA repair and cell survival.

4.3 AIM2-Like Receptors

AIM2-like receptors (ALRs) are a large family of structurally related proteins that are generally considered to act as intracellular DNA sensors alerting the innate immune system. Recent studies reveal that ALRs perform different functions outside the immune system. It has been demonstrated that DNA breaks are repaired more efficiently in mice and cells lacking ALRs ($ALR^{-/-}$ mice lack the entire ALR locus containing all 13 ALR genes on Chromosome 13),

resulting in the stronger resistance to the genotoxic effects of irradiation and chemotherapy (Brunette et al., 2012; Gray et al., 2016; Jiang et al., 2021). Mechanistically, nuclear ALRs limit DNA repair machinery access to damaged sites by binding the chromatin, and self-oligomerization promoted chromatin compaction. These findings reveal that ALRs could be the possible target for new interventions against genotoxic tissue injury, but more research into the different members of the ALR family is needed.

5 CONCLUSION AND FUTURE PERSPECTIVE

Targeting DDR factors in tumors has achieved outstanding success over the last decade, especially PARP inhibitors for cancer therapy. Recently, we have gained an improved understanding of the molecular mechanism of how DNA damage is interconnected to cellular innate immunity, which plays essential roles in the therapeutic efficacy of DNA repair targeted treatments (Pantelidou et al., 2019). Damaged nucleic acids also shape adaptive immune responses by activating innate immune cells. Accumulation of nucleic acids from necrotic cells can induce type I IFNs and other immune-regulatory cytokines production from bystander cells [e.g., dendritic cells (DCs)] to promote antitumor immunity through nucleic acid-sensing pathways. The DCs activated by the type I IFNs secretion will be transported to tumor-draining lymph nodes and cross-prime naïve $CD8^+$ T lymphocytes (Ellermeier et al., 2013; Duewell et al., 2014; Klarquist et al., 2014; Woo et al., 2014). The cancer-induced host response and tumor rejection relies heavily on the immunological responses to danger DAMPs signals.

Immune checkpoint blockade (ICB), as a promising therapeutic strategy, has made tremendous strides in recent years providing an alternative to irradiation therapy or traditional chemotherapies. Unfortunately, the efficacy of ICB is limited to only a subgroup of cancer patients (depending on the type of the tumor), with an overall response rate of about 20% for all malignancies to date (Hargadon et al., 2018; Chowell et al., 2021). ICB is effective in "hot" tumors with T cell infiltration rather than in "cold" tumors lacking T cell infiltration (Petitprez et al., 2020). Novel strategies for activating innate immunity within the TME to promote the antitumor immune responses have emerged in recent years, with the goal of eradicating the disease in "cold" tumors (Iurescia et al., 2018). Agonists of the nucleic acid-sensing pathways (such as cGAMP, agonists of STING) have been applied to eradicate tumor mass and induce a durable anti-tumor immune response (Chin et al., 2020; Pan et al., 2020). However, since some PRRs are involved in DDR and tumorigenesis, the impact of nucleic acid-sensing pathways on DNA repair cannot be ignored in therapeutic strategies aiming at promoting the activation of nucleic acid-sensing pathways.

As DDR inhibitors can trigger innate immune responses, DDR inhibition could be effective in combination with ICBs. The DDR inhibitors that target PARP have been investigated the most in anticancer immunotherapies. PARP inhibition could increase $CD8^+$ T-cell infiltration and IFN-γ generation in tumors, and promote the tumor regression when used accompanied with anti-PD-1 antibody (Pantelidou et al., 2019; Shen et al., 2019). Recently, many other regents inhibiting DDR components have been developed and used preclinically (Cleary et al., 2020). DDR inhibition strategies combined with other therapeutic strategies possess tremendous potential to improve the effectiveness of cancer treatment because of their immunomodulatory effect on radiation and chemotherapies and immune checkpoint blocking. Furthermore, in order to kill tumor cells more precisely, innovative approaches (such as nanoparticles, viral particles, and targeted deliveries) beneficial to the precise delivery of a chemotherapeutic drug, DDR inhibitors, or nucleic acid-sensing pathways agonists to tumors can be used to induce local specific antitumor immune responses, which could significantly expand the therapeutic window for their use in cancer immunotherapies (Gentili et al., 2015; Wilson et al., 2018; Wang et al., 2020; Xu et al., 2021).

AUTHOR CONTRIBUTIONS

BX and AL drafted the manuscript. All authors contributed to the article and approved the submitted version.

FUNDING

This work was supported by the National Natural Science Foundation of China (Grant No. 32100554) to BX.

REFERENCES

Abe, T., Marutani, Y., and Shoji, I. (2019). Cytosolic DNA-Sensing Immune Response and Viral Infection. *Microbiol. Immunol.* 63, 51–64. doi:10.1111/1348-0421.12669

Ablasser, A., Goldeck, M., Cavlar, T., Deimling, T., Witte, G., Röhl, I., et al. (2013). cGAS Produces a 2′-5′-linked Cyclic Dinucleotide Second Messenger that Activates STING. *Nature* 498, 380–384. doi:10.1038/nature12306

Alexopoulou, L., Holt, A. C., Medzhitov, R., and Flavell, R. A. (2001). Recognition of Double-Stranded RNA and Activation of NF-Kb by Toll-like Receptor 3. *Nature* 413, 732–738. doi:10.1038/35099560

Andreeva, L., Hiller, B., Kostrewa, D., Lässig, C., de Oliveira Mann, C. C., Jan Drexler, D., et al. (2017). cGAS Senses Long and HMGB/TFAM-bound U-Turn DNA by Forming Protein-DNA Ladders. *Nature* 549, 394–398. doi:10.1038/nature23890

Barrat, F. J., Meeker, T., Gregorio, J., Chan, J. H., Uematsu, S., Akira, S., et al. (2005). Nucleic Acids of Mammalian Origin Can Act as Endogenous Ligands for Toll-like Receptors and May Promote Systemic Lupus Erythematosus. *J. Exp. Med.* 202, 1131–1139. doi:10.1084/jem.20050914

Barton, G. M., and Kagan, J. C. (2009). A Cell Biological View of Toll-like Receptor Function: Regulation through Compartmentalization. *Nat. Rev. Immunol.* 9, 535–542. doi:10.1038/nri2587

Biau, J., Chautard, E., Verrelle, P., and Dutreix, M. (2019). Altering DNA Repair to Improve Radiation Therapy: Specific and Multiple Pathway Targeting. *Front. Oncol.* 9, 1009. Epub 2019/10/28. doi:10.3389/fonc.2019.01009

Bixel, K., and Hays, J. (2015). Olaparib in the Management of Ovarian Cancer. *Pgpm* 8, 127–135. Epub 2015/08/27. doi:10.2147/pgpm.s62809

Bouwman, P., and Jonkers, J. (2012). The Effects of Deregulated DNA Damage Signalling on Cancer Chemotherapy Response and Resistance. *Nat. Rev. Cancer* 12, 587–598. Epub 2012/08/25. doi:10.1038/nrc3342

Brunette, R. L., Young, J. M., Whitley, D. G., Brodsky, I. E., Malik, H. S., and Stetson, D. B. (2012). Extensive Evolutionary and Functional Diversity Among Mammalian AIM2-like Receptors. *J. Exp. Med.* 209, 1969–1983. doi:10.1084/jem.20121960

Burdette, D. L., Monroe, K. M., Sotelo-Troha, K., Iwig, J. S., Eckert, B., Hyodo, M., et al. (2011). STING Is a Direct Innate Immune Sensor of Cyclic Di-GMP. *Nature* 478, 515–518. doi:10.1038/nature10429

Burma, S., Chen, B. P., Murphy, M., Kurimasa, A., and Chen, D. J. (2001). ATM Phosphorylates Histone H2AX in Response to DNA Double-Strand Breaks. *J. Biol. Chem.* 276, 42462–42467. Epub 2001/09/26. doi:10.1074/jbc.c100466200

Caldecott, K. W. (2020). Mammalian DNA Base Excision Repair: Dancing in the Moonlight. *DNA Repair* 93, 102921. Epub 2020/10/23. doi:10.1016/j.dnarep.2020.102921

Cavassani, K. A., Ishii, M., Wen, H., Schaller, M. A., Lincoln, P. M., Lukacs, N. W., et al. (2008). TLR3 Is an Endogenous Sensor of Tissue Necrosis during Acute Inflammatory Events. *J. Exp. Med.* 205, 2609–2621. doi:10.1084/jem.20081370

Ceccaldi, R., Liu, J. C., Amunugama, R., Hajdu, I., Primack, B., O'Connor, M. I. R., et al. (2015). Homologous-recombination-deficient Tumours Are Dependent on Polθ-Mediated Repair. *Nature* 518, 258–262. doi:10.1038/nature14184

Chang, H. H. Y., Pannunzio, N. R., Adachi, N., and Lieber, M. R. (2017). Non-homologous DNA End Joining and Alternative Pathways to Double-Strand Break Repair. *Nat. Rev. Mol. Cell Biol* 18, 495–506. Epub 2017/05/18. doi:10.1038/nrm.2017.48

Chang, Z. L. (2010). Important Aspects of Toll-like Receptors, Ligands and Their Signaling Pathways. *Inflamm. Res.* 59, 791–808. doi:10.1007/s00011-010-0208-2

Chatterjee, N., and Walker, G. C. (2017). Mechanisms of DNA Damage, Repair, and Mutagenesis. *Environ. Mol. Mutagen.* 58, 235–263. Epub 2017/05/10. doi:10.1002/em.22087

Chen, X., Xu, X., Chen, Y., Cheung, J. C., Wang, H., Jiang, J., et al. (2021). Structure of an Activated DNA-PK and its Implications for NHEJ. *Mol. Cell* 81, 801–810. e803Epub 2021/01/02. doi:10.1016/j.molcel.2020.12.015

Cheng, B., Pan, W., Xing, Y., Xiao, Y., Chen, J., and Xu, Z. (2022). Recent Advances in DDR (DNA Damage Response) Inhibitors for Cancer Therapy. *Eur. J. Med. Chem.* 230, 114109. Epub 2022/01/21. doi:10.1016/j.ejmech.2022.114109

Cheng, Q., and Chen, J. (2010). Mechanism of P53 Stabilization by ATM after DNA Damage. *Cell Cycle* 9, 472–478. Feb 1Epub 2010/01/19. doi:10.4161/cc.9.3.10556

Cheradame, L., Guerrera, I. C., Gaston, J., Schmitt, A., Jung, V., Goudin, N., et al. (2021). STING Protects Breast Cancer Cells from Intrinsic and Genotoxic-Induced DNA Instability via a Non-canonical, Cell-Autonomous Pathway. *Oncogene* 40, 6627–6640. Epub 2021/10/10. doi:10.1038/s41388-021-02037-4

Chin, E. N., Yu, C., Vartabedian, V. F., Jia, Y., Kumar, M., Gamo, A. M., et al. (2020). Antitumor Activity of a Systemic STING-Activating Non-nucleotide cGAMP Mimetic. *Science* 369, 993–999. Epub 2020/08/21. doi:10.1126/science.abb4255

Chowell, D., Yoo, S.-K., Valero, C., Pastore, A., Krishna, C., Lee, M., et al. (2021). Improved Prediction of Immune Checkpoint Blockade Efficacy across Multiple Cancer Types. *Nat. Biotechnol.* 1, 1–8. Epub 2021/11/03. doi:10.1038/s41587-021-01070-8

Chu, W., Jin, W., Liu, D., Wang, J., Geng, C., Chen, L., et al. (2018). Diffusion-weighted Imaging in Identifying Breast Cancer Pathological Response to Neoadjuvant Chemotherapy: A Meta-Analysis. *Oncotarget* 9, 7088–7100. Epub 2018/02/23. doi:10.18632/oncotarget.23195

Ciccia, A., and Elledge, S. J. (2010). The DNA Damage Response: Making it Safe to Play with Knives. *Mol. Cell* 40, 179–204. Epub 2010/10/23. doi:10.1016/j.molcel.2010.09.019

Cimprich, K. A., and Cortez, D. (2008). ATR: an Essential Regulator of Genome Integrity. *Nat. Rev. Mol. Cell Biol* 9, 616–627. Epub 2008/07/03. doi:10.1038/nrm2450

Cleary, J. M., Aguirre, A. J., Shapiro, G. I., and D'Andrea, A. D. (2020). Biomarker-Guided Development of DNA Repair Inhibitors. *Mol. Cell* 78, 1070–1085. Jun 18Epub 2020/05/28. doi:10.1016/j.molcel.2020.04.035

Cussiol, J. R. R., Soares, B. L., and Oliveira, F. M. B. (2019). From Yeast to Humans: Understanding the Biology of DNA Damage Response (DDR) Kinases. *Genet. Mol. Biol.* 43, e20190071. Epub 2020/01/14. doi:10.1590/1678-4685-GMB-2019-0071

Dasari, S., and Tchounwou, P. B. (2014). Cisplatin in Cancer Therapy: Molecular Mechanisms of Action. *Eur. J. Pharmacol.* 740, 364–378. Epub 2014/07/25. doi:10.1016/j.ejphar.2014.07.025

de Oliveira Mann, C. C., Orzalli, M. H., King, D. S., Kagan, J. C., Lee, A. S. Y., and Kranzusch, P. J. (2019). Modular Architecture of the STING C-Terminal Tail Allows Interferon and NF-Kb Signaling Adaptation. *Cell Rep.* 27, 1165–1175. e1165. doi:10.1016/j.celrep.2019.03.098

De Ruysscher, D., Niedermann, G., Burnet, N. G., Siva, S., Lee, A. W. M., and Hegi-Johnson, F. (2019). Radiotherapy Toxicity. *Nat. Rev. Dis. Primers* 5, 13–20. doi:10.1038/s41572-019-0064-5

Delneste, Y., Beauvillain, C., and Jeannin, P. (2007). Immunité Naturelle. *Med. Sci. (Paris)* 23, 67–74. Epub 2007/01/11. doi:10.1051/medsci/200723167

Desouky, O., Ding, N., and Zhou, G. (2015). Targeted and Non-targeted Effects of Ionizing Radiation. *J. Radiat. Res. Appl. Sci.* 8, 247–254. doi:10.1016/j.jrras.2015.03.003

Dianov, G. L., and Hübscher, U. (2013). Mammalian Base Excision Repair: the Forgotten Archangel. *Nucleic Acids Res.* 41, 3483–3490. Apr 1Epub 2013/02/15. doi:10.1093/nar/gkt076

Diner, E. J., Burdette, D. L., Wilson, S. C., Monroe, K. M., Kellenberger, C. A., Hyodo, M., et al. (2013). The Innate Immune DNA Sensor cGAS Produces a Noncanonical Cyclic Dinucleotide that Activates Human STING. *Cell Rep.* 3, 1355–1361. doi:10.1016/j.celrep.2013.05.009

Dou, Z., Ghosh, K., Vizioli, M. G., Zhu, J., Sen, P., Wangensteen, K. J., et al. (2017). Cytoplasmic Chromatin Triggers Inflammation in Senescence and Cancer. *Nature* 550, 402–406. Epub 2017/10/05. doi:10.1038/nature24050

Du, M., and Chen, Z. J. (2018). DNA-induced Liquid Phase Condensation of cGAS Activates Innate Immune Signaling. *Science* 361, 704–709. Epub 2018/07/07. doi:10.1126/science.aat1022

Duewell, P., Steger, A., Lohr, H., Bourhis, H., Hoelz, H., Kirchleitner, S. V., et al. (2014). RIG-I-like Helicases Induce Immunogenic Cell Death of Pancreatic Cancer Cells and Sensitize Tumors toward Killing by CD8+ T Cells. *Cell Death Differ* 21, 1825–1837. Epub 2014/07/12. doi:10.1038/cdd.2014.96

Dupré, A., Boyer-Chatenet, L., Sattler, R. M., Modi, A. P., Lee, J. H., Nicolette, M. L., et al. (2008). A Forward Chemical Genetic Screen Reveals an Inhibitor of the Mre11-Rad50-Nbs1 Complex. *Nat. Chem. Biol.* 4, 119–125. doi:10.1038/nchembio.63

Ellermeier, J., Wei, J., Duewell, P., Hoves, S., Stieg, M. R., Adunka, T., et al. (2013). Therapeutic Efficacy of Bifunctional siRNA Combining TGF-B1 Silencing with RIG-I Activation in Pancreatic Cancer. *Cancer Res.* 73, 1709–1720. doi:10.1158/0008-5472.can-11-3850

Emadi, A., Jones, R. J., and Brodsky, R. A. (2009). Cyclophosphamide and Cancer: golden Anniversary. *Nat. Rev. Clin. Oncol.* 6, 638–647. Epub 2009/09/30. doi:10.1038/nrclinonc.2009.146

Ergun, S. L., Fernandez, D., Weiss, T. M., and Li, L. (2019). STING Polymer Structure Reveals Mechanisms for Activation, Hyperactivation, and Inhibition. *Cell* 178, 290–301. Epub 2019/06/25. doi:10.1016/j.cell.2019.05.036

Falck, J., Coates, J., and Jackson, S. P. (2005). Conserved Modes of Recruitment of ATM, ATR and DNA-PKcs to Sites of DNA Damage. *Nature* 434, 605–611. Epub 2005/03/11. doi:10.1038/nature03442

Feng, X., Tubbs, A., Zhang, C., Tang, M., Sridharan, S., Wang, C., et al. (2020). ATR Inhibition Potentiates Ionizing Radiation-Induced Interferon Response via Cytosolic Nucleic Acid-Sensing Pathways. *EMBO J.* 39, e104036. doi:10.15252/embj.2019104036

Ferguson, B. J., Mansur, D. S., Peters, N. E., Ren, H., and Smith, G. L. (2012). DNA-PK Is a DNA Sensor for IRF-3-dependent Innate Immunity. *elife* 1, e00047. doi:10.7554/eLife.00047

Fernandes-Alnemri, T., Yu, J.-W., Datta, P., Wu, J., and Alnemri, E. S. (2009). AIM2 Activates the Inflammasome and Cell Death in Response to Cytoplasmic DNA. *Nature* 458, 509–513. Epub 2009/01/23. doi:10.1038/nature07710

Fishelevich, R., Zhao, Y., Tuchinda, P., Liu, H., Nakazono, A., Tammaro, A., et al. (2011). Imiquimod-induced TLR7 Signaling Enhances Repair of DNA Damage Induced by Ultraviolet Light in Bone Marrow-Derived Cells. *J.I.* 187, 1664–1673. Epub 2011/07/19. doi:10.4049/jimmunol.1100755

Foote, K. M., Nissink, J. W. M., McGuire, T., Turner, P., Guichard, S., Yates, J. W. T., et al. (2018). Discovery and Characterization of AZD6738, a Potent Inhibitor of Ataxia Telangiectasia Mutated and Rad3 Related (ATR) Kinase with

Application as an Anticancer Agent. *J. Med. Chem.* 61, 9889–9907. doi:10.1021/acs.jmedchem.8b01187

Gaidt, M. M., Ebert, T. S., Chauhan, D., Ramshorn, K., Pinci, F., Zuber, S., et al. (2017). The DNA Inflammasome in Human Myeloid Cells Is Initiated by a STING-Cell Death Program Upstream of NLRP3. *Cell* 171, 1110–1124. e1118. doi:10.1016/j.cell.2017.09.039

Galluzzi, L., Humeau, J., Buqué, A., Zitvogel, L., and Kroemer, G. (2020). Immunostimulation with Chemotherapy in the Era of Immune Checkpoint Inhibitors. *Nat. Rev. Clin. Oncol.* 17, 725–741. Epub 2020/08/08. doi:10.1038/s41571-020-0413-z

Ganguly, D., Chamilos, G., Lande, R., Gregorio, J., Meller, S., Facchinetti, V., et al. (2009). Self-RNA-antimicrobial Peptide Complexes Activate Human Dendritic Cells through TLR7 and TLR8. *J. Exp. Med.* 206, 1983–1994. doi:10.1084/jem.20090480

Gao, P., Ascano, M., Wu, Y., Barchet, W., Gaffney, B. L., Zillinger, T., et al. (2013). Cyclic [G(2′,5′)pA(3′,5′)p] Is the Metazoan Second Messenger Produced by DNA-Activated Cyclic GMP-AMP Synthase. *Cell* 153, 1094–1107. doi:10.1016/j.cell.2013.04.046

Gavande, N. S., VanderVere-Carozza, P. S., Hinshaw, H. D., Jalal, S. I., Sears, C. R., Pawelczak, K. S., et al. (2016). DNA Repair Targeted Therapy: The Past or Future of Cancer Treatment? *Pharmacol. Ther.* 160, 65–83. Epub 2016/02/21. doi:10.1016/j.pharmthera.2016.02.003

Gavande, N. S., VanderVere-Carozza, P. S., Pawelczak, K. S., Mendoza-Munoz, P., Vernon, T. L., Hanakahi, L. A., et al. (2020). Discovery and Development of Novel DNA-PK Inhibitors by Targeting the Unique Ku-DNA Interaction. *Nucleic Acids Res.* 48, 11536–11550. doi:10.1093/nar/gkaa934

Gay, N. J., Symmons, M. F., Gangloff, M., and Bryant, C. E. (2014). Assembly and Localization of Toll-like Receptor Signalling Complexes. *Nat. Rev. Immunol.* 14, 546–558. Epub 2014/07/26. doi:10.1038/nri3713

Gentili, M., Kowal, J., Tkach, M., Satoh, T., Lahaye, X., Conrad, C., et al. (2015). Transmission of Innate Immune Signaling by Packaging of cGAMP in Viral Particles. *Science* 349, 1232–1236. Epub 2015/08/01. doi:10.1126/science.aab3628

Gentili, M., Lahaye, X., Nadalin, F., Nader, G. P. F., Puig Lombardi, E., Herve, S., et al. (2019). The N-Terminal Domain of cGAS Determines Preferential Association with Centromeric DNA and Innate Immune Activation in the Nucleus. *Cell Rep.* 26, 2377–2393. e2313. doi:10.1016/j.celrep.2019.01.105

Giglia-Mari, G., Zotter, A., and Vermeulen, W. (2011). DNA Damage Response. *Cold Spring Harbor Perspect. Biol.* 3, a000745. Epub 2010/10/29. doi:10.1101/cshperspect.a000745

Gillet, L. C. J., and Schärer, O. D. (2006). Molecular Mechanisms of Mammalian Global Genome Nucleotide Excision Repair. *Chem. Rev.* 106, 253–276. Epub 2006/02/09. doi:10.1021/cr040483f

Glück, S., Guey, B., Gulen, M. F., Wolter, K., Kang, T. W., Schmacke, N. A., et al. (2017). Innate Immune Sensing of Cytosolic Chromatin Fragments through cGAS Promotes Senescence. *Nat. Cell Biol* 19, 1061–1070. doi:10.1038/ncb3586

Gorecki, L., Andrs, M., Rezacova, M., and Korabecny, J. (2020). Discovery of ATR Kinase Inhibitor Berzosertib (VX-970, M6620): Clinical Candidate for Cancer Therapy. *Pharmacol. Ther.* 210, 107518. Epub 2020/02/29. doi:10.1016/j.pharmthera.2020.107518

Goubau, D., Deddouche, S., and Reis e Sousa, C. (2013). Cytosolic Sensing of Viruses. *Immunity* 38, 855–869. Epub 2013/05/28. doi:10.1016/j.immuni.2013.05.007

Goubau, D., Schlee, M., Deddouche, S., Pruijssers, A. J., Zillinger, T., Goldeck, M., et al. (2014). Antiviral Immunity via RIG-I-Mediated Recognition of RNA Bearing 5′-diphosphates. *Nature* 514, 372–375. doi:10.1038/nature13590

Grassberger, C., Ellsworth, S. G., Wilks, M. Q., Keane, F. K., and Loeffler, J. S. (2019). Assessing the Interactions between Radiotherapy and Antitumour Immunity. *Nat. Rev. Clin. Oncol.* 16, 729–745. doi:10.1038/s41571-019-0238-9

Gratia, M., Rodero, M. P., Conrad, C., Bou Samra, E., Maurin, M., Rice, G. I., et al. (2019). Bloom Syndrome Protein Restrains Innate Immune Sensing of Micronuclei by cGAS. *J. Exp. Med.* 216, 1199–1213. Epub 2019/04/03. doi:10.1084/jem.20181329

Gray, E. E., Winship, D., Snyder, J. M., Child, S. J., Geballe, A. P., and Stetson, D. B. (2016). The AIM2-like Receptors Are Dispensable for the Interferon Response to Intracellular DNA. *Immunity* 45, 255–266. Aug 16Epub 2016/08/09. doi:10.1016/j.immuni.2016.06.015

Hammel, P., Zhang, C., Matile, J., Colle, E., Hadj-Naceur, I., Gagaille, M.-P., et al. (2020). PARP Inhibition in Treatment of Pancreatic Cancer. *Expert Rev. Anticancer Ther.* 20, 939–945. Epub 2020/09/17. doi:10.1080/14737140.2020.1820330

Harding, S. M., Benci, J. L., Irianto, J., Discher, D. E., Minn, A. J., and Greenberg, R. A. (2017). Mitotic Progression Following DNA Damage Enables Pattern Recognition within Micronuclei. *Nature* 548, 466–470. doi:10.1038/nature23470

Hargadon, K. M., Johnson, C. E., and Williams, C. J. (2018). Immune Checkpoint Blockade Therapy for Cancer: An Overview of FDA-Approved Immune Checkpoint Inhibitors. *Int. Immunopharmacology* 62, 29–39. Epub 2018/07/11. doi:10.1016/j.intimp.2018.06.001

Hellmann, M. D., Li, B. T., Chaft, J. E., and Kris, M. G. (2016). Chemotherapy Remains an Essential Element of Personalized Care for Persons with Lung Cancers. *Ann. Oncol.* 27, 1829–1835. Epub 2016/07/28. doi:10.1093/annonc/mdw271

Henner, W. D., Grunberg, S. M., and Haseltine, W. A. (1982). Sites and Structure of Gamma Radiation-Induced DNA Strand Breaks. *J. Biol. Chem.* 257, 11750–11754. Epub 1982/10/10. doi:10.1016/s0021-9258(18)33827-4

Honda, K., Ohba, Y., Yanai, H., Negishi, H., Mizutani, T., Takaoka, A., et al. (2005). Spatiotemporal Regulation of MyD88-IRF-7 Signalling for Robust Type-I Interferon Induction. *Nature* 434, 1035–1040. doi:10.1038/nature03547

Hooy, R. M., and Sohn, J. (2018). The Allosteric Activation of cGAS Underpins its Dynamic Signaling Landscape. *Elife* 7, e39984. Epub 2018/10/09. doi:10.7554/eLife.39984

Hopfner, K.-P., and Hornung, V. (2020). Molecular Mechanisms and Cellular Functions of cGAS-STING Signalling. *Nat. Rev. Mol. Cell Biol* 21, 501–521. doi:10.1038/s41580-020-0244-x

Hornung, V., Ablasser, A., Charrel-Dennis, M., Bauernfeind, F., Horvath, G., Caffrey, D. R., et al. (2009). AIM2 Recognizes Cytosolic dsDNA and Forms a Caspase-1-Activating Inflammasome with ASC. *Nature* 458, 514–518. doi:10.1038/nature07725

Hou, F., Sun, L., Zheng, H., Skaug, B., Jiang, Q.-X., and Chen, Z. J. (2011). MAVS Forms Functional Prion-like Aggregates to Activate and Propagate Antiviral Innate Immune Response. *Cell* 146, 448–461. Epub 2011/07/26. doi:10.1016/j.cell.2011.06.041

Hove-Jensen, B. (1988). Mutation in the Phosphoribosylpyrophosphate Synthetase Gene (Prs) that Results in Simultaneous Requirements for Purine and Pyrimidine Nucleosides, Nicotinamide Nucleotide, Histidine, and Tryptophan in *Escherichia coli*. *J. Bacteriol.* 170, 1148–1152. doi:10.1128/jb.170.3.1148-1152.1988

Hu, B., Jin, C., Li, H.-B., Tong, J., Ouyang, X., Cetinbas, N. M., et al. (2016). The DNA-Sensing AIM2 Inflammasome Controls Radiation-Induced Cell Death and Tissue Injury. *Science* 354, 765–768. Epub 2016/11/16. doi:10.1126/science.aaf7532

Huang, R.-X., and Zhou, P.-K. (2020). DNA Damage Response Signaling Pathways and Targets for Radiotherapy Sensitization in Cancer. *Sig Transduct Target. Ther.* 5, 60. Epub 2020/05/02. doi:10.1038/s41392-020-0150-x

Ishikawa, H., and Barber, G. N. (2008). STING Is an Endoplasmic Reticulum Adaptor that Facilitates Innate Immune Signalling. *Nature* 455, 674–678. doi:10.1038/nature07317

Itoh, K., Watanabe, A., Funami, K., Seya, T., and Matsumoto, M. (2008). The Clathrin-Mediated Endocytic Pathway Participates in dsRNA-Induced IFN-β Production. *J. Immunol.* 181, 5522–5529. doi:10.4049/jimmunol.181.8.5522

Iurescia, S., Fioretti, D., and Rinaldi, M. (2018). Targeting Cytosolic Nucleic Acid-Sensing Pathways for Cancer Immunotherapies. *Front. Immunol.* 9, 711. Epub 2018/04/25. doi:10.3389/fimmu.2018.00711

Jiang, H., Xue, X., Panda, S., Kawale, A., Hooy, R. M., Liang, F., et al. (2019). Chromatin-bound cGAS Is an Inhibitor of DNA Repair and Hence Accelerates Genome Destabilization and Cell Death. *EMBO J.* 38, e102718. doi:10.15252/embj.2019102718

Jiang, H., Swacha, P., and Gekara, N. O. (2021). Nuclear AIM2-Like Receptors Drive Genotoxic Tissue Injury by Inhibiting DNA Repair. *Adv. Sci.* 8, 2102534. doi:10.1002/advs.202102534

Jobson, A. G., Lountos, G. T., Lorenzi, P. L., Llamas, J., Connelly, J., Cerna, D., et al. (2009). Cellular Inhibition of Checkpoint Kinase 2 (Chk2) and Potentiation of Camptothecins and Radiation by the Novel Chk2 Inhibitor PV1019 [7-nitro-1H-indole-2-carboxylic Acid {4-[1-(guanidinohydrazone)-Ethyl]-Phenyl}-

Amide]. *J. Pharmacol. Exp. Ther.* 331, 816–826. Epub 2009/09/11. doi:10.1124/jpet.109.154997

Kang, D.-c., Gopalkrishnan, R. V., Lin, L., Randolph, A., Valerie, K., Pestka, S., et al. (2004). Expression Analysis and Genomic Characterization of Human Melanoma Differentiation Associated Gene-5, Mda-5: a Novel Type I Interferon-Responsive Apoptosis-Inducing Gene. *Oncogene* 23, 1789–1800. Epub 2003/12/17. doi:10.1038/sj.onc.1207300

Karikó, K., Ni, H., Capodici, J., Lamphier, M., and Weissman, D. (2004). mRNA Is an Endogenous Ligand for Toll-like Receptor 3. *J. Biol. Chem.* 279, 12542–12550. doi:10.1074/jbc.M310175200

Kato, H., Takeuchi, O., Mikamo-Satoh, E., Hirai, R., Kawai, T., Matsushita, K., et al. (2008). Length-dependent Recognition of Double-Stranded Ribonucleic Acids by Retinoic Acid-Inducible Gene-I and Melanoma Differentiation-Associated Gene 5. *J. Exp. Med.* 205, 1601–1610. doi:10.1084/jem.20080091

Kawai, T., and Akira, S. (2011). Toll-like Receptors and Their Crosstalk with Other Innate Receptors in Infection and Immunity. *Immunity* 34, 637–650. doi:10.1016/j.immuni.2011.05.006

Kawai, T., Takahashi, K., Sato, S., Coban, C., Kumar, H., Kato, H., et al. (2005). IPS-1, an Adaptor Triggering RIG-I- and Mda5-Mediated Type I Interferon Induction. *Nat. Immunol.* 6, 981–988. doi:10.1038/ni1243

King, C., Diaz, H., Barnard, D., Barda, D., Clawson, D., Blosser, W., et al. (2014). Characterization and Preclinical Development of LY2603618: a Selective and Potent Chk1 Inhibitor. *Invest. New Drugs* 32, 213–226. Epub 2013/10/12. doi:10.1007/s10637-013-0036-7

Klarquist, J., Hennies, C. M., Lehn, M. A., Reboulet, R. A., Feau, S., and Janssen, E. M. (2014). STING-mediated DNA Sensing Promotes Antitumor and Autoimmune Responses to Dying Cells. *J.I.* 193, 6124–6134. Epub 2014/11/12. doi:10.4049/jimmunol.1401869

Klaschik, S., Tross, D., Shirota, H., and Klinman, D. M. (2010). Short- and Long-Term Changes in Gene Expression Mediated by the Activation of TLR9. *Mol. Immunol.* 47, 1317–1324. Epub 2009/12/17. doi:10.1016/j.molimm.2009.11.014

Kondo, T., Kobayashi, J., Saitoh, T., Maruyama, K., Ishii, K. J., Barber, G. N., et al. (2013). DNA Damage Sensor MRE11 Recognizes Cytosolic Double-Stranded DNA and Induces Type I Interferon by Regulating STING Trafficking. *Proc. Natl. Acad. Sci. U.S.A.* 110, 2969–2974. Epub 2013/02/08. doi:10.1073/pnas.1222694110

Kornberg, A., Lieberman, I., and Simms, E. S. (1955). Enzymatic Synthesis and Properties of 5-phosphoribosylpyrophosphate. *J. Biol. Chem.* 215, 389–402. Epub 1955/07/01. doi:10.1016/s0021-9258(18)66047-8

Kovacs, S. B., and Miao, E. A. (2017). Gasdermins: Effectors of Pyroptosis. *Trends Cell Biol.* 27, 673–684. Epub 2017/06/18. doi:10.1016/j.tcb.2017.05.005

Krejci, L., Altmannova, V., Spirek, M., and Zhao, X. (2012). Homologous Recombination and its Regulation. *Nucleic Acids Res.* 40, 5795–5818. Epub 2012/04/03. doi:10.1093/nar/gks270

Krokan, H. E., Standal, R., and Slupphaug, G. (1997). DNA Glycosylases in the Base Excision Repair of DNA. *Biochem. J.* 325 (Pt 1), 1–16. Epub 1997/07/01. doi:10.1042/bj3250001

Kryston, T. B., Georgiev, A. B., Pissis, P., and Georgakilas, A. G. (2011). Role of Oxidative Stress and DNA Damage in Human Carcinogenesis. *Mutat. Research/Fundamental Mol. Mech. Mutagenesis* 711, 193–201. Epub 2011/01/11. doi:10.1016/j.mrfmmm.2010.12.016

Kuchta, K., Knizewski, L., Wyrwicz, L. S., Rychlewski, L., and Ginalski, K. (2009). Comprehensive Classification of Nucleotidyltransferase Fold Proteins: Identification of Novel Families and Their Representatives in Human. *Nucleic Acids Res.* 37, 7701–7714. doi:10.1093/nar/gkp854

Kumagai, Y., Takeuchi, O., and Akira, S. (2008). TLR9 as a Key Receptor for the Recognition of DNA☆. *Adv. Drug Deliv. Rev.* 60, 795–804. doi:10.1016/j.addr.2007.12.004

Lammert, C. R., Frost, E. L., Bellinger, C. E., Bolte, A. C., McKee, C. A., Hurt, M. E., et al. (2020). AIM2 Inflammasome Surveillance of DNA Damage Shapes Neurodevelopment. *Nature* 580, 647–652. Epub 2020/05/01. doi:10.1038/s41586-020-2174-3

Li, M., and Yu, X. (2013). Function of BRCA1 in the DNA Damage Response Is Mediated by ADP-Ribosylation. *Cancer cell* 23, 693–704. doi:10.1016/j.ccr.2013.03.025

Li, X.-D., Wu, J., Gao, D., Wang, H., Sun, L., and Chen, Z. J. (2013b). Pivotal Roles of cGAS-cGAMP Signaling in Antiviral Defense and Immune Adjuvant Effects. *Science* 341, 1390–1394. Epub 2013/08/31. doi:10.1126/science.1244040

Li, X., Shu, C., Yi, G., Chaton, C. T., Shelton, C. L., Diao, J., et al. (2013a). Cyclic GMP-AMP Synthase Is Activated by Double-Stranded DNA-Induced Oligomerization. *Immunity* 39, 1019–1031. doi:10.1016/j.immuni.2013.10.019

Liang, F., Zhang, F., Zhang, L., and Wei, W. (2020). The Advances in Pyroptosis Initiated by Inflammasome in Inflammatory and Immune Diseases. *Inflamm. Res.* 69, 159–166. Epub 2020/01/15. doi:10.1007/s00011-020-01315-3

Limagne, E., Nuttin, L., Thibaudin, M., Jacquin, E., Aucagne, R., Bon, M., et al. (2022). MEK Inhibition Overcomes Chemoimmunotherapy Resistance by Inducing CXCL10 in Cancer Cells. *Cancer cell* 40, 136–152. Feb 14e112Epub 2022/01/21. doi:10.1016/j.ccell.2021.12.009

Liu, H., Zhang, H., Wu, X., Ma, D., Wu, J., Wang, L., et al. (2018). Nuclear cGAS Suppresses DNA Repair and Promotes Tumorigenesis. *Nature* 563, 131–136. Epub 2018/10/26. doi:10.1038/s41586-018-0629-6

Liu, R., Li, J., Shao, J., Lee, J.-H., Qiu, X., Xiao, Y., et al. (2021). Innate Immune Response Orchestrates Phosphoribosyl Pyrophosphate Synthetases to Support DNA Repair. *Cell Metab.* 33, 2076–2089. Epub 2021/08/04. doi:10.1016/j.cmet.2021.07.009

Liu, S., Cai, X., Wu, J., Cong, Q., Chen, X., Li, T., et al. (2015). Phosphorylation of Innate Immune Adaptor Proteins MAVS, STING, and TRIF Induces IRF3 Activation. *Science* 347, aaa2630. Epub 2015/02/01. doi:10.1126/science.aaa2630

Lövgren, T., Eloranta, M. L., Båve, U., Alm, G. V., Rönnblom, L. J. A., and Rheumatology, R. O. (2004). Induction of Interferon-α Production in Plasmacytoid Dendritic Cells by Immune Complexes Containing Nucleic Acid Released by Necrotic or Late Apoptotic Cells and Lupus IgG. *Arthritis Rheum.* 50, 1861–1872. doi:10.1002/art.20254

Luecke, S., Holleufer, A., Christensen, M. H., Jønsson, K. L., Boni, G. A., Sørensen, L. K., et al. (2017). cGAS Is Activated by DNA in a Length-dependent Manner. *EMBO Rep.* 18, 1707–1715. doi:10.15252/embr.201744017

Lugrin, J., and Martinon, F. (2018). The AIM2 Inflammasome: Sensor of Pathogens and Cellular Perturbations. *Immunol. Rev.* 281, 99–114. doi:10.1111/imr.12618

Mackenzie, K. J., Carroll, P., Martin, C.-A., Murina, O., Fluteau, A., Simpson, D. J., et al. (2017). cGAS Surveillance of Micronuclei Links Genome Instability to Innate Immunity. *Nature* 548, 461–465. Epub 2017/07/25. doi:10.1038/nature23449

Majer, O., Liu, B., and Barton, G. M. (2017). Nucleic Acid-Sensing TLRs: Trafficking and Regulation. *Curr. Opin. Immunol.* 44, 26–33. Epub 2016/12/03. doi:10.1016/j.coi.2016.10.003

Majewski, S., Jantschitsch, C., Maeda, A., Schwarz, T., and Schwarz, A. (2010). IL-23 Antagonizes UVR-Induced Immunosuppression through Two Mechanisms: Reduction of UVR-Induced DNA Damage and Inhibition of UVR-Induced Regulatory T Cells. *J. Invest. Dermatol.* 130, 554–562. doi:10.1038/jid.2009.274

Mateo, J., Lord, C. J., Serra, V., Tutt, A., Balmaña, J., Castroviejo-Bermejo, M., et al. (2019). A Decade of Clinical Development of PARP Inhibitors in Perspective. *Ann. Oncol.* 30, 1437–1447. Epub 2019/06/21. doi:10.1093/annonc/mdz192

Mateos-Gomez, P. A., Gong, F., Nair, N., Miller, K. M., Lazzerini-Denchi, E., and Sfeir, A. (2015). Mammalian Polymerase θ Promotes Alternative NHEJ and Suppresses Recombination. *Nature* 518, 254–257. doi:10.1038/nature14157

McLaughlin, M., Patin, E. C., Pedersen, M., Wilkins, A., Dillon, M. T., Melcher, A. A., et al. (2020). Inflammatory Microenvironment Remodelling by Tumour Cells after Radiotherapy. *Nat. Rev. Cancer* 20, 203–217. AprEpub 2020/03/13. doi:10.1038/s41568-020-0246-1

Miao, E. A., Rajan, J. V., and Aderem, A. (2011). Caspase-1-induced Pyroptotic Cell Death. *Immunological Rev.* 243, 206–214. doi:10.1111/j.1600-065x.2011.01044.x

Morchikh, M., Cribier, A., Raffel, R., Amraoui, S., Cau, J., Severac, D., et al. (2017). HEXIM1 and NEAT1 Long Non-coding RNA Form a Multi-Subunit Complex that Regulates DNA-Mediated Innate Immune Response. *Mol. Cel.* 67, 387–399. e385. doi:10.1016/j.molcel.2017.06.020

Moresco, E. M. Y., LaVine, D., and Beutler, B. (2011). Toll-like Receptors. *Curr. Biol.* 21, R488–R493. Epub 2011/07/12. doi:10.1016/j.cub.2011.05.039

Munster, P. N., Mahipal, A., Nemunaitis, J. J., Mita, M. M., Paz-Ares, L. G., Massard, C., et al. (2016). Phase I Trial of a Dual TOR Kinase and DNA-PK Inhibitor (CC-115) in Advanced Solid and Hematologic Cancers. *J. Clin. Oncol.* 34–2505. doi:10.1200/jco.2016.34.15_suppl.2505

Nastasi, C., Mannarino, L., and D'Incalci, M. (2020). DNA Damage Response and Immune Defense. *Ijms* 21, 7504. Epub 2020/10/16. doi:10.3390/ijms21207504

Ori, D., Murase, M., and Kawai, T. (2017). Cytosolic Nucleic Acid Sensors and Innate Immune Regulation. *Int. Rev. Immunol.* 36, 74–88. Epub 2017/03/24. doi:10.1080/08830185.2017.1298749

Oshiumi, H., Matsumoto, M., Funami, K., Akazawa, T., and Seya, T. (2003). TICAM-1, an Adaptor Molecule that Participates in Toll-like Receptor 3-mediated Interferon-β Induction. *Nat. Immunol.* 4, 161–167. doi:10.1038/ni886

Paludan, S. R., Reinert, L. S., and Hornung, V. (2019). DNA-stimulated Cell Death: Implications for Host Defence, Inflammatory Diseases and Cancer. *Nat. Rev. Immunol.* 19, 141–153. Epub 2019/01/16. doi:10.1038/s41577-018-0117-0

Pan, B. S., Perera, S. A., Piesvaux, J. A., Presland, J. P., Schroeder, G. K., Cumming, J. N., et al. (2020). An Orally Available Non-nucleotide STING Agonist with Antitumor Activity. *Science* 369, eaba6098. Epub 2020/08/21. doi:10.1126/science.aba6098

Pandey, N., and Black, B. E. (2021). Rapid Detection and Signaling of DNA Damage by PARP-1. *Trends Biochem. Sci.* 46, 744–757. Epub 2021/03/07. doi:10.1016/j.tibs.2021.01.014

Pantelidou, C., Sonzogni, O., De Oliveria Taveira, M., Mehta, A. K., Kothari, A., Wang, D., et al. (2019). PARP Inhibitor Efficacy Depends on CD8+ T-Cell Recruitment via Intratumoral STING Pathway Activation in BRCA-Deficient Models of Triple-Negative Breast Cancer. *Cancer Discov.* 9, 722–737. Epub 2019/04/25. doi:10.1158/2159-8290.cd-18-1218

Petitprez, F., Meylan, M., de Reyniès, A., Sautès-Fridman, C., and Fridman, W. H. (2020). The Tumor Microenvironment in the Response to Immune Checkpoint Blockade Therapies. *Front. Immunol.* 11, 784. Epub 2020/05/28. doi:10.3389/fimmu.2020.00784

Pike, K. G., Barlaam, B., Cadogan, E., Campbell, A., Chen, Y., Colclough, N., et al. (2018). The Identification of Potent, Selective, and Orally Available Inhibitors of Ataxia Telangiectasia Mutated (ATM) Kinase: the Discovery of AZD0156 (8-{6-[3-(Dimethylamino) Propoxy] Pyridin-3-Yl}-3-Methyl-1-(tetrahydro-2 H-Pyran-4-Yl)-1, 3-dihydro-2 H-Imidazo [4, 5-c] Quinolin-2-One). *J. Med. Chem.* 61, 3823–3841. doi:10.1021/acs.jmedchem.7b01896

Pinder, J. B., Attwood, K. M., and Dellaire, G. (2013). Reading, Writing, and Repair: the Role of Ubiquitin and the Ubiquitin-like Proteins in DNA Damage Signaling and Repair. *Front. Genet.* 4, 45. Epub 2013/04/05. doi:10.3389/fgene.2013.00045

Qin, S.-Y., Cheng, Y.-J., Lei, Q., Zhang, A.-Q., and Zhang, X.-Z. (2018). Combinational Strategy for High-Performance Cancer Chemotherapy. *Biomaterials* 171, 178–197. Epub 2018/04/27. doi:10.1016/j.biomaterials.2018.04.027

Ramakrishnan Geethakumari, P., Schiewer, M. J., Knudsen, K. E., and Kelly, W. K. (2017). PARP Inhibitors in Prostate Cancer. *Curr. Treat. Options. Oncol.* 18, 37. Epub 2017/05/26. doi:10.1007/s11864-017-0480-2

Roth, S., Rottach, A., Lotz-Havla, A. S., Laux, V., Muschaweckh, A., Gersting, S. W., et al. (2014). Rad50-CARD9 Interactions Link Cytosolic DNA Sensing to IL-1β Production. *Nat. Immunol.* 15, 538–545. doi:10.1038/ni.2888

Rupnik, A., Grenon, M., and Lowndes, N. (2008). The MRN Complex. *Curr. Biol.* 18, R455–R457. Epub 2008/06/05. doi:10.1016/j.cub.2008.03.040

San Filippo, J., Sung, P., and Klein, H. (2008). Mechanism of Eukaryotic Homologous Recombination. *Annu. Rev. Biochem.* 77, 229–257. Epub 2008/02/16. doi:10.1146/annurev.biochem.77.061306.125255

Serrone, L., Zeuli, M., Sega, F. M., and Cognetti, F. (2000). Dacarbazine-based Chemotherapy for Metastatic Melanoma: Thirty-Year Experience Overview. *J. Exp. Clin. Cancer Res.* 19, 21–34. Epub 2000/06/07.

Seth, R. B., Sun, L., Ea, C.-K., and Chen, Z. J. (2005). Identification and Characterization of MAVS, a Mitochondrial Antiviral Signaling Protein that Activates NF-Kb and IRF3. *Cell* 122, 669–682. doi:10.1016/j.cell.2005.08.012

Shang, G., Zhang, C., Chen, Z. J., Bai, X.-c., and Zhang, X. (2019). Cryo-EM Structures of STING Reveal its Mechanism of Activation by Cyclic GMP-AMP. *Nature* 567, 389–393. doi:10.1038/s41586-019-0998-5

Shen, J., Zhao, W., Ju, Z., Wang, L., Peng, Y., Labrie, M., et al. (2019). PARPi Triggers the STING-dependent Immune Response and Enhances the Therapeutic Efficacy of Immune Checkpoint Blockade Independent of BRCAness. *Cancer Res.* 79, 311–319. Epub 2018/11/30. doi:10.1158/0008-5472.can-18-1003

Shuck, S. C., Short, E. A., and Turchi, J. J. (2008). Eukaryotic Nucleotide Excision Repair: from Understanding Mechanisms to Influencing Biology. *Cell Res* 18, 64–72. Epub 2008/01/02. doi:10.1038/cr.2008.2

Smith, J., Mun Tho, L., Xu, N., and Gillespie, D. A. (2010). The ATM-Chk2 and ATR-Chk1 Pathways in DNA Damage Signaling and Cancer. *Adv. Cancer Res.* 108, 73–112. doi:10.1016/b978-0-12-380888-2.00003-0

Sommariva, M., De Cecco, L., De Cesare, M., Sfondrini, L., Ménard, S., Melani, C., et al. (2011). TLR9 Agonists Oppositely Modulate DNA Repair Genes in Tumor versus Immune Cells and Enhance Chemotherapy Effects. *Cancer Res.* 71, 6382–6390. Epub 2011/09/01. doi:10.1158/0008-5472.can-11-1285

Souliotis, V. L., Vlachogiannis, N. I., Pappa, M., Argyriou, A., Ntouros, P. A., and Sfikakis, P. P. (2020). DNA Damage Response and Oxidative Stress in Systemic Autoimmunity. *Int. J. Mol. Sci.* 21, 55. doi:10.3390/ijms21010055

Stracker, T. H., and Petrini, J. H. J. (2011). The MRE11 Complex: Starting from the Ends. *Nat. Rev. Mol. Cell Biol* 12, 90–103. Epub 2011/01/22. doi:10.1038/nrm3047

Sui, H., Zhou, M., Imamichi, H., Jiao, X., Sherman, B. T., Lane, H. C., et al. (2017). STING Is an Essential Mediator of the Ku70-Mediated Production of IFN-Λ1 in Response to Exogenous DNA. *Sci. Signal.* 10, eaah5054. doi:10.1126/scisignal.aah5054

Sui, H., Chen, Q., and Imamichi, T. (2021a). Cytoplasmic-translocated Ku70 Senses Intracellular DNA and Mediates Interferon-lambda1 Induction. *Immunology* 163, 323–337. doi:10.1111/imm.13318

Sui, H., Hao, M., Chang, W., and Imamichi, T. (2021b). The Role of Ku70 as a Cytosolic DNA Sensor in Innate Immunity and beyond. *Front. Cel. Infect. Microbiol.* 11, 761983. doi:10.3389/fcimb.2021.761983

Sun, L., Wu, J., Du, F., Chen, X., and Chen, Z. J. (2013). Cyclic GMP-AMP Synthase Is a Cytosolic DNA Sensor that Activates the Type I Interferon Pathway. *Science* 339, 786–791. doi:10.1126/science.1232458

Taffoni, C., Steer, A., Marines, J., Chamma, H., Vila, I. K., and Laguette, N. (2021). Nucleic Acid Immunity and DNA Damage Response: New Friends and Old Foes. *Front. Immunol.* 12, 660560. Epub 2021/05/14. doi:10.3389/fimmu.2021.660560

Takeuchi, O., and Akira, S. (2010). Pattern Recognition Receptors and Inflammation. *Cell.* 140, 805–820. Epub 2010/03/23. doi:10.1016/j.cell.2010.01.022

Tatematsu, M., Nishikawa, F., Seya, T., and Matsumoto, M. (2013). Toll-like Receptor 3 Recognizes Incomplete Stem Structures in Single-Stranded Viral RNA. *Nat. Commun.* 4, 1833. Epub 2013/05/16. doi:10.1038/ncomms2857

Tigano, M., Vargas, D. C., Tremblay-Belzile, S., Fu, Y., and Sfeir, A. (2021). Nuclear Sensing of Breaks in Mitochondrial DNA Enhances Immune Surveillance. *Nature* 591, 477–481. Epub 2021/02/26. doi:10.1038/s41586-021-03269-w

Timme, C. R., Rath, B. H., O'Neill, J. W., Camphausen, K., and Tofilon, P. J. (2018). The DNA-PK Inhibitor VX-984 Enhances the Radiosensitivity of Glioblastoma Cells Grown *In Vitro* and as Orthotopic Xenografts. *Mol. Cancer Ther.* 17, 1207–1216. doi:10.1158/1535-7163.mct-17-1267

Tisi, R., Vertemara, J., Zampella, G., and Longhese, M. P. (2020). Functional and Structural Insights into the MRX/MRN Complex, a Key Player in Recognition and Repair of DNA Double-Strand Breaks. *Comput. Struct. Biotechnol. J.* 18, 1137–1152. doi:10.1016/j.csbj.2020.05.013

Trinchieri, G., and Sher, A. (2007). Cooperation of Toll-like Receptor Signals in Innate Immune Defence. *Nat. Rev. Immunol.* 7, 179–190. Epub 2007/02/24. doi:10.1038/nri2038

Uematsu, N., Weterings, E., Yano, K.-i., Morotomi-Yano, K., Jakob, B., Taucher-Scholz, G., et al. (2007). Autophosphorylation of DNA-PKCS Regulates its Dynamics at DNA Double-Strand Breaks. *J. Cel. Biol.* 177, 219–229. doi:10.1083/jcb.200608077

Uziel, T., Lerenthal, Y., Moyal, L., Andegeko, Y., Mittelman, L., and Shiloh, Y. (2003). Requirement of the MRN Complex for ATM Activation by DNA Damage. *EMBO J.* 22, 5612–5621. Epub 2003/10/09. doi:10.1093/emboj/cdg541

Volkman, H. E., Cambier, S., Gray, E. E., and Stetson, D. B. (2019). Tight Nuclear Tethering of cGAS Is Essential for Preventing Autoreactivity. *Elife* 8, e47491. doi:10.7554/eLife.47491

Vyncke, L., Bovijn, C., Pauwels, E., Van Acker, T., Ruyssinck, E., Burg, E., et al. (2016). Reconstructing the TIR Side of the Myddosome: a Paradigm for TIR-TIR Interactions. *Structure* 24, 437–447. Epub 2016/02/16. doi:10.1016/j.str.2015.12.018

Wang, B., and Yin, Q. (2017). AIM2 Inflammasome Activation and Regulation: A Structural Perspective. *J. Struct. Biol.* 200, 279–282. Epub 2017/08/17. doi:10.1016/j.jsb.2017.08.001

Wang, Q., Wang, Y., Ding, J., Wang, C., Zhou, X., Gao, W., et al. (2020). A Bioorthogonal System Reveals Antitumour Immune Function of Pyroptosis. *Nature* 579, 421–426. Epub 2020/03/20. doi:10.1038/s41586-020-2079-1

Wang, Y., Fu, Z., Li, X., Liang, Y., Pei, S., Hao, S., et al. (2021a). Cytoplasmic DNA Sensing by KU Complex in Aged CD4+ T Cell Potentiates T Cell Activation and Aging-Related Autoimmune Inflammation. *Immunity* 54, 632–647. Apr 13e639Epub 2021/03/06. doi:10.1016/j.immuni.2021.02.003

Wang, Y., Wang, M., Djekidel, M. N., Chen, H., Liu, D., Alt, F. W., et al. (2021b). eccDNAs Are Apoptotic Products with High Innate Immunostimulatory Activity. *Nature* 599, 308–314. Epub 2021/10/22. doi:10.1038/s41586-021-04009-w

Watson, R. O., Manzanillo, P. S., and Cox, J. S. (2012). Extracellular *M. tuberculosis* DNA Targets Bacteria for Autophagy by Activating the Host DNA-Sensing Pathway. *Cell* 150, 803–815. Epub 2012/08/21. doi:10.1016/j.cell.2012.06.040

West, A. P., Khoury-Hanold, W., Staron, M., Tal, M. C., Pineda, C. M., Lang, S. M., et al. (2015). Mitochondrial DNA Stress Primes the Antiviral Innate Immune Response. *Nature* 520, 553–557. Epub 2015/02/03. doi:10.1038/nature14156

Wilson, D. R., Sen, R., Sunshine, J. C., Pardoll, D. M., Green, J. J., and Kim, Y. J. (2018). Biodegradable STING Agonist Nanoparticles for Enhanced Cancer Immunotherapy. *Nanomedicine: Nanotechnology, Biol. Med.* 14, 237–246. Epub 2017/11/12. doi:10.1016/j.nano.2017.10.013

Woo, S.-R., Fuertes, M. B., Corrales, L., Spranger, S., Furdyna, M. J., Leung, M. Y. K., et al. (2014). STING-dependent Cytosolic DNA Sensing Mediates Innate Immune Recognition of Immunogenic Tumors. *Immunity* 41, 830–842. Nov 20Epub 2014/12/18. doi:10.1016/j.immuni.2014.10.017

Woodrick, J., Gupta, S., Camacho, S., Parvathaneni, S., Choudhury, S., Cheema, A., et al. (2017). A New Sub-pathway of Long-patch Base Excision Repair Involving 5′ gap Formation. *Embo J.* 36, 1605–1622. doi:10.15252/embj.201694920

Woods, D., and Turchi, J. J. (2013). Chemotherapy Induced DNA Damage Response. *Cancer Biol. Ther.* 14, 379–389. Epub 2013/02/06. doi:10.4161/cbt.23761

Wu, J., Sun, L., Chen, X., Du, F., Shi, H., Chen, C., et al. (2013). Cyclic GMP-AMP Is an Endogenous Second Messenger in Innate Immune Signaling by Cytosolic DNA. *Science* 339, 826–830. doi:10.1126/science.1229963

Xiao, W., Singh, K. K., Chen, B., and Samson, L. (1993). A Common Element Involved in Transcriptional Regulation of Two DNA Alkylation Repair Genes (MAG and MGT1) of *Saccharomyces cerevisiae*. *Mol. Cell Biol* 13, 7213–7221. Epub 1993/12/01. doi:10.1128/mcb.13.12.7213-7221.1993

Xie, B., Liang, X., Yue, W., Ma, J., Li, X., Zhang, N., et al. (2021). Targeting Cytokinesis Bridge Proteins to Kill High-CIN Type Tumors. *Fundam. Res.* 1, 752–766. doi:10.1016/j.fmre.2021.08.015

Xie, H., Wang, W., Xia, B., Jin, W., and Lou, G. (2020). Therapeutic Applications of PARP Inhibitors in Ovarian Cancer. *Biomed. Pharmacother.* 127, 110204. Epub 2020/05/19. doi:10.1016/j.biopha.2020.110204

Xu, S., Wang, L., and Liu, Z. (2021). Molecularly Imprinted Polymer Nanoparticles: An Emerging Versatile Platform for Cancer Therapy. *Angew. Chem. Int. Ed. Engl.* 19 (60), 3858–3869. Epub 2020/08/14. doi:10.1002/anie.202005309

Yamamoto, M., Sato, S., Hemmi, H., Hoshino, K., Kaisho, T., Sanjo, H., et al. (2003). Role of Adaptor TRIF in the MyD88-independent Toll-like Receptor Signaling Pathway. *Science* 301, 640–643. Epub 2003/07/12. doi:10.1126/science.1087262

Yilmaz, D., Furst, A., Meaburn, K., Lezaja, A., Wen, Y., Altmeyer, M., et al. (2021). Activation of Homologous Recombination in G1 Preserves Centromeric Integrity. *Nature* 600, 748–753. Epub 2021/12/03. doi:10.1038/s41586-021-04200-z

Yoneyama, M., Kikuchi, M., Matsumoto, K., Imaizumi, T., Miyagishi, M., Taira, K., et al. (2005). Shared and Unique Functions of the DExD/H-Box Helicases RIG-I, MDA5, and LGP2 in Antiviral Innate Immunity. *J. Immunol.* 175, 2851–2858. Epub 2005/08/24. doi:10.4049/jimmunol.175.5.2851

Yoneyama, M., Kikuchi, M., Natsukawa, T., Shinobu, N., Imaizumi, T., Miyagishi, M., et al. (2004). The RNA Helicase RIG-I Has an Essential Function in Double-Stranded RNA-Induced Innate Antiviral Responses. *Nat. Immunol.* 5, 730–737. doi:10.1038/ni1087

Zandarashvili, L., Langelier, M. F., Velagapudi, U. K., Hancock, M. A., Steffen, J. D., Billur, R., et al. (2020). Structural Basis for Allosteric PARP-1 Retention on DNA Breaks. *Science* 368, eaax6367. Apr 3Epub 2020/04/04. doi:10.1126/science.aax6367

Zhang, C., Shang, G., Gui, X., Zhang, X., Bai, X.-c., and Chen, Z. J. (2019). Structural Basis of STING Binding with and Phosphorylation by TBK1. *Nature* 567, 394–398. Epub 2019/03/08. doi:10.1038/s41586-019-1000-2

Zhang, J.-Z., Liu, Z., Liu, J., Ren, J.-X., and Sun, T.-S. (2014a). Mitochondrial DNA Induces Inflammation and Increases TLR9/NF-Kb Expression in Lung Tissue. *Int. J. Mol. Med.* 33, 817–824. doi:10.3892/ijmm.2014.1650

Zhang, X., Shi, H., Wu, J., Zhang, X., Sun, L., Chen, C., et al. (2013). Cyclic GMP-AMP Containing Mixed Phosphodiester Linkages Is an Endogenous High-Affinity Ligand for STING. *Mol. Cel.* 51, 226–235. doi:10.1016/j.molcel.2013.05.022

Zhang, X., Wu, J., Du, F., Xu, H., Sun, L., Chen, Z., et al. (2014b). The Cytosolic DNA Sensor cGAS Forms an Oligomeric Complex with DNA and Undergoes Switch-like Conformational Changes in the Activation Loop. *Cell Rep.* 6, 421–430. Epub 2014/01/28. doi:10.1016/j.celrep.2014.01.003

Zhao, B., Du, F., Xu, P., Shu, C., Sankaran, B., Bell, S. L., et al. (2019). A Conserved PLPLRT/SD Motif of STING Mediates the Recruitment and Activation of TBK1. *Nature* 569, 718–722. Epub 2019/05/24. doi:10.1038/s41586-019-1228-x

Zheng, L., Asprodites, N., Keene, A. H., Rodriguez, P., Brown, K. D., and Davila, E. (2008). TLR9 Engagement on CD4 T Lymphocytes Represses γ-radiation-induced Apoptosis through Activation of Checkpoint Kinase Response Elements. *Blood* 111, 2704–2713. doi:10.1182/blood-2007-07-104141

Zhong, X., Thornton, K., and Reed, E. (2000). Computer Based Analyses of the 5'-flanking Regions of Selected Genes Involved in the Nucleotide Excision Repair Complex. *Int. J. Oncol.* 17, 375–380. Epub 2000/07/13. doi:10.3892/ijo.17.2.375

Zhu, M., Zhao, H., Limbo, O., and Russell, P. (2018). Mre11 Complex Links Sister Chromatids to Promote Repair of a Collapsed Replication fork. *Proc. Natl. Acad. Sci. U S A.* 115 (115), 8793–8798. Epub 2018/08/15. doi:10.1073/pnas.1808189115

Zierhut, C., Yamaguchi, N., Paredes, M., Luo, J.-D., Carroll, T., and Funabiki, H. (2019). The Cytoplasmic DNA Sensor cGAS Promotes Mitotic Cell Death. *Cell.* 178, 302–315. e323Epub 2019/07/13. doi:10.1016/j.cell.2019.05.035

Zimmer, A. S., Gillard, M., Lipkowitz, S., and Lee, J.-M. (2018). Update on PARP Inhibitors in Breast Cancer. *Curr. Treat. Options. Oncol.* 19, 21. Apr 11Epub 2018/04/13. doi:10.1007/s11864-018-0540-2

Conflict of Interest: The authors declare that the research was conducted in the absence of any commercial or financial relationships that could be construed as a potential conflict of interest.

Publisher's Note: All claims expressed in this article are solely those of the authors and do not necessarily represent those of their affiliated organizations, or those of the publisher, the editors and the reviewers. Any product that may be evaluated in this article, or claim that may be made by its manufacturer, is not guaranteed or endorsed by the publisher.

frontiers | Frontiers in Cell and Developmental Biology

REVIEW
published: 29 April 2022
doi: 10.3389/fcell.2022.886718

V(D)J Recombination: Recent Insights in Formation of the Recombinase Complex and Recruitment of DNA Repair Machinery

Shaun M. Christie, Carel Fijen* and Eli Rothenberg**

Department of Biochemistry and Molecular Pharmacology, NYU Grossman School of Medicine, New York, NY, United States

V(D)J recombination is an essential mechanism of the adaptive immune system, producing a diverse set of antigen receptors in developing lymphocytes via regulated double strand DNA break and subsequent repair. DNA cleavage is initiated by the recombinase complex, consisting of lymphocyte specific proteins RAG1 and RAG2, while the repair phase is completed by classical non-homologous end joining (NHEJ). Many of the individual steps of this process have been well described and new research has increased the scale to understand the mechanisms of initiation and intermediate stages of the pathway. In this review we discuss 1) the regulatory functions of RAGs, 2) recruitment of RAGs to the site of recombination and formation of a paired complex, 3) the transition from a post-cleavage complex containing RAGs and cleaved DNA ends to the NHEJ repair phase, and 4) the potential redundant roles of certain factors in repairing the break. Regulatory (non-core) domains of RAGs are not necessary for catalytic activity, but likely influence recruitment and stabilization through interaction with modified histones and conformational changes. To form long range paired complexes, recent studies have found evidence in support of large scale chromosomal contraction through various factors to utilize diverse gene segments. Following the paired cleavage event, four broken DNA ends must now make a regulated transition to the repair phase, which can be controlled by dynamic conformational changes and post-translational modification of the factors involved. Additionally, we examine the overlapping roles of certain NHEJ factors which allows for prevention of genomic instability due to incomplete repair in the absence of one, but are lethal in combined knockouts. To conclude, we focus on the importance of understanding the detail of these processes in regards to off-target recombination or deficiency-mediated clinical manifestations.

Keywords: V(D)J rearrangements, DNA repair, nonhomologous end joining, chromatin 3D architecture, recombinase activating gene

OPEN ACCESS

Edited by:
Feilong Meng,
Chinese Academy of Sciences (CAS), China

Reviewed by:
Ludovic Deriano,
Institut Pasteur, France
Jiazhi Hu,
Peking University, China

****Correspondence:***
Shaun M. Christie
shaun.christie@nyulangone.org
Carel Fijen
carolus.fijen@nyulangone.org
Eli Rothenberg
eli.rothenberg@nyulangone.org

Specialty section:
This article was submitted to Signaling, a section of the journal Frontiers in Cell and Developmental Biology

Received: *28 February 2022*
Accepted: *01 April 2022*
Published: *29 April 2022*

Citation:
Christie SM, Fijen C and Rothenberg E (2022) V(D)J Recombination: Recent Insights in Formation of the Recombinase Complex and Recruitment of DNA Repair Machinery. Front. Cell Dev. Biol. 10:886718. doi: 10.3389/fcell.2022.886718

INTRODUCTION

An essential trait of an effective adaptive immune response is the generation of a diverse set of antigen receptors. Developing lymphocytes undergo a process of regulated DNA cleavage and subsequent repair, termed V(D)J recombination, to progress from progenitor cells to immature B or T cells. In this review, we focus on the mechanism as it occurs in B cells, however, many aspects can

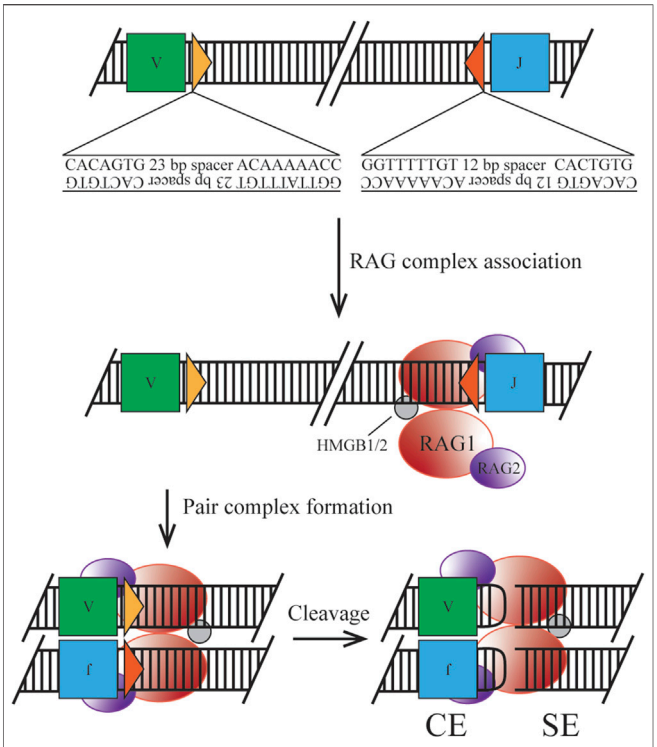

FIGURE 1 | Classical mechanism of RAG initiated cleavage. Ig loci segments are flanked by 12/23 RSS containing a heptamer and nonamer sequence for RAG complex association. Synapsis of two RSS sites allows for nicking, cleavage by transesterification, and hairpin formation to form the post cleavage complex.

be applied to T cells. Genes for the production of heavy and light chains of antigen receptors, termed variable (V), diversity (D), and joining (J), are clustered on chromosome 14 and 2/22, respectively, and require rearrangement to produce a large repertoire of functional surface receptors (Little et al., 2015; Delves and Roitt, 2000). Mechanistically, V(D)J recombination occurs in three distinct phases: recognition of recombination sites, induction of two double-strand breaks, and repair of the broken DNA by ligating the strands in a recombined configuration (**Figure 1**). In order to avoid off-target effects, the V(D)J recombination process is tightly regulated on a broad level by cell lineage, developmental stage, and cell cycle (Lin and Desiderio, 1994; Zhang et al., 2011; Little et al., 2015). Importantly, defects in V(D)J recombination can result in aberrant DNA joining events or loss of function, which in turn can lead to immunodeficiency and tumorigenesis, as we will describe in this review (Villa and Notarangelo, 2019).

Central to V(D)J recombination are two lymphocyte specific proteins: recombination activating genes (RAG) 1 and 2 (Teng and Schatz, 2015; Lescale and Deriano, 2017). These proteins were found to act as a tetrameric complex to mediate the cleavage phase at specific recombination signal sequences (RSSs) (Bailin et al., 1999). A multitude of these RSSs flank the V(D)J regions on the chromosome, allowing for a large variety of potential rearrangements. Chromatin remodelers and histone modifications guide the RAG proteins in their search for RSSs, as we will discuss in this review. RAG1 contains the catalytic motif essential for cleaving the DNA at the RSS, while RAG2 mediates and enhances chromosomal binding (Lescale and Deriano, 2017). Since the RAG proteins were first identified, evidence has mounted that implicates them in more than just DNA cleavage, with special roles for the complex in regulation and the hand-off to the Non-Homologous End Joining (NHEJ) repair pathway (Qui et al., 2001; Schultz et al., 2001; Lee et al., 2004). As the name indicates, NHEJ does not rely on a homologous template for repair: on the contrary, it aims to directly ligate two DNA ends together with minimal processing (Lieber, 2010; Wang et al., 2020; Zhao et al., 2020). NHEJ is the preferred pathway for V(D)J recombination, since templated Homologous Recombination would restore the original sequence, while alternative end joining pathways are too error-prone (Sallmyr and Tomkinson, 2018). Here, we will describe how the cell ensures a proper transition from the RAG-bound post-cleavage complex to the NHEJ repair complex. We also highlight some of the mechanisms the cell puts in place to make the repair phase more robust, thereby avoiding genomic instability.

In this review we aim to identify lingering gaps in the knowledge base and establish the need for continued research in the field due to the clinical implications of recombination dysfunction.

The Fundamentals of V(D)J Recombination

Effective Recombination Controls Differentiation

Each antigen receptor produced through recombination in B cells will contain a heavy (IgH) and light [IgL, (Igκ or Igλ)] chain consisting of VDJ segments for IgH and VJ segments for IgL. These gene clusters extend over 3 Mb, consisting of approximately 140 Vκ, 4 Jκ, 38 Vλ, and 5 Jλ loci for use in the IgL and approximately 150 V_H, 9 D_H, and 4 J_H loci for use in the IgH (Jung et al., 2006; Ji et al., 2010; Collins and Watson, 2018).

Due to expression and degradation mechanisms of the RAG proteins discussed below V(D)J recombination is restricted to G0/G1 phase of the cell cycle. At this point the IgH locus can undergo recombination, first between D_H-J_H segments before V_H-DJ_H joining. Successful rearrangement of the three segments allows for production of a pre-B cell receptor (pre-BCR) and further differentiation to the small pre-B stage where IgL rearrangement can begin. Gene usage during this recombination step is skewed toward Igκ segments over Igλ (2:1 up to 95:5) (Woloschak and Krco, 1987; Lycke et al., 2015). Surface expression of the BCR in the immature B cell activates a checkpoint to determine whether the receptor is autoreactive or non-functional. If either condition occurs, secondary recombination of the Igλ gene segments is used to substitute light chains until the autoreactivity is diminished. Molecular signatures of this recombination event are the usage of more upstream V regions and more downstream J regions (Villa and Notarangelo, 2019). Following proper reactivity, the mature B cell is released from the bone marrow.

RAG-Mediated DNA Cleavage

The heterotetrameric recombination complex that binds the antigen receptor loci at RSSs is composed of two RAG1 subunits and two RAG2 subunits (Kim et al., 2015). Two discrete RSSs, a heptamer and a nonamer, are required for efficient binding and cleavage. Heptamer sequences follow the pattern of CACAGTG, where only the first three nucleotides are highly conserved and required for cleavage. The stronger binding nonamer sequence, ACAAAAACC, contains several conserved positions required for initial protein complex interaction. RSSs are separated by a 12 or 23 base pair spacer, which exhibits low conservation, but has the potential to introduce a significant effect on recombination efficiency (Hirokawa et al., 2020; Lee et al., 2003). Binding must occur at a pair of RSSs following the 12/23 rule, forming the paired complex (PC), which can be mediated by random collision or locus contraction (see below) (Eastman et al., 1996). Discussed later in the clinical manifestation section, cryptic RSSs (cRSSs) are common throughout the genome and, due to the sequence variation allowed by the RAG complex, may induce off-target effects. For example, frequent RAG-mediated DSBs in *c-Myc* rely only on the presence of the CAC motif of an RSS heptamer (Hu et al., 2015). Upon binding to DNA, the RAG complex induces a conformational change to the 12- and 23-RSS sites to enable efficient cleavage by RAG1. The recombination complex also utilizes high mobility group box 1/2 (HMGB1/2) to promote DNA bending, enhancing synapsis and cleavage. Once the PC is established, cleavage first occurs on a single strand via a 5' nick at the heptamer-coding flank junction. This allows for a direct transesterification reaction where the 3' hydroxyl group attacks the phosphate of the bottom strand. Two cleavage events in the PC generate four broken DNA ends, where two are covalently sealed coding ends (CEs) and two are blunt signal ends (SEs). This reaction takes place without a required external energy source, as the hairpin formation energy is derived from the DNA breakage. The RAG-DNA complex does not form a covalent intermediate making it distinct from other site-specific recombinases and is more similar to bacterial transposases and HIV integrase than its mammalian counterparts (Little et al., 2015). The nicking reaction can occur within minutes but the hairpinning may require hours potentially indicating simultaneous nick locations within the locus (Yu et al., 2004).

Upon cleavage the RAG complex stays associated with the broken ends forming a post-cleavage complex (PCC). This structure permits CEs to dissociate first, under the correct conditions to enter the NHEJ pathway. SEs are retained in the complex until physical disassembly can occur due to RAG2 degradation, however, this process is only speculative (Mizuta et al., 2002). Joined SEs ultimately create a non-replicative episome which is routinely lost during cell division (Smith et al., 2019). As discussed in the clinical manifestation section regulation of this component is necessary as well, due to the potential for translocation or other off-target effects if the complex is retained.

Non-Homologous End Joining

NHEJ proceeds through a couple of seemingly simple steps. The exposed DNA ends are first recognized by the Ku heterodimer, a ring-shaped protein (Fell and Schild-Poulter, 2015). Together with the DNA-dependent protein kinase catalytic subunit (DNA-PKcs), Ku forms the DNA-PK holoenzyme (Yue et al., 2020). This complex binds to the break site and acts as a scaffold for other repair proteins. XRCC4 (together with its binding partner Ligase IV) and XLF are recruited to the break site (Mcelhinny et al., 2000) and aid the DNA ends in coming together, a transient process called synapsis (Reid et al., 2015; Graham et al., 2017; Zhao et al., 2019). Structural studies and super-resolution microscopy have shown that XRCC4 and XLF can accomplish this by forming filaments along the DNA, which helps bridge the two ends (Hammel et al., 2010; Ropars et al., 2011; Mahaney et al., 2013; Reid et al., 2015; Chen et al., 2021). Once the DNA ends are aligned, Ligase IV seals the backbones to complete repair (Conlin et al., 2017). Over the years, it has become clear that a host of accessory factors are implicated in NHEJ, some of which are functionally redundant. We will discuss the best studied accessory factors and the implications of their functional redundancies later in this review.

If NHEJ is unavailable, repair can proceed through Alternative End Joining (alt-EJ). Alt-EJ is a less well-defined process that involves a different set of proteins, most prominently DNA Polymerase Theta (PolQ), that mediate microhomology-based annealing of resected DNA ends (Sallmyr and Tomkinson, 2018). Alt-EJ is exceptionally error-prone and usually only serves as a backup pathway. It does not typically occur during V(D)J recombination, since the hand-off of the break sites to the NHEJ machinery is tightly arranged. Indeed, deficiency in core NHEJ factors often leads to cell death (Wang et al., 2020). If certain key proteins in the hand-off fail, however, alt-EJ may be employed and lead to genome instability and disease.

With this three step process established there is still information lacking on direct influences for the recruitment of a RAG complex to RSS regions as well as subsequent pairing to the partner RSS, regulation by non-catalytic regions of RAG proteins, and certain redundant features of NHEJ factors during the repair phase, each of which will be highlighted by the following sections.

V(D)J Regulation by RAG Non-Core Domains

RAG1 and RAG2 each contain various domains, where the smallest catalytically functional unit is denoted as the core region (**Figure 2**). These truncated constructs have been used in reconstituted functional studies due to their ease of purification. Deletion of the non-core regions allowed for recombination activity to occur, but at the cost of increased off-target effects and decreased efficiency and diversity (Talukder et al., 2004). Therefore, non-core regions are required for regulatory roles such as RSS recognition, complex stability, and handoff to repair factors. Earlier research using core proteins only and extrachromosomal substrates may require

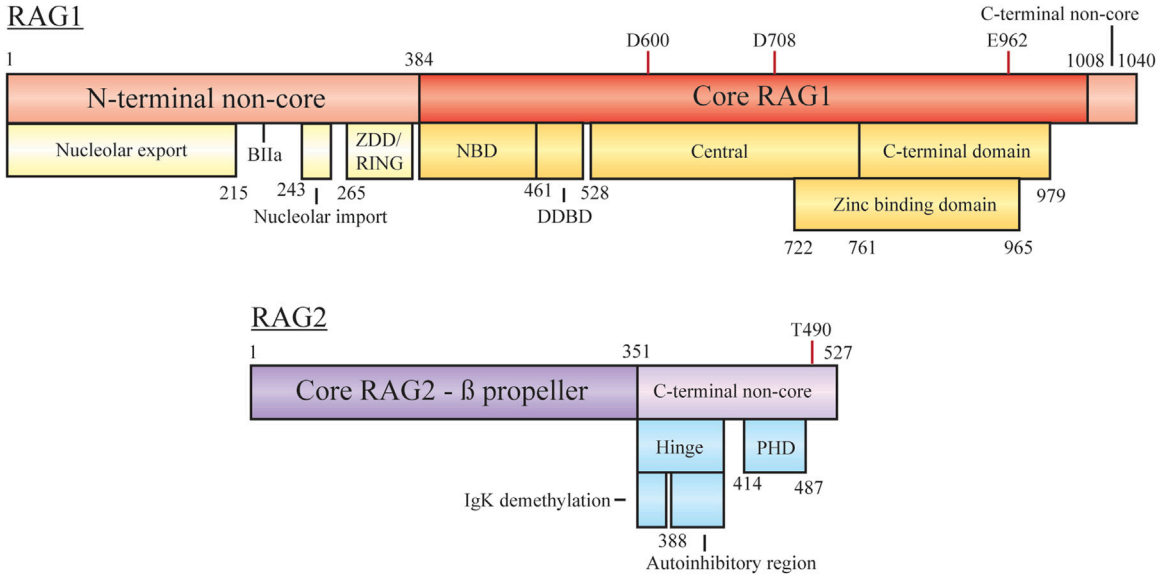

FIGURE 2 | Domain organization of RAG1 and RAG2, with minimal core regions shaded darker. Subdomains/functional regions are noted below each region. Residues involved in RAG1 catalytic activity and RAG2 degradation are highlighted. Abbreviations: ZDD, zinc dimerization domain; RING, really interesting new gene; NBD, nonamer binding domain; DDBD, dimerization and DNA-binding domain; PHD, plant homeodomain.

additional follow up studies to confirm physiological functions (Gigi et al., 2014).

RAG1 Non-Core Domain Function

RAG1 is a 1,040 aa protein consisting of a large N-terminal non-core domain (aa 1–384), the core region (384–1,008), and a short C-terminal non-core domain (1,008–1,040) (Schatz and Swanson, 2011; Little et al., 2015; Lescale and Deriano, 2017; Villa and Notarangelo, 2019). The functional core region contains the essential sites for DNA/RSS binding, homo- and hetero-dimerization and DNA cleavage (facilitated by D600, D708, and E962). The nonamer binding domain (NBD) interacts with the nonamer RSS, with the downstream dimerization and DNA binding domain (DDBD) providing a site for RAG1 homo-dimerization (Villa and Notarangelo, 2019). Regulation of contact with the heptamer RSS, ssDNA, and RAG2 is controlled by motifs within the central region. The C-terminal core region contains nonspecific DNA binding activity to mediate contact with the coding sequence flanking the RSS. A catalytic triad within the central and C-terminal domains coordinates metal ions (Mg^{2+}) to activate water for ssDNA nicking activity. A zinc binding domain (ZBD) also spanning the central and C-terminal regions (722–965) is important for interaction with RAG2.

In order to understand potential interaction partners of RAG1, Brecht et al. examined association via a proximity-dependent biotin identification screening (Brecht et al., 2020). Results here indicated interaction with multiple nucleolar factors suggesting localization to this region of the nucleus outside of G1 cell cycle phase. By sequestering the protein to the nucleolus, off-target recombination events were dampened and genome stability was promoted. Upon induced recombination and G1 cell cycle arrest, RAG1 was observed to be released from the nucleolar regions and allowed to bind partner RAG2 and RSSs. Truncation of the full length protein determined that two sequences within the N-terminal non-core region were responsible for nucleolar entry (residues 243–249) and export (1–215) (Brecht et al., 2020).

In addition to nucleolar localization, the N-terminal non-core domains of RAG1 are responsible for regulation of cellular protein levels, mediation of interaction with other factors, and coordination of zinc ions, all of which act to enhance recombination activity. The zinc dimerization domain in this region (265–380) acts as a counterpart to the core ZBD, but here facilitates homo-dimerization (Lescale and Deriano, 2017). Overlapping with this domain is a RING motif, at residues 264–389, which has the capability to act as an E3 ubiquitin ligase for both autoubiquitylation and modification of other proteins (Grazini et al., 2010). RAG1 autoubiquitylation at K233 has been shown to stimulate cleavage activity in a cell free assay and exhibit post-transcriptional regulation in mice studies (Singh and Gellert, 2015; Beilinson et al., 2021). Ubiquitin modification of other proteins occurs at different stages of recombination, such as polyubiquitylation of KPNA1 or the monoubiquitylation of histones (discussed below). Sequestering RAG1 after nuclear import may be achieved by KPNA1 interaction with the basic motif BIIa within residues 218–263, only relieved by KPNA1 ubiquitylation for sub-nuclear localization (Simkus et al., 2009). However, follow up reports have discussed ubiquitylation activity mediated by additional complexes rather than the isolated RING region (discussed below) (Kassmeier et al., 2012). At the C-terminus of RAG1 the non-core region is only 32 residues, but inhibition of hairpin formation is controlled by this motif (Grundy et al., 2010). Interaction of the RAG complex with modified histones

overcomes the inhibition possibly due to RAG2-mediated conformation changes associated with RAG2 C-terminal regions.

RAG2 Non-Core Domain Function

RAG2 is a 527 aa protein consisting of a core domain (1–351) and a C-terminal non-core domain (352–527). The core region is comprised of six Kelch-like motifs which form a six bladed ß-propeller responsible for efficient DNA cleavage (Schatz and Swanson, 2011; Little et al., 2015; Lescale and Deriano, 2017; Villa and Notarangelo, 2019). The second and sixth ß-strands are responsible for making contact with RAG1 (Little et al., 2015; Villa and Notarangelo, 2019). On its own RAG2 is monomeric, forming a 2:2 heterotetramer with RAG1 to form the RAG recombination complex (Bailin et al., 1999). As with RAG1, the non-core domain is not required for recombination activity, but regulates various parts of the recombination mechanism.

The RAG2 C-terminal non-core region is composed of two main components, an acidic hinge (351–408) and a plant homeodomain (PHD, 414–487). Although many studies have reported the RAG2 non-core region spans residues 387–527, assays with further truncations of the RAG2 core region have displayed efficient recombination with only residues 1–351 (Coussens et al., 2013; Kim et al., 2015). The acidic hinge, linking core RAG2 and the PHD, contains a high concentration of acidic residues contributing to flexibility of the region. Neutralization of the residues severely reduces the flexibility and leads to increased genomic instability as aberrant repair begins to occur (Coussens et al., 2013). Two separate regions within the acidic hinge are necessary to regulate recombination activity. Serial truncations of the hinge by Wu et al. lead to the discovery that the Igκ locus was hypermethylated upon deletion of residues 350–383 and occurred in a RAG1-independent manner (Wu et al., 2017). Demethylation of the chromosome in this context may assist in facilitating allelic exclusion, preventing further recombination on the locus. Coupled with this in the acidic hinge is an autoinihibitory function by residues 388–405, where relief is required to promote activity. As discussed below, histone recognition mediates this inhibition, with mutations bypassing the necessity for this interaction (Lu et al., 2015). The PHD component is responsible for interactions with chromatin, specifically at modified histones, based on full-length and truncated constructs submitted to ChIP-seq experiments (see below) (Teng et al., 2015). Mutations to this site, such as W453A, result in overall loss of genome localization and reduced recombination activity (Liu et al., 2007; Teng et al., 2015). At the far C-terminus phosphorylation of T490 promotes cell cycle-regulated degradation at the G1-S transition (Zhang et al., 2011). RAG2 T490A mutation can lead to persistent accumulation throughout the cell cycle as degradation is reduced. This overexpression results in continuous opportunities for RSS/cRSS target cleavage in the presence of RAG1 and recombination intermediates. The mutation also plays a role in stabilizing genomic interaction displayed by Rodgers et al. where slowed diffusion, measured in live cells via fluorescence recovery after photobleaching, was indicative of stronger interactions with modified histones (Rodgers et al., 2019).

Recruitment of RAGs to the Site of Recombination

Histone Modification

To begin the process of recombination, RAG proteins must first associate with an RSS within the Mb chromosomal antigen receptor locus. The limiting of initial RAG binding can be considered a regulatory mechanism to prevent DNA nicks at random sites within the genome and may be facilitated solely by 3D diffusion to scan for sites rich in modified histones which indicate active chromatin (Lovely et al., 2020). ChIP-seq experiments by Teng et al. and Ji et al. determined the binding pattern of RAG1 and RAG2 across V(D)J segments and the entire genome revealing chromatin features which may influence the recruitment of these proteins (Ji et al., 2010; Teng et al., 2015). Within the antigen receptor loci both RAG1 and RAG2 were observed to bind at J segments in the Igκ locus and both D and J segments in the IgH locus (Ji et al., 2010). In this region, an RSS is necessary for strong binding with mutation to the nonamer sequence reducing overall recruitment. Outside of these loci, however, RAG1 localization is poorly indicated by RSS presence alone, along with cRSSs and heptamers depletion from observed binding sites suggesting that other chromatin features may play a role in RAG complex recruitment. The genomic localization of RAG2 is significantly broader with binding sites dependent on regions with high levels of methylated histone 3 (H3K4me3) and physical association determined by co-immunoprecipitation (Teng et al., 2015; Rodgers et al., 2019). As noted above, interaction of RAG2 and H3K4me3 is facilitated by the PHD of RAG2 (Matthews et al., 2007; Teng et al., 2015) The necessity of H3K4me3 binding was then determined to be due to autoinhibition of the RAG complex by RAG2 (Grundy et al., 2010). Stimulation with exogenous H3K4me3 relieved the reduced binding and catalysis, with truncation of this site uncoupling the necessity for histone recognition. Studies by Lu et al. and Bettridge et al. determined allosteric conformational changes occur to both RAG1, at the DDBD and catalytic region, and RAG2 at the autoinhibitory region allowing for increased accessibility (Lu et al., 2015; Bettridge et al., 2017). Mutations to this region can bypass the need for histone recognition to promote activity but will likely increase off-target effects (Lu et al., 2015). While RAG2 and H3K4me3 display a linear correlation of interaction, the non-linear correlation of RAG1 and H3K4me3 suggests additional features. Maman et al. used additional ChIP-seq experiments to determine possible factors for RAG1 interaction (Maman et al., 2016). H3K4me3 overlap with RAG1 was determined to be RAG2-histone dependent making it insufficient to determine RAG1 binding throughout the genome and the role methylation plays in off-target binding. Another histone modification, H3K27Ac, was instead determined to be RAG2 independent and more so influenced by N-terminal regions of RAG1, but with little direct evidence the significance is unclear (Maman et al., 2016).

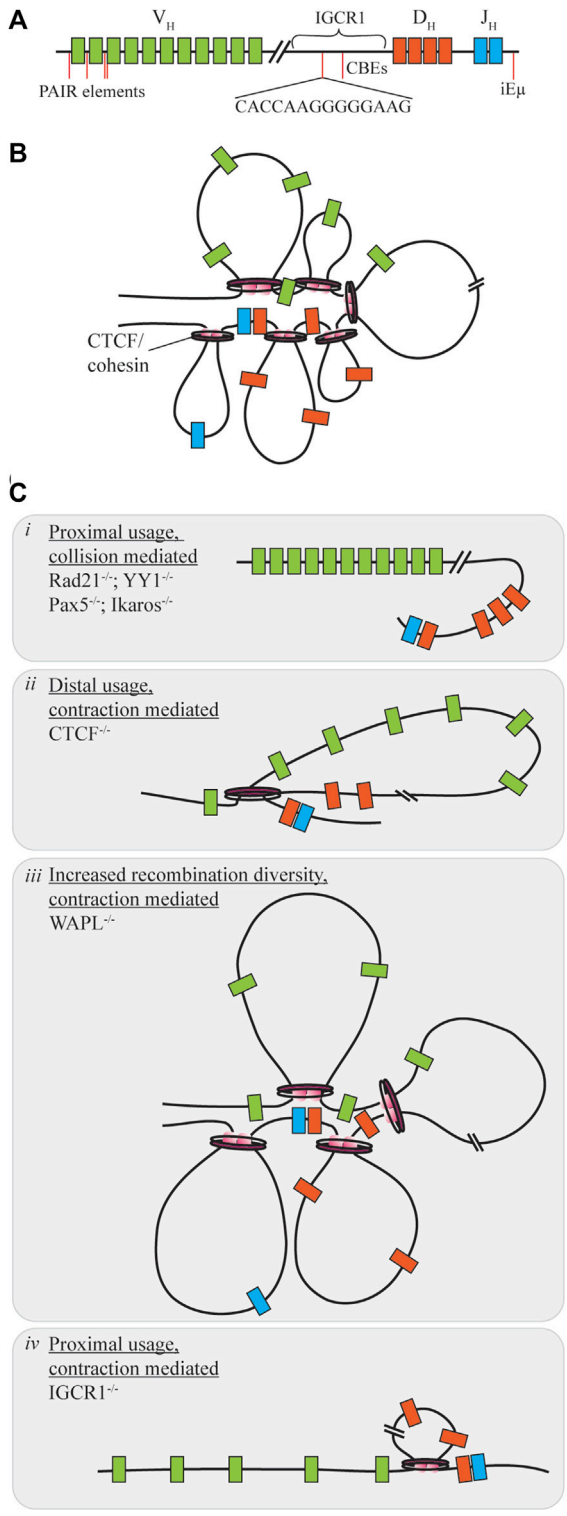

FIGURE 3 | Contraction mediated conformational changes of the Ig locus. **(A)** The IgH locus contains V, D, and J segments spread over 2.8 MB of the chromosome, with regulatory regions distrubuted throughout the locus. **(B)** Under normal conditions contraction of the locus allows for gene

(*Continued*)

FIGURE 3 | segments to be brought into close proximity as the rosette conformation is formed with varying loop sizes. **(C)** When proteins mediating this contraction are dysregulated V**(D)**J recombination diversity may be skewed towards one segment of the V_H region through collision (i) or contraction (ii, iv). Only under WAPL repression is diversity increased as cohesin-mediated loop size increases due to cohesin retention on chromatin (iii).

Pairing Through Locus Contraction

In addition to initial binding, the RAG-DNA complex must associate with a second, partner RSS to perform recombination. Regulation at this point is achieved through the physical proximity of the V gene segments, which are spread across over 2 Mb of DNA (**Figure 3A**). While proximal segments may be paired via random collision, large scale chromosomal conformational changes are utilized to direct pairing at both central and distal regions within the loci, skewing interaction partners and providing a diverse set of antigen receptors (**Figure 3B**). Various mechanisms of chromosomal looping enables regions to be brought into close proximity during pro- and pre-B stages via proteins such as YY1, Ikaros, Pax5 and CTCF.

Distal V_H utilization is facilitated by each of the proteins under slightly different mechanisms. Within the IgH locus are enhancer regions, intronic enhancer (iEμ) and a 3' regulatory region which provide sites for contraction protein binding. Yin Yang 1 (YY1) is a zinc finger protein with multiple functions in regards to transcription activation and repression (Liu et al., 2007). Knockouts of this protein during B-cell development yield a block at the pro-B cell stage due to insufficient V_H-DJ_H recombination without influencing expression of additional V(D)J recombination components (**Figure 3Ci**). Using ChIP and 3D DNA FISH Liu et al. were able to determine that YY1 binds to iEμ sites to provide a node for locus contraction (Liu et al., 2007). Deletion of iEμ does not inhibit YY1 binding to the overall chromosome loci, indicating that additional sequences and factors influence the contraction (Guo et al., 2011). In addition, YY1 may have heterotypic interactions with CTCF, however, changes to rearrangement if CTCF levels are decreased are not as pronounced as the knockdown of YY1 in reducing recombination efficiency (Degner et al., 2011; Weintraub et al., 2017). Ikaros, also a zinc finger protein, contributes various roles in differentiation control and chromosome accessibility (Reynaud et al., 2008). In a similar manner, reduction of Ikaros leads to overall low V_H-DJ_H recombination with heavily skewed usage of proximal V_H segments (**Figure 3Ci**). Pax5, a B-cell commitment factor for differentiation, controls transcription, but also functions by positioning chromatin towards the central nuclear regions ensuring active chromatin is in an extended state and promotes locus contraction (Ebert et al., 2011; Fuxa et al., 2004). When Pax5 is deleted, cells will have characteristic features of uncommitted progenitors, such as the ability to change differentiation pathway following cytokine stimulation, and exhibit reduced diversity due to a 50-fold reduction of distal V recombination (**Figure 3Ci**). Contraction by Pax5 is mediated through Pax5-activated intergenic repeats (PAIRs) over 750 kB of

the distal V_H gene which allow for interaction with iEμ sites (Verma-Gaur et al., 2012). *Via* Bio-ChIP-chip Ebert et al. showed that this mechanism is specifically lost in the pre-B cell stage where other mechanisms must be used to promote distal gene usage (Ebert et al., 2011).

CCCTC-binding factor (CTCF) is another zinc finger protein with diverse functions for transcriptional control, but also mediating chromosomal contacts across the genome (Phillips and Corces, 2009; Degner et al., 2011). Deletion of CTCF reduces overall B-cell maturation and arrests development at pre-B stage for those progressing that far. Mediation of contraction here is regulated by the presence of CTCF-binding elements (CBEs), 14 bp conserved targets within the Ig loci (Hu et al., 2015). Association of pairs of convergently oriented CBEs bound by CTCF and the cohesin complex form loop domains of the antigen receptor loci restricting the V segments (Zhao et al., 2016; Zhang et al., 2019). Cohesin, consisting of multiple subunits including Rad21, will form loops of various sizes by extrusion of chromatin in an ATP-dependent manner until reaching a CTCF bound CBE (Ba et al., 2020). The loop extrusion process is dynamic and allows for a subset of CTCF/cohesin formed loops to exist at any given time enhancing genetic diversity (Degner et al., 2011). Large chromosomal structural rearrangements also compete with the short range collisional recombination which is extinguished during CTCF downregulation as RAG proceeds to distal V_H regions without obstruction therefore limiting diversity (**Figure 3Cii**), yet in the Igκ locus proximal usage is increased (De Almeida et al., 2011; Ba et al., 2020; Zhang et al., 2022). In contrast, deletion of cohesin subunit Rad21 eliminates all recombination at most sites, except for proximal regions which form a synapse due to collisional diffusion (**Figure 3Ci**). Cohesin unloading is regulated by the expression of WAPL throughout the cell cycle. Pax5 repression of the WAPL promoter during pro- and pre-B cell stages allows for increased cohesin residence time on chromatin extending loop sizes by circumventing CBE obstructions (Hill et al., 2020; Dai et al., 2021). Under these circumstances, there is a general increase of recombination at all sites (**Figure 3Ciii**). For a comprehensive look into cohesin-mediated loop extrusion, we refer the reader to the recent review by Zhang et al., (2022).

Enhancer and intergenic regions of the antigen receptor loci are also important for CTCF mediated loop extrusion as deletion or mutation of these sites provides limited diversity and dysfunction. iEμ in the IgH locus is required for efficient recombination, where deletion increases proximal gene usage and reduced chromosomal relocation to the central nuclear regions to limit total accessibility (Guo et al., 2011). The intergenic control region 1 (IGCR1), between V_H and D_H segments, contains CBEs to suppress V_H usage prior to D_H-J_H rearrangement. Deletion of the IGCR1 region promotes proximal V_H usage, but also induces off-target breaks spreading up to 120 kb upstream of the proximal V_H segments for potential cRSS replacement (**Figure 3Civ**). CBEs within the V_H region prevent distal usage past these segments in the absence of IGCR1 regulation (Hu et al., 2015). The Vκ-Jκ locus contains additional DNase hypersensitive (HS) regions which influence chromosomal conformation change. Upon deletion of HS3-6 there is only a moderate decrease of middle gene usage, with overall insignificant changes to locus contraction. However, HS1-2 deletion results in at least a 7-fold increase of proximal gene usage with 3D DNA FISH indicating a 50% decreasing in overall contraction of the Ig locus (Xiang et al., 2013).

Hand-Off of the Post-Cleavage Complex to the DNA Repair Machinery

Cleavage by the RAG proteins triggers the DNA damage response. A proper hand-off to NHEJ machinery is essential for successful recombination: alt-EJ may lead to aberrant joining events and genomic instability, especially in p53-deficient environments. The idea that the role of the RAG proteins extends beyond the cleavage step, came when several RAG mutants were found to be proficient for cleavage but exhibited aberrant joining (Qui et al., 2001; Schultz et al., 2001; Lee et al., 2004). Exactly how the RAG proteins channel the repair to NHEJ is unclear, although three elements seem to be important for pathway choice. The first is the dependence of RAG activity on the cell cycle: by limiting recombination to G1, HR is not available (Zhang et al., 2011). Moreover, expression of PolQ is very low in G0 and G1, limiting the possibilities for alt-EJ as well (Yu et al., 2020). RAG2 residue T490 is a CDK phosphorylation site, that is, instrumental in targeting RAG2 for breakdown when the cell moves to S phase; indeed, the T490A mutation is enough to lead to aberrant recombination (Zhang et al., 2011). The second element is the ability of the RAG1 N-terminal domain to bind a multi-protein complex, containing Ku, that steers repair to NHEJ (Raval et al., 2008; Kassmeier et al., 2012). Ku was recently shown to suppress alt-EJ of RAG-induced DSBs, indicating it aids in shepherding breaks to NHEJ during V(D)J recombination (Liang et al., 2021). Other proteins in the complex are VprBP, DDB, Cul4A and RocI: these act as a RING E3 ligase that can ubiquitylate nearby proteins (Kassmeier et al., 2012). Disruption of VprBP (by conditional excision of two exons) leads to defects in recombination and increased mutations in the D and J segments in mice. Based on the mutational signature, the authors suggest that VprBP specifically regulates terminal transferase activity through a mechanism that involves ubiquitylation of an unknown target, and thus suppresses other error-prone repair pathways. The third element is the stability of the PCC, which was found early on to influence the choice of repair pathway: unstable PCCs are more prone to lead to alt-EJ instead (Lee et al., 2004). Stability of the PCC seems to be closely related to the conformation of the acidic hinge in the RAG2 C-terminus, an intrinsically disordered domain with a high negative charge. Mutations that neutralize this charge destabilize the PCC and allow repair through alt-EJ (Coussens et al., 2013). The RAG2 C-terminus has been shown to influence pathway choice on more occasions (Corneo et al., 2007; Gigi et al., 2014; Mijuskovic et al., 2015). The exact mechanism, however, still remains unclear. Interestingly, the RAG2 C-terminus was found to be redundant with XLF for what appears to be a function in stabilization of DNA ends: mice that are deficient for XLF but express the core RAG2 show severe defects in V(D)J recombination which in turn leads to lower numbers of

lymphocytes (Lescale et al., 2016a). This opens the intriguing possibility that the RAG proteins interact with XLF in the synaptic complex.

Although both proceed through NHEJ, the repair of coding and signal ends is slightly different. Signal ends are blunt (Roth et al., 1993), while coding ends are hairpins that need processing (Roth et al., 1992). After cleavage, the RAG proteins are more likely to stay bound to the signal ends, at least *in vitro* (Ramsden and Gellert, 1995; Livak and Schatz, 1996; Agrawal and Schatz, 1997; Hiom and Gellert, 1998). The sealed coding ends, which will be quickly bound by Ku, are a target for DNA-PKcs (**Figure 4A**). Once this enzyme binds to the break site, it will act as a regulator for further processing steps. As has recently been shown through a crystal structure of DNA-PKcs, the hairpin DNA substrate will trigger DNA-PKcs to phosphorylate itself, which results in a large conformational change that creates room for the Artemis endonuclease to bind (Liu et al., 2022). Artemis is capable of opening the hairpins, which it does asymmetrically to create a 3' 2 nucleotide overhang (Ma et al., 2002; Karim et al., 2020; Yosaatmadja et al., 2021). This overhang is the reason repaired coding ends typically show indels; it serves as a substrate for the TdT polymerase, which can add nucleotides to the overhang without the need for a template (Motea and Berdis, 2010). As such, 3' overhang elongation is an additional mechanism to create diversity at V(D)J junctions. The two ends, which may have diffused apart in the meantime, then need to be brought together in a synaptic complex for repair to proceed. The signal ends, on the contrary, are blunt and held together by the RAG proteins, obviating the need for a pre-processing step or formation of a synaptic complex. As a consequence, the aforementioned interaction between XRCC4 and XLF to form filaments that bridge DNA ends is not necessary for signal end repair (Roy et al., 2012). Signal end repair does, however, need kinase activity from either DNA-PKcs or ATM, probably to remove the RAG proteins from the break site (Zha et al., 2011b; Gapud et al., 2011; Gapud and Sleckman, 2011). In the absence of filament formation, signal end repair is also more dependent on XRCC4 than on XLF, which is in line with the role of XRCC4 to carry Ligase IV to the break site.

Functional Redundancies and Newly Identified Non-Homologous End Joining Factors

The core factors Ku, XRCC4 and Ligase IV are absolutely essential for NHEJ: knock-outs of these genes in mice lead to severe phenotypes or embryonic lethality (reviewed in Wang et al., 2020 and Zhao et al., 2020) (Wang et al., 2020; Zhao et al., 2020). There is, however, a considerable degree of functional redundancy among most other NHEJ factors. These redundancies make repair more robust, and prevent genomic instability associated with unrepaired breaks or alt-EJ pathways (Chang et al., 2017). A number of functional redundancies have been identified in mouse models: while a single knock-out of a redundant NHEJ factor may only lead to a mild phenotype, a more severe phenotype in a double knock-out suggests a functional redundancy between those two NHEJ factors. These redundancies have for years obscured the role some proteins play in NHEJ, like XLF (Li et al., 2008) or the more recently identified roles of PAXX (Ochi et al., 2015; Xing et al., 2015) and MRI (Hung et al., 2018). For this reason, functional redundancies with XLF have been particularly well studied and have shed some light on the molecular mechanism of end joining. For a relatively recent overview of the effect of single or double knock-outs in NHEJ we would like to refer to Wang et al., (2020). Here, we focus on redundancies of XLF with some of the newly identified NHEJ factors PAXX and MRI, and with ATM and H2AX.

PAXX, a paralog of XRCC4 and XLF, was discovered not so long ago as a player in NHEJ (Ochi et al., 2015; Xing et al., 2015). PAXX bears strong structural similarity to XRCC4 and XLF, but is slightly smaller. Consistent with a role in DNA repair, PAXX is recruited to damage sites; moreover, PAXX deficiency leads to an increased sensitivity to ionizing radiation in human somatic U2OS cells (Ochi et al., 2015). The conserved C-terminal region of PAXX binds to the N-terminal region of Ku80, revealing a mechanism for PAXX recruitment to DSBs (Ochi et al., 2015; Liu et al., 2017). This interaction is essential, since PAXX does not appear to have any DNA binding activity by itself. Considering its similarity to XRCC4 and XLF, it was surprising to find that PAXX does not participate in bridging of DNA ends. Rather, its interaction with Ku seems to promote the accumulation of XLF and Polymerase Lambda at DSBs (Craxton et al., 2018), as well as to promote further accumulation of Ku (Liu et al., 2017). In the context of simple DSBs, PAXX function seems to be redundant with XLF, whereas PAXX and XLF work together in the repair of more complex breaks (Xing et al., 2015). Interestingly, PAXX is dispensable for V(D)J recombination in a mouse pro-B cell line, as long as XLF is present (Kumar et al., 2016; Lescale et al., 2016b). This reveals a functional redundancy between these two proteins in the context of V(D)J recombination. Since XLF itself is redundant with ATM in the same context, one might wonder if PAXX, in turn, is also redundant with ATM. It turns out this is not the case, indicating that these proteins act at more than one stage and only some functions overlap (Kumar et al., 2016). Lescale et al. proposed a two-tier model of an initial synapsis stage and a subsequent ligation stage (Lescale et al., 2016b). In the synapsis stage, XLF forms filaments with XRCC4, bridging the break site (**Figure 4B**). ATM has a similar, but independent role. In the ligation stage, XLF stabilizes the ligation complex. Here PAXX has a similar function, thus creating the redundancy with XLF (**Figure 4C**). Gaps due to incompatible ends can then be filled in by Polymerase Lambda. In line with this redundancy, mouse models showed that PAXX is dispensable for normal development (Gago-Fuentes et al., 2018), but PAXX and XLF double knock-out mice died as embryos (Balmus et al., 2016; Liu et al., 2017; Abramowski et al., 2018). In summary, the role of PAXX in NHEJ fits with the general theme of redundancy.

Another recently identified player in NHEJ is the Modulator of Retroviral Infection (MRI). This small disordered protein interacts with DNA-PKcs, Ku, PAXX, XLF and XRCC4 through its N-terminal domain and with ATM and the MRN complex through its C-terminus (Arnoult et al., 2017; Hung et al., 2018). MRI is thought to stabilize these other proteins on the

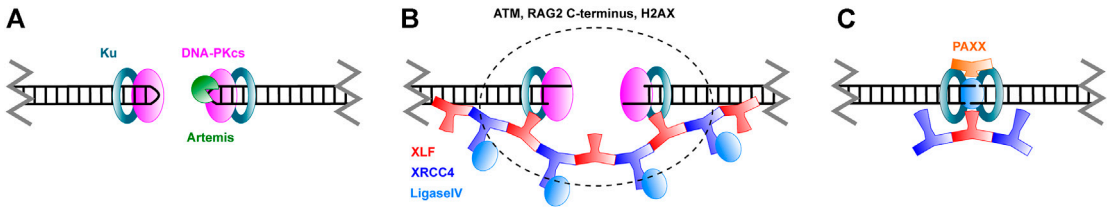

FIGURE 4 | Schematic overview of Non-Homologous End Joining. **(A)** Broken DNA ends are recognized by Ku and DNA-PKcs. Hairpins in coding ends are opened by the Artemis nuclease. **(B)** Ends are brought in close proximity in a process called synapsis. XLF and XRCC4 are thought to form filaments that mediate this process. As discussed in the text, ATM, the RAG2 C-terminus and H2AX also have a role in synapsis. **(C)** Ends are ligated by Ligase IV. PAXX joins in this stage of repair. Please note that, while care was taken to represent the architecture of the complexes as accurately as possible, many structural features still remain unknown.

chromatin around the break site, potentially by forming multimeric structures through its disordered regions (Hung et al., 2018). In mice, MRI deficiency alone does not result in a detectable phenotype. However, *MRI-/- XLF-/-* and *MRI-/- DNA-PKcs-/-* mice show embryonic lethality, while the double knock-out *MRI-/- PAXX-/-* does not result in a severe phenotype (Castaneda-Zegarra et al., 2020). This again indicates a degree of redundancy between different repair factors; the severe phenotype with DNA-PKcs and the milder phenotype with PAXX suggests that the major role of MRI is relatively early in repair, during the synapsis stage.

Interestingly, XLF is also functionally redundant with ATM (Zha et al., 2011a; Xing and Oksenych, 2019). The ATM kinase is an important regulator in NHEJ and the DNA damage response in general (Lee and Paull, 2021). It phosphorylates H2AX, which alters the local chromatin architecture to create a favorable environment for DNA repair processes. XLF also has redundant functions with H2AX directly. Consistent with all of this, the XLF/ATM redundancy only exists in the context of chromatin, and does not occur in assays that utilize extrachromosomal DNA (Zha et al., 2011a). It has been shown that H2AX keeps break sites together (Yin et al., 2009), and is therefore likely to have a role in the synapsis phase of repair, where the redundancy with XLF would then originate. The exact molecular mechanism, however, remains unclear. Rather than interacting directly with the coding and signal ends, phosphorylated H2AX could keep the double-strand breaks together in a confined space by forming a biomolecular condensate in the chromatin. The role of such condensates or repair foci has received a lot of attention recently [reviewed in (Fijen and Rothenberg, 2021)]. As discussed earlier, chromatin remodeling is also a key process in the initiation of recombination. Further research into the role of the chromatin architecture and biomolecular condensates throughout the recombination process could provide an interesting new perspective on the regulation and efficiency of V(D)J recombination.

Clinical Manifestation of V(D)J Recombination Defects

While healthy cells should be able to restrict recombination activity to G1 cell cycle phase, isolating RAG-mediated breaks to prevent off-target repair pathways, the large number of components involved during this mechanism can lead to harmful implications. Various types of immunodeficiency and potential tumorigenesis can be initiated by aberrant translocations and deletions through RAG complex mutation or deficiency.

Immunodeficiency

Deficiency in RAG proteins results in an overall lack of recombination efficiency and diversity, with lower expression leading to a harsher clinical outcome. This deficiency can lead to several phenotypes including severe combined immunodeficiency (SCID), combined immunodeficiency with granulomas or autoimmunity (CID-G/AI) and Omenn Syndrome (OS) (Schwarz et al., 1996; Schuetz et al., 2008). For an extensive analysis of the pathogenesis of these RAG-mediated deficiencies we refer the reader to the recent review from Bosticardo et al. (Bosticardo et al., 2021). SCID, and to the lesser extent CID-G/AI, can cause major vulnerability to minor infections, with current treatment through methods such as bone marrow transplant (Buckley, 2004). Recent large cohort studies for RAG deficiency show occurrence in 12% of SCID cases and 42% of atypical SCID cases (Dvorak et al., 2019). OS patients display a complex pathogenesis with symptoms similar to SCID, except an estimated 90% of cases are due to RAG mutations (Marrella et al., 2011). Over 60 naturally occurring mutations resulting in immunodeficiency have been mapped to just the core regions of RAGs with effects such as destabilized structures between RAGs or other components, decreased DNA binding, and catalytic deficiency (Kim et al., 2015). Two example mutations related to OS, V779M and C328G in RAG1, reduce recombination through different mechanisms, decreased cleavage efficiency and joint formation, respectively (Grazini et al., 2010; Matthews et al., 2015). Lee et al. and Tirosh et al. determined the recombination efficiency of RAG1 and RAG2, respectively, using mutations present in patient samples with varying disease type and severity (Lee et al., 2014; Tirosh et al., 2019). A high density of mutations occur in the NBD and mutations to this region or the heptamer binding motif of RAG1 tend to exhibit significantly lower activity even though the protein is catalytically active (Lee et al., 2014). In RAG2 samples, the overrepresentation occurs in the PHD, affecting histone interaction and the autoinhibitory

mechanism. Various mutations in RAGs may also circumvent the checkpoints related to autoreactivity leading to reduced functional circulating B-cells in addition to the reduced repertoire (Villa and Notarangelo, 2019). As noted in **Figure 3**, interfering with locus contraction leads to decreased antigen receptor diversity and mutations to proteins involved, such as cohesin subunits and Ikaros, have been associated with immune disease (Bjorkman et al., 2018; Kuehn et al., 2021). Recurrence of the same low activity mutations in RAGs or other proteins required for recombination could allow for prediction of disease severity in newly diagnosed patients and potential for personalized medicine for achieving a significant level of recombination based on genotype.

Tumorigenesis

Human lymphomas can involve RAG-mediated deletions or potential translocations between the Ig locus V(D)J segments and non-Ig locus. The main area of concern is the presence of cRSSs which mimic the RSS motif, but exist outside of the antigen receptor loci (Onozawa and Aplan, 2012; Hu et al., 2015; Teng et al., 2015). RAG-mediated cleavage at cRSS sites could be detrimental to cell viability as uncontrolled regions are disturbed. Notch-1, a ligand activator transcription factor which transduces signaling information from the cell surface to the nucleus, contains 14 cRSSs within the 30 kb locus (Mijuskovic et al., 2015). N-terminal truncation caused by cRSS-mediated deletion exhibits constitutive ligand independent intracellular activity. Using ChIP-seq data from Ji et al., RAG2-H3K4me-Notch-1 5' binding and colocalization indicates that RAG-mediated cleavage has a high likelihood of occurring in this region (Onozawa and Aplan, 2012). Multiple sets of cRSSs are also involved in the deletion of Jak1 exons 6–8, leading to activation with multiple roles in cell growth and survival (Mijuskovic et al., 2015). Additional RAG-mediated deletions have occurred at Trat1, Phlda1, Agpat9, CDKN2a/b, Ikaros, and have been attributed to *Tal1-Sil* fusion (Mullighan et al., 2008; Onozawa and Aplan, 2012; Larmonie et al., 2013; Mijuskovic et al., 2015). Even so, a majority of other oncogenic breakpoints detected in lymphomas do not contain cRSS sites and may be due to event at non-B form DNA structures (Raghavan et al., 2004).

Translocation due to off-target RAG-mediated events would be more detrimental to cell viability, but have eluded direct detection in the genome. Translocations themselves are common and likely due to recombination events, but as of July 2019, there have been no documented cases of leukemia and lymphomas which could be traced directly to a RAG-mediated transposition event (Zhang et al., 2017; Smith et al., 2019). Even translocations which involve the antigen receptor loci, such as *Bcl2-IgH* or *BCR-ABL1*, lack substantial evidence of initial RAG-mediated DSBs (Mossadegh-Keller et al., 2021; Yuan et al., 2021). This may be due to a lack of ability to screen for these type of lesions as the limitations of some sequencing methods may overlook certain breakpoint features, however, recent improvements to next generation sequencing and whole genome sequencing will allow for higher discovery rate of these off-target RAG induced breaks (Nordlund et al., 2020; Afkhami et al., 2021; Xiao et al., 2021). The excised signal circle (ESC) complex consisting of the SEs, RAG proteins, and other factors is another source of potential reintegration into the genome (Kirkham et al., 2019). This complex can be extremely dangerous for oncogenic upregulation due to the presence of V region adjacent promoters. More likely are asymmetric cleavage events ("cut and run"), where a closed ESC binds and cleaves at a cRSS before continuing on a series of unchaperoned DNA DSBs. These events have yet to proven *in vivo*, yet acute lymphoblastic leukemia patients have shown oncogenic activation through translocation events, such as *ETV6-RUNX1* gene fusion, which could be facilitated by RAG-mediated 'cut and run' events, however, more research is necessary to understand a direct involvement of RAGs in this type of tumorigenesis (Papaemmanuil et al., 2014; Kirkham et al., 2019). In addition, translocation of the DNA fragment of the ESC complex may not be due to new RAG-mediated cleavage events, but instead insertion at independently formed DSBs, leading to further genomic instability (Antoszewska-Smith et al., 2017; Rommel et al., 2017).

CONCLUDING REMARKS AND OUTLOOK

Historically, focus on V(D)J recombination research has been on the molecular mechanism of single recombination events, while more recently the regulation has gained more attention. Efficient V(D)J recombination is dependent on a tight regulation of locus recognition, DNA cleavage and repair. Here we discussed the latest insights regarding target binding and robustness of the NHEJ pathway, but details of some key processes remain to be established. RAG non-core domains have been only recently studied for their regulatory roles, noted here is the importance of these regions in sub-nuclear localization (PHD), efficient transition to repair (acidic hinge), and maintenance of protein degradation (RING). Additional research will be necessary to further investigate these roles and potential allosteric mechanisms influencing function. We discussed RSS binding and pairing, but Maman et al. determine histone modification itself is not enough for initial recruitment (Maman et al., 2016). Simple 3D diffusion may account for RSS association, however, the choice of a partner RSS may be influenced by several rounds of binding/release during locus contraction. The role of local chromatin architecture and condensate formation has been gaining significant traction lately, with the role of disordered protein domains and long non-coding RNAs being recognized (Fijen and Rothenberg, 2021). We see potential for advanced imaging techniques to resolve the recruitment dynamics and large-scale features of the recombination center and repair foci. We noted here that the repair-associated kinases ATM and DNA-PKcs are required for efficient recombination, but the specific contribution of each and potential redundant roles remain poorly understood. We anticipate that the phosphorylation profile of repair factors has an impact on stability of the recombination complex, joint formation, and repair factor recruitment. Dysregulation of these events have significant influence on off-target breaks or repair deficiency resulting in immunocompromising phenotypes and potential tumorigenesis. Certain mutations and RAG-mediated deletions are implicated in these disease states yet likely direct involvement of RAGs in oncogenic translocations fails to be detected. Extraction of this aberrant joining from the tumor

genome proves challenging, but would be vital for clinical therapeutics and personalized medicine.

AUTHOR CONTRIBUTIONS

SC, CF and ER wrote and edited the manuscript.

FUNDING

Research in the ER lab is supported by the NIH grants 1R35GM134947-01 (to ER), 1R01AI153040-01 (to ER), 1P01CA247773-01/549 (to ER), and V Foundation BRCA Research grants (to ER).

REFERENCES

Abramowski, V., Etienne, O., Elsaid, R., Yang, J., Berland, A., Kermasson, L., et al. (2018). PAXX and Xlf Interplay Revealed by Impaired CNS Development and Immunodeficiency of Double KO Mice. *Cell Death Differ* 25, 444–452. doi:10.1038/cdd.2017.184

Afkhami, M., Ally, F., Pullarkat, V., and Pillai, R. K. (2021). Genetics and Diagnostic Approach to Lymphoblastic Leukemia/Lymphoma. *Cancer Treat. Res.* 181, 17–43. doi:10.1007/978-3-030-78311-2_2

Agrawal, A., and Schatz, D. G. (1997). RAG1 and RAG2 Form a Stable Postcleavage Synaptic Complex with DNA Containing Signal Ends in V(D)J Recombination. *Cell* 89, 43–53. doi:10.1016/s0092-8674(00)80181-6

Antoszewska-Smith, J., Pawlowska, E., and Blasiak, J. (2017). Reactive Oxygen Species in BCR-ABL1-Expressing Cells - Relevance to Chronic Myeloid Leukemia. *Acta Biochim. Pol.* 64, 1–10. doi:10.18388/abp.2016_1396

Arnoult, N., Correia, A., Ma, J., Merlo, A., Garcia-Gomez, S., Maric, M., et al. (2017). Regulation of DNA Repair Pathway Choice in S and G2 Phases by the NHEJ Inhibitor CYREN. *Nature* 549, 548–552. doi:10.1038/nature24023

Ba, Z., Lou, J., Ye, A. Y., Dai, H.-Q., Dring, E. W., Lin, S. G., et al. (2020). CTCF Orchestrates Long-Range Cohesin-Driven V(D)J Recombinational Scanning. *Nature* 586, 305–310. doi:10.1038/s41586-020-2578-0

Bailin, T., Mo, X., and Sadofsky, M. J. (1999). A RAG1 and RAG2 Tetramer Complex Is Active in Cleavage in V(D)J Recombination. *Mol. Cel Biol* 19, 4664–4671. doi:10.1128/mcb.19.7.4664

Balmus, G., Barros, A. C., Wijnhoven, P. W. G., Lescale, C., Hasse, H. L., Boroviak, K., et al. (2016). Synthetic Lethality between PAXX and XLF in Mammalian Development. *Genes Dev.* 30, 2152–2157. doi:10.1101/gad.290510.116

Beilinson, H. A., Glynn, R. A., Yadavalli, A. D., Xiao, J., Corbett, E., Saribasak, H., et al. (2021). The RAG1 N-Terminal Region Regulates the Efficiency and Pathways of Synapsis for V(D)J Recombination. *J. Exp. Med.* 218, e20210250. doi:10.1084/jem.20210250

Bettridge, J., Na, C. H., Pandey, A., and Desiderio, S. (2017). H3K4me3 Induces Allosteric Conformational Changes in the DNA-Binding and Catalytic Regions of the V(D)J Recombinase. *Proc. Natl. Acad. Sci. U.S.A.* 114, 1904–1909. doi:10.1073/pnas.1615727114

Björkman, A., Du, L., Van Der Burg, M., Cormier-Daire, V., Borck, G., Pié, J., et al. (2018). Reduced immunoglobulin gene diversity in patients with Cornelia de Lange syndrome. *J. Allergy Clin. Immunol.* 141, 408–411. doi:10.1016/j.jaci.2017.06.043

Bosticardo, M., Pala, F., and Notarangelo, L. D. (2021). RAG Deficiencies: Recent Advances in Disease Pathogenesis and Novel Therapeutic Approaches. *Eur. J. Immunol.* 51, 1028–1038. doi:10.1002/eji.202048880

Brecht, R. M., Liu, C. C., Beilinson, H. A., Khitun, A., Slavoff, S. A., and Schatz, D. G. (2020). Nucleolar Localization of RAG1 Modulates V(D)J Recombination Activity. *Proc. Natl. Acad. Sci. U.S.A.* 117, 4300–4309. doi:10.1073/pnas.1920021117

Buckley, R. H. (2004). Molecular Defects in Human Severe Combined Immunodeficiency and Approaches to Immune Reconstitution. *Annu. Rev. Immunol.* 22, 625–655. doi:10.1146/annurev.immunol.22.012703.104614

Castañeda-Zegarra, S., Zhang, Q., Alirezaylavasani, A., Fernandez-Berrocal, M., Yao, R., and Oksenych, V. (2020). Leaky Severe Combined Immunodeficiency in Mice Lacking Non-homologous End Joining Factors XLF and MRI. *Aging* 12, 23578–23597. doi:10.18632/aging.202346

Chang, H. H. Y., Pannunzio, N. R., Adachi, N., and Lieber, M. R. (2017). Non-homologous DNA End Joining and Alternative Pathways to Double-Strand Break Repair. *Nat. Rev. Mol. Cel Biol* 18, 495–506. doi:10.1038/nrm.2017.48

Chen, S., Lee, L., Naila, T., Fishbain, S., Wang, A., Tomkinson, A. E., et al. (2021). Structural Basis of Long-Range to Short-Range Synaptic Transition in NHEJ. *Nature* 593, 294–298. doi:10.1038/s41586-021-03458-7

Collins, A. M., and Watson, C. T. (2018). Immunoglobulin Light Chain Gene Rearrangements, Receptor Editing and the Development of a Self-Tolerant Antibody Repertoire. *Front. immunol.* 9. doi:10.3389/fimmu.2018.02249

Conlin, M. P., Reid, D. A., Small, G. W., Chang, H. H., Watanabe, G., Lieber, M. R., et al. (2017). DNA Ligase IV Guides End-Processing Choice during Nonhomologous End Joining. *Cel Rep.* 20, 2810–2819. doi:10.1016/j.celrep.2017.08.091

Corneo, B., Wendland, R. L., Deriano, L., Cui, X., Klein, I. A., Wong, S.-Y., et al. (2007). Rag Mutations Reveal Robust Alternative End Joining. *Nature* 449, 483–486. doi:10.1038/nature06168

Coussens, M. A., Wendland, R. L., Deriano, L., Lindsay, C. R., Arnal, S. M., and Roth, D. B. (2013). RAG2's Acidic Hinge Restricts Repair-Pathway Choice and Promotes Genomic Stability. *Cel Rep.* 4, 870–878. doi:10.1016/j.celrep.2013.07.041

Craxton, A., Munnur, D., Jukes-Jones, R., Skalka, G., Langlais, C., Cain, K., et al. (2018). PAXX and its Paralogs Synergistically Direct DNA Polymerase λ Activity in DNA Repair. *Nat. Commun.* 9, 3877. doi:10.1038/s41467-018-06127-y

Dai, H.-Q., Hu, H., Lou, J., Ye, A. Y., Ba, Z., Zhang, X., et al. (2021). Loop Extrusion Mediates Physiological Igh Locus Contraction for RAG Scanning. *Nature* 590, 338–343. doi:10.1038/s41586-020-03121-7

De Almeida, C. R., Stadhouders, R., De Bruijn, M. J. W., Bergen, I. M., Thongjuea, S., Lenhard, B., et al. (2011). The DNA-Binding Protein CTCF Limits Proximal V Kappa Recombination and Restricts Kappa Enhancer Interactions to the Immunoglobulin Kappa Light Chain Locus. *Immunity* 35, 501–513. doi:10.1016/j.immuni.2011.07.014

Degner, S. C., Verma-Gaur, J., Wong, T. P., Bossen, C., Iverson, G. M., Torkamani, A., et al. (2011). CCCTC-binding Factor (CTCF) and Cohesin Influence the Genomic Architecture of the Igh Locus and Antisense Transcription in Pro-B Cells. *Proc. Natl. Acad. Sci. U.S.A.* 108, 9566–9571. doi:10.1073/pnas.1019391108

Delves, P. J., and Roitt, I. M. (2000). The Immune System. First of Two Parts. *N. Engl. J. Med.* 343, 37–49. doi:10.1056/nejm200007063430107

Dvorak, C. C., Haddad, E., Buckley, R. H., Cowan, M. J., Logan, B., Griffith, L. M., et al. (2019). The Genetic Landscape of Severe Combined Immunodeficiency in the United States and Canada in the Current Era (2010-2018). *J. Allergy Clin. Immunol.* 143, 405–407. doi:10.1016/j.jaci.2018.08.027

Eastman, Q. M., Leu, T. M. J., and Schatz, D. G. (1996). Initiation of V(D)J Recombination *In Vitro* Obeying the 12/23 Rule. *Nature* 380, 85–88. doi:10.1038/380085a0

Ebert, A., Mcmanus, S., Tagoh, H., Medvedovic, J., Salvagiotto, G., Novatchkova, M., et al. (2011). The Distal V(H) Gene Cluster of the Igh Locus Contains Distinct Regulatory Elements with Pax5 Transcription Factor-dependent Activity in Pro-B Cells. *Immunity* 34, 175–187. doi:10.1016/j.immuni.2011.02.005

Fell, V. L., and Schild-Poulter, C. (2015). The Ku Heterodimer: Function in DNA Repair and beyond. *Mutat. Research/Reviews Mutat. Res.* 763, 15–29. doi:10.1016/j.mrrev.2014.06.002

Fijen, C., and Rothenberg, E. (2021). The Evolving Complexity of DNA Damage Foci: RNA, Condensates and Chromatin in DNA Double-Strand Break Repair. *DNA Repair* 105, 11. doi:10.1016/j.dnarep.2021.103170

Fuxa, M., Skok, J., Souabni, A., Salvagiotto, G., Roldan, E., and Busslinger, M. (2004). Pax5 Induces V-To-DJ Rearrangements and Locus Contraction of the Immunoglobulin Heavy-Chain Gene. *Genes Dev.* 18, 411–422. doi:10.1101/gad.291504

Gago-Fuentes, R., Xing, M., Saeterstad, S., Sarno, A., Dewan, A., Beck, C., et al. (2018). Normal Development of Mice Lacking PAXX, the Paralogue of XRCC4 and XLF. *FEBS Open Bio* 8, 426–434. doi:10.1002/2211-5463.12381

Gapud, E. J., Dorsett, Y., Yin, B., Callen, E., Bredemeyer, A., Mahowald, G. K., et al. (2011). Ataxia Telangiectasia Mutated (Atm) and DNA-PKcs Kinases Have Overlapping Activities during Chromosomal Signal Joint Formation. *Proc. Natl. Acad. Sci. U.S.A.* 108, 2022–2027. doi:10.1073/pnas.1013295108

Gapud, E. J., and Sleckman, B. P. (2011). Unique and Redundant Functions of ATM and DNA-PKcs during V(D)J Recombination. *Cell Cycle* 10, 1928–1935. doi:10.4161/cc.10.12.16011

Gigi, V., Lewis, S., Shestova, O., Mijušković, M., Deriano, L., Meng, W., et al. (2014). RAG2 Mutants Alter DSB Repair Pathway Choice *In Vivo* and Illuminate the Nature of 'alternative NHEJ'. *Nucleic Acids Res.* 42, 6352–6364. doi:10.1093/nar/gku295

Graham, T. G. W., Walter, J. C., and Loparo, J. J. (2017). "Ensemble and Single-Molecule Analysis of Non-homologous End Joining in Frog Egg Extracts," in *DNA Repair Enzymes: Cell, Molecular, and Chemical Biology*. Editor B. F. Eichman (San Diego: Elsevier Academic Press Inc). doi:10.1016/bs.mie.2017.03.020

Grazini, U., Zanardi, F., Citterio, E., Casola, S., Goding, C. R., and Mcblane, F. (2010). The RING Domain of RAG1 Ubiquitylates Histone H3: a Novel Activity in Chromatin-Mediated Regulation of V(D)J Joining. *Mol. Cel* 37, 282–293. doi:10.1016/j.molcel.2009.12.035

Grundy, G. J., Yang, W., and Gellert, M. (2010). Autoinhibition of DNA Cleavage Mediated by RAG1 and RAG2 Is Overcome by an Epigenetic Signal in V(D)J Recombination. *Proc. Natl. Acad. Sci. U.S.A.* 107, 22487–22492. doi:10.1073/pnas.1014958107

Guo, C., Yoon, H. S., Franklin, A., Jain, S., Ebert, A., Cheng, H.-L., et al. (2011). CTCF-binding Elements Mediate Control of V(D)J Recombination. *Nature* 477, 424–430. doi:10.1038/nature10495

Hammel, M., Yu, Y., Fang, S., Lees-Miller, S. P., and Tainer, J. A. (2010). XLF Regulates Filament Architecture of the XRCC4·Ligase IV Complex. *Structure* 18, 1431–1442. doi:10.1016/j.str.2010.09.009

Hill, L., Ebert, A., Jaritz, M., Wutz, G., Nagasaka, K., Tagoh, H., et al. (2020). Wapl Repression by Pax5 Promotes V Gene Recombination by Igh Loop Extrusion. *Nature* 584, 142–147. doi:10.1038/s41586-020-2454-y

Hiom, K., and Gellert, M. (1998). Assembly of a 12/23 Paired Signal Complex: A Critical Control point in V(D)J Recombination. *Mol. Cel* 1, 1011–1019. doi:10.1016/s1097-2765(00)80101-x

Hirokawa, S., Chure, G., Belliveau, N. M., Lovely, G. A., Anaya, M., Schatz, D. G., et al. (2020). Sequence-dependent Dynamics of Synthetic and Endogenous RSSs in V(D)J Recombination. *Nucleic Acids Res.* 48, 6726–6739. doi:10.1093/nar/gkaa418

Hu, J., Zhang, Y., Zhao, L., Frock, R. L., Du, Z., Meyers, R. M., et al. (2015). Chromosomal Loop Domains Direct the Recombination of Antigen Receptor Genes. *Cell* 163, 947–959. doi:10.1016/j.cell.2015.10.016

Hung, P. J., Johnson, B., Chen, B.-R., Byrum, A. K., Bredemeyer, A. L., Yewdell, W. T., et al. (2018). MRI Is a DNA Damage Response Adaptor during Classical Non-homologous End Joining. *Mol. Cel* 71, 332–342. doi:10.1016/j.molcel.2018.06.018

Ji, Y., Resch, W., Corbett, E., Yamane, A., Casellas, R., and Schatz, D. G. (2010). The *In Vivo* Pattern of Binding of RAG1 and RAG2 to Antigen Receptor Loci. *Cell* 141, 419–431. doi:10.1016/j.cell.2010.03.010

Jung, D., Giallourakis, C., Mostoslavsky, R., and Alt, F. W. (2006). Mechanism and Control of V(D)J Recombination at the Immunoglobulin Heavy Chain Locus. *Annu. Rev. Immunol.* 24, 541–570. doi:10.1146/annurev.immunol.23.021704.115830

Karim, M. F., Liu, S., Laciak, A. R., Volk, L., Koszelak-Rosenblum, M., Lieber, M. R., et al. (2020). Structural Analysis of the Catalytic Domain of Artemis endonuclease/SNM1C Reveals Distinct Structural Features. *J. Biol. Chem.* 295, 12368–12377. doi:10.1074/jbc.ra120.014136

Kassmeier, M. D., Mondal, K., Palmer, V. L., Raval, P., Kumar, S., Perry, G. A., et al. (2012). VprBP Binds Full-Length RAG1 and Is Required for B-Cell Development and V(D)J Recombination Fidelity. *EMBO J.* 31, 945–958. doi:10.1038/emboj.2011.455

Kim, M.-S., Lapkouski, M., Yang, W., and Gellert, M. (2015). Crystal Structure of the V(D)J Recombinase RAG1-RAG2. *Nature* 518, 507–511. doi:10.1038/nature14174

Kirkham, C. M., Scott, J. N. F., Wang, X., Smith, A. L., Kupinski, A. P., Ford, A. M., et al. (2019). Cut-and-Run: A Distinct Mechanism by Which V(D)J Recombination Causes Genome Instability. *Mol. Cel* 74, 584–597. doi:10.1016/j.molcel.2019.02.025

Kuehn, H. S., Nunes-Santos, C. J., and Rosenzweig, S. D. (2021). Germline IKZF1 Mutations and Their Impact on Immunity: IKAROS-Associated Diseases and Pathophysiology. *Expert Rev. Clin. Immunol.* 17, 407–416. doi:10.1080/1744666x.2021.1901582

Kumar, V., Alt, F. W., and Frock, R. L. (2016). PAXX and XLF DNA Repair Factors Are Functionally Redundant in Joining DNA Breaks in a G1-Arrested Progenitor B-Cell Line. *Proc. Natl. Acad. Sci. U.S.A.* 113, 10619–10624. doi:10.1073/pnas.1611882113

larmonie, N. S. D., dik, w. a., meijerink, J. P. P., homminga, i., van dongen, J. J. M., and langerak, a. W. (2013). Breakpoint Sites Disclose the Role of the V(D)J Recombination Machinery in the Formation of T-Cell Receptor (TCR) and Non-TCR Associated Aberrations in T-Cell Acute Lymphoblastic Leukemia. *Haematologica* 98, 1173–1184. doi:10.3324/haematol.2012.082156

Lee, A. I., Fugmann, S. D., Cowell, L. G., Ptaszek, L. M., Kelsoe, G., and Schatz, D. G. (2003). A Functional Analysis of the Spacer of V(D)J Recombination Signal Sequences. *Plos Biol.* 1, E1. doi:10.1371/journal.pbio.0000001

Lee, G. S., Neiditch, M. B., Salus, S. S., and Roth, D. B. (2004). RAG Proteins Shepherd Double-Strand Breaks to a Specific Pathway, Suppressing Error-Prone Repair, but RAG Nicking Initiates Homologous Recombination. *Cell* 117, 171–184. doi:10.1016/s0092-8674(04)00301-0

Lee, J.-H., and Paull, T. T. (2021). Cellular Functions of the Protein Kinase ATM and Their Relevance to Human Disease. *Nat. Rev. Mol. Cel Biol* 22, 796–814. doi:10.1038/s41580-021-00394-2

Lee, Y. N., Frugoni, F., Dobbs, K., Walter, J. E., Giliani, S., Gennery, A. R., et al. (2014). A Systematic Analysis of Recombination Activity and Genotype-Phenotype Correlation in Human Recombination-Activating Gene 1 Deficiency. *J. Allergy Clin. Immunol.* 133, 1099–1108. doi:10.1016/j.jaci.2013.10.007

Lescale, C., Abramowski, V., Bedora-Faure, M., Murigneux, V., Vera, G., Roth, D. B., et al. (2016a). RAG2 and XLF/Cernunnos Interplay Reveals a Novel Role for the RAG Complex in DNA Repair. *Nat. Commun.* 7, 10529. doi:10.1038/ncomms10529

Lescale, C., and Deriano, L. (2017). The RAG Recombinase: Beyond Breaking. *Mech. Ageing Dev.* 165, 3–9. doi:10.1016/j.mad.2016.11.003

Lescale, C., Lenden Hasse, H., Blackford, A. N., Balmus, G., Bianchi, J. J., Yu, W., et al. (2016b). Specific Roles of XRCC4 Paralogs PAXX and XLF during V(D)J Recombination. *Cel Rep.* 16, 2967–2979. doi:10.1016/j.celrep.2016.08.069

Li, G., Alt, F. W., Cheng, H.-L., Brush, J. W., Goff, P. H., Murphy, M. M., et al. (2008). Lymphocyte-specific Compensation for XLF/cernunnos End-Joining Functions in V(D)J Recombination. *Mol. Cel* 31, 631–640. doi:10.1016/j.molcel.2008.07.017

Liang, Z., Kumar, V., Le Bouteiller, M., Zurita, J., Kenrick, J., Lin, S. G., et al. (2021). Ku70 Suppresses Alternative End Joining in G1-Arrested Progenitor B Cells. *Proc. Natl. Acad. Sci. U S A.* 118, e2103630118. doi:10.1073/pnas.2103630118

Lieber, M. R. (2010). The Mechanism of Double-Strand DNA Break Repair by the Nonhomologous DNA End-Joining Pathway. *Annu. Rev. Biochem.* 79, 181–211. doi:10.1146/annurev.biochem.052308.093131

Lin, W. C., and Desiderio, S. (1994). Cell Cycle Regulation of V(D)J Recombination Activating Protein RAG2. *Proc. Natl. Acad. Sci. U.S.A.* 91, 2733–2737. doi:10.1073/pnas.91.7.2733

Little, A. J., Matthews, A., Oettinger, M., Roth, D. B., and Schatz, D. G. (2015). "Chapter 2-The Mechanism of V(D)J Recombination," in *Molecular Biology of B Cells (Second Edition)*. Editors F. W. Alt, T. Honjo, A. Radbruch, and M. Reth. London: Academic Press.

Liu, L., Chen, X., Li, J., Wang, H., Buehl, C. J., Goff, N. J., et al. (2022). Autophosphorylation Transforms DNA-PK from Protecting to Processing DNA Ends. *Mol. Cel* 82, 177–189. doi:10.1016/j.molcel.2021.11.025

Liu, X., Shao, Z., Jiang, W., Lee, B. J., and Zha, S. (2017). PAXX Promotes KU Accumulation at DNA Breaks and Is Essential for End-Joining in XLF-Deficient Mice. *Nat. Commun.* 8, 13816. doi:10.1038/ncomms13816

Liu, Y., Subrahmanyam, R., Chakraborty, T., Sen, R., and Desiderio, S. (2007). A Plant Homeodomain in Rag-2 that Binds Hypermethylated Lysine 4 of Histone H3 Is Necessary for Efficient Antigen-Receptor-Gene Rearrangement. *Immunity* 27, 561–571. doi:10.1016/j.immuni.2007.09.005

Livak, F., and Schatz, D. G. (1996). T-cell Receptor Alpha Locus V(D)J Recombination By-Products Are Abundant in Thymocytes and Mature T Cells. *Mol. Cel Biol* 16, 609–618. doi:10.1128/mcb.16.2.609

Lovely, G. A., Braikia, F.-Z., Singh, A., Schatz, D. G., Murre, C., Liu, Z., et al. (2020). Direct Observation of RAG Recombinase Recruitment to Chromatin and the IgH Locus in Live Pro-B Cells. *bioRxiv*. doi:10.1101/2020.09.07.286484

Lu, C., Ward, A., Bettridge, J., Liu, Y., and Desiderio, S. (2015). An Autoregulatory Mechanism Imposes Allosteric Control on the V(D)J Recombinase by Histone H3 Methylation. *Cel Rep.* 10, 29–38. doi:10.1016/j.celrep.2014.12.001

Lycke, N., Bemark, M., and Spencer, J. (2015). "Chapter 33 - Mucosal B Cell Differentiation and Regulation," in *Mucosal Immunology*. Fourth Edition. Editors J. Mestecky, W. Strober, M. W. Russell, B. L. Kelsall, H. Cheroutre, and B. N. Lambrecht (Boston: Academic Press).

Ma, Y., Pannicke, U., Schwarz, K., and Lieber, M. R. (2002). Hairpin Opening and Overhang Processing by an Artemis/DNA-dependent Protein Kinase Complex in Nonhomologous End Joining and V(D)J Recombination. *Cell* 108, 781–794. doi:10.1016/s0092-8674(02)00671-2

Mahaney, B. L., Hammel, M., Meek, K., Tainer, J. A., and Lees-Miller, S. P. (2013). XRCC4 and XLF Form Long Helical Protein Filaments Suitable for DNA End protection and Alignment to Facilitate DNA Double Strand Break Repair. *Biochem. Cel Biol.* 91, 31–41. doi:10.1139/bcb-2012-0058

Maman, Y., Teng, G., Seth, R., Kleinstein, S. H., and Schatz, D. G. (2016). RAG1 Targeting in the Genome Is Dominated by Chromatin Interactions Mediated by the Non-core Regions of RAG1 and RAG2. *Nucleic Acids Res.* 44, 9624–9637. doi:10.1093/nar/gkw633

Marrella, V., Maina, V., and Villa, A. (2011). Omenn Syndrome Does Not Live by V(D)J Recombination Alone. *Curr. Opin. Allergy Clin. Immunol.* 11, 525–531. doi:10.1097/aci.0b013e32834c311a

Matthews, A. G. W., Briggs, C. E., Yamanaka, K., Small, T. N., Mooster, J. L., Bonilla, F. A., et al. (2015). Compound Heterozygous Mutation of Rag1 Leading to Omenn Syndrome. *PLoS One* 10, e0121489. doi:10.1371/journal.pone.0121489

Matthews, A. G. W., Kuo, A. J., Ramón-Maiques, S., Han, S., Champagne, K. S., Ivanov, D., et al. (2007). RAG2 PHD finger Couples Histone H3 Lysine 4 Trimethylation with V(D)J Recombination. *Nature* 450, 1106–1110. doi:10.1038/nature06431

Mijušković, M., Chou, Y. F., Gigi, V., Lindsay, C. R., Shestova, O., Lewis, S. M., et al. (2015). Off-Target V(D)J Recombination Drives Lymphomagenesis and Is Escalated by Loss of the Rag2 C Terminus. *Cell Rep* 12, 1842–1852. doi:10.1016/j.celrep.2015.08.034

Mizuta, R., Mizuta, M., Araki, S., and Kitamura, D. (2002). RAG2 Is Down-Regulated by Cytoplasmic Sequestration and Ubiquitin-dependent Degradation. *J. Biol. Chem.* 277, 41423–41427. doi:10.1074/jbc.m206605200

Mossadegh-Keller, N., Brisou, G., Beyou, A., Nadel, B., and Roulland, S. (2021). Human B Lymphomas Reveal Their Secrets through Genetic Mouse Models. *Front. Immunol.* 12, 683597. doi:10.3389/fimmu.2021.683597

Motea, E. A., and Berdis, A. J. (2010). Terminal Deoxynucleotidyl Transferase: The story of a Misguided DNA Polymerase. *Biochim. Biophys. Acta (Bba) - Proteins Proteomics* 1804, 1151–1166. doi:10.1016/j.bbapap.2009.06.030

Mullighan, C. G., Miller, C. B., Radtke, I., Phillips, L. A., Dalton, J., Ma, J., et al. (2008). BCR-ABL1 Lymphoblastic Leukaemia Is Characterized by the Deletion of Ikaros. *Nature* 453, 110–114. doi:10.1038/nature06866

Nick McElhinny, S. A., Snowden, C. M., Mccarville, J., and Ramsden, D. A. (2000). Ku Recruits the XRCC4-Ligase IV Complex to DNA Ends. *Mol. Cel Biol* 20, 2996–3003. doi:10.1128/mcb.20.9.2996-3003.2000

Nordlund, J., Marincevic-Zuniga, Y., Cavelier, L., Raine, A., Martin, T., Lundmark, A., et al. (2020). Refined Detection and Phasing of Structural Aberrations in Pediatric Acute Lymphoblastic Leukemia by Linked-Read Whole-Genome Sequencing. *Sci. Rep.* 10, 2512. doi:10.1038/s41598-020-59214-w

Ochi, T., Blackford, A. N., Coates, J., Jhujh, S., Mehmood, S., Tamura, N., et al. (2015). PAXX, a Paralog of XRCC4 and XLF, Interacts with Ku to Promote DNA Double-Strand Break Repair. *Science* 347, 185–188. doi:10.1126/science.1261971

Onozawa, M., and Aplan, P. D. (2012). Illegitimate V(D)J Recombination Involving Nonantigen Receptor Loci in Lymphoid Malignancy. *Genes Chromosom. Cancer* 51, 525–535. doi:10.1002/gcc.21942

Papaemmanuil, E., Rapado, I., Li, Y., Potter, N. E., Wedge, D. C., Tubio, J., et al. (2014). RAG-mediated Recombination Is the Predominant Driver of Oncogenic Rearrangement in ETV6-RUNX1 Acute Lymphoblastic Leukemia. *Nat. Genet.* 46, 116–125. doi:10.1038/ng.2874

Phillips, J. E., and Corces, V. G. (2009). CTCF: Master Weaver of the Genome. *Cell* 137, 1194–1211. doi:10.1016/j.cell.2009.06.001

Qui, J.-X., Kale, S. B., Schultz, H. Y., and Roth, D. B. (2001). Separation-of-function Mutants Reveal Critical Roles for RAG2 in Both the Cleavage and Joining Steps of V(D)J Recombination. *Mol. Cel* 7, 77–87. doi:10.1016/s1097-2765(01)00156-3

Raghavan, S. C., Swanson, P. C., Wu, X., Hsieh, C. L., and Lieber, M. R. (2004). A Non-B-DNA Structure at the Bcl-2 Major Breakpoint Region Is Cleaved by the RAG Complex. *Nature* 428, 88–93. doi:10.1038/nature02355

Ramsden, D. A., and Gellert, M. (1995). Formation and Resolution of Double-Strand Break Intermediates in V(D)J Rearrangement. *Genes Dev.* 9, 2409–2420. doi:10.1101/gad.9.19.2409

Raval, P., Kriatchko, A. N., Kumar, S., and Swanson, P. C. (2008). Evidence for Ku70/Ku80 Association with Full-Length RAG1. *Nucleic Acids Res.* 36, 2060–2072. doi:10.1093/nar/gkn049

Reid, D. A., Keegan, S., Leo-Macias, A., Watanabe, G., Strande, N. T., Chang, H. H., et al. (2015). Organization and Dynamics of the Nonhomologous End-Joining Machinery during DNA Double-Strand Break Repair. *Proc. Natl. Acad. Sci. U S A.* 112, E2575–E2584. doi:10.1073/pnas.1420115112

Reynaud, D., A Demarco, I., L Reddy, K., Schjerven, H., Bertolino, E., Chen, Z., et al. (2008). Regulation of B Cell Fate Commitment and Immunoglobulin Heavy-Chain Gene Rearrangements by Ikaros. *Nat. Immunol.* 9, 927–936. doi:10.1038/ni.1626

Rodgers, W., Byrum, J. N., Simpson, D. A., Hoolehan, W., and Rodgers, K. K. (2019). RAG2 Localization and Dynamics in the Pre-B Cell Nucleus. *PLoS One* 14, e0216137. doi:10.1371/journal.pone.0216137

Rommel, P. C., Oliveira, T. Y., Nussenzweig, M. C., and Robbiani, D. F. (2017). RAG1/2 Induces Genomic Insertions by Mobilizing DNA into RAG1/2-independent Breaks. *J. Exp. Med.* 214, 815–831. doi:10.1084/jem.20161638

Ropars, V., Drevet, P., Legrand, P., Baconnais, S., Amram, J., Faure, G., et al. (2011). Structural Characterization of Filaments Formed by Human Xrcc4-Cernunnos/XLF Complex Involved in Nonhomologous DNA End-Joining. *Proc. Natl. Acad. Sci. U.S.A.* 108, 12663–12668. doi:10.1073/pnas.1100758108

Roth, D. B., Menetski, J. P., Nakajima, P. B., Bosma, M. J., and Gellert, M. (1992). V(D)J Recombination: Broken DNA Molecules with Covalently Sealed (Hairpin) Coding Ends in Scid Mouse Thymocytes. *Cell* 70, 983–991. doi:10.1016/0092-8674(92)90248-b

Roth, D. B., Zhu, C., and Gellert, M. (1993). Characterization of Broken DNA Molecules Associated with V(D)J Recombination. *Proc. Natl. Acad. Sci. U.S.A.* 90, 10788–10792. doi:10.1073/pnas.90.22.10788

Roy, S., Andres, S. N., Vergnes, A., Neal, J. A., Xu, Y., Yu, Y., et al. (2012). XRCC4's Interaction with XLF Is Required for Coding (But Not Signal) End Joining. *Nucleic Acids Res.* 40, 1684–1694. doi:10.1093/nar/gkr1315

Sallmyr, A., and Tomkinson, A. E. (2018). Repair of DNA Double-Strand Breaks by Mammalian Alternative End-Joining Pathways. *J. Biol. Chem.* 293, 10536–10546. doi:10.1074/jbc.tm117.000375

Schatz, D. G., and Swanson, P. C. (2011). V(D)J Recombination: Mechanisms of Initiation. *Annu. Rev. Genet.* 45, 167–202. doi:10.1146/annurev-genet-110410-132552

Schuetz, C., Huck, K., Gudowius, S., Megahed, M., Feyen, O., Hubner, B., et al. (2008). An Immunodeficiency Disease withRAGMutations and Granulomas. *N. Engl. J. Med.* 358, 2030–2038. doi:10.1056/nejmoa073966

Schultz, H. Y., Landree, M. A., Qiu, J.-X., Kale, S. B., and Roth, D. B. (2001). Joining-deficient RAG1 Mutants Block V(D)J Recombination *In Vivo* and Hairpin Opening *In Vitro*. *Mol. Cel* 7, 65–75. doi:10.1016/s1097-2765(01)00155-1

Schwarz, K., Gauss, G. H., Ludwig, L., Pannicke, U., Li, Z., Lindner, D., et al. (1996). RAG Mutations in Human B Cell-Negative SCID. *Science* 274, 97–99. doi:10.1126/science.274.5284.97

Simkus, C., Makiya, M., and Jones, J. M. (2009). Karyopherin Alpha 1 Is a Putative Substrate of the RAG1 Ubiquitin Ligase. *Mol. Immunol.* 46, 1319–1325. doi:10.1016/j.molimm.2008.11.009

Singh, S. K., and Gellert, M. (2015). Role of RAG1 Autoubiquitination in V(D)J Recombination. *Proc. Natl. Acad. Sci. U.S.A.* 112, 8579–8583. doi:10.1073/pnas.1510464112

Smith, A. L., Scott, J. N. F., and Boyes, J. (2019). The ESC: The Dangerous By-Product of V(D)J Recombination. *Front. Immunol.* 10, 1572. doi:10.3389/fimmu.2019.01572

Talukder, S. R., Dudley, D. D., Alt, F. W., Takahama, Y., and Akamatsu, Y. (2004). Increased Frequency of Aberrant V(D)J Recombination Products in Core RAG-Expressing Mice. *Nucleic Acids Res.* 32, 4539–4549. doi:10.1093/nar/gkh778

Teng, G., Maman, Y., Resch, W., Kim, M., Yamane, A., Qian, J., et al. (2015). RAG Represents a Widespread Threat to the Lymphocyte Genome. *Cell* 162, 751–765. doi:10.1016/j.cell.2015.07.009

Teng, G., and Schatz, D. G. (2015). Regulation and Evolution of the RAG Recombinase. *Adv. Immunol.* 128, 1–39. doi:10.1016/bs.ai.2015.07.002

Tirosh, I., Yamazaki, Y., Frugoni, F., Ververs, F. A., Allenspach, E. J., Zhang, Y., et al. (2019). Recombination Activity of Human Recombination-Activating Gene 2 (RAG2) Mutations and Correlation with Clinical Phenotype. *J. Allergy Clin. Immunol.* 143, 726–735. doi:10.1016/j.jaci.2018.04.027

Verma-Gaur, J., Torkamani, A., Schaffer, L., Head, S. R., Schork, N. J., and Feeney, A. J. (2012). Noncoding Transcription within the Igh Distal V H Region at PAIR Elements Affects the 3D Structure of the Igh Locus in Pro-B Cells. *Proc. Natl. Acad. Sci. U.S.A.* 109, 17004–17009. doi:10.1073/pnas.1208398109

Villa, A., and Notarangelo, L. D. (2019). RAGgene Defects at the Verge of Immunodeficiency and Immune Dysregulation. *Immunol. Rev.* 287, 73–90. doi:10.1111/imr.12713

Wang, X. S., Lee, B. J., and Zha, S. (2020). The Recent Advances in Non-homologous End-Joining through the Lens of Lymphocyte Development. *DNA Repair* 94, 102874. doi:10.1016/j.dnarep.2020.102874

Weintraub, A. S., Li, C. H., Zamudio, A. V., Sigova, A. A., Hannett, N. M., Day, D. S., et al. (2017). YY1 Is a Structural Regulator of Enhancer-Promoter Loops. *Cell* 171, 1573–1588. doi:10.1016/j.cell.2017.11.008

Woloschak, G. E., and Krco, C. J. (1987). Regulation of κ/λ Immunoglobulin Light Chain Expression in normal Murine Lymphocytes. *Mol. Immunol.* 24, 751–757. doi:10.1016/0161-5890(87)90058-7

Wu, C., Dong, Y., Zhao, X., Zhang, P., Zheng, M., Zhang, H., et al. (2017). RAG2 Involves the Igκ Locus Demethylation during B Cell Development. *Mol. Immunol.* 88, 125–134. doi:10.1016/j.molimm.2017.06.026

Xiang, Y., Park, S.-K., and Garrard, W. T. (2013). Vκ Gene Repertoire and Locus Contraction Are Specified by Critical DNase I Hypersensitive Sites within the Vκ-Jκ Intervening Region. *J.I.* 190, 1819–1826. doi:10.4049/jimmunol.1203127

Xiao, W., Ren, L., Chen, Z., Fang, L. T., Zhao, Y., Lack, J., et al. (2021). Toward Best Practice in Cancer Mutation Detection with Whole-Genome and Whole-Exome Sequencing. *Nat. Biotechnol.* 39, 1141–1150. doi:10.1038/s41587-021-00994-5

Xing, M., and Oksenych, V. (2019). Genetic Interaction between DNA Repair Factors PAXX , XLF, XRCC4 and DNA-PKcs in Human Cells. *FEBS Open Bio* 9, 1315–1326. doi:10.1002/2211-5463.12681

Xing, M., Yang, M., Huo, W., Feng, F., Wei, L., Jiang, W., et al. (2015). Interactome Analysis Identifies a New Paralogue of XRCC4 in Non-homologous End Joining DNA Repair Pathway. *Nat. Commun.* 6, 6233. doi:10.1038/ncomms7233

Yin, B., Savic, V., Juntilla, M. M., Bredemeyer, A. L., Yang-Iott, K. S., Helmink, B. A., et al. (2009). Histone H2AX Stabilizes Broken DNA Strands to Suppress Chromosome Breaks and Translocations during V(D)J Recombination. *J. Exp. Med.* 206, 2625–2639. doi:10.1084/jem.20091320

Yosaatmadja, Y., Baddock, H. T., Newman, J. A., Bielinski, M., Gavard, A. E., Mukhopadhyay, S. M. M., et al. (2021). Structural and Mechanistic Insights into the Artemis Endonuclease and Strategies for its Inhibition. *Nucleic Acids Res.* 49, 9310–9326. doi:10.1093/nar/gkab693

Yu, K., Taghva, A., Ma, Y., and Lieber, M. R. (2004). Kinetic Analysis of the Nicking and Hairpin Formation Steps in V(D)J Recombination. *DNA Repair* 3, 67–75. doi:10.1016/j.dnarep.2003.09.006

Yu, W., Lescale, C., Babin, L., Bedora-Faure, M., Lenden-Hasse, H., Baron, L., et al. (2020). Repair of G1 Induced DNA Double-Strand Breaks in S-G2/M by Alternative NHEJ. *Nat. Commun.* 11, 5239. doi:10.1038/s41467-020-19060-w

Yuan, M., Wang, Y., Qin, M., Zhao, X., Chen, X., Li, D., et al. (2021). RAG Enhances BCR-ABL1 -positive Leukemic Cell Growth through its Endonuclease Activity *In Vitro* and *In Vivo*. *Cancer Sci.* 112, 2679–2691. doi:10.1111/cas.14939

Yue, X. Q., Bai, C. J., Xie, D. F., Ma, T., and Zhou, P. K. (2020). DNA-PKcs: A Multi-Faceted Player in DNA Damage Response. *Front. Genet.* 11, 12. doi:10.3389/fgene.2020.607428

Zha, S., Guo, C., Boboila, C., Oksenych, V., Cheng, H.-L., Zhang, Y., et al. (2011a). ATM Damage Response and XLF Repair Factor Are Functionally Redundant in Joining DNA Breaks. *Nature* 469, 250–254. doi:10.1038/nature09604

Zha, S., Jiang, W., Fujiwara, Y., Patel, H., Goff, P. H., Brush, J. W., et al. (2011b). Ataxia Telangiectasia-Mutated Protein and DNA-dependent Protein Kinase Have Complementary V(D)J Recombination Functions. *Proc. Natl. Acad. Sci. U.S.A.* 108, 2028–2033. doi:10.1073/pnas.1019293108

Zhang, L., Reynolds, T. L., Shan, X., and Desiderio, S. (2011). Coupling of V(D)J Recombination to the Cell Cycle Suppresses Genomic Instability and Lymphoid Tumorigenesis. *Immunity* 34, 163–174. doi:10.1016/j.immuni.2011.02.003

Zhang, X., Rastogi, P., Shah, B., and Zhang, L. (2017). B Lymphoblastic Leukemia/lymphoma: New Insights into Genetics, Molecular Aberrations, Subclassification and Targeted Therapy. *Oncotarget* 8, 66728–66741. doi:10.18632/oncotarget.19271

Zhang, Y., Zhang, X., Ba, Z., Liang, Z., Dring, E. W., Hu, H., et al. (2019). The Fundamental Role of Chromatin Loop Extrusion in Physiological V(D)J Recombination. *Nature* 573, 600–604. doi:10.1038/s41586-019-1547-y

Zhang, Y., Zhang, X., Dai, H. Q., Hu, H., and Alt, F. W. (2022). The Role of Chromatin Loop Extrusion in Antibody Diversification. *Nat. Rev. Immunol.* doi:10.1038/s41577-022-00679-3

Zhao, B., Watanabe, G., Morten, M. J., Reid, D. A., Rothenberg, E., and Lieber, M. R. (2019). The Essential Elements for the Noncovalent Association of Two DNA Ends during NHEJ Synapsis. *Nat. Commun.* 10, 3588. doi:10.1038/s41467-019-11507-z

Zhao, B., Rothenberg, E., Ramsden, D. A., and Lieber, M. R. (2020). The Molecular Basis and Disease Relevance of Non-homologous DNA End Joining. *Nat. Rev. Mol. Cel Biol* 21, 765–781. doi:10.1038/s41580-020-00297-8

Zhao, L., Frock, R. L., Du, Z., Hu, J., Chen, L., Krangel, M. S., et al. (2016). Orientation-specific RAG Activity in Chromosomal Loop Domains Contributes to Tcrd V(D)J Recombination during T Cell Development. *J. Exp. Med.* 213, 1921–1936. doi:10.1084/jem.20160670

Conflict of Interest: The authors declare that the research was conducted in the absence of any commercial or financial relationships that could be construed as a potential conflict of interest.

Publisher's Note: All claims expressed in this article are solely those of the authors and do not necessarily represent those of their affiliated organizations, or those of the publisher, the editors and the reviewers. Any product that may be evaluated in this article, or claim that may be made by its manufacturer, is not guaranteed or endorsed by the publisher.

frontiers | Frontiers in Cell and Developmental Biology

REVIEW
published: 17 May 2022
doi: 10.3389/fcell.2022.884873

DNA Damage Response and Repair in Adaptive Immunity

Sha Luo[1,2], *Ruolin Qiao*[1,2] *and Xuefei Zhang*[1]*

[1]*Biomedical Pioneering Innovation Center, Innovation Center for Genomics, Peking University, Beijing, China,* [2]*Academy for Advanced Interdisciplinery Studies, Peking University, Beijing, China*

The diversification of B-cell receptor (BCR), as well as its secreted product, antibody, is a hallmark of adaptive immunity, which has more specific roles in fighting against pathogens. The antibody diversification is from recombination-activating gene (RAG)-initiated V(D)J recombination, activation-induced cytidine deaminase (AID)-initiated class switch recombination (CSR), and V(D)J exon somatic hypermutation (SHM). The proper repair of RAG- and AID-initiated DNA lesions and double-strand breaks (DSBs) is required for promoting antibody diversification, suppressing genomic instability, and oncogenic translocations. DNA damage response (DDR) factors and DSB end-joining factors are recruited to the RAG- and AID-initiated DNA lesions and DSBs to coordinately resolve them for generating productive recombination products during antibody diversification. Recently, cohesin-mediated loop extrusion is proposed to be the underlying mechanism of V(D)J recombination and CSR, which plays essential roles in promoting the orientation-biased deletional end-joining . Here, we will discuss the mechanism of DNA damage repair in antibody diversification.

Keywords: antibody diversification, RAG-initiated V(D)J recombination, AID-initiated CSR and SHM, DNA damage repair, cohesin-mediated loop extrusion

OPEN ACCESS

Edited by:
Teng Ma,
Capital Medical University, China

Reviewed by:
Berit Jungnickel,
Friedrich Schiller University Jena, Germany
Michel Cogne,
University of Rennes 1, France

***Correspondence:**
Xuefei Zhang
xuefei_zhang10@pku.edu.cn

Specialty section:
This article was submitted to Signaling, a section of the journal Frontiers in Cell and Developmental Biology

Received: *27 February 2022*
Accepted: *31 March 2022*
Published: *17 May 2022*

Citation:
Luo S, Qiao R and Zhang X (2022) DNA Damage Response and Repair in Adaptive Immunity. Front. Cell Dev. Biol. 10:884873. doi: 10.3389/fcell.2022.884873

INTRODUCTION

The B-cell receptor (BCR) and antibody comprise two pairs of immunoglobulin heavy (IgH) and light (IgL) chains (Hwang et al., 2015). The N-terminal regions of IgH and IgL are the variable regions, which form the antigen-binding domain of BCR. The C-terminal region of IgH is the constant region that specifies the antibody effector function (**Figure 1A**) (Alt et al., 2013). In developing B cells, V(D)J recombination generates highly diverse antigen receptor repertoires by assembling the numerous IgH germline V_H (variable), D (diversity), and J_H (joining) gene segments in different combinations (**Figure 1B**). Also, IgL variable region exons are subsequently assembled by joining V_L and J_L segments (Ebert et al., 2015; Outters et al., 2015). In a given developing B cell, the unique IgH and IgL chains generate sets of mature B cells that express a highly diverse repertoire of BCR. In peripheral lymphoid organs, mature B cells can be activated by encountering antigens to undergo IgH class switch recombination (CSR) (**Figure 1C**) and V(D)J exon somatic hypermutation (SHM) (**Figure 1D**) to further diversify BCR/antibody affinity and function, enhancing antigen elimination (Methot and Di Noia, 2017; Yeap and Meng, 2019).

The mouse IgH locus spans 2.7 Mb with more than 100 functional V_Hs in the 2.4 Mb distal region, a 100 Kb intervening region, and a 60 Kb region with multiple Ds followed by 4 J_Hs (**Figure 2A**) (Ebert et al., 2015). V(D)J recombination is initiated by the Y-shaped recombination-activating gene (RAG) endonuclease (Liu et al., 2021). RAG is recruited to the V(D)J recombination center (RC), which includes the J_H-proximal DQ52, 4 J_Hs, and the intronic enhancer iEμ (Teng and Schatz, 2015).

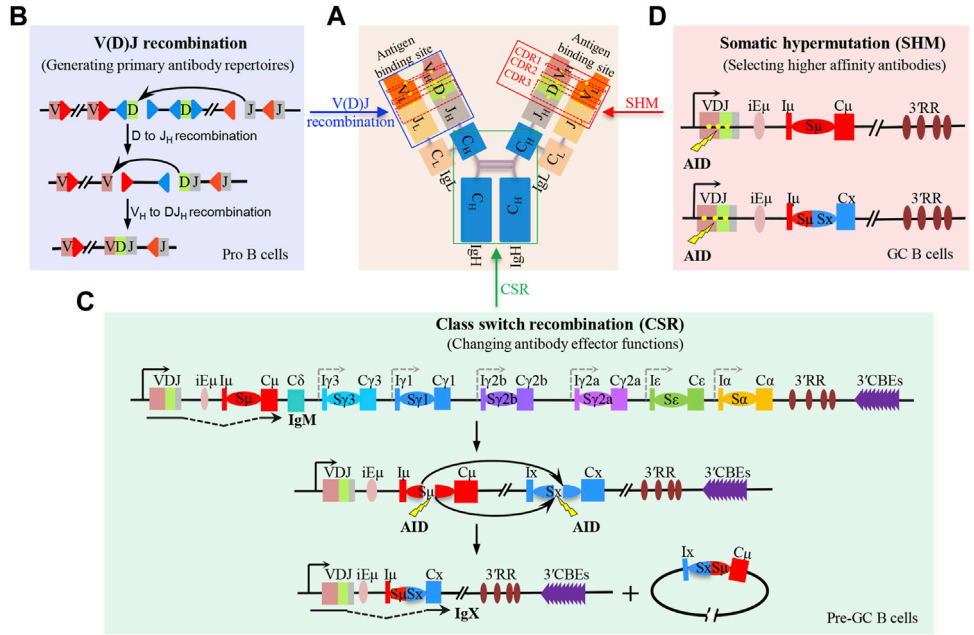

FIGURE 1 | V(D)J recombination, class switch recombination, and V(D)J exon somatic hypermutation-mediated antibody diversification. **(A)** Schematic structure of antibody which is composed of two pairs of immunoglobulin heavy (IgH) and light (IgL) chains. The blue box indicates the antibody variable region which binds to antigens. The green box indicates the antibody constant region, where the class switch recombination occurs. The red box indicates the mutated region including CDR1, CDR2, and CDR3 within the V(D)J exon; the yellow dots indicate the mutation sites. **(B)** Two-step process of RAG-initiated V(D)J recombination in progenitor (pro) B cells. **(C)** Process of AID-initiated class switch recombination (CSR) in mature B cells before entering the germinal center (GC), termed as pre-GC cells. **(D)** Process of AID-initiated V(D)J exon somatic hypermutation (SHM) in non-switched and switched GC B cells.

RAG binds and cleaves the recombination signal sequences (RSSs) (Kim et al., 2015; Ru et al., 2015; Kim et al., 2018; Ru et al., 2018) that flank V_H, D, and J_H gene segments (**Figure 2B**). The two blunt RSS ends are fused by classical non-homologous end-joining (C-NHEJ) directly to generate RSS joins as excision cycles, while the two coding ends are fused by C-NHEJ to generate the coding joins after DNA-PKcs and Artemis-mediated removal of coding end-associated hairpins (**Figures 2C–H**) (Zhao et al., 2020). V(D)J recombination is ordered, with Ds joining to J_Hs, prior to V_Hs joining to DJ_H intermediates to form V(D)J exons (**Figure 1B**) (Alt et al., 2013).

After V(D)J recombination is completed, immature B cells migrate to some peripheral lymphoid organs such as the spleen and further develop to become mature B cells (Nagasawa, 2006). Without stimulation or antigen activation, naïve B cells express the recombined V(D)J exon and its proximal Cμ exons that specify the IgM antibodies. Upon activation, mature B cells undergo CSR to replace the donor Cμ with one of the six sets of constant region exons (C_Hs) that lie 100–200 kb downstream, to change the antibody isotype with different pathogen-elimination functions (**Figure 1C**) (Yeap and Meng, 2019). Each C_H has an inducible (I) promoter exon, long (1–12 kb) repetitive switch (S) region, and several C_H exons (Hwang et al., 2015). Activation-induced cytidine deaminase (AID) (Muramatsu et al., 2000) initiates CSR by generating deamination lesions at frequent short DNA target motifs within donor Sμ, and a downstream acceptor S region (Hwang et al., 2015). The lesions are converted into DNA double-strand breaks (DSBs) by co-opting DNA damage repair factors. The upstream Sμ DSB ends are end-joined to the downstream acceptor S region DSB ends to complete CSR by C-NHEJ and alternative end-joining (A-EJ) (Boboila et al., 2012; Methot and Di Noia, 2017).

The switched and non-switched mature B cells can enter the lymphoid germinal centers (GCs), where they are further matured by introducing somatic hypermutation (SHM) into the V(D)J exons (**Figure 1D**) (Pilzecker and Jacobs, 2019; Roco et al., 2019). In response to antigen activation, AID targets the same deamination motifs in V(D)J exons that are mainly converted into mutational outcomes in GC B cells (Hwang et al., 2015). The mutated V(D)J exons that have higher binding affinity to the antigen are selected and expanded (Lau and Brink, 2020). This SHM process allows cellular selection to promote BCR/antibody affinity maturation.

V(D)J RECOMBINATION

RAG Initiates DNA Breaks for V(D)J Recombination

RAG endonuclease is a Y-shaped heterotetramer, which contains two units of RAG1 catalytic enzymes and two units of RAG2 regulatory co-factors (Kim et al., 2015; Ru et al., 2015; Kim et al., 2018; Ru et al., 2018). Both RAG1 and RAG2 are required for the physiological V(D)J recombination (Schatz et al., 1989; Oettinger

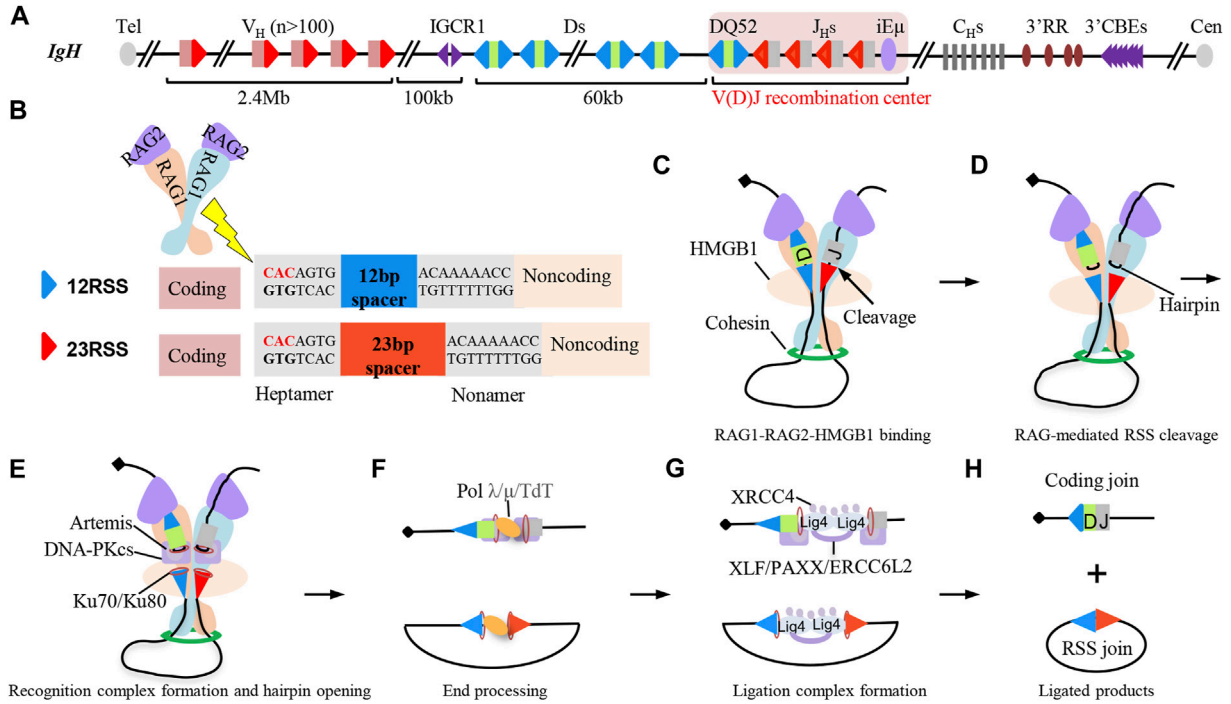

FIGURE 2 | Classical non-homologous end-joining (C-NHEJ) joins RAG-initiated recombination signal sequence (RSS) breaks to complete V(D)J recombination. **(A)** Schematic structure of the IgH locus in mice. There are over one hundred V_H segments, 9–12 D segments, and 4 J_H segments in mouse IgH locus. Each V_H is downstream flanked by 23RSS. Each D is flanked by 12RSS on both sides. Each J_H is upstream flanked by 12RSS. **(B)** Schematic structure of RAG endonuclease, 12RSS (blue triangles), and 23RSS (red triangles). RAG cleaves the heptamer of RSS sequences. **(C–H)** C-NHEJ-mediated end-joining process during D to J_H recombination. RAG and HMGB1 bind to a pair of D and J_H segments for cleavage, and the synapsis of D and J_H segments is promoted by loop extrusion-mediated RAG scanning process **(C)**. RAG cuts the synapsed RSSs associated with the D and J_H segments to generate a pair of blunt RSS ends and a pair of hairpin-associated coding ends **(D)**. Ku70/Ku80 complex binds to the RAG-initiated DSBs and recruits DNA-PKcs-Artemis complex to open the coding end-associated hairpins **(E)**. RAG-initiated breaks can further be processed by DNA polymerase λ/μ and terminal deoxynucleotidyl transferase (TdT) **(F)**. XRCC4 and ligase 4 are recruited to the breaks to ligate the processed DNA breaks, and other redundant C-NHEJ factors including XLF, PAXX, and ERCC6L2 are also involved in the ligation step **(G)**.Final D to J_H recombination products include the coding join and RSS join **(H)**.

et al., 1990). RAG1 has the DNA binding and cleaving activity to cut the heptamer of RSSs to generate blunt RSS ends and hairpin-associated coding ends (**Figures 2B–D**) (McBlane et al., 1995; van Gent et al., 1995; Alt et al., 2013). RAG1 interacts with numerous nucleolar proteins to modulate recombination activity in the nucleus (Brecht et al., 2020), and the N-terminal region of RAG1 regulates the efficiency and pathways of synapsis for V(D)J recombination (Beilinson et al., 2021). RAG2 has no DNA cleavage activity, but it is required to enhance RAG1 catalytic activity. RAG2 binds to DNA by recognizing trimethylation of lysine 4 on histone H3 (H3K4me3), which is a histone marker of active chromatin including promoters and enhancers (Matthews et al., 2007; Teng et al., 2015). The abundance of RAG2 protein is cell cycle-dependent which undergoes ubiquitin-dependent degradation when lymphocytes transit from G1 to the S phase (Li et al., 1996; Teng and Schatz, 2015). Also, RAG2 interacts with RAG1 to abolish RAG1 aggregation to initiate V(D)J recombination during the G1 phase (Brecht et al., 2020; Gan et al., 2021). The regulation of RAG2 promotes RAG-mediated V(D)J recombination in B cells during the G1 phase; meanwhile, it suppresses the generation of undesired DSBs and translocations to ensure the genome stability.

Loop Extrusion-Mediated RAG Scanning Promotes V(D)J Recombination

RAG not only binds the bona fide RSSs flanked by the V, D, and J gene segments for physiological V(D)J recombination but also can capture and cut cryptic targets besides RSSs at a low frequency (Hu et al., 2015), which might lead to translocations related to B- and T-cell lymphoma (Mahowald et al., 2008). RAG can generate robust recombination between Dβ1 and Jβ1-1 when the Dβ1 and Jβ1-1 segments of T-cell receptor β (TCRβ) are inserted into the c-Myc locus (c-Myc-DJβ cassette). Meanwhile, the c-Myc-DJβ cassette insertion activates RAG activity to capture and cut the cryptic targets (convergent-orientated "CAC" motifs) linearly. Interestingly, RAG cryptic targets are restricted to the 1.8 Mb c-Myc domain anchored by CTCF binding elements (CBEs). Also, RAG cryptic activity within a domain also applies to other domains across the genome (Hu et al., 2015). Moreover,

RAG extends its activity to the cryptic targets outside of a domain by deleting the CBE-mediated boundaries (Hu et al., 2015; Zhang Y. et al., 2019). This evidence suggests that RAG scans linearly to capture and cut the convergent-orientated CAC motifs within a domain.

The RAG scanning process can also explain the physiological D to J_H recombination and V_H to DJ_H recombination. The plasmid-based studies indicate that the RSS sequence, not RAG scanning, determines the utilization of D-RSSs (Gauss and Lieber, 1992), while the high-throughput HTGTS-V(D)J-seq analysis of large amounts of D-RSS-inverted *v-Abl* progenitor (pro)-B-cell lines supports that RSS orientation, not the RSS sequence, plays a key role in deletional D to J_H recombination, indicating that RAG scanning promotes the utilization of the downstream D-RSSs during physiological D to J_H recombination (**Figure 2C**) (Zhang Y. et al., 2019). J_H-RSS-bound RAG initiates scanning from RC to the upstream D segments until aligning and cutting one downstream D-RSS with J_H-RSS, leading to the generation of DJ_H recombination products (**Figures 2C–H**) (Zhang Y. et al., 2019). After DJ_H recombination, DJ_H-RSS-bound RAG initiates scanning to the upstream V_H segments and cuts a convergent-orientated V_H-RSS with DJ_H-RSS to complete the V_H to DJ_H recombination, which is supported by the V_H inversion experiments in mice (Hill et al., 2020; Dai et al., 2021). The V_H region inversion eliminates V_H utilization and increases the utilization of newly formed CAC motifs within the inverted region, which strongly supports that RAG scanning promotes the capture of convergent-orientated V_H-RSS in the physiological V_H to DJ_H recombination (Dai et al., 2021).

D to J_H joining occurs within the loop domain anchored upstream by the two divergent CBEs-formed IGCR1 between D and V_H and downstream by the ten tandem CBE-formed super anchor (3′CBEs) (Guo et al., 2011; Alt et al., 2013). V_H to DJ_H recombination needs the neutralization of IGCR1 anchor and V_H-associated CBEs, which allows RAG scanning to the upstream V_Hs (Guo et al., 2011; Alt et al., 2013; Jain et al., 2018). The depletion of CTCF in *v-Abl* pro-B cells increases the utilization of distal V_Hs, indicating that RAG scans through the CBEs after removing CTCF-mediated anchors in *v-Abl* pro-B cells (Ba et al., 2020). Moreover, the depletion of Wapl, a cohesin unloader, in *v-Abl* pro-B cells also increases the utilization of distal V_Hs (Dai et al., 2021), which is consistent with the downregulation of Wapl in normal pro-B cells. It is likely that downregulated Wapl might neutralize CBE-mediated blocks to enhance RAG scanning to the upstream V_Hs, leading to the generation of more diverse antibody repertoires during physiological V(D)J recombination. RAG activity mainly focuses on the targets within the dynamic chromatin impediments including the CTCF-bound chromatin, highly transcribed chromatin, RAG-bound chromatin, and even catalytic-dead Cas9-bound chromatin (Zhang Y. et al., 2019; Zhang et al., 2022). The aforementioned evidence strongly supports that cohesin-mediated loop extrusion is the underlying mechanism of RAG scanning-mediated V(D)J recombination.

DSB Response Factors Have Modest or No Effects on V(D)J Recombination

Intrinsic and extrinsic stress-induced DSBs are the most harmful DNA lesions to genome integrity, which trigger DNA damage response (DDR) by recruiting DDR factors to the DSBs for repairing. ATM and its downstream phosphorylated targets (H2AX, 53BP1, and MDC1) are the key DDR factors, which play crucial roles in repairing general DSBs and maintaining genome stability (Weitering et al., 2021).

RAG-initiated DSBs also recruit DDR factors during V(D)J recombination. ATM and ATM-phosphorylated p53 are recruited to the RAG-initiated DSBs to surveil the intermediates in V(D)J recombination, protecting against the potentially aberrant oncogenic translocations (Perkins et al., 2002). Also, coding joining is decreased with more un-joined coding ends in ATM-deficient pre-B cells, indicating that ATM stabilizes RAG-initiated DSBs during V(D)J recombination (Bredemeyer et al., 2006). 53BP1-deficient mice have relatively normal B-cell compartments and no substantial block in V(D)J recombination (Manis et al., 2004), while 53BP1-deficiency is also found to impair the distal V to DJ joining at the TCRα locus, suggesting a specific role of 53BP1 in maintaining genomic stability during long-range joining of DSBs (Difilippantonio et al., 2008). H2AX is recruited to the RAG-initiated DSBs at the TCRα locus (Chen et al., 2000), while it is not required for coding join formation or lymphocyte development (Bassing et al., 2002), suggesting that it only functions as a general surveillance machinery to prevent translocations during V(D)J recombination (Yin et al., 2009). MDC1-deficiency has no major block for V(D)J recombination or lymphocyte development (Lou et al., 2006). The recently identified shieldin complex, composed of MAD2L2/REV7, SHLD1, SHLD2, and SHLD3, is also dispensable for V(D)J recombination and lymphocyte development (Ghezraoui et al., 2018; Ling et al., 2020). Altogether, DDR factors have relatively modest or no effect on V(D)J recombination, suggesting the redundant roles of these DDR factors with others during V(D)J recombination (more discussion in the next section).

C-NHEJ Exclusively Joins RAG-Initiated Breaks During V(D)J Recombination

Intrinsic and extrinsic stress-induced DSBs are mainly repaired by homologous recombination (HR) and C-NHEJ. HR mainly functions in the late S and G2 phases, which uses sister chromatids as templates for error-free DNA repair. C-NHEJ repairs almost all DSBs outside of S and G2 phases and is the major DSB repair pathway in both dividing and non-dividing cells (Zhao et al., 2020).

RAG-initiated DSBs are exclusively repaired by C-NHEJ, resulting from the synapsis of breaks held by the RAG post-cleavage complex (PCC) (**Figure 2D**) (Teng and Schatz, 2015; Libri et al., 2021). RAG2 truncations or charge-neutralizing mutations switch the DSB repair pathway from C-NHEJ to alternative end-joining (A-EJ) and HR (Corneo et al., 2007; Coussens et al., 2013; Gigi et al., 2014). RAG interacts with the core NHEJ factors Ku70/Ku80 (**Figure 2E**) (Raval et al., 2008), and Ku70 suppresses A-EJ in G1-arrested pro-B cells (Liang et al., 2021). The deficiency of Ku70 has a severe combined immunodeficiency

(SCID) phenotype and severely impairs the formation of coding joins and RSS joins (Gu et al., 1997; Ouyang et al., 1997). The deficiency of Ku80 arrests lymphocyte development at early progenitor stages and induces a profound impairment in V(D)J recombination (Nussenzweig et al., 1996; Zhu et al., 1996). The Ku70/80 complex recruits another two core C-NHEJ factors, namely, XRCC4 and ligase 4, to the DSBs for end joining (**Figure 2G**). XRCC4 is a scaffolding protein to stabilize ligase 4 to form the ligation complex for ligating the DSB ends. XRCC4- or ligase 4-deficient mice die during the late embryonic development, resulting from the p53-dependent apoptosis (Barnes et al., 1998; Frank et al., 1998; Gao et al., 1998). Deleting p53 in XRCC4-deficient or ligase 4-deficient mice rescues the lethality, while has no rescues for the impaired V(D)J recombination and lymphocyte development (Frank et al., 1998; Gao et al., 2000). So the four core C-NHEJ factors are absolutely required for V(D)J recombination.

In addition to the conserved core C-NHEJ factors, there are several other C-NHEJ factors including DNA-PKcs, Artemis, XLF, and PAXX. DNA-PKcs is recruited to the RAG-initiated coding ends (Lieber, 2010) and phosphorylates Artemis to activate its endonuclease activity, leading to the removal of the coding end-associated hairpins (**Figure 2E**) (Ma et al., 2002). Before the DNA-PKcs-Artemis-processed coding ends get joined, DNA polymerases (Polμ, Polλ) and terminal deoxynucleotidyl transferase (TdT)-mediated nucleotide additions can further increase the junction diversity (**Figure 2F**) (Zhao et al., 2020). DNA-PKcs not only play roles in processing coding ends for coding joins, but also functions in RSS joins. The deficiency of DNA-PKcs and DDR factors severely impairs RSS joins, suggesting DNA-PKcs has redundant roles with DDR factors in RSS joins (Gapud et al., 2011; Zha et al., 2011b). In contrast to other C-NHEJ factors, XLF seems to be dispensable for V(D)J recombination as the deficiency of XLF has no measurable impact on V(D)J recombination (Li et al., 2008), while V(D)J recombination is almost abrogated by the deficiency of both XLF and ATM or one of its downstream DDR factors, suggesting functional redundancy of XLF with DDR factors during V(D)J recombination (Zha et al., 2011a; Liu et al., 2012; Oksenych et al., 2012). PAXX, a paralog of XLF, is also dispensable for V(D)J recombination, but the deficiency of both PAXX and XLF almost abrogates V(D)J recombination (Kumar et al., 2016). The new identified ERCC6L2 interacts with other C-NHEJ factors and plays functionally redundant roles with XLF during V(D)J recombination (**Figure 2G**) (Liu et al., 2020). These aforementioned C-NHEJ factors have relatively less influence on V(D)J recombination than the core C-NHEJ factor, resulting from the functional redundancy with DDR factors or other unknown factors.

CLASS SWITCH RECOMBINATION AND SOMATIC HYPERMUTATION

AID-Initiated DNA Lesions for CSR and V(D)J Exon SHM

AID is essential for both CSR and SHM (Muramatsu et al., 2000). As a paralog of the RNA-cytosine deaminase APOBEC family, AID is originally proposed to be an RNA editing enzyme (Muramatsu et al., 1999; Muramatsu et al., 2000), while large amount of evidence supports that AID functions as a DNA deaminase to deaminate deoxycytidine (dC) to deoxyuridine (dU) (Feng et al., 2020). AID preferentially targets the dC in short DGYW (D = A/G/T, Y=C/T, W = A/T) motifs within the V(D)J exons (**Figure 3A**) and S regions (**Figure 4A**) for SHM and CSR, respectively (Rogozin and Diaz, 2004). AID-initiated dU causes the mismatch with deoxyguanine (dG), which can be converted into the point mutation or DSB by base excision repair (BER) and mismatch repair (MMR) during SHM and CSR (**Figures 3C**, **4A**) (Hwang et al., 2015; Methot and Di Noia, 2017).

BER and MMR are two complex DNA repair processes which can function as error-free repair and error-prone repair (**Figures 3B,C**) (Hwang et al., 2015; Methot and Di Noia, 2017). BER repairs the AID-initiated dU from the recognition and excision of dU by UNG. APE cleaves the DNA to generate a nick at the UNG-initiated abasic site. The nick is further processed to generate a gap, which is filled by DNA polymerase β and sealed by DNA ligase 1/3. MMR repairs the AID-initiated dU from the recognition of the mismatch by MSH2/6, which further recruits MLH1 and PMS2. Exo1 excises the DNA sequences adjacent to the mismatch to generate a gap, which is filled by DNA polymerase δ and sealed by DNA ligase 1. Instead of accurate repair by BER and MMR (**Figure 3B**), mutagenic repair frequently occurs after AID-initiated dU during CSR and SHM (**Figures 3C**, **4A**). Recent studies indicate that FAM72a influences the usage of error-prone vs. error-free DNA repair by regulating UNG2 abundance during CSR and SHM (**Figures 3B,C**, **4A**) (Feng et al., 2021; Rogier et al., 2021).

DDR Factors Play Essential Roles for AID-Initiated CSR

DDR factors can also be recruited to the AID-initiated DNA lesions, and these DDR factors are required for CSR as the deficiency of the individual ATM, H2AX, or 53BP1 decreases the CSR frequency (Reina-San-Martin et al., 2003; Lumsden et al., 2004; Manis et al., 2004; Reina-San-Martin et al., 2004; Franco et al., 2006; Reina-San-Martin et al., 2007; Bothmer et al., 2010). 53BP1 and H2AX are the downstream targets of ATM, but 53BP1-deficiency has a much more dramatic effect than that of ATM- or H2AX-deficiency (Dong et al., 2015; Panchakshari et al., 2018). RIF1 is a downstream factor of 53BP1 to inhibit DSB end resection and RIF1-deficiency significantly decreases CSR (Chapman et al., 2013; Di Virgilio et al., 2013). The shieldin complex functions downstream of 53BP1-RIF1 pathway and the deficiency of shieldin components have similar phenotype as that of 53BP1-deficiency (Xu et al., 2015; Dev et al., 2018; Ghezraoui et al., 2018; Gupta et al., 2018; Noordermeer et al., 2018). This 53BP1 pathway can compete with MRN/CtIP activity to protect DNA ends during CSR (Mirman and de Lange, 2020). The deficiency of these DDR factors variably increases the resection of AID-initiated DSBs and increases the utilization of longer microhomology for end joining (Dong et al., 2015; Panchakshari et al., 2018). This evidence indicates that DDR

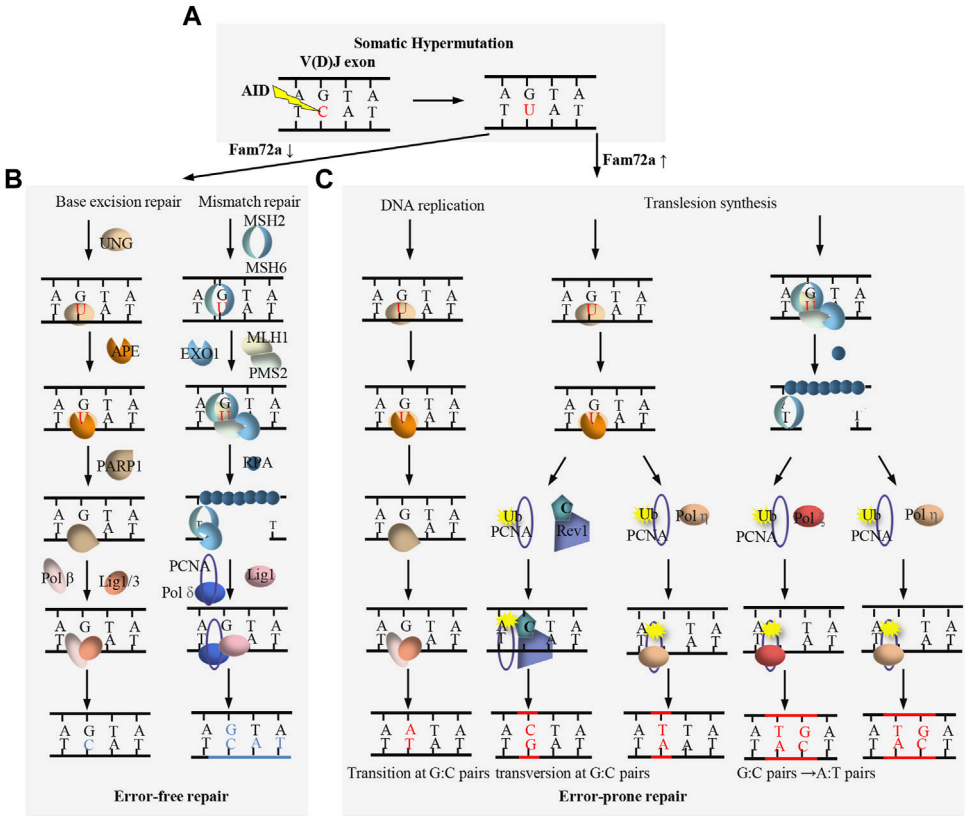

FIGURE 3 | Overview of DNA damage repair process during SHM. **(A)** AID targets the dC to generate dU within V(D)J exon. **(B)** FAM72a downregulation promotes base excision repair (BER)- and mismatch repair (MMR)-mediated error-free DNA repair. **(C)** FAM72a upregulation promotes BER- and MMR-mediated error-prone DNA repair, leading to the mutation of V(D)J exon during SHM.

factors inhibit resection to maintain the integrity of AID-initiated DSBs for the efficient C-NHEJ pathway (**Figure 4B**), while the deficiency of DDR factors switches the end joining from C-NHEJ to the less efficient A-EJ which is prone to use longer microhomology (**Figure 4C**).

End Joining of the AID-Initiated DSBs During CSR

The core C-NHEJ factor deficiency completely abolishes V(D)J recombination and blocks lymphocyte development, while core C-NHEJ factor-deficiency only decreases but not abrogates CSR, suggesting other less efficient end-joining pathways can join the AID-initiated breaks when C-NHEJ is absent during CSR (Yan et al., 2007; Boboila et al., 2012). This less efficient end-joining pathway is identified as A-EJ (Boboila et al., 2012) (**Figure 4C**).

C-NHEJ is the major DSB end-joining pathway during CSR (**Figure 4B**). The deficiency of the individual core C-NHEJ factor, Ku70, Ku80, XRCC4, or ligase 4, impairs CSR (Casellas et al., 1998; Manis et al., 1998; Pan-Hammarstrom et al., 2005; Yan et al., 2007; Han and Yu, 2008; Panchakshari et al., 2018). In addition to the core C-NHEJ factors, DNA-PKcs and Artemis are also necessary for joining AID-initiated DSBs during CSR (Franco et al., 2008). The deficiency of XLF impairs CSR (Zha et al., 2011a), while deficiency of PAXX, a paralog of XLF, has no influence on CSR (Kumar et al., 2016). ERCC6L2 is identified as a new NHEJ factor and ERCC6L2-deficiency impairs CSR. Surprisingly, ERCC6L2 deficiency does not increase the resection of AID-initiated break ends, but it significantly increases the inversional end joining during CSR (Liu et al., 2020). ERCC6L2 regulates the orientation-biased end joining without affecting the DSB end resection *via* an unprecedented mechanism during CSR.

A-EJ is activated when C-NHEJ or DDR factors are absent during CSR (**Figure 4C**). The deficiency of ligase 4 shares some similar features as that of DDR factor deficiency, including the increase of DSB resection, utilization of longer microhomology, and decrease of CSR frequency (Panchakshari et al., 2018). A-EJ is relatively less intelligible than C-NHEJ. PARP1 can respond to DNA damage and bind to the break sites during A-EJ (Wei and Yu, 2016). Then ligase 1 and ligase 3, the key joining factors of the A-EJ pathway, play redundant roles in joining AID-initiated DSBs during CSR (Lu et al., 2016; Masani et al., 2016). Several exonucleases and endonucleases can also enhance DSB resection and promote A-EJ during CSR (Bai et al., 2021; Sun et al., 2021). Further studies are required to figure out the whole picture of the A-EJ pathway in CSR and other physio-pathological processes.

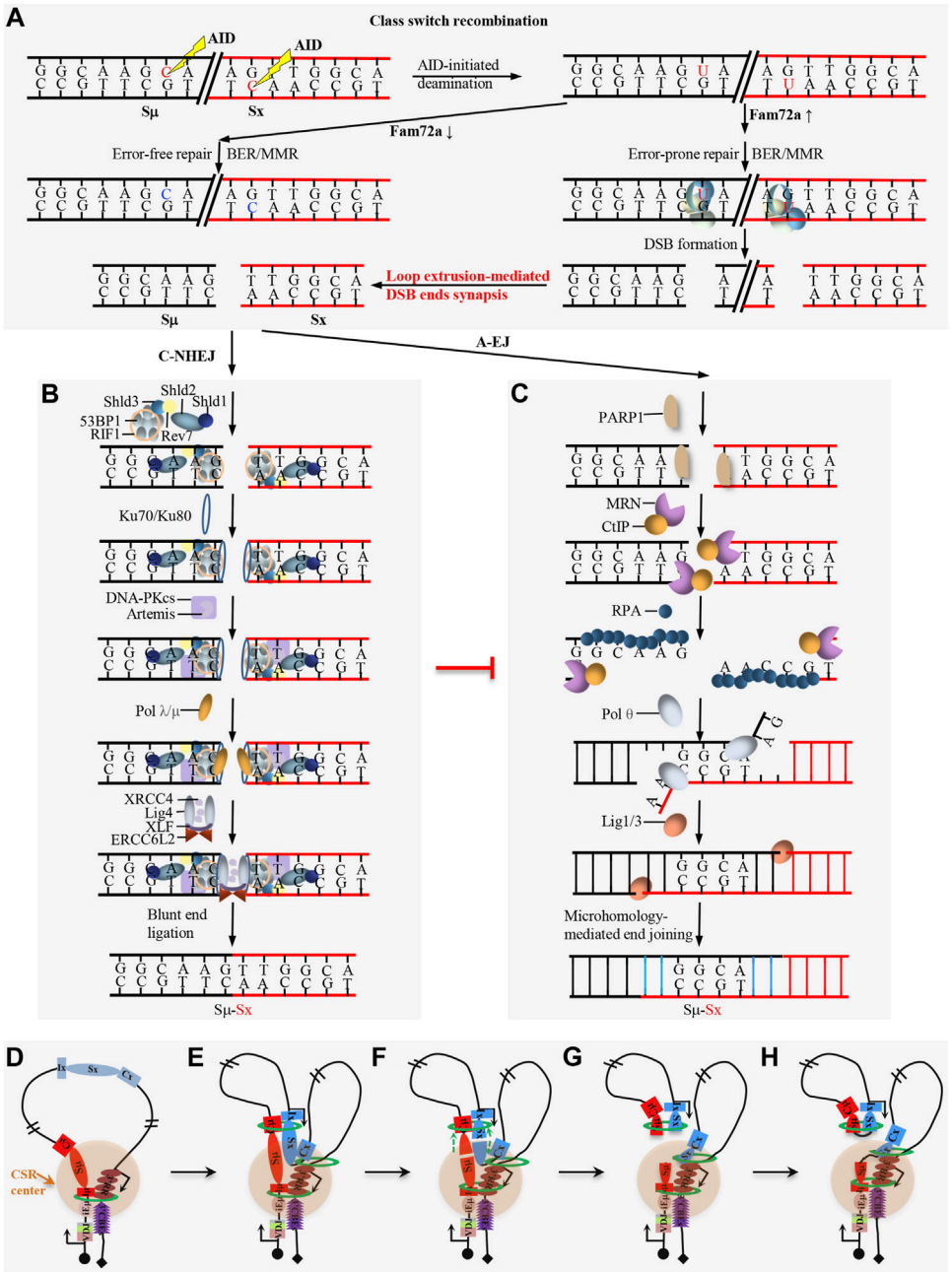

FIGURE 4 | Overview of DNA damage repair process during CSR. **(A)** FAM72a regulates the error-prone vs. error-free DNA repair during AID-initiated CSR. AID-initiated breaks are converted into double-strand breaks (DSBs) upon high level of FAM72a during CSR. **(B)** Overview of the DNA damage response (DDR) factors and C-NHEJ in promoting direct end joining during CSR. **(C)** Overview of the alternative end joining (A-EJ) in promoting DSB end resection and microhomology-mediated end joining during CSR. **(C–H)** Loop extrusion-mediated CSR model. Loop extrusion promotes CSR center formation **(D)**, acceptor S region activation **(E)**, Sμ–Sx synapsis **(F)**, and deletional end joining **(G–H)**.

Loop Extrusion-Mediated CSR

AID-initiated CSR occurs within the ~200 kb constant region of the IgH locus in mature B cells. Chromatin loop extrusion is proposed to be the underlying mechanism of CSR, which promotes the formation of the CSR center, transcriptional activation of acceptor S regions, synapsis of donor Sμ and an activated acceptor S region, and deletional joining of AID-initiated DSBs during CSR (**Figure 4D**) (Zhang X. et al., 2019; Zhang et al., 2021; Zhang et al., 2022). In addition to the physiological CSR process, the loop extrusion-mediated CSR model can also explain some abnormal switching events within the CSR center, including the IgH locus suicide recombination between Sμ and 3′RR (Peron et al., 2012), the ectopic S region switching after CBE insertion in the IgH constant region (Zhang X. et al., 2019) or 3′CBEs deletion (Zhang et al., 2021)

and the Sμ-Sγ3 switching after inserting Sμ, Sγ3, and core 3′RR in the Igκ locus (Le Noir et al., 2021).

In resting B cells, cohesin is loaded onto either the active iEμ-Sμ region or the downstream 3′RR enhancer region to initiate loop extrusion. Cohesin-mediated loop extrusion brings these two active regions, namely, iEμ-Sμ and 3′RR into proximity to form a basal loop, in which the iEμ-Sμ and 3′RR serve as dynamic loop anchors. This basal loop is termed as a dynamic CSR center (Zhang X. et al., 2019). When B cells get activated, loop extrusion brings the primed acceptor S region into the CSR center, where it gets transcriptionally activated by 3′RR. Then, the activated acceptor S region loads cohesin to initiate loop extrusion to bring the donor Sμ into close proximity with the activated acceptor S region, leading to the synapsis of two S regions in the CSR center (Zhang X. et al., 2019).

AID can target different locations of the synapsed donor Sμ and acceptor S region at different times within the CSR center. Once AID initiates a DSB within an S region, the DSB ends will be pulled toward the opposite direction by loop extrusion and stalled by the associated cohesin rings. The two pairs of ends held by cohesin rings will be joined deletionally to generate the productive CSR products (Zhang X. et al., 2019). The disruption of the synapsis structure by inserting CBEs that have a convergent orientation to 3′CBEs between donor Sμ and acceptor Sα significantly increases the inversional joining without influencing DSB end resection, which means that the loop extrusion-mediated perfect synapsis of the donor Sμ and acceptor S region is required for the deletional end-joining during CSR (Zhang X. et al., 2019). Loop extrusion-mediated deletional end-joining is consistent with the cohesin accumulation at DSBs (Kim et al., 2002; Strom et al., 2004). Loop extrusion is also proposed to be the underlying mechanism of DNA damage repair. Loop extrusion-mediated ATM scanning along the chromatin adjacent to the DSB site phosphorylates H2AX until reaching the loop anchor to form DNA damage repair foci (Arnould et al., 2021), which shares some similar features to the loop extrusion-mediated deletional end-joining during CSR (Zhang X. et al., 2019). Loop extrusion might have more general roles in DNA damage repair, DSB end joining, and recombination processes.

The Roles of DDR Factors in AID-Initiated SHM in GC B Cells

Upon activation by antigens, mature B cells can undergo CSR and SHM. CSR occurs prior to the mature B cells entering GC, where the V(D)J exons get mutated (Roco et al., 2019). Unlike the critical roles of DDR factors in CSR, ATM, 53BP1, and H2AX are dispensable for the V(D)J exon SHM. The deficiency of the individual ATM, 53BP1, or H2AX has no effect on the SHM frequency of the V(D)J exon (Reina-San-Martin et al., 2003; Manis et al., 2004; Reina-San-Martin et al., 2004). On the other hand, the checkpoint signaling *via* the ATR/Chk1 axis is downregulated by the transcription factor Bcl-6 in GC B cells, suggesting that negative regulation of the ATR/Chk1 axis is required for efficient SHM *in vivo* (Ranuncolo et al., 2007; Polo et al., 2008; Frankenberger et al., 2014; Bello and Jungnickel, 2021). However, Chk2 has opposite effects to Chk1 in the regulation of SHM. The deficiency of Chk2 decreases the SHM frequency, resulting from the defects of C-NHEJ and increase of the Chk1 activity (Davari et al., 2014). So, the ATR/Chk1/Chk2-mediated checkpoint signaling of the DNA damage response is crucial for the physiological SHM.

CONCLUSION

BCRs and antibodies play vital roles in protecting against antigens. The diversification of BCRs and antibodies from RAG-initiated V(D)J recombination, AID-initiated CSR, and V(D)J exon SHM is crucial for efficient elimination of antigens. However, the mechanisms of these complicated antibody diversification processes are still not well understood. The immunoglobulin genes must be tightly regulated to generate the large amounts of highly efficient antibodies, meanwhile, suppress the generation of undesired translocations or mutations. So, there are still many puzzling questions: how do B cells minimize the off-target effects of RAG and AID during antibody diversification and what are the mechanisms of their specificities? How DNA repair factors/pathways are differentially regulated for the general DNA damage and immunoglobulin gene recombination? Whether cohesin-mediated loop extrusion plays more roles in antibody diversification? Answers to these questions provide not only insights into the understanding of antibody diversification during B-cell development but also the basis for understanding the immune-related diseases. Moreover, the mechanism of antibody diversification has a wide range of applications for drug development of related diseases such as COVID-19 and HIV.

AUTHOR CONTRIBUTIONS

SL and XZ drafted the manuscript and prepared the figures. RQ helped in revising the manuscript.

FUNDING

This work was supported by the Beijing Advanced Innovation Center for Genomics at Peking University.

ACKNOWLEDGMENTS

We are grateful to Frederick W. Alt for his training. We thank Jiazhi Hu, Fei-Long Meng, Junchao Dong, and Li Zhou for reading the article. We thank members of the Zhang Laboratory for careful reading and helpful discussion.

REFERENCES

Alt, F. W., Zhang, Y., Meng, F.-L., Guo, C., and Schwer, B. (2013). Mechanisms of Programmed DNA Lesions and Genomic Instability in the Immune System. *Cell* 152 (3), 417–429. doi:10.1016/j.cell.2013.01.007

Arnould, C., Rocher, V., Finoux, A.-L., Clouaire, T., Li, K., Zhou, F., et al. (2021). Loop Extrusion as a Mechanism for Formation of DNA Damage Repair Foci. *Nature* 590 (7847), 660–665. doi:10.1038/s41586-021-03193-z

Ba, Z., Lou, J., Ye, A. Y., Dai, H.-Q., Dring, E. W., Lin, S. G., et al. (2020). CTCF Orchestrates Long-Range Cohesin-Driven V(D)J Recombinational Scanning. *Nature* 586 (7828), 305–310. doi:10.1038/s41586-020-2578-0

Bai, W., Zhu, G., Xu, J., Chen, P., Meng, F., Xue, H., et al. (2021). The 3′-flap Endonuclease XPF-ERCC1 Promotes Alternative End Joining and Chromosomal Translocation during B Cell Class Switching. *Cel Rep.* 36 (13), 109756. doi:10.1016/j.celrep.2021.109756

Barnes, D. E., Stamp, G., Rosewell, I., Denzel, A., and Lindahl, T. (1998). Targeted Disruption of the Gene Encoding DNA Ligase IV Leads to Lethality in Embryonic Mice. *Curr. Biol.* 8 (25), 1395–1398. doi:10.1016/s0960-9822(98)00021-9

Bassing, C. H., Chua, K. F., Sekiguchi, J., Suh, H., Whitlow, S. R., Fleming, J. C., et al. (2002). Increased Ionizing Radiation Sensitivity and Genomic Instability in the Absence of Histone H2AX. *Proc. Natl. Acad. Sci. U.S.A.* 99 (12), 8173–8178. doi:10.1073/pnas.122228699

Beilinson, H. A., Glynn, R. A., Yadavalli, A. D., Xiao, J., Corbett, E., Saribasak, H., et al. (2021). The RAG1 N-Terminal Region Regulates the Efficiency and Pathways of Synapsis for V(D)J Recombination. *J. Exp. Med.* 218 (10), e20210250. doi:10.1084/jem.20210250

Bello, A., and Jungnickel, B. (2021). Impact of Chk1 Dosage on Somatic Hypermutation *In Vivo*. *Immunol. Cel Biol* 99 (8), 879–893. doi:10.1111/imcb.12480

Boboila, C., Alt, F. W., and Schwer, B. (2012). Classical and Alternative End-Joining Pathways for Repair of Lymphocyte-specific and General DNA Double-Strand Breaks. *Adv. Immunol.* 116, 1–49. doi:10.1016/B978-0-12-394300-2.00001-6

Bothmer, A., Robbiani, D. F., Feldhahn, N., Gazumyan, A., Nussenzweig, A., and Nussenzweig, M. C. (2010). 53BP1 Regulates DNA Resection and the Choice between Classical and Alternative End Joining during Class Switch Recombination. *J. Exp. Med.* 207 (4), 855–865. doi:10.1084/jem.20100244

Brecht, R. M., Liu, C. C., Beilinson, H. A., Khitun, A., Slavoff, S. A., and Schatz, D. G. (2020). Nucleolar Localization of RAG1 Modulates V(D)J Recombination Activity. *Proc. Natl. Acad. Sci. U.S.A.* 117 (8), 4300–4309. doi:10.1073/pnas.1920021117

Bredemeyer, A. L., Sharma, G. G., Huang, C.-Y., Helmink, B. A., Walker, L. M., Khor, K. C., et al. (2006). ATM Stabilizes DNA Double-Strand-Break Complexes during V(D)J Recombination. *Nature* 442 (7101), 466–470. doi:10.1038/nature04866

Casellas, R., Nussenzweig, A., Wuerffel, R., Pelanda, R., Reichlin, A., Suh, H., et al. (1998). Ku80 Is Required for Immunoglobulin Isotype Switching. *EMBO J.* 17 (8), 2404–2411. doi:10.1093/emboj/17.8.2404

Chapman, J. R., Barral, P., Vannier, J.-B., Borel, V., Steger, M., and Tomas-Loba, A. (2013). RIF1 Is Essential for 53BP1-dependent Nonhomologous End Joining and Suppression of DNA Double-Strand Break Resection. *Mol. Cel* 49 (5), 858–871. doi:10.1016/j.molcel.2013.01.002

Chen, H. T., Bhandoola, A., Difilippantonio, M. J., Zhu, J., Brown, M. J., Tai, X., et al. (2000). Response to RAG-Mediated VDJ Cleavage by NBS1 and Gamma-H2ax. *Science* 290 (5498), 1962–1965. doi:10.1126/science.290.5498.1962

Corneo, B., Wendland, R. L., Deriano, L., Cui, X., Klein, I. A., Wong, S. Y., et al. (2007). Rag Mutations Reveal Robust Alternative End Joining. *Nature* 449 (7161), 483–486. doi:10.1038/nature06168

Coussens, M. A., Wendland, R. L., Deriano, L., Lindsay, C. R., Arnal, S. M., and Roth, D. B. (2013). RAG2's Acidic Hinge Restricts Repair-Pathway Choice and Promotes Genomic Stability. *Cell Rep* 4 (5), 870–878. doi:10.1016/j.celrep.2013.07.041

Dai, H. Q., Hu, H., Lou, J., Ye, A. Y., Ba, Z., Zhang, X., et al. (2021). Loop Extrusion Mediates Physiological Igh Locus Contraction for RAG Scanning. *Nature* 590 (7845), 338–343. doi:10.1038/s41586-020-03121-7

Davari, K., Frankenberger, S., Schmidt, A., Tomi, N. S., and Jungnickel, B. (2014). Checkpoint Kinase 2 Is Required for Efficient Immunoglobulin Diversification. *Cell Cycle* 13 (23), 3659–3669. doi:10.4161/15384101.2014.964112

Dev, H., Chiang, T. W., Lescale, C., de Krijger, I., Martin, A. G., Pilger, D., et al. (2018). Shieldin Complex Promotes DNA End-Joining and Counters Homologous Recombination in BRCA1-Null Cells. *Nat. Cel Biol* 20 (8), 954–965. doi:10.1038/s41556-018-0140-1

Di Virgilio, M., Callen, E., Yamane, A., Zhang, W., Jankovic, M., Gitlin, A. D., et al. (2013). Rif1 Prevents Resection of DNA Breaks and Promotes Immunoglobulin Class Switching. *Science* 339 (6120), 711–715. doi:10.1126/science.1230624

Difilippantonio, S., Gapud, E., Wong, N., Huang, C. Y., Mahowald, G., Chen, H. T., et al. (2008). 53BP1 Facilitates Long-Range DNA End-Joining during V(D)J Recombination. *Nature* 456 (7221), 529–533. doi:10.1038/nature07476

Dong, J., Panchakshari, R. A., Zhang, T., Zhang, Y., Hu, J., Volpi, S. A., et al. (2015). Orientation-specific Joining of AID-Initiated DNA Breaks Promotes Antibody Class Switching. *Nature* 525 (7567), 134–139. doi:10.1038/nature14970

Ebert, A., Hill, L., and Busslinger, M. (2015). Spatial Regulation of V-(D)J Recombination at Antigen Receptor Loci. *Adv. Immunol.* 128, 93–121. doi:10.1016/bs.ai.2015.07.006

Feng, Y., Li, C., Stewart, J. A., Barbulescu, P., Seija Desivo, N., Alvarez-Quilon, A., et al. (2021). FAM72A Antagonizes UNG2 to Promote Mutagenic Repair during Antibody Maturation. *Nature* 600 (7888), 324–328. doi:10.1038/s41586-021-04144-4

Feng, Y., Seija, N., Di Noia, J. M., and Martin, A. (2020). AID in Antibody Diversification: There and Back Again. *Trends Immunol.* 41 (7), 586–600. doi:10.1016/j.it.2020.04.009

Franco, S., Gostissa, M., Zha, S., Lombard, D. B., Murphy, M. M., Zarrin, A. A., et al. (2006). H2AX Prevents DNA Breaks from Progressing to Chromosome Breaks and Translocations. *Mol. Cel* 21 (2), 201–214. doi:10.1016/j.molcel.2006.01.005

Franco, S., Murphy, M. M., Li, G., Borjeson, T., Boboila, C., and Alt, F. W. (2008). DNA-PKcs and Artemis Function in the End-Joining Phase of Immunoglobulin Heavy Chain Class Switch Recombination. *J. Exp. Med.* 205 (3), 557–564. doi:10.1084/jem.20080044

Frank, K. M., Sekiguchi, J. M., Seidl, K. J., Swat, W., Rathbun, G. A., Cheng, H. L., et al. (1998). Late Embryonic Lethality and Impaired V(D)J Recombination in Mice Lacking DNA Ligase IV. *Nature* 396 (6707), 173–177. doi:10.1038/24172

Frankenberger, S., Davari, K., Fischer-Burkart, S., Bottcher, K., Tomi, N. S., Zimber-Strobl, U., et al. (2014). Checkpoint Kinase 1 Negatively Regulates Somatic Hypermutation. *Nucleic Acids Res.* 42 (6), 3666–3674. doi:10.1093/nar/gkt1378

Gan, T., Wang, Y., Liu, Y., Schatz, D. G., and Hu, J. (2021). RAG2 Abolishes RAG1 Aggregation to Facilitate V(D)J Recombination. *Cel Rep* 37 (2), 109824. doi:10.1016/j.celrep.2021.109824

Gao, Y., Ferguson, D. O., Xie, W., Manis, J. P., Sekiguchi, J., Frank, K. M., et al. (2000). Interplay of P53 and DNA-Repair Protein XRCC4 in Tumorigenesis, Genomic Stability and Development. *Nature* 404 (6780), 897–900. doi:10.1038/35009138

Gao, Y., Sun, Y., Frank, K. M., Dikkes, P., Fujiwara, Y., Seidl, K. J., et al. (1998). A Critical Role for DNA End-Joining Proteins in Both Lymphogenesis and Neurogenesis. *Cell* 95 (7), 891–902. doi:10.1016/s0092-8674(00)81714-6

Gapud, E. J., Dorsett, Y., Yin, B., Callen, E., Bredemeyer, A., Mahowald, G. K., et al. (2011). Ataxia Telangiectasia Mutated (Atm) and DNA-PKcs Kinases Have Overlapping Activities during Chromosomal Signal Joint Formation. *Proc. Natl. Acad. Sci. U S A.* 108 (5), 2022–2027. doi:10.1073/pnas.1013295108

Gauss, G. H., and Lieber, M. R. (1992). The Basis for the Mechanistic Bias for Deletional over Inversional V(D)J Recombination. *Genes Dev.* 6 (8), 1553–1561. doi:10.1101/gad.6.8.1553

Ghezraoui, H., Oliveira, C., Becker, J. R., Bilham, K., Moralli, D., Anzilotti, C., et al. (2018). 53BP1 Cooperation with the REV7-Shieldin Complex Underpins DNA Structure-specific NHEJ. *Nature* 560 (7716), 122–127. doi:10.1038/s41586-018-0362-1

Gigi, V., Lewis, S., Shestova, O., Mijuskovic, M., Deriano, L., Meng, W., et al. (2014). RAG2 Mutants Alter DSB Repair Pathway Choice *In Vivo* and Illuminate the Nature of 'alternative NHEJ. *Nucleic Acids Res.* 42 (10), 6352–6364. doi:10.1093/nar/gku295

Gu, Y., Seidl, K. J., Rathbun, G. A., Zhu, C., Manis, J. P., van der Stoep, N., et al. (1997). Growth Retardation and Leaky SCID Phenotype of Ku70-Deficient Mice. *Immunity* 7 (5), 653–665. doi:10.1016/s1074-7613(00)80386-6

Guo, C., Yoon, H. S., Franklin, A., Jain, S., Ebert, A., Cheng, H. L., et al. (2011). CTCF-binding Elements Mediate Control of V(D)J Recombination. *Nature* 477 (7365), 424–430. doi:10.1038/nature10495

Gupta, R., Somyajit, K., Narita, T., Maskey, E., Stanlie, A., Kremer, M., et al. (2018). DNA Repair Network Analysis Reveals Shieldin as a Key Regulator of NHEJ and PARP Inhibitor Sensitivity. *Cell* 173 (4), 972–988 e923. doi:10.1016/j.cell.2018.03.050

Han, L., and Yu, K. (2008). Altered Kinetics of Nonhomologous End Joining and Class Switch Recombination in Ligase IV-Deficient B Cells. *J. Exp. Med.* 205 (12), 2745–2753. doi:10.1084/jem.20081623

Hill, L., Ebert, A., Jaritz, M., Wutz, G., Nagasaka, K., Tagoh, H., et al. (2020). Wapl Repression by Pax5 Promotes V Gene Recombination by Igh Loop Extrusion. *Nature* 584 (7819), 142–147. doi:10.1038/s41586-020-2454-y

Hu, J., Meyers, R. M., Dong, J., Panchakshari, R. A., Alt, F. W., and Frock, R. L. (2016). Detecting DNA Double-Stranded Breaks in Mammalian Genomes by Linear Amplification-Mediated High-Throughput Genome-wide Translocation Sequencing. *Nat. Protoc.* 11 (5), 853–871. doi:10.1038/nprot.2016.043

Hu, J., Zhang, Y., Zhao, L., Frock, R. L., Du, Z., Meyers, R. M., et al. (2015). Chromosomal Loop Domains Direct the Recombination of Antigen Receptor Genes. *Cell* 163 (4), 947–959. doi:10.1016/j.cell.2015.10.016

Hwang, J. K., Alt, F. W., and Yeap, L. S. (2015). Related Mechanisms of Antibody Somatic Hypermutation and Class Switch Recombination. *Microbiol. Spectr.* 3 (1), 1. MDNA3-0037-2014. doi:10.1128/microbiolspec.MDNA3-0037-2014

Jain, S., Ba, Z., Zhang, Y., Dai, H. Q., and Alt, F. W. (2018). CTCF-binding Elements Mediate Accessibility of RAG Substrates during Chromatin Scanning. *Cell* 174 (1), 102–116. e114. doi:10.1016/j.cell.2018.04.035

Kim, J. S., Krasieva, T. B., LaMorte, V., Taylor, A. M., and Yokomori, K. (2002). Specific Recruitment of Human Cohesin to Laser-Induced DNA Damage. *J. Biol. Chem.* 277 (47), 45149–45153. doi:10.1074/jbc.M209123200

Kim, M. S., Chuenchor, W., Chen, X., Cui, Y., Zhang, X., Zhou, Z. H., et al. (2018). Cracking the DNA Code for V(D)J Recombination. *Mol. Cel* 70 (2), 358–370. e354. doi:10.1016/j.molcel.2018.03.008

Kim, M. S., Lapkouski, M., Yang, W., and Gellert, M. (2015). Crystal Structure of the V(D)J Recombinase RAG1-RAG2. *Nature* 518 (7540), 507–511. doi:10.1038/nature14174

Kumar, V., Alt, F. W., and Frock, R. L. (2016). PAXX and XLF DNA Repair Factors Are Functionally Redundant in Joining DNA Breaks in a G1-Arrested Progenitor B-Cell Line. *Proc. Natl. Acad. Sci. U S A.* 113 (38), 10619–10624. doi:10.1073/pnas.1611882113

Lau, A. W., and Brink, R. (2020). Selection in the Germinal center. *Curr. Opin. Immunol.* 63, 29–34. doi:10.1016/j.coi.2019.11.001

Le Noir, S., Bonaud, A., Herve, B., Baylet, A., Boyer, F., Lecardeur, S., et al. (2021). IgH 3' Regulatory Region Increases Ectopic Class Switch Recombination. *Plos Genet.* 17 (2), e1009288. doi:10.1371/journal.pgen.1009288

Li, G., Alt, F. W., Cheng, H. L., Brush, J. W., Goff, P. H., Murphy, M. M., et al. (2008). Lymphocyte-specific Compensation for XLF/cernunnos End-Joining Functions in V(D)J Recombination. *Mol. Cel* 31 (5), 631–640. doi:10.1016/j.molcel.2008.07.017

Li, Z., Dordai, D. I., Lee, J., and Desiderio, S. (1996). A Conserved Degradation Signal Regulates RAG-2 Accumulation during Cell Division and Links V(D)J Recombination to the Cell Cycle. *Immunity* 5 (6), 575–589. doi:10.1016/s1074-7613(00)80272-1

Liang, Z., Kumar, V., Le Bouteiller, M., Zurita, J., Kenrick, J., Lin, S. G., et al. (2021). Ku70 Suppresses Alternative End Joining in G1-Arrested Progenitor B Cells. *Proc. Natl. Acad. Sci. U S A.* 118 (21), e2103630118. doi:10.1073/pnas.2103630118

Libri, A., Marton, T., and Deriano, L. (2021). The (Lack of) DNA Double-Strand Break Repair Pathway Choice during V(D)J Recombination. *Front. Genet.* 12, 823943. doi:10.3389/fgene.2021.823943

Lieber, M. R. (2010). The Mechanism of Double-Strand DNA Break Repair by the Nonhomologous DNA End-Joining Pathway. *Annu. Rev. Biochem.* 79, 181–211. doi:10.1146/annurev.biochem.052308.093131

Ling, A. K., Munro, M., Chaudhary, N., Li, C., Berru, M., Wu, B., et al. (2020). SHLD2 Promotes Class Switch Recombination by Preventing Inactivating Deletions within the Igh Locus. *EMBO Rep.* 21 (8), e49823. doi:10.15252/embr.201949823

Liu, C., Zhang, Y., Liu, C. C., and Schatz, D. G. (2021). Structural Insights into the Evolution of the RAG Recombinase. *Nat. Rev. Immunol.* 39 (21), e105857. doi:10.1038/s41577-021-00628-6

Liu, X., Jiang, W., Dubois, R. L., Yamamoto, K., Wolner, Z., and Zha, S. (2012). Overlapping Functions between XLF Repair Protein and 53BP1 DNA Damage Response Factor in End Joining and Lymphocyte Development. *Proc. Natl. Acad. Sci. U S A.* 109 (10), 3903–3908. doi:10.1073/pnas.1120160109

Liu, X., Liu, T., Shang, Y., Dai, P., Zhang, W., Lee, B. J., et al. (2020). ERCC6L2 Promotes DNA Orientation-specific Recombination in Mammalian Cells. *Cell Res* 30 (9), 732–744. doi:10.1038/s41422-020-0328-3

Lou, Z., Minter-Dykhouse, K., Franco, S., Gostissa, M., Rivera, M. A., Celeste, A., et al. (2006). MDC1 Maintains Genomic Stability by Participating in the Amplification of ATM-dependent DNA Damage Signals. *Mol. Cel* 21 (2), 187–200. doi:10.1016/j.molcel.2005.11.025

Lu, G., Duan, J., Shu, S., Wang, X., Gao, L., Guo, J., et al. (2016). Ligase I and Ligase III Mediate the DNA Double-Strand Break Ligation in Alternative End-Joining. *Proc. Natl. Acad. Sci. U S A.* 113 (5), 1256–1260. doi:10.1073/pnas.1521597113

Lumsden, J. M., McCarty, T., Petiniot, L. K., Shen, R., Barlow, C., Wynn, T. A., et al. (2004). Immunoglobulin Class Switch Recombination Is Impaired in Atm-Deficient Mice. *J. Exp. Med.* 200 (9), 1111–1121. doi:10.1084/jem.20041074

Ma, Y., Pannicke, U., Schwarz, K., and Lieber, M. R. (2002). Hairpin Opening and Overhang Processing by an Artemis/DNA-dependent Protein Kinase Complex in Nonhomologous End Joining and V(D)J Recombination. *Cell* 108 (6), 781–794. doi:10.1016/s0092-8674(02)00671-2

Mahowald, G. K., Baron, J. M., and Sleckman, B. P. (2008). Collateral Damage from Antigen Receptor Gene Diversification. *Cell* 135 (6), 1009–1012. doi:10.1016/j.cell.2008.11.024

Manis, J. P., Gu, Y., Lansford, R., Sonoda, E., Ferrini, R., Davidson, L., et al. (1998). Ku70 Is Required for Late B Cell Development and Immunoglobulin Heavy Chain Class Switching. *J. Exp. Med.* 187 (12), 2081–2089. doi:10.1084/jem.187.12.2081

Manis, J. P., Morales, J. C., Xia, Z., Kutok, J. L., Alt, F. W., and Carpenter, P. B. (2004). 53BP1 Links DNA Damage-Response Pathways to Immunoglobulin Heavy Chain Class-Switch Recombination. *Nat. Immunol.* 5 (5), 481–487. doi:10.1038/ni1067

Masani, S., Han, L., Meek, K., and Yu, K. (2016). Redundant Function of DNA Ligase 1 and 3 in Alternative End-Joining during Immunoglobulin Class Switch Recombination. *Proc. Natl. Acad. Sci. U S A.* 113 (5), 1261–1266. doi:10.1073/pnas.1521630113

Matthews, A. G., Kuo, A. J., Ramon-Maiques, S., Han, S., Champagne, K. S., Ivanov, D., et al. (2007). RAG2 PHD finger Couples Histone H3 Lysine 4 Trimethylation with V(D)J Recombination. *Nature* 450 (7172), 1106–1110. doi:10.1038/nature06431

McBlane, J. F., van Gent, D. C., Ramsden, D. A., Romeo, C., Cuomo, C. A., Gellert, M., et al. (1995). Cleavage at a V(D)J Recombination Signal Requires Only RAG1 and RAG2 Proteins and Occurs in Two Steps. *Cell* 83 (3), 387–395. doi:10.1016/0092-8674(95)90116-7

Methot, S. P., and Di Noia, J. M. (2017). Molecular Mechanisms of Somatic Hypermutation and Class Switch Recombination. *Adv. Immunol.* 133, 37–87. doi:10.1016/bs.ai.2016.11.002

Mirman, Z., and de Lange, T. (2020). 53BP1: a DSB Escort. *Genes Dev.* 34 (1-2), 7–23. doi:10.1101/gad.333237.119

Muramatsu, M., Kinoshita, K., Fagarasan, S., Yamada, S., Shinkai, Y., and Honjo, T. (2000). Class Switch Recombination and Hypermutation Require Activation-Induced Cytidine Deaminase (AID), a Potential RNA Editing Enzyme. *Cell* 102 (5), 553–563. doi:10.1016/s0092-8674(00)00078-7

Muramatsu, M., Sankaranand, V. S., Anant, S., Sugai, M., Kinoshita, K., Davidson, N. O., et al. (1999). Specific Expression of Activation-Induced Cytidine Deaminase (AID), a Novel Member of the RNA-Editing Deaminase Family in Germinal center B Cells. *J. Biol. Chem.* 274 (26), 18470–18476. doi:10.1074/jbc.274.26.18470

Nagasawa, T. (2006). Microenvironmental Niches in the Bone Marrow Required for B-Cell Development. *Nat. Rev. Immunol.* 6 (2), 107–116. doi:10.1038/nri1780

Noordermeer, S. M., Adam, S., Setiaputra, D., Barazas, M., Pettitt, S. J., Ling, A. K., et al. (2018). The Shieldin Complex Mediates 53BP1-dependent DNA Repair. *Nature* 560 (7716), 117–121. doi:10.1038/s41586-018-0340-7

Nussenzweig, A., Chen, C., da Costa Soares, V., Sanchez, M., Sokol, K., Nussenzweig, M. C., et al. (1996). Requirement for Ku80 in Growth and Immunoglobulin V(D)J Recombination. *Nature* 382 (6591), 551–555. doi:10.1038/382551a0

Oettinger, M. A., Schatz, D. G., Gorka, C., and Baltimore, D. (1990). RAG-1 and RAG-2, Adjacent Genes that Synergistically Activate V(D)J Recombination. *Science* 248 (4962), 1517–1523. doi:10.1126/science.2360047

Oksenych, V., Alt, F. W., Kumar, V., Schwer, B., Wesemann, D. R., Hansen, E., et al. (2012). Functional Redundancy between Repair Factor XLF and Damage Response Mediator 53BP1 in V(D)J Recombination and DNA Repair. *Proc. Natl. Acad. Sci. U S A.* 109 (7), 2455–2460. doi:10.1073/pnas.1121458109

Outters, P., Jaeger, S., Zaarour, N., and Ferrier, P. (2015). Long-Range Control of V(D)J Recombination & Allelic Exclusion: Modeling Views. *Adv. Immunol.* 128, 363–413. doi:10.1016/bs.ai.2015.08.002

Ouyang, H., Nussenzweig, A., Kurimasa, A., Soares, V. C., Li, X., Cordon-Cardo, C., et al. (1997). Ku70 Is Required for DNA Repair but Not for T Cell Antigen Receptor Gene Recombination *In Vivo*. *J. Exp. Med.* 186 (6), 921–929. doi:10.1084/jem.186.6.921

Pan-Hammarstrom, Q., Jones, A. M., Lahdesmaki, A., Zhou, W., Gatti, R. A., Hammarstrom, L., et al. (2005). Impact of DNA Ligase IV on Nonhomologous End Joining Pathways during Class Switch Recombination in Human Cells. *J. Exp. Med.* 201 (2), 189–194. doi:10.1084/jem.20040772

Panchakshari, R. A., Zhang, X., Kumar, V., Du, Z., Wei, P. C., Kao, J., et al. (2018). DNA Double-Strand Break Response Factors Influence End-Joining Features of IgH Class Switch and General Translocation Junctions. *Proc. Natl. Acad. Sci. U S A.* 115 (4), 762–767. doi:10.1073/pnas.1719988115

Perkins, E. J., Nair, A., Cowley, D. O., Van Dyke, T., Chang, Y., and Ramsden, D. A. (2002). Sensing of Intermediates in V(D)J Recombination by ATM. *Genes Dev.* 16 (2), 159–164. doi:10.1101/gad.956902

Peron, S., Laffleur, B., Denis-Lagache, N., Cook-Moreau, J., Tinguely, A., Delpy, L., et al. (2012). AID-driven Deletion Causes Immunoglobulin Heavy Chain Locus Suicide Recombination in B Cells. *Science* 336 (6083), 931–934. doi:10.1126/science.1218692

Pilzecker, B., and Jacobs, H. (2019). Mutating for Good: DNA Damage Responses during Somatic Hypermutation. *Front. Immunol.* 10, 438. doi:10.3389/fimmu.2019.00438

Polo, J. M., Ci, W., Licht, J. D., and Melnick, A. (2008). Reversible Disruption of BCL6 Repression Complexes by CD40 Signaling in normal and Malignant B Cells. *Blood* 112 (3), 644–651. doi:10.1182/blood-2008-01-131813

Ranuncolo, S. M., Polo, J. M., Dierov, J., Singer, M., Kuo, T., Greally, J., et al. (2007). Bcl-6 Mediates the Germinal center B Cell Phenotype and Lymphomagenesis through Transcriptional Repression of the DNA-Damage Sensor ATR. *Nat. Immunol.* 8 (7), 705–714. doi:10.1038/ni1478

Raval, P., Kriatchko, A. N., Kumar, S., and Swanson, P. C. (2008). Evidence for Ku70/Ku80 Association with Full-Length RAG1. *Nucleic Acids Res.* 36 (6), 2060–2072. doi:10.1093/nar/gkn049

Reina-San-Martin, B., Chen, H. T., Nussenzweig, A., and Nussenzweig, M. C. (2004). ATM Is Required for Efficient Recombination between Immunoglobulin Switch Regions. *J. Exp. Med.* 200 (9), 1103–1110. doi:10.1084/jem.20041162

Reina-San-Martin, B., Chen, J., Nussenzweig, A., and Nussenzweig, M. C. (2007). Enhanced Intra-switch Region Recombination during Immunoglobulin Class Switch Recombination in 53BP1-/- B Cells. *Eur. J. Immunol.* 37 (1), 235–239. doi:10.1002/eji.200636789

Reina-San-Martin, B., Difilippantonio, S., Hanitsch, L., Masilamani, R. F., Nussenzweig, A., and Nussenzweig, M. C. (2003). H2AX Is Required for Recombination between Immunoglobulin Switch Regions but Not for Intra-switch Region Recombination or Somatic Hypermutation. *J. Exp. Med.* 197 (12), 1767–1778. doi:10.1084/jem.20030569

Roco, J. A., Mesin, L., Binder, S. C., Nefzger, C., Gonzalez-Figueroa, P., Canete, P. F., et al. (2019). Class-Switch Recombination Occurs Infrequently in Germinal Centers. *Immunity* 51 (2), 337–350. e337. doi:10.1016/j.immuni.2019.07.001

Rogier, M., Moritz, J., Robert, I., Lescale, C., Heyer, V., Abello, A., et al. (2021). Fam72a Enforces Error-Prone DNA Repair during Antibody Diversification. *Nature* 600 (7888), 329–333. doi:10.1038/s41586-021-04093-y

Rogozin, I. B., and Diaz, M. (2004). Cutting Edge: DGYW/WRCH Is a Better Predictor of Mutability at G:C Bases in Ig Hypermutation Than the Widely Accepted RGYW/WRCY Motif and Probably Reflects a Two-step Activation-Induced Cytidine Deaminase-Triggered Process. *J. Immunol.* 172 (6), 3382–3384. doi:10.4049/jimmunol.172.6.3382

Ru, H., Chambers, M. G., Fu, T. M., Tong, A. B., Liao, M., and Wu, H. (2015). Molecular Mechanism of V(D)J Recombination from Synaptic RAG1-RAG2 Complex Structures. *Cell* 163 (5), 1138–1152. doi:10.1016/j.cell.2015.10.055

Ru, H., Mi, W., Zhang, P., Alt, F. W., Schatz, D. G., Liao, M., et al. (2018). DNA Melting Initiates the RAG Catalytic Pathway. *Nat. Struct. Mol. Biol.* 25 (8), 732–742. doi:10.1038/s41594-018-0098-5

Schatz, D. G., Oettinger, M. A., and Baltimore, D. (1989). The V(D)J Recombination Activating Gene, RAG-1. *Cell* 59 (6), 1035–1048. doi:10.1016/0092-8674(89)90760-5

Strom, L., Lindroos, H. B., Shirahige, K., and Sjogren, C. (2004). Postreplicative Recruitment of Cohesin to Double-Strand Breaks Is Required for DNA Repair. *Mol. Cel* 16 (6), 1003–1015. doi:10.1016/j.molcel.2004.11.026

Sun, X., Bai, J., Xu, J., Xi, X., Gu, M., Zhu, C., et al. (2021). Multiple DSB Resection Activities Redundantly Promote Alternative End Joining-Mediated Class Switch Recombination. *Front Cel Dev Biol* 9, 767624. doi:10.3389/fcell.2021.767624

Teng, G., Maman, Y., Resch, W., Kim, M., Yamane, A., Qian, J., et al. (2015). RAG Represents a Widespread Threat to the Lymphocyte Genome. *Cell* 162 (4), 751–765. doi:10.1016/j.cell.2015.07.009

Teng, G., and Schatz, D. G. (2015). Regulation and Evolution of the RAG Recombinase. *Adv. Immunol.* 128, 1–39. doi:10.1016/bs.ai.2015.07.002

van Gent, D. C., McBlane, J. F., Ramsden, D. A., Sadofsky, M. J., Hesse, J. E., and Gellert, M. (1995). Initiation of V(D)J Recombination in a Cell-free System. *Cell* 81 (6), 925–934. doi:10.1016/0092-8674(95)90012-8

Wei, H., and Yu, X. (2016). Functions of PARylation in DNA Damage Repair Pathways. *Genomics Proteomics Bioinformatics* 14 (3), 131–139. doi:10.1016/j.gpb.2016.05.001

Weitering, T. J., Takada, S., Weemaes, C. M. R., van Schouwenburg, P. A., and van der Burg, M. (2021). ATM: Translating the DNA Damage Response to Adaptive Immunity. *Trends Immunol.* 42 (4), 350–365. doi:10.1016/j.it.2021.02.001

Xu, G., Chapman, J. R., Brandsma, I., Yuan, J., Mistrik, M., Bouwman, P., et al. (2015). REV7 Counteracts DNA Double-Strand Break Resection and Affects PARP Inhibition. *Nature* 521 (7553), 541–544. doi:10.1038/nature14328

Yan, C. T., Boboila, C., Souza, E. K., Franco, S., Hickernell, T. R., Murphy, M., et al. (2007). IgH Class Switching and Translocations Use a Robust Non-classical End-Joining Pathway. *Nature* 449 (7161), 478–482. doi:10.1038/nature06020

Yeap, L. S., and Meng, F. L. (2019). Cis- and Trans-factors Affecting AID Targeting and Mutagenic Outcomes in Antibody Diversification. *Adv. Immunol.* 141, 51–103. doi:10.1016/bs.ai.2019.01.002

Yin, B., Savic, V., Juntilla, M. M., Bredemeyer, A. L., Yang-Iott, K. S., Helmink, B. A., et al. (2009). Histone H2AX Stabilizes Broken DNA Strands to Suppress Chromosome Breaks and Translocations during V(D)J Recombination. *J. Exp. Med.* 206 (12), 2625–2639. doi:10.1084/jem.20091320

Zha, S., Guo, C., Boboila, C., Oksenych, V., Cheng, H. L., Zhang, Y., et al. (2011a). ATM Damage Response and XLF Repair Factor Are Functionally Redundant in Joining DNA Breaks. *Nature* 469 (7329), 250–254. doi:10.1038/nature09604

Zha, S., Jiang, W., Fujiwara, Y., Patel, H., Goff, P. H., Brush, J. W., et al. (2011b). Ataxia Telangiectasia-Mutated Protein and DNA-dependent Protein Kinase Have Complementary V(D)J Recombination Functions. *Proc. Natl. Acad. Sci. U S A.* 108 (5), 2028–2033. doi:10.1073/pnas.1019293108

Zhang, X., Yoon, H. S., Chapdelaine-Williams, A. M., Kyritsis, N., and Alt, F. W. (2021). Physiological Role of the 3'IgH CBEs Super-anchor in Antibody Class Switching. *Proc. Natl. Acad. Sci. U S A.* 118 (3). doi:10.1073/pnas.2024392118

Zhang, X., Zhang, Y., Ba, Z., Kyritsis, N., Casellas, R., and Alt, F. W. (2019a). Fundamental Roles of Chromatin Loop Extrusion in Antibody Class Switching. *Nature* 575 (7782), 385–389. doi:10.1038/s41586-019-1723-0

Zhang, Y., Zhang, X., Ba, Z., Liang, Z., Dring, E. W., Hu, H., et al. (2019b). The Fundamental Role of Chromatin Loop Extrusion in Physiological V(D)J Recombination. *Nature* 573 (7775), 600–604. doi:10.1038/s41586-019-1547-y

Zhang, Y., Zhang, X., Dai, H. Q., Hu, H., and Alt, F. W. (2022). The Role of Chromatin Loop Extrusion in Antibody Diversification. *Nat. Rev. Immunol.* 1, 1. doi:10.1038/s41577-022-00679-3

Zhao, B., Rothenberg, E., Ramsden, D. A., and Lieber, M. R. (2020). The Molecular Basis and Disease Relevance of Non-homologous DNA End Joining. *Nat. Rev. Mol. Cel Biol* 21 (12), 765–781. doi:10.1038/s41580-020-00297-8

Zhu, C., Bogue, M. A., Lim, D. S., Hasty, P., and Roth, D. B. (1996). Ku86-deficient Mice Exhibit Severe Combined Immunodeficiency and Defective Processing of V(D)J Recombination Intermediates. *Cell* 86 (3), 379–389. doi:10.1016/s0092-8674(00)80111-7

Conflict of Interest: The authors declare that the research was conducted in the absence of any commercial or financial relationships that could be construed as a potential conflict of interest.

Publisher's Note: All claims expressed in this article are solely those of the authors and do not necessarily represent those of their affiliated organizations, or those of the publisher, the editors, and the reviewers. Any product that may be evaluated in this article, or claim that may be made by its manufacturer, is not guaranteed or endorsed by the publisher.

frontiers | Frontiers in Cell and Developmental Biology

REVIEW
published: 26 May 2022
doi: 10.3389/fcell.2022.885537

The Oxidative Damage and Inflammation Mechanisms in GERD-Induced Barrett's Esophagus

Deqiang Han[1,2] *and Chao Zhang*[1]*

[1]Department of General Surgery, National Clinical Research Center for Geriatric Diseases, Xuanwu Hospital of Capital Medical University, Beijing, China, [2]Cell Therapy Center, Beijing Institute of Geriatrics, Xuanwu Hospital Capital Medical University, National Clinical Research Center for Geriatric Diseases, Beijing, China

Barrett's esophagus is a major complication of gastro-esophageal reflux disease and an important precursor lesion for the development of Barrett's metaplasia and esophageal adenocarcinoma. However, the cellular and molecular mechanisms of Barrett's metaplasia remain unclear. Inflammation-associated oxidative DNA damage could contribute to Barrett's esophagus. It has been demonstrated that poly(ADP-ribose) polymerases (PARPs)-associated with ADP-ribosylation plays an important role in DNA damage and inflammatory response. A previous study indicated that there is inflammatory infiltration and oxidative DNA damage in the lower esophagus due to acid/bile reflux, and gastric acid could induce DNA damage in culture esophageal cells. This review will discuss the mechanisms of Barrett's metaplasia and adenocarcinoma underlying oxidative DNA damage in gastro-esophageal reflux disease patients based on recent clinical and basic findings.

Keywords: Barrett's esophagus, DNA damage, transdifferentiation, polyADP-ribose polymerase 1, NF-kappa B

OPEN ACCESS

Edited by:
Weihua Zhou,
University of Michigan, United States

Reviewed by:
Qiang Chen,
Wuhan University, China
Zhifei Wang,
Zhejiang Provincial People's Hospital, China

***Correspondence:**
Chao Zhang
ghostzhang35@qq.com

Specialty section:
This article was submitted to Signaling, a section of the journal Frontiers in Cell and Developmental Biology

Received: *28 February 2022*
Accepted: *13 April 2022*
Published: *26 May 2022*

Citation:
Han D and Zhang C (2022) The Oxidative Damage and Inflammation Mechanisms in GERD-Induced Barrett's Esophagus. Front. Cell Dev. Biol. 10:885537. doi: 10.3389/fcell.2022.885537

INTRODUCTION

Barrett's esophagus (BE) most commonly arises from gastro-esophageal reflux disease (GERD), which is defined as the retrograde flow of gastric and (or) duodenal contents into the esophagus, inducing discomfort symptoms and (or) esophageal mucosal pathological lesions. The incidence rate of GERD varies from 10 to 20% in the Eastern and Western countries (El- Serag et al., 2014; Amadi et al., 2017; Maslyonkina et al., 2021; Mittal et al., 2021). Indeed, it is one of the most prevalent gastrointestinal functional disorders worldwide. Heartburn and regurgitation are the typical symptoms of GERD and the number of atypical manifests is estimated over 100, including non-cardiac chest pain, bronchial-pulmonary or ear, nose, and throat symptoms, and dental erosion. The understanding of the cellular and molecular mechanisms by which this metaplastic transformation occurs remains limited. Histological proof of BE is currently considered objective evidence of GERD, which is a common pre-malignant condition characterized by the replacement of the normal squamous epithelium by a metaplastic columnar-lined epithelium extending to the gastro-oesophageal junction (Barrett, 1950; McDonald et al., 2015). GERD is a chronic inflammation of the esophagus stimulated by repeated acid/bile acids. Chronic inflammation is likely to carry an increased risk of cancer via oxidative damage pathways (Farinati et al., 2010). Therefore, both GERD-induced reactive oxygen species (ROS) accumulation and chronic inflammatory infiltration are associated with BE formation. This review mainly focuses on the oxidative damage, inflammation mechanisms, and the reparative response in GERD-induced BE.

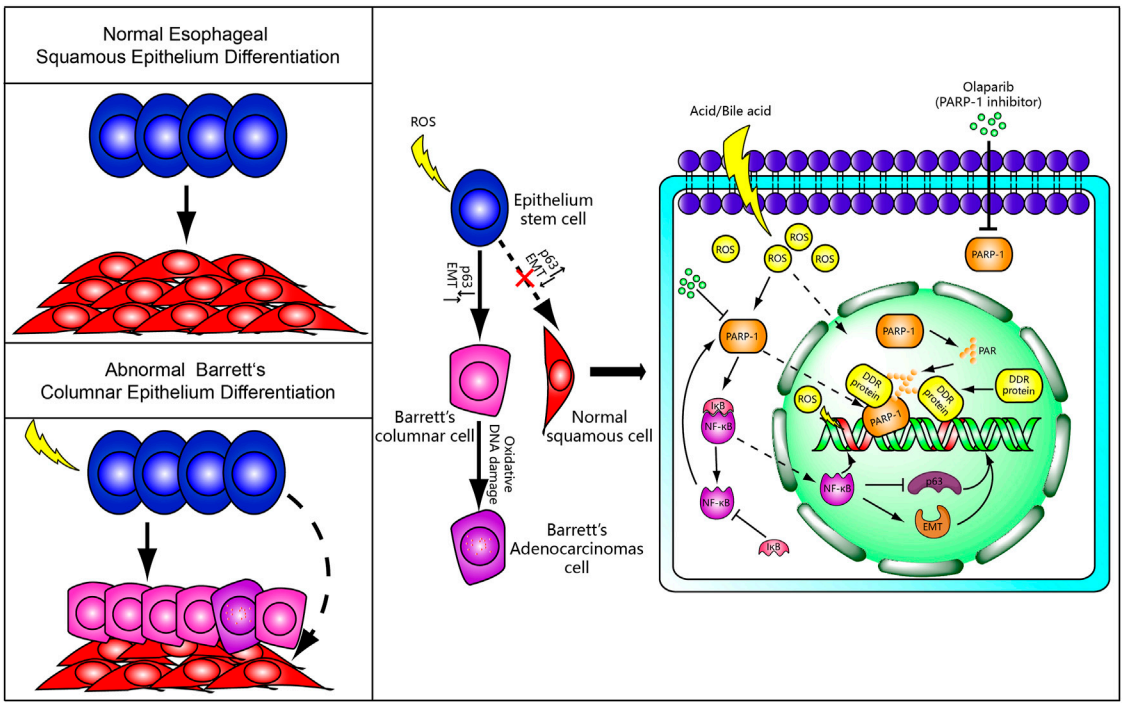

FIGURE 1 | A putative mechanism for Barrett's metaplasia and adenocarcinoma. Normally, epithelial stem cells differentiate into squamous epithelium cells. However, Barrett's columnar epithelium cells and adenocarcinoma cells replace the normal squamous cells by abnormal differentiation under chronic reflux-induced oxidative damage and inflammation. We speculate that PARP-1/NF-κB signaling and ADP-ribosylation-dependent DNA damage response may be involved in the occurrence of BE and incomplete DNA repair possibly lead to Barrett's adenocarcinoma. The PARP-1 inhibitor may serve as a molecular rescuer for BE formation.

INFLAMMATION INVOLVED IN GERD-INDUCED BARRETT'S ESOPHAGUS

GERD is a chronic inflammation of the esophagus stimulated by repeated acid/bile acids. Thus, esophagitis is the major pathological manifestation for patients with GERD and BE (Vaezi and Richter, 1996; Deshpande et al., 2021). Furthermore, chronic inflammation is likely to carry an increased risk of cancer via oxidative damage pathways (Farinati et al., 2010). Metaplasia is a pathological condition that commonly occurs in the presence of chronic inflammation (Kumar AKA et al., 2007), including typical Barrett's metaplasia (Colleypriest et al., 2009). Therefore, there is a strong association between GERD-induced reactive oxygen species (ROS) accumulation, chronic inflammatory infiltration, and BE formation. Some cell fate and development-related genes transcriptionally change in the conditions of such chronic inflammation, including BMP4, PTGS2, SHH, CDX1, CDX2, Notch, and SOX9 (Jiang et al., 2017; Peters et al., 2019).

The reflux-induced epithelial injury could be repaired by squamous cell regeneration and differentiated columnar epithelium in the distal esophagus. It is reviewed that different types of cells have been proposed to develop intestinal metaplasia during GERD-induced BE by direct or indirect trans-differentiation. Many signaling pathways may also be involved in this process (Peters et al., 2019). Columnar epithelium may be an intermediate stage in the formation of specialized intestinal metaplasia that pSMAD/CDX2 interaction is essential for the switch toward an intestinal phenotype (Mari et al., 2014). An inflammatory environment induced by damage leads to increased sonic hedgehog signaling and decreased Notch signaling mediated by PGE2, NF-κB, TNF, and other molecules. In addition, genetic variations are involved in BE. Variants of GSTP1 (such as rs1695A > G missense variant) are frequently linked to risks of infiltration and esophageal adenocarcinoma (EAC) due to the reduction of antioxidant enzymatic activity (Peng et al., 2021). Therefore, the detailed molecular mechanism of oxidative damage and inflammation involved in GERD-induced BE should be further explored.

ROLE OF P63 IN BARRETT'S ESOPHAGUS

BE may arise and develop from various stem cells, including residual embryonic stem cells, submucosal gland stem cells, gastric cardia stem cells, gastro-oesophageal junction, or basal squamous progenitor cells (Badgery et al., 2020). BE is defined as the replacement of the normal squamous epithelium by a metaplastic columnar-lined epithelium. Abnormal differentiation of multipotential stem cells into columnar-lined epithelium was considered one of the potential mechanisms (Tosh and Slack, 2002). p63, the p53 gene family member, has been termed as the master regulator of epithelial cells that determines the differentiation of progenitor cells into

squamous epithelium cells. In $p63^{-/-}$ mice, the stratified squamous epithelium fails to form, while the esophagus is lined by simple columnar epithelium (Daniely et al., 2004; Koster et al., 2004). Consistently, BE lacks the staining of p63 (Daniely et al., 2004; von Holzen and Enders, 2012). Thus, Barrett's stem cells may not be derived from the $p63^{+}$ embryonic esophageal progenitor cells and the adult squamous esophageal stem cells. The other possibility would be that p63 is downregulated in originally $p63^{+}$ adult squamous esophageal stem cells in BE. Indeed, downregulation of p63 was observed upon exposure to bile salts and acid in normal and cancer esophageal cells in culture (Roman et al., 2007). Thus, it is more likely that $p63^{+}$ adult squamous esophageal stem cells lost p63 expression in BE due to the repeated acid/bile acid stimulation in GERD patients. Molecular mechanisms for p63 downregulation in BE need to be further investigated.

DNA DAMAGE REPAIR IN GERD-INDUCED BARRETT'S ESOPHAGUS

The pathological mechanism of GERD is relatively clear, including the lower esophageal sphincter and cardia relaxation, lower esophageal sphincter pressure, and (or) esophageal insufficiency, esophageal hiatal hernia, leading to gastric acid, pepsin, and bile reflux into the esophagus. Bile salts or hydrochloric acid treatment could increase the levels of ROS, inducing an increase in the levels of 8-hydroxydeoxyguanosine (8-OH-dG) and p-H2AX which are markers of oxidative DNA damage and DNA double-strand breaks, respectively (Zhang et al., 2009; Dvorak et al., 2007). It is well established that oxidative DNA damage is usually induced by ROS which is primarily generated from normal intracellular metabolism in mitochondria and peroxisomes (Cadet et al., 2010). Increased studies from clinical biopsies have shown that oxidative stress exists in the GERD model as well as BE (Dvorak et al., 2007; Räsänen et al., 2007). Chronic exposures to high levels of ROS from overwhelming reflux and the deteriorative ability of bolus clearance in the esophagus, these excessive active free radicals to attack genomic DNA and consequently induce various types of DNA lesions. These lesions, including DNA single-stand breaks and double-strand breaks, may lead to genomic instability and various diseases (Olinski et al., 2002; Sedelnikova et al., 2010). Recent studies reported that oxidative DNA damage exists in Barrett's mucosa, and the magnitude of damage is beyond the repair capacity of a cell (Cardin et al., 2013). Since GERD patients developed BE or EAC with an approximately 6–8 fold increased risk than normal people, BE patients carry an increased risk of EAC varying between 30–125 times that of the general population (Altorki et al., 1997). Both CD133 and 8-OH-dG formation were detected at the apical surface of columnar epithelial cells of biopsy specimens of patients with BE and BE adenocarcinoma with significantly higher expression levels. This study indicated that oxidative and nitrative DNA damage and CD133 localization would contribute to BE-derived carcinogenesis (Thanan et al., 2016). Corresponding to the repair of oxidative DNA damage, apurinic/apyrimidinic endonuclease 1 (APE1), one of the key enzymes generated by ROS, is frequently overexpressed in EAC. Moreover, Barrett's and EAC cells could be protected against oxidative DNA damage by regulating JNK and p38 kinases (Hong et al., 2016; Peng et al., 2021). In this regard, the relationship between oxidative DNA damage and BE progress should be further explored. Next, we will especially discuss the role of the ROS/PARP-1/NF-κB pathway in the formation of BE and Barrett's adenocarcinoma.

THE ROLE OF PARP-1 IN BARRETT'S ESOPHAGUS

Oxidative stress triggers DNA strand breakage in BE, leading to the activation of the nuclear enzyme poly(ADP-ribose) polymerase (PARPs) which catalyze poly(ADP-ribose)relation (PARylation) at the sites of damage (Liu and Yu, 2015). These enzymes use NAD^{+} as the substrate and the negatively charged ADP-ribose (ADP) group is covalently added to the target proteins. The most common target sites for PARylation are the side chains of arginine, aspartic acid, and glutamic acid residues. After catalyzing the addition of the first ADPr onto the target proteins, other ADPrs can be covalently polymerized onto the first ADPr leading to the formation of both linear and branched polymers, called poly(ADP-ribose) (PAR) (Schreiber et al., 2006). Among the PARP family, PARP-1 is the prototypical and most abundant nuclear-expressed PARPs, which can PARylate various target proteins, including histones, DNA polymerases, DNA ligase, and PARP-1 itself. The PAR chains generated by PARP-1 form various regulatory complexes during DNA damage response and metabolism (Kim et al., 2005; Malanga and Althaus, 2005; Schreiber et al., 2006). PARP-1 can be excessively activated in situations where oxidative DNA damage is beyond the repair capacity of PARP-1. These conditions lead to excessive consumption of NAD^{+}. Since NAD^{+} synthesis requires ATP molecules, the reduction of cellular NAD^{+} and ATP levels leads to the collapse of cellular metabolism and, consequently, cell death (Schreiber et al., 2006). Thus, the PARP-1 upregulation may present a double-edged sword in the process of DNA damage response.

Recently, the role of PARP-1-dependent DNA damage response in the formation of BE and the pathological process of GERD-induced esophageal cancer is very limited. Our preliminary results show that PARP1 overexpression is probably taken as a resistance factor of BE epithelial cells to H_2O_2 or bile acid-induced oxidative damage and cell death. PARP1 also positively regulates the viability of esophageal epithelial cells, which reveals a potential candidate for a therapeutic strategy for BE (Zhang et al., 2018). PARP-1 is also known to be a co-activator of NF-κB, playing a key role in pro-inflammation by contributing to inflammatory processes through the regulation of transcription factors (Hassa and Hottiger, 1999; Liu et al., 2012). NF-κB was one of the first mediators of inflammation to be identified as a target for PARP-1 mediated PARylation (Aguilar-Quesada et al., 2007). In $PARP^{-/-}$ mice and cell lines, NF-κB activity is severely compromised in absence of activation by upstream PARP-1 (Oliver et al., 1999),

and in an oxazolone-induced contact hypersensitivity model, PARP-1 inhibition reduces the extent of inflammation by modulating oxidative stress and impairing the activation of NF-κB (Brunyánszki et al., 2010). PARP-1 may serve as a negative regulator of p63 by activating NF-κB in Barrett's cell. Hence, oxidative stress-induced high PARP-1 activity in the BE-related stem cells may downregulate p63.

FUTURE PERSPECTIVES

The widely present evidence of oxidative DNA damage in BE from human tissue and cell models was recently reported (Dvorak et al., 2007; Peng et al., 2014; Hong et al., 2016). It is assumed that the development of BE is associated with oxidative DNA damage response. The long-term excessive acid/base-induced ROS stimulation in GERD may lead to activation of the PARP-1/NF-κB pathway with inflammatory infiltration of the epithelial stem cells. The inflammatory cells then tend to differentiate into Barrett's esophageal epithelium (columnar epithelium) via transcription factor p63 and EMT. Whereas, DNA damage itself can lead to carcinogenesis with incomplete ADP-ribosylation-dependent DNA damage response. All these events can be associated with a heterogeneity of esophageal epithelial cells and tumor occurrence and development, eventually leading to EAC (**Figure 1**). This presumably suggests that antagonists of PARP-1/NF-κB might have beneficial effects on Barrett's metaplasia in GERD patients. However, to the best of our knowledge, there has been no research on the effects of oxidative DNA damage-related agents on Barrett's cell lines or animal models, which necessitates more studies.

We speculate that PARP-1/NF-κB signaling and ADP-ribosylation-dependent DNA damage response may be involved in the occurrence of BE and incomplete DNA repair due to low levels of ADP-ribosylation possibly lead to Barrett's adenocarcinoma. However, there are still many open questions existing in the field that require further studies. 1) The degree of oxidative DNA damage, the level of PARP-1/NF-κB signaling, and NAD^+ between esophageal stem cells, esophageal squamous cells, Barrett's esophageal columnar cells, and adenocarcinoma cells by acid, bile acid, and oxidative stress treatment should be further investigated. 2) Adding extrinsic NF-κB or activating PARP-1/NF-κB signaling to detect the DNA damage repair and inflammatory response between PARP-1 knockout esophageal stem cell lines and wild-type cell lines with induced ROS. So what is the detailed mechanism among NF-κB/ΔNp63/EMT in the development of BE and EAC. 3) What is the exact role of PARP-1 in esophageal stem cells, Barrett's esophageal columnar cells, and adenocarcinoma cells.

AUTHOR CONTRIBUTIONS

DH drafted the manuscript; CZ revised the manuscript, and all authors read and approved the final manuscript.

FUNDING

National Natural Science Foundation of China (81800483 to CZ) and Beijing Hospitals Authority Youth Programme (QMS20200803 to CZ).

REFERENCES

Aguilar-Quesada, R., Munoz-Gamez, J., Martin-Oliva, D., Peralta-Leal, A., Quiles-Perez, R., Rodriguez-Vargas, J., et al. (2007). Modulation of Transcription by PARP-1: Consequences in Carcinogenesis and Inflammation. *Cmc* 14 (11), 1179–1187. doi:10.2174/092986707780597998

Altorki, N. K., Oliveria, S., and Schrump, D. S. (1997). Epidemiology and Molecular Biology of Barrett's Adenocarcinoma. *Semin. Surg. Oncol.* 13 (4), 270–280. doi:10.1002/(sici)1098-2388(199707/08)13:4<270::aid-ssu9>3.0.co;2-2

Amadi, C., Gatenby, P., and Oesophagus, B. (2017). Barrett's Oesophagus: Current Controversies. *Wjg* 23 (28), 5051–5067. doi:10.3748/wjg.v23.i28.5051

Badgery, H., Chong, L., Iich, E., Huang, Q., Georgy, S. R., Wang, D. H., et al. (2020). Recent Insights into the Biology of Barrett's Esophagus. *Ann. N.Y. Acad. Sci.* 1481 (1), 198–209. doi:10.1111/nyas.14432

Barrett, N. R. (1950). Chronic Peptic Ulcer of the Oesophagus and 'oesophagitis'. *Br. J. Surg.* 38 (150), 175–182. doi:10.1002/bjs.18003815005

Brunyánszki, A., Hegedűs, C., Szántó, M., Erdélyi, K., Kovács, K., Schreiber, V., et al. (2010). Genetic Ablation of PARP-1 Protects against Oxazolone-Induced Contact Hypersensitivity by Modulating Oxidative Stress. *J. Invest. Dermatol.* 130 (11), 2629–2637. doi:10.1038/jid.2010.190

Cadet, J., Douki, T., and Ravanat, J.-L. (2010). Oxidatively Generated Base Damage to Cellular DNA. *Free Radic. Biol. Med.* 49 (1), 9–21. doi:10.1016/j.freeradbiomed.2010.03.025

Cardin, R., Piciocchi, M., Tieppo, C., Maddalo, G., Zaninotto, G., Mescoli, C., et al. (2013). Oxidative DNA Damage in Barrett Mucosa: Correlation with Telomeric Dysfunction and P53 Mutation. *Ann. Surg. Oncol.* 20 (Suppl. 3), S583–S589. doi:10.1245/s10434-013-3043-1

Colleypriest, B. J., Palmer, R. M., Ward, S. G., and Tosh, D. (2009). Cdx Genes, Inflammation and the Pathogenesis of Barrett's Metaplasia. *Trends Mol. Med.* 15 (7), 313–322. doi:10.1016/j.molmed.2009.05.001

Daniely, Y., Liao, G., Dixon, D., Linnoila, R. I., Lori, A., Randell, S. H., et al. (2004). Critical Role of P63 in the Development of a normal Esophageal and Tracheobronchial Epithelium. *Am. J. Physiology-Cell Physiol.* 287 (1), C171–C181. doi:10.1152/ajpcell.00226.2003

Deshpande, N. P., Riordan, S. M., Gorman, C. J., Nielsen, S., Russell, T. L., Correa-Ospina, C., et al. (2021). Multi-omics of the Esophageal Microenvironment Identifies Signatures Associated with Progression of Barrett's Esophagus. *Genome Med.* 13 (1), 133. doi:10.1186/s13073-021-00951-6

Dvorak, K., Payne, C. M., Chavarria, M., Ramsey, L., Dvorakova, B., Bernstein, H., et al. (2007). Bile Acids in Combination with Low pH Induce Oxidative Stress and Oxidative DNA Damage: Relevance to the Pathogenesis of Barrett's Oesophagus. *Gut* 56 (6), 763–771. doi:10.1136/gut.2006.103697

El-Serag, H. B., Sweet, S., Winchester, C. C., and Dent, J. (2014). Update on the Epidemiology of Gastro-Oesophageal Reflux Disease: a Systematic Review. *Gut* 63 (6), 871–880. doi:10.1136/gutjnl-2012-304269

Farinati, F., Piciocchi, M., Lavezzo, E., Bortolami, M., and Cardin, R. (2010). Oxidative Stress and Inducible Nitric Oxide Synthase Induction in Carcinogenesis. *Dig. Dis.* 28 (4-5), 579–584. doi:10.1159/000320052

Hassa, P. O., and Hottiger, M. O. (1999). A Role of Poly (ADP-Ribose) Polymerase in NF-kappaB Transcriptional Activation. *Biol. Chem.* 380 (7-8), 953–959. doi:10.1515/BC.1999.118

Hong, J., Chen, Z., Peng, D., Zaika, A., Revetta, F., Washington, M. K., et al. (2016). APE1-mediated DNA Damage Repair Provides Survival Advantage for Esophageal Adenocarcinoma Cells in Response to Acidic Bile Salts. *Oncotarget*, 7(13):16688–166702. doi:10.18632/oncotarget.7696

Jiang, M., Li, H., Zhang, Y., Yang, Y., Lu, R., Liu, K., et al. (2017). Transitional Basal Cells at the Squamous-Columnar junction Generate Barrett's Oesophagus. *Nature* 550 (7677), 529–533. doi:10.1038/nature24269

Kim, M. Y., Zhang, T., and Kraus, W. L. (2005). Poly(ADP-ribosyl)ation by PARP-1: `PAR-Laying' NAD+ into a Nuclear Signal. *Genes Dev.* 19 (17), 1951–1967. doi:10.1101/gad.1331805

Koster, M. I., Kim, S., Mills, A. A., DeMayo, F. J., and Roop, D. R. (2004). p63 Is the Molecular Switch for Initiation of an Epithelial Stratification Program. *Genes Dev.* 18 (2), 126–131. doi:10.1101/gad.1165104

Kumar Aka, V., Fausto, N., Mitchell, R., and Robbins (2007). *Basic Pathology*. 8th edn. Elsevier Saunders.

Liu, C., and Yu, X. (2015). ADP-ribosyltransferases and Poly ADP-Ribosylation. *Cpps* 16 (6), 491–501. doi:10.2174/1389203716666150504122435

Liu, L., Ke, Y., Jiang, X., He, F., Pan, L., Xu, L., et al. (2012). Lipopolysaccharide Activates ERK-PARP-1-RelA Pathway and Promotes Nuclear Factor-Kb Transcription in Murine Macrophages. *Hum. Immunol.* 73 (5), 439–447. doi:10.1016/j.humimm.2012.02.002

Malanga, M., and Althaus, F. R. (2005). The Role of poly(ADP-Ribose) in the DNA Damage Signaling Network. *Biochem. Cell Biol.* 83 (3), 354–364. doi:10.1139/o05-038

Mari, L., Milano, F., Parikh, K., Straub, D., Everts, V., Hoeben, K. K., et al. (2014). A pSMAD/CDX2 Complex Is Essential for the Intestinalization of Epithelial Metaplasia. *Cell Rep.* 7 (4), 1197–1210. doi:10.1016/j.celrep.2014.03.074

Maslyonkina, K. S., Konyukova, A. K., Alexeeva, D. Y., Sinelnikov, M. Y., and Mikhaleva, L. M. (2021). Barrett's Esophagus: The Pathomorphological and Molecular Genetic Keystones of Neoplastic Progression. *Cancer Med.* 11 (2), 447–478.

McDonald, S. A. C., Lavery, D., Wright, N. A., and Jansen, M. (2015). Barrett Oesophagus: Lessons on its Origins from the Lesion Itself. *Nat. Rev. Gastroenterol. Hepatol.* 12 (1), 50–60. doi:10.1038/nrgastro.2014.181

Mittal, S. K., Abdo, J., Adrien, M. P., Bayu, B. A., Kline, J. R., Sullivan, M. M., et al. (2021). Current State of Prognostication, Therapy and Prospective Innovations for Barrett's-related Esophageal Adenocarcinoma: a Literature Review. *J. Gastrointest. Oncol.* 12 (4), 1197–1214. doi:10.21037/jgo-21-117

Olinski, R., Gackowski, D., Foksinski, M., Rozalski, R., Roszkowski, K., and Jaruga, P. (2002). Oxidative DNA Damage: Assessment of the Role in Carcinogenesis, Atherosclerosis, and Acquired Immunodeficiency Syndrome1 1This Article Is Part of a Series of Reviews on "Oxidative DNA Damage and Repair." the Full List of Papers May Be Found on the Homepage of the Journal. *Free Radic. Biol. Med.* 33 (2), 192–200. doi:10.1016/s0891-5849(02)00878-x

Oliver, F. J., Menissier-de Murcia, J., Nacci, C., Decker, P., Andriantsitohaina, R., Muller, S., et al. (1999). Resistance to Endotoxic Shock as a Consequence of Defective NF-Kappa B Activation in Poly (ADP-Ribose) Polymerase-1 Deficient Mice. *EMBO J.* 18 (16), 4446–4454. doi:10.1093/emboj/18.16.4446

Peng, D., Zaika, A., Que, J., and El-Rifai, W. (2021). The Antioxidant Response in Barrett's Tumorigenesis: A Double-Edged Sword. *Redox Biol.* 41, 101894. doi:10.1016/j.redox.2021.101894

Peng, S., Huo, X., Rezaei, D., Zhang, Q., Zhang, X., Yu, C., et al. (2014). In Barrett's Esophagus Patients and Barrett's Cell Lines, Ursodeoxycholic Acid Increases Antioxidant Expression and Prevents DNA Damage by Bile Acids. *Am. J. Physiology-Gastrointestinal Liver Physiol.* 307 (2), G129–G139. doi:10.1152/ajpgi.00085.2014

Peters, Y., Al-Kaabi, A., Shaheen, N. J., Chak, A., Blum, A., Souza, R. F., et al. (2019). Barrett Oesophagus. *Nat. Rev. Dis. Primers* 5 (1), 35. doi:10.1038/s41572-019-0086-z

Räsänen, J. V., Sihvo, E. I. T., Ahotupa, M. O., Färkkilä, M. A., and Salo, J. A. (2007). The Expression of 8-hydroxydeoxyguanosine in Oesophageal Tissues and Tumours. *Eur. J. Surg. Oncol. (Ejso)* 33 (10), 1164–1168. doi:10.1016/j.ejso.2007.03.003

Roman, S., Pétré, A., Thépot, A., Hautefeuille, A., Scoazec, J.-Y., Mion, F., et al. (2007). Downregulation of P63 upon Exposure to Bile Salts and Acid in normal and Cancer Esophageal Cells in Culture. *Am. J. Physiology-Gastrointestinal Liver Physiol.* 293 (1), G45–G53. doi:10.1152/ajpgi.00583.2006

Schreiber, V., Dantzer, F., Ame, J.-C., and de Murcia, G. (2006). Poly(ADP-ribose): Novel Functions for an Old Molecule. *Nat. Rev. Mol. Cell Biol* 7 (7), 517–528. doi:10.1038/nrm1963

Sedelnikova, O. A., Redon, C. E., Dickey, J. S., Nakamura, A. J., Georgakilas, A. G., and Bonner, W. M. (2010). Role of Oxidatively Induced DNA Lesions in Human Pathogenesis. *Mutat. Res.* 704 (1-3), 152–159. doi:10.1016/j.mrrev.2009.12.005

Thanan, R., Ma, N., Hiraku, Y., Iijima, K., Koike, T., Shimosegawa, T., et al. (2016). DNA Damage in CD133-Positive Cells in Barrett's Esophagus and Esophageal Adenocarcinoma. *Mediators Inflamm.* 2016, 7937814. doi:10.1155/2016/7937814

Tosh, D., and Slack, J. M. W. (2002). How Cells Change Their Phenotype. *Nat. Rev. Mol. Cell Biol* 3 (3), 187–194. doi:10.1038/nrm761

Vaezi, M., and Richter, J. (1996). Role of Acid and Duodenogastroesophageal Reflux in Gastroesophageal Reflux Disease. *Gastroenterology* 111 (5), 1192–1199. doi:10.1053/gast.1996.v111.pm8898632

von Holzen, U., and Enders, G. H. (2012). A surprise Cell of Origin for Barrett's Esophagus. *Cancer Biol. Ther.* 13 (8), 588–591. doi:10.4161/cbt.20088

Zhang, C., Ma, T., Luo, T., Li, A., Gao, X., Wang, Z.-G., et al. (2018). Dysregulation of PARP1 Is Involved in Development of Barrett's Esophagus. *Wjg* 24 (9), 982–991. doi:10.3748/wjg.v24.i9.982

Zhang, H. Y., Hormi-Carver, K., Zhang, X., Spechler, S. J., and Souza, R. F. (2009). In Benign Barrett's Epithelial Cells, Acid Exposure Generates Reactive Oxygen Species that Cause DNA Double-Strand Breaks. *Cancer Res.* 69 (23), 9083–9089. doi:10.1158/0008-5472.can-09-2518

Conflict of Interest: The authors declare that the research was conducted in the absence of any commercial or financial relationships that could be construed as a potential conflict of interest.

Publisher's Note: All claims expressed in this article are solely those of the authors and do not necessarily represent those of their affiliated organizations, or those of the publisher, the editors, and the reviewers. Any product that may be evaluated in this article, or claim that may be made by its manufacturer, is not guaranteed or endorsed by the publisher.

Advantages of publishing in Frontiers

OPEN ACCESS
Articles are free to read for greatest visibility and readership

FAST PUBLICATION
Around 90 days from submission to decision

HIGH QUALITY PEER-REVIEW
Rigorous, collaborative, and constructive peer-review

TRANSPARENT PEER-REVIEW
Editors and reviewers acknowledged by name on published articles

Frontiers
Avenue du Tribunal-Fédéral 34
1005 Lausanne | Switzerland

Visit us: www.frontiersin.org
Contact us: frontiersin.org/about/contact

REPRODUCIBILITY OF RESEARCH
Support open data and methods to enhance research reproducibility

DIGITAL PUBLISHING
Articles designed for optimal readership across devices

FOLLOW US
@frontiersin

IMPACT METRICS
Advanced article metrics track visibility across digital media

EXTENSIVE PROMOTION
Marketing and promotion of impactful research

LOOP RESEARCH NETWORK
Our network increases your article's readership